

BEDROCK GEOCHEMISTRY OF PORPHYRY COPPER
DEPOSITS, HIGHLAND VALLEY, BRITISH COLUMBIA

by

MOSES AYODELE DELESON OLADE

B. Sc., (Hons.), University of Ibadan, Nigeria, 1969

M. Sc., University of Alberta, 1972

A THESIS SUBMITTED IN PARTIAL FULFILLMENT

OF THE REQUIREMENTS FOR THE DEGREE OF

DOCTOR OF PHILOSOPHY

in the department

of

GEOLOGICAL SCIENCES

We accept this thesis as conforming to
the required standard

The University of British Columbia

October 1974

In presenting this thesis in partial fulfilment of the requirements for an advanced degree at the University of British Columbia, I agree that the Library shall make it freely available for reference and study.

I further agree that permission for extensive copying of this thesis for scholarly purposes may be granted by the Head of my Department or by his representatives. It is understood that copying or publication of this thesis for financial gain shall not be allowed without my written permission.

Department of GEOLOGICAL SCIENCES

The University of British Columbia
Vancouver 8, Canada

Date 7th Nov. 1974

ABSTRACT

The feasibility of utilizing bedrock and mineral geochemistry in the exploration for porphyry copper deposits has been investigated in the Highland Valley copper district. More than 1500 bedrock samples collected from the vicinity of the Valley Copper, Bethlehem-JA, Lornex, Highmont and Skeena deposits together with 60 fresh unmineralized samples covering the Guichon Creek batholith (Northcote, 1968) were analyzed for more than 20 elements using total and partial digestion. An efficacious sulphide-selective technique, not used previously in bedrock geochemistry was developed during this investigation.

Chemical variations in fresh rocks of the Guichon Creek batholith are consistent with a model of fractional crystallization of a calc-alkaline dioritic magma. Cu, like other femic elements (Zn, Mn, V, Ti, Ni, Co, Fe, Mg), generally decreases with increasing magmatic fractionation. This geochemical pattern is commonly characteristic of unmineralized intrusions suggesting that ore metals were not derived by differentiation of a Cu-rich Guichon Creek magma as proposed by previous workers. Results of isotopic studies (Field *et al.*, 1973) are however, consistent with a model of derivation of ore metals from a subcrustal source, most probably subducted oceanic crust or upper mantle.

Detailed bedrock geochemistry around mineralization reveals that S and Cu show the highest geochemical contrast, with halos extending up to 0.5km from mineralized zones. Of these two elements,

S shows the more consistent pattern. Dispersions of the lithophile elements (Rb, Sr, Ba, K, Ca, Na) are controlled by type and intensity of wall-rock alteration, with halos extending slightly beyond ore zones but within the alteration envelope. Distribution of the femic elements (Zn, Mn, V, Ti, Ni, Co, Fe, Mg) is controlled principally by primary lithology, although minor hydrothermal redistribution is apparent. Hg defines a broad anomaly at Bethlehem-JA but is absent at Valley Copper. B anomalies are well developed at Lornex and Highmont but less prominent at Valley Copper and Bethlehem-JA. Results of factor analysis are consistent with subjective interpretations of metal associations and ore-forming processes.

Mineral geochemistry indicates that biotite, magnetite and quartz-feldspar phases from mineralized samples are enriched in Cu but depleted in Ni, Zn, Mn, Co and Mg, relative to background samples. Better geochemical contrast is obtained with whole-rock than mineral analysis, consequently the use of mineral phases offers no advantages for exploration in the Highland Valley.

In exploration for porphyry copper deposits of the Highland Valley type, S, Cu, Rb, Sr, Ba, K, Na, B and Hg in bedrock can be useful in delineating intensely altered and mineralized zones.

TABLE OF CONTENTS

	Page
ABSTRACT	i
TABLE OF CONTENTS	ii
LIST OF TABLES	ix
LIST OF FIGURES (Volume 1)	xiii
LIST OF FIGURES (Volume 11)	xviii
LIST OF PLATES	xxiii
ACKNOWLEDGEMENTS	xxvi
 CHAPTER ONE:	 1
<u>INTRODUCTION</u>	2
GENERAL STATEMENT	2
LOCATION AND ACCESS	3
OBJECTIVES OF STUDY	3
BEDROCK GEOCHEMISTRY IN MINERAL EXPLORATION - PREVIOUS WORK	5
(a) Regional Geochemical Patterns	5
(b) Hydrothermal Dispersion Patterns	7
(c) Mineral Geochemical Patterns	9
 CHAPTER TWO:	 12
<u>GEOLOGIC SETTING OF GUICHON CREEK BATHOLITH</u>	12
I: GUICHON CREEK BATHOLITH	13
REGIONAL SETTING	13
PETROLOGY AND STRUCTURE	14
ECONOMIC MINERALIZATION	19

II: HIGHLAND VALLEY	21
INTRODUCTION	21
GEOLOGY OF MINERAL DEPOSITS	21
(a) Bethlehem-JA	21
(b) Valley Copper	25
(c) Lornex and Skeena	27
(d) Highmont	30
CHAPTER THREE:	35
<u>WALL-ROCK ALTERATION</u>	35
INTRODUCTION	36
(a) General Statement	36
(b) Methods of Study and Terminology	36
BETHLEHEM-JA	38
(a) Main Stage Pervasive Alteration	41
Potassic Alteration	41
Argillic Alteration	42
Propylitic Alteration	43
(b) Late Stage Alteration	44
Zeolites	44
Epidote	46
(c) Sulphide Zoning	46
VALLEY COPPER	49
(a) Pervasive Argillic Alteration	49
(b) Vein Alteration	51
(i) Early Phase Veining	51
Barren Quartz Veins	52
Quartz-Potash Feldspar Veins	52
(ii) Main Phase Veining	52
Quartz-Sericite Veins	52
Potash Feldspar Alteration	53
(iii) Late Phase Veining	54
(c) Sulphide Zoning	54

	Page
LORNEX	56
(a) Early Stage Pervasive Alteration	56
Propylitic	59
Propy-Argillic Zone	59
Argillic Zone	60
(b) Main Stage Alteration	61
Quartz-Sericite Alteration	61
Potash-Feldspar Veining	62
Gypsum Veining	62
(c) Sulphide Zoning	63
SKEENA	63
HIGHMONT	63
(a) Pervasive Alteration	66
Propylitic Alteration	66
Propy-Argillic Alteration	66
Argillic Alteration	69
(b) Vein Alteration	70
Quartz-Sericite Alteration	70
Quartz-Potash Feldspar Veining	
Quartz-Tourmaline-Biotite Alteration	70
Gypsum Veining	70
(c) Sulphide Zoning	71
FACTORS CONTROLLING WALL-ROCK ALTERATION	71
(a) Host Rock Composition	71
(b) Intensity of Faulting and Fracturing	74
(c) Composition of Mineralizing Solutions	75
(d) Structural Levels of Ore Formation	76
SUMMARY AND CONCLUSIONS	77
CHAPTER FOUR:	80
<u>SAMPLING AND ANALYTICAL TECHNIQUES</u>	80
SAMPLE COLLECTION	81
(a) Outcrop Sampling	81
(b) Drill-Core Sampling	83
SAMPLE PREPARATION	84

	Page
(a) Crushing and Grinding	84
(b) Mineral Separation	84
ANALYTICAL TECHNIQUES	85
(a) Emission Spectrography	86
(b) X-Ray Fluorescence Spectrometry	86
Major Elements	86
Minor Elements	89
(c) Ion-Selective Electrodes	89
Total-Extractable Halogens	89
Water-Extractable Halogens	91
(d) Atomic Absorption Spectrophotometry	91
HF-HClO ₄ -HNO ₃ Digestion	93
HNO ₃ -HClO ₄ Digestion	99
Pre-Analytical Treatment for Hg Determination	99
(i) Sulphide Selective Decompositions	99
Aqua Regia	99
H ₂ O ₂ -Ascorbic Acid	100
KClO ₃ -HCl	100
POTASSIUM CHLORATE-HYDROCHLORIC ACID: A SULPHIDE SELECTIVE LEACH FOR BEDROCK GEOCHEMISTRY	102
(a) Introduction	102
(b) Analytical Procedure	102
(c) Experimental Work and Results	102
(d) Discussion	106
(e) Applications to Geochemical Exploration	111
(f) Conclusions	
CHAPTER FIVE:	114
<u>REGIONAL GEOCHEMISTRY</u>	114
INTRODUCTION	115
RESULTS	115
(a) Major Elements	115
(b) Trace Elements	122
(i) Introduction	122
(ii) Distribution of Copper	124
(iii) Distribution of S, Rb, Sr, Cl and F	126
DISCUSSION	140
SUMMARY AND CONCLUSIONS	145

CHAPTER SIX:	147
<u>METAL DISPERSION IN BEDROCK AROUND MINERALIZATION</u>	147
INTRODUCTION	148
DATA HANDLING	148
RESULTS	150
BETHLEHEM-JA	150
(a) Geochemical Patterns Related to Primary Lithology	150
(b) Geochemical Patterns Related to Hydrothermal Alteration	157
(c) Geochemical Patterns Related to Mineralization	161
(i) Distribution of Ore Elements	161
(ii) Distribution of Pathfinder Elements	163
(d) R-mode Factor Analysis	166
(e) General Discussion and Summary	171
VALLEY COPPER	173
(a) Geochemical Patterns Related to Hydrothermal Alteration	179
(b) Geochemical Patterns Related to Mineralization	182
(i) Ore Elements	182
(ii) Pathfinder Elements	186
(c) R-mode Factor Analysis	186
(d) General Discussion and Summary	191
LORNEX	193
(a) Geochemical Patterns Related to Lithology	197
(b) Geochemical Patterns Related to Hydrothermal Alteration	200
(c) Geochemical Patterns Related to Lornex Fault	202
(d) Geochemical Patterns Related to Mineralization	206
(e) R-mode Factor Analysis	209
(i) Surface samples	209
(ii) Subsurface samples	215
(f) General Discussion and Summary	216
HIGHMONT	220
(a) Geochemical Patterns Related to Lithology	220
(b) Geochemical Patterns Related to Hydrothermal Alteration	225
(c) Geochemical Patterns Related to Mineralization	225
(d) R-mode Factor Analysis	229
SKEENA	235
Distribution of Cu, Zn, Mn, CaO, Fe ₂ O ₃ , K ₂ O	235

DISCUSSION	240
Applications to Mineral Exploration	247
CONCLUSIONS	251
CHAPTER SEVEN:	253
<u>MICRO-GEOCHEMICAL DISPERSION IN MINERALS</u>	253
INTRODUCTION	254
METHODS OF STUDY	255
RESULTS	259
(a) Biotite	259
(b) Magnetite	261
(c) Quartz-Feldspar	263
DISCUSSION	263
(a) Form of Trace Elements in Mineral Phases	265
(b) Chemical Variations Related to Modal Composition	269
(c) Variations Related to Chemical Composition of Mineral Phases Biotites	275
(d) Chemical Variations Related to Mineralization	279
(i) Biotites	279
(ii) Magnetites	281
(iii) Quartz-Feldspar	283
GEOCHEMICAL CONTRAST	285
SUMMARY AND CONCLUSIONS	287
CHAPTER EIGHT:	289
<u>ORE-FORMING PROCESSES AT HIGHLAND VALLEY</u>	289
INTRODUCTION	290
(a) General Statement	290
(b) Ore Genetic Models for Porphyry Copper Deposits	290
ORIGIN OF GUICHON CREEK BATHOLITH AND SOURCE OF METALS	292

	Page
(a) Provenance of Guichon Creek Magma and Associated Metals	292
(b) Level of Emplacement and Volatile Pressures	297
NATURE OF ALTERATION-MINERALIZATION PROCESSES	300
(a) Mineral Stability Fields	300
(b) Bedrock Geochemical Evidence	301
DISCUSSION	301
CONCLUSIONS	310
CHAPTER NINE:	311
SUMMARY AND CONCLUSIONS	312
(a) Regional Geochemistry	312
(b) Detailed Bedrock Geochemistry	313
(c) Mineral Geochemistry	315
(d) Sulphide Selective Digestion	316
(e) Ore-forming Processes at Highland Valley	318
(f) Applications of Bedrock Geochemistry in Exploration	318
REFERENCES	322
APPENDIX A	337
B	349
C	361
D	378

VOLUME II

Maps depicting metal distribution patterns at Bethlehem-JA, Valley
Copper, Lornex, Highmont and Skeena.

LIST OF TABLES

Table		Page
I	Units and Phases of the Guichon Creek batholith.	15
II	Size production, capacity, grade and ore mineralogy of mineral deposits, Guichon Creek batholith	20
III	Summary of sampling and chemical analysis	82
IV	Spectrographic equipment and standard operating conditions	87
V	Spectral lines and precision at the 95% confidence level of emission spectrographic analysis	88
VI	Operating conditions for Philips 1010 X-ray spectrometer	90a
VII	Equipment and stock reagents in ion-selective electrode analysis	90b
VIII	Comparison of fluorine and chlorine contents of U.S.G.S. standard rocks	92
IX	Operating conditions for Techtron AA-4 spectrophotometer	94
X	Operating conditions for the Perkin Elmer 303 spectrophotometer	95
XI	Operating conditions for the Jarrell-Ash 82-270 spectrophotometer	96
XII	Analytical precision of $\text{HF}/\text{HClO}_4/\text{HNO}_3$ digestion at the 95% confidence level estimated from paired samples	97
XIII	Comparison of trace and major element contents of U.S.G.S. standard rocks	98
XIV	Effect of composition of standards on atomic absorption	101
XV	Comparison of leaches on ultramafic standard UM1, UM2 and UM4	105
XVI	Effect of amount of KClO_3 added on release of copper with KClO_3 -HCl leach	108
XVII	Effect of grinding on release of copper and zinc with KClO_3 -HCl leach	109
XVIII	Comparison of analytical results obtained from KClO_3 -HCl digests using atomic absorption and colorimetry	112

	Page
XIX Means, ranges and mean normative composition of intrusive units, Guichon Creek batholith	117
XX Means and ranges of trace elements in rocks of Guichon Creek batholith	123
XXI Abundances of sulphur, rubidium and strontium in rocks of Guichon Creek batholith	128
XXII Abundances of mercury in rocks of Guichon Creek batholith	129
XXIII Abundances of chlorine and fluorine in rocks of Guichon Creek batholith	135
XXIV Means and ranges of trace elements at Bethlehem-JA, 2800 Level	151
XXV Means and ranges of some metal concentrations in principal lithologic units, Bethlehem-JA 2800 Level	154
XXVI Correlation matrix of trace and major element contents, Bethlehem-JA 2800 Level	156
XXVII Chemical variations associated with types of alteration, Bethlehem-JA 2800 Level	158
XXVIII Relationships among copper, potassium and potential pathfinder elements, Bethlehem-JA 2800 Level	167
XXIX Element associations of different factor models, trace and major element content of rocks, Bethlehem-JA, 2800 Level	168
XXX R-mode Varimax Factor Matrix, Bethlehem-JA 2800 Level	169
XXXI Comparison of mean content and geochemical contrast in background and anomalous samples, Bethlehem-JA 2800 Level	172
XXXII Means, deviations and ranges of trace and major elements of Valley Copper	176
XXXIII Chemical variations associated with types of alteration, Valley Copper 3600 Level	180
XXXIV Correlation coefficients, Valley Copper 3600 Level	187
XXXV Element associations of different factor models, Valley Copper 3600 Level	188

XXXVI	Varimax Factor Matrix, Valley Copper 3600 Level	189
XXXVII	Comparisons of mean element content in background and mineralized samples, Valley Copper 3600 Level	192
XXXVIII	Means and ranges of trace and major elements, Lornex property	196
XXXIX	Means and ranges of metal concentrations in lithologic units, Lornex Surface	198
XL	Means and ranges of element abundances associated with alteration types, Lornex Subsurface	201
XLI	Metal concentrations along the Lornex Fault	204
XLII	Correlation coefficients, Lornex Subsurface	210
XLIII	R-mode Varimax Factor Matrix, Lornex Surface	211
XLIV	Metal associations of different factor models, Lornex Subsurface	212
XLV	Correlation Coefficients, Lornex Subsurface	213
XLVI	R-mode Varimax Factor Matrix, Lornex Subsurface	214
XLVII	Comparison of variability in copper contents of background and mineralized samples, Lornex	218
XLVIII	Comparison of metal contents and contrast in background and mineralized areas, Lornex property	219
XLIX	Means and ranges of trace and major elements at Highmont	223
L	Means and ranges of metal concentrations in lithologic units, Highmont Surface	224
LI	Metal concentrations associated with types of alteration, Highmont property	226
LII	Correlation matrix, Highmont Subsurface	230
LIII	Metal associations of different factor models, Highmont Subsurface	231
LIV	Varimax Factor Matrix, Highmont Subsurface	232

LV	Comparison of variability in copper contents of background and mineralized samples, Highmont	236
LVI	Comparison between metal concentrations in background and mineralized zones, Highmont	237
LVII	Comparison of relative contrast and extent of halos at Highland Valley deposits	248
LVIII	Trace element and modal content of whole rock samples	258
LIX	Trace and major element contents of minerals	260
LX	Student T test of background and anomalous samples	262
LXI	KClO ₃ -HCl extractable metal in mineral phases	264
LXII	Correlation matrix for modal analysis and trace element content of rocks and minerals	276
LXIII	Comparison of geochemical contrast in whole rock and mineral separates	286
LXIV	Rb, Sr, Rb/Sr, K/Rb, and Sr ⁸⁷ /Sr ⁸⁶ abundances of some Cordilleran intrusions	296

LIST OF FIGURES

FIGURE	Page
1: Location of study area	4
2: Geology of Guichon Creek batholith	16
3: Simplified modal variations in rocks of the Guichon Creek batholith	18
4: Generalized geology of Highland Valley	22
5: General geology of Bethlehem-JA, 2800 Level	24
6: General geology of Valley Copper	26
7: Generalized geology of Lornex and Skeena Mines	28
8: Simplified geology across a section at Lornex mine	29
9: Simplified geology of Highmont property	31
10: Simplified geology across a section at Highmont	33
11: Generalized alteration map, Bethlehem-JA, 2800 Level	39
12: Generalized alteration across a section of Bethlehem-JA	40
13: Distribution of zeolite alteration at Bethlehem-JA	45
14: Generalized sulphide zoning at Bethlehem-JA	47
15: Generalized vertical distribution of sulphides at Bethlehem-JA	48
16: Generalized alteration map, Valley Copper 3600 Level	50
17: Generalized alteration map, Lornex 4900 Level	57
18: Generalized alteration in a section across Highmont	58
19: Sulphide distribution at Lornex mine	64
20: Wall-rock alteration map, Skeena mine	65
21: Generalized alteration map, Highmont property	67
22: Generalized alteration map in a section across Highmont	68

FIGURE

Page

23a:	Mineral zoning and copper grade at Highmont property	72
23b:	Distribution of MoS_2 in relation to mineral zoning at Highmont	73
24:	Comparison of % of total metal extracted by partial extraction techniques	104
25:	Relationship between the amount of metal extracted and time of grinding	107
26:	Location of samples used in regional study, Guichon Creek batholith	116
27:	Variation diagrams in Guichon Creek rocks showing major element concentrations versus Larsen differentiation index	119
28:	AFM variation diagram for rocks of Guichon Creek batholith	120
29:	$\text{CaO-Na}_2\text{O-K}_2\text{O}$ variations for rocks of Guichon Creek batholith	121
30a:	Distribution of Copper in relation to Larsen differentiation index	125
30b:	Regional distribution of aqua regia extractable copper in rocks of Guichon Creek batholith	125
31:	Relationship between Copper and Iron in rocks of Guichon Creek batholith	127
32:	Relationship between rubidium and potassium in rocks of Guichon Creek batholith	131
32b:	Plots of K/Rb versus K in rocks of Guichon Creek batholith	132
33:	Plots of K/Rb and Ca/Sr versus Larsen differentiation index	133
34:	Variation diagrams in Guichon Creek rocks showing trace element concentrations plotted against LDI	137
35:	Relationship between Iron and Zinc in rocks of Guichon Creek batholith	138

FIGURE

Page

36:	Relationship between Iron and Manganese in rocks of the Guichon batholith	139
37a:	Variation of Nickel with Iron in rocks of Guichon Creek batholith	141
37b:	Variation of Nickel with Magnesium in Guichon Creek batholith	141
38a:	Relationship between Cobalt and Iron in Guichon Creek batholith	142
38b:	Relationship between Cobalt and Magnesium in Guichon Creek rocks	142
39:	Relationship between Zinc and Magnesium contents of rocks, Bethlehem-JA 2800 Level	155
40:	Plot of Rubidium versus Potassium, Bethlehem-JA 2800 Level	160
41:	Plot of Strontium versus Calcium, Bethlehem-JA 2800 Level	160
42:	Log probability plot of Copper at Bethlehem-JA	162
43:	Relationship between total and water-extractable Chlorine in rocks, Bethlehem-JA, 2800 Level	165
44a:	Schematic diagram showing extent and relative intensity of primary halos, Bethlehem-JA 2800 Level	174
44b:	Schematic diagram showing distribution of factor scores, Bethlehem-JA 2800 Level	175
45:	Log probability plot of Copper at Valley Copper	183
46:	Relationship between Copper and Potassium at Valley Copper 3600 Level	185
47a:	Schematic diagram showing extent and relative intensity of primary halos, Valley Copper 3600 Level	194
47b:	Schematic diagram showing distribution of factor scores, Valley Copper 3600 Level	195
48:	Plot of Barium versus Potassium in background samples, Lornex Surface	199
49:	Manganese versus Iron in unmineralized samples, Lornex Surface	199

FIGURE

Page

50:	Relationship between Mercury and Zinc along Lornex Fault	205
51:	Log probability plot of Copper at Lornex	207
52:	Schematic diagram showing extent and relative intensity of primary halos, Lornex Subsurface	221
53:	Schematic diagram showing distribution of factor scores, Lornex Subsurface	222
54:	Log probability plot of Copper at Highmont	227
55:	Schematic diagram showing extent and relative intensity of primary halos, Highmont Subsurface	239
56:	Schematic diagram showing distribution of factor scores, Highmont Subsurface	238
57:	Location of rock and mineral samples, Highland Valley	256
58:	Proportions of total Copper and Zinc extracted from biotites by KCLO_3 -HCl digestion	266
59:	Proportions of total Copper and Zinc extracted from magnetites by KCLO_3 -HCl digestion	267
60:	Proportions of total Copper and Zinc extracted from quartz-feldspar phases by KCLO_3 -HCl digestion	268
61:	Relationship between whole-rock copper and modal proportions of biotite	270
62:	Relationship between modal and Copper contents of biotites	271
63:	Plot of modal biotite versus Copper from biotite in whole rock	272
64:	Relationship between whole-rock Copper and percent accessory minerals in rocks	273
65:	Covariance of Copper and modal K-feldspar in whole rocks	274
66:	Plot of modal biotite versus Zinc from biotite in whole rocks	277
67:	Copper versus Iron in biotites	278

FIGURE

Page

68:	Copper versus Magnesium in biotites	278
69:	Relationship between total Copper in whole rocks and biotites	280
70:	Relationship between Copper contents of whole rocks and magnetites	282
71:	Relationship between Copper contents of whole rocks and quartz-feldspar fractions	284
72:	Plot of Potassium versus Rubidium and K/Rb ratios in rocks of Guichon Creek batholith	293
73:	Plot of Rubidium versus Strontium in rocks of Guichon Creek batholith	294
74:	Plot of normative Ab-Or-Qz proportions for the Guichon Creek samples compared with boundary curves and minima at 2, 4, 7 and 10 kb P_{H_2O}	298
75:	Gain and loss of principal rock constituents through alteration and mineralization, Valley Copper	302
76:	Model for chemical and mineral zoning and evolution of ore-forming fluids	307
77:	Location of samples, Bethlehem-JA Suboutcrop Level	338
78:	Location of samples, Bethlehem-JA 2800 Level	341
79:	Location of samples, Bethlehem-JA 2400 Level	346
80:	Location of samples, Valley Copper Suboutcrop Level	350
81:	Location of samples, Valley Copper 3600 Level	353
82:	Location of samples, Valley Copper, 3300 Level	358
83:	Location of samples, Lornex Surface (in pocket ^{in tube in Special Collections})	362
84:	Location of drill-core samples, Lornex mine	369
85:	Location of samples, Highmont Surface (in pocket ^{in tube in Special Collections})	379
86:	Location of drill-core samples, Highmont property	392

LIST OF FIGURES

VOLUME II

(Maps depicting trace and major element dispersions around mineralization)

Bethlehem-JA (2800 Level except where indicated)

FIGURE

- A1 Zinc
- A2 Manganese
- A3 Titanium
- A4 Vanadium
- A5 Magnesia
- A6 Silica
- A7 Potash
- A8 Rubidium
- A9 Barium
- A10 Calcium
- A11 Strontium
- A12a Rubidium/Strontium
- A12b Barium/Strontium
- A13 Soda
- A14 Iron
- A15 Copper (Suboutcrop Level)
- A16 Copper (2800 Level)
- A17 Copper (2400 Level)
- A18 Sulphide Copper
- A19 Sulphide Iron
- A20 Molybdenum

FIGURE

A21	Sulphur
A22	Mercury
A23	Boron
A24	Chlorine
A25	Water-extractable chlorine
A26	Fluorine
A27	Water-extractable Fluorine
A28	Factor R-1
A29	Factor R-2
A30	Factor R-3
A31	Factor R-4

VALLEY COPPER (3600 Level except where indicated)

FIGURE

A32	Zinc
A33	Manganese
A34	Manganese (3300 Level)
A35	Strontium
A36a	Barium
A36b	Barium/Strontium
A37	Magnesia
A38	Iron
A40	Calcium
A41	Soda
A42	Rubidium
A43	Potash
A44	Rubidium/Strontium
A45	Silica

FIGURE	A46	Copper (Suboutcrop)
	A47	Copper (3600)
	A48	Copper (3300)
	A49	Sulphide Copper
	A50	Sulphide Iron
	A51	Molybdenium
	A52	Sulphur
	A53	Boron
	A54	Chlorine
	A55	Fluorine
	A56	Factor R-1
	A57	Factor R-2
	A58	Factor R-3
	A59	Factor R-4

Lornex (Subsurface, except where indicated)

	A60	Zinc
	*A60b	Zinc (Surface)
	A61	Iron
	*A61b	Iron (Surface)
	A62	Manganese
	*A62b	Manganese (Surface)
	A63a	Strontium
	A63b	Calcium
	A64	Sodium
	A65a	Barium
	A65b	Potash

FIGURE	A66	Silver
	A67	Lead
	A68	Cadmium
	*A69	Copper (surface)
	A70	Copper
	A71	Molybdenum
	*A71b	Boron (surface)
	A72	Factor R-1
	A73	Factor R-2
	A74	Factor R-3
	A75	Factor R-4

Highmont (Subsurface except where indicated)

	A76	Zinc
	A77	Manganese
	A78	Iron
	A79	Soda
	*A80	Copper (surface)
	A81	Copper
	A82	Molybdenum
	*A83	Boron (surface)
	A84	Boron
	A85	Factor R-1
	A86	Factor R-2
	A87	Factor R-3
	A88	Factor R-4

FIGURE A89 Factor R-5

Skeena

FIGURE A90 Copper, Zinc, Manganese

A91 Calcium, Iron, Potash

* ~~In tube in~~ Special Collections Cabinet 8

LIST OF PLATES

PLATE		Page
1:	Conglomeration of (?) secondary perthitic K-feldspar in Bethlehem quartz diorite of the potassic zone, Bethlehem-JA	78
2:	Sericite alteration of plagioclase and alkali feldspars in potassic zone of Bethlehem-JA	78
3:	Coarse-grained sheaves of interlocking chlorite in the propylitic zone of Bethlehem-JA	78
4:	Medium- to coarse-grained crystal of epidote (vein-filling material) in the propylitic zone of Bethlehem-JA	78
5:	Pervasive sericite (+ minor kaolinite) and quartz remnants in the argillic zone of Valley Copper deposit	78
6:	Alteration of coarse biotite grains to fibrous sericite in the argillic zone of Valley Copper deposit	78
7:	Very coarse grained sericite (vein material) in the phyllic zone of Valley Copper deposit	79
8:	Fine-grained epidote partially replacing a biotite grain in propylitized rock of Lornex mine	79
9:	Fine to medium-grained sericite and kaolinite in the argillic zone of Lornex mine	79
10:	Quartz and chlorite replacements of a biotite grain in the propylitic zone of Highmont deposit	79
11:	Weak argillization of plagioclase (with minor carbonate) at Highmont property	79
12:	Radiating tourmaline crystals (schorl) in a breccia matrix at Highmont	79
13:	Disseminated sulphide grains (mainly bornite with minor chalcopyrite) in mineralized samples at Highmont (reflected light)	288
14:	Bornite inclusions in chloritized biotite (a) transmitted light (b) reflected light	288
15:	Opaque grains (sulphide) occurring at the margins of a chloritized biotite (transmitted light)	288

ACKNOWLEDGEMENTS

This research project formed part of the applied geo-chemistry research programme being undertaken at the Geological Sciences Centre, U.B.C., under the direction of Dr. W.K. Fletcher, to whom the writer is grateful for suggesting, actively supervising and channeling generous funds for the thesis.

Grateful acknowledgement is made to A. Dhillon, D. Marshall, and M. Waskett-Myers for analyzing many of the samples. Able assistance was provided in the field by P. Marcello and M. Waskett-Myers.

I wish to thank members of the mining industry - notably Bethlehem Mining Corporation, Canex Placer, Cominco, Highmont Mining Corporation, Lornex Mining Corporation, and Quintana Minerals Exploration for providing access to their properties and for financial and material assistance. Specifically, I wish to mention, R.F. Anderson and P.P. Tsaparas (Bethlehem Mining Corporation), J.M. Allen and M. Osatenko (Cominco), A. Reed (Highmont Mining Corporation), M. Skopos, G. Waldén and G. Smith (Lornex Mining Corporation), and W.J. McMillan (B.C. Dept. of Mines).

I am thankful to Drs. A.J. Sinclair, A. Soregaroli, K.C. McTaggart, W.J. McMillan and T. Brown for constructive criticism of earlier drafts of the thesis. I am indebted to my colleagues, Messrs. P. Doyle, S. Hoffman and R. Lett for useful discussions of geochemical and statistical problems.

Financial support for the project was provided partly by

the National Research Council of Canada (PRAI Grant # P-7303) and NRC Grant 67-7714 awarded to Dr. K. Fletcher. During this investigation, I benefited from various fellowships for which I am grateful.

CHAPTER ONE

INTRODUCTION

GENERAL STATEMENT

Bedrock geochemistry, as a tool in detailed mineral exploration, is still in an experimental stage (Hawkes and Webb, 1962; Boyle, 1967). According to Boyle and Garrett (1970), research on the nature and extent of primary halos around specific types of mineral deposits is required to establish bedrock geochemistry as a practical exploration technique.

Porphyry-type deposits are major sources of copper and molybdenum in the Canadian Cordillera and other parts of the world. Compared with other types of deposits, such as massive sulphides (Shikawa et al., 1962, 1974; Sakrison, 1971; Nairis, 1971; Pantazis and Govett, 1973; Goodfellow, 1974; Thurlow, 1974) or vein-type mineralization (Boyle, 1961, 1965, 1968; Bolter and Al-Shaieb, 1971; Ineson, 1969, 1970; Dass et al., 1973; Bailey and McCormick, 1974), relatively less research work has been undertaken or published on lithogeochemical halos around porphyry-type deposits (see Coope, 1973). However, notable exceptions are the recent studies of Theodore and Nash (1973) on trace element dispersion around the Copper Canyon deposits, Oyarzun et al. (1974) on primary halos of Rb and Sr around Chilean porphyry copper deposits, Warren et al. (1974) on Ba and Sr dispersion in wallrocks of the Island Copper deposit in B.C., and Gunton and Nichol (1974).

The porphyry copper-molybdenum deposits of the Guichon

Creek batholith (Valley Copper, Bethlehem-JA, Lornex and Highmont) were chosen for this investigation by virtue of their economic significance and the availability of previous studies of geology and geochemistry by Northcote (1969) and Brabec (1970) respectively. Their location in an easily accessible area of southern British Columbia (Fig. 1) and the relative abundance of outcrops and drill cores, were further advantages.

LOCATION AND ACCESS

The Highland Valley district is located in the central part of the Guichon Creek batholith, approximately 250 miles north-east of Vancouver, B.C. (Fig. 1). Main access to the area is provided by a 28 mile paved secondary road from the town of Ashcroft, and from the east, through Logan Lake, a small mining town recently developed by Lornex Mining Corporation. As a result of intensive mining and exploration activities, the entire Highland Valley district is easily accessible by numerous unpaved roads and trails.

OBJECTIVES OF STUDY

Objectives of this study are to:

(1) determine the nature, extent and factors controlling epigenetic dispersion of major and trace elements in wall rocks surrounding porphyry copper-molybdenum deposits.

(2) determine relationships between distribution of Cu and potential pathfinders, such as Hg, Cl, F, B, and Rb and Sr.

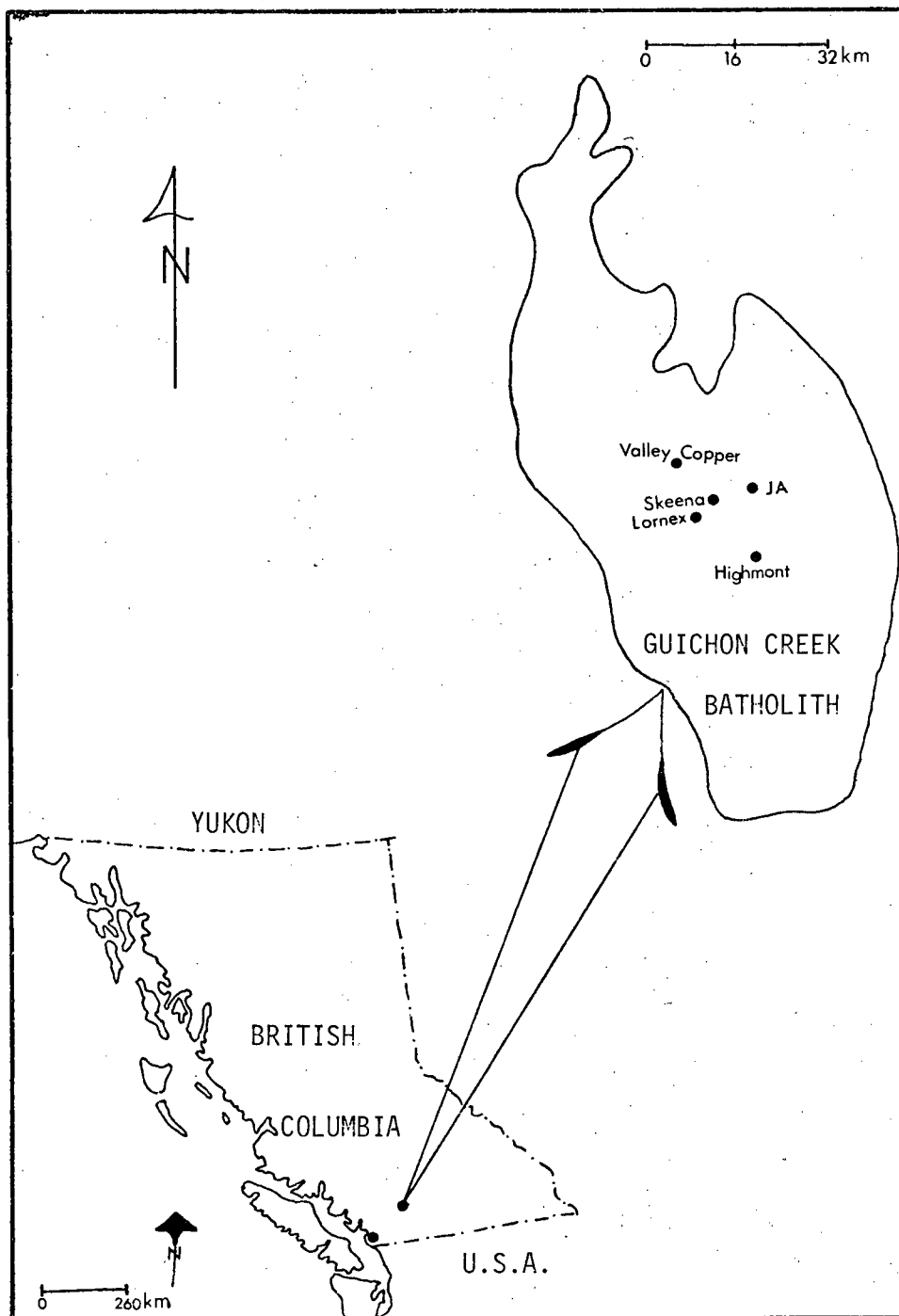


FIGURE 1: Location of Study Area

(3) investigate, and if appropriate, develop partial extraction techniques as a means of selectively extracting sulphide Cu, and thereby improving geochemical contrast between anomalous and background areas.

(4) assess the value of chemical analysis of constituent minerals, rather than whole rocks, in improving contrast between anomalous and background environments.

BEDROCK GEOCHEMISTRY IN MINERAL EXPLORATION - PREVIOUS WORK

Use of bedrock geochemistry as an exploration tool grew largely from the work of A.E. Fersman and his colleagues in the U.S.S.R. in the early part of this century. Since their pioneer work, considerable research and refinement of the technique have been undertaken in the U.S.S.R. and other parts of the world. Boyle and Garrett (1970), Sakrison (1971) and Coope (1973) have recently reviewed the status of lithogeochemistry in mineral exploration.

The following review of relevant literature emphasises the results of studies on exploration for porphyry copper deposits. The review is subdivided into three sections: (1) regional geochemical surveys; (2) detailed chemical and mineralogical patterns around ore deposits; and (3) micro-dispersion of trace metals in mineral phases.

(a) Regional Geochemical Patterns

Various types of mineral deposits, including porphyry coppers, are believed to be genetically related to their host rocks

(Krauskopf, 1967). Consequently, numerous bedrock geochemistry studies have been focussed on differentiating barren from potentially ore-bearing intrusives.

Goldschmidt (1954) assembled a vast amount of data on trace element abundances in crustal rocks, and devised 'rules' that govern their behaviour in silicate melts. A critical review of this subject is presented by Burns and Fyfe (1967).

Empirical data on systematic variations of trace elements during magmatic differentiation have been presented by Wager and Mitchell (1951) and Wager and Brown (1967) for the Skaergaard intrusion, and other differentiated igneous suites (Cornwall and Rose, 1957; McDougall and Lovering, 1963).

Warren and Delavault (1960) found that aqua-regia-extractable Cu in plutons containing porphyry Cu deposits (including Guichon Creek batholith) was appreciably higher than in barren intrusives of similar composition.

Brabec and White (1971) investigated the distribution of aqua-regia-extractable Cu and Zn in more than 300 fresh samples from the Guichon Creek batholith. Their results indicate a general decrease in Cu and Zn from the outer margins to the central zone where rock phases containing the main porphyry Cu deposits are impoverished in Cu. They concluded that, a relatively high Cu content of an intrusive phase is not necessarily indicative of its superior ore potential.

Kesler et al. (1973), using ion-selective electrodes,

evaluated the possible use of water-leachable Cl and F in 'fingerprinting' intrusions that are potentially ore-bearing. Their sampling included two porphyry-copper-bearing intrusives, plutonic bodies with associated contact deposits and other barren intrusions in the Caribbean and Central America. The results, which are a measure of the abundance and concentration of fluid inclusions and other water-soluble rock constituents, do not indicate there is any simple relation between abundance of Cl and the occurrence of mineralization. However, average F values are higher in mineralized than unmineralized intrusion.

Rabinovich et al. (1958) and Tauson et al. (1970) reported that the Mo contents of intrusives that carry Mo mineralization in the U.S.S.R. are not higher than those of barren plutons of similar composition.

(b) Hydrothermal Dispersion Patterns

Metasomatism of ore and associated metals into country rock during metallization is instrumental in the development of hydrothermal dispersion patterns in wall rocks of mineral deposits. Hawkes and Webb (1962) and Bradshaw et al. (1970) have discussed the factors controlling epigenetic dispersion patterns.

Theodore and Nash (1973) studied the distribution of 20 trace elements in wall rocks surrounding the Copper Canyon porphyry copper deposits. The orebodies are localized within metasedimentary rocks intruded by a relatively barren granodiorite stock. They

found that concentrations of Cu, Mo and other trace elements were higher in the barren intrusion than in the mineralized metasediments. Thus they conclude that a geochemical anomaly of Cu in bedrock does not necessarily coincide with Cu ore at Copper Canyon.

Armbrust (1971) and Oyarzun et al. (1974) found that Rb is enriched and Sr depleted in central zones of intense potassic alteration and mineralization at several Chilean porphyry Cu deposits. Warren et al. (1974) reported that Ba and Sr values are depleted in ore zones of the Island Copper deposit in British Columbia.

Davis and Guilbert (1973), investigating radio-element (K, U, Th) distribution in several porphyry-type deposits in southwest U.S.A. found that in mineralized plutons, enhanced K and U levels are centrally located and spatially associated with intense potassic alteration and mineralization. Thus, they conclude that radiometric measurements of K and U are viable tools in the search for porphyry-type deposits.

Gunton and Nichol (1974) studied the distribution of 18 major, minor and trace elements in volcanic and plutonic rocks associated with the Ingerbelle and Copper Mountain Cu deposits. On a reconnaissance basis, they found that increased contents of P, Rb and Sr and to a lesser extent Na and K in volcanic rocks adjacent to the ore-bearing Copper Mountain stock. On a local scale, a broad zone of Na enrichment is associated with intense alteration at Ingerbelle deposit as opposed to localized zones of K enrichment in the Copper Mountain deposits.

Mineralogical zoning patterns around porphyry Cu deposits have been investigated by numerous workers, notably, Lowell and Guilbert (1970), Rose (1970), Nielsen (1968) and Carson and Jambor (1974). Hausen and Kerr (1971) employed X-ray diffraction methods in outlining distribution of alteration minerals in porphyry Cu-Mo deposits in Arizona, Montana and Washington. They conclude that alteration patterns correlate with the distribution of Cu and Mo, and permit the projection of previously unknown mineralization.

(c) Mineral Geochemical Patterns

The trace element contents of various mineral phases have been utilized in the exploration of porphyry Cu deposits. The basis for these applications is that constituent minerals might better reflect the presence of mineralization or give better geochemical contrast than whole rocks.

Parry and Nackowski (1963) found that Cu contents of biotites from intrusions in porphyry Cu areas tended to be relatively high. Similar conclusions were reached by Putman and Burnham (1963) and Graybeal (1973) in their studies of Cu contents in biotites and hornblendes of plutonic rocks in Arizona. In the Sierrita and Santa Rita Mountains of southern Arizona, rocks from intrusions that are genetically associated with Cu deposits contain as much as 300 p.p.m., whereas biotites separated from these rocks contain as much as 1% Cu. Lovering et al. (1970), therefore conclude that Cu anomalies in biotite provide a more reliable guide to Cu mineralization than

do whole rocks.

Al-Hashimi and Brownlow (1970) reported relatively high Cu contents in biotites from mineralized Boulder batholith. This enrichment is attributed to the presence of epigenetic sulphide inclusions. However, the authors conclude that because of the erratic distribution of Cu in biotites, bedrock provides a better and more consistent guide to mineralization.

Parry (1972) found no clear distinction between the Cl content of biotites and their occurrence in mineralized or barren plutons, except that biotites with less than 0.2% Cl came from plutons with little or no Cu mineralization.

Hamil and Nackowski (1971) investigated magnetites from several intrusives in Utah and Nevada, and found that low abundances of Ti and Zn in magnetite correlate with major porphyry Cu mineralization. Theobald and Thompson (1962) noted that magnetite from rocks presumably associated with Cu mineralization at Butte, Montana are relatively impoverished in Zn. In contrast, high concentrations of Cu and Zn were reported by de Grys (1970) in magnetite from intrusives associated with porphyry Cu mineralization. Stanley (1964) found that the Cu contents of wall rocks in the Granduc deposit in B.C. were not related to the proportion of magnetite. Huff (1971) found no significant Cu anomalies in magnetites derived from intrusives associated with Cu mineralization in the Lone Star district in Arizona.

In conclusion, various workers have obtained different results using similar techniques. This emphasizes the need for studies to be carried out in different environments. Lines of further productive research involve the use of minor and trace elements, such as Rb, Sr, and Ba, and volatiles in delineating zones associated with hydrothermal alteration and mineralization in porphyry copper deposits.

CHAPTER TWO

GEOLOGIC SETTING OF GUICHON CREEK BATHOLITH

I. GUICHON CREEK BATHOLITH

REGIONAL SETTING

The Guichon Creek batholith is a concentrically zoned, granitoid pluton, elongated slightly west of north, underlying an area of approximately 480 square miles. It intrudes sedimentary and volcanic rocks of the Permian Cache Creek and Upper Triassic Nicola Groups, within a tectonic setting that is considered either eugeosynclinal (Danner and Nestall, 1971) or as an oceanic-island arc couple (Dercourt, 1972; Monger et al., 1972). The batholith is overlain unconformably by Middle Jurassic to Tertiary volcanic and sedimentary rocks, and bounded on the west and east by faults of regional extent (Carr, 1962).

The age of the batholith has been determined precisely by stratigraphic and geochronometric methods. Forty-five K-Ar (Folinsbee et al., 1965; Baadsgaard et al., 1961; Leech et al., 1964; Wanless et al., 1965; 1968; Dirom, 1965; Northcote, 1969; Blanchflower, 1971; Jones et al., 1972) and two Rb-Sr (Christmas et al., 1969) age determinations on rocks from the batholith indicate that the various igneous phases are, within limits of analytical error, 200 m.y. old. However, geologic evidence presented by Northcote (1969) suggests that the zoned pluton is progressively younger from the border inward. Rocks of the batholith have not undergone any significant metamorphism since emplacement.

PETROLOGY AND STRUCTURE

Petrology of the Guichon Creek batholith has been described by numerous workers, notably White *et al.*, (1957), Carr (1966), Northcote (1969), McMillan (1972) and Hylands (1972). The batholith is composed of nine igneous phases delineated by variations in texture (Table I and Fig. 2). These phases, which vary in composition from diorite to quartz monzonite are grouped into units on modal similarities and contact relations (Hylands, 1972).

Border Unit forms the outer zone of the batholith, and is composed of hybrid, highly variable to uniformly fine-grained diorite that is commonly enriched in mafic minerals.

Highland Valley Unit, which comprises the Guichon and Chataway Phases, forms a complete ring within the Border Unit (Fig. 2). Medium-grained Guichon quartz diorite is characterized by anhedral quartz grains and unevenly distributed clusters of mafic minerals. Average modal composition is estimated by Northcote (1969) as follows: plagioclase (An_{33-46}) constitutes 50%, orthoclase 10%, quartz 18%, biotite and hornblende 17%, pyroxene and accessory minerals 5%. The equigranular Chataway granodiorite is characterized by evenly distributed equant grains of hornblende and biotite which both constitute 12% of the mode (McMillan, 1972).

Intermediate Unit lies between the Highland Valley Unit and the core of the batholith. It is composed of the Bethlehem and Skeena granodiorites and Witches Brook and Bethlehem Porphyry dykes. The Bethlehem and Skeena granodiorites are characterized by randomly

TABLE I: Units and phases of the Guichon Creek batholith (Modified after, Northcote, 1969; Hylands, 1972; McMillan, 1972).

UNITS	PHASES	ROCK TYPES	MODE OF EMPLACEMENT	RELATIVE AGE
Core	Gnawed Mountain	dacite to quartz latite porphyry	dyke	youngest
	Bethsaida	granodiorite to quartz monzonite	epizonal-plutonic	
Intermediate	Bethlehem Porphyry	latite, dacite, quartz diorite, microgranite	dyke	
	Witches Brook	granodiorite to quartz monzonite	dyke	
	Skeena	quartz diorite to granodiorite	epi-mesozonal-plutonic	
	Bethlehem	quartz diorite to granodiorite	mesozonal-plutonic	
Highland Valley	Chataway	quartz diorite to granodiorite	mesozonal-plutonic	
	Guichon	quartz diorite to granodiorite	mesozonal-plutonic	
Border	Hybrid	diorite to quartz diorite	mesozonal-plutonic	oldest

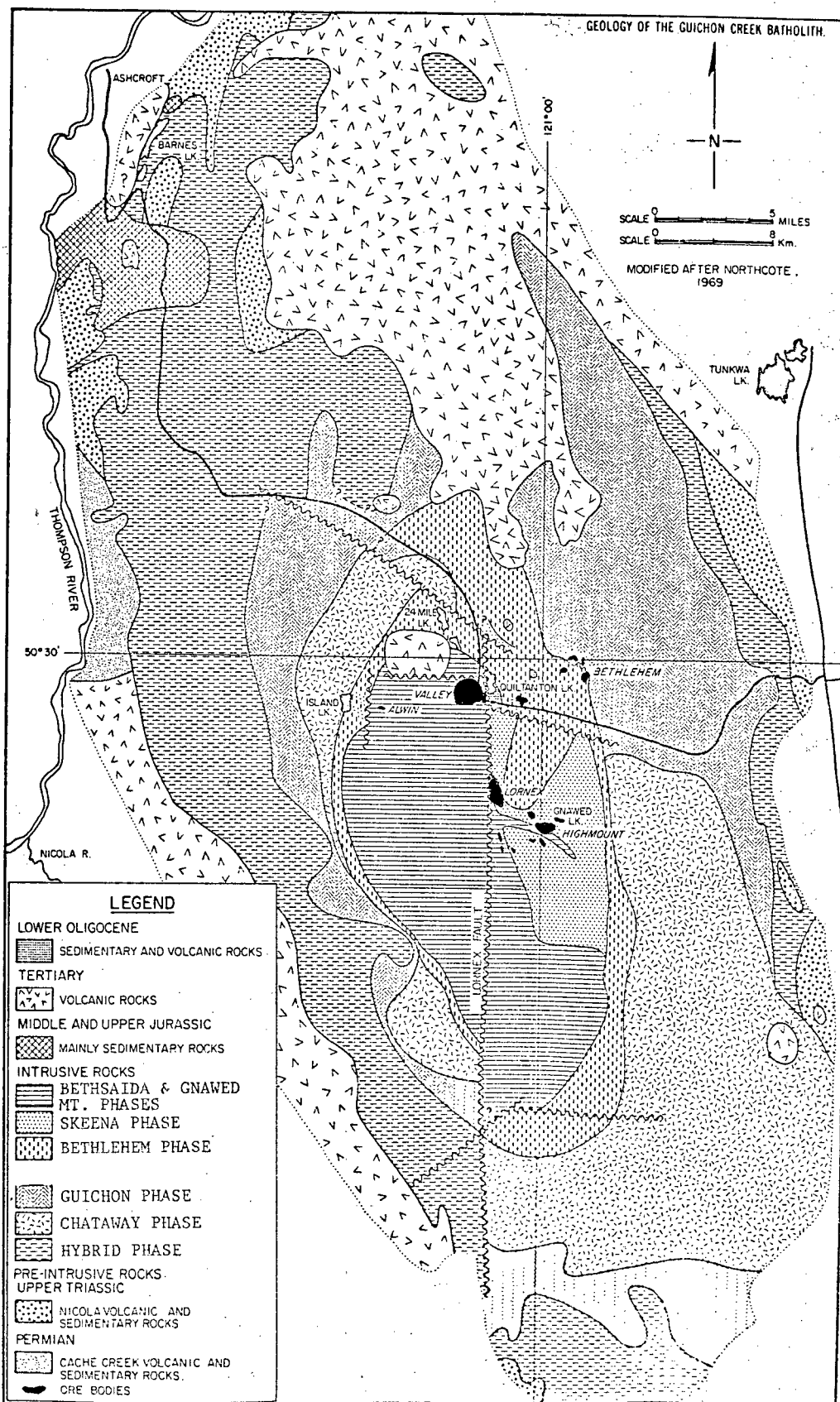


FIGURE 2: Geology of Guichon Creek batholith
(Modified after McMillan, 1972)

distributed, coarse, poikilitic hornblende crystals, set in a matrix of fine- to medium- grained felsic minerals. However, the Skeena differs from the Bethlehem granodiorite in possessing coarse-grained, subhedral quartz phenocrysts and interstitial, ragged micro-perthite. An estimated modal composition is: plagioclase 4%, orthoclase 10%, quartz 21%, and mafic minerals 8% (Northcote, 1969). Rocks of the Witches Brook and Bethlehem Porphyry Phases occur as dykes and small stocks with varying mineralogy and texture (Table I).

Core Unit comprises the Bethsaida and Gnawed Mountain Phases. The Bethsaida granodiorite to quartz monzonite is coarse-grained, commonly porphyritic and consists of subhedral phenocrysts of quartz (16 - 45%), plagioclase (38 - 57%), interstitial micro-perthite (5 - 14%) and coarse biotite "books" (3 - 7%) (Northcote, 1969). Rocks of the Gnawed Mountain Phase occur mainly as porphyry dykes with varying texture; plagioclase and quartz phenocrysts are set in an aplitic groundmass. Mafic minerals, mainly biotite, constitute less than 5% of the mode.

Variations in mineralogical composition within the constituent rock units of the batholith are depicted in Fig. 3. Hornblende, anorthite content of plagioclase, accessory minerals and biotite decrease, whereas quartz content increases from the border to core of the pluton. Pyroxene is not found in rocks younger than the Highland Valley Unit. K-feldspar shows no systematic variations throughout the batholith. Textural change is manifested by increasing

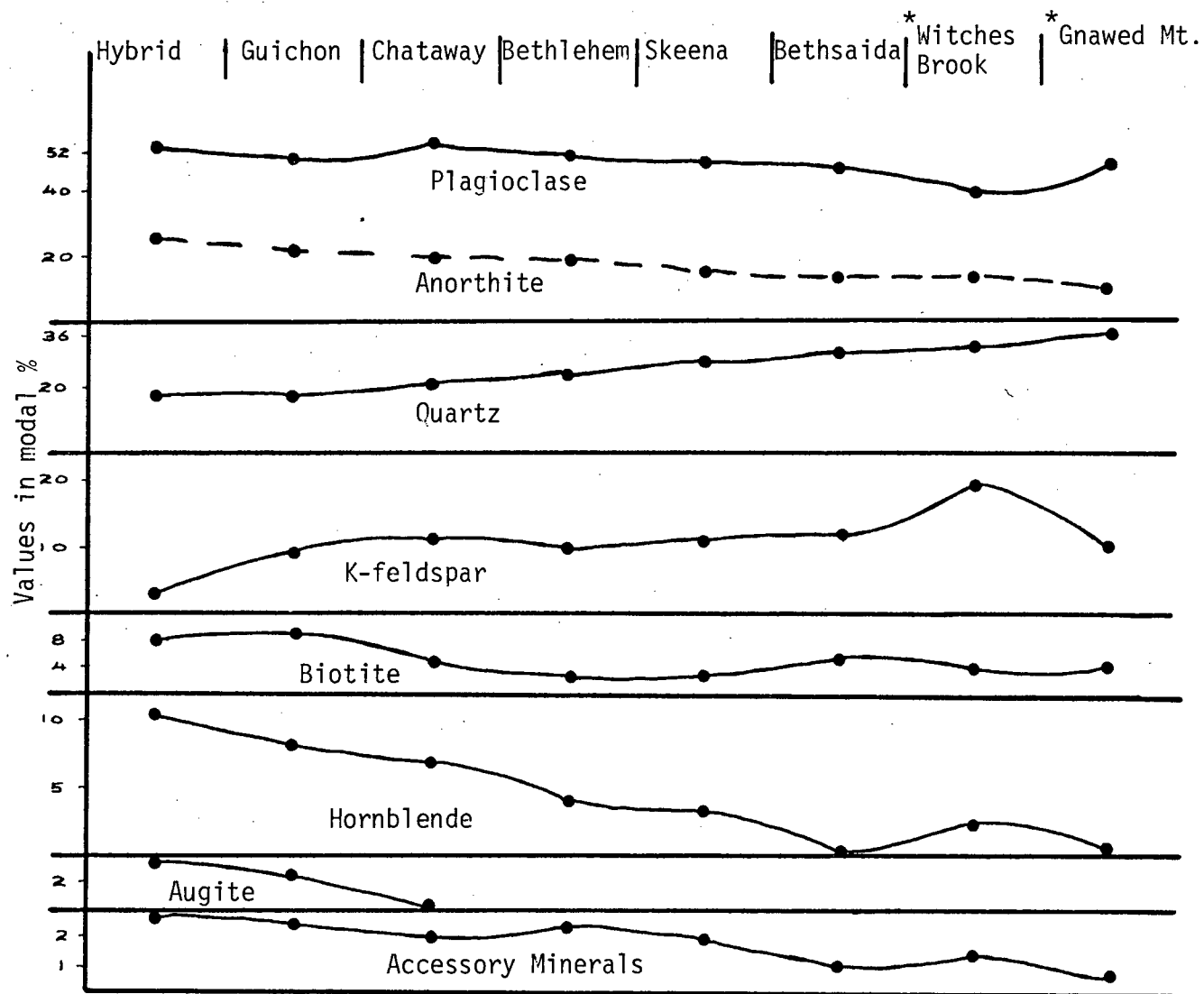


FIGURE 3: Simplified modal variations in rocks of the Guichon Creek Batholith (Data partly from Northcote, 1969); *Highly variable composition.

grain size toward the core. Specific gravity of rocks also decreases inwards (Northcote, 1969).

Structurally, the batholith is a semi-concordant dome dipping steeply on all sides, (Northcote, 1969). Geophysical evidence (Ager et al., 1973) suggests that, at greater depths, the batholith is a flattened funnel-shaped structure slightly tilted to the west. Structural features within the batholith include minor and major faults, prominent among which are the 16 km long, north-trending Lornex Fault and the west-northwest trending Highland Valley Fault (McMillan, 1972). Other local structural elements with a predominant northerly trend, include lineaments, fractures, breccia pipes and dyke swarms. These probably all result from stress patterns imposed by the underlying basement (Bergey et al., 1971) or pressure from the intruding magma.

ECONOMIC MINERALIZATION

The Guichon Creek batholith is host to several large producing and pre-producing porphyry copper deposits. Lornex, Bethlehem-Huestis and Bethlehem-Jersey mines are presently in production; Valley Copper, Highmont, Trojan (South Seas), Bethlehem-Iona, Bethlehem-JA and Alwin are in advanced stages of production planning, whereas East Jersey and Skeena have been mined out. Aggregate tonnage of these deposits exceeds 1.8 billion tons of material grading approximately 0.4% Cu equivalent (Table II). Other prospects and showings abound in the Highland Valley district. Although Craigmont,

TABLE II: Size, production capacity, grade and ore mineralogy of mineral deposits, Guichon Creek batholith (Data from Canadian Mines Handbook, 1971 - 1972, and Northern Miner Press)

	Tonnage X10 ⁶	Production tons/day	Grade of % Cu	Grade % MoS ₂	Principal Ore Minerals
Bethlehem - East Jersey	3		1.14		bornite
Bethlehem - Jersey	30	16,000	0.60		bornite, chakopyrite
Bethlehem - Huestis	26		0.65		bornite, chalcopyrite
Bethlehem - Iona	10.2		0.53		chalcopyrite, bornite
Bethlehem - Lake Zone	190		0.48		bornite, chalcopyrite
Valley Copper	1000		0.48		
Lornex	293	38,000	0.43	0.014	chalcopyrite, bornite, molybdenite
Highmont*	150		0.28	0.015	chalcopyrite, bornite, molybdenite
Bethlehem-JA	300		0.45	0.017	chalcopyrite, bornite, molybdenite
Krain	35.5		0.37		chalcopyrite (bornite)
Trojan (South Seas)	17.4		0.75		bornite
Alwin	1.2		2.31		chalcopyrite
Skeena	0.15		3.50		chalcopyrite
Craigmont	14.6	5,600	1.72		

* Highmont comprises two major deposits.

a producing mine located immediately south of the batholith, is a pyrometasomatic deposit, it is regarded as genetically related to Guichon Creek batholith (Christmas et al., 1969; A.J. Sinclair, oral communication).

Most of the orebodies are localized within intense zones of shattering and brecciation, usually along or near contacts between intrusive units or in the vicinity of porphyry dyke swarms and breccia pipes. Principal ore minerals are bornite, chalcopyrite and molybdenite which occur as fracture fillings, either within quartz and quartz-carbonate veins or clay/sericite gangue, and as disseminations within altered host rocks.

II. HIGHLAND VALLEY

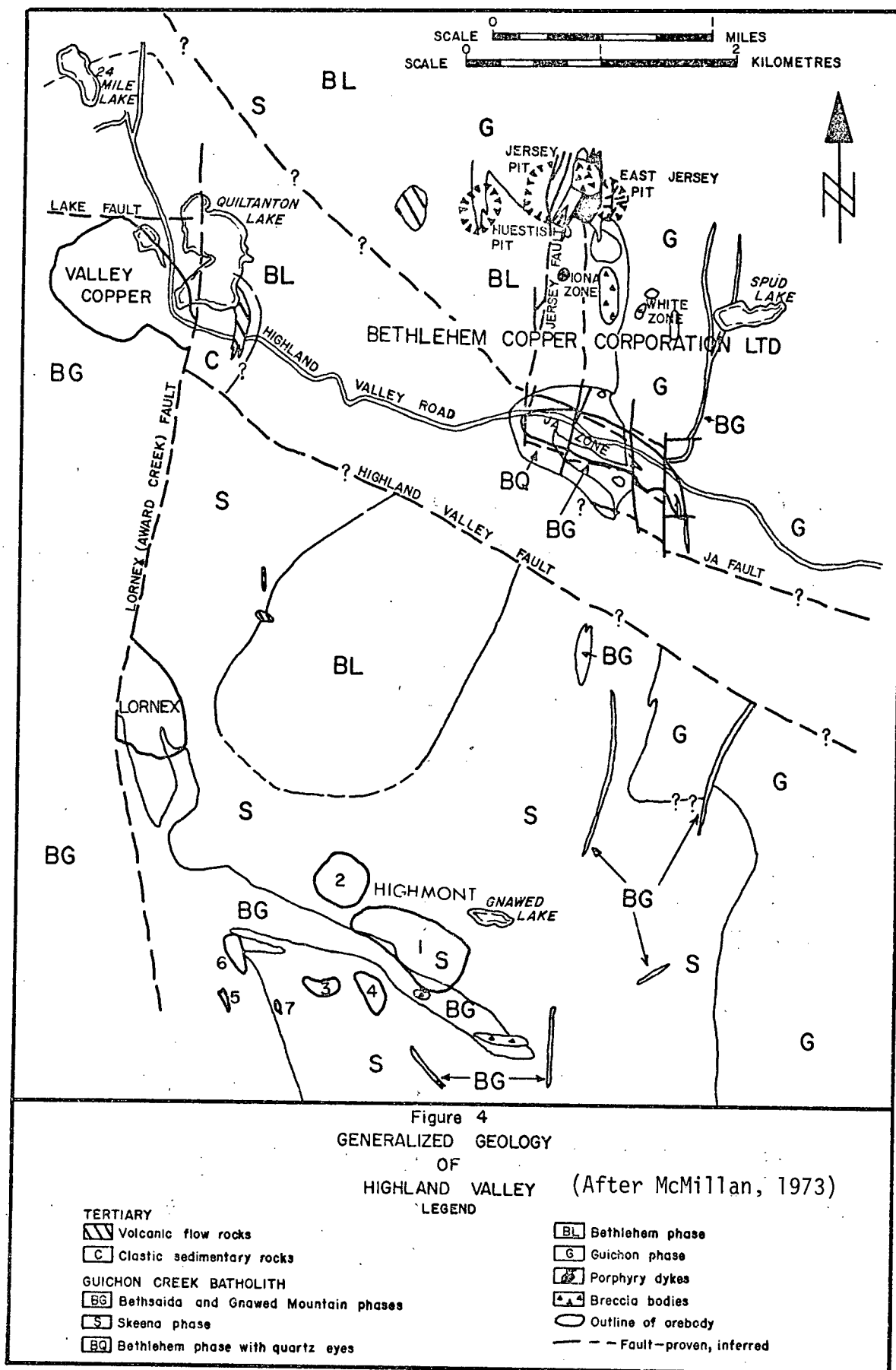
INTRODUCTION

The following discussion of geology at Highland Valley is based solely on the work of McMillan (1971, 1972, 1973; oral communications) and private company reports. However, these sources have been corroborated by field observations while collecting rock samples and petrographic examination of relevant thin sections. General geology of the Highland Valley and location of deposits are shown in Fig. 4.

GEOLOGY OF MINERAL DEPOSITS

(a) Bethlehem-JA

The recently discovered Bethlehem-JA deposit contains estimated reserves of more than 300 million tons of 0.45% Cu. The



orebody is approximately 900 by 400 m, with its long axis striking east-west. It is localized along the contact between quartz diorite of the Guichon Phase and granodiorite of the younger Bethlehem Phase, within and north of a small quartz latite porphyry dyke (Fig. 5). In thin section, the porphyry consists of phenocrysts of plagioclase, K-feldspar and quartz, set in a fine-grained groundmass. Results of modal analysis (1000 counts) of three samples are as follows: plagioclase (42 - 47%), orthoclase (18 - 23%), quartz (25 - 28%) and biotite (2 - 3%). Except for higher content of quartz adjacent to the porphyry, rocks of the Bethlehem and Guichon Phase are not different in composition from those described by Northcote (1969).

Structurally, the deposit is characterized mainly by north and northwest-trending faults and fractures. Most prominent of these faults is the northwest-trending 'JA' or 'Brook' Fault (Figs. 4 and 5).

Economic mineralization is most intense along the shattered contact between the Guichon and Bethlehem Phases, although approximately two-thirds of the orebody lie within the latter. Principal ore minerals are chalcopyrite, bornite and molybdenite which occur as veins, veinlets (1 - 5 mm wide), fracture coatings and disseminations. Pyrite and specularite are the only other metallic minerals.

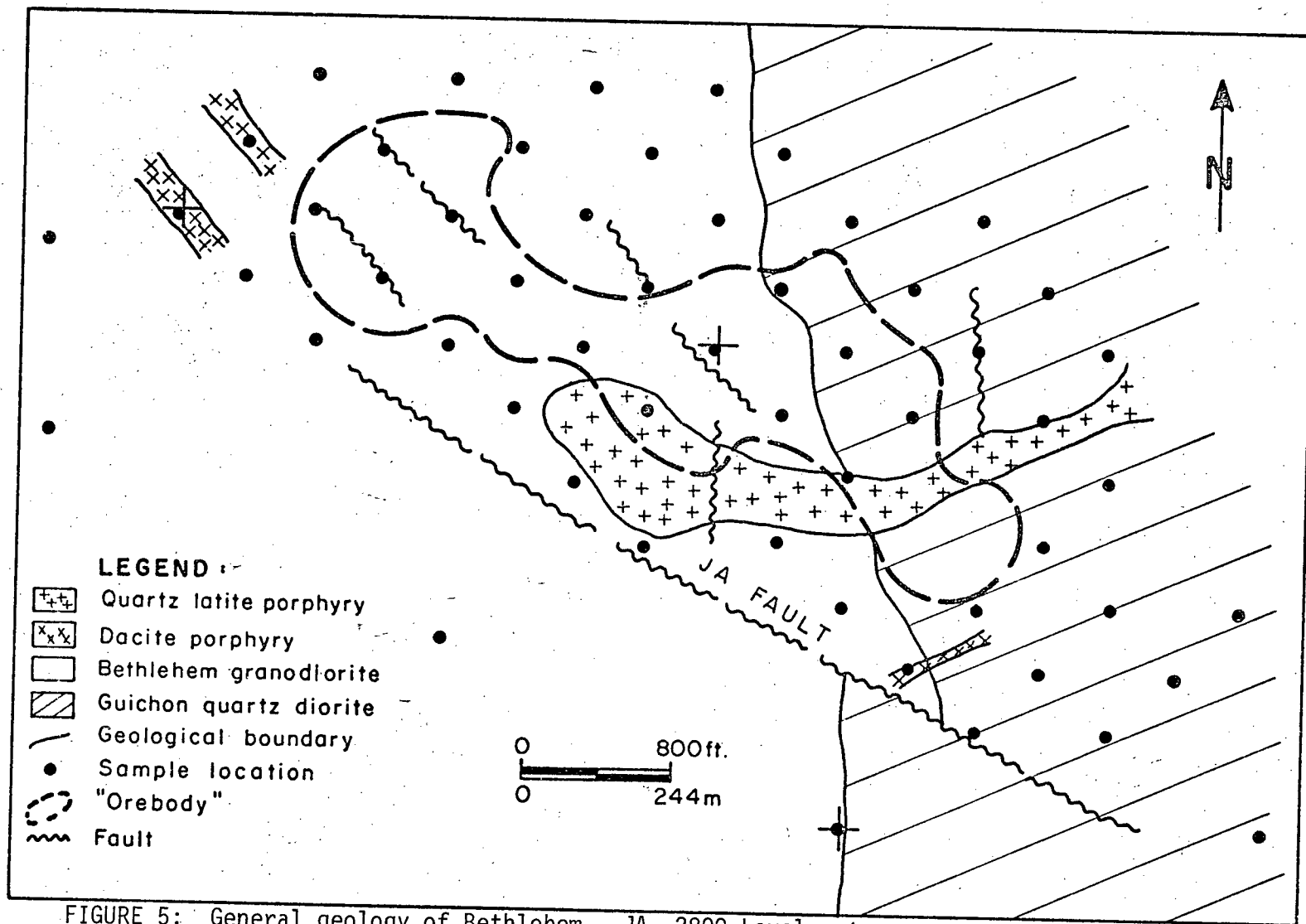


FIGURE 5: General geology of Bethlehem - JA, 2800 Level. (Modified after Bethlehem mining staff.)

(b) Valley Copper

Valley Copper orebody has a roughly elliptical plan of approximately 1000 by 1300 m, with the long axis striking north-westerly (Allen and Richardson, 1970). It contains more than 1 billion tons of 0.48% Cu. The deposit is situated entirely within porphyritic granodiorite to quartz monzonite of the Bethsaida Phase (McMillan, 1972) (Fig. 6). Local textural and mineralogical variants include mafic patches enriched in biotite and magnetite, and conspicuously porphyritic zones with aplitic matrix. Other volumetrically insignificant rock types include small pre- and post-ore felsite and lamprophyre dykes. Jones et al. (1972) obtained a K-Ar age of 132 m.y. on a post-ore lamprophyre dyke.

Structurally, the deposit lies west of the Lornex Fault, near its junction with the west-trending Lake and Highland Valley Faults (Fig. 6). Carr (1967) considers the Valley Copper and Lornex deposits as segments of the same orebody that were offset by post-ore movement on the Lornex Fault. According to McMillan (1971), two dominant fault systems are evident in the underground working; one striking south-southeast with steep northeasterly dips, and one sub-horizontal set.

Ore-grade mineralization is localized within zones of intense shattering and brecciation. Bornite, chalcopyrite and molybdenite are the principal ore minerals. Pyrite, sphalerite and hematite are relatively uncommon, but up to 2% specular hematite

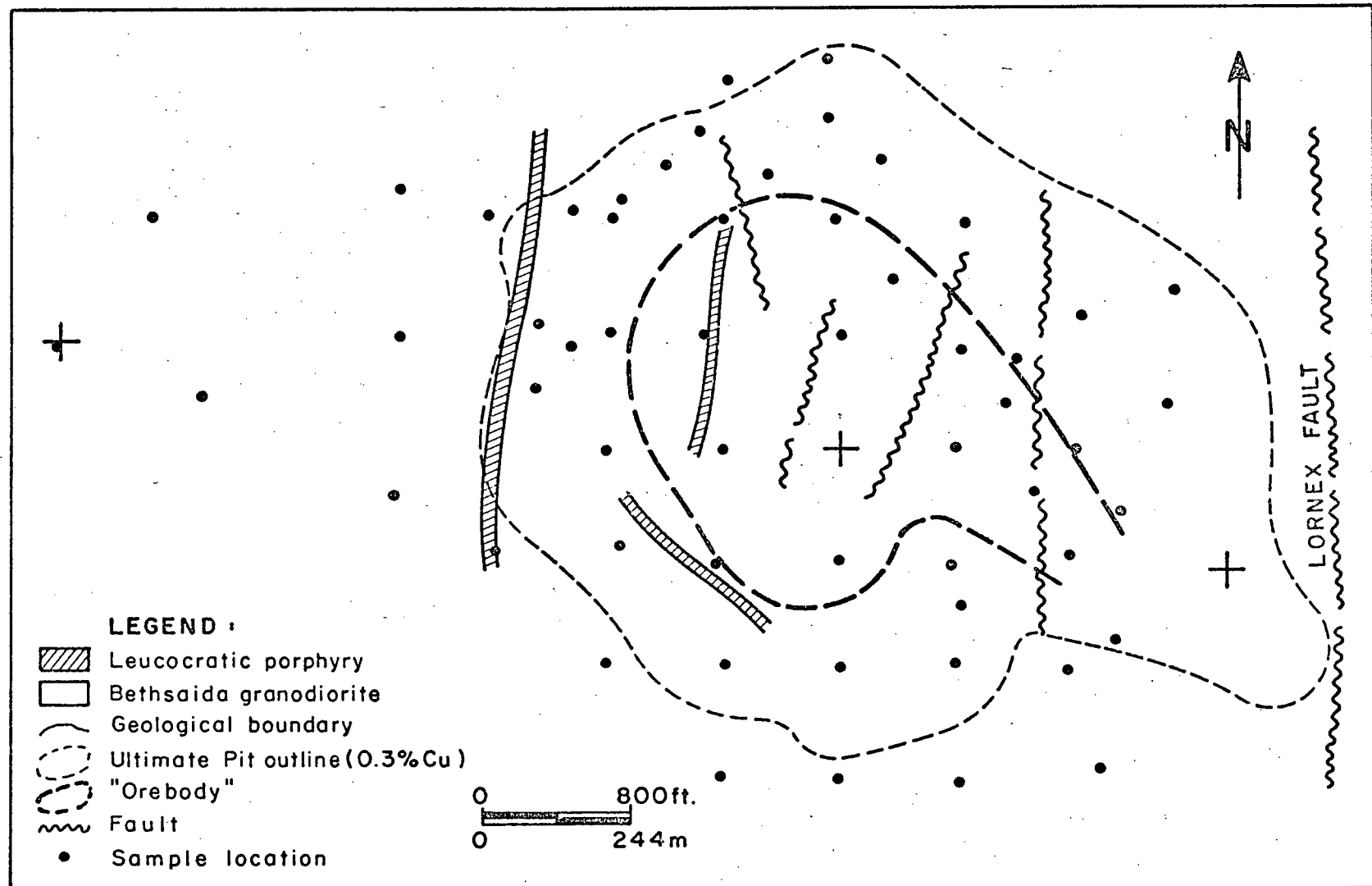


FIGURE 6: General geology of Valley Copper (After McMillan, 1971, 1973).

occurs within the deposit (Allen and Richardson, 1970).

(c) Lornex and Skeena

Lornex ore deposit is 500 x 1300 m with an elliptical outline in which the long axis is oriented north-westerly. Currently in production, its ore reserves exceed 300 million tons of about 0.43% Cu and 0.014% MoS₂. The orebody lies mainly within the Skeena granodiorite adjacent to a contact with Bethsaida quartz monzonite (Fig. 7).

Skeena granodiorite is medium to coarse grained and composed of anhedral quartz, plagioclase (An₃₀₋₃₄), coarse poikilitic hornblende, biotite and interstitial perthitic orthoclase. Modal proportions as estimated from eight samples are; plagioclase (58 - 65%), orthoclase (5 - 14%), quartz (18 - 25%), biotite (3 - 6%), hornblende (2 - 5%) and accessories (1 - 2 %).

Bethsaida granodiorite is characterized by coarse-grained subhedral quartz phenocrysts (23 - 30%), plagioclase (54 - 65%), interstitial orthoclase (6 - 15%), coarse biotite (2 - 7%), hornblende (1%) and accessory minerals (1%). Near the southern end of the deposit, a quartz-plagioclase porphyry of the Gnawed Mountain Phase intrudes the Skeena granodiorite (Fig. 7). The porphyry is composed of large crowded phenocrysts of anhedral quartz and plagioclase, set in an aplitic groundmass. Other minor rock types include small aplite and felsite dykes. Subsurface geology of a section across the orebody is presented in Fig. 8.

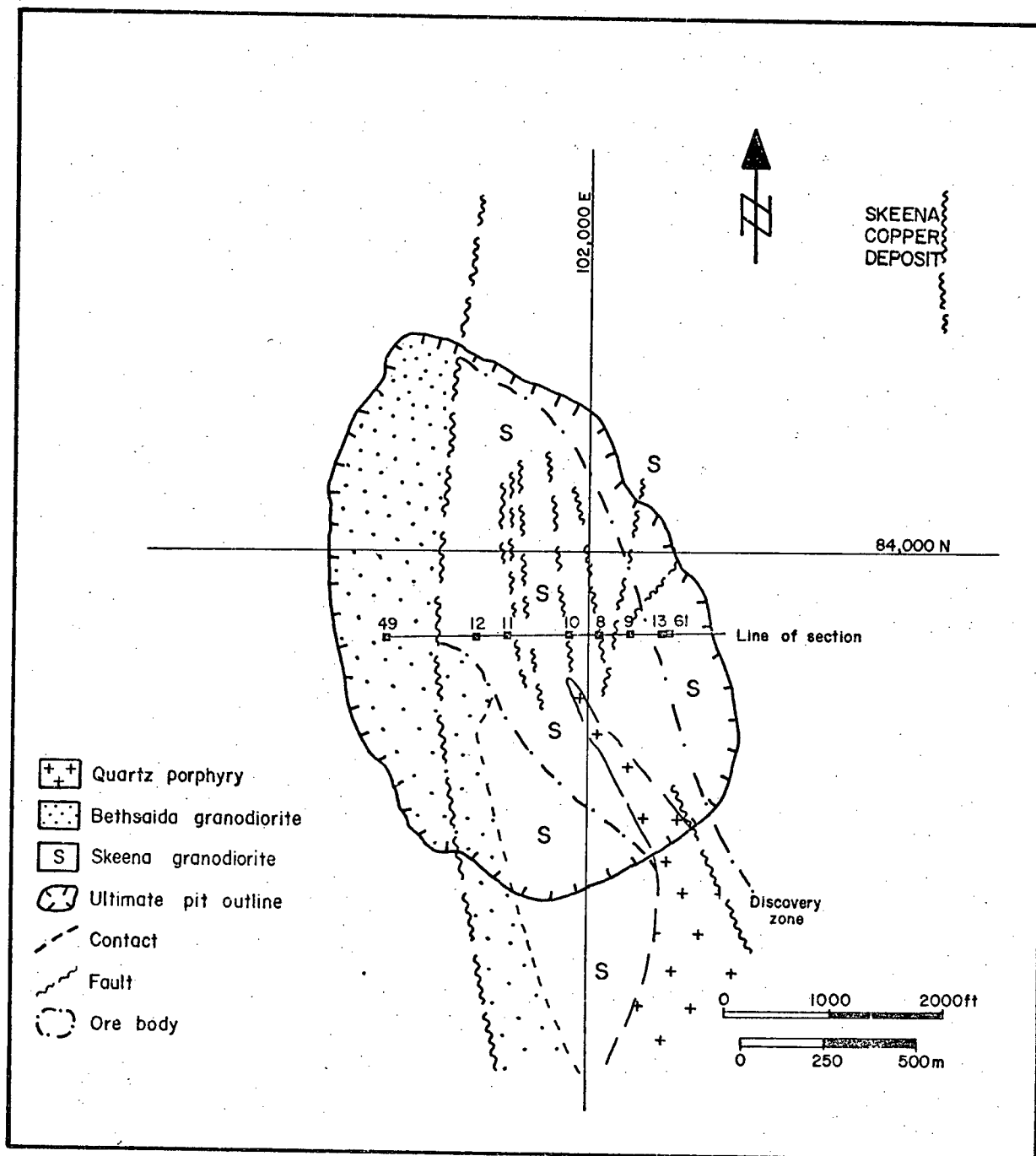


FIGURE 7: Generalized geology of Lornex and Skeena mines (After Lornex mining staff).

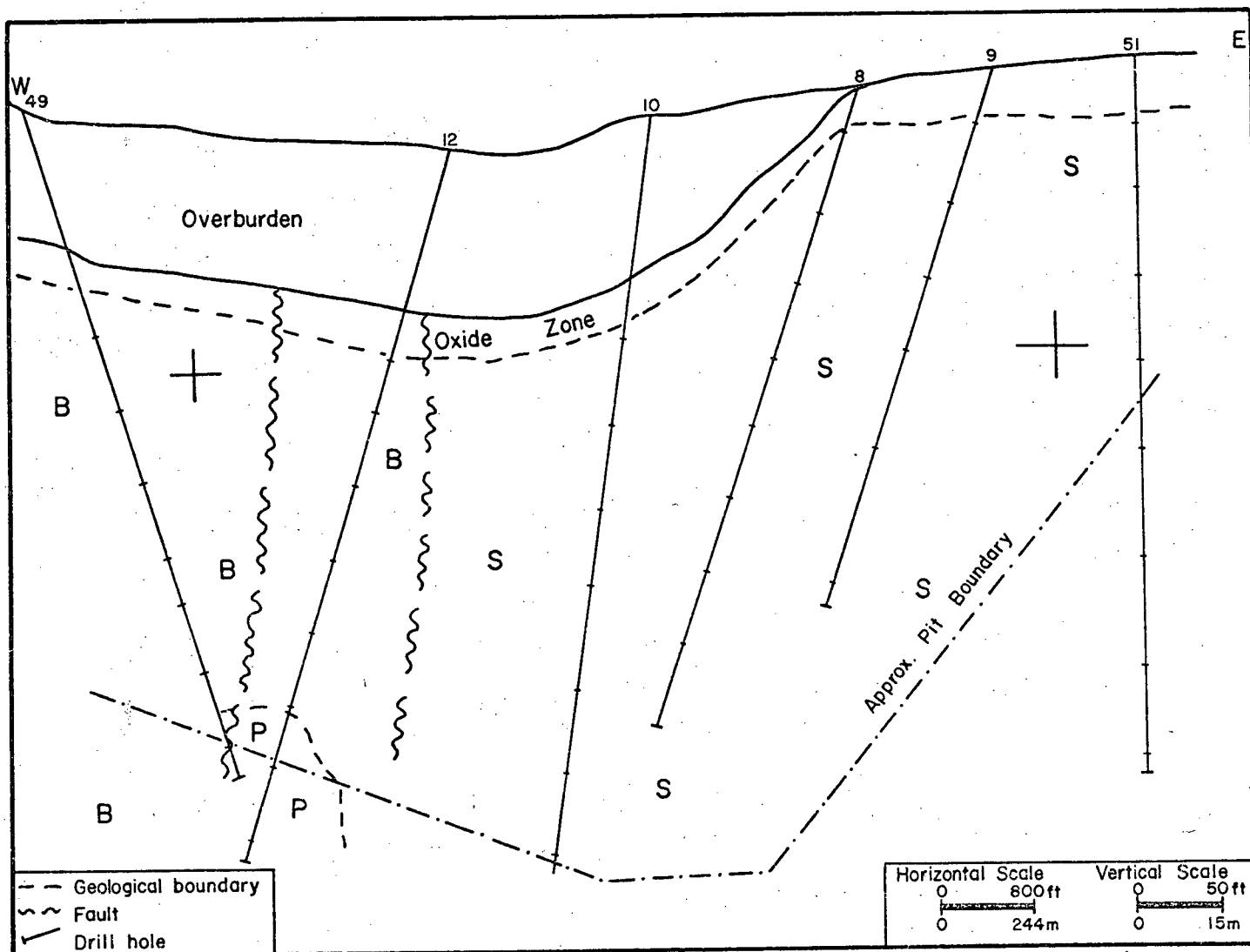


FIGURE 8: Simplified geology across a section at Lornex mine (P = Quartz porphyry; B = Bethsaida granodiorite; S = Skeena granodiorite).

Structurally, the Lornex orebody is bounded on the west by the Lornex Fault dipping west at $80 - 85^{\circ}$. Faults are numerous within the orebody (Fig. 7), and exhibit three main trends, north, east and northwest; all with moderate to steep dips. Several of these faults are characterized by wide zones of gouge and breccia.

Ore-grade mineralization occurs within intensely brecciated zones and along contacts between rock phases. The porphyry dyke is only weakly mineralized. Principal ore minerals are chalcopyrite, bornite and molybdenite, although minor amounts of chalcocite, pyrite and covellite have been reported (McMillan, 1972). Main modes of occurrence are; as fracture fillings, in quartz-carbonate veins up to 10 cm wide, and disseminations in altered host rock. Molybdenite tends to occur separately, in quartz veinlets and "moly-slips" on fault planes.

The Skeena Mine is a vein-type deposit in a porphyry copper environment. It is localized along a major, north-trending, 50 m-wide shear zone within rocks of the Skeena Phase (Fig. 7). Ore minerals include chalcopyrite, pyrite and malachite in quartz-carbonate veins.

(d) Hightmont

The Hightmont deposits comprise five low-grade mineralized zones lying on either side of a porphyry dyke of the Gnawed Mountain Phase (Fig. 9). The zones have maximum dimensions of 360 to 1100 m and are oriented sub-parallel to the west-northwest trending dyke. Grade of mineralization is approximately 0.3% Cu and 0.015% MoS_2 .

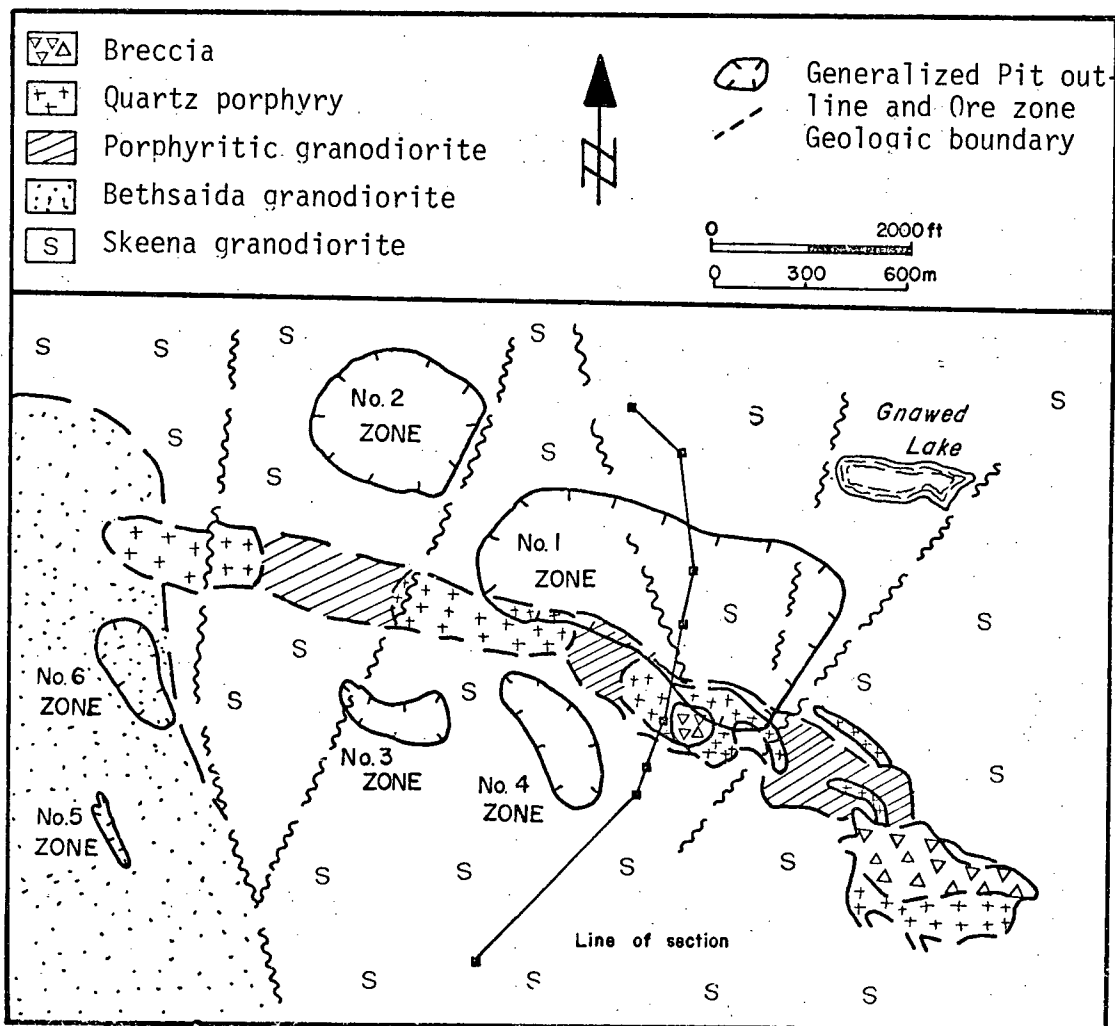


FIGURE 9: Simplified geology of Highmont Property (After Bergey et al. 1971)

(Table I). Estimated reserves are in the range of 150 million tons.

The Highmont property is underlain primarily by quartz diorite to granodiorite of the Skeena Phase (Fig. 4). The contact with the Bethsaida granodiorite crosses the westernmost part and a 120 m wide composite dyke extends 3 km eastward from this contact across the property (McMillan, 1972) (Fig. 9). The dyke consists of porphyritic granodiorite which is cut by irregular porphyry bodies and local offshoots which extend as dykes into the surrounding Skeena quartz diorite. Modal analysis of four samples of the porphyritic granodiorite indicates a variable composition as follows: anhedral quartz phenocrysts (20 - 28%), subhedral plagioclase (52 - 60%), orthoclase (4 - 11%), coarse biotite (5 - 9%) and accessory minerals (1 - 2%). The quartz porphyry is similar in mineralogy to that described at Lornex. Breccia zones within the dyke are composed of angular and rounded fragments of Skeena quartz diorite and porphyry, set in an autoclastic matrix of finely comminuted rock and mineral fragments and tourmaline (schorl). Several of the fragments were veined by quartz prior to brecciation.

Skeena and Bethsaida Phases are similar to those described for Lornex. Other rock types within the property include aplite and lamprophyre dykes. Subsurface geology across a section of the property is presented in Fig. 10.

Structurally, the Highmont deposits are characterized by numerous north-northwest, north and north-northeast trending faults (Bergey et al., 1971) (Fig. 9).

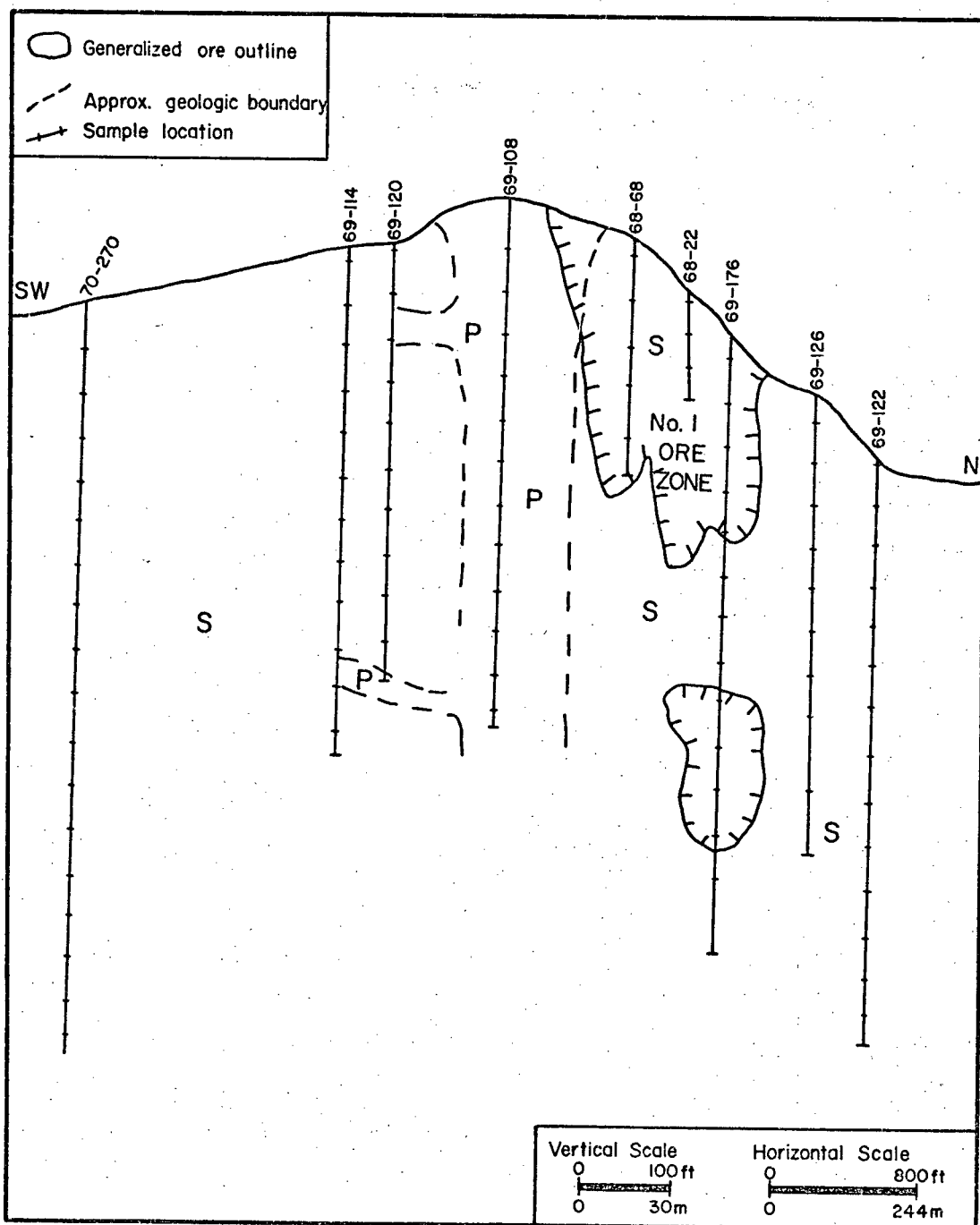


FIGURE 10: Simplified geology across a section at Highmont (P=Quartz porphyry; S=Skeena granodiorite. See Fig. 9 for line of section)

Copper-molybdenum mineralization occurs within all rock types, north and south of the main dyke (Fig. 9). Principal ore minerals are chalcopyrite, bornite and molybdenite. Pyrite and specularite are the other metallic minerals. Ore minerals occur as veins and fracture fillings, within quartz and clay gangue (Bergey et al., 1971). Sulphide disseminations also occur within altered host rock near fractures.

CHAPTER THREE
WALL-ROCK ALTERATION

INTRODUCTION

(a) General Statement

Hydrothermal alteration and sulphide zoning in wall rocks associated with ore deposits are closely-related products of ore-forming and metasomatic processes. (Rose, 1970; Lowell and Guilbert, 1970). Because the formation of metasomatic minerals generally involves enrichment, depletion or redistribution of elements in wall rocks, an adequate understanding of their nature and distribution is intrinsic to proper interpretation and understanding of local epigenetic dispersion halos around orebodies. In porphyry copper environments, alteration zones are normally broader than the mineralization, and thus constitute larger targets for ore search, using mineralogical and chemical methods.

(b) Methods of Study and Terminology

Approximately 1500 samples collected from outcrops and drill cores for the purpose of geochemical analyses were utilized in mapping of alteration and sulphide distribution patterns. Emphasis was placed on large-scale patterns, as contrasted to alteration around individual veins (Rose, 1970). Mineralogical, textural and other megascopic physical properties of all samples were recorded in the field, and approximately 200 of these were examined by X-ray diffraction. X-ray analysis of fine-grained clay minerals without the use of D.T.A. (Differential Thermal

Analysis) or heat treatment facilities allows only an approximate identification. However, this apparent drawback is compensated by the large number of samples that can be analyzed per unit time. The terms, sericite, kaolinite and montmorillonite refer respectively, to the presence of a 10\AA mica group mineral, a 7\AA kaolinite group mineral and a 14\AA montmorillonite-type mineral. 7\AA kaolinite and 7\AA chlorite peaks were resolved by scanning at low speeds of $1^\circ 2\theta/\text{min}$ or less, using Cu K α radiation. Kaolinite occurs at 7.16\AA ($12.3^\circ 2\theta$) and chlorite at 7.08\AA ($12.5^\circ 2\theta$). Preliminary experiments on quantitative determination of modal content using X-ray diffraction produced unsatisfactory results. This is attributed to the problem of preferred orientation in layered silicates resulting in poor reproducibility (Bristol, 1968, 1972). More than 100 thin sections of fresh and altered rocks were examined for relationships between primary and secondary (alteration) minerals. Many drill holes that were not sampled were also logged for their alteration mineralogy.

The terminology presently used in the geologic literature for describing alteration minerals is in a state of flux (Fountain, 1972). To avoid confusion, the terms used in the following discussion are here defined on the basis of mineral assemblages (modified after Lowell and Guilbert, 1970; Carson and Jambor, 1974).

propylitic: chlorite-epidote-calcite-albite-(adularia)

propylargillic: chlorite-sericite-montmorillonite-epidote
(kaolinite)

argillic: kaolinite-sericite-montmorillonite-(chlorite, quartz)

phyllic: quartz-sericite-pyrite with less than 5% kaolinite
or K-feldspar

potassic: secondary K-feldspar-sericite-biotite (anhydrite,
chlorite)

The term pervasive alteration is used here only for alteration which is evenly disseminated through the rock and shows no apparent relationship to veins or fractures (Fountain, 1972). Vein alteration is used here only for alteration which displays an obvious relation to veins or fractures. Deuteric alteration effects which are not directly related to hydrothermal processes are not described in this presentation. Northcote (1969) has shown that deuteric alteration which involves minor chloritization of mafic minerals and saussuritization, is widespread within the batholith. All alteration processes are considered as hypogene. Supergene alteration effects are either absent or negligible.

BETHLEHEM-JA

Guilbert and Lowell (1974) have briefly described the hydrothermal alteration patterns at Bethlehem-JA. They recognize three types of silicate alteration; potassic (K-feldspar-sericite-phlogopite-biotite-chlorite), phyllic (quartz-sericite-chlorite) and propylitic (chlorite-epidote-carbonates). McMillan (1973) mapped potassic alteration at the centre of the property, coinciding with the porphyry dyke, and epidote-zeolite alteration at the periphery.

In this study, two stages of alteration are recognized,

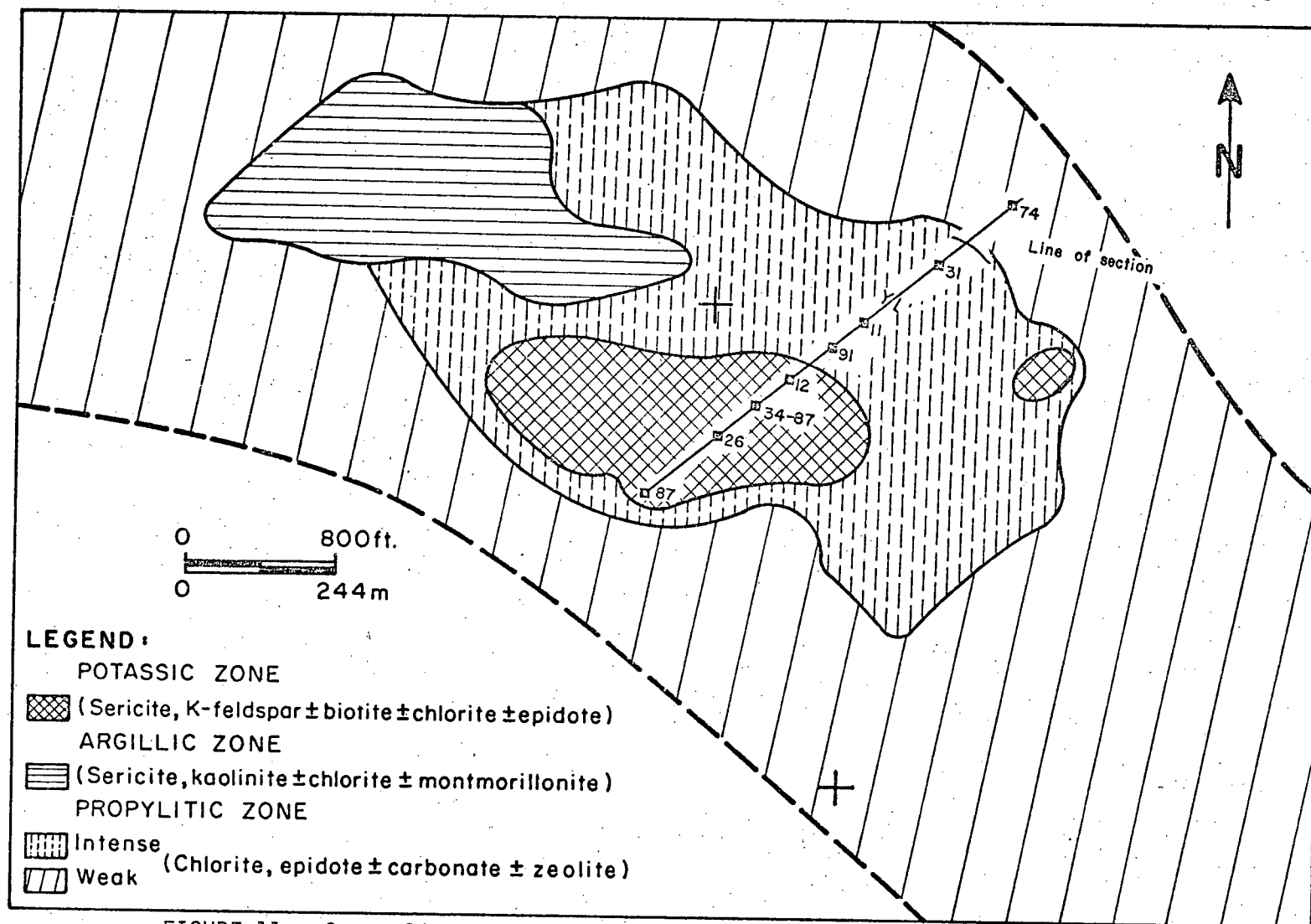


FIGURE 11: Generalized alteration map, Bethlehem-JA, 2800 Level

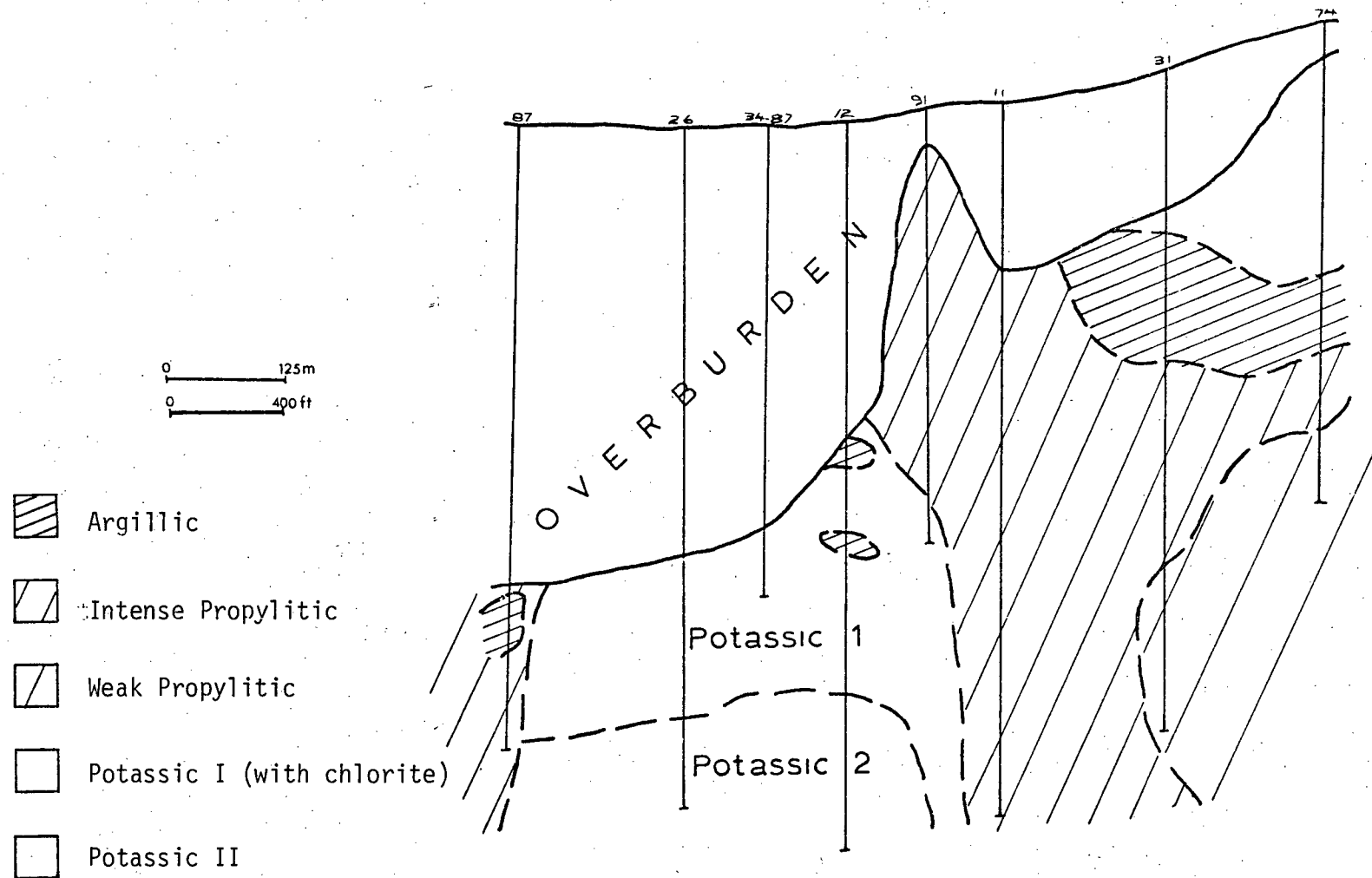


FIGURE 12: Generalized alteration across a section of Bethlehem-JA (see Fig.11 for line of section)

each stage comprising one or more types of alteration that are considered to be products of temporally related metasomatic processes. The two stages are; - an early main stage of pervasive alteration associated with the major episode of Bethlehem-JA mineralization, and a later, lesser stage of zeolite alteration and epidote veining.

(a) Main Stage Pervasive Alteration

Main stage alteration comprises three main types; potassic, argillic and propylitic.

Potassic Alteration: Potassic alteration is confined to the porphyry dyke and adjacent rocks of the Bethlehem Phase (Figs. 11 and 12). The characteristic mineral assemblage is sericite-K-feldspar-biotite. At the outer margins of the potassic zone, chlorite appears and gradually increases in abundance outward.

The exact nature of K-feldspar - whether it is secondary or primary - is not certain (K.C. McTaggart, oral comm.). Diagnostic textural evidence, such as complete replacement of plagioclase grains is not apparent. K-feldspar occurs mainly as interstitial grains, similar to that of primary K-feldspar in fresh Bethlehem rocks. However, the following lines of evidence might support a secondary origin for most of the K-feldspar (A. Soregaroli, oral communication). Firstly, the Bethlehem rocks in the potassic zone contain 20 - 26% K-feldspar (modal analysis of 4 samples) compared to a mean modal value of 10% and a range of 5 - 15% in

fresh rocks (Northcote, 1969). Secondly, K-feldspar occurs in clusters, commonly forming rims around plagioclase but not obviously replacing them (Plate 1). Thirdly, the K-feldspar is dominantly perthite or microcline compared with the dominant microperthite in fresh rocks (Westermann, 1970). Furthermore, twinning of K-feldspar is common in the potassic zone but rare in fresh Bethlehem rocks (Westermann, 1970).

Sericite occurs as fine-grained replacements of plagioclase feldspar and mafic minerals (Plate 2). Fine-grained, colourless to slightly pleochroic biotite (phlogopite) occurs as individual flakes within the groundmass. It is sparse and erratic in distribution, generally constituting less than 3% of the rock. Towards the outer part and bottom of the zone (Fig. 12) chlorite occurs as a replacement of mafic minerals, and in association with sericite and K-feldspar, constitutes 5 - 10% of the rock.

Argillic Alteration: - This type of alteration, which occurs within the northwest portion of the property, is not concentrically arranged around the potassic zone (Fig. 11). There is a close association between zones of intense shearing within Bethlehem rocks and the distribution of argillic alteration. The characteristic mineral assemblage is sericite-kaolinite-montmorillonite with minor chlorite, carbonate and epidote. On the basis of this mineral association, as determined by X-ray diffraction, and the absence of abundant pyrite and secondary quartz, this zone is considered argillic and not phyllic as proposed by Guilbert and Lowell (1974).

Megascopically, in rocks of the argillic zone, plagioclase feldspars are chalky green and soft. In thin section, sericite is seen to be evenly distributed throughout the rock as a microscopic fine-grained replacement of feldspars. Fine-grained sheared quartz occurs as remnants. In zones of intense deformation, the original texture of the rock is destroyed. However, in zones of moderate argillic alteration, the crystal outline and twinning of plagioclase feldspars are discernible. Kaolinite occurs as very fine-grained dust in plagioclase feldspar. Montmorillonite and kaolinite were only positively identified by X-ray diffraction technique. In the transitional zone between propylitic and argillic zones, chlorite and epidote are associated with clay minerals.

Propylitic Alteration: Propylitic alteration is most widespread within the property, especially in rocks of the Guichon Phase. The propylitic zone is classified into two subzones on the basis of intensity of alteration (Fig. 11). The characteristic mineral assemblage is chlorite-epidote-carbonates-zeolite. In the intense propylitic zone, altered rocks are totally impregnated with coarse radiating chlorite sheaves ranging in size from 1-3 mm. In thin section, intensely altered rocks contain 40-80% chlorite which occurs as replacements of rock constituents and as inclusions within plagioclase feldspar (Plate 3). Epidote also replaces plagioclase grains.

In weakly to moderately altered rocks, mafic minerals are partly or wholly replaced by chlorite, and plagioclase is dusted

with epidote and minor sericite. Chlorite, epidote and carbonate also occur as veinlets within this zone. Quartz and alkali feldspars are apparently fresh.

The propylitic zone grades outwards into either fresh rock or into rocks in which regional deuteritic alteration is evident.

(b) Late Stage Alteration

Zeolites: Within the JA deposit, zeolites occur abundantly as veins, seams, and replacement minerals. General distribution patterns suggest no close spatial association between zeolite alteration effects and the main stage alteration and metallization processes. Cross-cutting relationships suggest that zeolite formation was probably post-mineralization, and related to the waning stage of hydrothermal activity. Such prolific development of zeolites is commonly characteristic of hot spring activity.

Although zeolites are ubiquitous within the property, they are most abundant towards the outer margins of the deposit (Fig. 13). Minerals constituting the zeolite assemblage are leonhardite, heulandite, stilbite and chabazite. Leonhardite is the most common, and occurs as thick seams of pinkish-white soft material that ranges in width from less than 1 to 10 cm. Commonly, it is pervasively developed, replacing primary and secondary minerals. Stilbite is next in abundance, and occurs as thin films of salmon-pink colour, occupying fractures. Chabazite rarely occurs as small, colourless, euhedral crystals filling vugs, and commonly associated with calcite and leonhardite. These zeolites are seldom spatially associated

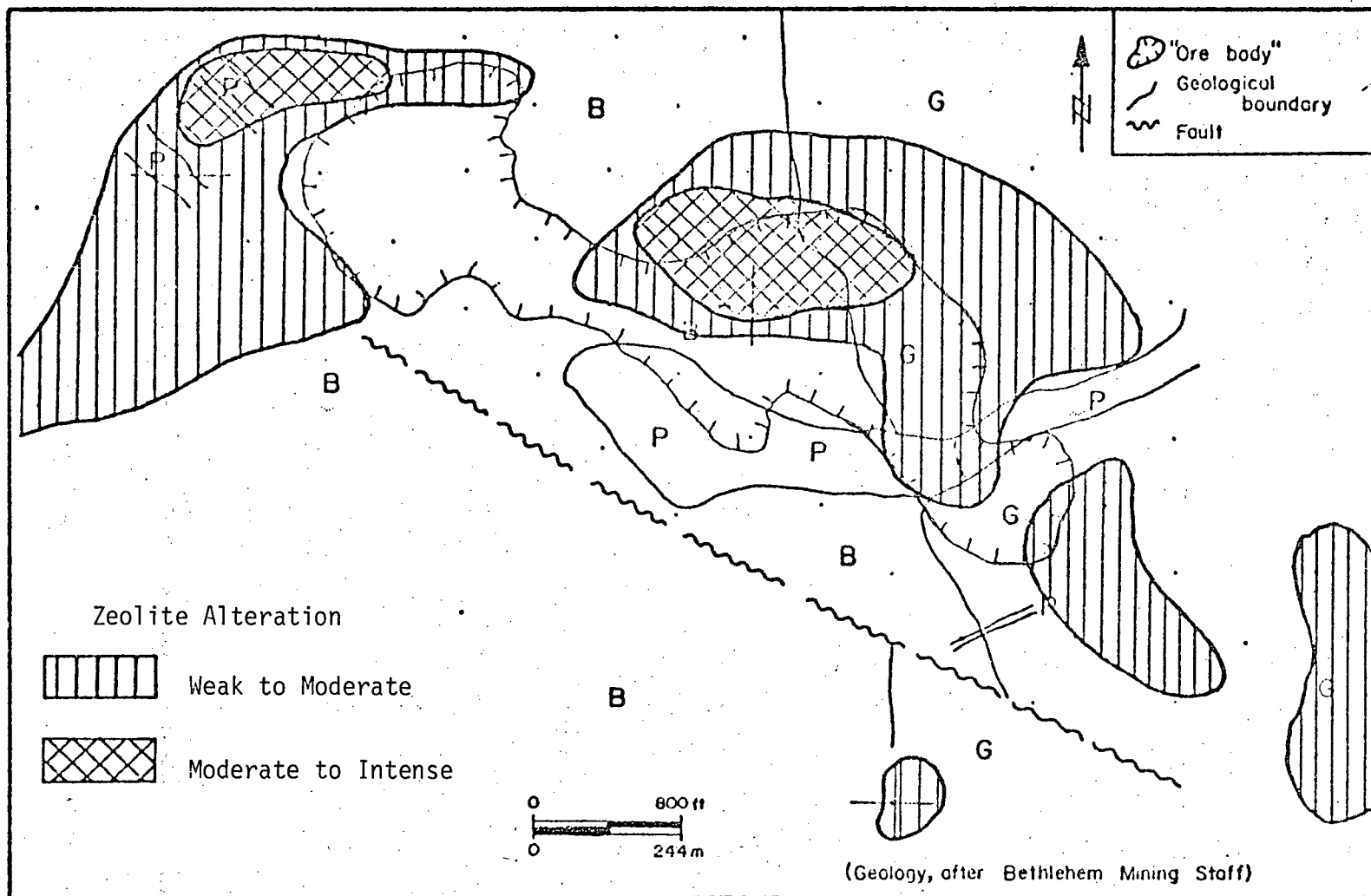


FIGURE 13: Distribution of zeolite alteration at Bethlehem-JA

with sulphides, which further attests to their post-mineralization origin.

Epidote: Veins of very coarse epidote ranging in width from 1 - 10 cm generally cross-cut earlier alteration (Plate 4), which suggest post-mineralization emplacement (W.J. McMillan, pers. comm.).

Sulphide Zoning

Spatial distribution of metallic minerals is shown in Fig. 14 and Fig. 15. Generally, chalcopyrite is the dominant sulphide mineral within the orebody, with an average ratio of 5:1 chalcopyrite to bornite (Guilbert and Lowell, 1974); and even in the bornite zone, bornite rarely exceeds chalcopyrite. The bornite is centrally located and coincides with the relatively low grade porphyry dyke and potassic alteration, an association characteristic of many porphyry copper deposits (Lowell and Guilbert, 1970). Quartz-molybdenite veinlets are also wide-spread within this zone. (Fig. 14).

The chalcopyrite zone, which is the most extensive, is characterized by chalcopyrite - pyrite - molybdenite, with sparse bornite. This zone passes outwards into the pyrite zone in which pyrite constitutes less than 2% of the mode.

Vertical zoning is generally defined by a decrease in chalcopyrite and increase in pyrite with depth (Fig. 15).

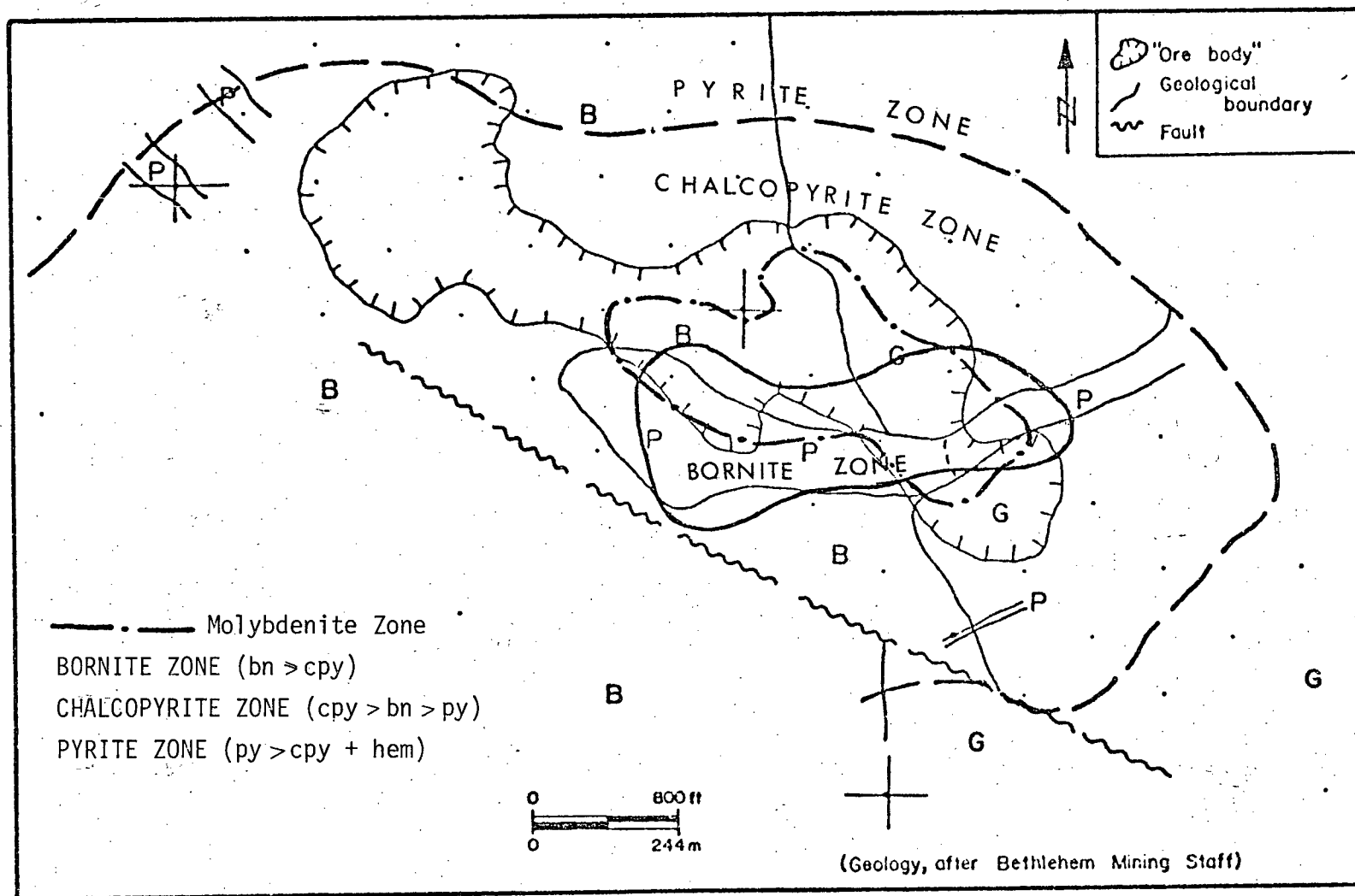


FIGURE 14: Generalized sulphide zoning at Bethlehem-JA, 2800 Level

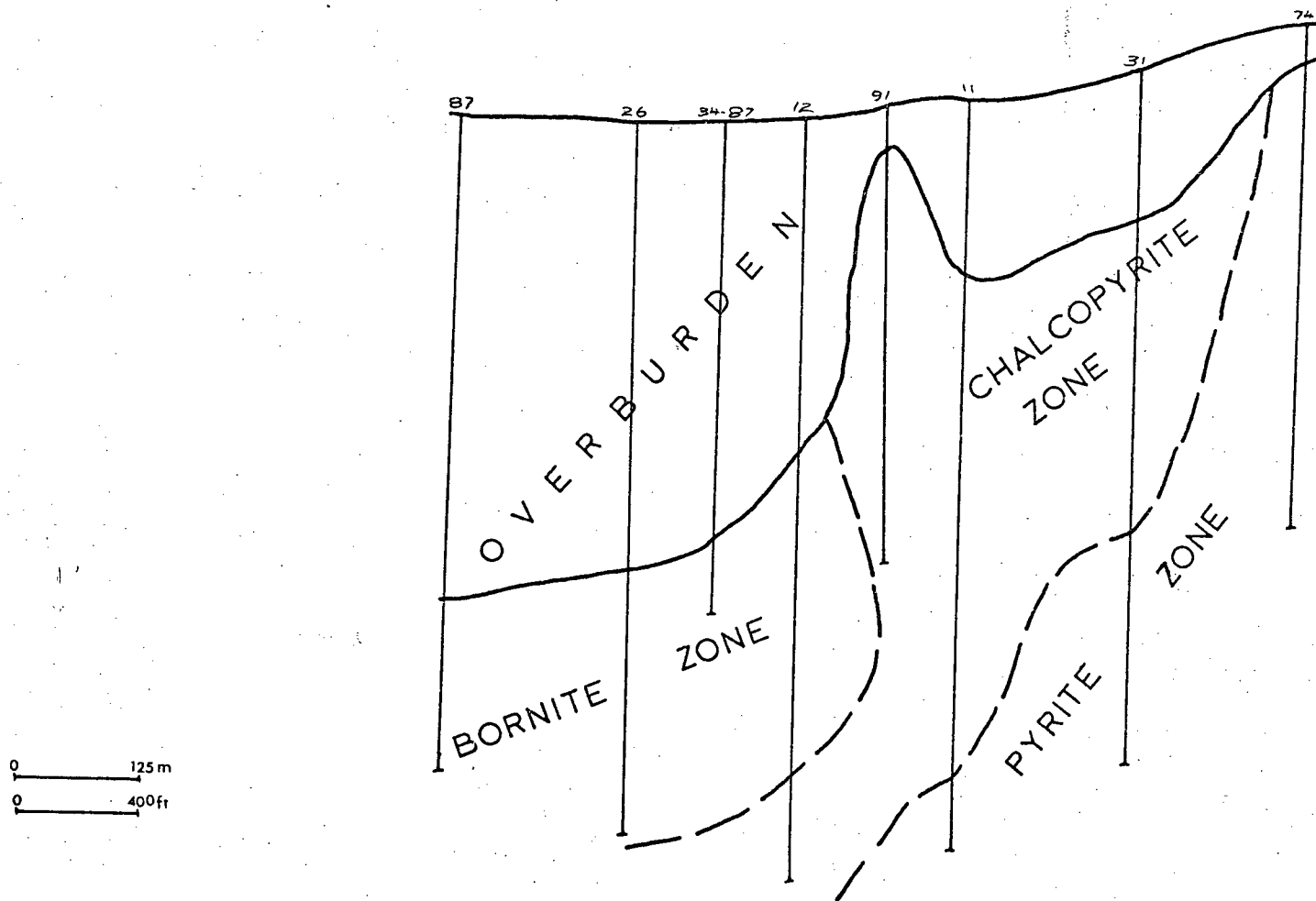


FIGURE 15: Generalized vertical distribution of sulphides at Bethlehem-JA

VALLEY COPPER

Hydrothermal alteration and sulphide distribution patterns at Valley Copper deposit have been well described by Allen and Richardson (1970), McMillan (1971, 1972), and briefly by Guilbert and Lowell (1974). Results of the present study confirm earlier findings, although a few modifications are suggested.

Two main stages of alteration characterize the Valley Copper deposit - an early stage of pervasive argillic alteration, on which a later stage of vein alteration has been superimposed. Vein alteration can also be classified into three substages, in accordance with the sequence of emplacement; a relatively early phase of barren quartz and quartz-potash feldspar veining; a main phase of quartz-sericite and sericite veining, and a late phase of gypsum and relatively young quartz veining. Pervasive argillic alteration is associated with only minor disseminated mineralization, whereas quartz-sericite veining is intimately associated with the ore-forming stage.

(a) Pervasive Argillic Alteration

Pervasive argillic alteration occurs throughout and for a short distance beyond the ore-body (Fig. 16), and probably represents a product of "ground preparation" prior to the main stage of alteration and metallization. Propylitic alteration is rare, probably due to the leucocratic nature of the host rocks.

Intensity of argillic alteration generally increases

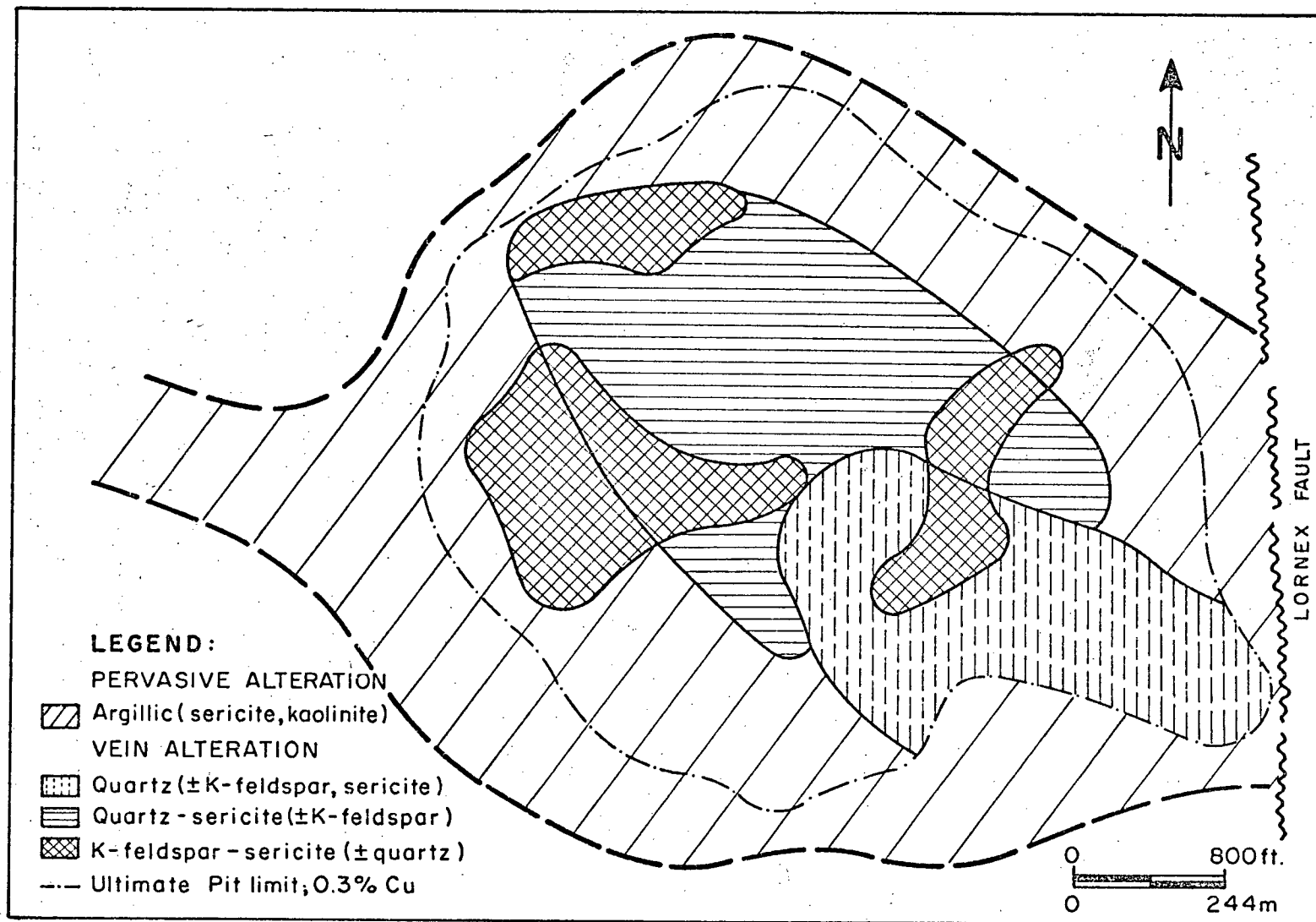


FIGURE 16: Generalized alteration map, Valley Copper 3600 Level (Modified after McMillan, 1971)

from west to east and is accompanied by a slight change in mineralogy. Where argillic alteration is weak to moderate, the plagioclase feldspar is white, relatively hard, and partially replaced by sericite, kaolinite and carbonate. Microscopically, sericite occurs as microcrystalline grains which rarely exceed 1mm (Plate 5). Kaolinite occurs mainly as 'dust' in the plagioclase feldspar. As estimated from X-ray diffractograms, kaolinite constitutes about 20-50% of the mode. Quartz and potash feldspar are commonly unaltered, whereas biotite is replaced by sericite and minor chlorite. Where argillic alteration is intense, especially in the eastern sector of the orebody adjacent to the Lornex Fault, kaolinite content decreases to about 10 - 15%, and sericite is relatively coarser. The plagioclase feldspars are chalky in various shades of white and green and completely replaced by fine-aggregates of sericite, carbonate and kaolinite. Primary K-feldspar and biotite are in many instances completely altered to sericite (Plate 6). Quartz occurs as remnants, commonly containing numerous fractures filled with sericite.

Montmorillonite is relatively uncommon, and has only been identified in a few samples from the outer margins of the argillic zone. Minor albite persistently accompanies weak to moderate argillic alteration in many samples.

(b) Vein Alteration

(1) Early Phase Veining

The early phase of vein alteration at Valley Copper is

characterized by a centrally-located stockwork of barren quartz veins and quartz veins with potash feldspar selvages.

Barren Quartz Veins: As shown in Figure 16, these veins occupy a low-grade stockwork zone in the southeast of the deposit. They consist predominantly of barren coarse-grained quartz varying in width from 1 mm to 5 cm, and commonly containing minute pods of sericite and/or K-feldspar.

Quartz-Potash Feldspar Veins: At the northeast part of the barren quartz zone, K-feldspar envelopes around quartz veins are very common. The pink potash feldspar selvages range in width from less than 1 to 10 mm and pass outward into weakly argillized rock. Like the quartz veins which they border, the potash feldspar envelopes are generally barren, although a few contain chalcopyrite and minor molybdenite (McMillan, 1971).

(11) Main Phase Veining

This phase of alteration is characterized by quartz-sericite and sericite veins formed during the main ore-forming stage. Bornite and chalcopyrite occur predominantly as veins and pods in association with quartz or as disseminated intergrowths with sericite.

Quartz-Sericite Veins: Quartz-sericite and sericite veins occur almost throughout the ore zone, but are developed most intensely in a zone nested upon the central quartz-rich zone (Fig. 16). Quartz-sericite veins vary from quartz veins with coarse-grained

sericite envelopes varying in width from 1mm to 5 cm, to vuggy quartz-sericite zones with hair-line or no apparent central quartz vein, to quartz veins containing only a few pods of sericite (McMillan, 1971). These veins generally pass outwards into argillized rocks or potash-feldspar selvages. Where many veins coalesce, pervasive sericite zones commonly develop, up to several metres wide.

Microscopically, vein sericite relatively is very coarse grained, usually forming rosettes 1 to 5 mm long and 0.5 to 3 mm wide of vein-filling and replacement material (Plate 7). Euhedral to subhedral crystals of quartz which are commonly fractured and filled with fine-grained sericite, intergrow with very coarse sericite (Plate 8). Most of the sulphide minerals are intimately associated with the quartz-sericite veins. Minor secondary biotite accompanies sericite alteration.

Potash Feldspar Alteration: Potash feldspar generally occurs as envelopes around quartz-sericite veins, passing outwards into argillized rock. Locally the host rock is flooded with pervasive salmon-pink K-feldspar (McMillan, 1971). Generalized distribution of potash feldspar alteration is shown in Figure 16. It is strongly developed along the western margins of the quartz-sericite zone, where it also extends into the zone of pervasive argillic alteration.

In thin section, subhedral potash feldspar (mainly microcline) ranges in size between 1 and 5 mm, and occurs as vein filling or replacements of plagioclase and in association with

coarsely crystalline sericite.

The presence of K-feldspar envelopes around sericite and in equilibrium with kaolite is contrary to the stability field relationships established for these minerals by Hemley and Jones (1964). A similar anomalous relationship has been documented by Fournier (1967) at Ely, Nevada, and attributed to a resurgence of abnormally high silica activities of ore-forming fluids.

(iii) Late Phase Veining

Late phase veining comprises gypsum veins and relatively young quartz veins which cut quartz-sericite veins. The nature and distribution of gypsum veins are not clear although they occur abundantly at depth, below the so-called 'gypsum line' (McMillan, 1971). They crosscut all the earlier veins and are associated with minor anhydrite.

(c) Sulphide Zoning

McMillan (1971) has investigated the distribution of chalcopyrite-bornite ratios within the Valley Copper deposit. The generalized distribution map (Fig. 16b) shows that the low-grade, quartz-rich core is characterized by chalcopyrite - sparse bornite - molydenite, passing outwards into bornite-chalcopyrite - low pyrite, and finally to chalcopyrite - sparse bornite - minor pyrite at the outer part of the deposit. Pyrite, which generally constitutes less than 1% of sulphide content within the orebody, forms a halo around the northern part of the deposit. Minor hematite occurs

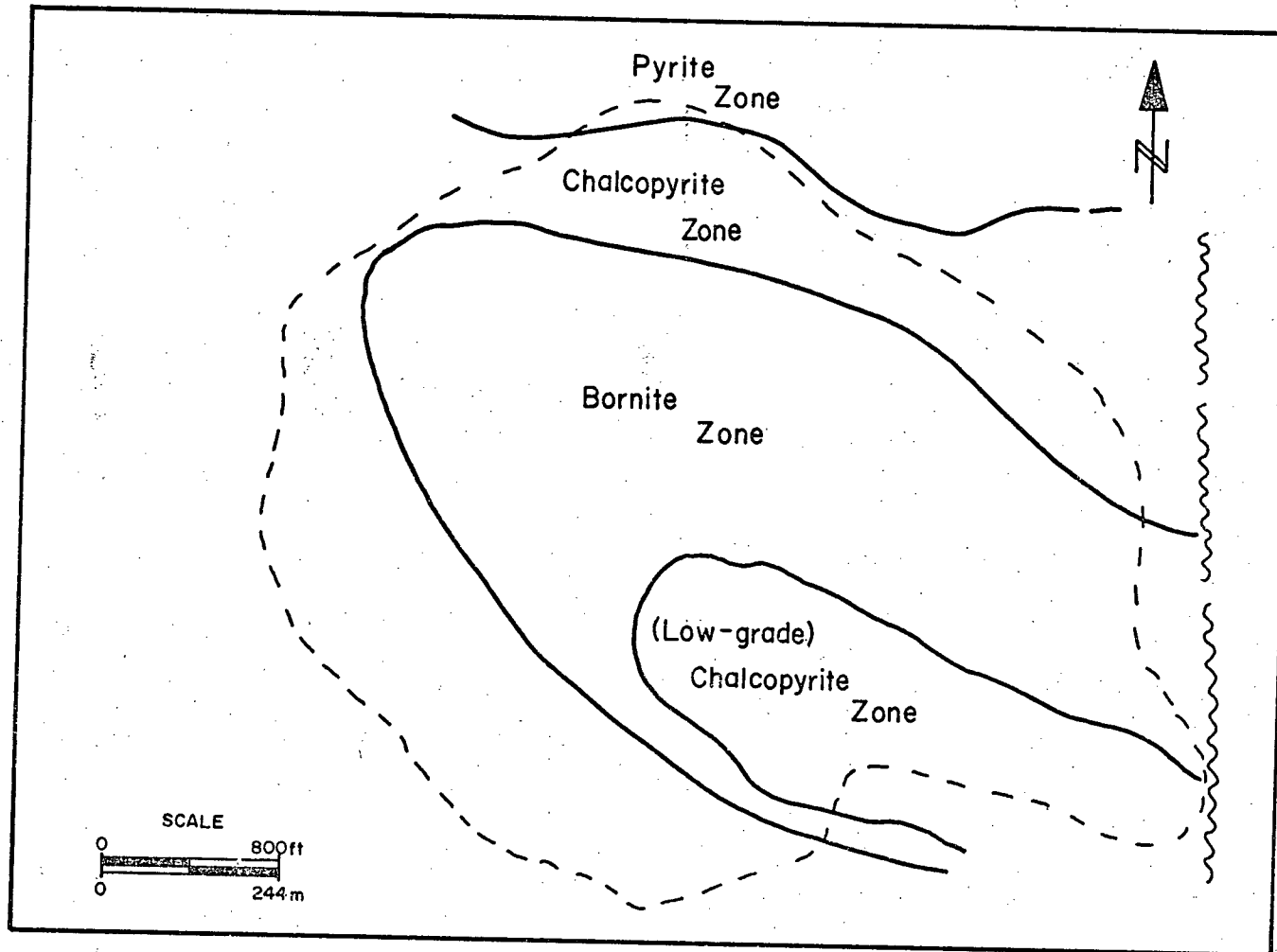


FIGURE 16b: Generalized sulphide zoning, Valley Copper 3600 Level
(Modified after McMillan, 1971)

throughout the orebody.

LORNEX

Wall-rock alteration patterns at Lornex are similar to those of Valley Copper except for the extensive development of propylitic and propy-argillic assemblages, which are partly attributable to wall rock at Lornex (Skeena granodiorite) containing up to 15% mafic content; a readily available source of Mg and Fe needed for the formation of propylitic minerals. Also, the well-developed vein alteration effects at Valley Copper are only moderately developed at Lornex, although wide gouge zones with quartz-sericite alteration are prominent. Fipkie (1972) studied the alteration patterns in samples across the orebody and his findings are generally consistent with the results of this study.

Two stages of alteration are present at Lornex; - an early stage of well-developed pervasive argillic and propylitic alteration, on which has been superimposed a main stage of intense, structurally controlled quartz-sericite alteration, K-feldspar and gypsum veining. Fig. 17 is a generalized composite map of alteration at Lornex, based upon observations in the open-pit and studies of drill-core samples. Generalized alteration patterns in a section across the orebody are presented in Fig. 18.

(a) Early Stage Pervasive Alteration

Three main alteration zones characterize the early stage

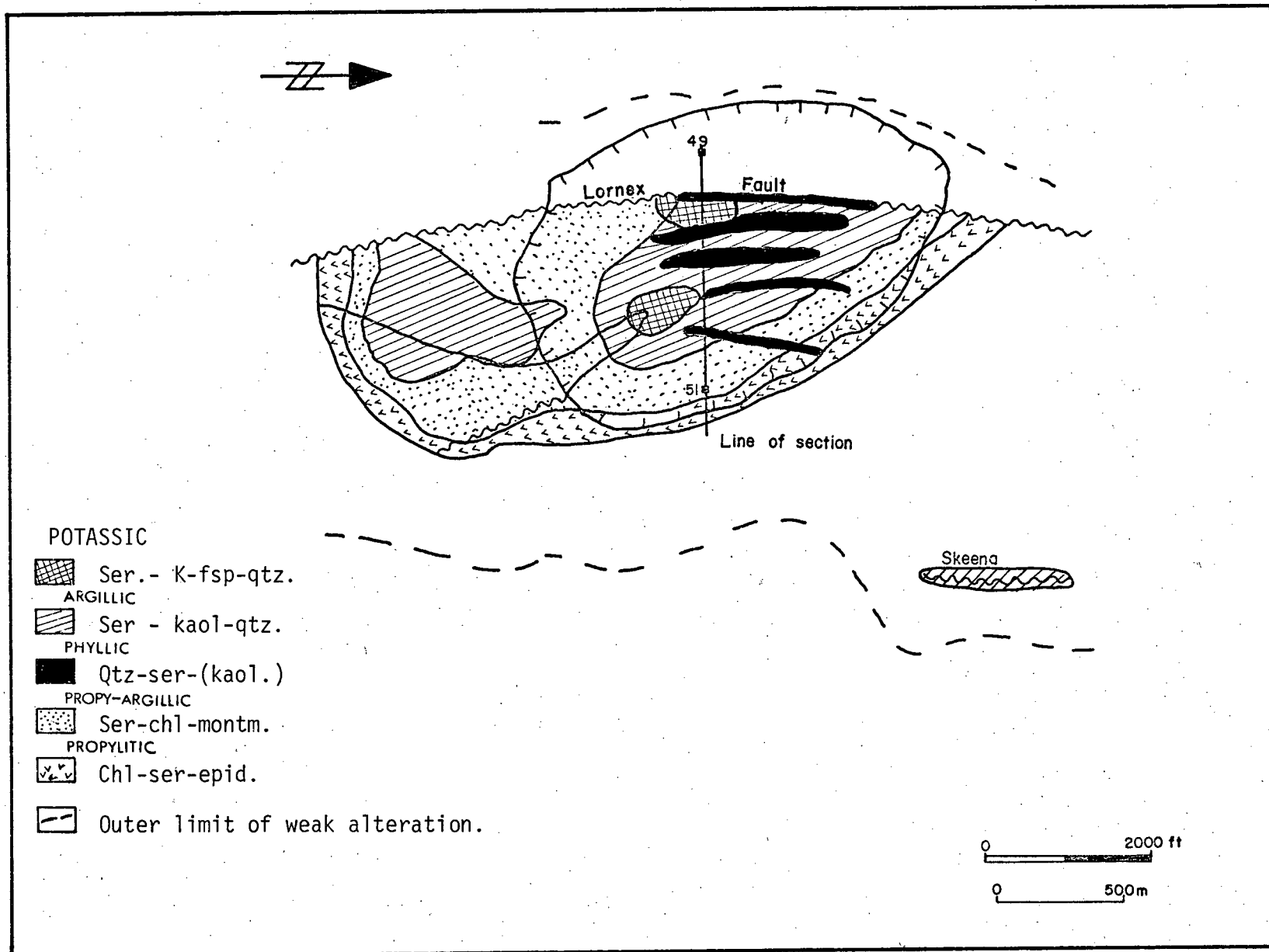


FIGURE 17: Generalized alteration map, Lornex 4900 Level.

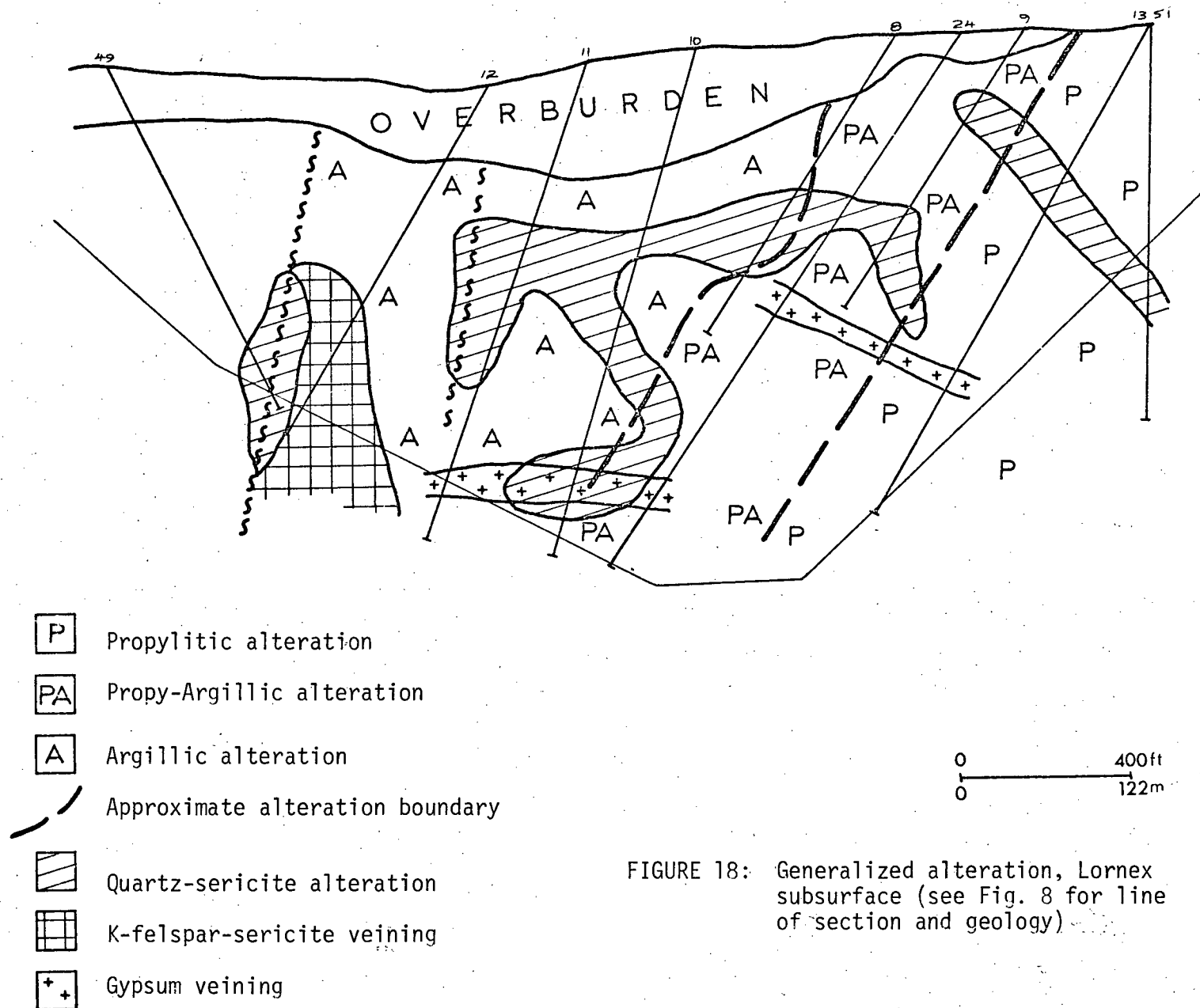


FIGURE 18: Generalized alteration, Lornex subsurface (see Fig. 8 for line of section and geology)

hydrothermal activity; propylitic, propy-argillic (mixed propylitic and argillic) and argillic. Compared to early stage alteration at Valley Copper, that of Lornex is apparently associated with more sulphide mineralization, probably as a result of numerous microfractures superimposed on the earlier phase of hydrothermal activity.

Propylitic Zone: This zone occurs along the outer margins of the orebody, generally extending from the 5000 level bench (1972 levels) to the surface (Fig. 17 and 18). The dominant propylitic mineral assemblage is epidote-chlorite-carbonate. Minor sericite, montmorillonite and zeolites are present within this zone.

In hand specimen, rocks of this zone are various shades of green, as a result of the high epidote and chlorite content. In zones of intense propylitic alteration, epidote occurs as medium-grained masses replacing plagioclase, biotite and hornblende grains (Plate 8). Biotite is generally altered to chlorite, leucoxene and quartz. K-feldspar and quartz remain unaltered. Further east, away from the orebody (Fig. 17), propylitic alteration is less intense and plagioclase feldspars remain relatively fresh although preferential replacement of calcic cores by fine-grained sericite is common. Locally, carbonates (calcite, siderite) are present. Pyrite, hematite and minor chalcopyrite are the predominant metallic minerals in this zone.

Propy-Argillic Zone:

This zone, which represents a transition between the

propylitic and argillic zones, is characterized by significant increase in montmorillonite and sericite and a general decrease in epidote, although chlorite is still widespread. Plagioclase feldspar is commonly replaced by sericite, montmorillonite and allophane. Mafic minerals are altered to sericite, chlorite and epidote. Inter-layered sericite-chlorite-montmorillonite is locally present. Associated metallization represented by chalcopyrite and minor bornite is low grade except where later fracture-filled mineralization is superimposed.

Argillic Zone: Pervasive argillic alteration is most widespread within the orebody and coincides with the major zone of mineralization.. Intense fracturing and faulting within this zone have caused the development of extensive areas with quartz-sericite alteration; consequently it is often difficult to differentiate between argillic and phyllic alteration within the orebody. South of the Lornex Pit (Fig. 17) argillic alteration is well-developed within an area presently considered as protore (Discovery Zone; Carr, 1967).

Megascopically, the argillized rocks are creamy-white and fragile, as a result of the pervasive fracturing and shearing. They are characterized by chalky-white to waxy green feldspars. The intensity of argillic alteration progressively increases from the east to west, and this is accompanied by progressive destruction of plagioclase, and lastly potash feldspar. In areas of moderate to weak argillic alteration, the plagioclase feldspars are partly

altered to kaolinite, montmorillonite and waxy-green sericite (Plate 9). Crystal outlines and twinning are generally preserved. Mafic minerals breakdown into sericite, minor chlorite and leucoxene or quartz. Wherever argillic alteration is intense, the plagioclase feldspars are completely replaced by fine- to medium-grained sericite, quartz and kaolinite with sericite the dominant mineral. With increasing alteration intensity towards the west near the Lornex Fault (Fig. 17 and Fig. 18), the alkali feldspars also are completely altered to sericite and kaolinite. Only primary quartz with sericite in fractures remain. Mafic minerals are also converted to sericite, rutile and leucoxene. The metallic minerals associated with argillized rocks are ore-grade bornite and chalcopyrite, as disseminates or fracture fillings.

(b) Main Stage Alteration

The distribution of main stage alteration products is controlled by structural features which probably developed after the early stage alteration processes. Main stage alteration is classified into quartz-sericite and K-feldspar types.

Quartz-Sericite Alteration: This type of alteration occurs as envelopes around sulphide-bearing veins and within fault-gouge zones which range from less than 1 to 100 m in width. Distribution of some of the zones with intense quartz-sericite alteration is shown in Figures 17 and 18. These zones cross-cut earlier types of pervasive alteration, and show a dominant northerly trend coin-

ciding with the strike of faults and fractures. Where quartz-sericite alteration is intense and extensive, primary textures of the rocks are completely destroyed. All plagioclase feldspars are converted to sericite, carbonate and quartz. However, kaolinite and minor chlorite may survive as relicts of the earlier pervasive alteration. Commonly, alkali feldspars are partially or completely replaced by sericite and quartz. Mafic minerals also are altered to sericite. In DDH 8 (Fig. 18), muscovite co-exists with sericite and quartz. A few gouge zones contain dark green talc. Pyrite is a common sulphide in association with quartz and sericite. Ore-grade chalcopyrite and lesser amount of bornite predominate within the ore-bearing veins and gouges.

Potash feldspar Veining: Potash feldspar veins with argillic or quartz-sericite selvages occur abundantly in two areas of the ore-body; one near the centre of the deposit within and north of the quartz porphyry dyke (Fig. 17), and at depth adjacent to the Lornex Fault (Fig. 18). In the latter the K-feldspar veins occur above and within a (?) porphyry dyke (Fig. 8). The veins and envelopes consist of perthite and microcline within pervasively argillized rock. Cross-cutting relationships suggest that the phase of K-feldspar veining is relatively younger than pervasive argillic alteration.

Gypsum Veining: As at Valley Copper, the nature of gypsum veining and its relationship to other forms of alteration is not evident. Figure 18 shows that it is generally encountered in deep

boreholes, cross cutting quartz-sericite and potassic alteration. Occurrence of anhydrite has not been reported.

Sulphide Zoning

Staff geologists at the Lornex Mine have established that a core, in which bornite exceeds chalcopyrite, is enveloped by a zone in which chalcopyrite exceeds bornite (Fig. 19). A pyrite halo, characterized by sparsely disseminated pyrite, coincides with the outer part of the deposit and zones of propylitic and propy-argillic alteration.

SKEENA

A drill-hole that cuts through the Skeena quartz lode was examined for hydrothermal alteration patterns. As shows in Figure 20, argillic alteration increases in intensity towards the lode. The characteristic mineral assemblage is sericite-kaolinite-montrimollonite. Potash feldspar is relatively unaltered. Chlorite occurs at the outer fringes of the drill-hole. The main sulphide minerals are pyrite and chalcopyrite in quartz-carbonate veins.

HIGHMONT

Compared to other major porphyry copper deposits in the Highland Valley, the intensity of hydrothermal alteration at Highmont is relatively weak, although alteration zoning is moderately well-developed.

Hydrothermal alteration affects are classified into two stages; an early pervasive alteration (argillic and propylitic)

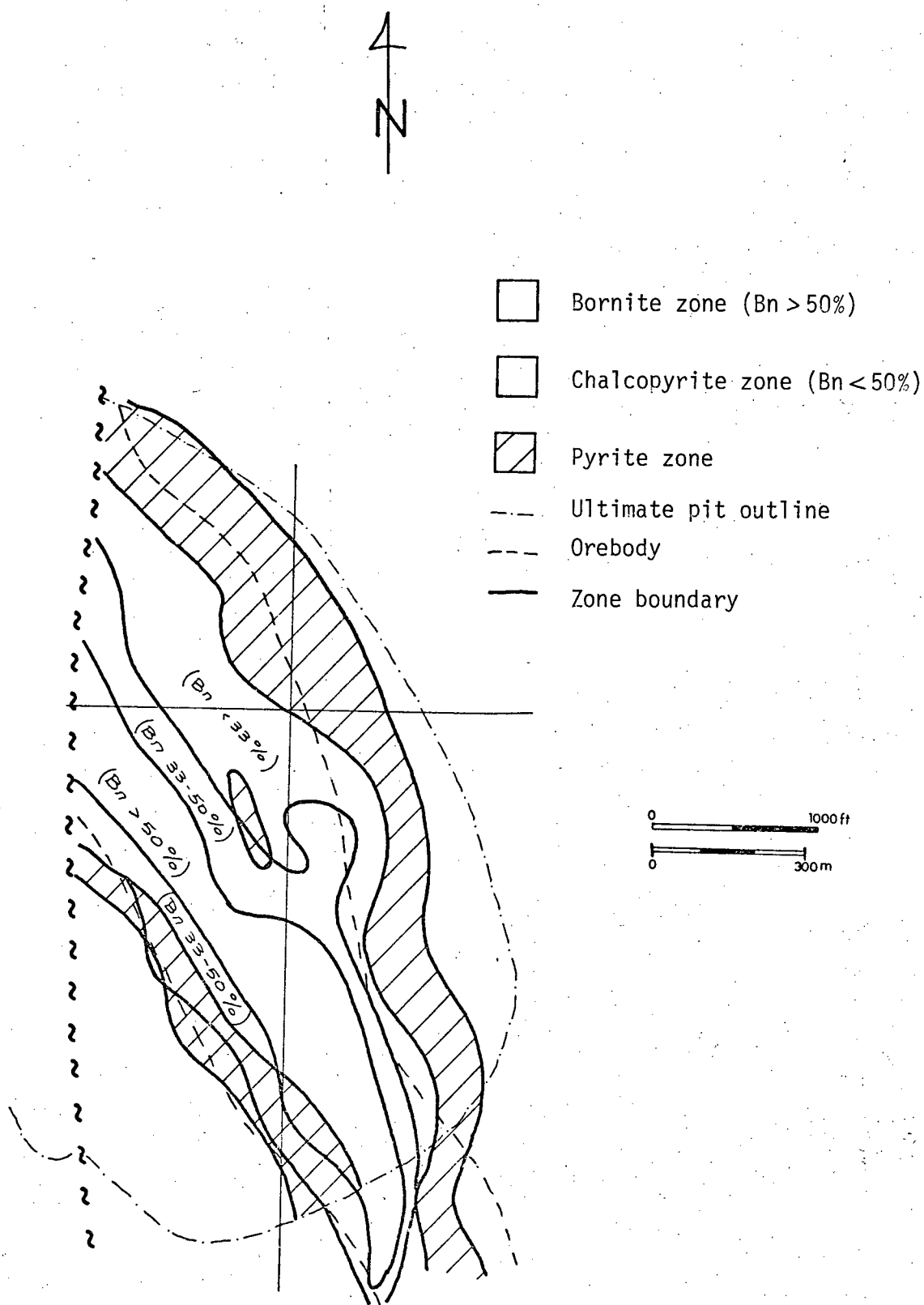
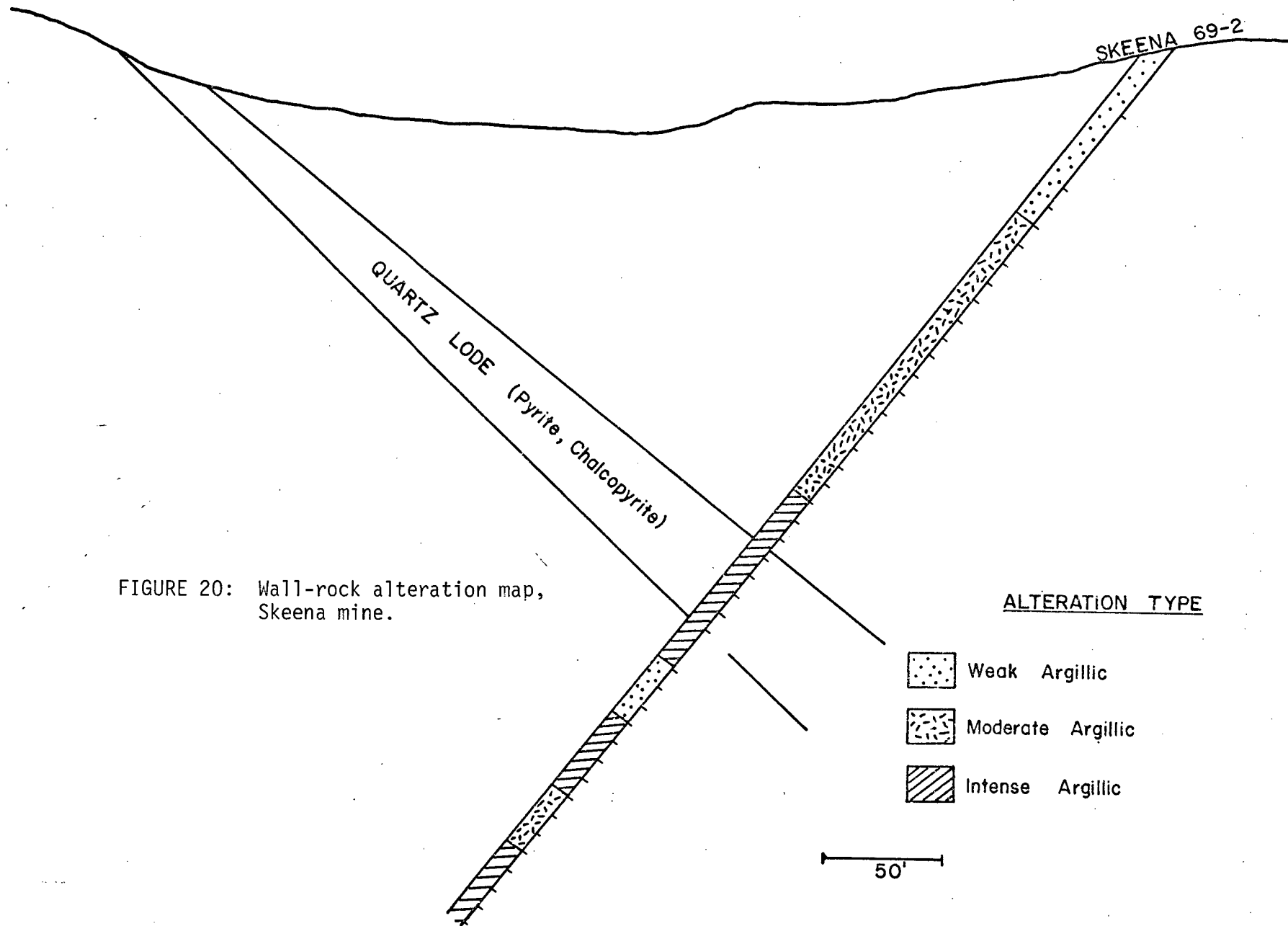


FIGURE 19: Sulphide distribution at Lornex mine (After Lornex mining staff)



and a later phase of vein alteration (K-feldspar and quartz-sericite). Tourmaline-biotite with minor sericite alteration is confined to breccia pipes and their immediate surroundings.

(a) Pervasive Alteration

Pervasive alteration effects are classified into propylitic, propy-argillic and argillic types.

Propylitic Alteration: Propylitic alteration is confined mainly to the outer margins of the Nos. 1 and 2 ore zones and the areas surrounding the other small deposits south of the main dyke (Fig. 21). Relatively weak propylitic alteration is characterized by the mineral assemblage chlorite-carbonate-epidote-zeolite. Plagioclase feldspars are generally fresh except for selective partial replacement of calcic cores by carbonate. Biotite is altered to chlorite and quartz (Plate 10). Epidote occurs commonly as veinlets rather than replacements of plagioclase feldspar. Quartz and alkali feldspars are relatively unaltered. Pyrite and lesser chalcopyrite are disseminated within the altered rocks.

Propy-Argillic Alteration: This type of alteration is most closely associated with sulphide mineralization. The characteristic mineral assemblage is a sericite-chlorite-montmorillonite-carbonate. Veins of epidote, and albite replacements of plagioclase are also common within this zone.

Figs. 21 and 22 show the distribution of propy-argillic alteration, north and south of the argillic alteration zone. It is

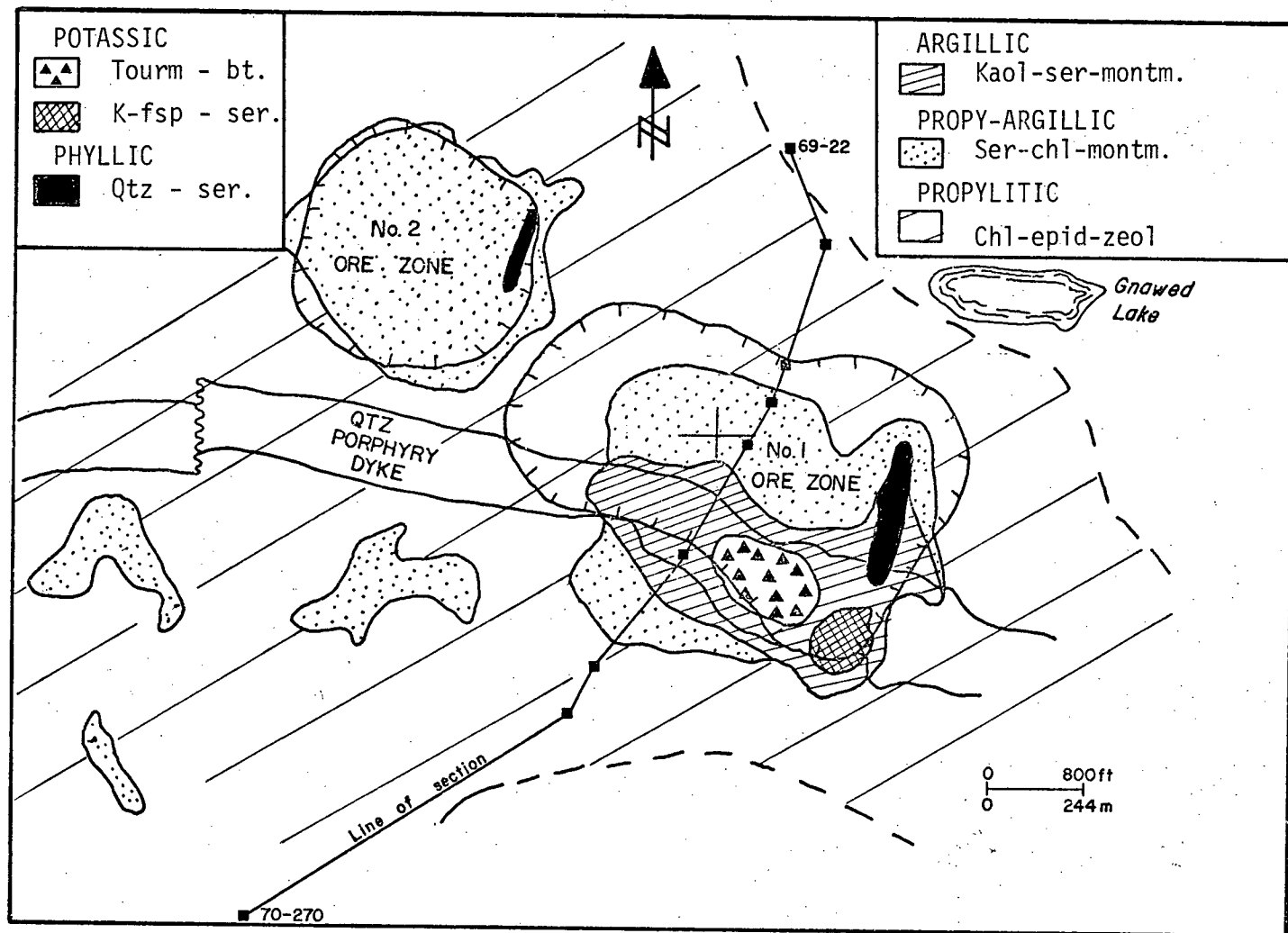


FIGURE 21: Generalized alteration map, Highmont property.

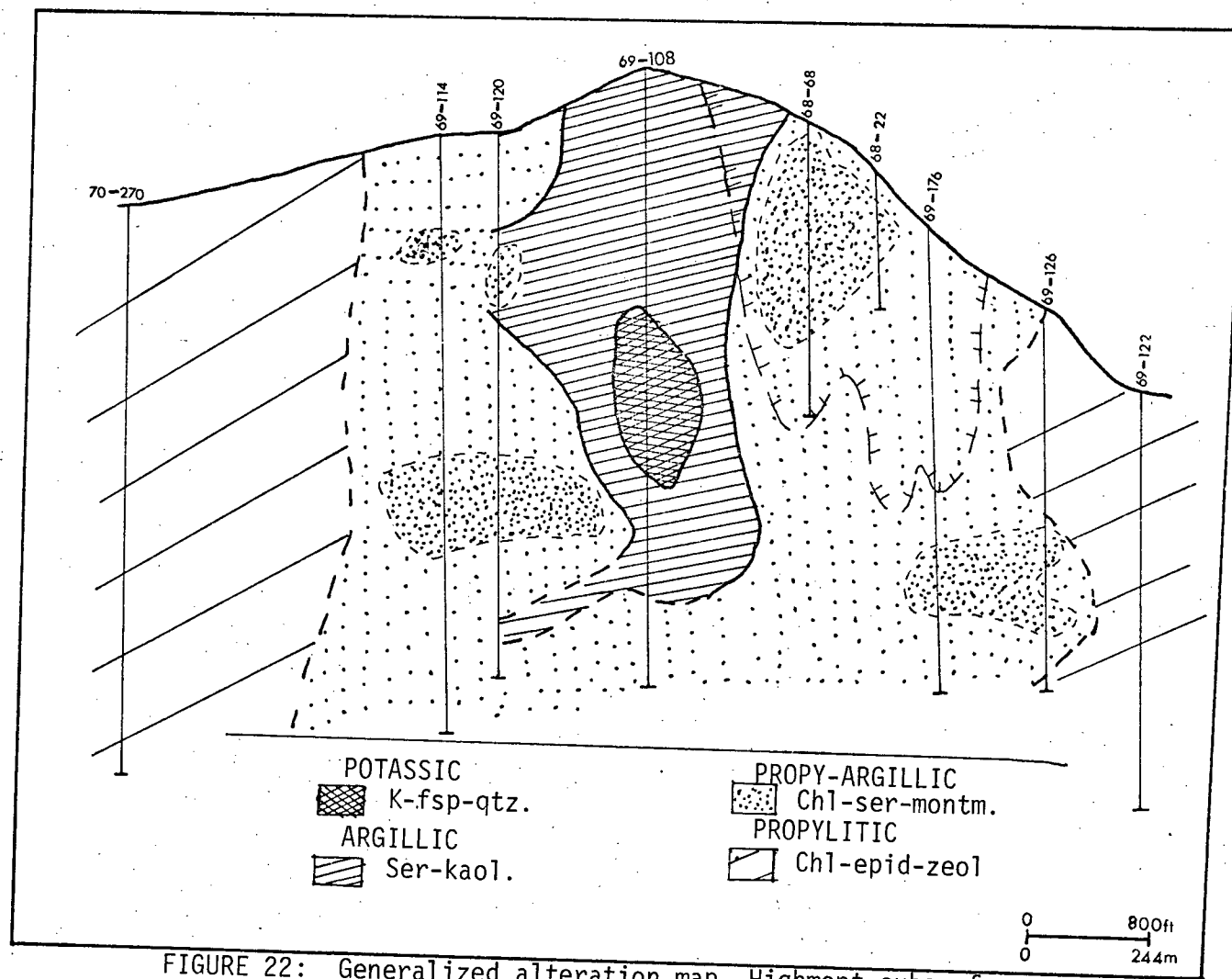


FIGURE 22: Generalized alteration map, Highmont subsurface.
(See Fig 21 for line of section)

most prominent in the No. 2 Ore zone (Fig. 21) but also occurs in the small deposits in the south-western part of the property. Plagioclase feldspar in intensely altered rocks is partly or completely replaced by sericite and carbonate, preserving only the crystal outlines. Calcite occurs as replacement of primary minerals, and as veinlets. Mafic minerals (generally) are replaced by sericite, leucoxene and chlorite. Alkali feldspars are commonly dusted with sericite, whereas quartz remains fresh. Epidote replaces plagioclase feldspar and hornblende, but is most common as veins. The principal sulphide mineral is chalcopyrite with minor bornite and disseminated pyrite.

Argillic Alteration: The argillic zone is centred upon the quartz porphyry dyke (Figs. 21 and 22), forming an annulus around zones with potassic, tourmaline and quartz-sericite alteration. This distribution pattern reflects the influence of wall-rock composition upon alteration type. The characteristic mineral assemblage is kaolinite-montmorillonite-sericite-(carbonate). Where argillic alteration is well-developed, the plagioclase feldspars are completely replaced by fine-grained kaolinite, sericite and minor montmorillonite (Plate 11). Carbonate occurs as replacement patches and veins within plagioclase feldspar. Under conditions of weak to moderate argillic alteration, alternate crystal zones within plagioclase feldspar are selectively replaced by kaolinite, thus accentuating the crystal zoning. Alkali feldspars generally remain fresh although commonly they are dusted with

sericite and kaolinite. Mafic minerals break down to sericite and leucoxene.

(b) Vein Alteration

Quartz-Sericite Alteration: Quartz-sulphide veins with potash feldspar envelopes are common within the zone of argillic alteration, in association with the main porphyry dyke (Fig. 22). Figure 21 shows a small potassic zone within the porphyry dyke and southeast of the No. 1 ore zone, in which extensive, K-feldspar/aplite veining locally grade into pervasive alteration. Tourmaline also occurs in association with some of the quartz-potash feldspar veins which often contain chalcopyrite.

Quartz-Tourmaline-Biotite Alteration: Tourmaline (schorl) is associated with breccia pipes and surrounding rocks. The breccia zones are spatially and genetically related to the quartz porphyry dyke (Carr, 1966). Tourmaline occurs as elongated and radiating crystals cementing the breccia fragments and as disseminations within the surrounding porphyry (Plate 12). The breccias are also silicified as a result of the introduction of anhedral secondary quartz into the matrix. Plagioclase feldspars are commonly dusted with sericite. Sparse, fine-grained secondary biotite is associated with tourmaline impregnation. Quartz-sulphide veins also contain disseminated tourmaline.

Gypsum Veining: Gypsum veins have been encountered in a few drill-holes, especially Hole 69-108, although the nature of their

distribution and relationship to other forms of alteration are not clear. They are generally associated with zones of intense argillic alteration.

Sulphide Zoning

Zonal distribution of metallic sulphides is summarized in Figure 23. The data were obtained mainly from company files. In the two major orebodies mineral zoning is parallel to the dyke. East of the No. 1 ore zone and immediately north of the dyke, the author observed that the predominant sulphide is chalcopyrite, and thus a chalcopyrite zone is suggested (Fig. 23a). Generally, in a zone north of and parallel to the dyke bornite and chalcopyrite occur in roughly equal amounts; this zone grades outwards to one of chalcopyrite, sparse pyrite and rare bornite, and finally to a pyritic zone in which pyrite locally amounts to 1 percent of the rock (Bergey et al., 1971). The MoS_2 zone is slightly displaced south of the Cu zone in Nos. 1 and 2 ore zones (Fig. 23b).

FACTORS CONTROLLING WALL-ROCK ALTERATION

Host rock composition, structural features and chemistry of mineralizing solutions influence the nature and intensity of wall-rock alteration in Highland Valley.

(a) Host Rock Composition

The effects of host rock lithology on alteration are apparent in all the Highland Valley deposits. Propylitic alteration

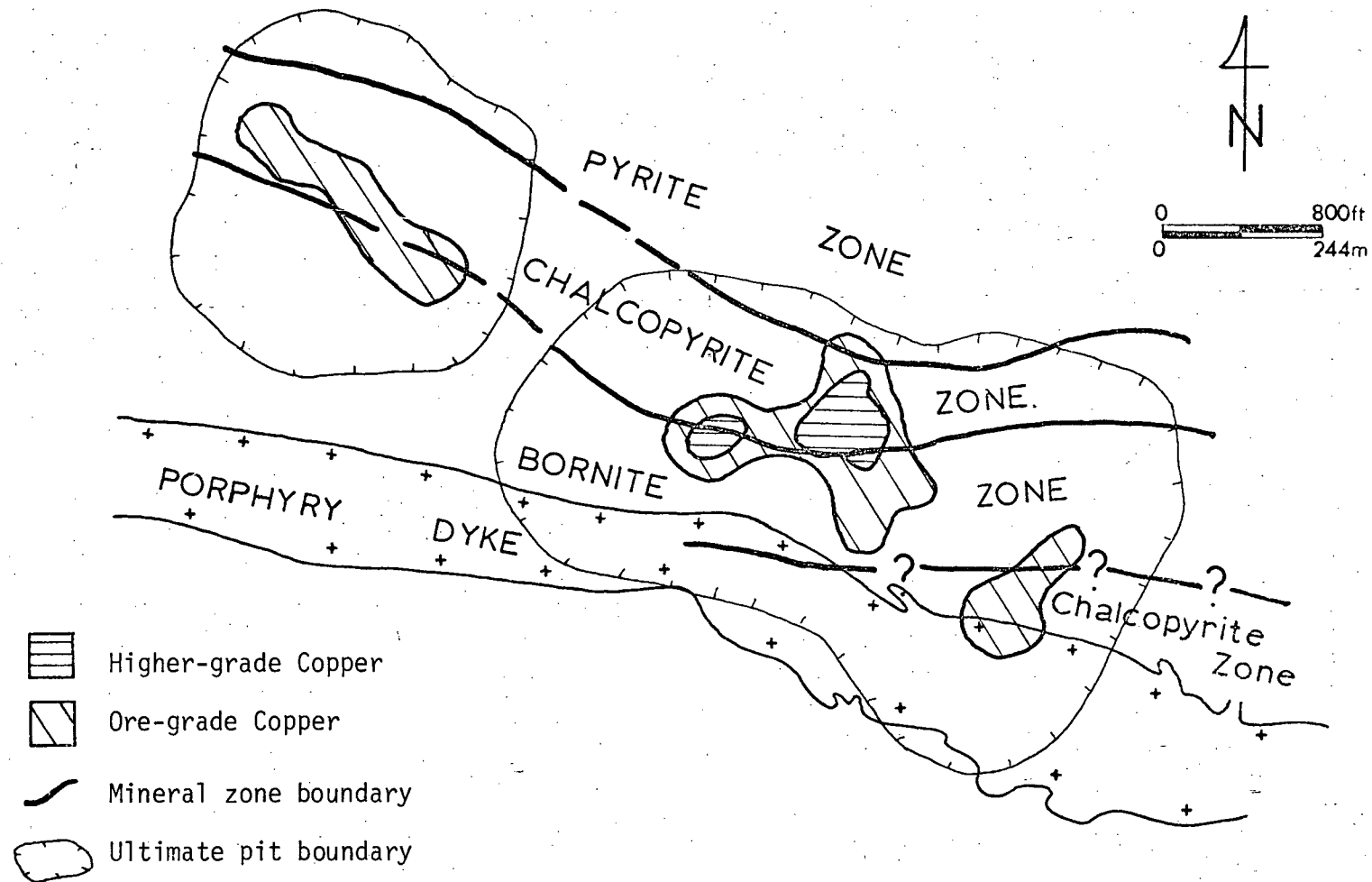


FIGURE 23a: Mineral zoning and copper grade at Highmont property
(Data from company files, Highmont Mining Corporation)

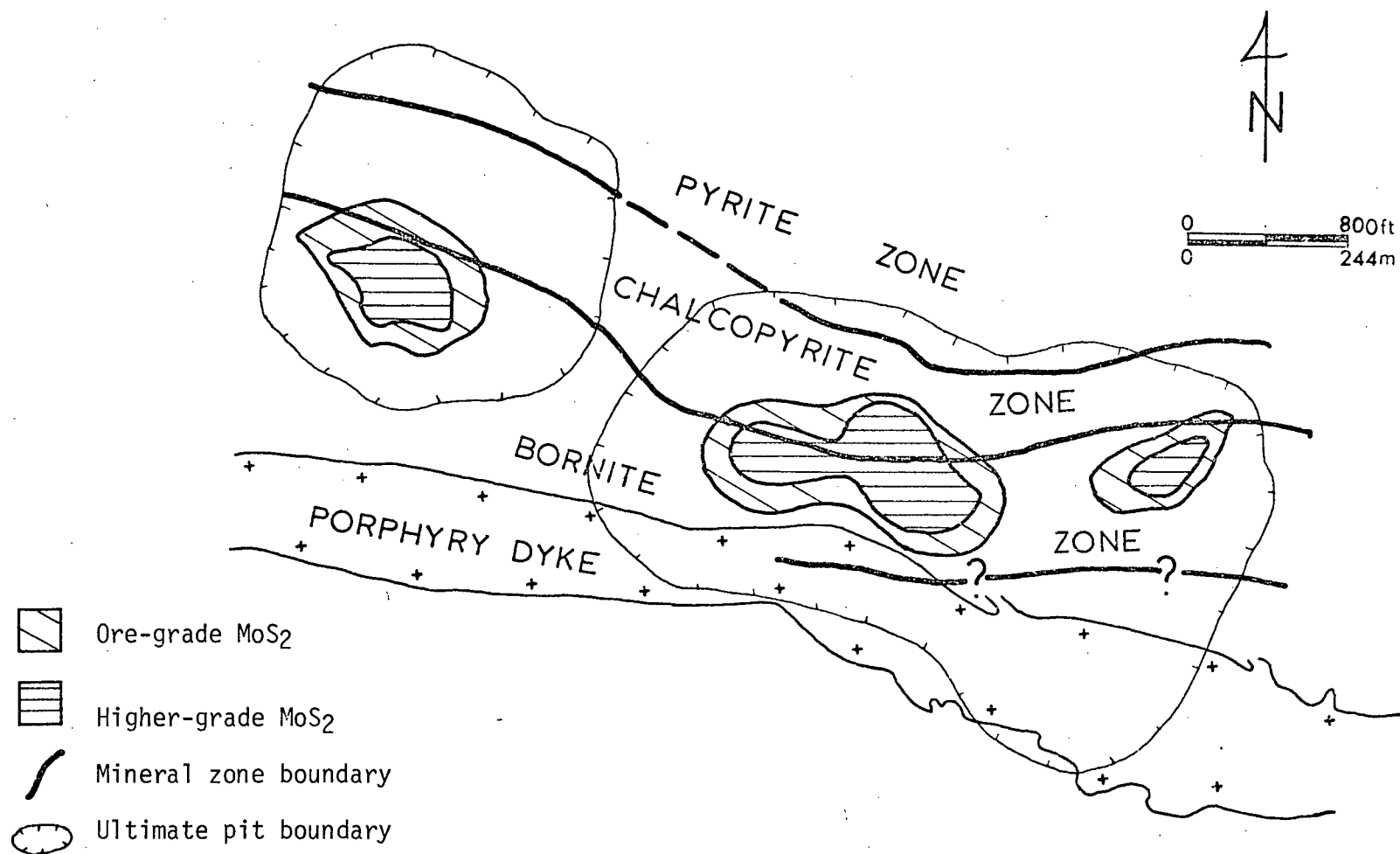


FIGURE 23b: Distribution of MoS_2 in relation to mineral zoning at Highmont
(Data from company files, Highmont Mining Corporation)

is rare at Valley Copper partly because of the more leucocratic composition of the host rock (Bethsaida granodiorite). A similar reasoning applies to the rarity of propylitic alteration within porphyry dykes at Highmont and Lornex. In these leucocratic rocks adequate Mg and Fe were not available for formation of abundant chlorite. Hence, sericite, kaolinite and carbonate are the dominant alteration products. Hydrothermal addition of K^+ and SiO_2 , probably from deep-seated sources led to extensive development of quartz, sericite and K-feldspar.

At Bethlehem-JA, potassic alteration is associated with the felsic porphyry and adjacent Bethlehem Phase. In contrast, propylitic alteration is most intense in the more mafic rocks of the Guichon Phase.

Argillic alteration is best developed in leucocratic Bethsaida rocks immediately east of the Lornex Fault at Lornex mine and within the main porphyry dyke at Highmont. In contrast, rocks of the Skeena phase are commonly associated with propylitic and propy-argillic alteration.

(b) Intensity of Faulting and Fracturing

Wherever intense faulting and fracturing are developed, the general tendency is towards quartz-sericite alteration and

veining. This relationship is reflected in all the deposits. At Valley Copper, zones with intense fracturing and crackle brecciation are flooded with quartz-sericite veins. Gouge zones at Lornex and Highmont are commonly characterized by quartz-sericite alteration. At Bethlehem-JA, argillic alteration is closely associated with zones of intense shearing.

From the foregoing, it is apparent that zones of structural weakness permit an easy infiltration of hydrothermal solutions. Consequently, development of extensive hydrolytic base leaching is associated with formation of sericite, kaolinite and quartz. These also are the most preferred sites for ore deposition.

(c) Composition of Mineralizing Solutions

Chemical and physical properties of ore-forming fluids influence alteration patterns. As mineralizing fluids migrate from centres of mineralization, they cool and react with wall rocks. These processes culminate in changes in pH, Eh, sulfur fugacity, temperature and pressure of the solutions. These changes partly account for the zoning and decreasing intensity of alteration from the centre to periphery of the deposits. At Valley Copper, where there is only one type of host rock, alteration patterns grade inwards from weak to moderate argillic at the outer margins, to intense phyllic and potassic alteration at the core. At Lornex, and Highmont, weak propylitic alteration at the periphery grades inwards into propy-argillic and finally into argillic alteration.

(d) Structural Levels of Ore Formation

Although the porphyry copper deposits of the Highland Valley are generally considered as products of relatively deep-seated hydrothermal processes (Guilbert and Lowell, 1974; Brown, 1969), W.J. McMillan (oral communication) has suggested that the deposits were formed at different structural levels. For example, the Highmont and Jersey deposits which are spatially associated with breccia pipes (Carr, 1966) are considered to have formed at structurally higher levels in the crust than neighbouring deposits. The deposits can be arranged in the following sequence, from those formed at relatively deep to shallow structural levels; Valley Copper, Lornex, Bethlehem-JA, Highmont and Jersey. This sequence corresponds roughly with decreasing intensity of wall-rock alteration, ore size and grade.

Carr (1966) suggested that the breccia zones at the Jersey and Highmont deposits were formed when volatile pressures exceeded lithostatic pressure, culminating in the escape of volatiles. Thus, the relatively weak alteration and ore size of these deposits might partly be attributed to the inability of volatile solutions to react intensely with host rocks. In contrast, ore deposits formed at deeper structural levels show evidence of intensive and extensive reaction of volatile solutions with wall rocks. From the foregoing discussion, it is apparent that variations in wall-rock alteration can be partly attributed to the nature of ore emplacement, which might consequently influence the nature and extent of geochemical

halos associated with these deposits.

SUMMARY AND CONCLUSIONS

(1) Except at Valley Copper where propylitic alteration is rare, mineral deposits of the Highland Valley are characterized by zonal distribution of alteration patterns; propylitic at the periphery, grading inwards into pervasive argillic and/or phyllic alteration. Potassic alteration is generally centrally located, in association with porphyry dykes. Structural features dominantly control the distribution of quartz-sericite alteration.

(2) Except at Jersey deposit (White et al., 1957), biotite is not an important mineral in potassic zones of Highland Valley porphyry copper deposits.

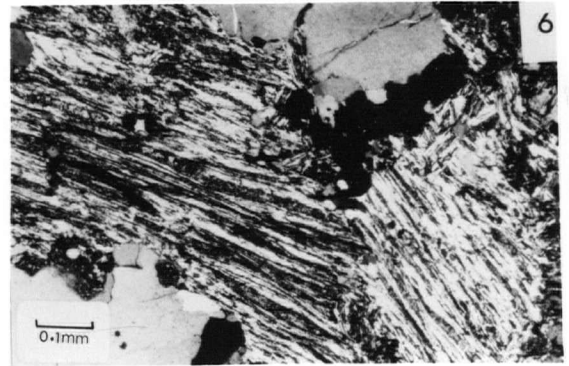
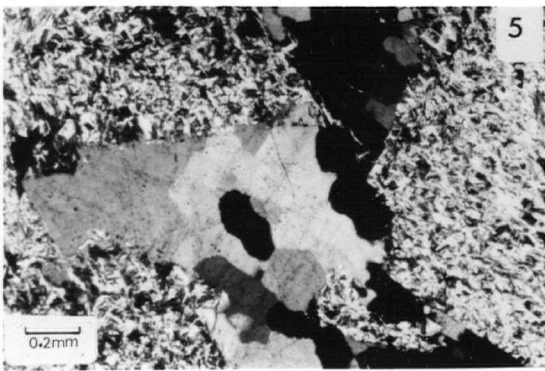
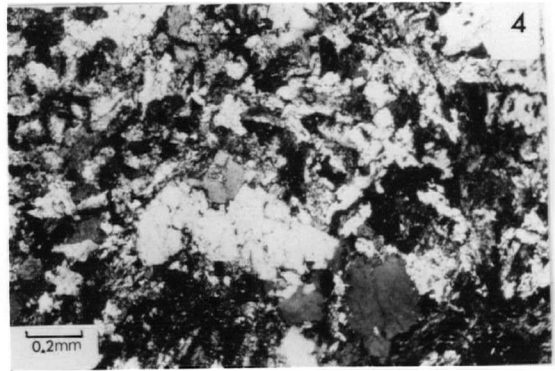
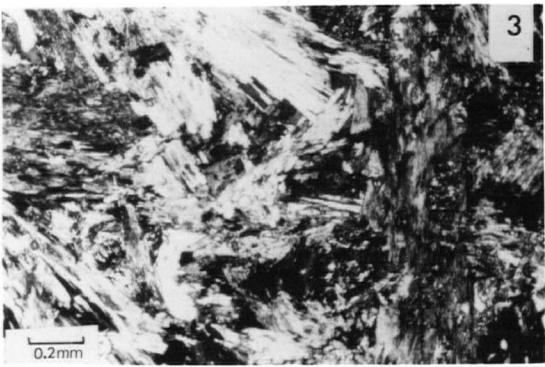
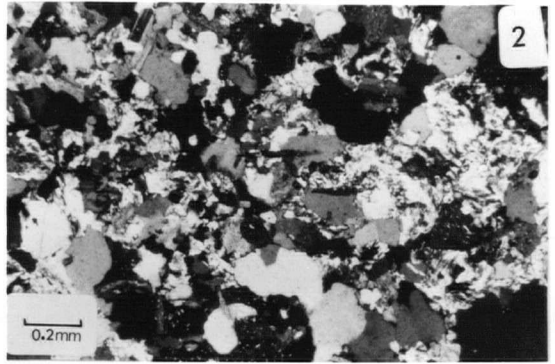
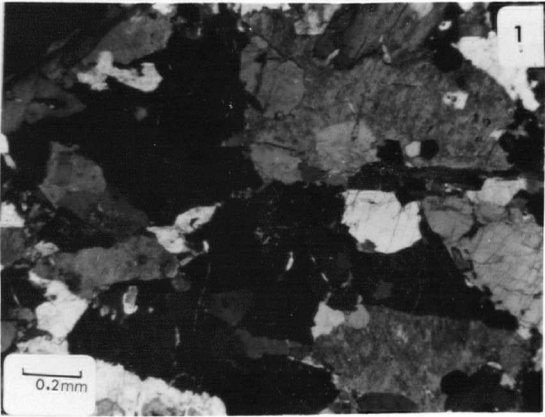
(3) Economic mineralization is most commonly associated with zones of intense argillic (or propy-argillic) and quartz-sericite alteration, whereas potassic and propylitic zones are relatively devoid of mineralization.

(4) Intensity of wall-rock alteration correlates with grade and size of mineralization.

(5) Although the inability to quantify alteration patterns, and the fine-grained mineralogy characteristic of alteration zones are major limitations, large-scale mapping of wall-rock alteration can be useful in delineating zones most suitable for detailed exploration.

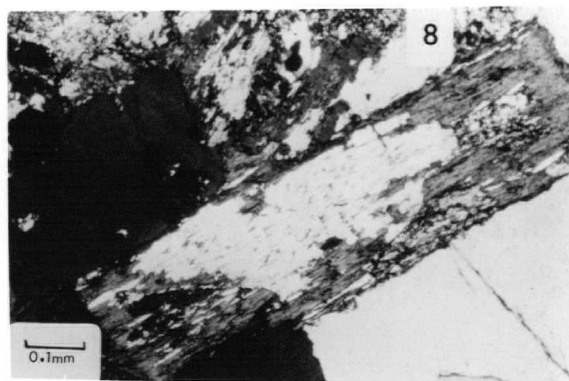
- PLATE 1: Conglomeration of (?) secondary perthitic K-feldspar
in Bethlehem quartz diorite of the potassic zone,
Bethlehem-JA.
- PLATE 2: Sericite alteration of plagioclase and alkali feldspars
in potassic zone of Bethlehem-JA. (s = sericite)
- PLATE 3: Course-grained sheaves of interlocking chlorite in the
propylitic zone of Bethlehem-JA.
- PLATE 4: Medium- to coarse-grained crystals of epidote (vein-filling
material) in the propylitic zone of Bethlehem-JA.
- PLATE 5: Pervasive sericite (+ minor kaolinite) and quartz
remnants in the argillic zone of Valley Copper deposit.
- PLATE 6: Alteration of coarse biotite grains to fibrous sericite
in the argillic zone of Valley Copper deposit.

(All plates crossed nicols)



- PLATE 7: Very coarse-grained sericite (vein material) in the phyllic zone of Valley Copper deposit.
- PLATE 8: Fine-grained epidote partially replacing a biotite grain in propylitized rock of Lornex mine.
- PLATE 9: Fine to medium-grained sericite and kaolinite in the argillic zone of Lornex mine.
- PLATE 10: Quartz and chlorite replacements of a biotite grain in the propylitic zone of Highmont deposit.
- PLATE 11: Weak argillization of plagioclase (with minor carbonate) at Highmont property.
- PLATE 12: Radiating tourmaline crystals (schort) in a breccia matrix at Highmont.

(All plates crossed nicols)



CHAPTER FOUR

SAMPLING AND ANALYTICAL TECHNIQUES

SAMPLE COLLECTION

During May to August 1972 and June 1973, approximately 1800 bedrock samples (excluding duplicates) were collected from the Highland Valley district. Table III summarizes the number and nature of samples.

(a) Outcrop Sampling

Sampling of outcrops was undertaken at Highmont, Lornex, Skeena and Bethlehem properties. Sample locations are presented in the Appendix. Outcrops at Highmont, although not abundant, are uniformly distributed, and samples were collected from most of them. At Lornex, outcrops are plentiful and relatively fresh, west of Lornex Fault, whereas to the east, open-pit development, construction and dumps have obliterated many. Thus, the topmost part of drill cores (suboutcrops) were used to supplement outcrop samples.

All samples comprise 4 to 5kg of half fist-sized rock chips collected over a surface area of about 10m^2 . Weathered surfaces were removed, and fresh chips placed in heavy-duty plastic bags. Most of the outcrop samples were collected beyond zones of visible mineralization and were apparently unaltered. Subsequent thin section examination however, reveals that sericite "dusting" of plagioclase is widespread. This can be attributed to regional deuteric alteration that is ubiquitous in rocks of the batholith (Northcote, 1969). For comparison, limonite-rich samples (oxidized

TABLE III: Summary of sampling and chemical analysis.

Property	Type of Sample	No. of Samples	Analytical techniques*
Highmont	Outcrop		
	Fresh rock	192	AAT, ES, AAM
	Limonite-rich rock	28	AAT, ES
	Drill Core	550	XRFT, AAM, AAT, FAA, ES
	TOTAL	<u>760</u>	
Lornex	Outcrop	90	AAT, ES, AAM
	Drill Core	425	AAT, ES, AAM
	TOTAL	<u>515</u>	
Skeena	Outcrop	20	AAT, ES, AAM
	Drill Core	40	AAT, ES, AAM
	TOTAL	<u>60</u>	
Bethlehem (JA Zone)	Suboutcrop	58	AAT, ES
	2800 Level	54	AAT, AAM, FAA, XRFM, XRFT, ISE
	2400 Level	48	AAT, ES
	(Others)		
(Others)	Outcrop	106	AAT, AAM, ES
	Drill Core	120	AAT, AAM, ES
	TOTAL	<u>386</u>	
Valley Copper	Suboutcrop	61	AAT, ES
	3600 Level	59	AAT, AAM, FAA, XRFM, XRFT, ISE
	3300 Level	41	AAT, ES
	TOTAL	<u>161</u>	

* XRFT - X-ray fluorescence - Rb, Sr, S, Zr

XRFM - X-ray fluorescence - SiO_2 , P_2O_5 , Al_2O_3 , TiO_2

AAT - Atomic absorption - Cu, Zn, Mn, Ag, Ni, Co, Pb, Cd

AAM - Atomic absorption - MgO, CaO, Fe_2O_3 , Na_2O , K_2O

FAA - Flameless atomic absorption - Hg

ES - Emission spectrography - B, V, Sr, Mo, Ti, Ba, Sr, Ga

ISE - Ion-selective electrodes - Cl, F

zone) were collected from several localities along with fresh bedrock at Highmont. In more than 20 localities, duplicate samples were collected for evaluating sampling error (Garrett, 1969).

(b) Drill-Core Sampling

Drill-core chip samples were collected at intervals of 3m (10ft) in sections across Highmont, Valley Copper, Lornex, Skeena and Bethlehem properties. Each sample comprises several 5 cm long chips collected over a distance of 3m around the sampling point. No discrimination was made between fresh and altered samples.

Valley Copper and Bethlehem-JA are buried almost completely beneath glacial and alluvial overburden. A modified sampling pattern, in which samples were collected from several evenly-spaced drill holes at constant elevations or "levels", was employed. In each deposit three levels were sampled; a "Suboutcrop Level" which represents the topmost part of drill holes beneath the oxidation zone, and two other levels, each designated by its elevation above sea level. Duplicate samples were collected in approximately 40% of the drill-holes, using sample locations 3m above the original sampling point. At Valley Copper and Bethlehem-JA, samples were obtained within and as far from the orebody as available drill holes permit. It is believed that the number of drill-holes in background areas is adequate for purposes of this study.

Megascopic features of all samples were recorded in the field, including rock type, mineralogy, alteration, visible mineralization and fracturing. Locations of drill-core samples at the

various mining properties are presented in the Appendix.

SAMPLE PREPARATION

(a) Crushing and Grinding

Chip samples were fed into a Bico "Chipmunk" jaw crusher. Crushed material was then pulverized to less than 2mm in a ceramic rotary grinder. After splitting, approximately 50g were further ground to minus 100 mesh in a high speed ceramic ball mill. To estimate sample homogeneity, replicates of the fine rock powder were obtained by grinding separately three additional splits of every fiftieth pulverized sample. Material remaining from the ceramic grinder was reserved for mineral separation studies. A piece of every rock sample was also preserved for reference.

(b) Mineral Separation

Mineral separation was performed on the minus 35 plus 120 mesh fractions of samples obtained by sieving the pulverized material from the ceramic grinder. Each sample weighed approximately 1kg. Samples were washed by transferring portions into large beakers filled with tap water, and stirred thoroughly with a rubber-tipped heavy glass rod. The material was allowed to settle for a minute and the supernatant liquid decanted. This operation was repeated a dozen times. Samples were then washed with distilled water and dried in an oven at 110°C. Magnetite, iron fillings and other mineral grains with magnetite inclusions were removed with a hand magnet before passing the material through a Frantz isodynamic

separator using a forward slope of 20° and side slope of 15° . In this way it was possible to obtain a preliminary separation of biotite and hornblende from quartz and feldspar.

Additional purification was achieved using heavy liquids - bromoform or tetrabromoethane (S.G.=2.9) and methylene iodide (S.G.=3.3). A conical 500-1000 ml separating funnel was half-filled with bromoform, and small portions of samples were carefully added through a filtration funnel. The liquid was swirled within the separatory funnel from time to time for about an hour in order to obtain complete separation of light and heavy fractions. The heavy fraction was then released and filtered through a No. 1 or 41 Whatman filter paper. Mineral fractions were washed with acetone and dried in air or under a lamp.

Biotite was separated from hornblende using methylene iodide in a smaller 50-100 ml separating funnel. However, hornblende content of most samples was small, and adequate separates were obtained only from two samples. Better than 95% purity was attained by handpicking remaining impurities, such as zircon and apatite, under a binocular microscope.

ANALYTICAL TECHNIQUES

Rock samples were analyzed by emission spectrography, X-ray fluorescence spectrometry, flame and flameless atomic absorption spectrophotometry and ion-selective electrodes. Elements determined by the above procedures are summarized in Table III. Routinely, a blank, a sample of UBC standard rock, and a duplicate

were included in every batch of 24 analyzed samples.

(a) Emission Spectrography

Semi-quantitative procedures for spectrographic analysis are described by Doyle (1972) and Hoffman (1972). A powdered rock sample, mixed 1:1 with graphite containing 100 p.p.m. indium as internal standard, was loaded into a graphite cup electrode, sealed with sugar solution, and excited by a 12 ampere DC arc for 20 seconds. Spectra were recorded on spectrographic plates and element concentrations estimated visually by comparison with master plates of known concentration. Operating conditions are summarized in Table IV, after Doyle (1972). Analytical precision estimated from replicate analysis of UBC standard rock (Stanton, 1966) is presented in Table V.

(b) X-Ray Fluorescence Spectrometry

Major Elements: 0.28g powdered sample was mixed thoroughly with 1.5g flux containing lithium tetraborate, lithium carbonate and lanthanum oxide (Norrish and Hutton, 1969). The mixture was fused for approximately 20 minutes in a graphite crucible at 1150°C and the melt then rapidly poured onto an aluminum-coated plate where it solidified to give a glass bead. The bead was pulverized in a Spex ball mill for 15 minutes, the powder bound with a few drops of polyvinyl alcohol (PVA), and then compressed into a pellet, backed by a mixture of 1:1 boric acid and bakelite. A load of 20,000 lbs was used in pellet compaction. The resulting sample is a pellet approximately 3cm in diameter and 5 mm thick.

TABLE IV: Spectrographic equipment and standard operating conditions.

Spectrograph	Hilga-Watts Automatic Quartz Spectrograph
Source	Electromatic products (ARL), Model P6KS, Type 2R47
Arc/Spark stand	Spex Industries #9010
Microdensitometer	ARL Spectroline Scanner #2200
Anode	Graphite, National L3709SPK
Cathode	Graphite, National L3803AGKS
3-step neutral filter	Spex Industries #1090; 5%, 20% and 100% transmittance
Neutral filter	Spex Industries #9022; 20% transmittance
Emulsion	Spectrum analysis #1
Wavelength range	2775 to 4800 angstroms
Mask	17 mm
Slit width	15 microns
Arc current	12 amperes
Arc gap	6 mm
Exposure time	30 seconds
Plate processing	Developer Kodak D-19 at 23°C
Plate processing	Stopbath Kodak 30 seconds
Plate processing	Fixer Kodak 5 minutes
Plate processing	5 minutes

TABLE V: Spectral lines and *precision at the 95% confidence level of
emission spectrographic analysis
(24 analyses of UBC standard rock)

Element	Spectral Lines (Angstroms)	Mean Value (ppm)	Precision ± %
B	2497.73	n.d	-
Sr	4607.33	711	42
Ti	3372.80	1281	66
V	3185.40	36	34
Mo	3170.35	n.d	-
Ba	4554.04	590	39
Ga	2943.64	18	33
Sn	2839.90	n.d	-

n.d = below detection limit

* After Stanton (1966)

Minor Elements: 3g of minus 100 mesh powder was bound with a few drops of PVA, and then pelletized, using the procedures described earlier.

Analytical determinations were made using a Philips PW 1010 spectrometer. Operating conditions are summarized in Table VI. Calibration curves were obtained from U.S.G.S. standard rocks G-2, GSP-1, AGV-1, BCR-1 and W-1. Recommended values for these standards were obtained from Flanagan (1973). Analytical precision for major elements is better than $\pm 8\%$ at the 95% confidence level. For Rb, Sr and S, precision at the 95% confidence level is $\pm 2\%$, $\pm 1\%$ and $\pm 15\%$ respectively, based on data from 18 paired samples (Garrett, 1969).

(c) Ion-Selective Electrodes

Total Extractable Halogens: The analytical procedure is slightly modified from that of Haynes and Clark (1972). 0.25g sample was mixed with 1g 2:1 sodium carbonate — potassium nitrate in a 40 ml nickel crucible; fused at 900°C for 20 min and then cooled for 10 min. 20 ml of boiling water were added, and the crucible covered and left overnight. Contents of the crucible were stirred to detach the adhering cake, and then washed into a 100 ml volumetric flask. Preliminary experiments indicated that there was no difference between results obtained from filtered and unfiltered solutions. Unfiltered sample solutions were therefore diluted to 100 ml with de-ionized water after addition of 1.5 ml concentrated nitric acid.

TABLE VI: Operating conditions for Philips FW 1010 X-ray spechometer

Element	X-Ray Tube Target	kV	mA	Peak (20)	B-G (20)	F.T. (sec.)	XTAL	CTR	CTRV(KV)	X-RP	PHLV	PHW	Atten.	Collim.
SiO ₂	Cr	50	30	78.11	-	20	EDDT	F.P.	4.64	Vac.	200	450	2	Coarse
Al ₂ O ₃	Cr	50	30	112.7	-	10	EDDT	F.P.	4.64	Vac.	180	300	2	Coarse
P ₂ O ₅	Cr	50	30	58.8	-	20	EDDT	F.P.	4.55	Vac.	250	300	2	Coarse
K ₂ O	Cr	50	30	20.36	-	10	EDDT	F.P.	4.55	Vac.	200	450	2	Fine
MgO	Cr	50	30	14.50	-	100	RAP	F.P.	4.85	Vac.	250	400	2	Coarse
CaO	Cr	40	20	113.3	-	10	LIF	F.P.	4.35	Vac.	150	500	2	Fine
TiO ₂	Cr	40	20	86.14	-	10	LIF	F.P.	4.25	Vac.	180	300	2	Fine
Fe ₂ O ₃	Cr	40	20	57.49	-	10	LIF	F.P.	4.25	Vac.	300	350	2	Fine
Rb	Mo	50	30	26.58	25.90	40	LIF	Scint.	2.675	Air	270	400	5	Fine
Sr	Mo	50	30	25.09		40	LIF	Scint.	2.675	Air	270	400	5	Fine
S	Cr	44	30	45.20	44.20	40	EDDT	F.P.	4.60	Vac.	100	200	3	Coarse
Zr	W	50	30	22.51	-	10	LIF	Scint.	2.675	Air	250	600	5	Coarse

Explanation of Abbreviations.

B-G - Background position
 F.T. - Fixed Counting Time
 XTAL - Analyzing Crystal
 EDDT - Ethylene-Diamine-d-Tartrate
 LIF - Lithium Fluoride
 RAP - Rubidium Acid Phthalate
 CTR - Counter (X-ray detector)

F.P. - Flow Proportional Counter
 Scint. - Scintillation Counter
 CTRV - Counter Voltage
 X-RP - X-ray Path
 Vac. - Vacuum
 PHLV - Pulse Height Level Voltage
 PHW - Pulse Height Window
 Atten. - Attenuation
 Collim - Collimator

TABLE VII: Equipment and stock reagents in ion-selective electrode analysis

Equipment

Orion 407 meter or equivalent
Orion 94-17 chloride electrode or equivalent
Orion 94-02 double junction reference electrode
Orion 94-09 fluoride electrode
Orion sleeve-type reference electrode (for F)
Orion 90-00-01, 90-00-02, 90-00-03 reference electrode filling solutions
40 ml capacity nickel crucibles and lids
Magnetic stirrer and teflon stirring rods

Stock Reagents

Fluoride buffer solution: dissolve 59g sodium citrate dehydrate and 20g potassium nitrate in water and dilute to 1 liter.

Fluoride standard (1000Hg/ml): dissolve 1.105g sodium fluoride in water and dilute to 500 ml.

Chloride standard (10,000 Hg/ml): dissolve 16.48 g sodium chloride in water and dilute to 500 ml.

Flux: thoroughly mix 2:1 sodium carbonate:potassium nitrate

In determination of fluorine, 10 ml sodium citrate were added to an equal volume of sample solution in a 50 ml plastic beaker. The solution was stirred for 5 min with a small magnetic stirrer at medium speed, fluoride and reference electrodes inserted, and a millivolt (mV) reading (expanded scale) was taken with an Orion 407 meter. The millivolt reading was compared to similar readings from a series of standards containing appropriate concentrations of fluorine (0.1, 0.5 and 1.0 p.p.m.) in a similar sodium citrate matrix (Haynes and Clark, 1972).

For determination of chlorine, chloride and reference electrodes were inserted in the same sample solution, and readings obtained using the "known addition" method (Orion Research, 1970). Operating conditions, equipment, and reagents are summarized in Table VII. Results obtained by these procedures for U.S.G.S. standard rocks GSP-1 and AGV-1 are compared with recommended values (Flanagan, 1973) in Table VIII.

Water-Extractable Halogens: The analytical procedure is described in detail by Van Loon et al. (1973). 1g sample was weighed into a 50 ml plastic beaker, and 5 ml de-ionized water added. The solution was stirred for 2-3 min, the electrodes inserted and a millivolt reading taken after allowing a response time-interval of an additional 20 sec. Millivolt readings were compared to similar readings from a series of standards.

(d) Atomic Absorption Spectrophotometry

Techtron AA-4 and Perkin Elmer 303 spectrophotometers were

TABLE VIII: Comparison of fluorine and chlorine contents of U.S.G.S. standard rocks.

Sample No.	This Study		Recommended Values*	
	F (p.p.m.)	Cl (p.p.m.)	F (p.p.m.)	Cl (p.p.m.)
GSP-1	3000	384	3200	300
	2860	384		
	3260	312		
	2900	320		
AGV-1	660	272	435	110
	580	269		
	600	258		

* After Flanagan (1973)

utilized in major and trace element determinations, except for Hg which was determined by a flameless procedure on a Jarrell-Ash 82-270. Operating conditions for the three instruments are summarized in Tables IX, X and XI.

HF - HClO₄ - HNO₃ Digestion: Total decomposition was accomplished in two ways: a rapid "teflon tube" and a routine "teflon dish" procedure. In the former, working solutions were prepared by decomposing 0.1g of minus 100 mesh powder in 1 ml hydrofluoric acid and 1 ml nitric-perchloric acid mixture using teflon test tubes. Acid digestions were evaporated to dryness at 200°C on a sandbath and residues redissolved in 1 ml hydrochloric acid. Sample solutions were made up to 10 ml with 1.5M HCl and analyzed for Cu and Zn. 1 ml was diluted to 10 ml with distilled water and analyzed for Ca, K, Na and Fe. To suppress molecular and ionization interferences, lanthanum and cesium solutions were added to both sample solutions and standards. Analytical precision at the 95% confidence level is summarized in Table XII.

In the routine "teflon dish" procedure, 0.5g samples were taken to dryness with 10 ml hydrofluoric acid and 5 ml 3:2 nitric-perchloric acid mixture in teflon dishes. Residues were leached with 5 ml 6M hydrochloric acid and made up to volume in a 25 ml volumetric flask. As shown in Table XII, analytical precision is better than that obtained with the rapid procedure. Accuracy of the total digestion is evaluated by duplicate analysis of U.S.G.S. standard rocks (Table XIII).

TABLE IX: Operating conditions for techtron AA-4 spectrophotometer

Element	Current (mA)	Wavelength (Å)	Slit width (Å)
Cu	3	3247.5	1.7
Zn	6	2138.6	3.3
Fe	5	3719.9	0.8
Mn	10	2794.8	3.3
Mg	4	2852.1	1.7
Na	5	5890.0	3.3
Ca	10	4226.7	0.8
K	10	5889.9	6.6

Flame height 2.3 (arbitrary units)

Acetylene flow gauge 2.5 (arbitrary units)

Air pressure 20 p.s.i.

TABLE X: Operating conditions for the Perkin Elmer 303 spectrophotometer

	Cu	Pb	Zn	Ni	Co	Fe	Mn	Cd	Ag		Ca	Na
Slit	4	4	5	3	3	3	4	4	4	4	4	3
Scale	1	2	1	1	1	1	1	1	10	1	1	1
Damping	2	2	2	2	2	2	2	2	1	1	1	1
Current (mA)	14	14	14	20	20	20	15	15	5	20	20	20
Wavelength (Å)	3248	2175	2146	2324	2407	3719	2800	2283	3280	3853	2125	2956
Range	UV	UV	UV	UV	UV	UV	UV	UV	UV	VIS	VIS	VIS
H ₂ Lamp	-	+	-	+	+	-	-	+	+	-	-	-
Filter	-	-	-	-	-	-	-	-	-	+	-	-

- Not required

+ Required

Flame height 2.3 (arbitrary units)

Main air pressure 30 p.s.i.

Auxiliary air pressure 4 p.s.i.

Acetylene pressure 4 flow units

Meter response 2

TABLE XI: Operating conditions for the Jarrell-Ash 82-270 spectrophotometer.

Hg Determination

Lamp current	5 mA
Gain	3
Mode	Absorbance
Scale expansion	300
Damping	2
Wavelength (Å)	2550.0
Cell dimensions	
length	21 cm
diameter	3 cm
Slit	75 μ
Chart speed	2 inches/minute
Mainostat Pump speed	5

TABLE XII: *Analytical precision of HF/HClO₄/HNO₃ digestion at the 95% confidence level estimated from paired samples.

Element	Teflon tube procedure Precision (\pm %)	Teflon dish procedure Precision (\pm %)
	70 samples	10 samples
Cu	20	8
Zn	15	4
Fe	21	10
Ca	18	2
Na ₂ O	9	2
K ₂ O	19	3
MgO	-	1

(-) Data not available

* After Garrett (1969)

TABLE XIII: Comparison of trace and major element contents of U.S.G.S.
standard rocks.

	Recommended Values			This Study (mean of 2 values)		
	G-2	GSP-1	AGV-1	G-2	GSP-1	AGV-1
Metal content (p.p.m.)						
Cu	12	33	60	13	37	63
Zn	85	98	84	82	96	85
Mn	260	331	763	182	209	560
Ni	5	13	19	9*	5*	11*
Co	6	6	14	7*	8*	17*
Metal content (wt. %)						
CaO	1.94	2.02	4.90	1.98	2.18	4.86
MgO	0.76	0.96	1.53	0.77	0.99	1.53
Fe as Fe ₂ O ₃	2.65	4.33	6.76	2.65	4.30	6.20
Na ₂ O	4.07	2.80	4.26	4.07	2.95	4.25
K ₂ O	4.51	5.53	2.89	4.14	4.99	2.89

*Values obtained with background correction (H₂ lamp) on Perkin Elmer 303 instrument.

**Flanagan (1973)

HNO₃ - HClO₄ Digestion: 0.5g samples were digested with 10 ml 4:1 nitric:perchloric acid mixture in 100 ml beakers. Samples were refluxed for an hour at low heat and then evaporated to dryness. Residues were taken up in 5 ml 6M hydrochloric acid and diluted to 20 ml with distilled water in calibrated test tubes. Prior to instrumental analysis, sample solutions were allowed to settle overnight and the clear supernatant solution decanted. Analytical precision at the 95% confidence level for Cu, Zn and Mn is $\pm 25\%$, $\pm 16\%$ and $\pm 31\%$ respectively.

Pre-analytical treatment for Hg Determination: The analytical procedure is slightly modified from that of Jonasson et al. (1973). 0.5g sample was weighed into a test tube and 10 ml concentrated nitric acid added. The sample was allowed to stand for 10 min, and 30 ml deionized water added. The solution was then heated in a water bath at 90°C for 2 hr, with occasional swirling. After cooling to room temperature, 10 ml of 5% w/v stannous chloride in concentrated hydrochloric acid were added and the solution aerated. Evolved Hg was determined by comparison with similarly treated standards. Analytical precision at the 95% confidence level in 12 replicates of UBC standard rock, with a mean value of 38 p.p.b., is $\pm 42\%$.

(1) Sulphide Selective Decompositions

Aqua Regia: 0.1g samples were digested to dryness with 5 ml aqua regia (3:1 hydrochloric:nitric acids) in 100 ml beakers at 130°C $\pm 10^\circ\text{C}$. Residues were leached with 2 ml distilled water and 2 ml hydrochloric acid, transferred to a 10 ml volumetric flask and made

up to the mark with distilled water.

H₂O₂ - Ascorbic Acid: This procedure is described in detail by Lynch (1971). 0.2g samples were weighed into test tubes calibrated at 10 ml. 7 ml H₂O₂- ascorbic acid mixture were added and samples allowed to stand approximately 18 hr (overnight) with occasional mixing. Sample solutions were diluted to 10 ml with de-ionized water, mixed and centrifuged for 5 min to obtain clear supernatant solutions. Working solutions were analyzed using standards made up in H₂O₂ - ascorbic acid.

KClO₃ - HCl: 0.2g of minus 100 mesh samples were weighed into test tubes (22 x 175mm) and an approximately equal weight of potassium chlorate added, followed by 2 ml concentrated hydrochloric acid. After standing for 30 min the solution was diluted to 10 ml with distilled water, mixed and then centrifuged to obtain a clear supernatant solution.

Standard solutions, initially prepared in potassium chlorate-hydrochloric acid were found to deteriorate within three days, hence, standards were subsequently prepared in 1.5M HCl, after experiments indicated that matrix effects between standards do not significantly affect absorption (Table XIV). Analytical precision for this procedure is estimated as $\pm 7\%$ at the 95% confidence level, on the basis of six replicate analysis of UBC standard rock containing 17 p.p.m. leachable Cu.

This efficacious technique has not been used previously in bedrock geochemistry. Hence, a detailed description of experi-

TABLE XIV: Effect of composition of standards on atomic absorption.

ug/ml Cu	Percent Absorption		
	1.5 MHCl	KClO ₃ -MHCl	H ₂ O ₂ -Asc.
0.5	4.14	4.52	5.27
1.0	8.20	8.64	10.36
2.0	15.40	16.40	19.02
4.0	28.40	29.80	34.64

mental results are presented in the following section.

*POTASSIUM CHLORATE - HYDROCHLORIC ACID: A SULPHIDE

SELECTIVE LEACH FOR BEDROCK GEOCHEMISTRY

(a) Introduction

Geochemical contrast between mineralized and unmineralized bedrock can often be enhanced by use of sulphide selective leaches. Digestion with aqua regia (Stanton, 1966) or hydrogen peroxide - ascorbic acid (Lynch, 1971) has been used for this purpose, but a potassium chlorate-hydrochloric acid leach described by Dolezal et al. (1968), has not been evaluated in this context. As part of this research programme, an analytical procedure utilizing potassium chlorate and concentrated hydrochloric acid was developed under the supervision of Dr. K. Fletcher. Data obtained by using this method is compared to data obtained with other partial extraction techniques - nitric-perchloric, aqua regia, and hydrogen peroxide-ascorbic acid.

(b) Analytical Procedure (as described earlier)

(c) Experimental Work and Results

A series of twenty-six granodiorite samples containing copper contents ranging from 5 to 10,000 ppm and zinc ranging from 18 to 50 ppm were analyzed for Cu, Zn, Mn using two cold leaches;

* Extract from a paper of same title: Olade and Fletcher (1974), Journal of Geochemical Exploration, v. 3, (in press).

two hot acid extractions, and "total" digestion with HF-HNO₃-HClO₄.

Results presented in Figures 24A to 24D show consistent differences in relative release of copper and zinc with all leaches except HNO₃-HClO₄. This is particularly striking with KClO₃-HCl which liberates up to 100% Cu_t¹, compared to a maximum of 28% Zn_t. On the average the ratio of Cu_x:Zn_x increases in the order KClO₃-HCl > H₂O₂-Asc. > aqua regia > HNO₃ - HClO₄. Results obtained with HNO₃-HClO₄ are, however, erratic.

Another obvious relationship is the well-defined trend for Cu_x to increase with Cu_t, to 95-100% when Cu_t is greater than 700 p.p.m. The same trend is apparent in data obtained with H₂O₂ - Asc. and aqua regia. However, the minimum value of Cu_x increases from about 20% of Cu_t with KClO₃-HCl to a corresponding value of 70% with aqua regia. As would be expected this trend is accompanied by a decrease in the value for which Cu_x becomes approximately equal to Cu_t (i.e. Cu_x equals 95-100% Cu_t). With the H₂O₂-Asc. leach, Cu_x:Cu_t declines in samples containing more than 1000 ppm Cu_t to a minimum of about 30%.

To further evaluate the efficiency of the KClO₃-HCl procedure, G.S.C. ultramafic standards UM1, UM2 and UM4 were analyzed. Table XV compares this data with results reported by Cameron (1972)

¹The following abbreviations are used throughout: Me_t - total metal content; Me_x - metal leached with KClO₃-HCl; H₂O₂ - Asc.; aqua regia or HNO₃ - HClO₄.

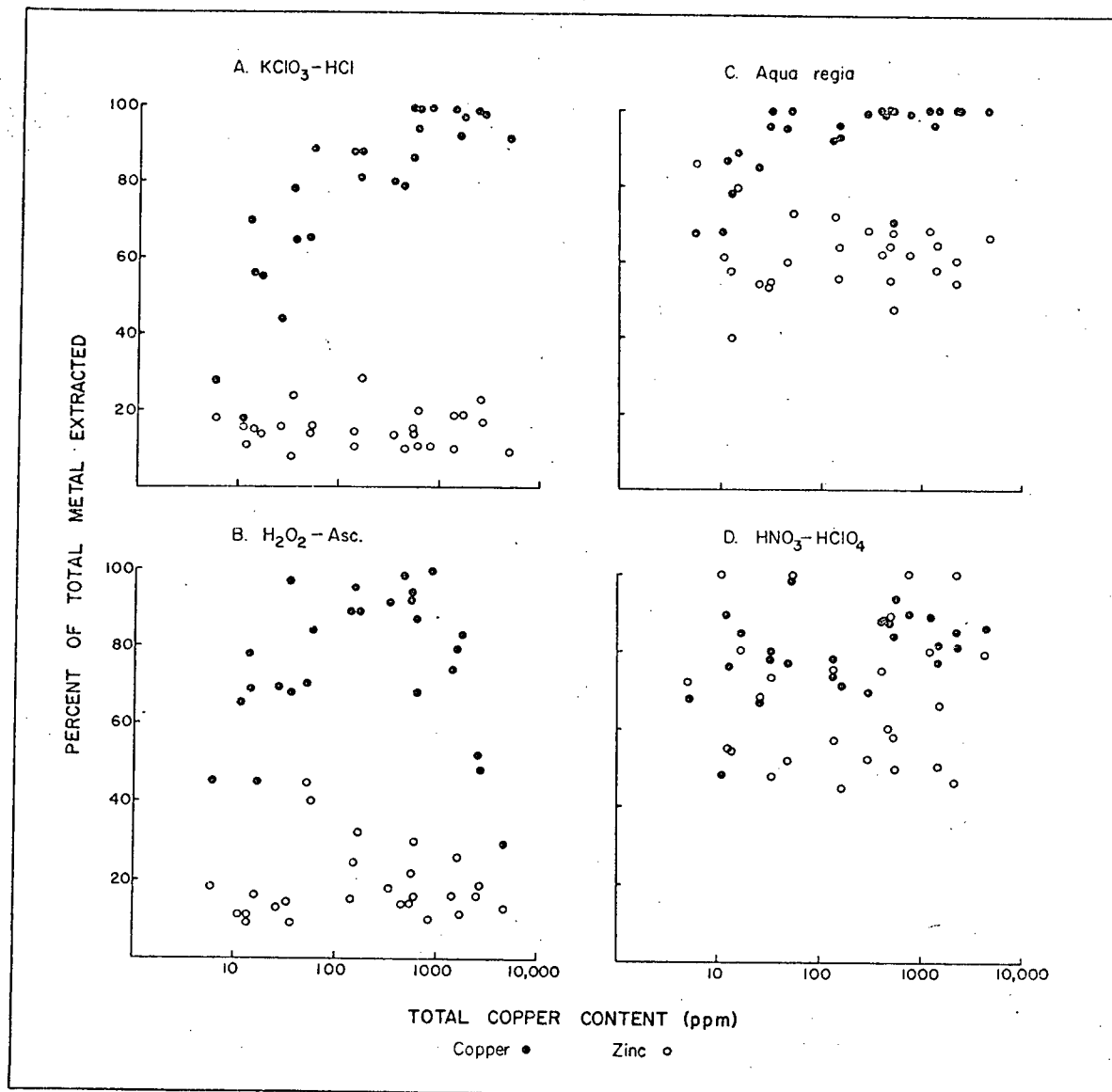


FIGURE 24: Comparison of % of total metal extracted by partial extraction techniques.

TABLE XV: Comparison of leaches on ultramafic standards UM1,
UM2 and UM4.

Method	Metal content (ppm)		
	UM1	UM2	UM4
I*	3896	951	594
Cu II	4147	946	538
III	.41%	.095%	.058%
I	8013	2590	1945
Ni II	8337	2901	1915
III	0.96%	0.39%	0.25%
I	236	120	76
Co II	288	120	66
III	362	178	108
Zn I	35	14	18
III	97	32	63

*I KClO_3 -HCl leach, mean of two determinations

II H_2O_2 -Asc., data from Cameron (1972)

III Total metal, data from Cameron (1972)

for H_2O_2 - Asc. extractable metal. Values are generally within 10% of those reported. However, for UM2 and UM4 results are consistently high.

In view of the promising results obtained on the granodiorite and ultramafic samples, additional experiments were undertaken to evaluate the influence of several experimental parameters on extraction with KClO_3 -HCl.

Neither the extraction period (Fig. 25) nor the amount of KClO_3 used (Table XVI) has an appreciable effect on liberation of copper. Furthermore, for copper the reaction with both mineralized and unmineralized samples appears to be complete within 5 minutes. In contrast, for zinc there is a gradual release with reaction time. Experiments with pure silica sand indicate that the observed trend is not attributable to contamination from the tungsten carbide ball mill during grinding.

Influence of grain size was evaluated by grinding two -80 + 100 mesh samples for 30 min in a tungsten carbide ball mill. Copper and zinc were then leached from portions of both the original and ground material (Table XVII). Results show no significant effect for Cu_x whereas there is a marked increase in Zn_x after grinding.

(d) Discussion

According to Dolezal et al. (1968) addition of potassium chlorate to hydrochloric acid facilitates dissolution of many sulphides - arsenopyrite, chalcopyrite, cinnabar, molybdenite and pyrite are specifically mentioned by their reaction in statu

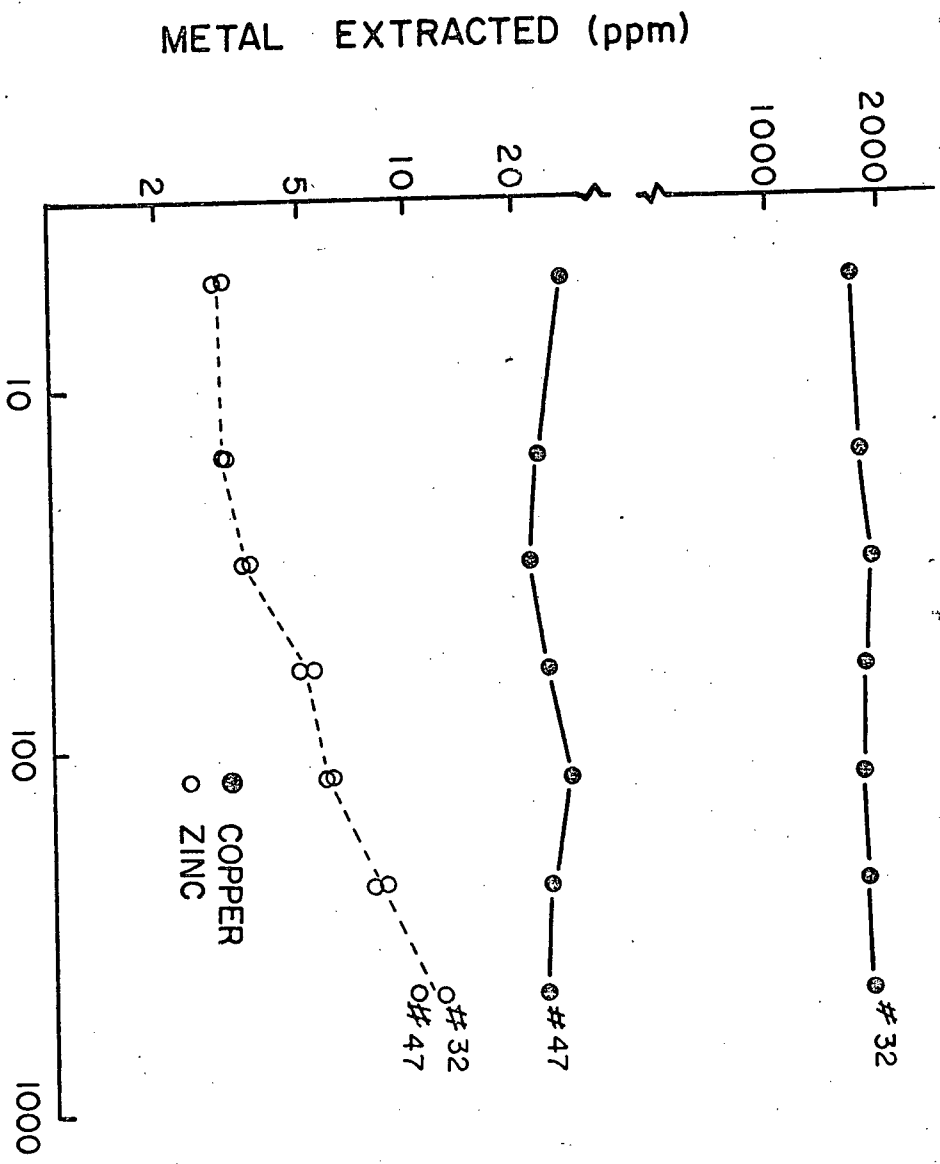


FIGURE 25: Relationship between the amount of metal extracted and time of grinding.

TABLE XVI: Effect of amount of KClO_3 added on release of copper with KClO_3 -HCl leach.

g KClO_3 added ³	Copper released (ppm)*	
	#47	#32
HCl only	7.2	734
.1g	25.4	2038
.2g	25.0	2022
.5g	26.0	1802

* #47 Total copper content 29.3 ppm

#32 Total copper content 2059 ppm

TABLE XVII: Effect of grinding on release of copper and zinc
with KClO_3 -HCl leach.

Treatment	Metal released (ppm)	
	Copper	Zinc
Unground (-80 + 100 mesh)	25.6	7.2
Ground*	24.5	16.8
Total	29.3	30.5
Unground (-80 + 100 mesh)	2012	5.8
Ground	1936	14.2
Total	2059	33.2

* Ground for 30 minutes in a tungsten carbide ball mill

nascendi. In contrast, most silicates are only weakly attacked by cold hydrochloric acid. Consequently, $\text{KClO}_3\text{-HCl}$ should be sulphide selective and discriminate against metal held in silicate lattice of fresh igneous rock. Experimental studies on magnetite separates suggest that $\text{KClO}_3\text{-HCl}$ does not remove appreciable zinc from magnetite.

It is extremely difficult to assess the efficiency of a sulphide selective leach since there is no simple, independent method of estimating silicate versus sulphide metal. In this study, criteria based on the geochemical behaviour of copper and zinc are used to compare selectivity of the leaches. Copper, a strongly chalcophile element is generally believed to be present largely as sulphide inclusions even in unmineralized bedrock (Putman, 1972; Graybeal, 1973). Putman (1973) for example, calculates an upper limit of 5 ppm for 'silicate' copper in biotites of granitic rocks. In contrast, zinc, which is less strongly chalcophile, probably occurs predominantly within silicate lattices of unmineralized samples. On this basis it seems reasonable to suppose that:

- (i) an efficient copper sulphide selective attack will give a high $\text{Cu}_x : \text{Zn}_x$ ratio in samples unmineralized with respect to zinc.
- (ii) $\text{Cu}_x : \text{Cu}_t$ will increase with Cu_t as copper sulphide content increases, until in strongly mineralized samples Cu_x equals Cu_t within the limits of analytical error.

Evaluated against these criteria the $\text{KClO}_3\text{-HCl}$, $\text{H}_2\text{O}_2\text{-Asc.}$, and aqua regia leaches, all appear to be selective (Figs. 24A to 24C). However, the $\text{Cu}_x:\text{Zn}_x$ ratio is greatest with $\text{KClO}_3\text{-HCl}$ and at a minimum with aqua regia. Also $\text{Cu}_x:\text{Cu}_t$ for samples with low copper content is lowest with $\text{KClO}_3\text{-HCl}$ and at a maximum with aqua regia. On this basis $\text{KClO}_3\text{-HCl}$ is least damaging to silicates and most selective leach for sulphide copper.

(e) Applications to Geochemical Exploration

From a practical standpoint, $\text{KClO}_3\text{-HCl}$ appears to have several advantages over other sulphide selective leaches (i) for porphyry copper mineralization, the method appears to be more sulphide selective than either $\text{H}_2\text{O}_2\text{-Asc.}$ or aqua regia; (ii) hot concentrated acids are not involved; and (iii) the procedure is extremely rapid and simple, and hence suited to routine application. Furthermore, the $\text{KClO}_3\text{-HCl}$ procedure could also be utilized in the field. Determinations can be made by either colorimetry (Stanton, 1966) or by copper ion electrode. Results obtained by colorimetry in 26 granodiorite samples compare favourably with atomic absorption results (Table XVIII).

However, further studies on the action of $\text{KClO}_3\text{-HCl}$ on a wider range of sulphides (spalerite, molybdenite etc.) and host rocks (volcanics, ultramafics, etc.) are required before its general use can be recommended.

(f) Conclusions

A $\text{KClO}_3\text{-HCl}$ leach is shown to be sulphide-selective and

TABLE XVIII: Comparison of analytical results obtained from KClO_3 -
HCl digests using atomic absorption and colorimetry
(Stanton, 1966)

Sample No.	Cu (ppm) in KClO_3 -HCl Leaches	
	Atomic Absorption	Colorimetric
2	50	50
7	2772	3000
10	2	* < 50
19	470	600
22	351	500
28	647	700
29	2754	2400
30	8	* < 50
31	4281	5000
34	12	* 50
35	1545	1100
36	23	* < 50
50	1775	1500
61	883	1050
114	150	100
115	572	600
118	263	400
119	1598	1250
173	26	* < 50
176	33	* < 50
178	125	< 50
746	2	* < 50
757	151	100
776	544	450
Duplicate #2	49	50

*Lowest detection limit is 50 ppm

to have advantages over other procedures in estimating sulphide copper content of granodiorites. On three ultramafic standards, cobalt, copper and nickel values are within 10% of results obtained using an ascorbic acid-hydrogen peroxide leach.

CHAPTER FIVE

REGIONAL GEOCHEMISTRY

INTRODUCTION

Identification of lithogeochemical halos in igneous environments is dependent on a broad understanding of the chemistry and evolution of magmas, and the nature of primary processes which give rise to genetically related metal concentrations.

Brabec (1970) and Brabec and White (1971) have investigated distribution of major and trace elements in fresh rocks and minerals from the Guichon Creek batholith. Their findings suggest that metallization processes which gave rise to porphyry copper deposits are closely related to petrochemical evolution of the pluton. To further the understanding of relationships between major and trace elements and to provide adequate background geochemical data, 60 fresh rock samples (Fig. 26) collected and described by Northcote (1968) and Brabec (1970), and supplemented by samples from the author's collections were analyzed for selected major elements. In addition, results of 20 major element analyses compiled by Brabec (1970) are included in the plots of chemical variation diagrams.

RESULTS

(a) Major Elements

Results of major element analyses are presented together with normative composition in Table XIX, and as functions of the Larsen Differentiation Index ($LDI = 1/3SiO_2 + K_2O - CaO + MgO +$

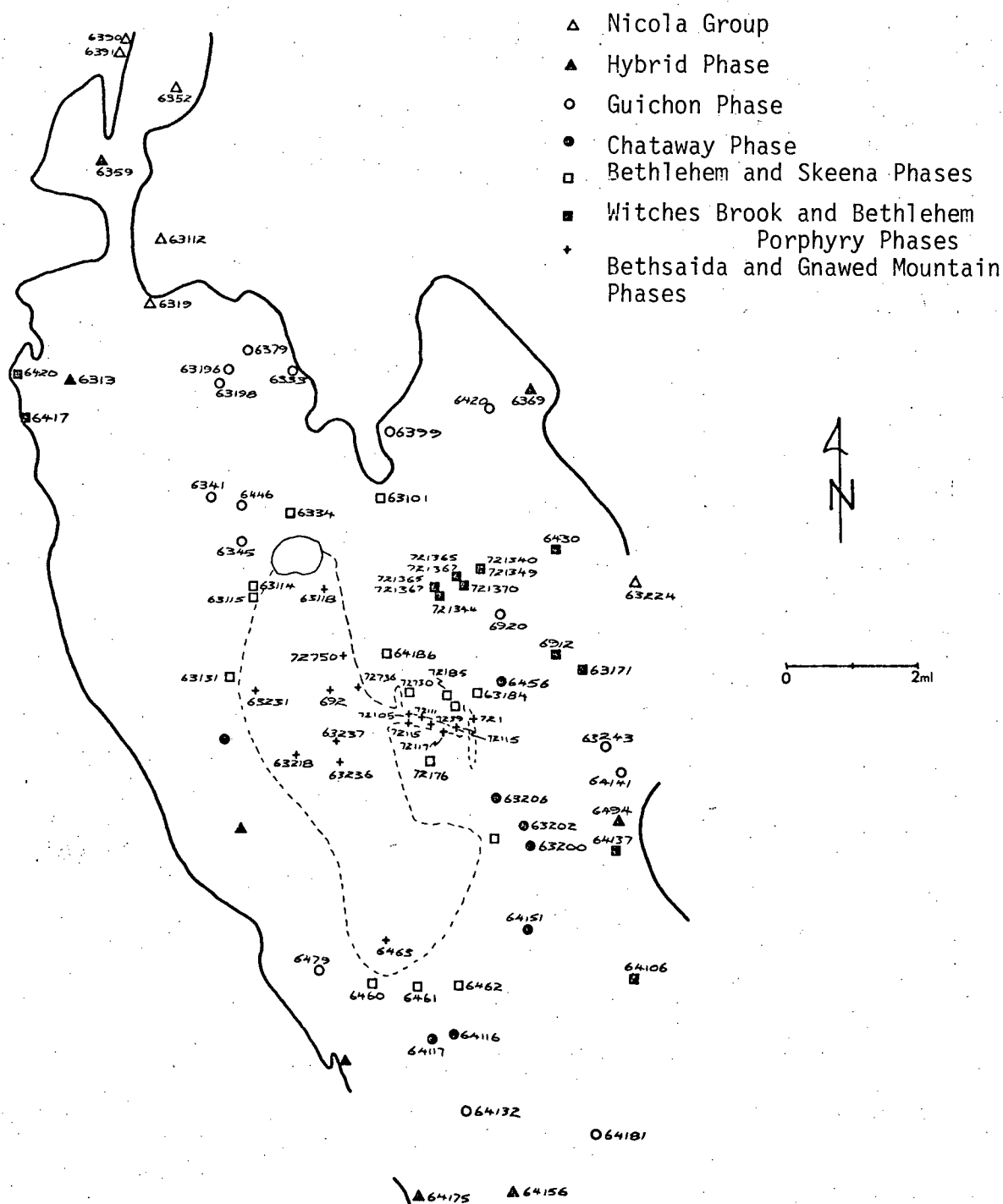


FIGURE 26: Location of samples used in regional study, Guichon Creek batholith (After Brabec, 1970; Northcote, 1968)

TABLE XIX: ¹Means, ranges and mean normative composition
of intrusive units, Guichon Creek batholith (Values in wt. %)

								ESTHERSHEM PORPHYRY		BETHSAIDA		Porphyritic Porphyry	
	NICOLA VOLCANICS	HYBRID	GUICHON	CHATAWAY	BATHLESHEM	SEBENA	WITCHES BROOK	Petocratic	Leucocratic				
	(5)	(6)	(6)	(10)	(9)	(6)	(8)	(4)	(5)	(7)	(3)	(4)	
SiO ₂	56.12 50.40 - 68.32	60.02 59.25-61.24	62.24 59.60-64.20	64.37 61.46-67.48	66.04 65.32-66.80	66.21 67.36-69.50	69.23 69.03-77.86	66.00 63.24-68.34	74.32 69.51-77.86	69.79 66.61-70.63	70.67 68.27-72.55	73.14 72.61-74.32	
Al ₂ O ₃	16.08 14.50-18.41	16.91 15.03-17.60	17.00 16.24-17.74	16.37 15.12-17.52	16.87 15.11-17.60	15.51 14.46-16.16	15.54 11.95-16.50	15.85 14.57-16.32	13.72 11.0-16.16	15.92 14.61-17.02	14.22 12.76-15.39	14.41 13.26-15.01	
*Fe ₂ O ₃	0.47 3.51 - 11.20	0.41 5.59-7.00	5.04 4.49-6.63	4.04 3.25-5.80	3.35 3.11-3.72	2.00 2.80-3.47	3.03 1.26-3.85	4.18 3.41-4.65	1.39 0.45- 1.3	1.91 1.34-2.30	2.49 1.42-3.01	1.17 0.95-1.55	
CaO	6.73 3.36-10.84	5.78 4.95-6.60	5.15 4.37-6.10	4.26 3.84-5.27	4.05 3.07-5.21	3.04 3.73-3.91	3.37 0.35-4.02	3.55 3.20-4.57	2.01 0.35-4.52	2.83 2.15-2.92	3.51 2.67-4.12	2.12 1.78-2.54	
MgO	4.89 1.17-9.59	3.16 2.20-3.82	2.31 1.04-3.28	1.89 1.30-2.30	1.31 1.10-1.63	1.02 0.80-1.53	1.36 0.60-1.78	1.48 0.92-1.83	0.41 0.12-0.87	0.54 0.40-0.82	0.85 0.57-1.03	0.34 0.23-0.46	
Na ₂ O	3.39 2.20-4.22	3.61 3.40-4.21	4.06 3.83-4.58	4.29 3.86-4.98	4.52 3.89-4.89	4.78 4.38-5.15	3.87 3.37-4.15	4.73 4.72-4.92	4.17 3.37-4.72	4.83 4.33-5.31	4.78 4.76-4.85	4.74 4.52-4.85	
K ₂ O	0.82 0.20-1.32	1.71 0.97-2.30	1.99 0.99-2.64	1.02 1.52-2.89	1.83 1.32-2.60	1.73 1.30-1.95	2.19 1.63-3.29	2.56 1.77-3.41	3.15 0.21-3.68	1.96 1.60-2.29	1.81 1.74-1.87	2.08 1.07-2.24	
TiO ₂	0.60 0.53-1.34	0.74 0.64-0.80	0.65 0.54-0.72	0.49 0.40-0.62	0.37 0.30-0.41	0.35 0.22-0.41	0.39 0.28-0.46	0.42 0.34-0.49	0.29 0.18-0.43	0.27 0.22-0.39	0.29 0.24-0.31	0.20 0.18-0.22	
P ₂ O ₅	0.15 0.14-0.17	0.16 0.14-0.22	0.17 0.14-0.22	0.16 0.14-0.22	0.14 0.13-0.14	0.14 0.13-0.15	0.11 0.09-0.15	0.14 0.14-0.15	0.12 0.09-0.15	0.13 0.09-0.14	0.12 0.12-0.13	0.12 0.11-0.13	
MnO	0.15 0.07-0.19	0.11 0.09-0.14	0.08 0.06-0.10	0.07 0.06-0.07	0.07 0.06-0.07	0.05 0.04-0.05	0.05 0.02-0.06	0.02 0.02-0.03	0.02 0.01-0.03	0.06 0.04-0.07	0.15 0.03-0.05	0.04 0.03-0.06	
³ C.I.P.W. Norms													
Quartz	12.45	15.38	16.63	21.65	22.69	24.94	29.37	19.34	33.49	28.88	28.60	33.41	
Orthoclase	5.00	10.30	11.96	11.67	11.00	10.36	13.08	15.33	18.71	10.69	10.80	12.51	
Albite	29.57	31.32	34.94	36.64	38.39	40.96	33.09	40.56	35.45	41.74	40.84	40.81	
Anorthite	27.04	25.35	22.66	20.67	19.50	16.78	15.17	14.64	9.24	13.48	12.11	9.91	
² Pyroxene	18.04	12.22	9.31	4.84	3.79	2.61	4.36	6.23	1.03	1.73	5.00	1.03	
Magnetite	5.99	3.83	2.83	3.05	2.67	2.36	2.02	2.79	0.92	1.41	1.82	0.86	
Ilmenite	1.57	1.43	1.26	0.96	0.27	0.67	0.75	0.61	0.55	0.52	0.56	0.39	
Apatite	0.37	0.39	0.41	0.39	0.34	0.34	0.34	0.34	0.29	0.32	0.29	0.29	
Corundum	-	-	-	-	-	-	1.02	-	0.08	1.25	-	0.80	
Rutile	0.01	0.01	0.01	0.01	-	-	-	0.01	-	-	-	-	
Hematite	-	-	-	0.14	-	-	-	-	-	-	-	-	

*Total Fe as Fe₂O₃ *FeO calculated by using FeO/Fe₂O₃ ratios in 24 samples
(Brabec, 1970).

¹Arithmetic means

²Total normative ortho- and clino-pyroxenes.

³Calculated by computer program (CORN) provided by A.L. Sinclair.

Fe as FeO) in Fig. 27. As shown in Table XIX, abundances of most major elements vary in accordance with relative ages of the rock units as deduced from contact relationships by Northcote (1969). Thus the intrusive units generally become more felsic from the relatively oldest to the youngest. Rocks of the Witches Brook and Chataway Phases show the greatest variations in element values.

Chemical variation diagrams (Fig. 27) show that SiO_2 and Na_2O concentrations increase with LDI, whereas MgO , CaO total Fe as Fe_2O_3 , TiO_2 , Al_2O_3 and P_2O_5 show a concomitant decrease. K_2O shows no appreciable change with LDI, except for dyke rocks of the Witches Brook and Bethlehem Porphyry Phases which exhibit considerable enrichment. Furthermore, excluding the aforementioned K-rich rocks, concentrations of K_2O in the remainder of the batholith range from 0.21 - 2.89% with a mean value of 1.8%. These values are low compared to the average value of 3.04% quoted by Turekian and Wedepohl (1961) for high-Ca granites. A lack of enrichment in K_2O values in the relatively younger units of the batholith is reflected in the near constant average modal proportions of K-feldspar, and decreasing values of modal biotite with decreasing age and increasing differentiation (Northcote, 1969).

On an AFM diagram (Fig. 28), enrichment in total alkalis relative to MgO and CaO is evident. This trend is similar to those found in typical calc-alkaline volcanic-plutonic complexes (Nockolds and Allen, 1953). However, on the CaO - Na_2O - K_2O variation diagram (Fig. 29), two trends are present. The first, manifested by dyke rocks of the Witches Brook and Bethlehem Porphyry Phases,

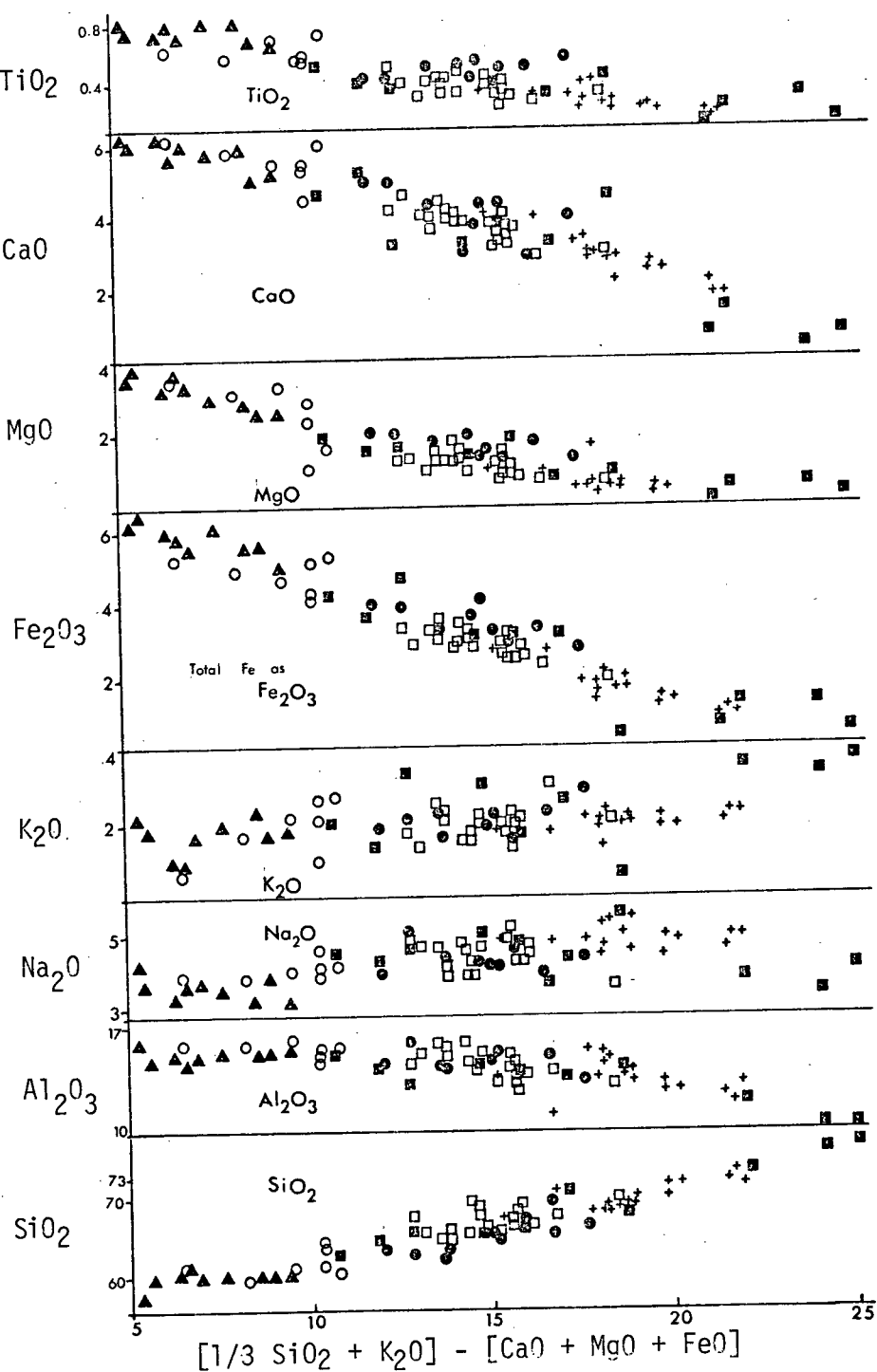


FIGURE 27: Variation diagrams in Guichon Creek rocks showing major element concentrations (wt.%) versus Larsen differentiation index (For legend, see Fig. 28)

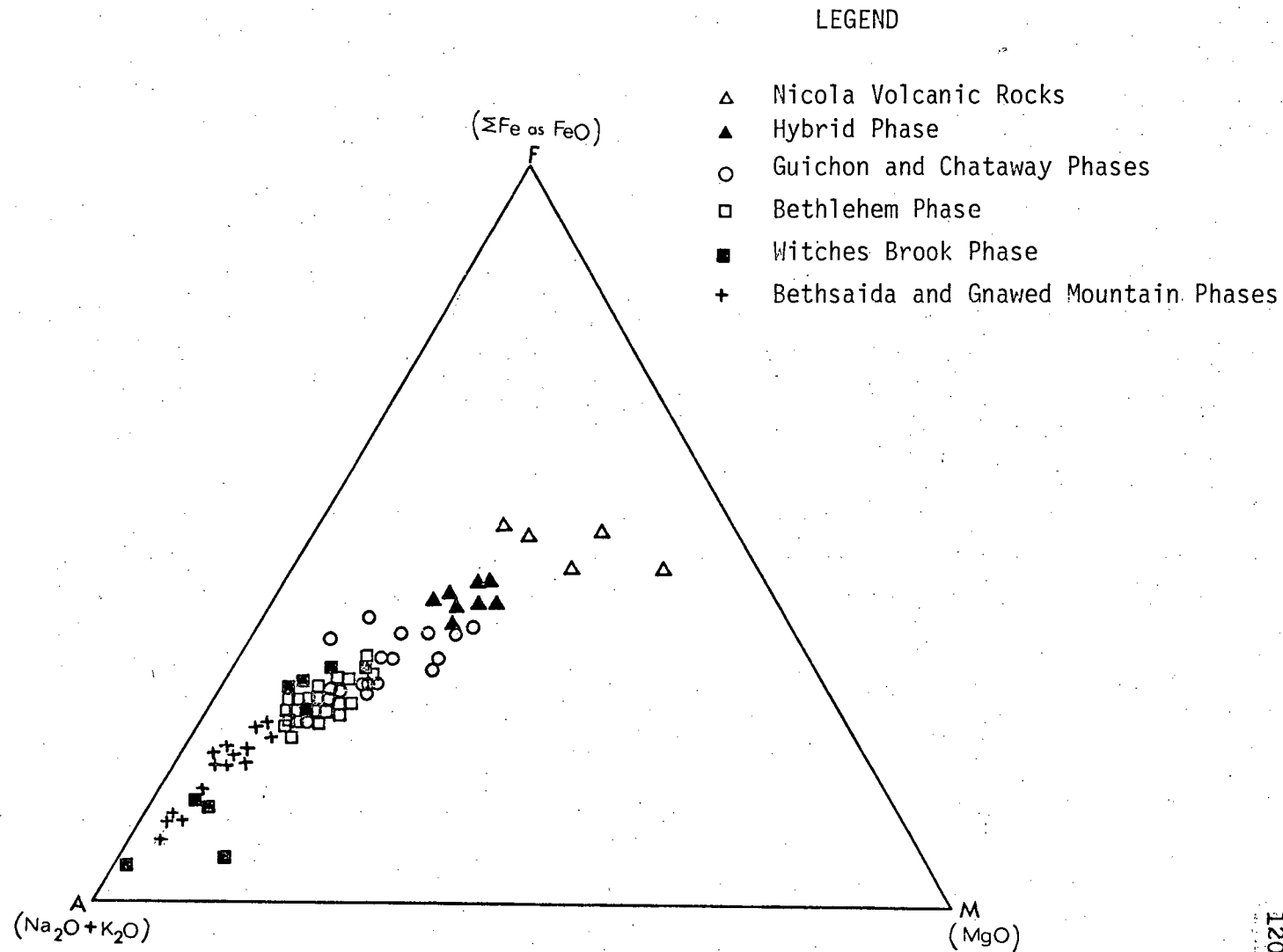


FIGURE 28: AFM variation diagram for rocks of Guichon Creek batholith.

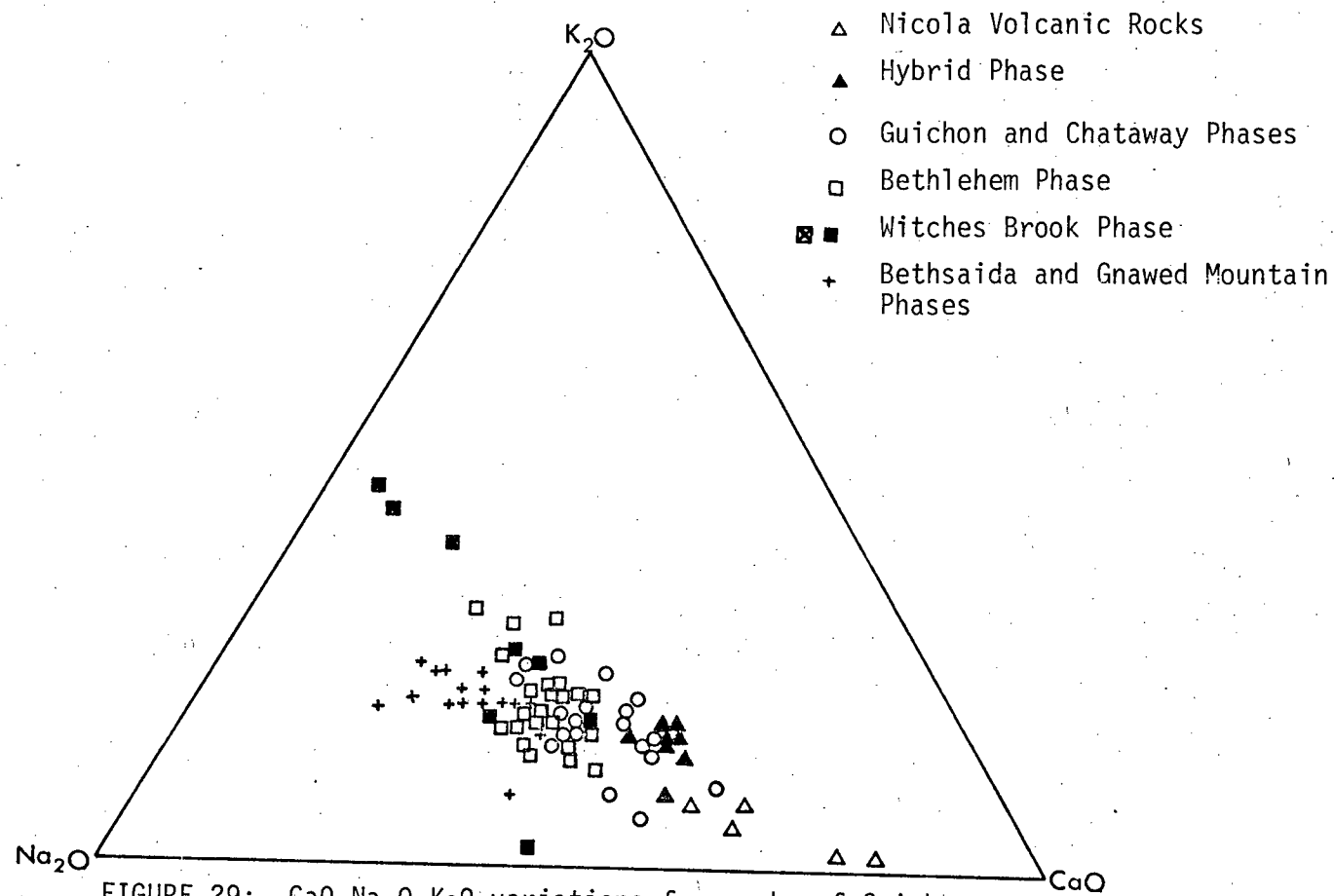


FIGURE 29: CaO-Na₂O-K₂O variations for rocks of Guichon Creek batholith

shows enrichment in K_2O relative to CaO and Na_2O (normal calc-alkaline trend), whereas the other trend is toward Na_2O enrichment. According to Larsen and Poldervaart (1961) and Taubeneck (1967), the latter trend is commonly characteristic of petrochemical differentiation in rocks of trondhjemitic affinity.

In both the AFM and $CaO-Na_2O-K_2O$ variation diagrams, 5 analyses of Nicola volcanic rocks plot along the same "liquid line of descent" (Nockolds and Allen, 1953) as rocks of the Guichon Creek batholith (Figs. 28 and 29).

(b) Trace Elements

(1) Introduction

Abundance data for selected trace elements are summarized in Table XX. These results provide data on background values for elements of specific interest, and also corroborate major element trends. Trace elements of especial interest are; (1) Cu, S and Mo ore metals; (2) potential pathfinders, Hg, (Hawkes and Webb, 1962; Friedrich, 1971), B (Boyle, 1971), Rb (Armbrust et al., 1971) Sr, Ba (Warren et al., 1974), Cl, F (Kesler et al., 1973) and Ag; and (3) elements related to primary lithologies, Zn, Ni, Co, V and Mn.

Brabec (1970) studied background trace-element content of rocks within the batholith, and his data will be referred to wherever appropriate. However, it should be noted that the majority of Brabec's (op. cit.) data were obtained by sulphide-selective aqua regia digestion rather than total extraction employed in this study.

Mo, Ag and Pb are generally below detection limit whereas

TABLE XX: *Means and Ranges of Trace Elements in rocks of Guichon Creek
Batholith.

	NICOLA VOLCANICS	HYBRID	GUICHON	CHATAWAY	BETHLEHEM	SKEENA	WITCHES BROOK	BETHLEHEM PORPHYRY	BETHSAIDA	GNAWED MOUNTAIN	ALL GUICHON SAMPLES
	(4)	(5)	(4)	(7)	(6)	(5)	(7)	(7)	(6)	(7)	(54)
¹ Cu	24 4 - 52	51 12-1143	67 30-95	45 16-240	33 11-195	26 9-45	47 10-88	43 22-127	19 4-135	8 3-15	39
**Cu	15	57	65	43	32	-	42	-	10	-	43
¹ Zn	92 39-141	74 68-81	60 47-76	45 37-72	39 33-46	33 22-35	30 17-41	19 10-31	29 15-37	28 2-33	40
**Zn	36	31	27	25	19	-	17	-	22	-	27
¹ Ni	40 4 - 134	33 15-44	27 16-38	20 9-32	12 6-24	8 6-10	10 6 - 14	7 4 - 9	5 5 - 6	5 3 - 6	14
¹ Co	14 5 - 25	13 11 - 35	12 11-13	11 8-15	8 6 - 9	8 6 - 10	6 5 - 9	5 2 - 7	5 3 - 7	5 4 - 7	8
² Mo	2	2	2	2	2	2	2	2	2	2	2
¹ Pb	5	5	5	5	5	5	5	5	5	5	5
¹ Ag	0.1	0.1	0.1	0.1	0.1	0.1	0.1	0.1	0.1	0.1	0.1
² B	14 10 - 15	5	15 5 - 20	5	5	5	5	5	5	8 5 - 10	5
² Ba	200 100-400	500 400-600	300 200-500	500 300-600	560 500-800	550 500-600	600 500-600	-	520 500-700	-	504
² V	150 20-200	83 50-100	50 40-60	39 20-50	34 30-40	26 20-40	40 30-50	25 10-40	15 10-20	15 10-20	45

¹HF-HClO₄-HNO₃ total digestion

²Emission spectrography

* Geometric mean

** Aqua regia extractable metal
(Brabec, 1970)

Ba and B do not show significant variations and results of Hg are extremely erratic (Table XXII). Consequently, results for these elements are not discussed further.

(ii) Distribution of Copper

With the exception of rocks from the Witches Brook and Bethlehem Porphyry Phases, mean Cu contents generally decrease from the relatively older units at the outer margins to relatively younger at the core (Table XX). Brabec and White (1970) reported a similar distribution for aqua-regia-extractable Cu in 300 samples from the batholith (Table XX and Fig. 30b). A plot of Cu values versus LDI shows a considerable scatter, although a trend towards decreasing Cu as LDI increases is evident (Fig. 30a).

Geochemical behaviour of Cu in silicate melts during magmatic differentiation is not well understood (Al-Hashimi and Brownlow, 1970). Wager and Mitchell (1951) in their classical study of Skaergaard intrusion, found that during the early and main phases of magmatic differentiation, Cu contents of the constituent minerals and whole rock increased, whereas after 90% solidification (Wager and Brown, 1967), most minerals were suddenly depleted in Cu. Simultaneously, whole-rock S showed a sharp increase, although whole-rock Cu did not change appreciably. The redistribution of Cu and increase in S were attributed to a separation of an immiscible sulphide phase which occurred near the end of the fractionation process. Similar, though less extensive studies on other intrusives tend to confirm the pattern observed for the Skaergaard

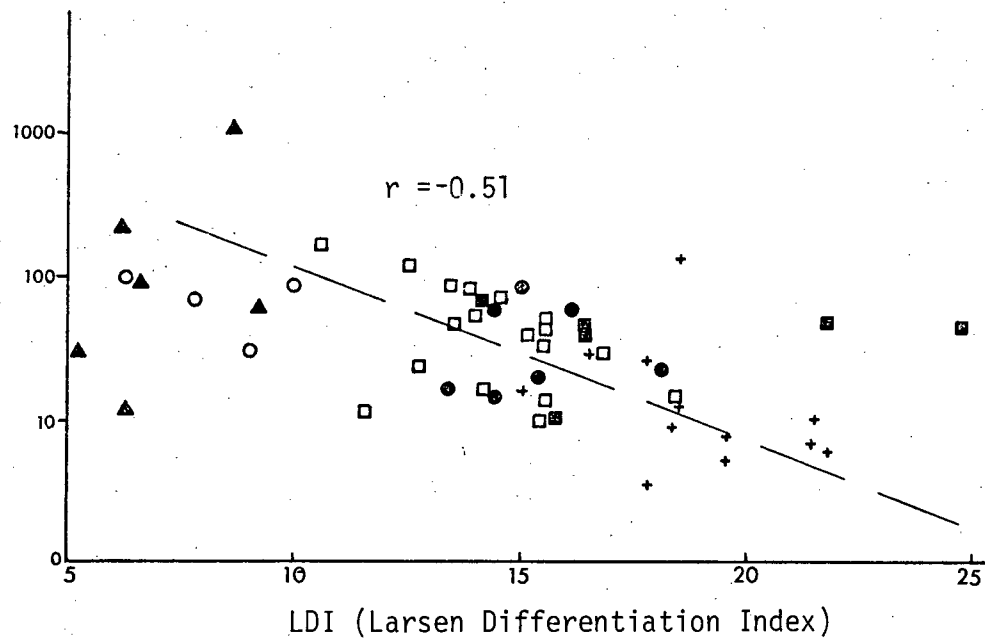
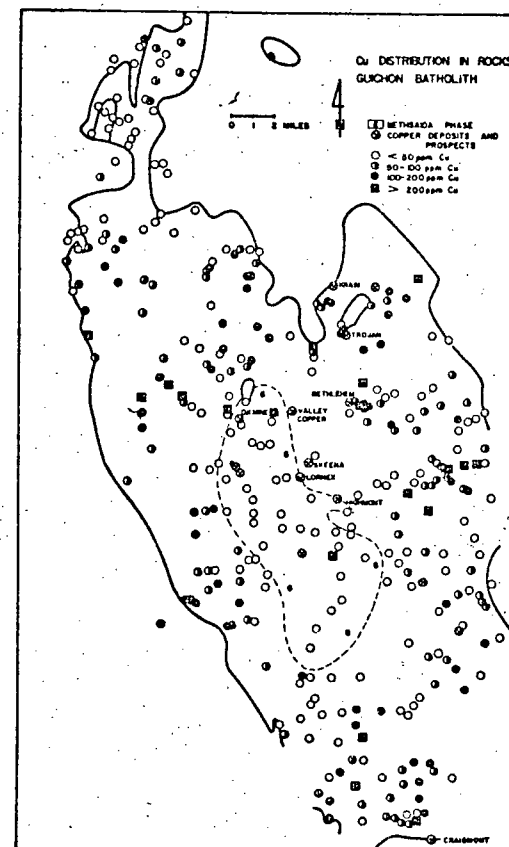


FIGURE 30a: Distribution of Copper in relation to Larsen differentiation index (Legend as for Fig. 29)

FIGURE 30b: Regional distribution of aqua regia extractable Copper in rocks of Guichon Creek batholith (After Brabec and White, 1971)



30b.

rocks (Cornwall and Rose, 1967; McDougall and Lovering, 1963).

In the Guichon Creek batholith, the tendency for Cu to decrease generally with increasing fractionation parallels the behaviour of Fe and Mg (Fig. 34). A plot of Cu versus Fe shows a significant but relatively weak correlation ($r = 0.41$) (Fig. 31). This suggests that Cu^{++} (0.72A) may to some extent substitute for Fe^{++} (0.74A) in silicates and oxides. However, from theoretical considerations, Ringwood (1955) has concluded that due to differences in electronegativities, Cu^{++} would form weaker bonds than Fe^{++} , resulting in a concentration of Cu in residual melts. Curtis (1964) pointed out that crystal-field effects could result in the exclusion of Cu from crystal structures in preference for Fe. Cu is strongly chalcophile, and generally combines with S to form sulphide grains. These commonly occur as inclusions in silicates or may even concentrate as ore deposits. Results of sulphide-selective, partial extraction techniques further support the dominant sulphide mode of occurrence of Cu (Olade and Fletcher, 1974). On this basis Zlobin et al. (1967) have concluded that the positive correlations between Cu and Fe reflects only similarity in geochemical behaviour rather than ionic substitution.

(iii) Distribution of S, Rb, Sr, Cl and F

S content of 38 unmineralized samples is presented in Table XXI. Average S content in the various intrusive units are not appreciably different, although the porphyritic rocks of the youngest Gnawed Mountain Phase are relatively enriched in S. Mean

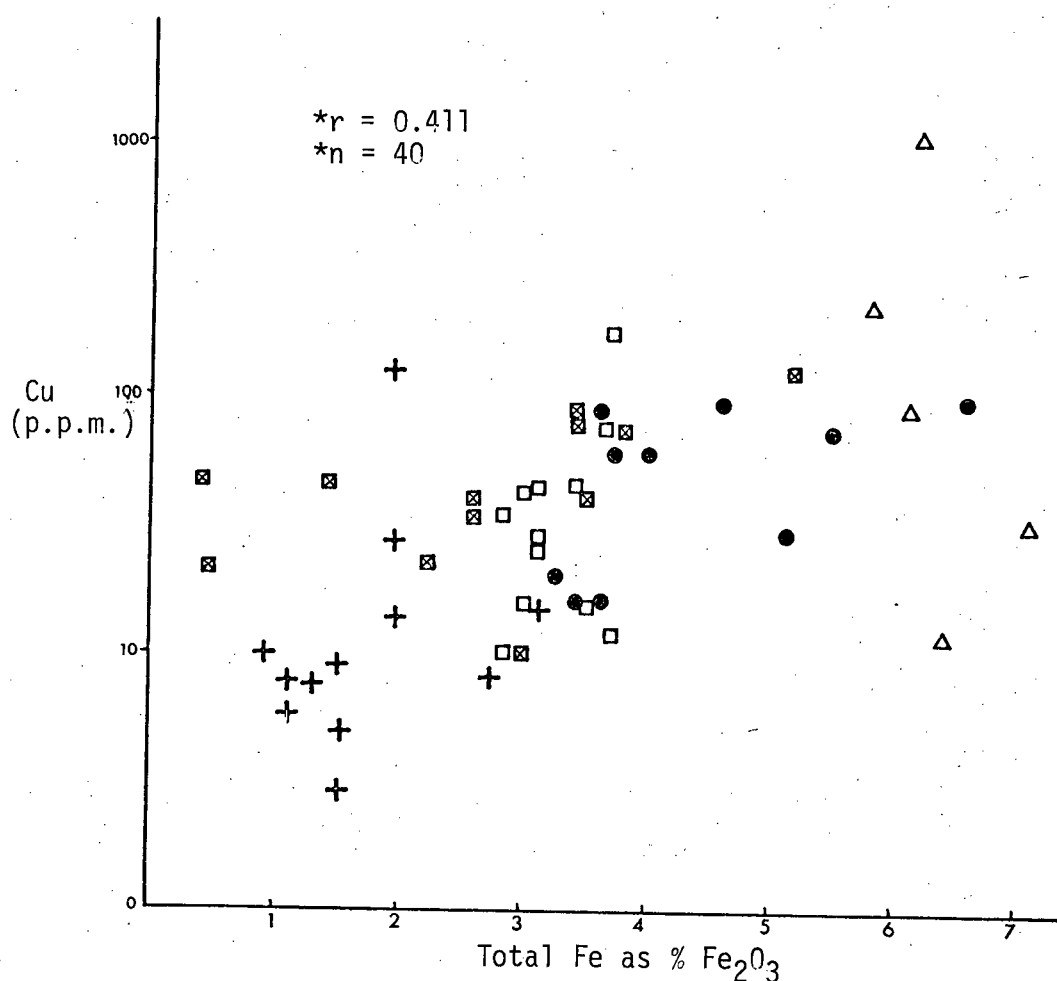


FIGURE 31: Relationship between Copper and Iron in rocks of Guichon Creek batholith. (Legend as for Fig. 29)

*(excluding Witches Brook and Bethlehem Porphyry Phases)

TABLE XXI: ¹Abundances of sulphur, rubidium and strontium in rocks of
Guichon Creek Batholith.

*Sample Number	Rock Unit	Sulphur (in ppm)	Rubidium (in ppm)	Strontium (in ppm)
0-6319	NICOLA	346	35	264
0-63221		382	37	282
0-63224		530	36	201
1-6352	HYBRID	310	82	255
1-6470		354	18	566
1-6494		475	51	582
21-63140	CHATAWAY	444	5	784
21-63206		282	37	727
21-64117		340	70	681
21-64151		609	52	734
21-6456		293	74	692
22-6479	GUICHON	363	52	746
22-64132		340	24	597
22-6920		621	42	750
22-6333		341	48	710
22-6341		d.n.a.	76	719
22-64141		395	4	1000
22-64201		298	51	756
22-63243		373	67	696
22-64181		553	71	609
4-64186	BETHLEHEM	380	80	603
4-6467		440	82	581
4-6461		500	18	857
4-63101		459	42	892
41-63184	SKEENA	300	52	625
41-63214		413	26	680
41-72185		291	36	655
5-64105	WITCHES	312	132	420
5-6430	BROOK	333	103	562
51-721453	BETHLEHEM	555	82	249
51-721365	PORPHYRY	247	86	368
51-721367		524	85	331
51-721370		d.n.a.	46	733
51-721358		376	4	865
6-6463	BETHSAIDA	272	35	528
6-72750		371	35	599
8-72111	GNAWED	751	35	591
8-72115	MOUNTAIN	377	36	635
8-721		475	32	612
8-7215		273	38	567

*Sample Number (After Northcote, 1960; and Brabec, 1970)

d.n.a. - Data Not Available

¹X-ray fluorescence analysis

TABLE XXII: ** Abundances of mercury in rocks of Guichon Creek
batholith

* Sample Number	Rock Unit	Mercury (in p.p.b.)
0-6319	Nicola	100
0-6319		4
1-6925		4
1-63186		4
1-63167		4
21-6346	Chataway	4
21-63140		110
21-64151		120
21-63202		35
22-6333	Guichon	55
22-6341		112
22-64132		4
22-64201		85
4-64132	Bethlehem	5
4-6462		155
41-72185	Skeena	5
41-63184		71
5-6430	Witches Brook	4
5-6912		4
5-64120		4
51-721340	Bethlehem	5
51-721353	Porphyry	20
51-721358		5
51-721370		6
6-63237	Bethsaida	80
6-6463		65
6-63128		270
8-721	Gnawed Mountain	10
8-72111		10
8-72115		10
8-72105		5

* Sample numbers (after Northcote 1968; and Brabec, 1970)

** Flameless atomic absorption analyses

value for all Guichon rocks is 390 ppm which is similar to the value of 300 ppm cited as the world average for S in intermediate igneous rocks (Turekian and Wedepohl, 1961).

Rb concentrations in 39 samples range from 4 to 132 ppm (Table XXI) and average 38 ppm. Compared with the average value of 110 p.p.m. for intermediate igneous rocks, the Guichon Creek batholith is impoverished in Rb. However, values are comparable to those obtained for the Sierra Nevada batholith (Kistler *et al.*, 1971) and the Coast Mountain intrusions (Culbert, 1972). When rock units within the batholith are compared, surprisingly there is no consistent difference in mean values although the K-rich rocks of the Witches Brook Phase are relatively enriched in Rb. Geochemical behaviour of Rb is influenced by the abundance of K (Nockolds and Allen, 1953; Goldschmidt, 1954) for which Rb substitutes in alkali feldspars and micas (Heier and Adams, 1964). A plot of K_2O versus Rb shows a strong positive correlation ($r = 0.77$; Fig. 32a). Thus, absence of appreciable variations in Rb levels is closely related to a similar behaviour by K (Fig. 27). However, a preliminary plot of K_2O against K/Rb ratios show a negative slope ($r = -0.41$) which suggests enrichment of Rb relative to K_2O in rocks with high K_2O values (Fig. 32b), although rocks with high K levels are not the most differentiated.

The K/Rb ratio is generally considered as a reliable index of differentiation in most igneous rock suites (Taubeneck, 1965). However, for the Guichon Creek batholith, K/Rb ratios show no consistent patterns when plotted against LDI (Fig. 33). This is

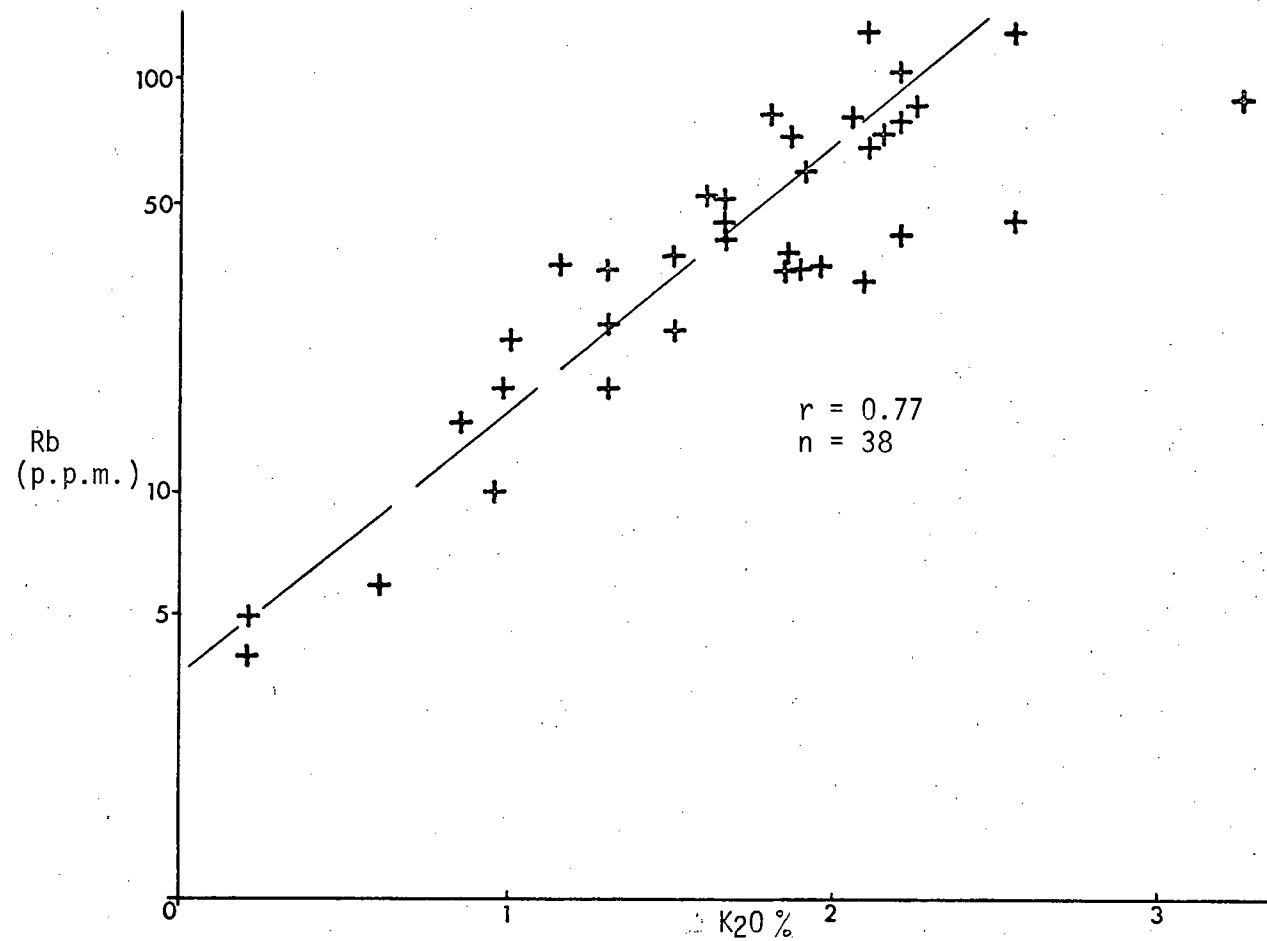


FIGURE 32: Relationship between rubidium and potassium in rocks of Guichon Creek batholith.

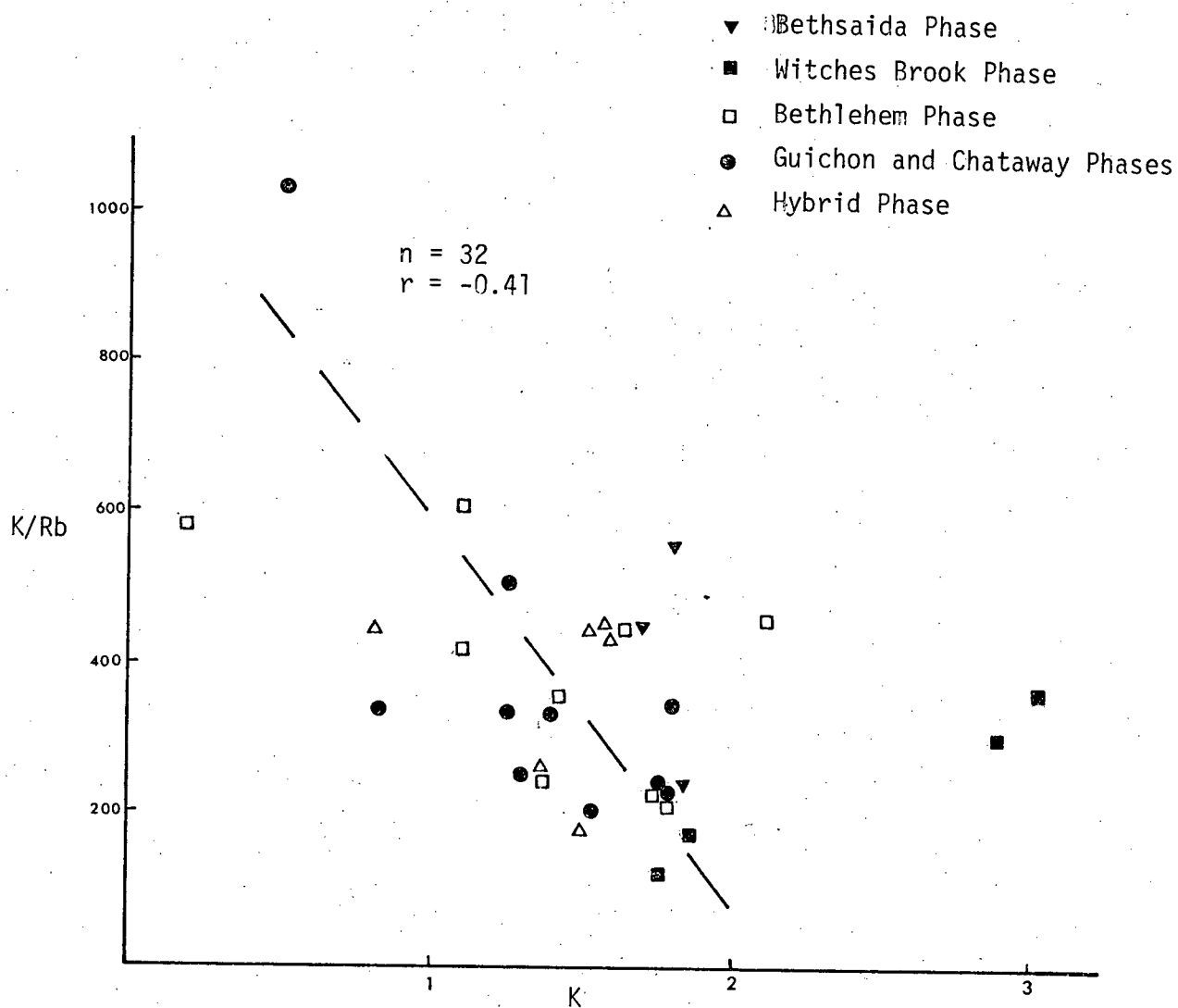
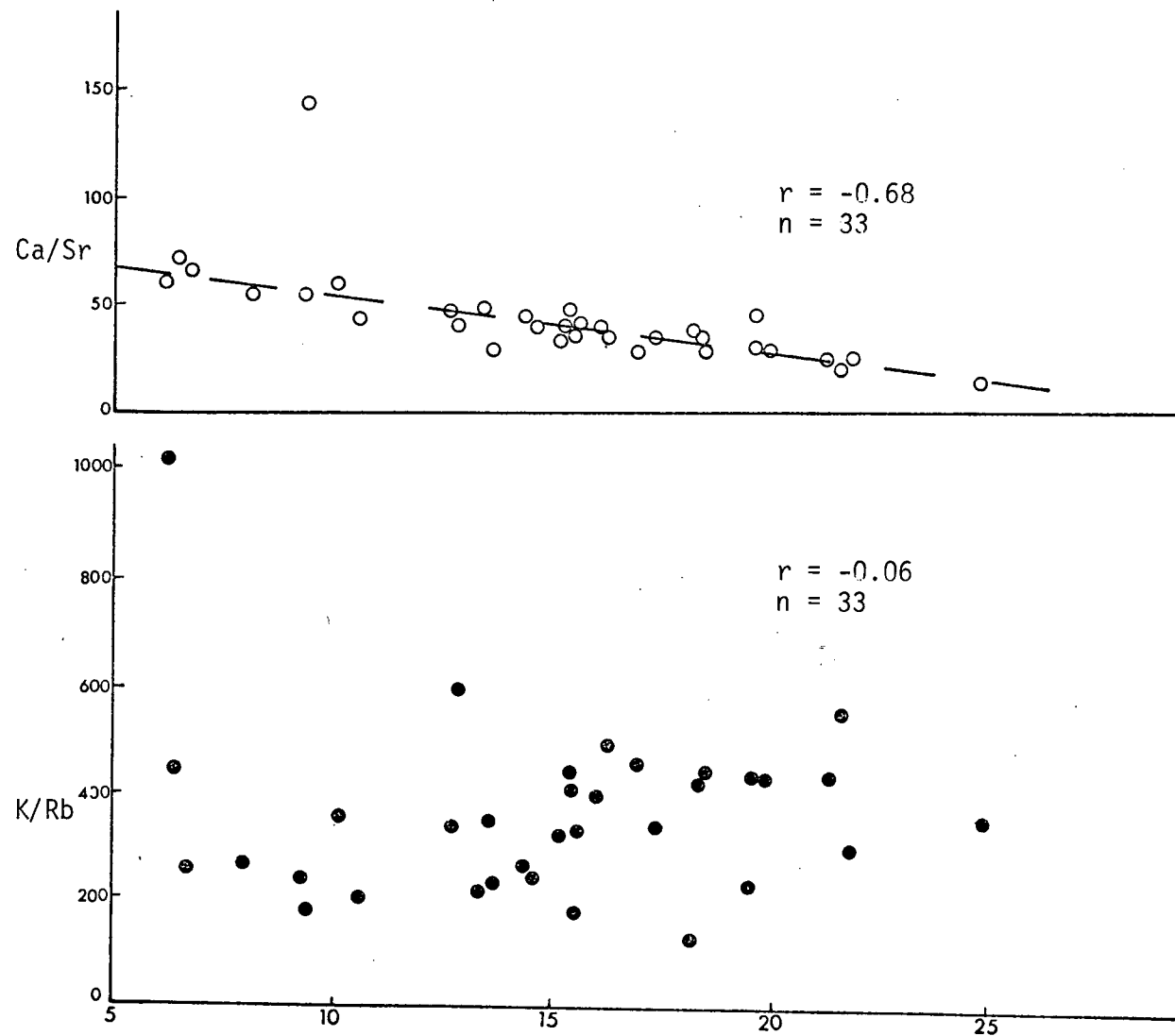


FIGURE 32b: Plots of K/Rb vs K in rocks of Guichon Creek batholith.



LDI (Larsen Differentiation Index)
 FIGURE 33 : Plots of K/Rb and Ca/Sr versus Larsen differentiation index.

attributed to the relatively low and near uniform concentrations of both elements in the intrusive units.

Sr concentrations range from 249 to 1000 p.p.m. and average 686 p.p.m. These values are high relative to the average of 440 p.p.m. cited by Turekian and Wedepohl (1961) for high-Ca granitic rocks. As shown in Table XXIV, mean Sr values are slightly lower in the more felsic rocks. During magmatic processes, Sr tends to substitute for Ca and K in feldspars. Thus, the apparent decrease of mean Sr concentrations with increasing differentiation might reflect a corresponding decrease in Ca levels. A plot of Ca/Sr ratios against LDI indicates a decrease with increasing differentiation (Fig. 33). This relationship suggests that Sr is enriched relative to Ca in more felsic rocks.

Abundance of Cl and F in 12 samples are tabulated in Table XXIII. Cl content is highest in the more mafic Hybrid and Guichon Phases, and values generally decrease in the more felsic rocks. F concentrations range from 108 to 380 p.p.m. with an erratic distribution. Compared to the world average of 130 p.p.m. Cl and 520 p.p.m. F (Turekian and Wedepohl, 1961; Kuroda and Sandell, 1953) for intermediate rocks, results indicate that the Guichon Creek batholith is relatively enriched in Cl but impoverished in F. Kuroda and Sandell (1953) and Allmann and Kortnig (1972) suggest that the halogen content of igneous rocks may be related to regional tectonic and crustal features, such as island arcs.

TABLE XXIII: Abundances of *chlorine and *fluorine in rocks of
Guichon Creek batholith

Intrusive Unit	Sample Number	Chlorine (p.p.m.)	Fluorine (p.p.m.)
Hybrid	1-6470	880	380
Guichon	22-6432	544	380
	22-6341	465	284
Bethlehem	4-6462	240	108
	4-63184	280	140
Skeena	41-72185	100	240
Witches Brook	5-721370	128	256
Bethsaida	6-6463	132	176
	6-64631	132	180
	6-72750	80	208
Gnawed Mountain	8-7215	92	172
	8-72111	120	224

* Ion-selective electrode analyses

(iv) Distribution of Zn, Mn, Ni, Co and V

Zn values generally decrease from more than 80 p.p.m. in the Hybrid Phase to less than 20 p.p.m. in the relatively younger Bethsaida and Gnawed Mountain Phases. A similar distribution was reported by Brabec and White (1971) for aqua regia-extractable Zn (Table XX). Although a plot of Zn versus LDI shows considerable scatter, two trends with no genetic significance are evident (Fig. 34). The first which is considered "spurious", has a relatively steep slope and includes rocks of the Hybrid, Witches Brook and Bethlehem Porphyry Phases. The second trend considered "normal" joins rocks of the other phases. The "spurious" trend is attributed to extensive contamination of the Hybrid Phase by relatively Zn-rich Nicola rocks, and strong depletion of Zn in the K-rich dyke rocks of the Witches Brook and Bethlehem Porphyry Phases. During magmatic processes, Zn generally substitutes for Fe^{++} in silicates and oxides because of similarity in ionic properties. A plot of Zn versus Fe shows a strong positive correlation (Fig. 35). Comparable results have been reported for other granitic rocks (Haack, 1969; Blaxland, 1971). Results of partial extraction techniques also indicate that Zn, unlike Cu, is principally associated with the silicate fraction (Brabec, 1971; Foster, 1973; Olade and Fletcher, 1974).

Mn distribution shows the same trends as Zn. Values generally decrease with increasing differentiation (Table XIX and Fig. 34). Fig. 36 demonstrates the covariance of Mn and Fe. This

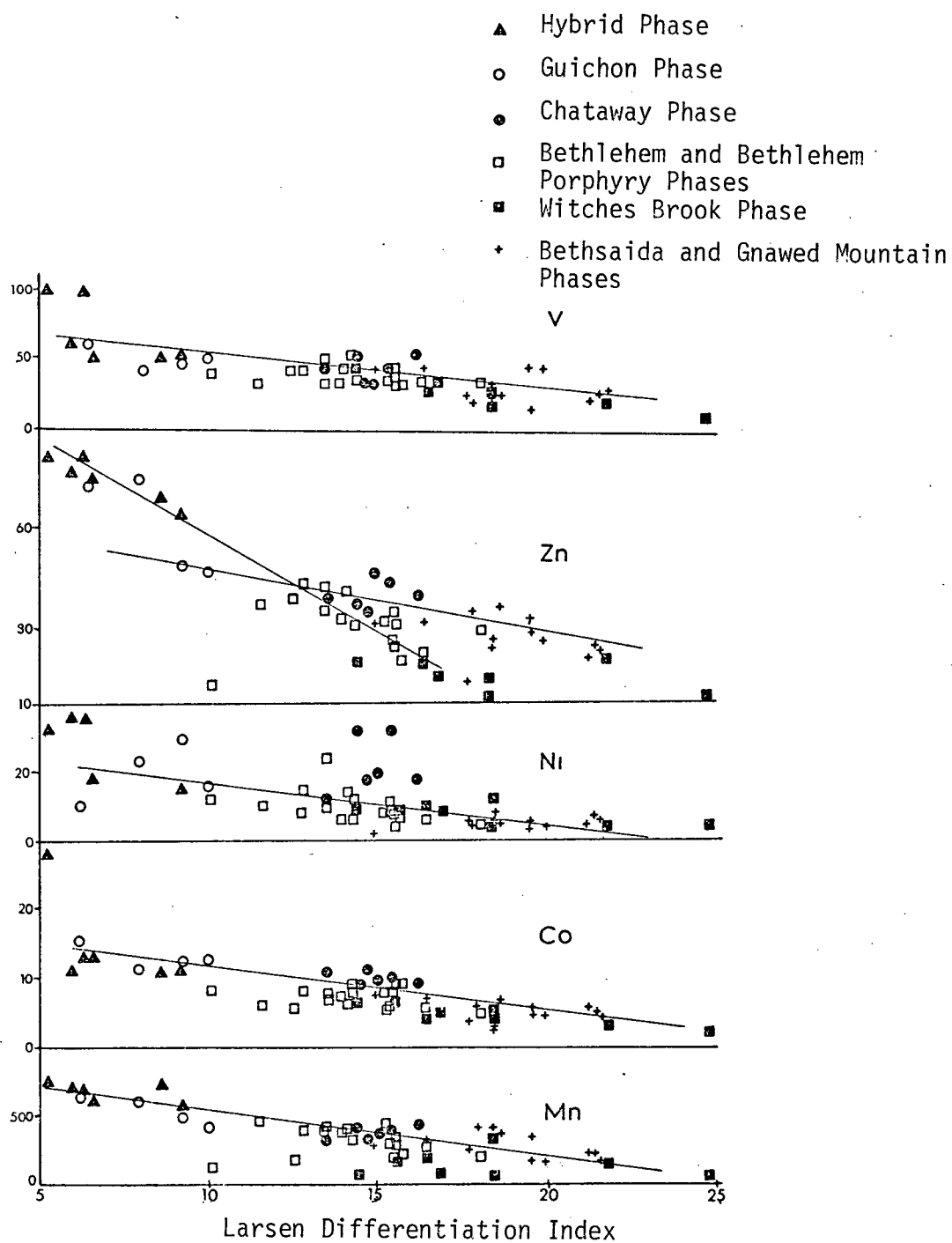


FIGURE 34: Variation diagrams in Guichon Creek rocks showing trace element concentrations plotted against LDI

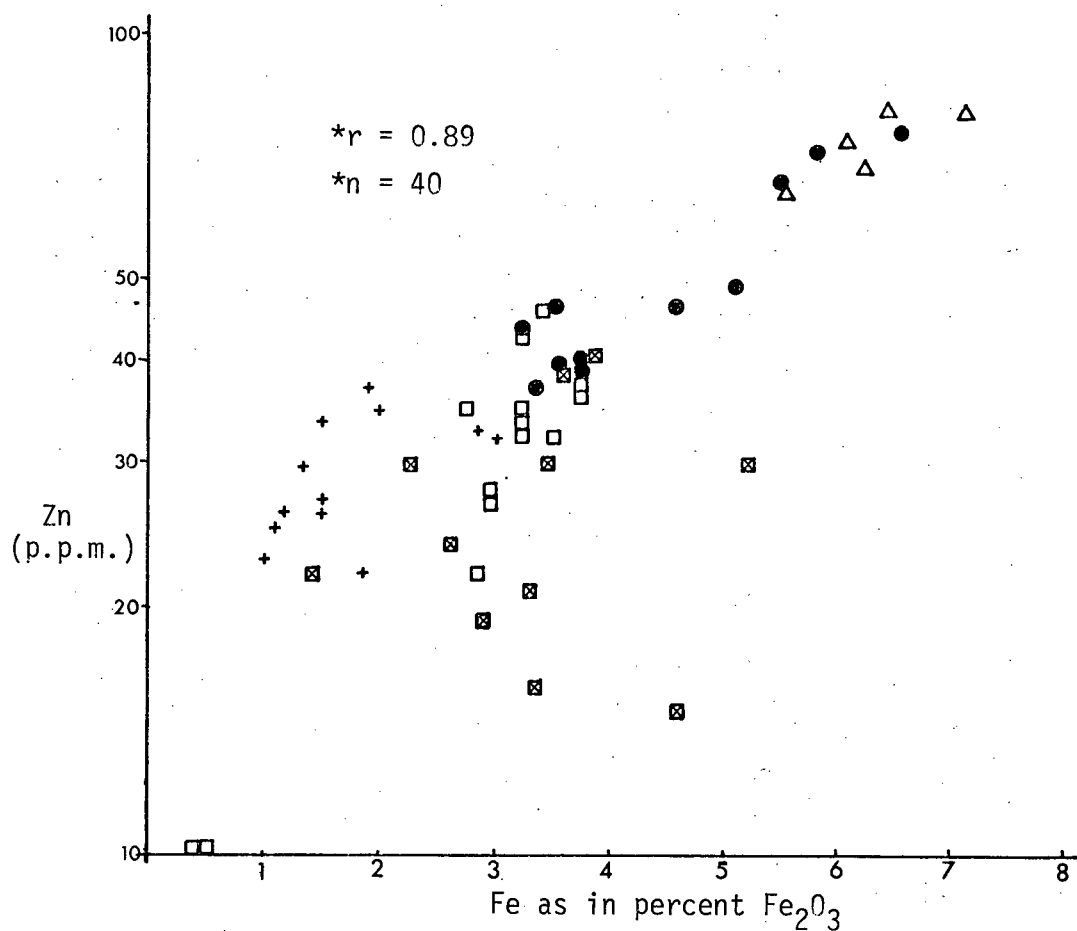
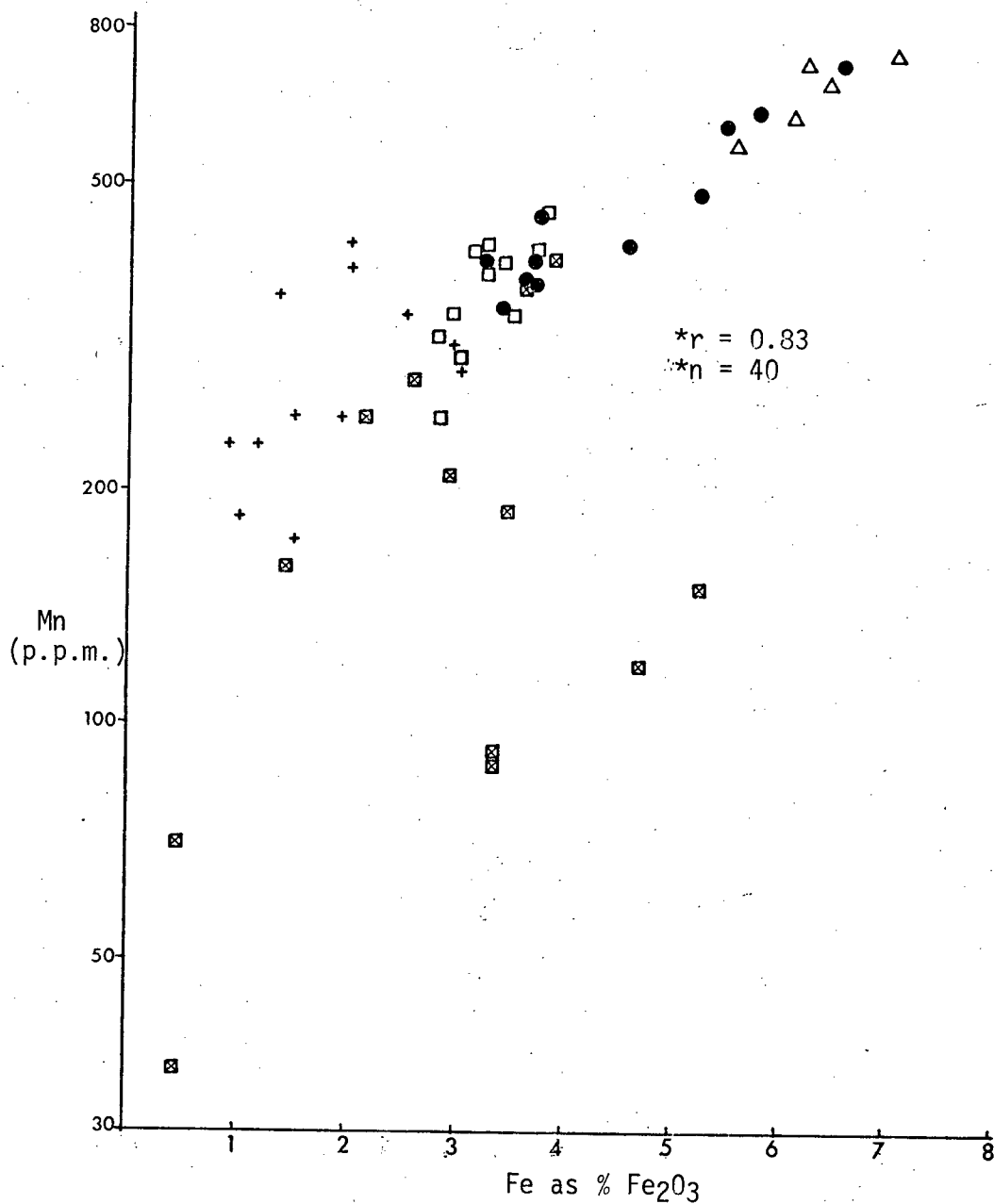


FIGURE 35: Relationship between Iron and Zinc in rocks of Guichon Creek batholith (52 samples)
*(excluding Witches Brook and Bethlehem Porphyry Phases) (Legend as for Fig. 29)



relationship is consistent with Mn^{++} (ionic size 0.80\AA) substituting for Fe^{++} (ionic size 0.74\AA) in feric silicates.

Mean values for Ni, Co and V for constituent rock units of the batholith are summarized in Table XX. Plots of these elements against LDI indicate a general decrease with increasing magmatic differentiation (Fig. 34). A significant positive correlation between Ni and Co and Fe and Mg (Fig. 37 and 38) is consistent with Ni and Co substituting for Fe and Mg in ferromagnesian silicates.

DISCUSSION

Petrochemical trends suggest that the zonal and compositional variations exhibited by rocks of Guichon Creek batholith conform with a model of fractional crystallization of a magma of intermediate composition by progressive fractionation of plagioclase of intermediate composition, hornblende and biotite. Plagioclase fractionation generally depletes the Ca content of derivative fluids, whereas biotite and hornblende fractionation tends to enrich Si and alkali content and deplete Fe, Mg and Ti levels of derivative fluids (Peto, 1973; Smith, 1974).

The most striking aspect of the petrochemical evolution of the batholith is the absence of K_2O enrichment in the most differentiated and relatively youngest rocks - the Bethsaida and Gnawed Mountain Phases. Low values of K_2O and lack of enrichment with increasing differentiation suggest either that the pluton is not highly differentiated or that the parental magma is

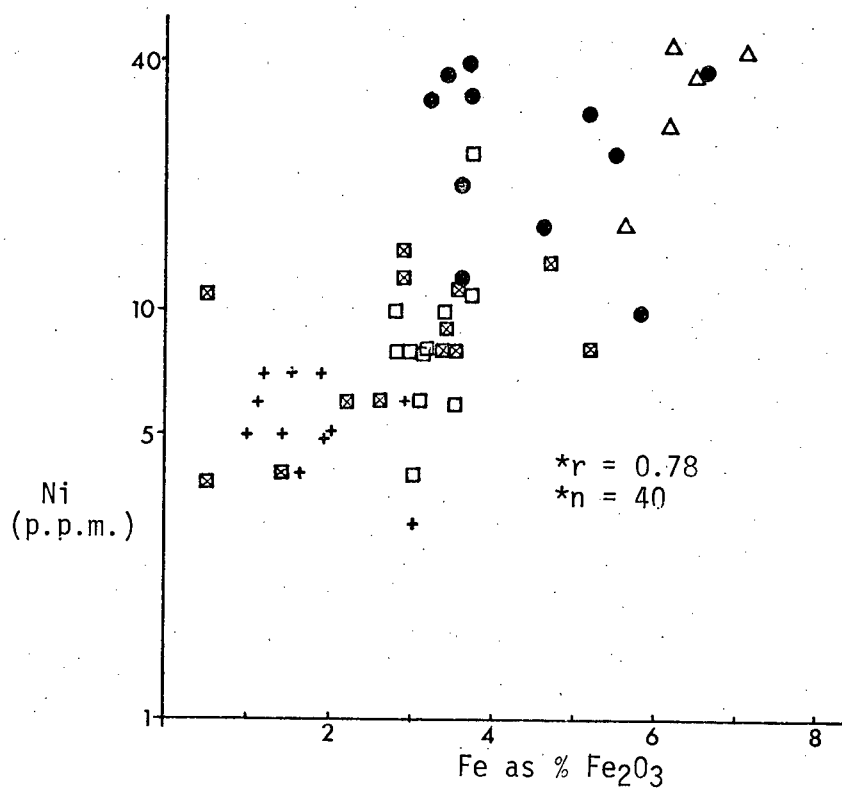


FIGURE 37a: Variation of Nickel with Iron in rocks of Guichon Creek batholith (Legend as for Fig. 29)

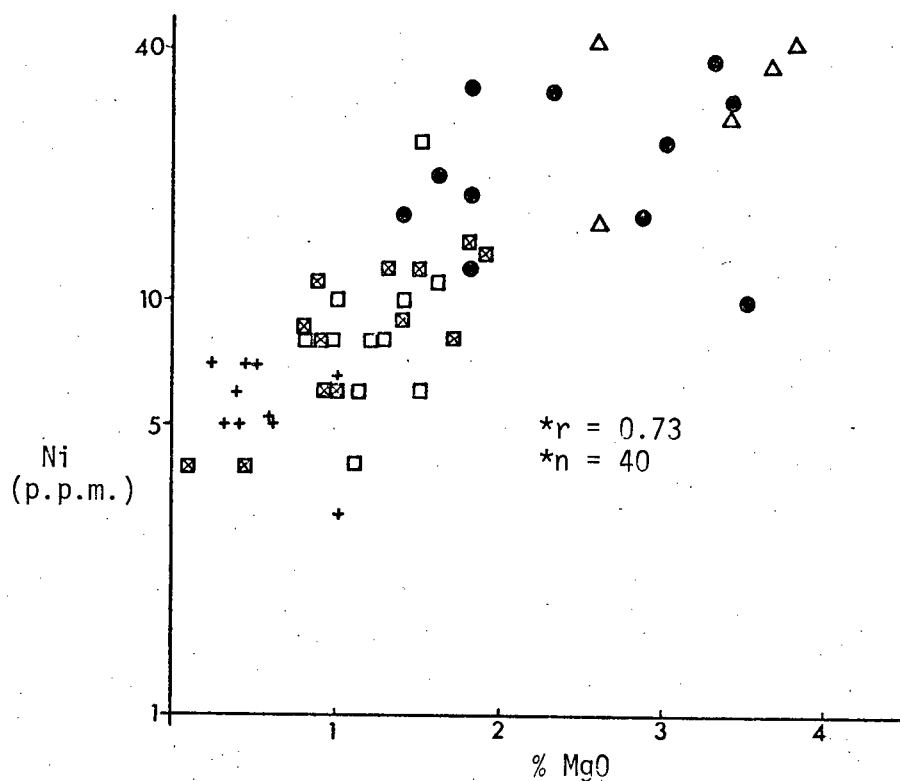


FIGURE 37b: Variation of Nickel with Magnesium in Guichon Creek batholith (*excluding Witches Brook and Bethlehem Porphyry Phases)

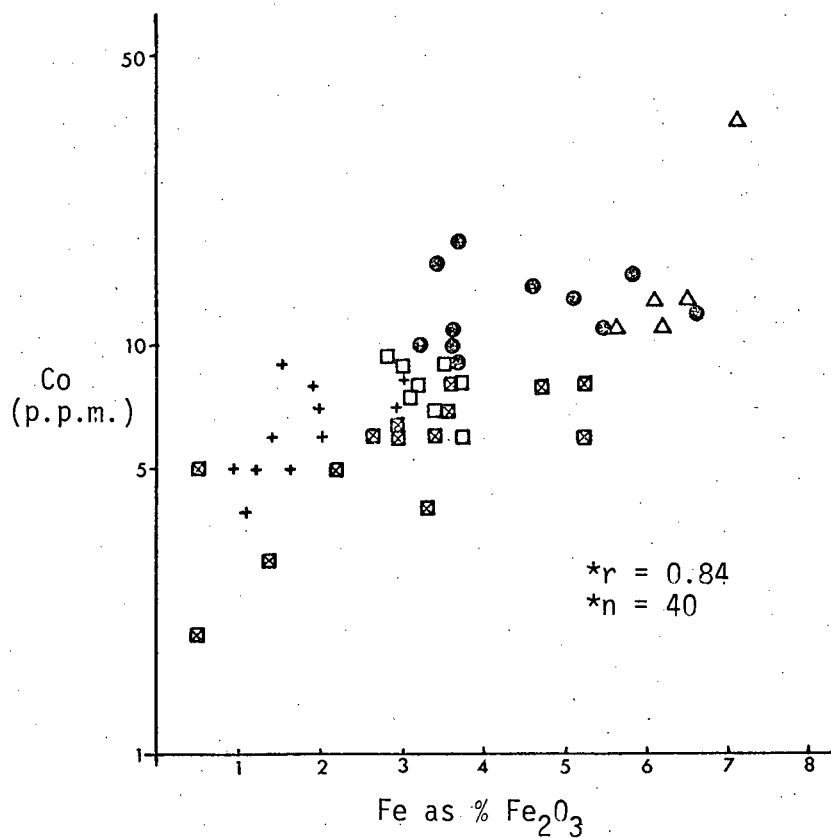


FIGURE 38a: Relationship between Cobalt and Iron in Guichon rocks (*excluding Witches Brook and Bethlehem porphyry phases). Legend as for Fig. 29.

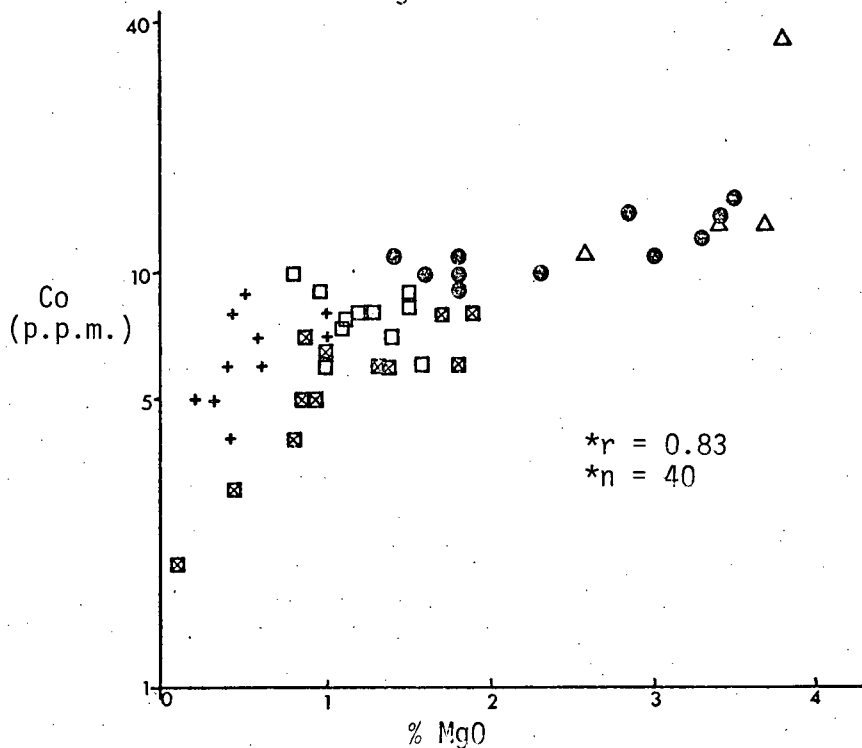


FIGURE 38b: Relationship between Cobalt and Magnesium in Guichon rocks (*excluding witches Brook and Bethlehem Porphyry Phases) (Legend as for Fig. 29)

relatively K-poor (Taubeneck, 1967). The latter is probably the case because petrographic evidence (Northcote, 1969) and petrochemical variation diagrams (Figs. 27 and 34) support magmatic differentiation. Absence of appreciable variations in Rb and K/Rb with increasing differentiation might be related to similar behaviour by K_2O . Furthermore, the tendency for Na_2O concentrations to increase with increasing differentiation (trondhjemitic trend) is commonly characteristic of K-poor magmas (Larsen and Poldervaart, 1961; Taubeneck, 1965).

Petrochemical evidence suggests that the K-rich dyke rocks of the Witches Brook Phase and some of the Bethlehem porphyries are either not cogenetic with the remainder of the batholith or might be related to local 'high-level' phenomena during evolution of the batholith (Northcote, 1969).

Trace element distribution in igneous rocks is generally controlled by abundance of major elements and the ability of the trace elements to enter appropriate crystal lattices. Trace elements capable of entering the structures of rock-forming minerals are removed from the magma, and thus eliminated from any further possibility of concentration into ore deposits (Levinson, 1974; p. 50). The behaviour of Cu suggests that Cu does not readily enter into crystal lattices of femic silicates. Because of its strongly chalcophile nature, Cu fractionates into the residual melt to combine with S (Wager and Mitchell, 1951). With increasing differentiation and volatile content, and an adequate supply of S, copper

sulphides might concentrate as ore deposits if the magma is Cu-rich. The spatial and temporal association between porphyry Cu deposits and the most differentiated and relatively youngest intrusive units in the batholith may be relevant in this context. Thus, according to Brabec and White (1971), the low Cu content of the most differentiated rocks of the Bethsaida Phase might be equated with the presence of epigenetic Cu deposits. However, the tendency for Cu to decrease with increasing differentiation parallels that of the femic elements (Zn, Ni, Co, Mn and V), and is most characteristic of Cu-poor magmas (Sheraton and Black, 1973). However, it is not clear whether the role of the batholith is one of structural control rather than a source of metals (Noble, 1970). These aspects of ore genesis are discussed further in Chapter 8.

Zn, Ni, Co, Mn and V are less chalcophile than Cu and more readily enter lattices of ferromagnesian minerals. Consequently they are removed from the magma during differentiation. Low abundances of Mo, Pb and Ag in rocks of the batholith reflect the initial concentrations in the magma. However, for Mo, magmatic differentiation resulted in concentration in the residual melt which formed MoS_2 deposits. Hg, B, Cl and F are enriched in volatile fractions of residual melts and subsequently are concentrated in zones of mineralization as hydrothermal minerals or in fluid inclusions.

From the foregoing, it is concluded that petrochemical trends could be useful in identifying rocks that are most differentiated and capable of being associated genetically with ore deposits. In the Guichon Creek batholith, the most differentiated

rocks may be identified easily by concentric zone relations and petrologic criteria. However, as Peto (1973) has shown, many plutons, for example, the Similkameen and Iron Mask batholiths in British Columbia are not concentrically zoned and petrological criteria might not be very useful in determining the differentiation sequence and cogenesis of the intrusive units. In this situation petrochemical studies could be useful in reconnaissance exploration. Furthermore, the close relationship between trace element levels and magmatic differentiation emphasises the need to assign for exploration purposes, different threshold and background levels to each intrusive phase.

SUMMARY AND CONCLUSIONS

(1) Major element variations are consistent with a model of fractional crystallization of a calc-alkaline dioritic magma by progressive fractionation of plagioclase, biotite and hornblende. By this process, derivative fluids were enriched in Si and Na and depleted in Ca, Fe, Mg and Ti.

(2) Dyke rocks of the Witches Brook Phase differ considerably in major and trace element contents, and might represent either a product of local 'high-level' crystallization or otherwise not cogenetic with other intrusive units of the batholith.

(3) The relatively low and near uniform K concentrations and the trondhjemitic trend exhibited by rocks of the batholith is suggestive of a K-deficient magma.

(4) Variations in Mn, Zn, Ni, Co and V are intimately associated with degree of fractionation. Strong positive correlations with Fe and Mg indicate partitioning of these elements into silicate fractions during magmatic evolution.

(5) Cu content generally decreases from the relatively oldest to youngest and most differentiated units. This pattern of variation parallels those of other 'femic' elements, reflecting normal differentiation trends which is most characteristic of unmineralized intrusions. This suggests that the Guichon Creek magma was not particularly rich in Cu, as this should be reflected by increasing Cu contents with increasing differentiation.

(6) Close relationships between metal values and degree of fractionation emphasize the need for assigning different background values to each intrusive unit during geochemical exploration.

(7) Petrochemical variation diagrams can be useful in identifying intrusive units that are most differentiated and capable of being genetically and spatially associated with mineral deposits.

CHAPTER SIX

METAL DISPERSION IN BEDROCK AROUND MINERALIZATION

INTRODUCTION

This section of the study reports on the nature, extent and applications of epigenetic dispersion patterns around Cu mineralization in the Highland Valley. Four major porphyry-type deposits (Bethlehem-JA, Valley Copper, Lornex and Highmont) and a small vein (Skeena) were investigated. More than 1300 samples collected from background and mineralized areas were analyzed for approximately 25 trace and major elements. Sample locations and plans are presented in the Appendix. At Valley Copper and Bethlehem-JA, analyses were obtained from samples collected from three levels. Except where metal contents are obviously different for the three levels, results are only presented for one level to avoid duplication. At Lornex and Highmont, geochemical data are presented for surface and drillcore samples, whereas at Skeena only results from drill cores are documented.

Geochemical patterns are examined in relation to primary lithology, hydrothermal alteration and mineralization, using major element data as indices where applicable. Except at Lornex, Pb, Ag, Ni, Cd, Sn, W and Bi levels are generally below their detection limits and are therefore not discussed further.

DATA HANDLING

All analytical data were computer-coded and histograms for all elements were prepared using a computer program (GHIST) provided by Dr. W.K. Fletcher. Means, standard deviations and other

statistical parameters are obtained with the histograms. Cumulative probability plots were prepared for most elements using a computer program (PROB) provided by Dr. A.J. Sinclair. The nature of frequency distribution patterns for all elements was determined from probability plots and verified by the Chi-square test for normality.

Preliminary "Calcomp" plots of element distribution were prepared by computer. Using transparent overlays, geochemical maps were prepared by manual contouring where smooth trends are evident. However, if metal distribution is erratic, discrete symbols are used. The choice of contour intervals was based on probability plots as described by Sinclair (1974). All geochemical maps were transferred from overlays to base maps.

Relationships among metal distributions were examined by factor analysis. R-mode factor analysis uses a measure of similarity among all pairs of variables to extract linear combinations which are termed "factors", of some or all of these variables. Standard programs (FAN) available at the Computing Centre, UBC were used to carry out the R-mode analysis. Prior to analysis, all metal distributions were standardized ($X = 0$; $s = 1$) to prevent bias arising from variations of concentration ranges for elements, in estimating factor loadings. Q-mode analysis was also used, but results were similar to those of R-mode, and are therefore not discussed.

RESULTS

BETHLEHEM-JA

Means, standard deviations and ranges of metal concentrations are recorded in Tables XXIV and XXV, and Figs. A1 - A27. Because of similarity in distribution patterns, only results for the 2800 level are discussed.

(a) Geochemical Patterns Related to Primary Lithology

Rocks of the Guichon Phase in the eastern part of the property are characterized by enhanced levels of Zn, Mn, Ti, V and Co compared to the more felsic rocks of the Bethlehem Phase in the west. Lowest concentrations are encountered in rocks of the JA porphyry in the central portion of the property (Figs. A1 - A4). Table XXV compares the means and ranges of these elements in the lithologic units. A student t-test suggests that the Guichon Phase is significantly different from the Bethlehem Phase in Zn, Ti, V, Co and MgO at the .05 confidence level.

Variations in Zn, Mn, V, Ti and Co are strongly controlled by obvious variations in the amounts of ferro-magnesian minerals present in the rock units. This is reflected in the distribution of MgO and Fe_2O_3 (Figs. A5 and A14) which are highest in the Guichon Phase and lowest in the felsic porphyry. In contrast SiO_2 levels are relatively enriched in the porphyry (Fig. A6). Because of similarity in ionic properties, Zn, V, Ti, Mn, and Co generally substitute for Mg and Fe in crystal lattices (Goldschmidt, 1954). A plot of Zn

TABLE XXIV: ⁴Means, deviations and ranges of trace elements at
Bethlehem J-A (Values in ppm except where indicated)

Elements	Analytical Technique	BETHLEHEM JA		
		Number of samples		
		(58) Sub out- crop level	(54) 2800 level	(48) 2400 level
¹ Cu	AA	1164 3.7 316-4289	1070 3.7 290-3950	1296 3.4 386-4349
³ Sulphide Cu	AA		1234 4.1 305-4977	
^{3*} Sulphide Fe	AA		0.62 0.45 0.17-1.07	
Mo	ES	3 4.9 0.7-16	5 5.4 0.8-24	6 6.3 1-40
¹ Ag	AA	0.12 2.2 0.05-0.26	0.12 2.1 .05-0.24	0.11 1.7 0.06-0.19
¹ Zn	AA	19 1.7 11-32	18 1.6 11-29	16 1.6 10-25
¹ Mn	AA	150 1.6 96-244	157 1.6 98-250	135 1.6 82-222

TABLE XXIV: (cont.)

		BETHLEHEM JA		
		Number of samples		
Elements	Analytical Technique	(58)	(54)	(48)
		Sub out- crop level	2800 level	2400 level
¹ Co	AA	7 1.6 4-11	7 1.7 4-12	6 1.8 3-10
V	ES	40 1.5 26-62	41 1.5 27-61	38 1.7 22-67
Ti	ES	1159 1.6 738-1820	1144 1.8 747-1752	1086 1.6 660-1788
* S	XRF		0.39 4.2 0.09-1.65	
** Hg	AA		7 4.8 1.4-34	
B	ES	10 1.9 5-19	9 2.0 5-19	10 1.7 5-19
Cl	ISE		254 1.6 156-414	
H ₂ O-Ex. Cl	ISE		6 2.1 3-13	
F	ISE		216 1.8 118-395	

TABLE XXIV: (cont.)

BETHLEHEM JA

Elements	Analytical Technique	Number of samples		
		(58) Sub out- crop level	(54) 2800 level	(48) 2400 level
H ₂ O-Ex	ISE		7	
F ²			1.5	
			5-11	
Rb	SRF		50	
			1.4	
			36-71	
Sr	XRF		579	
			1.6	
			371-902	
Ba	ES	493	490	442
		1.4	1.3	1.5
		358-679	371-645	289-676
* CaO	AA		2.82	
			0.86	
			1.96-3.68	
² * MgO	AA		1.40	
			0.62	
			0.78-2.03	
² * Total Fe as Fe ₂ O ₃	AA		3.31	
			1.19	
			2.12-4.50	
² * Na ₂ O	AA		4.27	
			1.39	
			2.88-5.67	
² * K ₂ O	AA		1.91	
			0.97	
			0.94-2.88	
* SiO ₂	XRF		62.34	
			3.40	
			58.94-65.74	

1 HNO₃-HClO₄ digestion

2 Total digestion

3 KClO₃-HCl digestion

4 Geometric Means except where indicated

R=Range = Mean \pm 1 standard deviation

* Values in weight percent

* Arithmetic mean

** Values in parts per billion

AA Atomic Absorption

ES Emission Spectrography

XRF X-ray fluorescence

ISE Ion-selective electrodes

TABLE XXV: Means and ⁴ranges of some metal concentrations in
principal lithologic units, Bethlehem JA 2800 level.

154

No. of samples	Guichon Phase (24)	Bethlehem Phase (25)	Porphyry (5)
1* CaO	3.12 (2.43 - 3.83)	2.78 (1.96 - 3.59)	1.51 (0.79 - 2.23)
1* MgO	1.91 (1.52 - 2.30)	1.11 (0.71 - 1.51)	0.89 (0.28 - 2.06)
1* Fe ₂ O ₃	4.26 (3.30 - 5.23)	2.84 (2.01 - 3.68)	1.72 (0.99 - 2.43)
1* Na ₂ O	4.42 (2.94 - 5.89)	4.25 (3.02 - 5.48)	3.69 (1.46 - 5.93)
1* K ₂ O	1.80 (1.20 - 2.40)	1.81 (0.76 - 2.85)	3.31 (2.19 - 4.42)
3* SiO ₂	61.32 (58.79 - 63.84)	62.38 (59.59 - 65.16)	67.40 (60.46 - 74.34)
2** Ti	1426 (1052 - 1933)	1032 (663 - 1604)	769 (551 - 1073)
1** Zn	24 (17 - 33)	16 (11 - 25)	9 (4 - 17)
1** Mn	183 (123 - 273)	145 (90 - 235)	123 (70 - 218)
2** V	53 (42 - 67)	37 (25 - 53)	26 (15 - 44)
2** Ba	500 (382 - 655)	484 (357 - 655)	474 (423 - 529)
1** Co	9 (5 - 15)	6 (3 - 12)	2 (1 - 4)

¹ Atomic absorption; ² Emission spectrography; ³ X-ray fluorescence

⁴ Mean \pm 1 standard deviation;

* Arithmetic mean and values in wt. % ** Geometric mean and values in p.p.m.

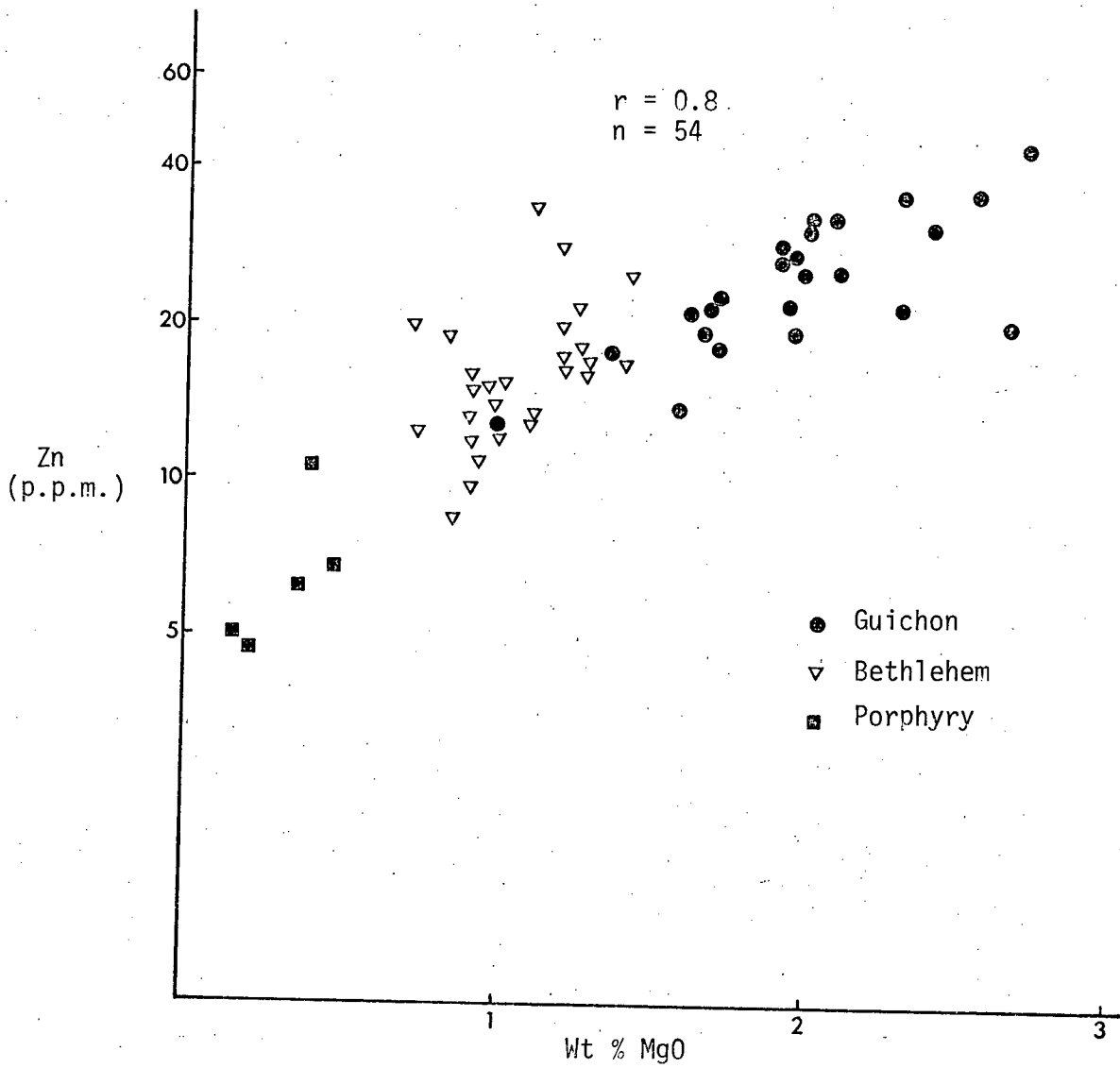


FIGURE 39: Relationship between Zinc and Magnesium contents of rocks, Bethlehem JA 2800 Level

TABLE XXVI: Correlation matrix of trace and major element contents,
Bethlehem-JA, 2000 level.

	Cu	Zn	Mn	B				
Cu	.99954							
Zn	-.17304	1.00060						
Mn	-.08821	.70569	.99950		Ti	V	Mo	Ba
B	.17534	-.08741	.26099	1.00312				
Ti	-.02395	.37407	.23664	.00294	1.00266			
V	.06393	.59796	.38553	-.01200	.73945	1.00072		
Mo	.24779	-.42504	-.21650	.41546	.02325	-.12000	.99786	
Ba	.28497	.17725	.20064	.08678	-.02377	.21502	-.26073	.99987
Rb	.39869	-.25715	-.17821	.40102	-.27188	-.26620	.30357	.25576
Sr	-.31809	.49496	.14047	-.44377	.30441	.39906	-.38328	-.13303
SiO ₂	-.02448	-.46823	-.37635	-.06268	-.21722	-.57306	.12143	-.3366
Sulphur	.37856	-.10216	-.22540	.1606	.08114	.14723	.28063	.19499
Hg	.19603	-.41770	-.37295	-.00698	-.41813	-.43877	.11914	.09174
Cl	.11912	-.11408	-.20008	.00269	-.08649	.00461	.03507	.21814
F	.02946	.33724	.24848	.14132	.15053	.30901	.00509	.09509
CaO	-.28405	.49951	.37657	-.27521	.37868	.61489	-.22675	.01624
MgO	-.27303	.81286	.57275	-.17222	.50752	.72904	-.37592	.10495
Fe ₂ O ₃	-.10600	.69187	.40099	-.05521	.46693	.68195	-.38210	.27928
Na ₂ O	-.55648	.28908	.22334	-.25600	-.02849	.03967	-.33053	-.17246
K ₂ O	.42838	-.38177	-.16425	.33321	-.33699	-.38265	.22188	.32358
	Rb	Sr	SiO ₂	Sulphur	Hg	Cl	F	CaO
Rb	.99331							
Sr	-.74479	1.00016						
SiO ₂	.01898	-.10320	1.00041					
Sulphur	.34663	-.36924	-.25455	.99840				
Hg	.43567	-.51587	.06094	.35545	.99870			
Cl	.16246	.00430	-.16746	.15457	.27078	.99890		
F	-.01779	.07752	-.35036	.10521	-.13684	.08307	.99998	
CaO	-.64840	.57978	-.50424	-.18517	-.37364	-.06558	.05099	1.00125
MgO	-.24205	.45885	-.51692	-.13165	-.40320	.00063	.22681	.56958
Fe ₂ O ₃	-.10108	.24190	-.54686	.30898	-.16539	-.04919	.12946	.49933
Na ₂ O	-.39741	.54661	-.08889	-.44937	-.23561	-.13174	-.03265	.24064
K ₂ O	.86388	-.86842	.08008	.31937	.51824	.07468	-.07819	-.68327
	MgO	Fe ₂ O ₃	Na ₂ O	K ₂ O				
MgO	1.00028							
Fe ₂ O ₃	.70812	1.00032						
Na ₂ O	.38373	-.01334	.99929					
K ₂ O	-.38884	-.16304	-.49880	.99960				

versus MgO (Fig. 39) shows a strong positive correlation ($r = 0.81$). Relationships among MgO and Fe_2O_3 and Ti, V, Mn, Co and Zn are shown in Table XXVI. All the aforementioned trace elements show consistently weaker correlations with Fe_2O_3 than MgO. This relatively weak relationships are attributed to the modes of occurrence of Fe, not only in silicates but also in sulphides (pyrite, chalcopyrite and bornite). Compared with other trace elements, Mn shows a relatively weaker correlation with MgO and Fe_2O_3 . This is attributed to partial hydrothermal redistribution within the ore zone (Fig. A2).

Compared with regional data, rocks of the Guichon and Bethlehem Phases within the property are obviously depleted in Zn and Mn.

(b) Geochemical Patterns Related to Hydrothermal Alteration

Hydrothermal alteration effects at Bethlehem-JA are associated with enrichment in K_2O , Rb and Ba and to varying extent, depletion of CaO, Na_2O , Fe, Sr and Mn. Results in relation to types of alteration are summarized in Table XVII.

K_2O levels generally increase from values less than 1.3% at the outer margins of the property, to values exceeding 3.7% at the core, within and north of the porphyry dyke (Fig. A7). Rb content follows K_2O , increasing from less than 40 p.p.m. at the periphery, to more than 140 p.p.m. at the core (Fig. A8). An east-west trending belt of enhanced K_2O and Rb contents coincide with the zone of pervasive potassic alteration (Sericite-K-feldspar).

TABLE XXVII: ¹Chemical variations associated with types of alteration, Bethlehem-JA, 2800 level

No. of samples	Unaltered Bethlehem Phase (7)	Propylitic Zone (16)	Argillic Zone (10)	Potassic Zone (6)
Metal Content (p.p.m.)				
Cu	² 33 (11 - 195)	1084 (386 - 3044)	1466 (471 - 4557)	1926 (323 - 12217)
Zn	³ 19 (16 - 22)	25 (17 - 38)	16 (11 - 22)	10 (4 - 24)
Mn	² 442 (364 - 542)	205 (147 - 287)	130 (97 - 176)	133 (54 - 324)
B	5	8 (5 - 15)	10 (4 - 24)	14 (5 - 39)
Tl	1250 (1000 - 1500)	1345 (977 - 1851)	1041 (916 - 1184)	748 (429 - 1308)
V	50 (40 - 60)	50 (39 - 65)	40 (33 - 49)	25 (11 - 56)
Mo	2	4 (1 - 13)	9 (3 - 32)	10 (1 - 90)
Ba	560 (500 - 800)	508 (398 - 649)	487 (381 - 621)	562 (322 - 980)
Rb	43 (34 - 80)	41 (38 - 65)	47 (35 - 63)	81 (54 - 121)
Sr	693 (580 - 829)	686 (570 - 828)	617 (528 - 721)	235 (111 - 500)
*S		0.15 (0.05 - 0.54)	0.59 (0.24 - 1.45)	0.37 (0.07 - 1.99)
**Hg		4 (2 - 9)	8 (1 - 44)	41 (8 - 214)
F		246 (161 - 375)	268 (169 - 426)	165 (75 - 366)
Cl		278 (196 - 394)	280 (171 - 458)	231 (81 - 1859)
Metal Content (wt. %)				
Fe ₂ O ₃	3.35 (3.11 - 3.72)	4.09 (3.08 - 5.09)	2.90 (2.02 - 3.79)	1.86 (0.69 - 3.88)
MgO	1.31 (1.10 - 1.63)	1.97 (1.51 - 2.42)	1.19 (0.81 - 1.56)	0.74 (0.17 - 1.65)
CaO	4.05 (3.07 - 5.21)	3.17 (2.51 - 3.82)	2.83 (1.63 - 3.83)	1.48 (0.64 - 2.32)
Na ₂ O	4.52 (3.86 - 4.90)	4.42 (3.37 - 5.48)	3.82 (2.74 - 5.11)	2.91 (1.78 - 4.05)
K ₂ O	1.83 (1.32 - 2.40)	1.77 (1.17 - 2.37)	1.62 (1.10 - 2.14)	3.84 (2.28 - 5.39)
SiO ₂	65.04 (65.30 - 66.84)	61.05 (58.42 - 63.69)	62.17 (60.88 - 63.47)	65.08 (57.65 - 72.50)

¹Values presented as geometric means and ranges, except for major elements.

*Values in wt. %

²HF-HClO₄ digestion (Total)

**Values in p.p.b.

³Aqua-regia digestion (Zabec, 1970)

Ba, to some extent follows K_2O , although the zone of enrichment is confined to a narrow central sector of the orebody (Fig. A9).

CaO , Sr and Na_2O values show trends that are the reverse of K_2O and Rb distribution. Enhanced levels occur at the periphery of the property and decrease progressively inwards (Figs. A10, A11 and A13). Lowest concentrations occur at the centre of the property coinciding in part with the porphyry dyke and in part with zone of intense potassic alteration and metallization. Distribution of Rb/Sr and Ba/Sr ratios are similar to those of Rb and Ba respectively, in that ratios increase progressively from the outer margins to the core (Figs. A12a and A12b). Fe_2O_3 and Mn are to some extent depleted within the ore zone reflecting leaching of these elements during formation of potassic and argillic alteration zones (Figs. A14 and A2).

Distribution of anomalous Rb , Ba and Sr is strongly influenced by the type and intensity of wall-rock alteration as reflected by abundances of K_2O and CaO respectively (Figs. 40 and 41). High Rb and Ba levels are associated with a zone enriched in K -feldspar and sericite (Fig. 11), whereas at the outer margins, where propylitic minerals are dominant, Rb and, to a lesser extent, Ba levels are relatively low. This relationship is amply demonstrated by the strong positive correlation between K_2O and Rb ($r = 0.86$) (Fig. 40), and a relatively weaker but significant correlation between K_2O and Ba ($r = 0.33$). These correlations are consistent with the tendency for Rb and, to a lesser extent, Ba to substitute for K in lattices of alkali feldspars. The relationship

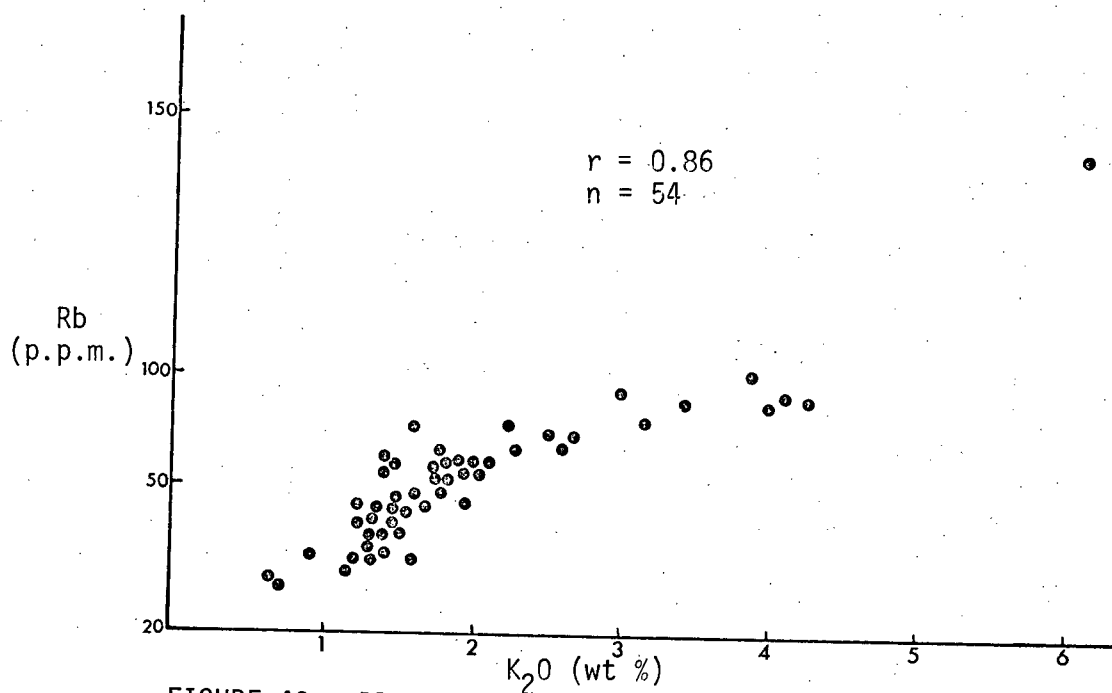


FIGURE 40: Plot of Rubidium versus Potassium, Bethlehem JA, 2800 level.

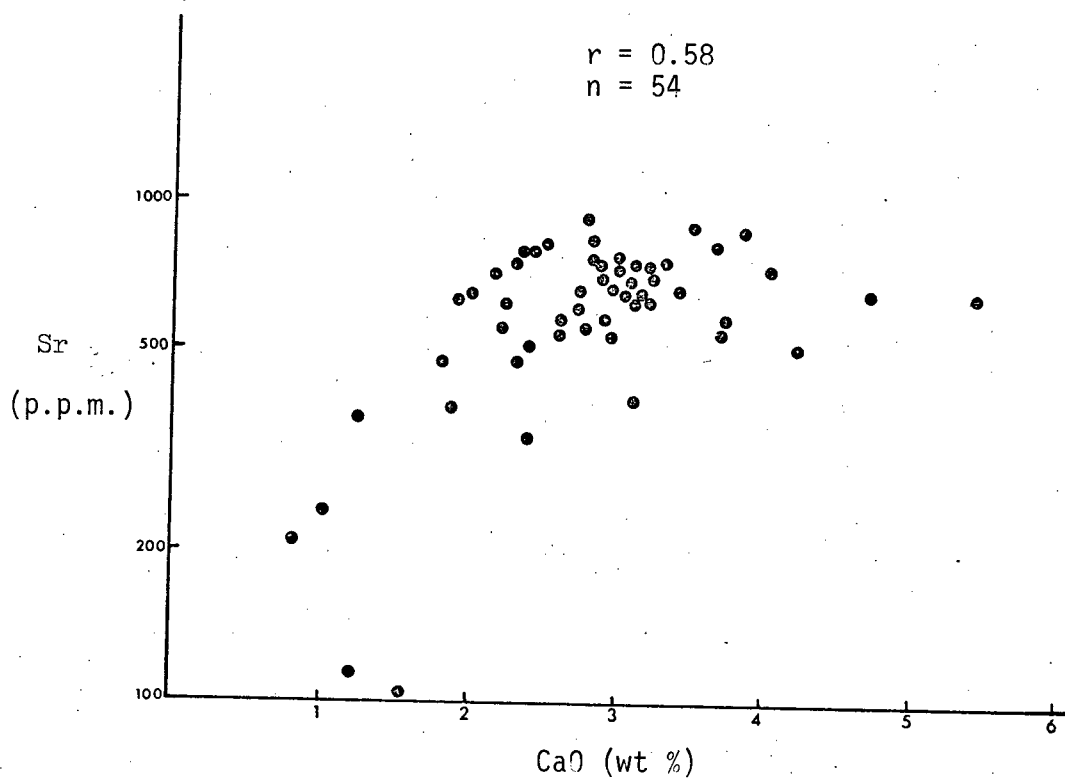


FIGURE 41: Plot of Strontium versus Calcium, Bethlehem JA 2800 level

between Sr and CaO ($r = 0.58$) is also consistent with their geochemical affinity.

(c) Geochemical Patterns Related to Mineralization

(i) Distribution of Ore Elements (Cu, Fe, Mo, S)

Copper. Cumulative log probability plot of Cu in 160 samples indicates the presence of two populations (Fig. 42); a lower population (B) representing 13% of the data, and an upper population (A) comprising 87%. Mean values for populations B and A are 126 and 1410 p.p.m. respectively. Compared with the regional data of Brabec (1970), populations A and B are both 'high-copper' population. Spatial distribution of population B is very erratic, whereas population A is confined to a broad inner zone of the property. The significance of population B is not certain, whereas population A represents 'ore'. Despite the erratic distribution of Cu, values exceeding 2000 p.p.m. are confined mainly to the ore zone at the 2800 and 2400 levels (Figs. A16 and A17). At the Suboutcrop level, effects of oxidation and enrichment might account for the scattered occurrence of anomalous values outside the ore zone (Fig. A15). As anticipated, sulphide-held Cu ($KClO_3$ -HCl extraction) shows a similar distribution as HNO_3 - $HClO_4$ extractable Cu (Fig. A18).

Sulphide-held Fe: Enhanced values of sulphide-held Fe ($> 0.75\%$) are confined to an elongated belt extending from the eastern periphery of the property to the central part of the orebody (Fig.

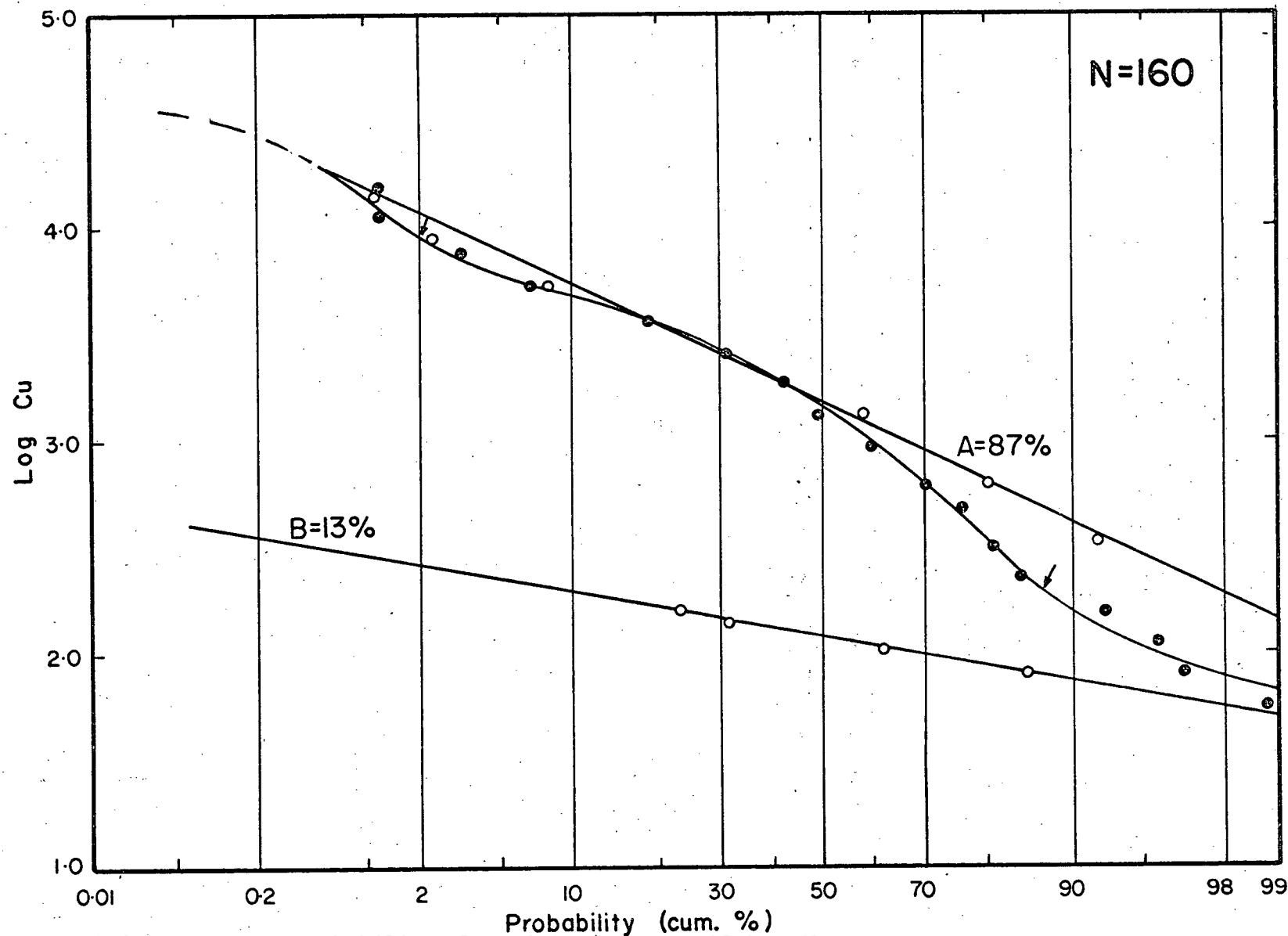


FIGURE 42: Log probability plot of Copper at Bethlehem-JA

A19). This corresponds to the area where pyrite and chalcopryrite are most abundant. A comparison with the distribution map of total Fe_2O_3 (Fig. A14) isolates the lithological variability which results in high Fe contents in Guichon rocks to the east of the mineralization.

Molybdenum: Mo dispersion is erratic. Enhanced levels (> 100 p.p.m.) occur at the southern fringe of the orebody, coinciding with the low-grade core on the porphyry dyke (Fig. A20). Elsewhere, values are generally less than 10 p.p.m. Distribution of Mo is consistent with metal zoning patterns in which molybdenite is confined to the central zone (Fig. 14). The erratic behaviour of Mo is attributed to its mode of occurrence as molybdenite within tiny quartz veinlets.

Sulphur: S distribution generally increases from less than 0.1% at the periphery to more than 4% in the ore zone (Fig. A21). Regional background content is less than 0.04%. Maximum concentrations are attained in the orebody along the Bethlehem-Guichon contact. This coincides with the distribution of sulphide-held Fe. Since chalcopryrite contains more S than bornite, the distribution of high S values is consistent with sulphide zoning patterns described in Chapter 3 (Fig. 14). S shows significant correlations with Cu ($r = 0.38$), Fe ($r = 0.31$) and Mo ($r = 0.28$)

(ii) Distribution of Pathfinder Elements (Hg, B, Cl, F)

Hg distribution defines a broad zone of anomalous values

(> 40 p.p.b.) at the centre of the property coinciding in part, with the zone of mineralization and intense potassic alteration. The periphery of the property is characterized by background concentrations, generally less than 10 p.p.b. (Fig. A22).

B dispersion is extremely erratic, although 2 samples with values exceeding 40 p.p.m. occur at the fringes of the ore zone (Fig. A23). There appears to be a subtle effect of rock composition on B content in that most of the high values (> 19 p.p.m.) occur in rocks of Guichon Phase in the eastern part of the property.

Cl abundance ranges from 32 to 640 p.p.m. and average 256 p.p.m. (Table XXIV). Values progressively increase from less than 200 p.p.m. at the periphery to more than 500 p.p.m. at the centre of the property (Fig. A24). An east-west-trending belt of anomalous Cl (> 400 p.p.m.) generally coincides with the orebody. Distribution of water-leachable Cl differs in that enhanced values (> 13 p.p.m.) are only well developed along the southern half of the ore zone (Fig. A25). Since Cl occurs predominantly as chloride in fluid inclusions, it is most logical to presume that enhanced Cl levels in the ore zone are associated with abundant fluid inclusions. Compared with regional data, Cl appears to be depleted in Guichon rocks at the eastern periphery of the deposit. Water-leachable Cl shows a relatively weak but significant positive correlation with total Cl ($r = 0.45$) (Fig. 43).

Anomalous F levels (> 395 p.p.m.) are confined to two small areas within the centre and western extremity of the orebody (Fig. A26). With the exception of the two anomalies, values

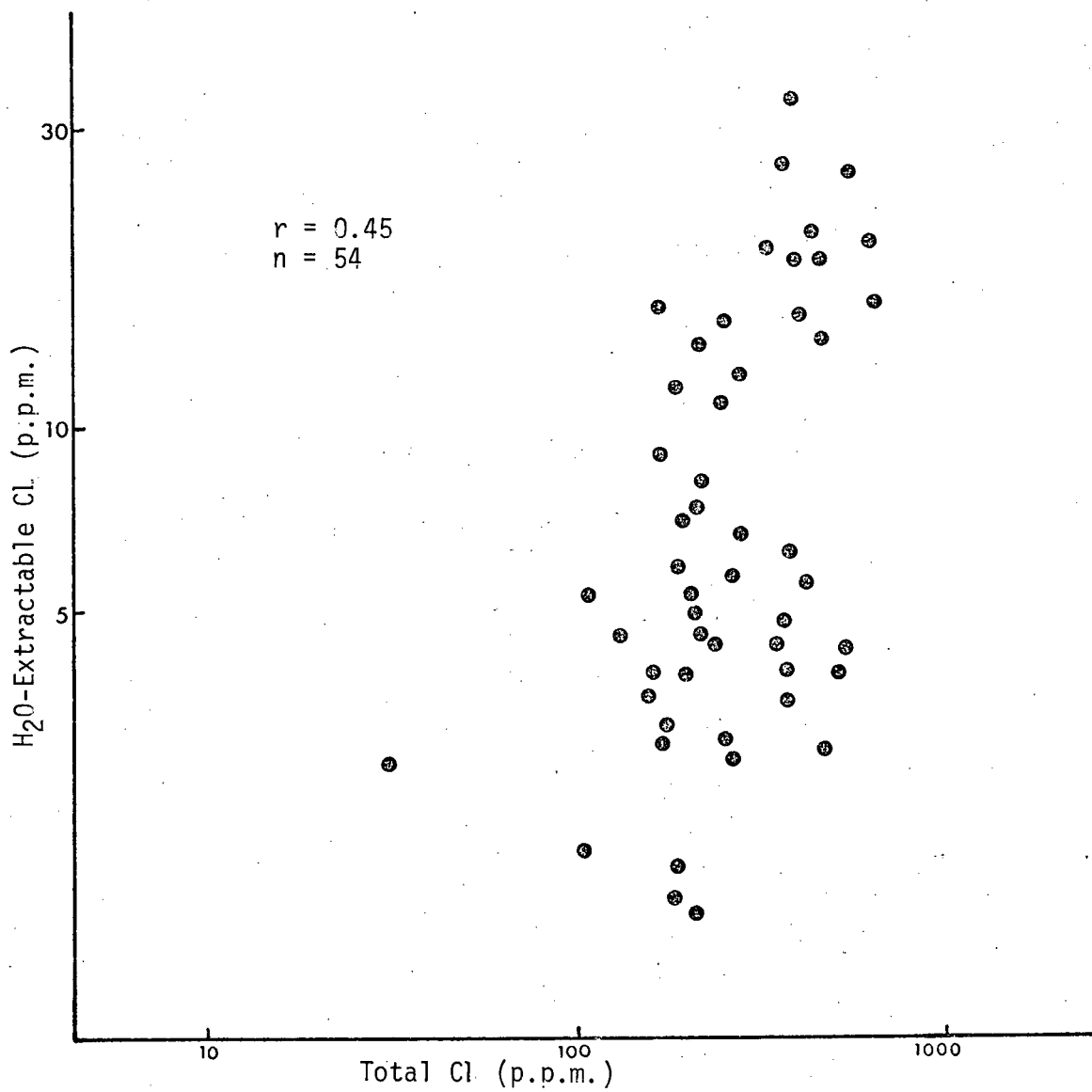


FIGURE 43: Relationship between total and water-extractable Chlorine in rocks, Bethlehem-Ja 2800 Level

exceeding 216 p.p.m. occur predominantly in Guichon Phase rocks. Distribution of water-extractable F is very erratic (Fig. A27) and shows no obvious correlation with total F ($r = -0.18$).

Relationships between Cu and potential pathfinder elements are summarized in Table XXVIII. No obvious correlation is apparent between Cu and Hg, B, Cl or F. However, there is positive relationship between K_2O and Hg, B and Cu. Rb, Ba and Sr, which are also pathfinders, show only weak correlation with Cu, but are strongly correlated with K_2O . The lack of correlation between Cu and volatile elements is probably related to the erratic distribution of Cu sulphides in fracture-fillings and as disseminations. In contrast, K_2O is associated with pervasive development of potassic minerals within and beyond the ore zone. In view of the close spatial and temporal relationships between potassic alteration and metallization, a correlation between K_2O and pathfinder elements also reflects an association with mineralization, albeit indirect.

(d) R-mode Factor Analysis

Results of R-mode analysis of 20 variables in 54 samples from the 2800 level are summarized in Tables XXIX and XXX and Figs. A28 to A31. Element associations characteristic of 3-, 4-, and 5- factor models are tabulated in Table XXIX. These models account for 58, 66 and 72% of total data variance respectively. Apart from the discrete 'Cl factor', the 5-factor model is not appreciably different from the 4-factor model. On the basis of geology, mineralization and hydrothermal effects, a 4-factor model is considered adequate. Although variability in F and Cl data is largely unaccounted for (Table XXX).

TABLE XXVIII: Relationships among copper, potassium and potential
pathfinder elements, Bethlehem JA, 2800 level

Variables	Correlation Coefficient
	(r)
Hg - Cu	0.20
B - Cu	0.18
Cl - Cu	0.12
F - Cu	0.03
Rb - Cu	<u>0.40</u>
Sr - Cu	<u>-0.32</u>
Ba - Cu	<u>0.29</u>
Cu - K	<u>0.43</u>
Hg - K	<u>0.52</u>
B - K	<u>0.33</u>
Rb - K	<u>0.86</u>
Sr - K	<u>-0.87</u>
Ba - K	<u>0.32</u>

_____ significant at .05 confidence level

===== significant at .01 confidence level

TABLE XXIX: Element associations of different factor models, trace and major element content of rocks, Bethlehem-JA, 2800, level

Factor	Factor Model		
	3	4	5
1	V	Fe	Fe
	Fe	Zn	Zn
	Mg	Mg	Mg
	Zn	V	V
	Ca	Mn	Mn
	Ti	Ba	<u>vs</u>
	<u>vs</u>	Si	Si
2	Si		
	Mo	K	K
	B	Rb	Rb
	Rb	<u>vs</u>	Hg
	Cu	Ca	<u>vs</u>
	S	Ti	Sr
	K		Ca
3	<u>vs</u>		Ti
	Na		
	Sr		
	K	Cl	B
	Ba	Hg	Mo
	Hg	<u>vs</u>	F
	Rb	B	
4		Cu	Cu
		S	S
		Mo	<u>vs</u>
		<u>vs</u>	Na
5		Na	
			Cl

TABLE XXX: R-mode Varimax Factor Matrix, Bethlehem JA, 2800 level.

Variable	Factor 1	Factor 2	Factor 3	Factor 4	Commun- ality
Cu	-0.0412	0.3199	0.1362	-0.5751	0.4533
Zn	-0.8112	-0.1915	-0.1542	0.3207	0.8213
Mn	-0.6654	-0.0833	-0.4923	0.3032	0.7839
B	-0.1044	0.4590	-0.5621	-0.3503	0.6603
Ti	-0.4841	-0.5056	-0.2039	-0.3612	0.6621
V	-0.7925	-0.4330	-0.0400	-0.2541	0.8817
Mo	0.3255	0.0593	-0.3324	-0.6837	0.6874
Ba	-0.4788	0.4340	0.3423	0.0263	0.5354
Rb	0.0332	0.8246	0.0443	-0.3054	0.7764
Sr	-0.2084	-0.7886	0.0604	0.3798	0.8132
Si	0.7482	0.0047	-0.1765	0.0729	0.5964
S	-0.1932	0.2084	0.3576	-0.6619	0.6468
Hg	0.2773	0.4932	0.5318	-0.1244	0.6184
Cl	-0.0461	0.0764	0.5438	-0.1496	0.3260
F	-0.4052	0.0255	-0.1739	-0.1213	0.2098
Ca	-0.5021	-0.6447	-0.0505	0.1432	0.6908
Mg	-0.7964	-0.3002	-0.0621	0.2688	0.8005
Fe	-0.8287	-0.1375	0.1722	-0.0161	0.7355
Na	-0.0445	-0.3096	-0.1168	0.7108	0.6168
K	0.1172	0.8916	0.0878	-0.2655	0.8873
Eigenvalue as %	36	30	13	21	

(i) Factor 1 (Fe, Zn, Mg, V, Mn vs Si)

This factor simply reflects lithology. High scores are associated with rocks of the Guichon Phase in the eastern portion of the property. In contrast, the more felsic rocks of the Bethlehem Phase and 'JA Porphyry' are characterized by lower scores (Fig. A28).

(ii) Factor 2 (K, Rb, vs Sr, Ca, Ti)

This factor which associates K and Rb reflects potassic alteration. High scores characterize the central part of the property where intense and pervasive potassic alteration is prevalent (Fig. A29). In contrast low factor scores occur at the periphery where propylitic and argillic alteration are dominant.

(iii) Factor 3 (Cl, Hg vs B)

This factor mainly reflects the effects of mineralization and lithology on volatile elements. Highest scores are found in a broad central zone coinciding with the orebody (Fig. A30). In contrast low factor scores occur in Guichon rocks in the eastern part of the deposit, where B values are relatively high.

(iv) Factor 4 (Cu, S, Mo vs Na)

The association of chalcophile elements, Cu and Mo with S suggests an 'ore factor'. High scores are associated with the ore zone where Na is obviously depleted. Low scores are generally confined to the unmineralized periphery of the property (Fig. A31).

(e) General Discussion and Summary

Results indicate that variations in the 'femic group' of elements (Mg, Zn, Mn, V, Ti, Co) are related to differences in content of ferromagnesian minerals in the lithologic units. Highest values are encountered in the more mafic rocks of Guichon Phase. In contrast lower values and high Si are associated with the felsic porphyry and Bethlehem rocks. Fe distribution is explicable in terms of lithology, hydrothermal alteration and epigenetic introduction as sulphides. K, Rb and Ba are enhanced in the zone of potassic alteration, whereas Ca, Na and Sr are depleted. These relationships reflect the geochemical affinity of these elements in magmatic and hydrothermal processes. Anomalous values of Cu, S, Hg and Cl occur in a broad central zone coinciding with the orebody. Results of factor analysis and subjective interpretation are consistent.

Geochemical contrast between regional background and anomalous environments is summarized in Table XXXI. Regional background represents fresh samples collected by Northcote (1968). Local background comprises a suite of samples from the periphery of the deposit, including the Bethlehem and Guichon Phases. It is evident that most of the ore and potential pathfinder elements show appreciable contrast. However, Cu, S and Hg show the best contrast between anomalous and local background concentrations. Contrast between anomalous and local background is higher for Cu and lower for S in Bethlehem than Guichon rocks reflecting the high back-

TABLE XXXI: Comparison of ¹mean element content and geochemical contrast
in background and anomalous samples, Bethlehem-JA, 2800 level.

No. of samples	Regional background (Guichon) (4)	Regional background (Bethlehem) (6)	Local Back- ground (All rock units) (14)	Mineralized zone (All rock units) (15)	² Contrast (Guichon)	² Contrast (Bethlehem)	² Contrast (Local Back- ground)
Cu	67	33	387	2168	32	66	5.6
Mo	2	2	5	11	5	5	2.2
S	373	448	860	5552	15	12	6.5
Hg	*	*	4 p.p.b.	16 p.p.b.	-	-	4
B	5	5	7	12	2.4	2.4	1.7
Cl	*	*	200	313	-	-	1.6
F	*	*	178	235	-	-	1.3
Rb	50	43	41	56	1.1	1.3	1.4
Sr	935	693	672	448	**2.1	**1.5	**1.5
Ba	300	560	421	545	1.8	**1.02	1.3
Zn	27	19	24	15	**1.8	**1.3	**1.6
Mn	422	372	201	152	**2.8	**1.85	**1.3

¹Geometric means; values in p.p.m.

²Contrast = Anomalous/Background

*Regional data inadequate

**Negative contrast.

ground content of Cu and low S in Guichon rocks. Distribution of both Cu and S are however erratic (coefficient of variation, Cu = 1.22, and S = 1.17) reflecting their modes of occurrence as fracture-fillings and veins.

Figs. 44a and 44b are schematic diagrams showing the extent of geochemical dispersion of trace elements and distribution of factor scores. Compared with regional background concentrations only Cu and S anomalies extend beyond the sampled area and the alteration aureole for at least 0.5km from the orebody. Anomalous values for other elements (Hg, Rb, Sr, Ba and Cl) are confined mainly to the orebody, or occur within the alteration envelope (Fig. 44a). Distribution of positive scores of Factor 4 (Cu, S, Mo vs Na) is almost as extensive as that of anomalous Cu and S, whereas positive scores of Factor 2 (K, Rb vs Ca, Tl) and Factor 3 (Hg, Cl vs B) are confined to the mineralized zone (Fig. 44b).

VALLEY COPPER

Means, standard deviations and ranges of element concentrations in the Suboutcrop, 3600 and 3300 levels are recorded in Table XXXII and Figs. A31 to A55. However, because of similarity in metal distribution at the three levels, only data for the 3600 level are discussed. At Valley Copper, there is only one major host rock - Bethsaida granodiorite. Although variations in modal proportions of rock constituents can slightly influence metal concentrations, this parameter cannot be documented mineralogically or by major element analysis because of alteration effects. Hence,

FIGURE 44b: Schematic diagram showing distribution of factor scores, Bethlehem-JA 2800 Level

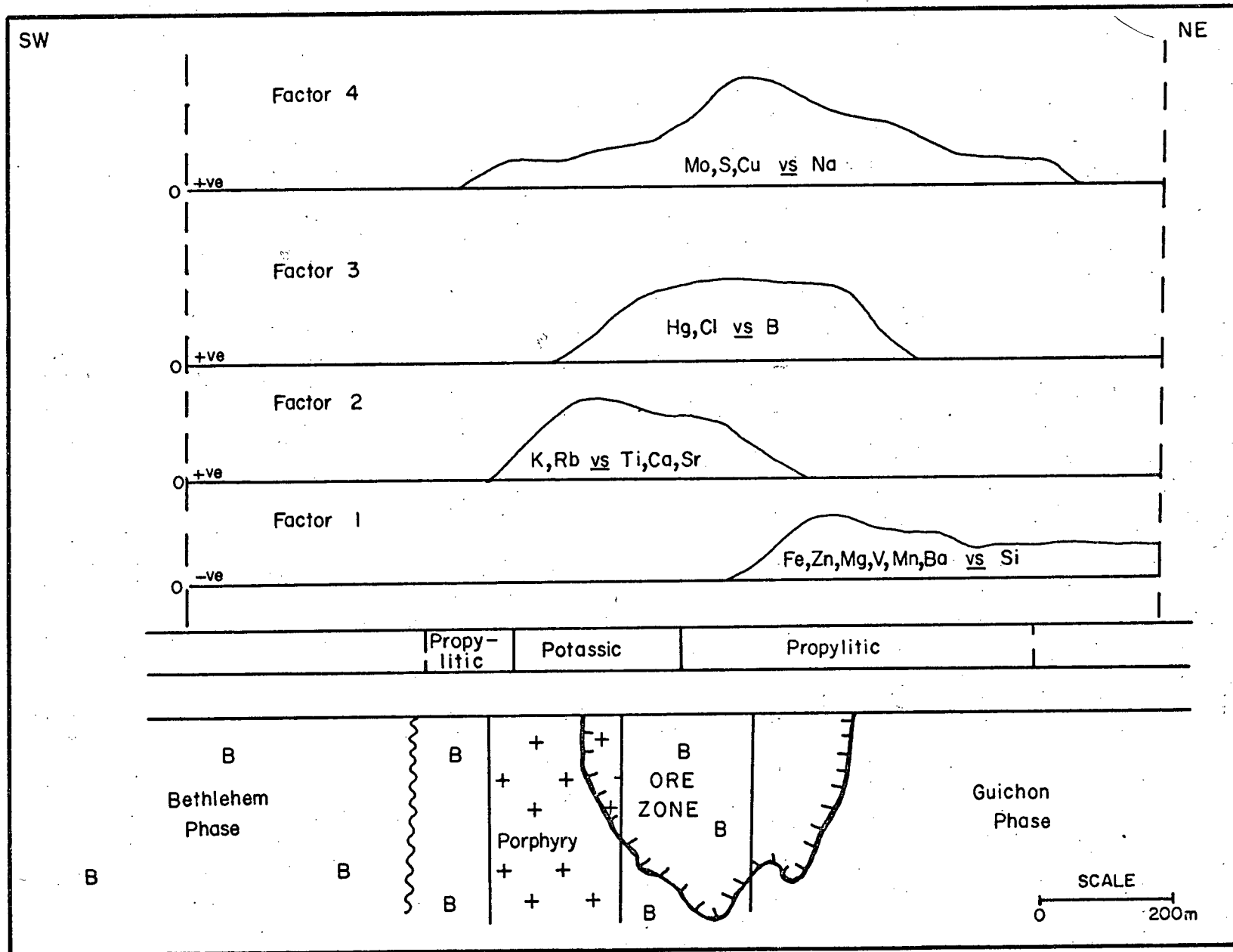


TABLE XXXII: ⁴ Means, deviations and ranges of trace and major elements at Valley Copper (Values in ppm except where indicated)

Elements	Analytical Technique	VALLEY COPPER		
		Number of samples		
		(61) Suboutcrop level	(59) 3600 level	(41) 3300 level
¹ Cu	AA	2115 3.5 607-7370	1936 3.7 526-7120	1482 4.7 314-6996
³ Sulphide Cu	AA		2194 3.6 619-7773	
^{3*} Sulphide Fe	AA		0.54 0.17 0.36-0.72	
¹ Mo	ES	4 5.2 0.87-23	5 4.9 0.93-23	3 4.3 0.78-15
¹ Ag	AA	0.18 2.9 0.06-0.54	0.21 3.1 0.07-0.68	0.23 1.7 0.07-0.77
¹ Zn	AA	18 1.5 12-28	19 2.3 8-45	15 1.8 8-27
¹ Mn	AA	224 1.6 139-362	223 1.8 130-384	225 1.4 164-309
¹ Co	AA	- - -	- - -	- - -

TABLE XXXII: (cont.)

		VALLEY COPPER		
		Number of samples		
Elements	Analytical Technique	(61) Suboutcrop level	(59) 3600 level	(41) 3300 level
V	ES	28 1.3 21-38	29 1.4 21-41	29 1.4 21-41
Ti	ES	948 1.5 613-1467	976 1.4 690-1377	910 1.5 619-1337
*S	XRF		0.45 2.61 0.17-1.16	
**Hg	AA		2.4 2.9 0.83-7.16	
B	ES	8 1.7 5-14	8 1.7 4-13	7 1.6 4-11
Cl	ISE	(GM)	240 1.4 173-333	
H ₂ O-Ex. Cl	ISE		2.3 1.8 1.3-4.3	
F	ISE		1.392 1.4 272-564	
H ₂ O-Ex. F	ISE		5.2 1.5 3.5-7.7	
Rb	XRF		59 1.2 48-73	

TABLE XXXII: (cont.)

		VALLEY COPPER		
		Number of samples		
Elements	Analytical Technique	(61) Suboutcrop level	(59) 3600 level	(41) 3300 level
Sr	XRF		562 1.8 304-1044	
Ba	Es	568 1.3 433-745	545 1.2 436-681	584 1.4 425-803
2* CaO	AA		1.95 0.80 1.14-2.75	
2* MgO	AA		0.42 0.11 0.31-0.53	
2 Total Fe as *Fe ₂ O ₃	AA		1.83 0.52 1.32-2.35	
2* Na ₂ O	AA		2.78 1.19 1.60-3.96	
2* K ₂ O	AA		2.78 0.71 2.07-2.50	
* SiO ₂	XRF		67.01 4.14 62.87-71.15	

1 HNO₃-HClO₄ digestion

2 Total digestion

3 KClO₃-HCl digestion

4 Geometric Means except where indicated

* Values in weight percent

* Arithmetic Mean

** Values in parts per billion.

AA = Atomic Absorption

ES = Emission Spectrography

XRF = X-Ray Fluorescence

ISE = Ion-selective electrodes

R = Range (Mean + standard deviation)

geochemical dispersion is discussed only in relation to hydrothermal alteration and mineralization.

(a) Geochemical Patterns Related to Hydrothermal Alteration

Variations in trace and major element contents are influenced by intensity and types of alteration; weak to moderate argillic at the periphery; intense potassic/phyllitic at the centre and northwest, and silicification at the southeastern sector of the property (see Fig. 16). Metal concentrations in relation to alteration types are summarized in Table XXXIII.

(i) Zn, Mn, Sr, Ba, MgO, Fe_2O_3 , CaO and Na_2O decrease progressively from the outer margins where argillic alteration (sericite-kaolinite) is dominant, to the central zone of intense phyllitic alteration (Figs. A32 - A41). The rate of metal depletion is highest for Mn, Sr, Na_2O and CaO (Table XXXIII). Mn distribution at the 3300 level is generally more uniform than at the 3600 level (Figs. A33 and A34). This corresponds to a decrease in intensity of hydrothermal alteration as the base of the orebody is approached. Although Ba and Sr both decrease from the periphery to core of the deposit, Ba/Sr ratios increase in the same direction (Fig. A36b); that is, the rate of Sr depletion is higher than that of Ba. The similarity in geochemical behaviour of Zn, Mn, MgO, Fe_2O_3 , Sr, CaO and Na_2O at Valley Copper is demonstrated by their significant positive correlations (Table XXXIV).

(ii) In contrast to the above elements, Rb and K_2O levels increase respectively from less than 51 p.p.m. and 1.8% at the

TABLE XXXIII: ¹Chemical variations associated with types of alteration,
Valley Copper 3600 level

	Unaltered Bethsaida Phase	Argillic Zone	Phyllic Zone	Potassic Zone	Quartz-rich Zone
No. of Samples	(6)	(11)	(12)	(10)	(7)
Metal Content (p.p.m.)					
Cu	² 19 (4 - 135)	506 (64 - 1000)	3869 (2300 - 6506)	2379 (877 - 6452)	1444 (597 - 3494)
Zn	³ 22 (11 - 32)	26 (7 - 101)	16 (7 - 37)	20 (15 - 26)	15 (10 - 23)
Mn	² 362 (290 - 420)	333 (218 - 508)	176 (78 - 397)	252 (160 - 398)	173 (132 - 229)
B	5	9 (4 - 19)	8 (5 - 13)	6 (4 - 9)	7 (4 - 12)
Ti	600 (400 - 700)	893 (703 - 1136)	1015 (685 - 1504)	1009 (681 - 1495)	1178 (827 - 1677)
V	15 (10 - 20)	24 (17 - 33)	31 (21 - 44)	34 (24 - 50)	24 (17 - 33)
Mo	2	6 (1 - 29)	7 (1 - 33)	5 (2 - 13)	5 (2 - 12)
Ba	520 (500 - 700)	556 (470 - 659)	481 (389 - 594)	564 (447 - 711)	535 (446 - 541)
Rb	35 (33 - 37)	57 (45 - 71)	69 (62 - 75)	61 (46 - 76)	45 (39 - 52)
Sr	588 (550 - 627)	641 (418 - 980)	396 (161 - 969)	617 (391 - 975)	529 (420 - 665)

(Cont. next page)

(Table XXXIII Contd)

*S	0.03 (0.27 - 0.37)	0.12 (0.04 - 0.38)	0.35 (0.18 - 0.68)	0.23 (0.08 - 0.69)	(0.13 (0.08 - 0.21)
**Hg	-	3 (1 - 8)	3 (1 - 8)	2 (1 - 4)	2 (1 - 4)
F	-	301 (219 - 415)	428 (334 - 547)	384 (257 - 573)	347 (236 - 510)
Cl	-	264 (207 - 335)	312 (233 - 418)	223 (186 - 276)	245 (174 - 344)

Metal Content (wt. %)

Fe ₂ O ₃	1.91 (1.34 - 2.30)	1.70 (1.32 - 2.07)	1.82 (1.28 - 2.35)	2.20 (1.73 - 2.67)	1.19 (0.92 - 1.46)
MgO	0.54 (0.40 - 0.82)	0.42 (0.30 - 0.53)	0.39 (0.28 - 0.51)	0.50 (0.36 - 0.65)	0.34 (0.28 - 0.41)
CaO	2.83 (2.16 - 2.98)	2.66 (1.67 - 3.64)	2.08 (1.34 - 2.81)	1.85 (1.39 - 2.30)	1.66 (1.15 - 2.16)
Na ₂ O	4.85 (4.55 - 5.31)	3.03 (1.24 - 4.82)	2.07 (1.34 - 2.81)	2.62 (1.95 - .04)	3.16 (2.69 - 3.62)
K ₂ O	1.90 (1.80 - 2.29)	2.44 (1.61 - 3.27)	3.26 (2.63 - 3.89)	3.05 (2.12 - 4.23)	2.08 (1.66 - 2.51)
SiO ₂	69.79 (68.61-70.88)	65.83 (62.98-68.68)	67.29 (62.51-72.09)	66.68 (63.82-69.53)	71.55 (69.29-73.81)

* Values in wt. %

** Values in p.p.b.

¹ Means and ranges (mean \pm 1 standard deviation)² HF-HClO₄ digestion³ Aqua regia digestion (Brabec, 1970)

outer margins of the property, to values exceeding 71 p.p.m. and 3.2% respectively at the central zone of intense phyllic/potassic alteration (Fig. A42 and A43). Rb/Sr ratios follow closely Rb distribution, although the anomalous zone is slightly displaced eastwards reflecting Sr dispersion (Fig. A44). Dependence of Rb concentrations on K abundance is demonstrated by a positive correlation ($r = 0.64$).

(iii) Although enhanced SiO_2 values ($>66\%$) occur in a broad central zone of the property, maximum values ($>70\%$) are associated with the zone of silicification (barren quartz veins) towards the southeast of the deposit (Fig. A45). This zone is also characterized by slightly lower Sr, MgO, Fe_2O_3 , Na_2O , K_2O and Rb than background areas (Table XXXIII).

(b) Geochemical Patterns Related to Mineralization

(1) Ore Elements (Cu, Fe, Mo, S)

Copper: (Figs. A46 - A48) A cumulative log probability plot of Cu in 161 samples (Fig. 45) shows that Cu distribution comprises two populations, A and B, in the proportion of 93 and 7% respectively; separated by a threshold value of 400 p.p.m. Mean values for populations A and B are 3162 and 25 p.p.m. respectively. Population B corresponds to local background, and is similar to the "low-copper" population obtained by Brabec (1970) for regional data. Its distribution though not symmetric, is confined to the periphery of the deposit. Population A corresponds to mineralization, and

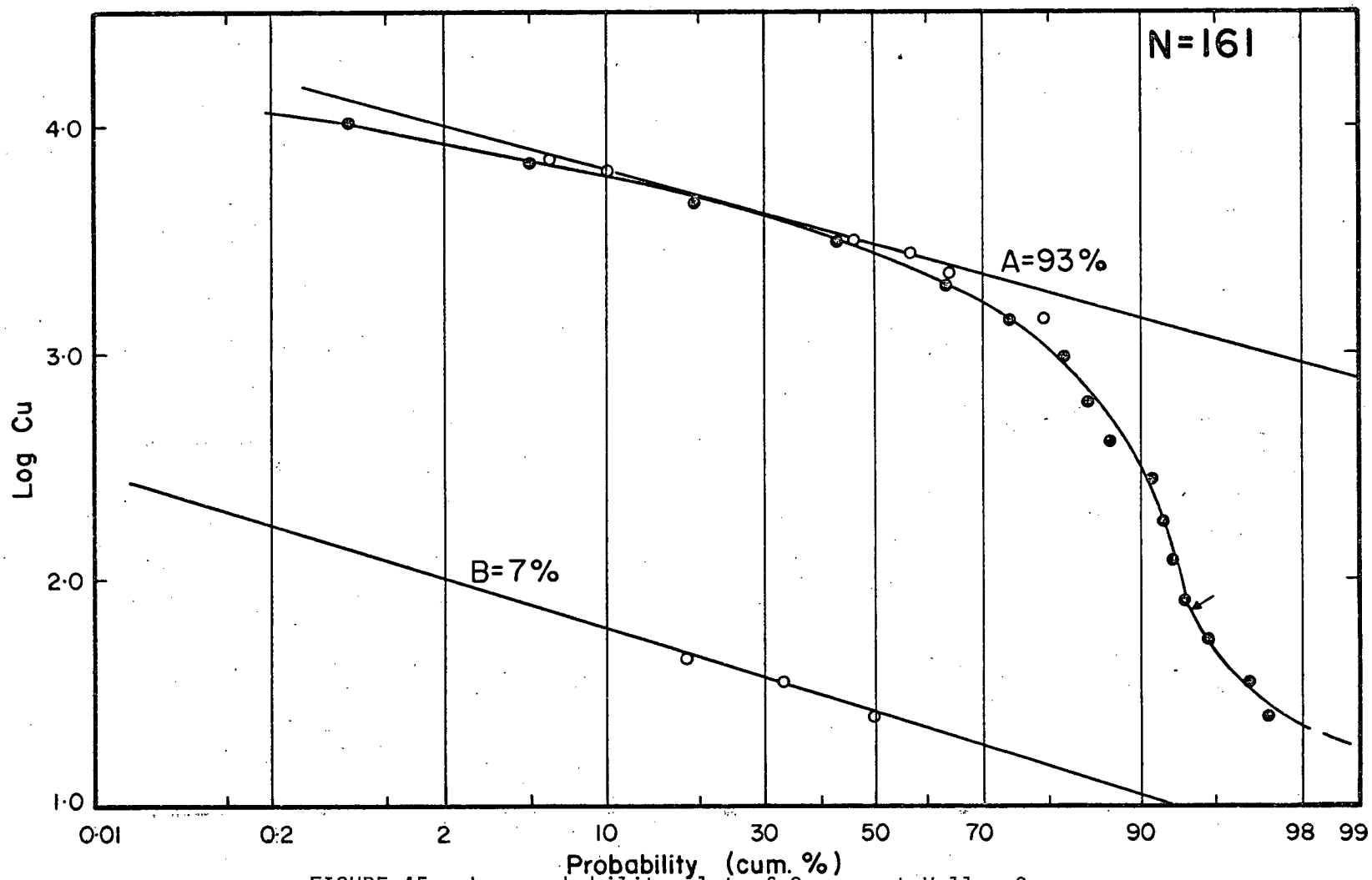


FIGURE 45: Log probability plot of Copper at Valley Copper.

is confined to the central mineralized zone (Figs. A46 - A48). As expected, sulphide Cu as determined by $\text{KClO}_3\text{-HCl}$ digestion is similar in distribution to "total" ($\text{HNO}_3\text{-HClO}_4$) Cu (Fig. A49). Relationship between Cu and quartz-sericite alteration is demonstrated by positive correlation between Cu and K_2O (Fig. 46).

Sulphide-held Fe: Abundance of sulphide Fe is generally low ($< 0.9\%$), reflecting the low content of sulphide-held Fe in bornite (Cu_5FeS_4) compared to high content in chalcopyrite (CuFeS_2) at Bethelhem-JA. Values exceeding 0.5% are confined to a linear belt in the northwest where pyrite and chalcopyrite are relatively abundant (Fig. A50). Within the ore zone, values are generally less than 0.3% .

Molybdenum: Although Mo distribution is erratic, enhanced values (> 23 p.p.m.) are confined principally to the borders of the Cu-rich zone (Fig. A51). This distribution suggests metal zoning that has not been disclosed by previous mineralogical studies.

Sulphur: Anomalous levels of S ($> 1\%$) occur in the northwest and eastern parts of the property, where chalcopyrite and pyrite are more abundant (Fig. A52), and coincide with enhanced levels of sulphide-held Fe. (See Fig. A50). The central part of the orebody, in which bornite predominates, is associated with relatively lower S values ($< 1\%$). Thus, in general, distribution of S is consistent with sulphide zoning patterns described in Chapter 3 (Fig. 16b).

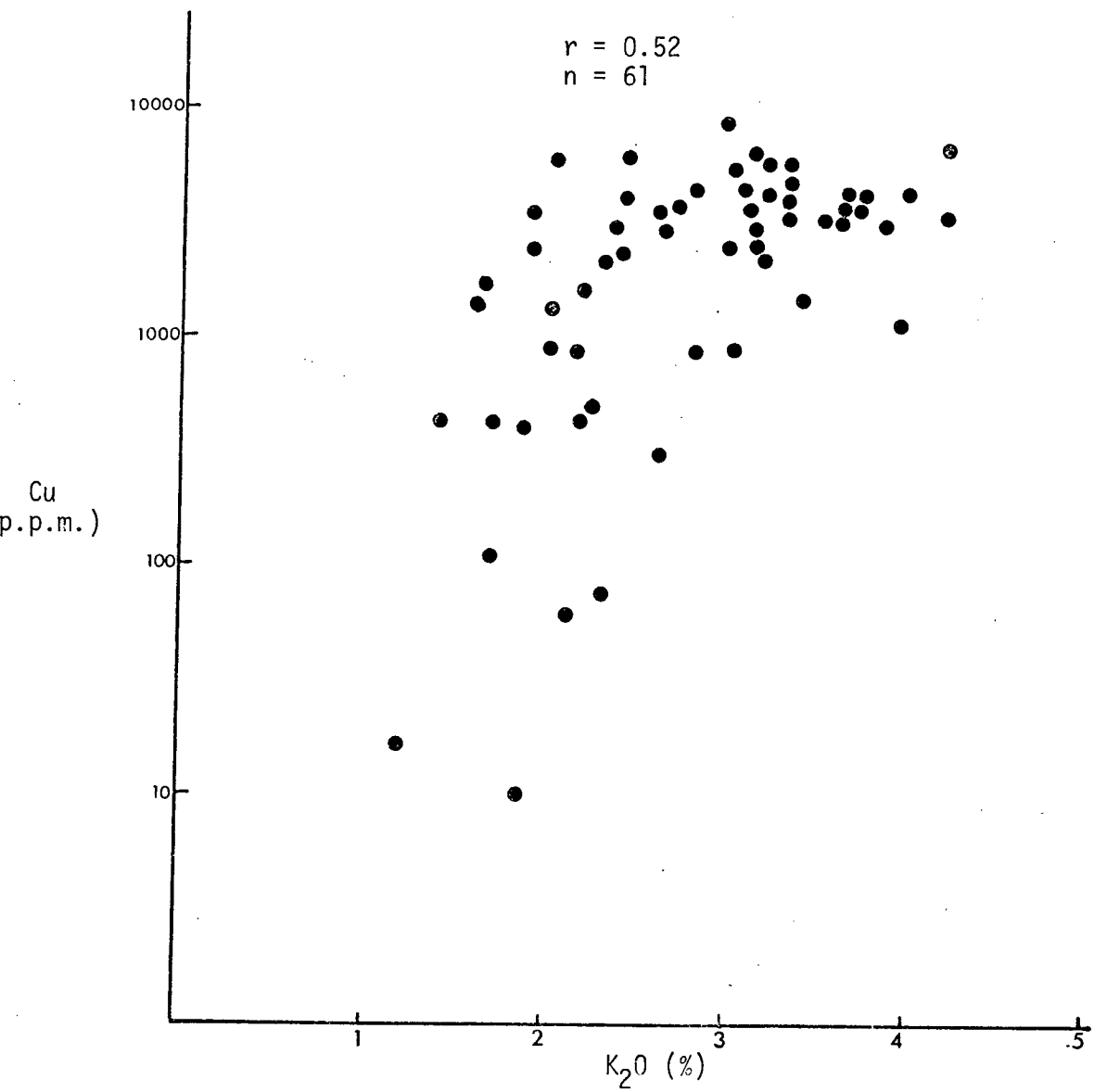


FIGURE 46: Relationship between Copper and Potassium at Valley Copper 3600 Level

(ii) Pathfinder Elements (Hg, B, Cl, F)

Hg values range from 1 to 52 p.p.b. and average 3 p.p.b. Only 6 out of 61 values exceed 7 p.p.b. (mean + 1 standard deviation), and no trends are apparent.

B dispersion is erratic, although values exceeding 11 p.p.m. are generally confined to the outer margins of the ore zone especially on the northwestern fringe (Fig. A53).

Cl levels do not show appreciable variations with most values lying in the range of 200 to 330 p.p.m. However, the few erratic values exceeding 330 p.p.m. are confined mainly to the ore-body (Fig. A54). Concentrations of water-extractable Cl range from 1-11 p.p.m. and average 2 p.p.m. High F values (> 564 p.p.m.) occur principally in the area immediately northwest of the ore zone (Fig. A55). Elsewhere F levels are less than 400 p.p.m. Water-soluble F ranges from 2 to 11 p.p.m. and average 5 p.p.m. No trends are evident and no obvious relationship exists between water-leachable F and total F, although a weak but significant positive correlation is apparent between water-extractable Cl and total Cl ($r = 0.32$).

(c) R-mode Factor Analysis

Results of R-mode analysis of 17 variables in 61 samples from the 3600 level are summarized in Tables XXXV and XXXVI and Figs. A56 and A59. Element associations of 3-, 4- and 5- factor models are compared in Table XXXV. These models account for 52, 61 and 66% of total data variability respectively. In view of known

TABLE XXXIV: Correlation Coefficients, Valley Copper 3600 Level (61 samples)

	Cu	Zn	Mn	Ti				
Cu	1.00111							
Zn	-.09361	1.00026						
Mn	-.39456	.33785	1.00040					
Ti	.01792	.15575	-.01470	1.00237	MO	RA	RB	SR
Ko	.24672	.05675	-.10567	.12393	.99541			
Za	-.14442	.12542	.14369	-.08094	-.04652	.99903		
Rb	.37740	.12089	.12647	.12232	.11787	-.27221	.99827	
Sr	-.26812	-.13824	.22664	-.19647	-.01470	.03285	-.29744	1.00064
SiO ₂	.09192	-.22788	-.70357	-.01000	.02269	-.20817	-.34770	-.22679
Sulphur	.31459	-.01684	.00612	-.13831	.27055	-.04437	.26239	.13736
CL	.16146	-.03333	-.21862	.00140	-.06280	-.13436	-.03408	-.27440
Fluorine	.28018	.09258	.09167	.11768	.11324	-.13848	.22627	.00918
CaO	-.38200	.19159	.77431	-.04650	.06439	.13281	.07514	.29501
MgO	-.13108	.43593	.44522	.09750	-.00056	.19606	.11181	.20758
Fe ₂ O ₃	.13128	.42963	.46563	.04807	.17619	.12471	.31695	.13936
Na ₂ O	-.42909	-.00011	.08870	-.22651	-.17826	.23922	-.60460	.31261
K ₂ O	.51606	.19298	-.08456	.04022	.09952	-.18691	.63246	-.08751
	SiO ₂	Sulphur	CL	F				
SiO ₂	1.00083							
Sulphur	-.28130	1.00061						
CL	.24300	-.19320	.99923					
Fluorine	-.13977	.37444	-.29287	.99867	CAO	MGO	FE ₂ O ₃	Na ₂ O
CAO	-.60646	.20511	-.32643	.14866	.99892			
MgO	-.38657	-.5547	-.22062	.20122	.28790	.99969		
Fe ₂ O ₃	-.59311	.31720	-.31070	.36293	.25726	.68561	.99975	
Na ₂ O	-.00597	-.13928	-.09350	-.21901	-.03647	.07204	.05967	.99807
K ₂ O	-.13096	.32400	-.04018	.33291	-.14842	.18374	.31122	-.59873

TABLE XXXV: Element associations of different factor models, Valley
Copper 3600 level.

FACTOR	FACTOR MODEL		
	3	4	5
1	Mn	Ca	Ca
	Fe	Mn	Mn
1	Ca	Sr	<u>vs</u>
	Mg	<u>vs</u>	Si
	Zn	Si	Cu
	<u>vs</u>	Cu	
	Si		
2	Cu	S	K
	S	Cu	Rb
	K	F	<u>vs</u>
	F	Fe	Sr
		K	
3		<u>vs</u>	
		Cl	
	K	Rb	S
	Rb	K	F
	<u>vs</u>	<u>vs</u>	<u>vs</u>
4	Sr	Na	Cl
	Na	Sr	
		Zn	Mg
		Mg	Fe
		Fe	Zn
5			Mo
			Ti

TABLE XXXVI: Varimax Factor Matrix, Valley Copper, 3600 Level

Variable	FACTOR 1	FACTOR 2	FACTOR 3	FACTOR 4	COMMUNALITY
Cu	-0.4396	0.6129	0.3939	-0.0249	0.7247
Zn	0.1376	-0.0433	0.0731	0.7799	0.6344
Mn	0.8817	-0.0974	-0.0308	0.2886	0.8712
Ti	-0.1100	-0.0979	0.2767	0.3549	0.2242
Mo	-0.1179	0.4091	0.0798	0.0432	0.1895
Ba	0.0521	-0.0201	-0.4616	0.3409	0.3324
Rb	0.2005	0.2619	0.8052	0.1306	0.7742
Sr	0.4066	0.2640	-0.5078	-0.2458	0.5532
Si	-0.7828	-0.2050	-0.0799	-0.2546	0.7261
S	0.1814	0.7053	0.1172	-0.1401	0.5637
Cl	-0.2723	-0.5516	0.2713	-0.0357	0.4533
F	0.1025	0.6063	0.1730	0.1132	0.4208
Ca	0.8951	0.300	-0.0395	0.0028	0.8035
Mg	0.3378	0.2216	-0.1445	0.7045	0.6804
Fe	0.3661	0.5153	-0.0237	0.6328	0.8006
Na	0.0186	-0.1440	-0.8426	0.0523	0.7337
K	-0.0686	0.4855	0.6273	0.1965	0.6726
Eigenvalue in %		30	24	26	20

geologic and mineralogic evidence, a 4- factor model is considered appropriate, although it does not account for a large proportion of the variance in Mo, Ti and Ba (Table XXXVI).

(i) Factor 1 (Ca, Mn, Sr vs Si, Cu)

This factor reflects argillic alteration. High factor scores coincide with the outer margins of the property which are relatively unmineralized and characterized by weak to moderate pervasive argillic alteration. In contrast, low scores occur in the central zone of intense quartz-sericite alteration and metallization (Fig. A56).

(ii) Factor 2 (S, Cu, F, Fe, K vs Cl)

Association of Cu and S suggests an "ore factor". However, high factor scores are concentrated along a curved belt immediately north and northwest, and on the fringes of the orebody, where a chalcopyrite/pyrite zone in conjunction with K-feldspar alteration is dominant (see Figs. 16, A50 and A52). Low scores are found in the centre of the orebody where bornite is the dominant sulphide, and in the barren quartz zone to the southeast (A57).

(iii) Factor 3 (Rb, K vs Na, Sr)

This factor reflects potassic alteration. High scores are confined to the central and northwest parts of the deposit (Fig. A58). In contrast, low scores occur at the outer margins especially in the west, and in the southeast where barren quartz veins are conspicuously developed.

(iv) Factor 4 (Zn, Mg, Fe)

The significance of this factor which associates the femic elements (Zn, Mg, Fe) is not well understood. High scores occur along a linear belt immediately north and within the ore zone, whereas low scores are confined to the centre and southeast. Distribution of this factor closely follows that of Zn (Fig. A32). However, its association with Mg and Fe most probably reflects the distribution of secondary biotite which is known to occur in the northern fringes of the orebody, although its detailed distribution has not been documented.

(d) General Discussion and Summary

Results indicate that Zn, Mn, Sr, Ba, Mg, Fe, Ca and Na generally decrease from the outer margins to core of intense alteration and metallization. In contrast, Rb and K are enriched in the central zone of potassic/phyllitic alteration. Enhanced Si and impoverished Sr, Ba, Mg, Fe, Na, K and Rb are characteristic of the silicified zone in the southeast. The apparent depletion of 'femic' and lithophile elements in zones of intense phyllic and argillic alteration is attributed to the breakdown of biotite and plagioclase into sericite and kaolinite. The base elements are leached and transferred to the outer margins of the deposits by outward-migrating solutions.

Maximum levels of Cu are associated with the central zone of intense mineralization, whereas high S and sulphide-selective Fe are confined to the northwest rim of the deposit where pyrite and

TABLE XXXVII: Comparison of ¹mean element content in background and mineralized samples, Valley Copper 3600 level.

No. of Samples	Regional Background (Bethsaida) (9)	Local Background (Bethsaida) (10)	Mineralized Zone (12)	³ Contrast (Regional)	³ Contrast (Local)
Cu	19	265	4580	241	17
Mo	2	7	9	4.5	1.3
S	322	830	2930	9	3.5
Hg	*	3 p.p.b.	3 p.p.b.	-	1
B	5	9	7	1.4	** 1.3
Cl	*	265	288	-	1.1
F	*	310	413	-	1.3
Rb	35	54	66	1.9	1.3
Sr	588	642	462	** 1.3	** 1.4
Ba	520	556	514	** 1.0	** 1.1
Zn	22	21	14	** 1.6	** 1.5
Mn	362	337	155	** 2.3	** 2.1
² K ₂ O	1.90	2.29	3.09	1.6	1.3
² Na ₂ O	4.35	3.28	2.03	** 2.1	** 1.6
² CaO	2.83	2.47	1.42	** 2.0	** 1.7
² Fe ₂ O ₃	1.91	1.68	1.85	** 1.0	1.0

* Regional data inadequate

** Negative contrast

¹ Geometric means and values in p.p.m. except where indicated.

² Arithmetic means and values in wt. %.

³ Contrast = Anomalous/Background

chalcopyrite are most abundant. Contrary to expectations, Hg and Cl do not show anomalous patterns at Valley Copper. B and F are generally erratic, although high values occur within the ore zone. Results of factor analysis are consistent with subjective interpretations of metal associations in relation to geologic processes.

Geochemical contrast between background and anomalous samples is summarized in Table XXXVII. Regional background comprises fresh Bethsaida samples collected by Northcote (1968). Local background consists of samples at the periphery of the deposit. Relative to regional and local background, Cu and S show the best contrast, whereas B and Hg show no contrast. Relatively pronounced negative contrast is shown by Sr, Na and Ca, and positive contrast for Rb and K. Although, both Cu and S are generally erratic, Cu shows a greater variation as reflected by their coefficients of variation, (Cu = 1.12; S = 0.77). Compared with regional background data, it is apparent that halos of Cu and S extend beyond the sample area and at least 0.5 km from the ore zone on all sides; and also extend beyond the alteration aureole. In contrast the halos of the other elements are of limited extent (Fig. 47a). Negative scores of Factors 1 (Ca, Mn, Sr vs Si, Cu), 2 (S, Cr, F, Fe, K vs Cl) and positive scores of Factor 3 (Rb, K vs Na, Sr) extend beyond the ore zone and as far as the periphery of the alteration envelope (Fig. 47b)

LORNEX

Results for surface and drill-core samples are presented

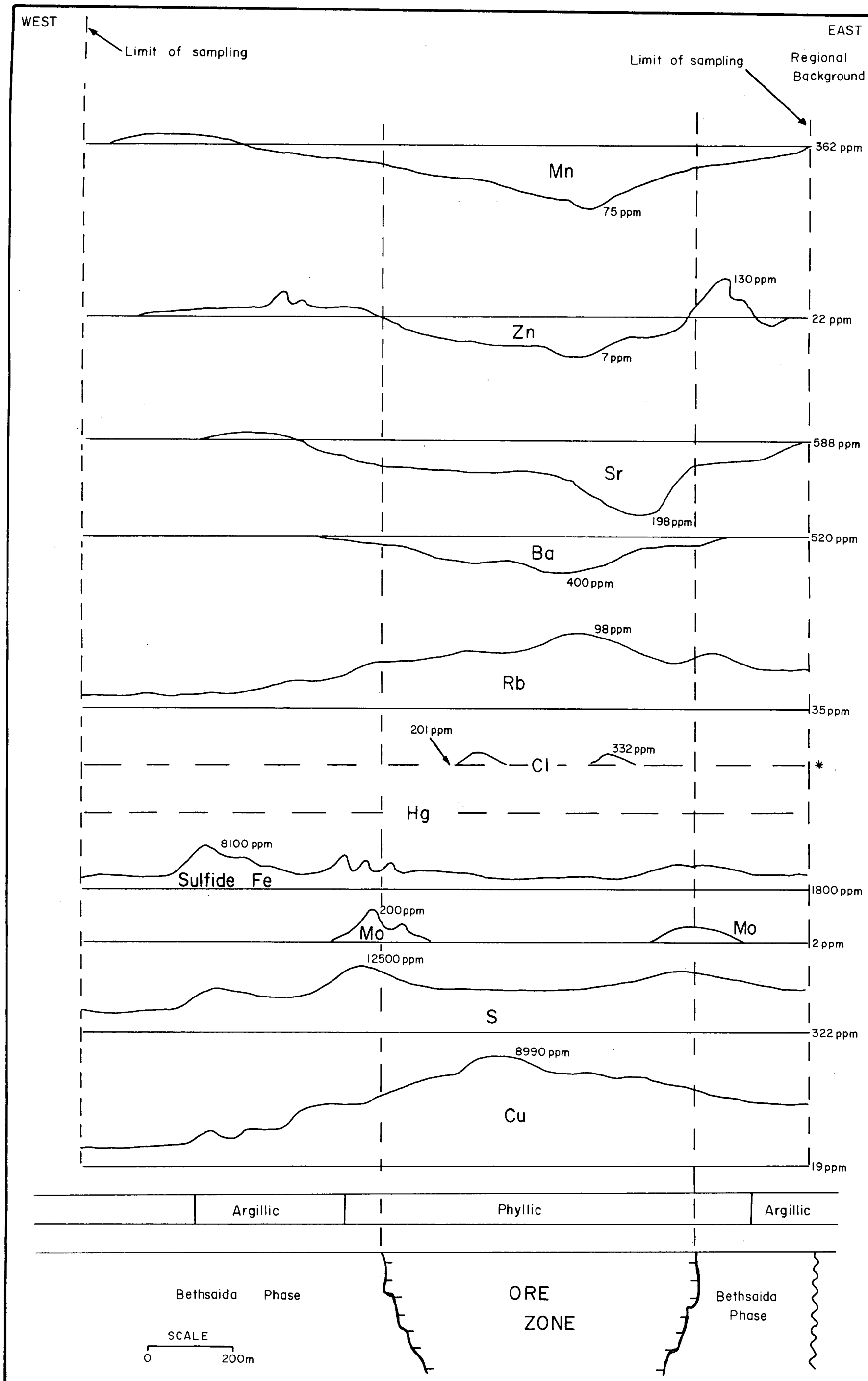


FIGURE 47a : Schematic diagram showing extent and relative intensity of primary halos, Valley Copper 3600 Level (*Regional data inadequate)

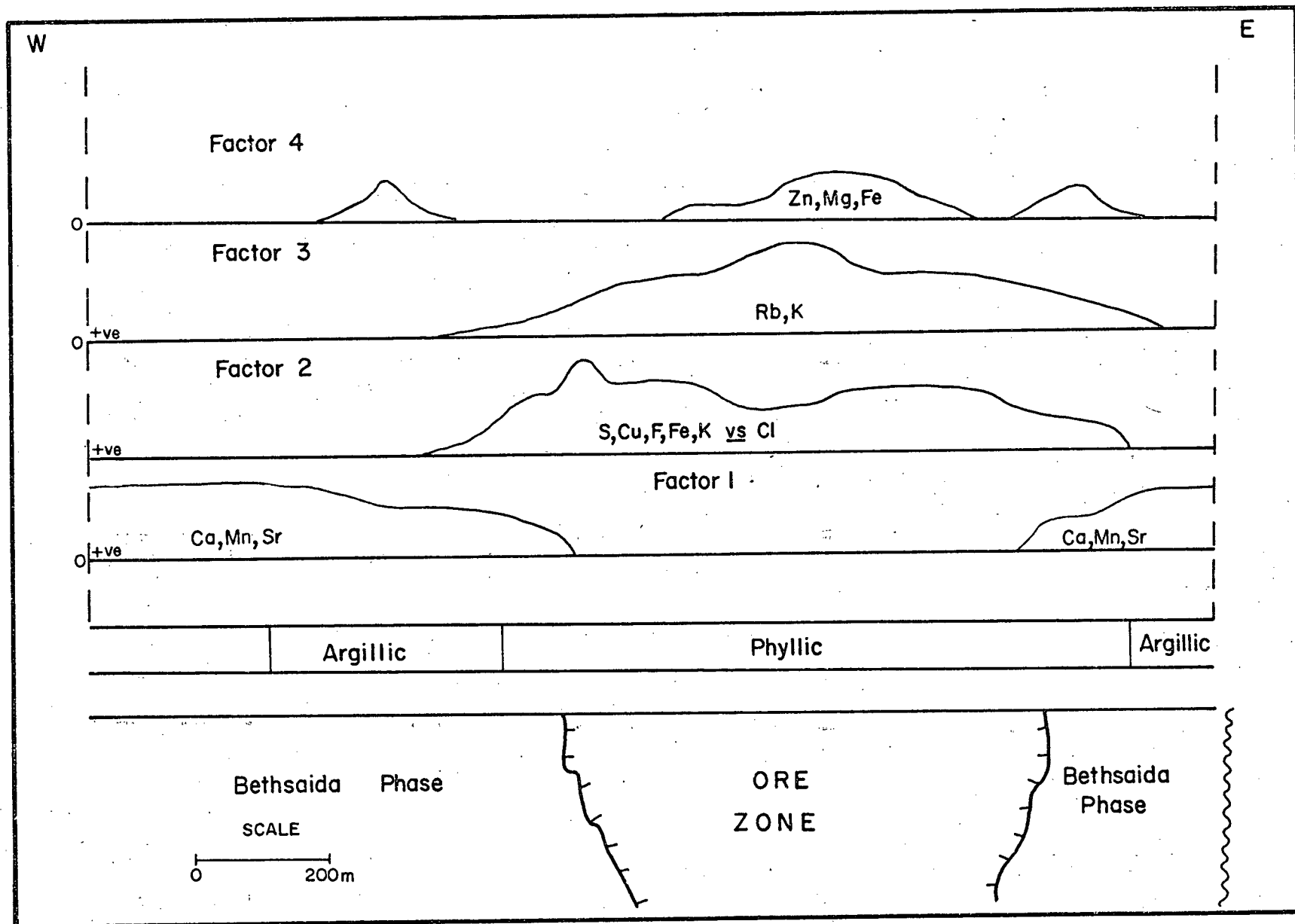


FIGURE 47b: Schematic diagram showing distribution of factor scores, Valley Copper, 3600 level.

TABLE XXXVIII: *Means and ranges of trace and major elements, Lornex property.

No. of samples	Surface Samples	Subsurface Samples	All Samples
	(103)	(85)	(188)
Metal Content (p.p.m)			
Cu	44 (4 - 456)	978 (75 - 12655)	180 (10 - 3200)
Zn	23 (14 - 36)	35 (12 - 105)	27 (12 - 64)
Mn	240 (160 - 359)	260 (91 - 742)	249 (116 - 534)
B	8 (4 - 16)	16 (8 - 31)	10 (5 - 24)
Sr	573 (394 - 835)	458 (283 - 742)	518 (333 - 806)
Ti	780 (473 - 1284)	1138 (783 - 1653)	925 (570 - 1501)
V	28 (18 - 43)	33 (18 - 59)	31 (19 - 49)
Mo	3 (1 - 8)	9 (2 - 51)	3 (1 - 19)
Ba	461 (307 - 694)	420 (244 - 722)	443 (275 - 711)
Metal Content (wt. %)			
Fe ₂ O ₃	1.85 (1.16 - 2.54)	1.85 (0.74 - 2.96)	1.85 (0.95 - 2.75)
CaO	2.99 (2.29 - 3.69)	2.27 (0.90 - 3.64)	2.66 (1.65 - 3.78)
Na ₂ O	3.71 (2.98 - 4.44)	2.49 (1.38 - 3.60)	3.16 (2.06 - 4.26)
K ₂ O	1.47 (0.92 - 2.01)	1.95 (1.34 - 2.55)	1.68 (1.06 - 2.31)

* Geometric means, except for major elements.

in Figs. A57 to A71 and Table XXXVIII. Apparently, half of the surface samples are fresh and unmineralized, whereas the remainder (51 samples) are weakly altered samples collected from the periphery of the Lornex orebody and from the sub-economic deposit (Discovery Zone) south of the main orebody (see Appendix). The latter group of samples are designated "mineralized surface" samples, in contrast to mineralized subsurface (drill-core) samples. B, Sr, Ti, V, Mo and Ba were determined by semi-quantitative emission spectrography; Cu, Zn, Mn, Ag, Pb, Ca, Cd and Ni by atomic absorption (HNO_3 - HClO_4 digestion); and Ca, Fe, Na and K by atomic absorption analysis of HF - HClO_4 digests, using the 'rapid teflon tube' procedure. Sample locations and plans are presented in the Appendix.

(a) Geochemical Patterns Related to Lithology

Variations in Ti, V, Fe_2O_3 , CaO, Ba, Na_2O and K_2O in unmineralized surface samples at Lornex are principally related to variations in abundance of ferromagnesian minerals and feldspars. Rocks of the Skeena Phase in the eastern part of the property are enhanced in Ti, V, Fe_2O_3 and CaO (Table XXXIX), which reflects the greater abundance of femic minerals and the more calcic plagioclase composition. In contrast, rocks of the Bethsaida Phase are characterized by higher concentrations of Na_2O , K_2O and Ba. A plot of Ba versus K_2O shows a strong positive relationship (Fig. 48). However, surprisingly, Mn shows a negative correlation with Fe_2O_3 . (Fig. 49). This relationship is attributed to the abnormally high

TABLE XXXIX: *Means and ** ranges of metal concentrations in Lithologic units, Lornex Surface (unmineralized).

No. of samples	Skeena Phase	Bethsaida Phase
	(19)	(33)
Metal content (p.p.m.)		
Cu	13 (3 - 60)	14 (3 - 58)
Zn	20 (15 - 26)	20 (16 - 25)
Mn	172 (132 - 226)	266 (213 - 330)
Sr	597 (466 - 764)	606 (466 - 788)
Ti	728 (512 - 1036)	533 (318 - 820)
V	33 (26 - 42)	17 (13 - 23)
Ba	428 (290 - 632)	510 (365 - 712)
Metal content (wt. %)		
Fe ₂ O ₃	2.12 (1.46 - 2.77)	1.47 (1.31 - 1.64)
CaO	3.50 (2.97 - 4.02)	2.68 (2.20 - 3.15)
Na ₂ O	3.70 (3.34 - 4.05)	4.05 (3.75 - 4.35)
K ₂ O	1.13 (0.55 - 2.29)	1.42 (0.82 - 1.82)

* Geometric means, except for major elements

** Mean \pm standard deviation.

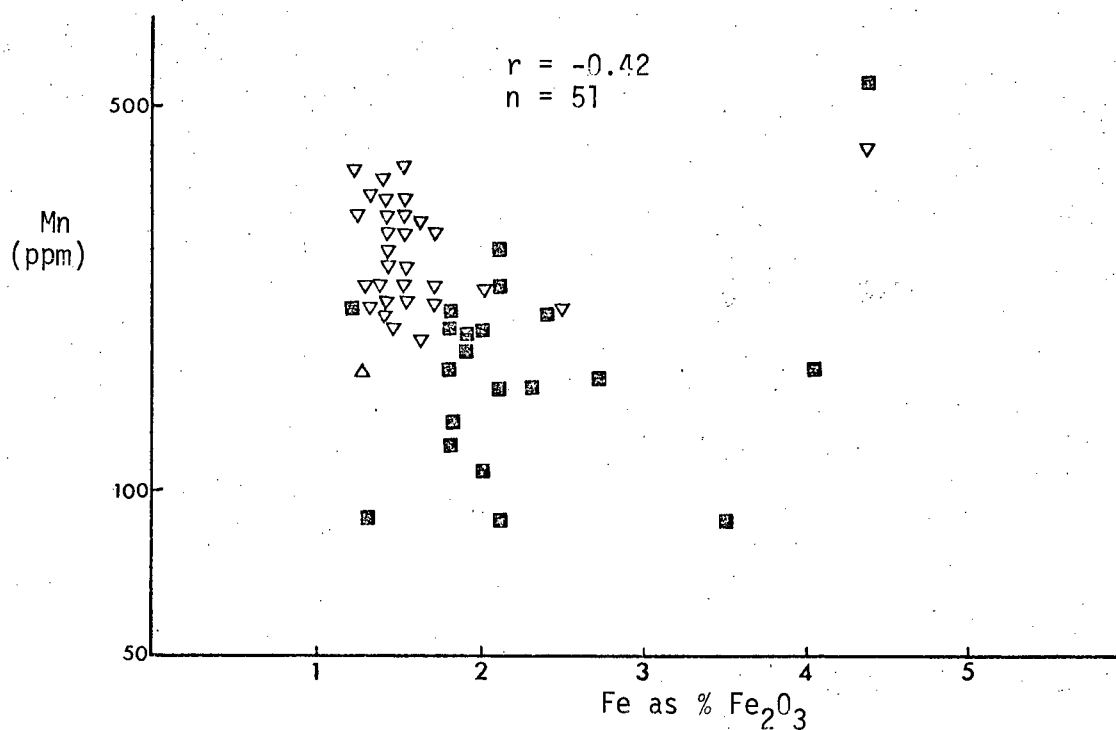


FIGURE 49: Manganese versus Iron in unmineralized samples, Lornex Surface.

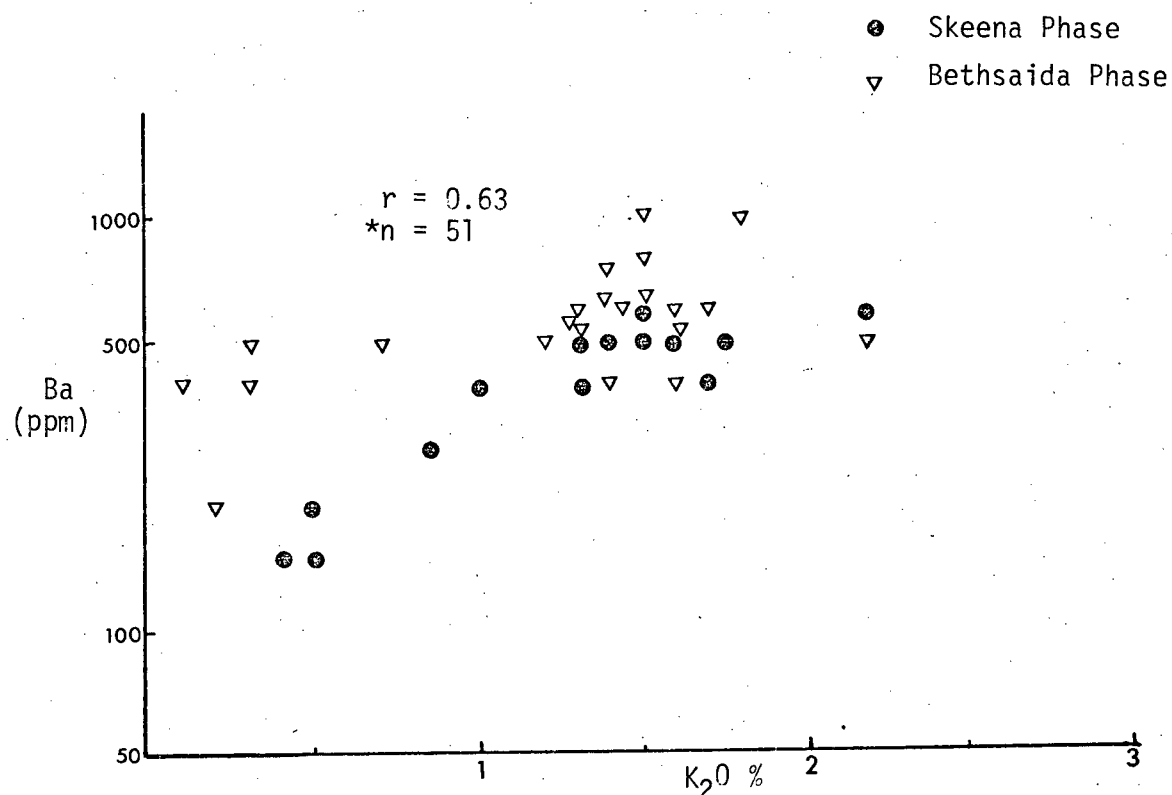


FIGURE 48: Plot of Barium versus Potassium in background samples, Lornex Surface.
(*several samples plot at the same point)

concentrations of Mn in biotite of Bethsaida Phase (Chapter 7, Table LIX). A student t-test suggests that, at the .05 confidence level, significant difference exists between fresh Skeena and Bethsaida Phases in Mn, Ti, V, Ba, Fe_2O_3 , CaO and Na_2O , but no significant difference in Cu, Zn, Mo, Sr and K_2O . Metal concentrations in fresh Skeena and Bethsaida within Lornex property do not differ appreciably from regional data.

(b) Geochemical Patterns Related to Hydrothermal Alteration

Effects of hydrothermal alteration are most evident in drill-core samples which penetrate the ore zone, and to a lesser extent in mineralized surface samples. Table XL shows the concentrations of trace and major elements in relation to alteration types. Zn, Mn and Fe_2O_3 levels in surface samples are relatively enriched in the propylitic zone at the periphery of the deposit relative to background Skeena rocks to the east (Figs. A60b, A61b & A62b) in pocket). The enhanced trace-element values are attributed to substitution for Fe in chlorite, epidote pyrite and siderite, that are relatively abundant in this zone. In contrast to the above distribution, the Discovery Zone lying south of the main orebody is characterized by lower values because of the felsic composition of the porphyry host rock and argillic alteration. The relationships between Zn and Mn, and Fe_2O_3 are demonstrated by positive correlations. (Zn and Fe_2O_3 , $r = 0.52$; Mn and Fe_2O_3 , $r = 0.48$). Ba, Sr and K_2O do not show systematic variations related to alteration in surface samples.

TABLE XI: *Means and **ranges of element abundances associated with alteration types, Lornex Subsurface.

No. of samples	Unaltered Skeena Phase	Propylitic Zone	Propy-Argillic Zone	Argillic Zone	Phyllic Zone
	(6)	(15)	(15)	(20)	(8)
Metal content (p.p.m.)					
Cu	1 26 (9 - 45)	999 (245 - 4065)	2754 (1462 - 5186)	3501 (2250 - 5448)	752 (54 - 10314)
Zn	2 19 (22 - 35)	40 (17 - 92)	38 (26 - 56)	22 (12 - 40)	23 (12 - 32)
Mn	1 312 (250 - 340)	275 (166 - 453)	201 (135 - 298)	229 (116 - 451)	218 (104 - 436)
B	5 -	10 (5 - 20)	14 (7 - 28)	17 (10 - 30)	30 (19 - 48)
Sr	653 (625 - 680)	490 (298 - 807)	432 (299 - 625)	520 (300 - 900)	252 (180 - 353)
Ti	1000 (900 - 1200)	978 (734 - 1303)	1275 (917 - 1772)	1473 (1053 - 2060)	944 (595 - 1496)
V	.35 (30 - 40)	32 (26 - 38)	36 (25 - 52)	44 (35 - 56)	14 (3 - 62)
Mo	2 -	5 (1 - 21)	8 (3 - 22)	14 (35 - 56)	10 (3 - 32)
Ba	550 (500 - 600)	528 (381 - 732)	485 (324 - 727)	317 (234 - 585)	371 (267 - 515)
Metal content (wt. %)					
Fe ₂ O ₃	2.98 (2.80 - 3.47)	3.09 (2.57 - 3.61)	1.83 (1.31 - 2.34)	1.49 (1.14 - 1.85)	1.68 (1.03 - 2.34)
CaO	3.84 (3.73 - 3.91)	2.48 (1.97 - 2.98)	1.69 (0.81 - 2.56)	2.60 (0.83 - 4.37)	1.06 (0.53 - 1.60)
Na ₂ O	4.78 (4.38 - 5.19)	2.80 (1.89 - 3.71)	2.83 (2.21 - 3.46)	2.56 (1.65 - 3.46)	1.30 (0.1 - 2.60)
K ₂ O	1.73 (1.30 - 1.96)	1.79 (1.41 - 2.18)	2.05 (1.36 - 2.74)	1.93 (1.34 - 2.51)	3.52 (2.76 - 4.26)

* Geometric means, except for major elements

** Mean \pm 1 standard deviation

¹ HF-HClO₄ digestion: ² Aqua regia digestion (Brabec, 1970)

In subsurface samples, Zn and Fe_2O_3 values decrease westwards from the eastern border of the orebody, and lowest values are attained in the zone of intense argillic, phyllic and potassic alteration close to the Lornex Fault (Figs. A60 and A61). Mn shows a slightly different distribution. Lowest values are encountered in a central zone (Holes 8, 9 and 10) where argillic alteration is prevalent (Fig. A62).

Sr distribution closely follows those of CaO and Na_2O in that highest values (> 600 p.p.m. Sr, $> 4\%$ CaO and $> 2.8\%$ Na_2O) are confined to Hole 10 where gypsum and quartz-carbonate-sulphide veins are relatively abundant. Lowest values of these elements are confined to the eastern periphery of the deposit and immediately east of Lornex Fault (Figs. A63a, A63b and A64). Ba distribution is similar to that of K_2O (Figs. A65a and A65b). Maximum values (> 800 p.p.m. Ba and $> 2.6\%$ K_2O) occur immediately east of Lornex Fault where K-feldspar veins are abundant, and in Holes 8 and 9 where sericite with muscovite is common.

(c) Geochemical Patterns Related to Lornex Fault

The north-trending Lornex Fault transects the Lornex property and extends for more than 16 km across the Guichon Creek batholith. Gouge zones associated with the fault are up to 100 m wide, adjacent to the Lornex orebody. Gouge samples collected from the fault were analyzed by X-ray diffraction, and results indicate that the dominant minerals are quartz and sericite. X-ray patterns suggest, but do not confirm, the presence of sphalerite.

There is no evidence of secondary coatings of Fe and/or Mn oxides.

Anomalous trace and major element patterns are associated with gouge samples from the Lornex Fault adjacent to the Lornex orebody (Table XLI). Many elements that are not abundant within the orebody are relatively enriched along the fault. Thus Zn values in excess of 1000 p.p.m. are common, in contrast to values of less than 30 p.p.m. immediately west of the fault (Fig. A60). Mn, Ag, Pb, Cd, Hg and CaO, and to a lesser extent Mo, are enriched in the fault gouge (Figs. A61, A66, A67, A68, A71 and A63). In contrast, Cu, Ni, Co and Fe_2O_3 do not show such enrichment. Fig. 50 shows that Hg closely follows Zn, probably in sphalerite. Samples collected from the fault gouge about 500m north of the orebody do not show anomalous metal concentrations, suggesting that the anomaly might be directly related to the Lornex orebody.

The Lornex Fault adjacent to Lornex orebody is unique in the Highland Valley for associated anomalous metal concentrations. This fault is a major crustal feature in the area (Ager *et al.*, 1973) and its influence on the localization of the Lornex and Valley Copper deposits can not be over-emphasized. Structural evidence (McMillan, 1971) suggests pre- and post- mineralization movements occurred along the fault. The present locations of the two deposits have been attributed to post-mineralization left-lateral movement on the fault (Carr, 1967). This contention is to some extent supported by the sharp truncation of geochemical anomalies by the fault in the Lornex property. Lack of Cu enrichment along the fault, suggests

TABLE XLI: Metal concentrations along the Lornex Fault.

	¹ Background Samples (15)		Lornex Fault Samples (10)	
	Means	Ranges	Means	Ranges
Metal content (p.p.m.)				
*Hg	6	4 - 12	145	26 - 784
Zn	20	17 - 23	449	121 - 1656
Ag	.01	-	0.24	0.16 - 0.35
Ni	2	1 - 3	1	-
Pb	1	-	167	57 - 490
Co	1	1 - 2	1	-
Cd	1	1	1	2 - 36
Mn	373	243 - 573	5022	1858 - 13573
Cu	12	8 - 15	27	14 - 52
B	9	4 - 18	38	22 - 63
Sr	606	438 - 838	270	174 - 417
Ti	809	583 - 1123	794	512 - 1229
V	24	18 - 32	6	2 - 24
Mo	2	1 - 2	10	4 - 24
Ba	682	395 - 1176	324	230 - 458
Metal content (wt. %)				
Fe ₂ O ₃	1.41	1.27 - 1.56	1.36	0.94 - 1.79
CaO	2.11	1.59 - 2.63	3.87	2.85 - 4.62
Na ₂ O	3.32	2.15 - 4.50	0.72	0.5 - 1.93
K ₂ O	1.51	1.27 - 1.75	2.48	1.87 - 3.09

* Values in p.p.b.

¹ Samples immediately west of fault

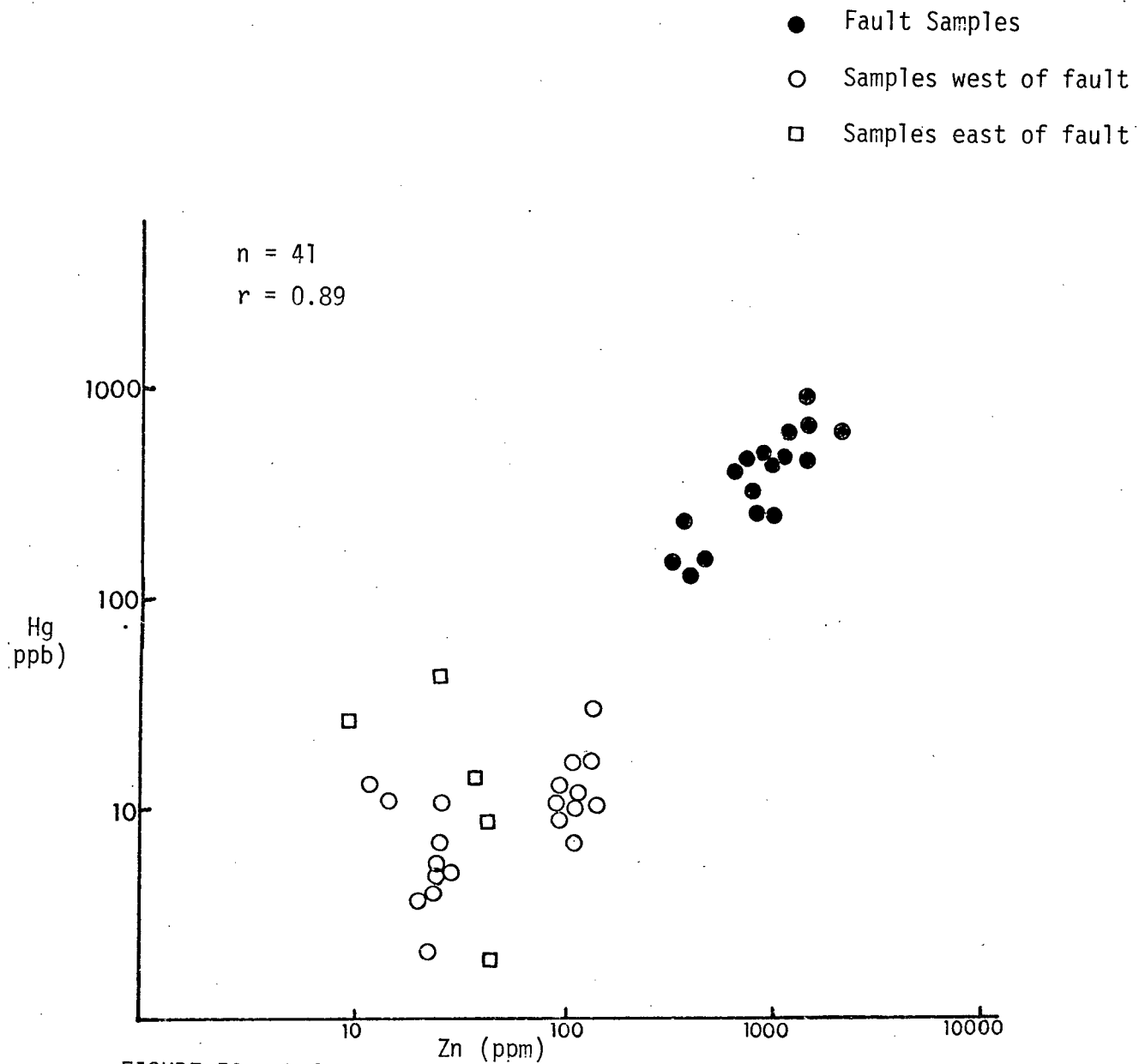


FIGURE 50: Relationship between Mercury and Zinc along Lornex Fault.

that anomalous metal values are not due to post-mineralization movement and crushing of sulphides within the fault zone. Because of appreciable vertical movement on the fault, the present surface represents a deeply-eroded level. On this basis, metal concentrations might represent; (1) a leakage halo, suggesting that the fault served as a pathway for upward migrating solutions; or (2) supergene concentrations by downward migrating surface waters. The latter is less likely since acid groundwaters should also have concentrated Cu and Fe as commonly characteristic of supergene enrichment in porphyry copper deposits in southwest U.S.A. Consequently, the anomaly along the Lornex Fault is believed to represent a leakage halo as defined by Hawkes and Webb (1962).

(d) Geochemical Patterns Related to Mineralization

Copper: Cumulative probability plot of Cu in 188 samples shows a characteristic curved pattern suggestive of a mixture of two lognormal populations A and B in proportion of 60 and 40% respectively (Fig. 51). The value separating the two populations is estimated as 75 p.p.m. The lower population (B) with a mean value of 6 p.p.m. represents background surface samples, especially rocks of the Bethesda Phase. The upper population, with a mean value of 1750 p.p.m. corresponds to mineralized subsurface and surface samples. The lower and upper populations correspond to the low-copper and high-copper populations of Brabec's (1970) regional data.

Cu content of surface samples east of Lornex deposit increases from less than 21 p.p.m. in background Skeena to enhanced

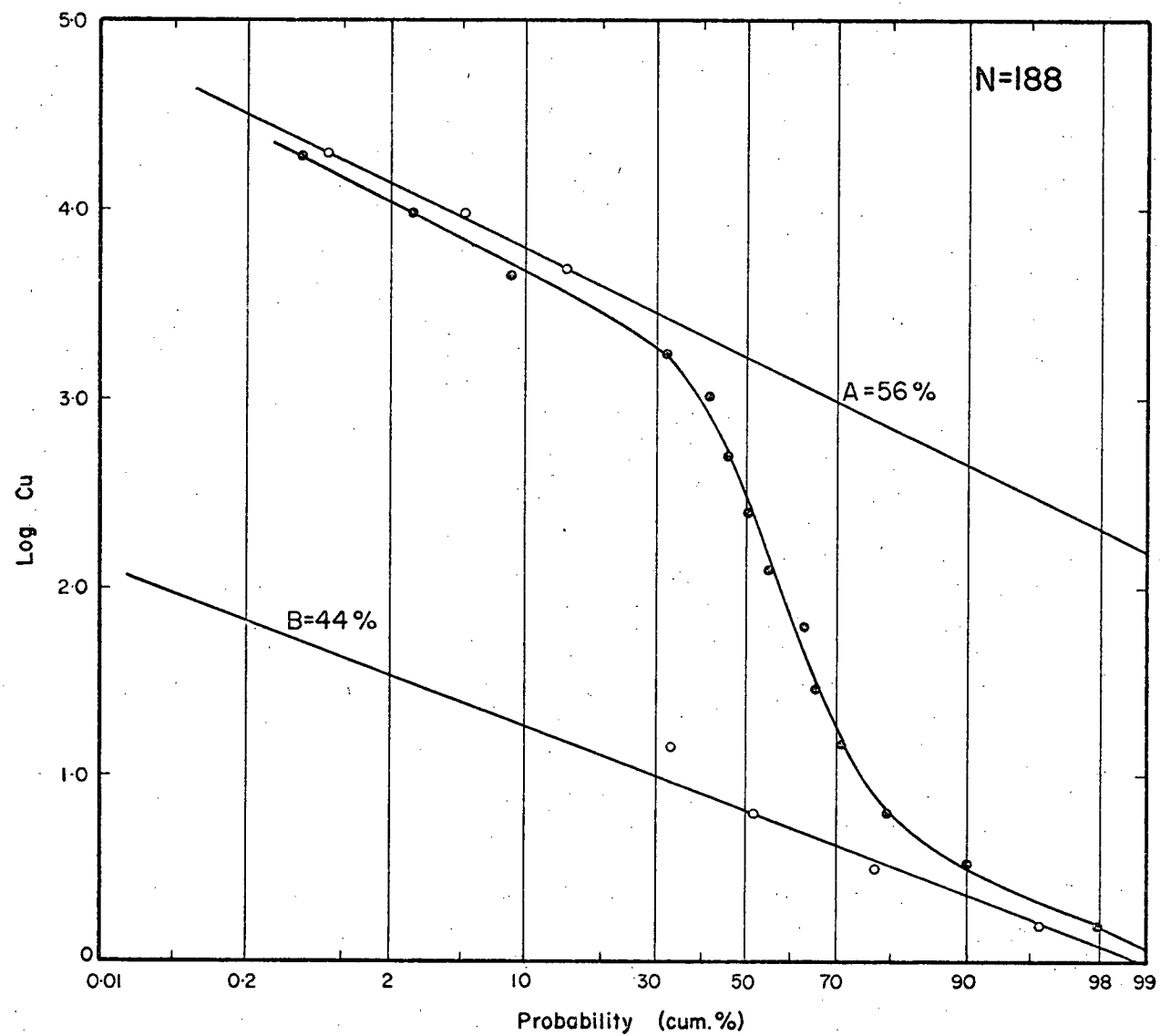


FIGURE 51: Log probability plot of Copper at Lornex.

values ranging from 80 to 2000 p.p.m. at the periphery of the ore-body (Fig. A69 in pocket). Near the Skeena Cu vein, values are generally background (3-24 p.p.m.) In contrast, to the above distribution, Bethsaida Phase rocks west of the Lornex Fault are characterized by low Cu values (< 21 p.p.m.). In subsurface samples, Cu abundance increases from less than 100 p.p.m. at the periphery of mineralization in the east, to values exceeding 5000 p.p.m. in the ore zone close to the Lornex Fault (Fig. A70).

Molybdenum: Except for a few erratic values exceeding 20 p.p.m. within the ore zone, Mo in surface samples is below detection limit (< 2 p.p.m.). In subsurface samples, high values (> 100 p.p.m.) are encountered in Hole 10. Elsewhere, values are generally less than 10 p.p.m. (Fig. A71a). Mo shows significant positive correlations with Cu ($r = 0.40$) and Fe ($r = 0.41$), reflecting their close association within the ore zone.

Other Elements: (Ti, V, B): Enhanced Ti (> 2000 p.p.m.) and V (> 50 p.p.m.) levels, relative to background values of less than 1000 and 30 p.p.m. respectively, are characteristic of the ore zone in Holes 12, 10 and 9. A significant correlation between V and Ti ($r = 0.45$) demonstrates their covariance. However, no overall significant relationship exists between Ti and Fe_2O_3 ($r = 0.09$), and only a weak one between V and Fe_2O_3 ($r = 0.37$). Nevertheless the positive relationships between Cu and V ($r = 0.49$) and Cu and Ti ($r = 0.38$) are significant. Enhanced levels of Ti and V are believed to be related to the occurrence of epigenetic magnetite whose occurrence

has been reported by McMillan (1972), although its detailed distribution has not been documented.

B content in surface samples east of the deposit generally increases westwards from values less than 5 p.p.m. to more than 50 p.p.m. at the periphery of the orebody (Fig. A71b, in pocket). Maximum value (400 p.p.m.) occur in two samples of quartz porphyry in the Discovery Zone. In drill-core samples, values ranging from 20 to 100 p.p.m. are common within the mineralized zone in Holes 12 and 10.

(e) R-mode Factor Analysis

Factor analysis was applied separately to 13 elements in 103 surface and 85 subsurface samples. A 3-factor model that accounts for 66% of total data variability was chosen for surface samples because of the apparent simplicity of metal distribution. Results are tabulated in Tables XLII and XLIII. Factor maps are not provided for surface samples. Element associations of 3-, 4- and 5- factor models for subsurface samples are recorded in Table XLIV. A 4-factor model that accounts for 71% of total data variance was chosen. Correlation coefficients and varimax factors matrix are recorded in Tables XLV and XLVI.

(i) Surface Samples

Metal associations of each factor are summarized as follows:

Factor 1: B, Mo, Cu vs Na, Sr

TABLE XLII: Correlation coefficients, Lornex Surface (103 samples)

	Zn	Mn	Cu	B	Sr			
Zn	1.00008							
Mn	.35471	1.00171						
Cu	.26211	.31128	.99973					
B	-.14621	.33697	.53366	.99982				
Sr	.24075	-.37264	-.47431	-.57135	.99751	Ti	V	Mo
Ti	.19533	.11540	.28962	.34636	.00363	1.00082		
V	.34466	.01381	.27183	.20152	.03148	.65622	.99727	
Mo	.01445	.22111	.62600	.61041	-.37531	.34175	.27803	1.00036
Ba	.12628	.14195	-.05715	-.23472	-.04336	-.09422	-.06181	-.27296
CAO	.43088	-.11792	-.08345	-.27365	.27002	.24147	.45437	-.24150
Fe ₂ O ₃	.14722	-.11821	-.29023	-.12725	.22473	.11613	.36501	-.23653
Na ₂ O	.06946	-.40059	-.58741	-.52696	.75398	-.28978	-.29302	-.54069
K ₂ O	.07878	.35875	.31445	.23395	-.57951	.18253	.20167	.15968
	BA	CAO	FE ₂ O ₃	NA ₂ O	K ₂ O			
BA	.99603							
CAO	.35643	1.00233						
Fe ₂ O ₃	-.14378	.51422	.99848					
Na ₂ O	-.01745	.10442	.13803	1.00018				
K ₂ O	.57224	.27595	-.06428	-.51759	1.00035			

TABLE XLIII: R-mode Varimax Factor Matrix, Lornex Surface
(3-Factor Model)

Variable	FACTOR 1	FACTOR 2	FACTOR 3	Communality
Zn	-0.0216	0-0.5992	0.2122	0.4045
Mn	0.4425	0.0024	0.4201	0.3723
Cu	0.7752	-0.1043	0.1119	0.6243
B	0.8225	0.0530	-0.1089	0.6911
Sr	-0.7081	-0.3253	-0.3826	0.7540
Ti	0.4454	-0.6347	-0.1378	0.6203
V	0.3296	-0.8217	-0.0736	0.7893
Mo	0.8097	-0.0387	-0.2037	0.6986
Ba	-0.2289	-0.0369	0.8518	0.7793
Ca	-0.2963	-0.7685	0.3463	0.7984
Fe	-0.2641	-0.6003	-0.1324	0.4477
Na	-0.8097	0.0070	-0.2897	0.7396
K	0.3775	-0.1292	0.8117	0.8181
Eigenvalue in %	46	30	24	

TABLE XLIV: Metal Associations of Different Factor Models, Lornex
Subsurface.

Factor Model			
FACTOR	3	4	5
1	Na	Na	K
	Sr	Sr	B
	<u>vs</u>	<u>vs</u>	<u>vs</u>
	K	K	Na
2	B	B	Sr
	V	V	V
	Ti	Ti	Ti
	Cu	Cu	Cu
	<u>vs</u>	<u>vs</u>	<u>vs</u>
	Mn	Mn	Mn
3	Zn	Zn	Zn
	Mo	Mo	
	Fe	Fe	Ba
	<u>vs</u>	<u>vs</u>	<u>vs</u>
4	Ba	Ba	Mo
		Ca	Ca
		Zn	Zn
5			Fe

TABLE XLV: Correlation Coefficients, Lornex Subsurface (85 samples)

	Zn	Mn	Cu	B				
Zn	.99907							
Mn	.43083	1.00010						
Cu	-.06213	-.44652	.99993		SR	TI	V	MO
B	.12799	.11402	.24503	1.00088				
Sr	-.03205	.06261	-.20071	-.47660	1.00165			
Ti	-.31363	-.32695	.38287	.09894	.01410	1.00187		
V	-.50424	-.49967	.48870	-.19051	.24054	.45421	1.00243	
Mo	-.07721	-.22820	.39740	.25080	-.13271	.10279	.29072	1.00121
Ba	-.12483	.04726	-.31713	-.35403	.03305	.03526	.00856	-.56400
CAO	.43728	-.23708	.25943	-.00753	-.13207	-.02426	-.00144	.06868
Fe ₂ O ₃	-.19019	.14063	.04045	-.12355	.46190	-.08887	.37263	.40641
Na ₂ O	-.25491	-.16913	-.23802	-.60573	.56869	.03610	.28580	-.22924
K ₂ O	.18976	.15909	.20910	.40040	-.47570	.03681	-.10949	-.04096
	BA	CAO	FE ₂ O ₃	Na ₂ O				
Ba	1.00232							
CAO	-.02891	1.00067						
Fe ₂ O ₃	-.25315	-.18439	1.00019					
Na ₂ O	.24555	-.17574	.17867	.99979				
K ₂ O	.23106	.14711	-.18223	-.59371	.99879			

TABLE XLVI: R-mode Varimax Factor Matrix, Lornex Subsurface

(4 - factor Model)

	FACTOR 1	FACTOR 2	FACTOR 3	FACTOR 4	Communality
Zn	-0.1371	-0.5809	0.0648	-0.6531	0.7870
Mn	-0.1064	-0.8011	0.0108	0.2244	0.7035
Cu	-0.2335	0.6542	0.3712	-0.2838	0.7267
B	-0.7672	-0.0570	0.3228	0.0830	0.7029
Sr	0.8066	-0.0714	0.1061	0.0935	0.6757
Ti	-0.1161	0.6882	-0.0636	0.1419	0.5112
V	0.2823	0.7897	0.2051	0.1411	0.7653
Mo	-0.1281	0.2587	0.8063	-0.0295	0.7341
Ba	0.0933	0.0494	-0.8361	0.1193	0.7244
Ca	-0.0539	0.1246	-0.0019	-0.9023	0.8327
Fe	0.4039	-0.0256	0.6373	0.3217	0.6734
Na	0.8324	0.1397	-0.2215	0.1296	0.7783
K	-0.7388	0.0006	-0.1799	-0.0509	0.5809
Eigenvalue in %	31	29	23	17	

Factor 2: V, Ca, Ti, Fe, Zn

Factor 3: Ba, K

Factor 1 is an 'ore association'. Most pronounced scores coincide with the subeconomic deposit (Discovery Zone) lying south of the Lornex orebody. Low factor scores coincide with fresh Bethsaida rocks west of Lornex Fault.

Factor 2 reflects lithology and propylitic alteration. High scores are associated with rocks of Skeena Phase east of Lornex deposit, with maximum values in the propylitic zone marginal to the orebody. In contrast, the more felsic Bethsaida rocks west of the Lornex Fault, and argillized quartz porphyry in the Discovery Zone are associated with low scores.

Factor 3 reflects degree of K-feldspar destruction in host rocks. High scores are confined to fresh Bethsaida and Skeena rocks to the west and east of the Lornex orebody respectively. In contrast, low scores are associated with the Discovery Zone and the periphery of the main orebody where K-feldspar has been destroyed by propylitic and argillic alteration.

(ii) Subsurface Samples

Element associations for the 4 factors are summarized as follows:

Factor 1: Na, Sr vs K, B

Factor 2: V, Ti, Cu vs Mn, Zn

Factor 3: Mo, Fe vs Ba

Factor 4: Ca, Zn

Factor 1 reflects hydrothermal alteration. High factor scores occur at the periphery of the orebody in Hole 51 (Fig. A72). Low scores are associated with the central zone and ground adjacent to the Lornex Fault where intense potassic and phyllic alteration are prevalent.

Factor 2: Distribution of this factor is almost the reverse of Factor 1. It reflects Cu mineralization (Cu sulphides in association with magnetite). High scores are confined to a broad central zone of intense metallization and alteration. Low scores occur at the periphery of the deposit (Fig. A73).

Factor 3 reflects Mo mineralization. Most pronounced scores occur in Holes 10 and 8 where Mo mineralization is most intense (Fig. A74). Low scores are associated with Bethsaida rocks and potassic alteration immediately east of the Lornex Fault.

Factor 4: High scores of this factor occur along the Lornex Fault and periphery of the orebody in Hole 51. Low scores coincide with the area immediately east of the fault (Fig. A75). This factor mainly reflects metal enrichment along the Lornex Fault.

(f) General Discussion and Summary

Background concentrations of V, Ti, CaO and Fe_2O_3 are higher in rocks of the Skeena Phase in the eastern part of the property than in fresh Bethsaida rocks west of Lornex Fault. This is consistent with the higher modal content of ferromagnesian minerals in rocks of the Skeena Phase. However, Mn is relatively higher in rocks of Bethsaida Phase reflecting the abnormally high Mn content.

of biotites in the Bethsaida Phase (Chapter 7, Table LIX).

Hydrothermal effects are associated with extensive leaching of Zn, Mn, Fe, Na, Sr and Ba in the central zone of intense argillic alteration. This is attributed to complete breakdown of ferromagnesian minerals and plagioclase to sericite and kaolinite. In contrast, the peripheral propylitic zone with abundant chlorite, epidote and pyrite is relatively enhanced in Zn, Fe and Mn. Anomalous concentrations of K and Ba are associated with potassic alteration immediately east of the Lornex Fault. The sharp truncation of geochemical anomalies by the Lornex Fault is consistent with geologic evidence which suggests post-mineralization movement along the fault. Compared to adjacent lithologies, gouge along the Lornex Fault is enriched in Zn, Mn, Hg, Pb, Ag and CaO but show no enhancement in Cu, Fe, Co and Ni.

Epigenetic metallization is associated with pronounced anomalies of Cu, Mo, B, Ti and V. Relatively high Ti and V reflect magnetite within the ore zone. Variability in Cu values is examined in Table XLVII. Coefficients of variation in local background samples are higher than in mineralized samples. This is attributed to the more uniform distribution of fractures in ore zones than areas peripheral to mineralization.

Geochemical contrast between background and mineralized environments is summarized in Table XLVIII. Cu and Mo show best contrast. In the eastern part of the property Cu and B halos extend at least 1000m from the orebody, but are sharply truncated in the west by the Lornex Fault. Dispersion of the other elements does

TABLE XLVII: Comparison of variability in copper contents of background and mineralized samples, Lornex.

Drill-hole #	No. of samples	Log. mean	Log. std. deviation	*Coefficient of variation
Background samples				
Hole 49	69	1.025	0.707	0.69
Hole 51	67	2.746	0.539	0.20
Mineralized Samples				
Hole 12	72	3.482	0.313	0.08
Hole 8	78	3.549	0.234	0.06
Hole 10	94	3.556	0.175	0.05
Hole 9	49	3.451	0.317	0.09

*Coefficient of variation = standard deviation/mean

TABLE XLVIII: Comparison of ¹metal contents and contrast in background and mineralized areas, Lornex property (Values in p.p.m. except where indicated.)

No. of samples	³ Regional background (Skeena)	⁴ Local background (Skeena)	Mineralized Zone	Contrast (regional)	Contrast (local)
	(6)	(51)	(60)		
Cu	26	149	2180	84	14
Zn	19	33	29	1.5	1.5
Mn	312	253	193	*1.6	*1.
Mo	2	5	13	6.5	2.6
B	5	11	18	3.6	1.6
Ti	1000	1022	1237	1.2	1.2
V	35	35	40	1.1	1.1
Sr	653	545	433	*1.5	*1.3
Ba	550	445	383	*1.4	*1.2
² K ₂ O	1.73	1.47	1.88	1.1	1.3
² Na ₂ O	4.78	3.29	2.10	*2.3	*1.6

¹Geometric means except for major elements.

²Arithmetic means and values in wt. %.

³Fresh samples of Skeena Phase collected by Northcote (1968).

⁴Samples at the periphery of the deposit.

*Negative contrast.

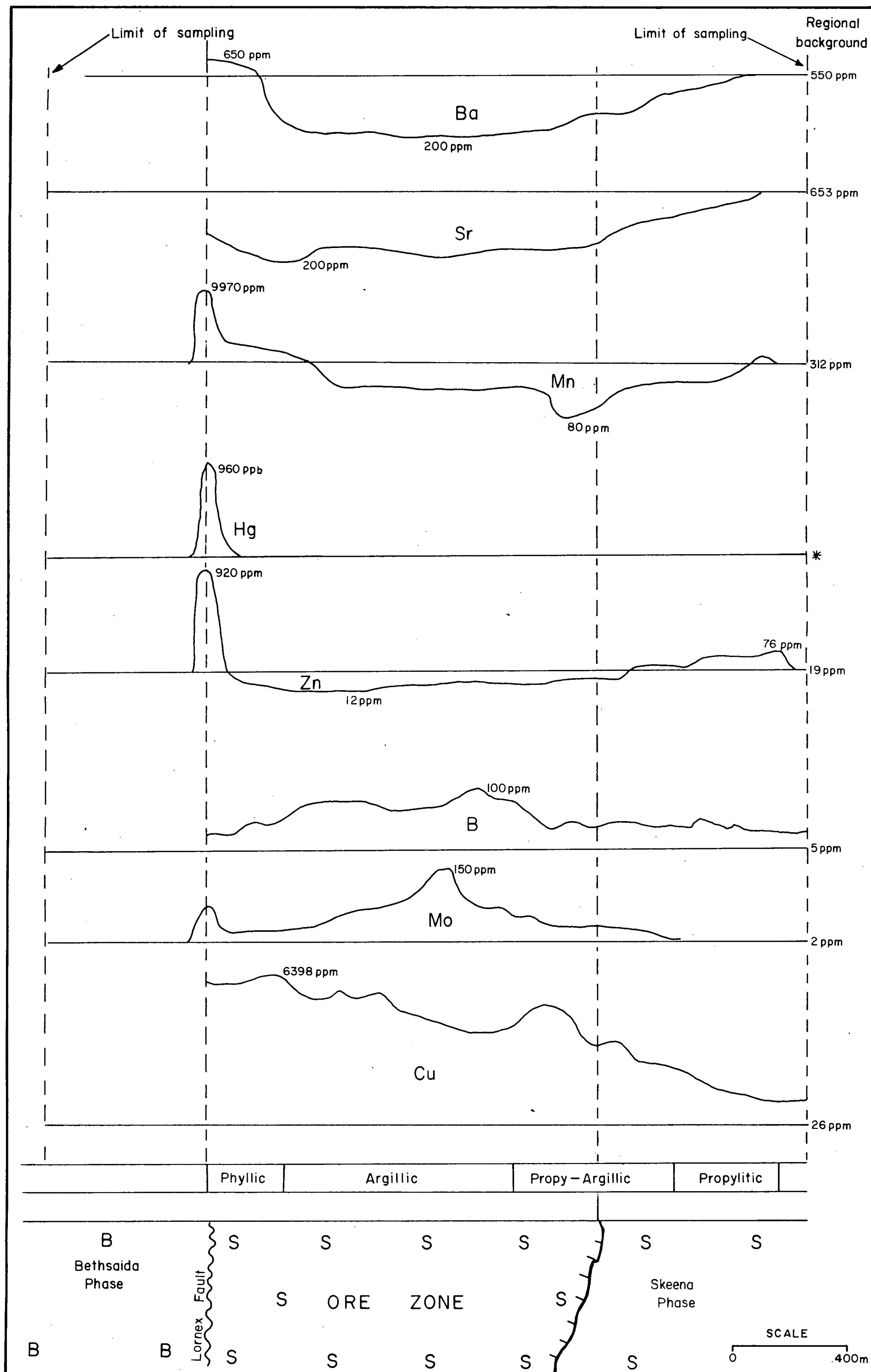
not extend beyond the periphery of the ore zone (Fig. 52). In surface samples, positive scores of Factor 1 (B, Mo, Cu vs Na, Sr) are as extensive as the halos of Cu and B. Because of sampling limitations, positive factor scores in subsurface samples are confined to the alteration envelope (Fig. 53).

HIGHMONT

Results of trace and major element analyses in surface and drill-core samples are summarized in Table XLIX and Figs. A76 to A86. Surface samples comprise outcrop samples from background areas and suboutcrop samples from the No. 2 Ore Zone (West Pit) and the periphery of the main orebody (No. 1 Ore Zone or East Pit). Subsurface samples were collected from a cross-section which includes background and mineralized zones. Sample locations and plans are presented in the Appendix. Analytical techniques are the same as described for Lornex.

(a) Geochemical Patterns Related to Lithology

Rocks of the Skeena Phase within Highmont are characterized by higher Zn, Mn, Ti, V, Fe_2O_3 , K_2O and CaO and lower Na and Sr relative to the more felsic rocks of the Bethsaida Phase and Gnawed Mountain Porphyry (Table L). A Student t-test suggests that these differences are only significant for Ti, V and Fe_2O_3 at the .05 confidence level. The relatively higher levels of the 'femic' elements are attributed to the relatively higher modal proportions of ferromagnesian minerals in Skeena rocks. Compared with the Bethsaida Phase, the Gnawed Mountain Porphyry is characterized by lower



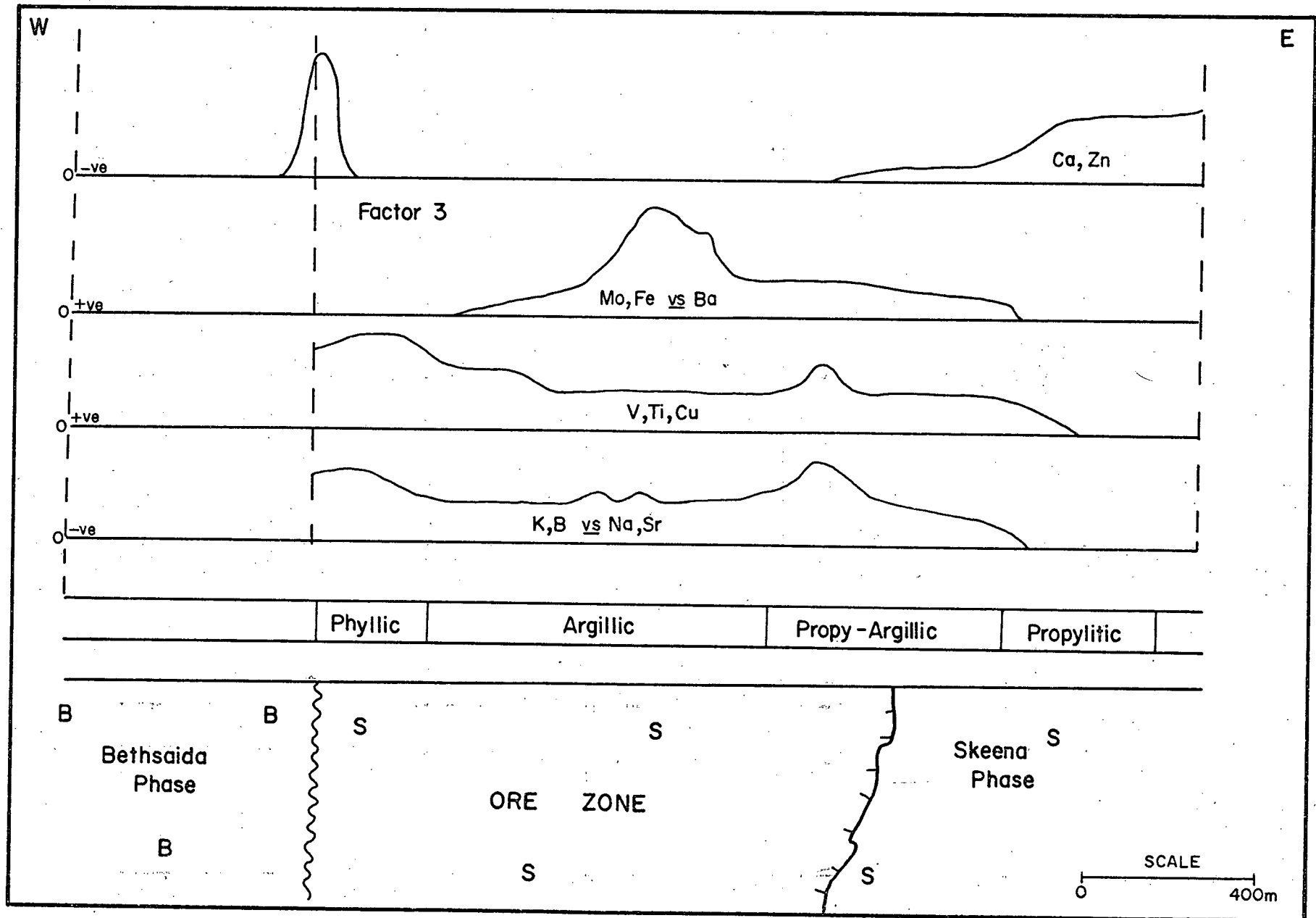


FIGURE 53: Schematic diagram showing distribution of factor scores, Lornex Subsurface.

TABLE XLIX: ¹Means and ²ranges of trace and major elements at Highmont.

No. of samples	Surface Samples (188)	Subsurface Samples (95)	All Samples (283)
Metal content (p.p.m.)			
Cu	108 (19 - 634)	111 (15 - 809)	109 (19 - 676)
Zn	18 (11 - 30)	19 (15 - 26)	18 (11 - 30)
Mn	176 (116 - 268)	230 (152 - 349)	178 (117 - 272)
B	12 (4 - 35)	10 (5 - 24)	12 (4 - 37)
Sr	761 (504 - 1148)	620 (450 - 855)	768 (494 - 1194)
Ti	1464 (1000 - 2143)	999 (659 - 1513)	1482 (1010 - 2174)
V	38 (26 - 55)	33 (25 - 44)	35 (26 - 52)
Mo	2 (1 - 7)	4 (1 - 11)	3 (1 - 8)
Ba	642 (405 - 1015)	500 (281 - 887)	627 (391 - 1007)
Metal content (wt. %)			
Fe ₂ O ₃	1.92 (1.25 - 2.59)	2.04 (1.53 - 2.55)	1.93 (1.31 - 2.56)
CaO	2.69 (2.05 - 3.33)	3.12 (1.62 - 4.63)	2.83 (1.79 - 3.87)
Na ₂ O	3.71 (3.21 - 4.21)	3.82 (3.20 - 4.44)	3.75 (3.17 - 4.34)
K ₂ O	1.34 (0.82 - 1.86)	1.37 (0.89 - 1.84)	1.35 (0.82 - 1.83)

¹Geometric means except²Mean \pm 1 standard deviation;

TABLE L: Means and ²ranges of metal concentrations in lithologic units,
Highmont surface (fresh and weakly mineralized samples). Values
in p.p.m. except where indicated).

No. of samples	Skeena Phase (103)	Bethsaida Phase (21)	Porphyry (46)
Cu	*103 (18 - 586)	*65 (13 - 322)	*120 (17 - 850)
Zn	20 (12 - 33)	17 (11 - 27)	14 (3 - 30)
Mn	195 (131 - 290)	186 (122 - 284)	142 (91 - 222)
B	10 (4 - 22)	9 (4 - 20)	21 (4 - 98)
Sr	774 (512 - 1167)	778 (556 - 1088)	798 (526 - 1210)
Ti	1644 (1203 - 2246)	1174 (790 - 1743)	1326 (863 - 2038)
V	42 (32 - 55)	34 (23 - 50)	32 (20 - 52)
*Mo	*2 (1 - 8)	*2 (1 - 13)	*1 (1 - 3)
Ba	666 (448 - 990)	554 (332 - 926)	654 (362 - 941)
¹ Fe ₂ O ₃	2.14 (1.67 - 2.60)	1.71 (1.07 - 2.36)	1.20 (0.68 - 2.11)
¹ CaO	2.86 (2.35 - 3.38)	2.77 (2.18 - 3.34)	2.04 (1.40 - 2.96)
¹ Na ₂ O	3.59 (3.17 - 4.01)	3.70 (3.09 - 4.30)	3.96 (3.41 - 4.58)
¹ K ₂ O	1.37 (1.02 - 1.72)	1.15 (0.37 - 1.92)	0.94 (0.42 - 2.10)

*Geometric means except where indicated.

¹Arithmetic means, and values in wt. %.

²Mean \pm 1 standard deviation.

CaO, K₂O, Fe₂O₃, Zn, Mn and higher Ti, B, Ba and Na₂O. Except for B, Mn and Ti these differences are not significant at the .05 confidences level. Metal concentrations in fresh Skeena and Bethsaida rocks within Highmont property do not differ appreciably from regional data.

(b) Geochemical Patterns Related to Hydrothermal Alteration

Hydrothermal alteration is most pronounced in drill-core samples. Table ~~ALII~~ shows metal concentrations in relation to alteration types. Enhanced Zn (>25 p.p.m.) and Mn (>250 p.p.m.) concentrations occur in a central zone which includes the Nos. 1 and 4 Ore Zones in both sides and within the central porphyry dyke (Figs. A76 and A77). Low values occur at depth in the dyke (Hole 69-108), and Hole 69-126 which transects a small quartz porphyry north of the ore zone. A significant positive correlation between Mn and Zn ($r = 0.64$) demonstrates the similarity in their distribution.

Fe₂O₃ and Na₂O are relatively depleted in the central dyke (Hole 69-108) and the quartz porphyry (Hole 69-126). In contrast, high values are associated with the ore zone where propy-argillic alteration (chlorite-sericite-albite-epidote) is associated with pyrite and other sulphides (Figs. A78 and A79). CaO and K₂O show no consistent trends related to alteration. Sr values are depleted within the ore zone.

(c) Geochemical Patterns Related to Mineralization

Copper: Cumulative log probability plot of Cu values in 283 samples shows two populations, A and B, in the proportion of 80 and 20%

TABLE LI: *Metal concentrations associated with types of alteration,
Highmont property.

No. of samples	Skeena Phase	Propylitic Zone	Propy-Argillic Zone	Argillic Zone
	(6)	(22)	(12)	(12)
Metal content (p.p.m.)				
Cu	¹ 26 (9 - 45)	299 (93 - 967)	742 (193 - 2847)	125 (28 - 545)
Zn	² 19 (22 - 35)	24 (16 - 30)	21 (16 - 27)	18 (12 - 28)
Mn	¹ 312 (250 - 340)	309 (242 - 395)	232 (188 - 286)	297 (202 - 438)
B	5 -	22 (7 - 32)	18 (4 - 65)	17 (8 - 36)
Sr	653 (625 - 680)	615 (409 - 923)	558 (407 - 763)	508 (364 - 709)
Ti	1000 (900 - 1200)	1280 (871 - 1881)	1062 (685 - 1)	1041 (585 - 1850)
V	35 (30 - 40)	35 (28 - 42)	38 (31 - 47)	27 (15 - 48)
Mo	2 -	7 (2 - 23)	7 (2 - 26)	3 (1 - 5)
Ba	550 (500 - 600)	442 (200 - 976)	550 (317 - 955)	518 (263 - 1019)
Metal content (wt. %)				
Fe ₂ O ₃	2.98 (2.80 - 3.47)	2.14 (1.79 - 2.49)	2.94 (2.39 - 3.88)	1.89 (1.18 - 2.59)
CaO	3.84 (3.73 - 3.91)	3.25 (0.44 - 6.06)	3.23 (2.17 - 4.09)	2.84 (1.98 - 3.07)
Na ₂ O	4.78 (4.38 - 5.19)	3.61 (3.02 - 4.60)	3.95 (2.69 - 4.80)	3.45 (3.26 - 4.04)
K ₂ O	1.73 (1.30 - 1.96)	1.49 (0.87 - 2.11)	1.46 (1.00 - 1.92)	1.32 (1.09 - 1.59)

*Means and ranges (range = mean \pm 1 standard deviation)

¹HF-HClO₄ digestion

²Aqua regia digestion (Brabec, 1970)

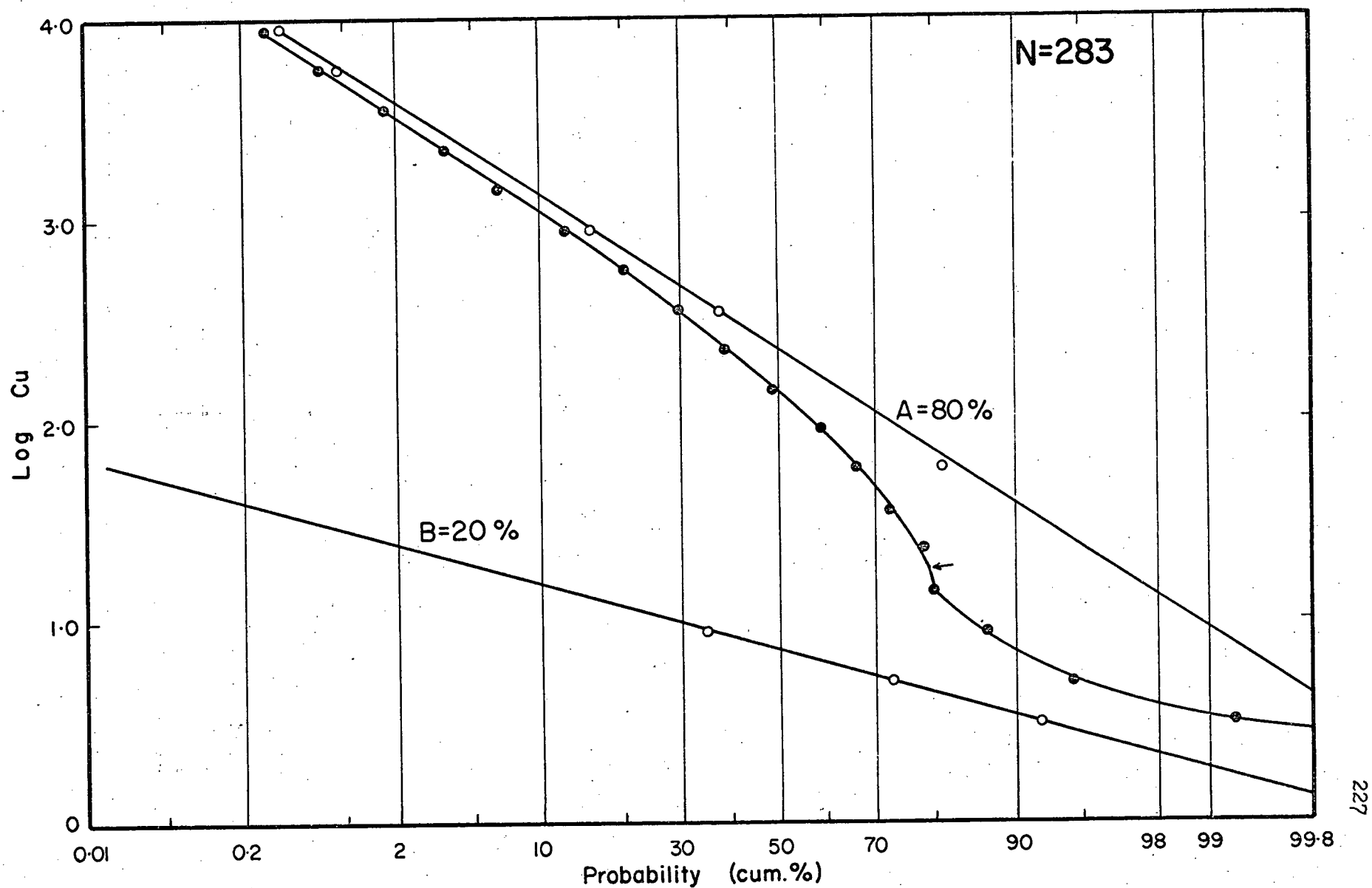


FIGURE 53: Log probability plot of Copper at Highmont.

respectively (Fig. 54). The value separating the two populations is 18 p.p.m. Population B, with a mean value of 7 p.p.m., represents background samples comprising surface and drill-core samples. Population A, with a mean of 224 p.p.m., corresponds to anomalous samples.

Cu distribution in surface samples is erratic because of the numerous Cu showings in the region, especially south of the porphyry dyke. In this area, enhanced Cu levels (>250 p.p.m.) are dominant (Fig. A80). In contrast background concentrations (<18 p.p.m.) occur north and northeast of the major orebodies (Nos. 1 and 2 ore zones). As the mineralized zones are approached from the north, Cu levels increase to a range of 100 to 400 p.p.m.

In subsurface samples, local background Cu content (<35 p.p.m.) is associated with peripheral drill holes (69-122 and 70-270) and most of the central porphyry dyke. Anomalous values are encountered immediately north and south of the dyke, defining Nos. 1 and 4 Ore Zones respectively (Fig. A81).

Molybdenum: Mo concentration is generally below the detection limit (<2 p.p.m.) in surface samples. In the subsurface, low values (<5 p.p.m.) occur in marginal holes (Holes 70-270, 69-122 and 69-126) and within parts of the porphyry dyke (Hole 69-108). Enhanced levels (>8 p.p.m.) are associated with mineralized zones, north and south of the porphyry dyke (Fig. A82). Correlation between Mo and Cu ($r = 0.58$) in subsurface samples reflects overall similarity in their distribution.

Boron: Anomalous B in surface samples (10-2000 p.p.m.) occurs dominantly within the NW-SE trending porphyry dyke and associated breccia pipes (Fig. A83). At the periphery of the main orebody, enhanced B levels (10-80 p.p.m.) are common. Elsewhere, B content is less than 5 p.p.m. In subsurface samples, B concentrations are less than 20 p.p.m. in marginal holes (Hole 70 - 270, 69-122 and 69-126). High values (> 50 p.p.m.) are encountered in the porphyry dyke (69-108) and adjoining mineralized zones (Fig. A84). High B levels in surface and subsurface samples are attributed to the presence of tourmaline (schorl). Although B shows no significant relationship with Cu ($r = 0.19$), there is a weak but significant positive correlation between B and Mo in subsurface samples ($r = 0.38$).

(d) R-mode Factor Analysis

R-mode analysis was applied to 13 variables in 95 subsurface samples at Highmont. Results are presented in Tables LII to LIV and Figs. A85 to A89. Element associations of 3-, 4- and 5- factor models are summarized in Table L. These models explain 52, 63 and 72% of data variability respectively. A 5-factor model is consistent with known geologic and mineralogic data.

Element associations characteristic of each factor are as follows:

Factor 1: Cu, Mo, B

Factor 2: Zn, Mn, Ca

TABLE LII: Correlation matrix, Highmont Subsurface

	Zn	Mn	Cu	B				
Zn	.99839							
Mn	.63934	1.00076						
Cu	.32258	.25570	1.00089		Sr	Ti	V	Mo
B	.18425	.39096	.41295	.99687				
Sr	.00252	-.28141	-.13930	-.21331	.99967			
Ti	.15578	.35187	.13500	.15009	.12885	.99850		
V	.24638	.19431	.07990	.09190	.31157	.58066	.99872	
Mo	.11170	.26642	.56574	.38321	-.15268	.30713	.19683	.99748
Ba	-.08272	-.03955	-.04567	-.06424	.16583	.26564	.35218	.12646
CAO	.44874	.36177	.08738	.19354	.15449	.17598	.30918	.04597
Fe ₂ O ₃	-.08629	.08882	-.11244	.03956	-.01755	.13698	.05503	-.10649
Na ₂ O	.17580	-.13934	-.08547	-.20041	.00978	-.32062	-.18991	-.26631
K ₂ O	-.12524	.06171	.11443	-.01578	-.22561	.17159	.15564	.26620
	Ba	CAO	Fe ₂ O ₃	Na ₂ O				
Ba	1.00174							
CAO	.20101	.99917						
Fe ₂ O ₃	-.10591	.10270	.99972					
Na ₂ O	-.06622	-.02028	-.27265	.99974				
K ₂ O	.39181	.15626	-.25672	-.25141	1.00081			

TABLE LIII: Metal associations of different factor models,
Highmont Subsurface.

FACTOR ANALYSIS			
FACTOR	3	4	5
1	Cu B Mo Mn <u>vs</u>	Mo Cu B <u>vs</u> Sr	Cu Mo B
2	Sr Ca Zn V Mn	Zn Ca Mn	Zn Mn Ca
3	Ba K Ti V <u>vs</u> Na	Ba K V	K Ba
4		Na <u>vs</u> Ti	Sr V Ti
5			Fe Na

TABLE LIV: Varimax Factor Matrix, Highmont Subsurface.

	FACTOR 1	FACTOR 2	FACTOR 3	FACTOR 4	FACTOR 5	Communality
Zn	0.2093	-0.8300	-0.1838	-0.0980	0.2392	0.8332
Mn	0.3048	-0.7913	0.0141	0.1797	-0.2097	0.7955
Cu	0.8367	-0.1241	-0.0410	-0.0056	0.1372	0.7327
B	0.6265	-0.2580	-0.1140	0.1335	-0.2128	0.5352
Sr	-0.1852	0.1128	-0.1595	-0.8452	0.1135	0.7997
Ti	0.2672	-0.2565	0.2730	-0.4775	-0.4450	0.6377
V	0.1348	-0.3104	0.2838	-0.6892	-0.2150	0.7167
Mo	0.8227	0.0058	0.2395	-0.0555	-0.0871	0.7448
Ba	-0.0838	-0.0392	0.7106	-0.3572	0.0221	0.6415
Ca	-0.0786	-0.7296	0.1887	-0.1974	-0.1382	0.6145
Fe	-0.2093	-0.0962	-0.3241	-0.0024	-0.7635	0.7411
Na	-0.2487	-0.1302	-0.2313	0.0389	-0.7442	0.6876
K	0.1208	-0.0090	0.8832	0.1819	-0.0188	0.8282
Eigenvalue in %						
	23	23	19	18	17	

Factor 3: K, Ba

Factor 4: Sr, V, Ti

Factor 5: Fe, Na

Factor 1 is an ore association. Most pronounced scores are associated with mineralized zones on both sides of the central porphyry dyke (Fig. A85). Minimum factor scores are confined to marginal holes (Hole 70-270 and 69-122).

Factor 2: The significance of this factor is not well understood. Its distribution is similar to that of Zn and Mn, in that high values are confined to a broad central zone encompassing the porphyry dyke and adjacent mineralized zones. Low factor scores are confined to peripheral holes (Fig. A86).

Factor 3 reflects the distribution of potassic minerals. High scores are associated with the central porphyry dyke containing relatively abundant K-feldspar veins and argillic alteration in which sericite is a dominant mineral. Low scores occur within the ore zone and fresh Skeena rocks at the periphery (Fig. A87).

Factor 4 broadly reflects lithology. High scores are associated with Skeena rocks north and south of the central dyke. In contrast low scores characterize the central porphyry dyke (Hole 69-108) and the small felsite dyke in Hole 69-126 (Fig. A88).

Factor 5 corresponds with intense propylitic alteration. High scores occur within the ore zone where propylitic minerals (chlorite-sericite-albite) are associated with pyrite and other sulphides.

Low factor scores are associated with areas outside the ore zone where rocks are either fresh or affected by argillic and potassic alteration (Fig. A89).

General Discussion and Summary

Concentrations of Zn, Ti, V and Fe_2O_3 are higher in fresh Skeena rocks relative to the more felsic rocks of the Bethsaida and Gnawed Mountain Porphyry Phases. This is attributed to greater abundance of ferromagnesian silicates in Skeena rocks.

Hydrothermal effects within the propylitic zone is relatively weak, and associated with subtle changes in metal concentrations relative to fresh rocks. Argillic alteration is associated generally with leaching of Mn, Zn, Fe, Ca, Na, Sr and Ba. This is attributed to the breakdown of plagioclase and ferromagnesian minerals to kaolinite and sericite. Furthermore, the close spatial association between argillic alteration and the quartz porphyry partly accounts for the lower concentrations of 'femic' elements within the argillic zone. In the mineralized zone where propy-argillic alteration is dominant, concentrations of Ba, Zn, Sr, Ti, V, Ca and K are higher than those of the argillic zone but lower than those of the propylitic zone. This reflects the intermediate nature of the propy-argillic zone. Nevertheless, Fe and Na are higher in this zone relative to the propylitic and argillic zones. This is consistent with the higher albite and pyrite contents.

Anomalous concentrations of Cu, Mo and B are associated with the mineralized zones. This is related to the occurrence of

sulphides in association with tourmaline. Cu in local background samples is more erratic than in mineralized zones where fracturing and intensity of epigenetic metallization is more uniformly distributed (Table LV).

Geochemical contrast between background and anomalous samples is presented in Table LVI. Cu, Mo and B show the best contrast. However, halos of Cu and B are generally the most extensive (Fig. 55), exceeding 200m in the north and 500 m in the south. Distribution of positive scores of all factors are confined to the mineralized zones and the alteration envelope on both sides of the main porphyry dyke (Fig. 56).

SKEENA

Results of analysis of samples from a drill hole which transects one of the main quartz lodes at the Skeena Cu deposit are presented in Figs. A90 and A91. Pb, Cd, Co, Ni, B, Sr, Mo, V, Ti and Ba and Na_2O show no appreciable trends and are not discussed further.

Distribution of Cu, Zn, Mn, CaO, Fe_2O_3 , K_2O

In the hanging wall, background contents of Cu, Zn and Mn are generally less than 20 p.p.m. for Cu and Zn, and 300 p.p.m. for Mn. Within 20m of the quartz lode, Cu, Zn, and Mn concentrations rise sharply (Fig. A90). However, the intensely altered wall rock (sericite-quartz-kaolinite) closest to the vein shows relatively lower values, defining an aureole of metal depletion.

TABLE IV: Comparison of variability in copper contents of background and mineralized samples, Highmont.

D.D.H. #	No. of samples	Log. mean	Log. std. deviation	* Coefficient of variation
Local Background Samples				
70 - 270	86	1.100	0.624	0.57
69 - 126	45	1.865	0.776	0.42
69 - 114	57	2.089	0.620	0.30
69 - 108	59	2.246	0.606	0.27
Anomalous Samples				
69 - 120	50	2.735	0.303	0.11
68 - 22	12	2.695	0.286	0.10
68 - 68	26	3.245	0.561	0.17

*Coefficient of variation = standard deviation/mean

TABLE LVI: Comparison between *metal concentrations in background and mineralized zones, Highmont.

No. of samples	Regional background (Skeena) (6)	Local background (Skeena) (31)	Mineralized Zone (33)	Contrast (regional)	Contrast (local)
Cu	26	24	369	14	15
Zn	19	18	22	1.1	1.2
Mn	312	200	274	1.4	**1.4
Mo	2	2	6	3	.3
B	5	6	17	3.4	3
V	35	36	36	1.0	1.0
Ti	1000	983	1106	1.1	1.1
Ba	550	586	482	**1.1	**1.2
Sr	653	676	557	**1.2	**1.2
³ Fe ₂ O ₃	2.98	2.02	2.25	**1.3	1.1
³ Na ₂ O	4.78	3.76	3.86	1.2	1.0

¹Fresh Skeena rocks collected by Northcote (1968).

²Samples from the periphery of the deposit.

³Arithmetic means and values in wt. %.

* Geometric means except where indicated.

** Negative contrast.

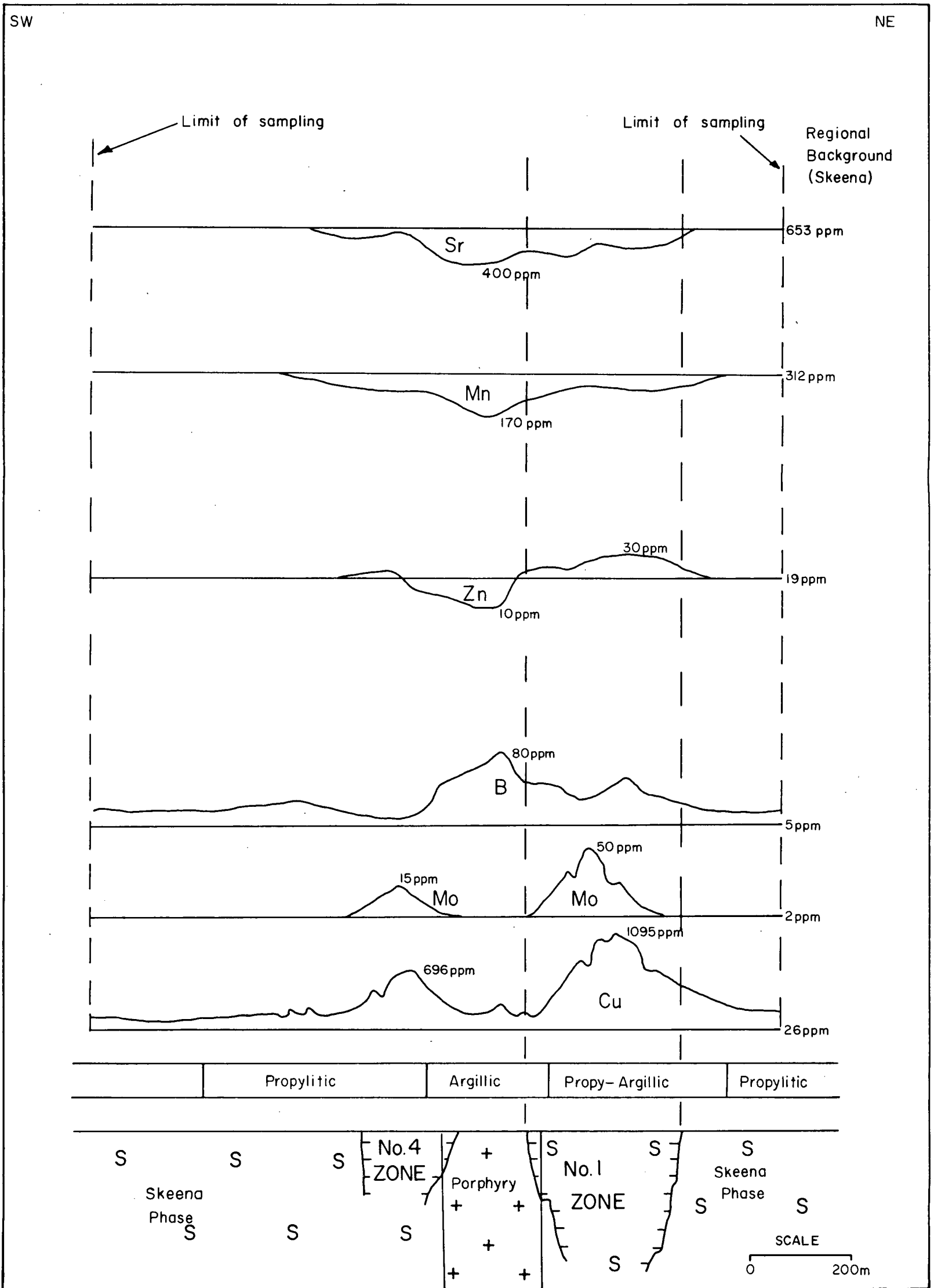
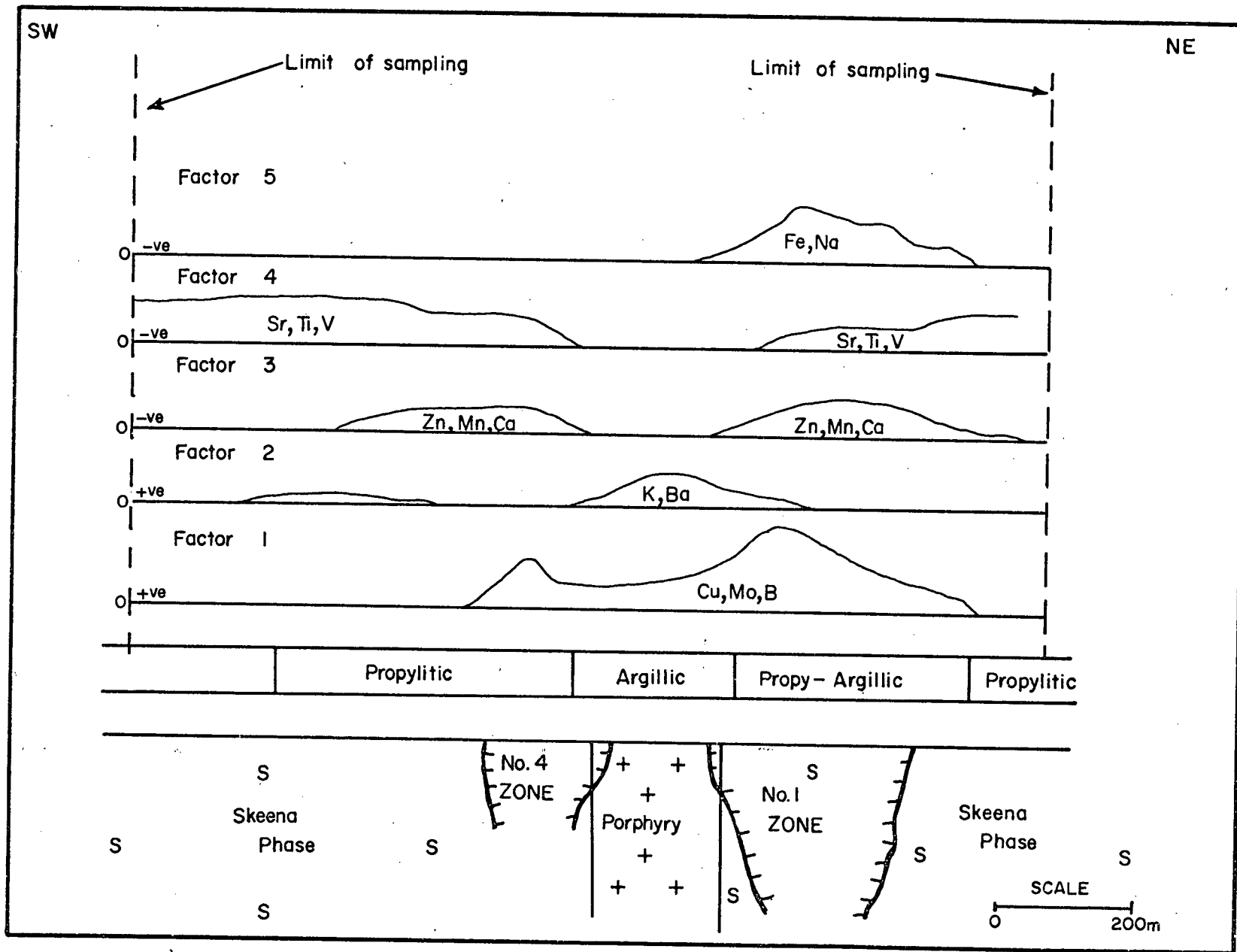


FIGURE 55: Schematic diagram showing extent and relative intensity of primary halos, Highmont Subsurface.

FIGURE 56: Schematic diagram showing the distribution of factor scores, Highmont Subsurface



In the footwall, geochemical halos for trace elements do not decay to background levels but remain consistently higher than values in the hanging wall. This is attributed to greater abundance of fractures and veins in the footwall. The apparent depletion of trace metals in wall rock adjacent to the lode is attributed to leaching during hydrothermal and metallization processes.

Major element concentrations (CaO , Fe_2O_3 , and K_2O) in the hanging wall decrease as the profile enters the alteration envelope (Fig. A91). Highest values are encountered within the ore vein reflecting abundance of pyrite, carbonate, and sericite. In the footwall, values decrease away from the lode, and at a distance of 10m become lower than levels in the hanging wall. Towards the bottom of the drill hole, values again increase, defining another zone similar to that surrounding the main lode.

DISCUSSION

This section compares and contrasts the nature of metal dispersion in the various deposits, and discusses the factors responsible for the observed differences, and applications of the geochemical patterns to mineral exploration.

Results of primary metal dispersion around porphyry-type deposits at Highland Valley indicate that variations in the abundance of 'femic group' of elements (Fe, Mg, Ti, V, Zn, Mn, Co) are controlled dominantly by primary lithologies. This relationship is attributed to the strong geochemical coherence of the trace elements with Fe and Mg. Because of similarity in ionic properties, these

elements tend to substitute for Fe and Mg in crystal lattices of ferromagnesian minerals (Goldschmidt, 1954). Except at Bethlehem-JA where Zn and Mn are impoverished, concentrations of these elements are similar to those obtained in regional samples. Thus, the host rocks surrounding the deposits are not peculiar in 'femic' metal concentrations relative to rocks of similar composition within the batholith.

Despite the dominant control of lithology on the distribution of the 'femic' elements, minor redistribution by hydrothermal processes is apparent at these deposits in which a major host rock is dominant. Thus at Valley Copper, Zn, Mn, Fe and Mg are obviously depleted in central zones of intense alteration relative to the periphery of the deposit. At Lornex, Zn, Mn and Fe are enhanced in the peripheral propylitic zone relative to adjoining fresh Skeena rocks. At Bethlehem-JA this effect has been masked by the apparent coincidence of propylitic alteration with the more mafic rocks of Guichon Phase. Hydrothermal mobilization of the femic elements is attributed to the breakdown of ferromagnesian minerals into sericite, epidote or chlorite. Where sericite is the dominant alteration mineral such as at Valley Copper, the femic elements are depleted whereas in propylitic zones with chlorite and/or epidote they are enriched or remain unchanged in concentration, for example, Lornex and Bethlehem-JA.

The lithophile elements (Rb, Sr, Ba), in association with K, Na and Ca, are most susceptible to metasomatic changes during metallization and hydrothermal processes. Results of factor analysis

have consistently associated Na and Sr which are most commonly impoverished wherever alteration is intense. Unlike K, Rb and Ba, these elements are not tied to visible alteration minerals, and thus constitute sensitive indicators of metasomatic processes.

Ba dispersion patterns are not consistent in the deposits examined in this study. At Valley Copper, values decrease from the outer margins to the core of intense alteration. In contrast, at Bethlehem-JA, higher values are encountered within the ore zone. At Lornex, values generally decrease from the periphery to the core of intense argillic alteration, although enhanced values are encountered within the potassic zone. The inconsistent behaviour of Ba is related to its geochemical affinity with K-feldspar, which is a common mineral in alteration zones of porphyry-type deposits. Nevertheless, the lack of overall correlation between K and Ba, suggests that Ba distribution, outside the potassic zone, is not controlled by K concentrations. At Bethlehem-JA, Valley Copper and a large portion of Lornex orebody, Ba/Sr ratios consistently increase from less than 1 in background areas to more than 1 in mineralized zones. Where Ba and Sr both decrease, the greater depletion of Sr than Ba is attributed to greater solubility of Sr relative to Ba in thermal solutions (Tooker, 1963). The only exception to the above distribution pattern is where gypsum or carbonate veins are locally abundant, as in the bottom of Hole 10 at Lornex. Thus, the use of Ba/Sr ratios produce more consistent and reliable patterns that are devoid of obvious mineralogical control than either Ba or Sr alone.

Rb consistently follows K at Bethlehem-JA and Valley Copper. Enhanced levels of both elements are associated with zones of intense potassic and phyllic alteration where K-feldspar and sericite are dominant. This covariant relationship is attributed to similarity in ionic properties and geochemical behaviour during magmatic and hydrothermal processes (Nockolds and Allen, 1953; Heier and Adams, 1964). The source of enhanced values of Rb is uncertain. However, two possibilities are suggested. (1) Wall rock metasomatism might result in bilateral exchange of material between centres of hydrothermal activity and outlying host rocks. (2) Hydrothermal fluids contribute Rb directly from deep-seated sources. Magmatic differentiation commonly culminates in the enrichment of Rb in residual fluids that might ultimately become hydrothermal solutions (Holland, 1972). Guilbert and Lowell (1974) among others have suggested that K-feldspar in potassic zones of porphyry copper deposits could be related to deep-seated, late-magmatic crystallization which accounts for its early paragenesis in the sequence of secondary mineral formation. If this supposition is correct, the association between K and Rb may suggest a magmatic-hydrothermal source for the latter.

In general, depletion of major and trace elements especially Zn, Mn, Sr and Na in zones of intense metasomatism is consistent with the model of mass flow of acidic hydrothermal solutions through grain boundaries, pores and other discontinuities in rocks. This culminates at the metasomatic leaching of base elements and

deposition at the 'outer front' as reaction with wall rock neutralizes the solutions (Korzhinskii, 1968). Consequently, negative anomalies are most commonly characteristic of primary dispersion of femic and lithophile elements.

Distribution of Cu and Mo are erratic in all the deposits. This is attributed to sampling problems associated with their irregular mode of occurrence mainly as fracture-fillings and veinlets. Relative abundance of Cu is influenced by bornite to chalcopyrite ratios. Higher Cu levels are encountered at Valley Copper where bornite is dominant, whereas abundant chalcopyrite at Bethlehem-JA is reflected in relatively lower Cu values. Mo and Cu distribution also reflects metal zoning patterns at Valley Copper and Bethlehem-JA; Mo in both cases is peripheral to Cu.

Distribution of sulphide-held Cu as determined by KClO_3 -HCl digestion is similar to that of total Cu because most of the Cu occurs as sulphides. In contrast, sulphide Fe isolates the effect of lithology from mineralization, and delineates zones with most abundant pyrite and/or chalcopyrite, or pyrite halos at Valley Copper and Bethlehem-JA.

S shows pronounced anomalies and more consistent patterns than Cu or Mo. This is attributed to the fact that S not only occurs in Cu or Mo sulphides but also in Fe sulphides (pyrite) which smoothens its dispersion patterns. Relative abundance of S is also influenced by bornite: : chalcopyrite content as reflected by results at Valley Copper and Bethlehem-JA. Pronounced anomalies of S in bedrock around porphyry Cu deposits have important implications for the use of SO_2

gas in prospecting for these deposits. Rouse and Stevens (1971) have found SO_2 anomalies in soil gas and air over the Highland Valley deposits. Most pronounced SO_2 anomalies occurred at Lornex, and a lesser one at Valley Copper, possibly reflecting the lower bornite:chalcopyrite ratios at Lornex.

Geochemical behaviour of potential pathfinder elements (Hg, B, Cl, F) is not consistent. Hg defines a broad anomaly at Bethlehem-JA but no such pattern is apparent at Valley Copper. Gott and McCarthy (1966), in a study of the porphyry Cu deposit near Ely, Nevada, found that Hg was enriched in rocks around the ore deposits and depleted in the central ore-bearing intrusive rocks. This distribution pattern was attributed to the higher temperature prevailing in the centre of the ore deposit which caused volatile Hg to move outward, forming a halo around the deposit. Brown (1967) reported Hg anomalies in soils over porphyry Mo deposits in the Canadian Cordillera. McCarthy (1973) noted that Robbins (1972) and the staff of U.S. Geological Survey, working independently, found no significant anomalies of Hg in air around porphyry Cu deposits in Arizona. Similar results were obtained by McNerney and Buseck (1973). It is apparent from these citations that the behaviour of Hg in porphyry-type deposits is not consistent, as typified by results obtained at Highland Valley. Low Hg levels at Valley Copper and enhanced concentrations at JA might be attributed to one or more of the following: (1) higher temperature of ore formation at Valley Copper caused the volatilization and loss of Hg. Relative high temp-

eratures at Valley Copper are suggested by fluid inclusion studies giving temperature over 350°C (Field et al., 1973) and up to 500°C by sulphur isotope geothermometry (J. Briskey, oral comm.). At Bethlehem-JA, no geothermometric evidence is presently available, but the abundance of zeolites within the deposit is reminiscent of low-temperature 'hot-spring' - type activity (Meyer and Hemley, 1967); (2) Loss or escape from fine-grained clay (Kaolinite) and sericite alteration minerals at Valley Copper compared to its retention in coarser and more structured alteration minerals (K-feldspar, chlorite, epidote) at Bethlehem-JA.

Total Cl defines a moderate anomaly at Bethlehem-JA but is erratic and low at Valley Copper. This behaviour is contrary to expectations, as the size and grade of mineralization at Valley Copper and greater abundance of quartz-sericite veins should be accompanied by greater abundance of fluid inclusions. Nevertheless, the low Cl concentrations at Valley Copper, might be due to volatilization and loss as described above for Hg, or low salinity of fluid inclusions. F distribution at Valley Copper and JA is erratic, which may be related to the erratic occurrence of epigenetic fluorite. There is no significant correlation, however, between F and Cu. H_2O - extractable Cl and F show even more erratic distribution and no obvious relationship with mineralization. Kesler et al (1973) also found no apparent correlation between contents of H_2O - leachable Cl and F and the ore-bearing potential of intrusive rocks.

B dispersion, though erratic, shows consistent relationship with mineralization. This is most obvious at Lornex and Highmont,

although high B concentrations in the latter are associated with tourmaline.

From the foregoing discussion of primary dispersion at Highland Valley, it is evident that the closely-related processes of hydrothermal alteration and metallization have introduced major changes in metal abundances around porphyry-type deposits. Hydrothermal effects involving the formation of potassic minerals (sericite, K-feldspar) and associated metal redistributions and additions show consistent association with mineralization. Because of the fine-grained mineralogy of alteration zones, the intimate relationship between metallization and metasomatic effects has important implications for application of bedrock geochemistry to the search for porphyry-type deposits at Highland Valley and other areas.

Applications to Mineral Exploration

Applications of regional geochemical data to exploration have been examined in Chapter 5. Here, detailed lithogeochemical surveys are discussed. Table LVII summarizes geochemical contrast and relative extent of halos at the various deposits.

One of the principal objectives of detailed lithogeochemical surveys in prospecting is to delineate mineralized zones that are most suitable for further detailed exploration or mine development. On the basis of geochemical results obtained in this study, the following observations are relevant to prospecting for porphyry-type deposits in the Guichon Creek batholith and other

TABLE LVII: Comparison of relative contrast and extent of halos at
Highland Valley deposits.

	Bethlehem - JA		Valley Copper		Lornex		Highmont	
	² Contrast	¹ Extent of halos	² Contrast	¹ Extent of Halos	² Contrast	¹ Extent of Halos	² Contrast	¹ Extent of Halos
Cu	66	3	241	3	84	3	14	3
Mo	5	1	5	1	7	1		
S	12	3	9	3	-	-	-	-
Hg	-	2	-	0	-	-	-	-
B	2	1	1	0	4	3	3	3
Cl	-	1	1	0	-	-	-	-
F	-	1	1	0	-	-	-	-
Rb	1	2	1	2	-	-	-	-
Sr	*2	2	*1	2	*2	2	*1	2
Ba	*1	2	*1	2	*1	2	*1	1
Zn	*1	0	*2	2	2	2	1	1
Mn	*2	0	*2	2	*2	2	1	1
Ti	-	0	-	-	1	1	*1	0
V	-	0	-	-	1	1	1	0

¹Extent of halos

0 = Nonexistent

1 = Narrow; confined to ore zone

2 = Extensive; within alteration aureole

3 = Very Extensive; beyond alteration aureole

*Negative contrast

- Not applicable

²Contrast in relation to regional background

similar calc-alkaline intrusions, using bedrock, residual soils and glacial overburden close to its source.

(1) S shows the most consistent and probably the broadest halos, extending at least 0.5 km from the ore zones at Valley Copper and Bethlehem-JA. Pronounced S anomalies in bedrock suggests that SO_2 in soil gas or air can be useful in delineating mineralized zones at Highland Valley.

(2) Cu shows an extensive halo and high contrast, but its distribution is erratic. Its erratic behaviour is attributed to mode of occurrence principally as fracture-fillings and veinlets. Consequently, a large number of samples is required to overcome the sampling problem and to establish reliable anomalies.

(3) Distribution of sulphide-held Fe using KClO_3 -HCl attack can be utilized in delineating pyrite halos peripheral to porphyry-type deposits (e.g. JA and Valley Copper). KClO_3 -HCl-extractable Cu corresponds to Cu held in sulphides, and hence constitutes a technique of improving geochemical contrast between background and mineralized environments.

(4) In view of the close spatial and temporal relationships between alteration involving potassic minerals (sericite, K-feldspar) and Cu mineralization in the majority of porphyry-type deposits in

North America (Guilbert and Lowell, 1973), the distribution of Rb, Sr, Ba or K, Ca, Na can be useful in outlining zones of most intense hydrothermal activity and metallization. Sr and Na have the greatest potential in this regard, because they are not tied to specific alteration minerals as are Rb, K and Ba. Moreover, the use of these lithophile elements has obvious advantages over mineralogical techniques because of the fine-grained texture of most alteration minerals.

(5) The use of element ratios, such as Ba/Sr and Rb/Sr, has obvious advantages in eliminating irregularities in metal distribution that might be attributed to mineralogical control or analytical/sampling errors. Ba/Sr ratios exceeding 1 and Rb/Sr ratios more than 0.1 broadly define mineralized zones in the Highland Valley, independent of rock and alteration types.

(6) Although no Hg anomaly occurs at Valley Copper, a pronounced and broad one is associated with Bethlehem-JA. Thus Hg in bedrock, soils and soil gas and air might be useful in delineating orebodies similar to JA.

(7) B constitutes a potential pathfinder for deposits associated with breccia pipes and quartz porphyries as at Highmont and Lornex.

(8) Cl and F, either as total or water-extractable, show no consistent relationship with mineralization. Moreover, contrast

between background and mineralized areas is very weak. Consequently, the use of halogens in bedrock, soil or air probably has no potential for exploration in the Highland Valley.

(9) In the absence or scarcity of outcrops, suboutcrop samples collected by drilling below overburden can be utilized for bedrock geochemical studies, especially in heavily drift-covered areas.

(10) Factor analysis constitutes a potent tool in analyzing relationships among elements in multi-element geochemical studies. In this study it has proved useful in isolating element associations related to distinct processes, such as hydrothermal alteration or mineralization. Furthermore, results of factor analysis have been consistent with subjective interpretations and known geologic and mineralogic evidence.

CONCLUSIONS

In all the porphyry copper deposits examined in this study similar geochemical patterns apply. Variations in contents of 'femic' elements (Zn, Mn, Ti, V, Fe, Mg) are related principally to primary lithologies, although effects of hydrothermal redistribution are apparent. The lithophile elements Sr, Ba, Na and Ca are sensitive indicators of hydrothermal processes. These elements are consistently depleted in zones of intense argillic and phyllic alteration, and metallization, whereas K and Rb, not appreciably depleted

in these zones, are enriched in potassic and phyllic zones which are, in some deposits, associated with mineralization. Cu and S show the most extensive anomalies and highest contrast. Hence, they are useful in delineating mineralized zones. Hg and B constitute useful pathfinders for some porphyry copper deposits such as JA, Lornex and Highmont. On the basis of pronounced S and Hg anomalies in bedrock, SO_2 and Hg in soil gas and air can be useful in rapid or reconnaissance exploration for porphyry type deposits in the Guichon Creek batholith.

CHAPTER SEVEN

MICRO-GEOCHEMICAL DISPERSION IN MINERALS

INTRODUCTION

In recent years, numerous workers have investigated the use of trace element contents of mineral phases, especially biotite, in geochemical exploration (see Levinson, 1974, pp. 336-341). However, the emphasis of the majority of these studies has been to use metal contents of minerals in differentiating barren from potentially ore-bearing intrusions (Parry and Nackowski, 1963; Putman and Burnham, 1963; Al-Hashimi and Brownlow, 1970; Blaxland, 1971). Relatively few workers have assessed application of mineral geochemistry to either defining primary halos around orebodies, or in enhancing geochemical contrast between background and mineralized environments.

Lovering et al. (1970), investigating Cu content of biotite in a large ore-bearing stock at Sierrita Mountains, Arizona, found that Cu concentrations increased from a few p.p.m. in the northern part to as much as 1% near Cu deposits at the southern end. Corresponding Cu content of bedrock showed only a subtle increase from 5 to 300 p.p.m. The authors concluded that trace element content of biotite is a more sensitive and extensive indicator of mineralization. Darling (1971) reported that the concentrations of Cu and other trace elements in biotite increased as the Pine Creek W-Mo-Cu orebody is approached, although he did not present corresponding data for whole rocks. Bradshaw and Stoyel (1968) investigated trace element variations in biotites and feldspars from granitic wall rocks of ore veins in southwest England. Their results

indicate that trace element contents of mineral phases showed similar, but less well-defined anomalies than whole rock data.

Trace element contents of magnetites have also been investigated as a guide to mineralization (see Levinson, 1974). High concentrations of Cu and Zn were reported by de Grys (1970) in magnetites from intrusions associated with porphyry Cu mineralization. In contrast, Theobald and Thompson (1962) noted that magnetites from rocks presumably associated with Cu mineralization at Butte, Montana were relatively impoverished in Zn. Hamil and Nackowski (1971) reported high abundances of Ti and Zn in magnetites associated with major Pb-Zn mineralization, and low values with major Cu deposits. Stanley (1964) found no correlation between Cu content and modal proportion of magnetite in whole rocks from the Granduc Cu deposit.

Objectives of the present investigation are twofold; (1) to examine the nature of micro-dispersion of trace elements in minerals from background and mineralized environments; and (2) to determine if geochemical contrast between background and anomalous samples can be enhanced by chemical analysis of mineral fractions, utilizing total and partial extraction techniques.

METHODS OF STUDY

A suite of 26 granodiorites was selected from outcrop samples obtained from Highmont and Lornex properties (Fig. 57). Samples were separated into 3 groups on the basis of Cu content and proximity to mineralization. 10 samples containing less than

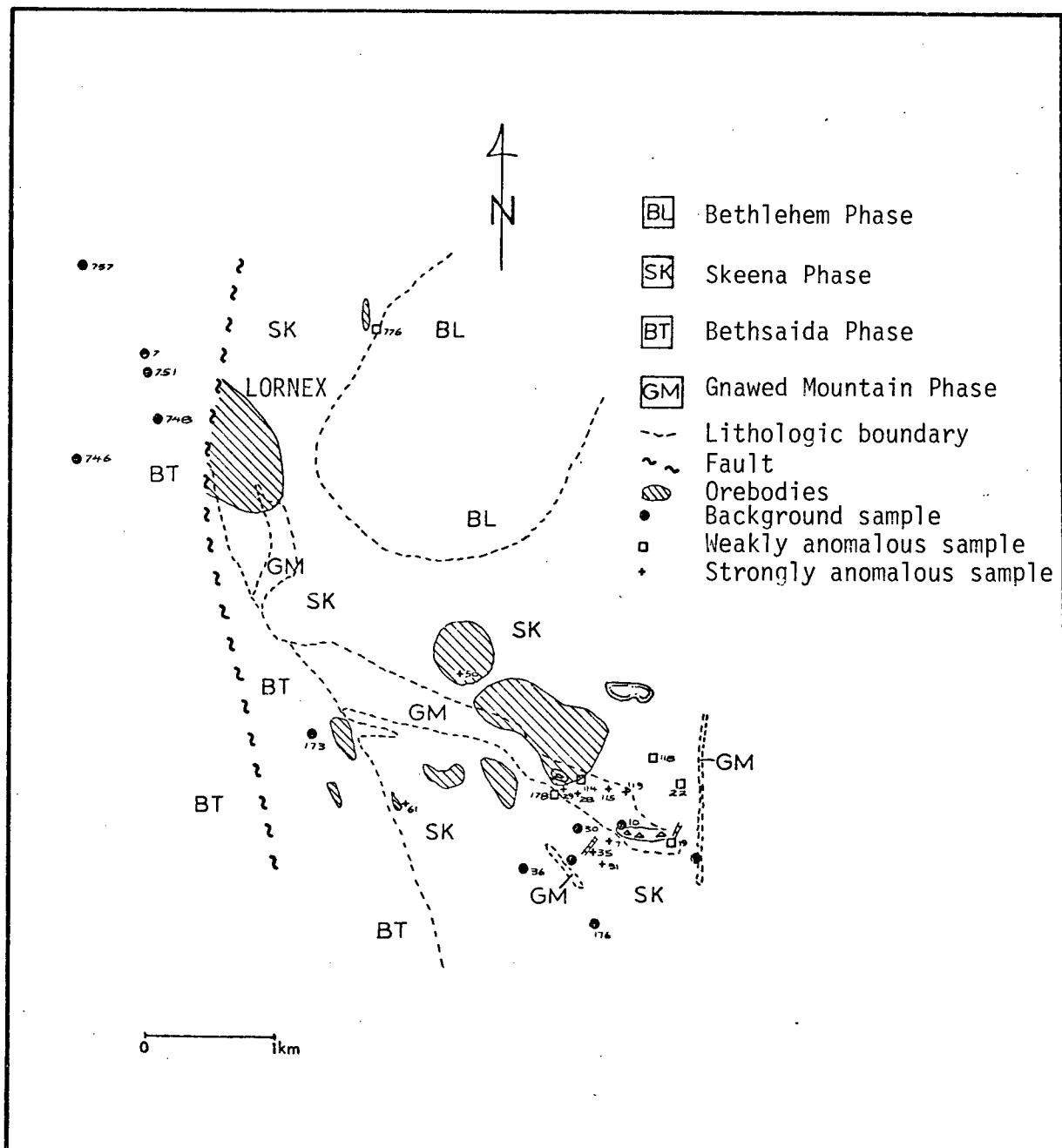


FIGURE 57: Location of rock and mineral samples, Highland Valley (Map after McMillan, 1973)

100 p.p.m. whole-rock Cu are considered as "background"; 7 samples with Cu values ranging from 100 to 600 p.p.m. are termed "weakly anomalous"; and the remaining 9 samples with Cu values ranging from 601 to 5000 p.p.m. are designated "strongly anomalous". Fourteen of the samples are equigranular rocks of the Skeena Phase, and the remainder are porphyritic rocks of the Bethsaida and Gnawed Mountain Phases.

Biotite, quartz-feldspar and magnetite fractions were separated by methods described in Chapter 4. Preliminary petrographic examination indicated that the majority of samples contained little or no hornblende (Table LVIII), nevertheless hornblende was removed as an impurity. On the basis of chemical analysis, all mineral fractions are considered more than 90% pure. However, the K content of biotites suggest a varying degree of chloritization, especially in "anomalous" samples. No obvious relationship exists between K content of biotites and concentrations of trace elements (Table LIX). This is consistent with the observations of Putman and Burnham (1963) and Graybeal (1973) that chloritization of biotite does not appreciably affect trace element content.

Original samples were examined microscopically, and modal data obtained for 21 (Table LVIII). However, 4 samples were too altered to obtain reliable modal analysis, and were replaced by other samples with similar Cu levels, for which modal and chemical data were available. Plagioclase feldspars in anomalous samples are weakly to moderately sericitized, although crystal form and twinning can still be observed. Biotites are generally fresh, although a few

TABLE LVIII: ¹Trace Element and Modal Content of Whole Rock Samples

SAMPLE NUMBER	Trace Cu	Elements Zn	(ppm) Mn	Modal Composition (vol. %)**					
				Biotite	Horn- blende	K-feld- spar	Plagio- cline	Quartz	Accessories
GM 2	56	30	254						
GM 10	11	31	250						
SK 30	14	20	279	6.24	0.43	15.92	58.28	18.28	0.81
SK 34	27	43	493	2.90	4.56	5.61	63.77	21.52	1.64
SK 36	34	30	345	3.40	1.1	14.8	55.43	25.00	0.03
BT 173	33	18	241	3.90	1.0	10.41	55.93	27.90	0.90
BT 176	51	31	353	7.55	0.06	6.70	57.13	25.82	2.14
BT 746	6	35	404	6.70	0.0	15.47	54.27	23.24	0.28
BT 748	18	36	445	3.36	0.44	6.83	65.60	22.72	1.03
BT 751	14	28	382	1.84	0.0	5.84	64.02	27.05	0.83
SK 19	542	42	366	2.05	4.28	3.21	68.13	21.19	1.14
SK 22	441	38	292	4.40	2.55	4.4	58.94	25.68	1.26
GM 114	185	18	132	3.02	0.0	3.02	66.12	24.45	0.37
GM 118	327	31	304	5.90	0.0	5.90	62.00	19.12	0.93
SK 178	147	37	383	0.75	1.89	0.75	66.38	25.28	0.47
BT 757	155	20	345	6.00	0.0	6.00	69.00	15.67	5.21
SK 776	539	24	214	3.23	0.0	3.23	62.95	22.05	0.35
SK 7	2821	38	342	6.70	0.10	0.83	67.78	22.50	2.08
*SK 28	609	27	352						
SK 29	2784	25	193	6.44	0.01	7.20	65.81	20.27	0.81
*SK 31	4689	35	311						
*SK 35	1400	37	349						
SK 50	1828	22	284	3.19	0.0	1.39	62.52	31.66	1.39
SK 61	823	24	347	3.66	5.11	7.78	57.34	20.88	0.18
GM 115	609	34	234	12.10	0.0	6.30	53.86	28.75	0.74
GM 119	1748	23	196	5.93	1.25	5.93	52.41	33.86	0.98

SK = Skeena Phase; BT = Bethsaida Phase; GM Gnwed Mountain
Phase (-) Data not available *Altered sample.

¹Total digestion **More than 1000 point counts per sample

are partly chloritized or sericitized. Sulphide inclusions occur within and around the margins of many of the biotites, including those with background Cu content. Examination of polished-thin sections show that pyrite, bornite and chalcopyrite are the dominant sulphides (Plate 13). In "anomalous" samples, K-feldspar is altered to varying extent, and difficult to identify. Vein quartz in some of the mineralized samples contains interstitial opaque inclusions which may be sulphides or oxides. Modal ratio of quartz to feldspar in most samples is approximately 1:3.

In the following data presentation and discussion, "anomalous" and "background" samples refer to anomalous and background bedrock samples and their mineral fractions.

RESULTS

Results of chemical analysis of whole rock, biotite, quartz-feldspar and magnetite fractions for total Cu, Zn, Mn, Co and Ni and sulphide-held Cu, Zn and Mn are presented in Tables LVIII to LX. Appropriate correlation diagrams and coefficients are shown in Figs. 58 to 71 and Table LXI. Cu concentrations in bedrock range from 6 to 4689 p.p.m. Geometric means for background and all anomalous samples are 21 and 745 p.p.m. respectively (Table LVIII).

(a) Biotite

Trace element contents of biotites are tabulated in Table LXIX. Cu values range from 44 to 5617 p.p.m., and average 98 p.p.m. for background and 1624 p.p.m. for anomalous samples. Background mean value for Cu is similar to the mean value of 113 p.p.m. obtained

TABLE LIX: Trace and major element contents of minerals.

Biotite									Magnetite			Quartz-Feldspar				
	Cu	Zn	Rn	Co	Al	Fe ₂ O ₃	K ₂ O		Cu	Zn	Co	Cu	Zn	K ₂ O	Na ₂ O	CaO
<u>Background Samples</u>									(n = 10)							
SK 2	123	275	2322	64	36	15.57	12.26	1.66	153	94	36	66	22	0.74	4.59	2.53
SK 10	52	182	1515	35	75				110	122	20	16	32	0.63	5.50	1.65
SK 30	44	279	3617	69	45	12.25	12.72	2.31	35	30	49	18	16	1.66	4.47	3.27
SK 34	49	455	4960	72	31	13.70	13.91	2.10	43	65	48	16	21	1.48	4.20	3.15
SK 36	149	172	1934	42	39	14.01	7.07	1.42	66	44	44	62	29	1.70	3.79	2.78
ET 173	110	187	4346	42	27				47	43	22	135	26	1.53	3.45	2.45
ET 176	164	277	3695	70	51	14.10	13.15	3.62	71	48	60	38	13	1.73	4.17	3.07
ET 746	105	902	8774	67	34				58	118	39	12	8	1.58	4.59	2.37
ET 748	39	931	11225	59	31				86	108	46	24	15	1.73	4.52	2.18
ET 751	226	565	8866	57	33	14.60	12.36	2.25	87	88	45	18	8	1.54	4.70	2.43
Mean	98	349	4195	56	40				67	68	40	29	17			
<u>Weakly Anomalous Samples</u>									(n = 7)							
SK 19	513	365	3403	62	40	15.54	15.48	4.20	832	64	34	408	34	1.66	4.00	2.51
SK 22	474	390	4368	65	47	15.32	7.59	3.05	220	64	38	513	21	1.48	4.42	3.27
SK 114	673	248	4407	45	25				846	61	34	142	20	2.09	4.67	1.80
SK 118	711	216	2164	55	34				110	48	37	486	26	1.32	3.52	2.74
SK 172	483	259	2484	47	38	15.00	10.05	1.81	110	56	38	29	16	1.78	4.50	2.66
SK 757	2644	299	3417	60	54				93	55	49	127	11	1.45	4.75	2.73
SK 776	1750	312	3171	76	32	16.78	13.63	2.43	390	38	59	318	12	1.65	4.29	2.87
Mean	683	292	3250	58	37				251	54	40	210	19			
<u>Strongly Anomalous Samples</u>									(n = 9)							
SK 7	531	421	5821	54	21	12.54	15.20	4.36	544	55	24	2420	26	1.58	3.25	1.85
SK 28	2645	326	2898	42	34				567	73	26	1056	20	1.66	4.52	1.56
SK 29	2576	326	5256	46	12				629	68	36	2365	22	1.70	4.49	2.04
SK 31	5517	294	3296	49	31				5451	73	36	3465	28	1.29	4.04	2.25
SK 35	5310	181	2038	45	44	16.01	8.55	2.55	305	51	41	2195	29	1.84	3.12	2.17
SK 50	2736	198	1953	53	29				175	48	29	384	18	1.56	4.34	3.13
SK 61	1858	209	2798	53	24				122	39	37	662	22	1.43	4.12	3.15
SK 115	2510	315	3246	43	17				245	67	36	793	23	1.47	4.67	2.17
SK 119	3022	288	3410	47	23				4246	64	37	1637	21	1.42	4.44	2.24
Mean	2549	275	3208	49	24				576	59	33	1440	23			
Mean (All Anomalous)		288	3227	52	29				401	57	36	619	21			

by Brabec (1970) for fresh biotites in the Guichon Creek batholith, and to the average values of 75 and 90 p.p.m. cited by Putman and Burnham (1963) and Parry and Nackowski (1963) for unmineralized biotites from Arizona and Basin and Range province respectively. Cu contents of biotites from anomalous samples are considerably higher than those from background samples (Table LXIX). Lovering et al. (1970) reported Cu values as high as 1% in biotites from mineralized rocks in Arizona. Similar high Cu values have been documented by Al-Hashimi and Brownlow (1970) and Graybeal (1973).

Levels of Co, Mn, Ni and Zn are consistently lower in anomalous than background samples. However, the Student's t-test indicates that difference is only significant for Ni at the .05 confidence level. (Table LX).

(b) Magnetite

Average Cu concentrations in magnetites from background and anomalous samples are 67 and 401 p.p.m. respectively. Cu values exceeding 4000 p.p.m. occur in two samples (Table LIX). Brabec (1970) obtained a mean Cu value of 398 p.p.m. for magnetites from the whole batholith. This mean value is conspicuously high, perhaps indicating that magnetites from the relatively older and more mafic rock phases contain high Cu values comparable to those found in gabbros and ultramafics (Wager and Mitchell, 1951). Differences in analytical techniques might also account for the discrepancy. Lyakhovich (1959) reported mean Cu values of 5 to 80 p.p.m. in magnetites from unmineralized intrusives in the U.S.S.R.

TABLE LX: Student's T test of ¹background and ²anomalous samples.

Background vs Anomalous	T - Value	D.F.
WrCu <u>vs.</u> WrCu	9.26*	24
WrZn <u>vs.</u> WrZn	1.62	20
WrMn <u>vs.</u> WrMn	1.85	19
BtCu <u>vs.</u> BtCu	9.25*	24
BtZn <u>vs.</u> BtZn	1.01	11
BtMn <u>vs.</u> Bt Mn	1.15	12
BtCo <u>vs.</u> Bt Co	0.94	24
BtNi <u>vs.</u> BtNi	2.07*	24
FQCu <u>vs.</u> FQCu	6.64*	24
FQZn <u>vs.</u> FQZn	1.32	24
MgCu <u>vs.</u> MgCu	5.34*	20
MgZn <u>vs.</u> MgZn	1.13	11
MgCo <u>vs.</u> MgCo	1.08	24

Wr = Whole rock; Bt = Biotite; Mg = Magnetite; FQ = Quartzfeldspar; D.F. = Degree of freedom

* Significant at the .05 confidence level.

¹ 10 samples ² 16 samples

Al-Hashimi (1969) noted that Cu levels in magnetites from the Boulder batholith range from less than 1 to 230 p.p.m. and average 40 p.p.m.

Magnetites, are regarded as efficient concentrators of Zn (Theobald et al., 1962; de Grys, 1970). However, Zn content of magnetites examined in this study ranges from 30 to 122 p.p.m. Levels of Zn and Co are consistently lower in anomalous than background samples, although a Student's t-test suggests the difference is not significant at the .05 confidence level.

(c) Quartz-Feldspar

Cu concentrations in quartz-feldspar fractions range from 12 to 3465 p.p.m. and average 29 and 619 p.p.m. for background and anomalous samples respectively. Mean Cu content of background samples is similar to mean values of 25 and 50 p.p.m. reported by Brabec (1970) and Bradshaw and Stoyel (1968) respectively. Average abundances of Zn in background and mineralized samples are not significantly different (Table LX).

DISCUSSION

Putman and Burnham (1963) and Putman (1972) have shown that variations in bulk chemical composition (major and trace elements) between samples from a plutonic body have three main sources: (1) variations in modal composition of the rock, with or without changes in mineralogy; (2) variations in chemical composition of constituent minerals; and (3) variations related to endogenous processes, for example, hydrothermal alteration, mineralization, weathering or

TABLE LXI: KClO_3 -HCl extractable metal in mineral phases.
(Values in p.p.m.)

	Biotite			Magnetite		Quartz-Feldspar	
	Cu	Zn	Mn	Cu	Zn	Cu	Zn
Background Samples (n = 10)							
GM 2	116	36	419	53	6	57	4
GM 10	32	27	305	-	-	11	6
SK 30	26	28	313	15	3	6	9
SK 34	22	42	311	46	3	8	6
SK 36	147	23	185	31	4	23	6
BT 173	112	21	839	30	4	106	8
BT 176	143	45	743	46	4	22	8
BT 746	79	191	2471	29	4	7	5
BT 748	69	161	2532	41	4	20	8
BT 751	214	62	546	42	4	12	5
Weakly Anomalous Samples (n = 7)							
SK 19	820	50	566	519	15	382	8
SK 22	468	65	767	139	3	386	3
SK 114	683	62	1257	641	9	107	6
SK 118	638	31	249	62	5	456	7
SK 178	384	35	268	92	5	15	6
SK 757	2297	66	856	113	13	78	5
SK 776	1557	36	233	167	6	287	3
Strongly Anomalous Samples (n = 9)							
SK 7	459	43	512	921	5	1714	3
SK 28	2671	70	674	388	5	696	7
SK 29	2995	67	1174	676	10	1868	4
SK 31	5093	58	1573	1061	6	3253	6
SK 35	5022	24	255	251	3	1139	8
SK 50	2891	40	320	142	4	355	4
SK 61	2199	18	390	61	7	610	4
GM 115	2583	53	839	179	5	737	6
GM 119	2938	29	681	674	4	1392	7

metamorphism.

Composition of mineral phases is discussed in relation to these factors.

(a) Form of Trace Elements in Mineral Phases

The form of trace elements in mineral phases was examined by sulphide-selective KClO_3 -HCl digestion. Results are presented in Table LXI and Figs. 58 to 60. In background biotite samples with less than 100 p.p.m. Cu, the proportion of Cu extracted ranges from 40 to 80%. In contrast, more than 80% of total Cu is extracted from background samples containing more than 100 p.p.m. Cu, and all anomalous samples with Cu values ranging from 384 to 5093 p.p.m. (Fig. 58). In magnetites, considerable overlap is evident in the proportion of Cu extracted from background (34 - 75%) and anomalous (20 - 100%) samples (Fig. 59). On the other hand, the proportions of Zn extracted from biotites and magnetites, and Mn from biotites (Table LXI) are generally less than 30% in both background and anomalous samples (Figs. 58 and 59 and Table LXI).

In quartz-feldspar phases, the proportion of Cu extracted in background samples range from 33 to 84%. In anomalous samples, proportion of Cu extracted increases from 60% at 100 p.p.m. total Cu to more than 95% at 500 p.p.m. (Fig. 60). This is followed by a decline in % extraction at more than 1000 p.p.m. total Cu. The extraction of Zn in anomalous quartz-feldspar samples is generally less than 35%, whereas in background samples a considerable scatter is apparent, with extraction ranging from 18 to 62% of total Zn. However, the 4 samples with more than 40% extraction are very low

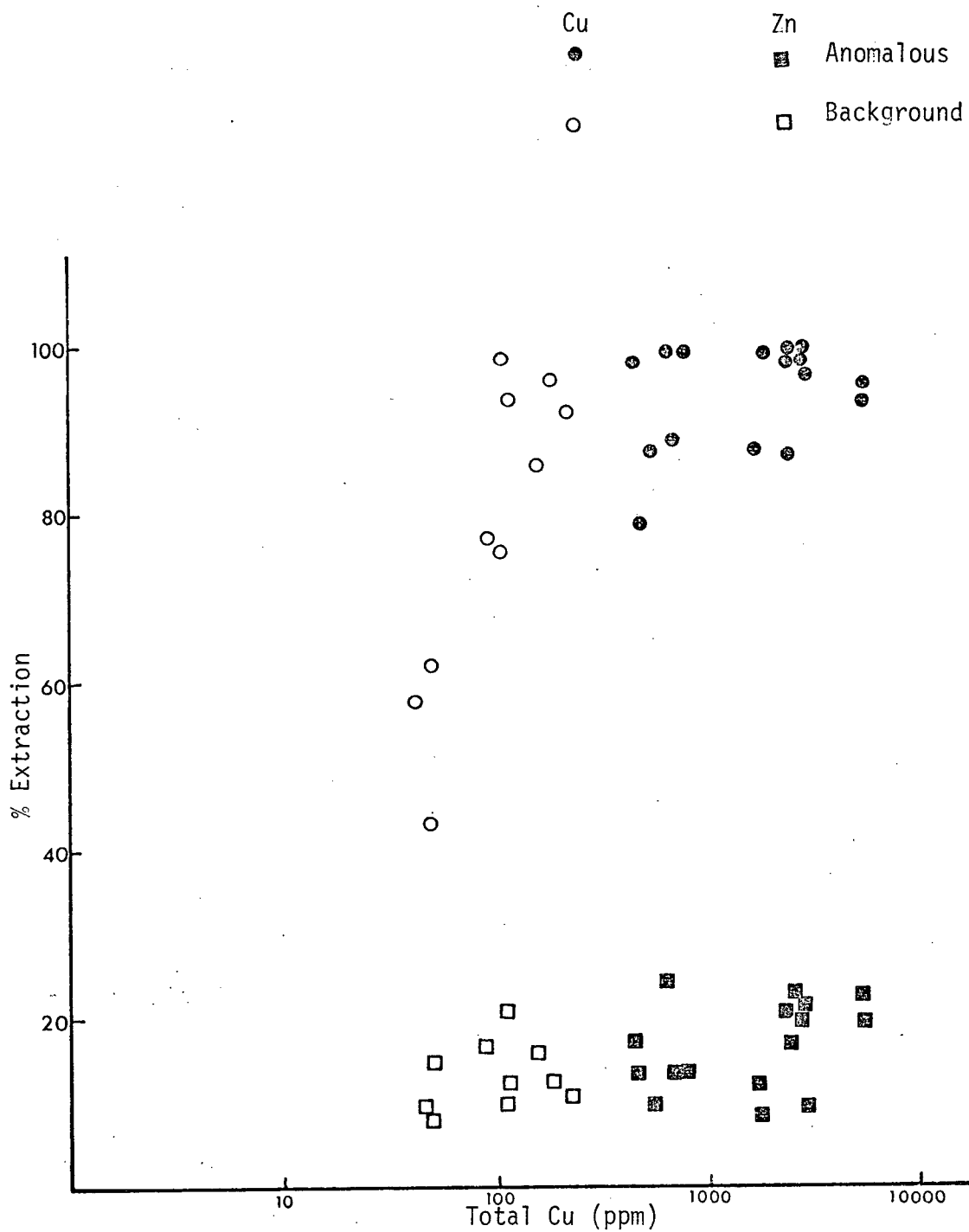


FIGURE 58: Proportions of total Copper and Zinc extracted from biotites by $\text{KClO}_3\text{-HCl}$ digestion.

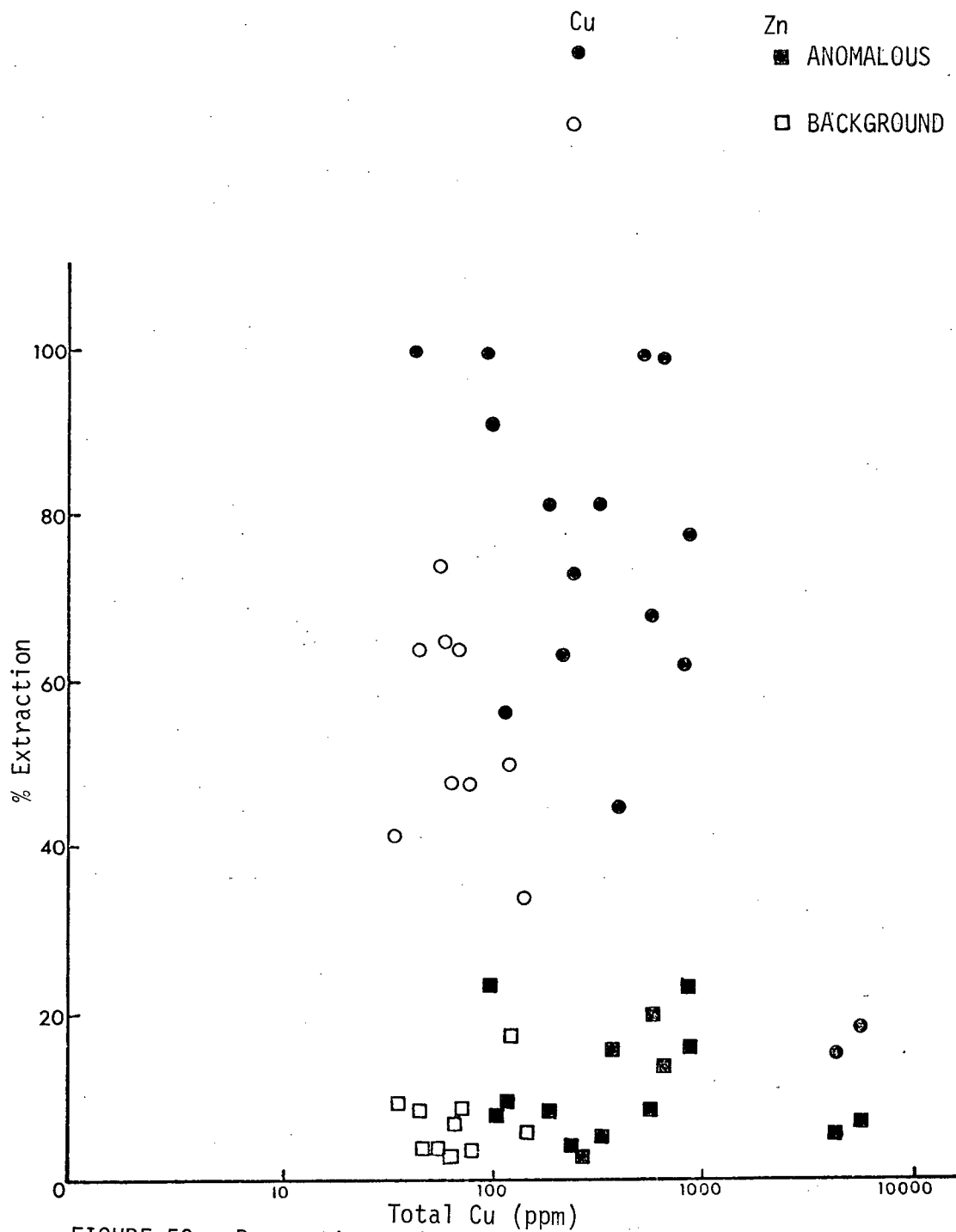


FIGURE 59: Proportions of total Copper and Zinc extracted from magnetites by $\text{KClO}_3\text{-HCl}$ digestion.

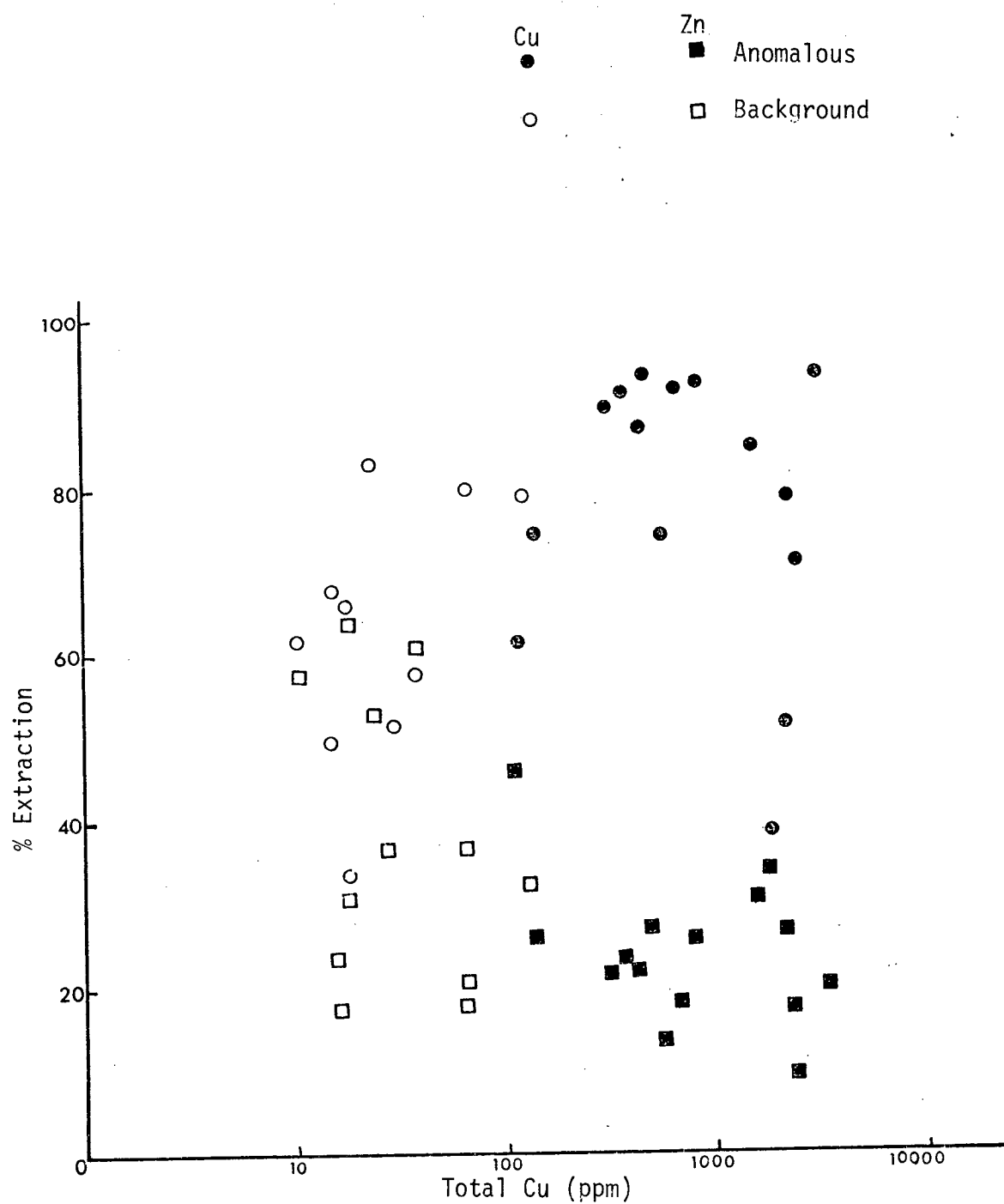


FIGURE 60: Proportions of total Copper and Zinc extracted from quartz-feldspar phases by $\text{KClO}_3\text{-HCl}$ digestion.

in total Zn (8-15 p.p.m.), consequently the high % extraction is attributed to poor analytical precision at low concentrations.

Results of sulphide-selective leach suggest that Cu occurs dominantly as sulphides in mineral phases from anomalous samples. Some background samples also contain appreciable sulphide-held Cu. In contrast Zn in all mineral phases and Mn in biotites occur mainly in non-sulphide form, presumably in substitution for Fe and Mg in crystal lattices.

(b) Chemical Variations Related to Modal Composition

Although there are no significant correlations between abundance of biotite and either whole-rock or biotite Cu (Fig. 61 and 62), the amount of Cu contributed by biotite to whole-rock samples increases with increasing modal biotite (Fig. 63). This positive relationship is strongest for biotites from mineralized samples, and reflects the occurrence of epigenetic Cu, mostly as sulphide inclusions.

A plot of whole-rock Cu versus modal proportion of accessory minerals (mainly opaque) exhibits no significant correlation for all samples, although a rather weak ($r = 0.53$) positive correlation exists between whole-rock Cu in background samples and modal accessory minerals (Fig. 64). Fig. 65 shows that the amount of K-feldspar generally decreases with increasing Cu content of whole rocks. This reflects increasing intensity of hydrothermal alteration of K-feldspar to sericite in mineralized samples.

Whole-rock Zn shows no obvious correlation with biotite

All Samples	$r = 0.21$	$n = 21$
Anomalous samples	$r = 0.30$	$n = 13$
Background samples	$r = -0.07$	$n = 8$

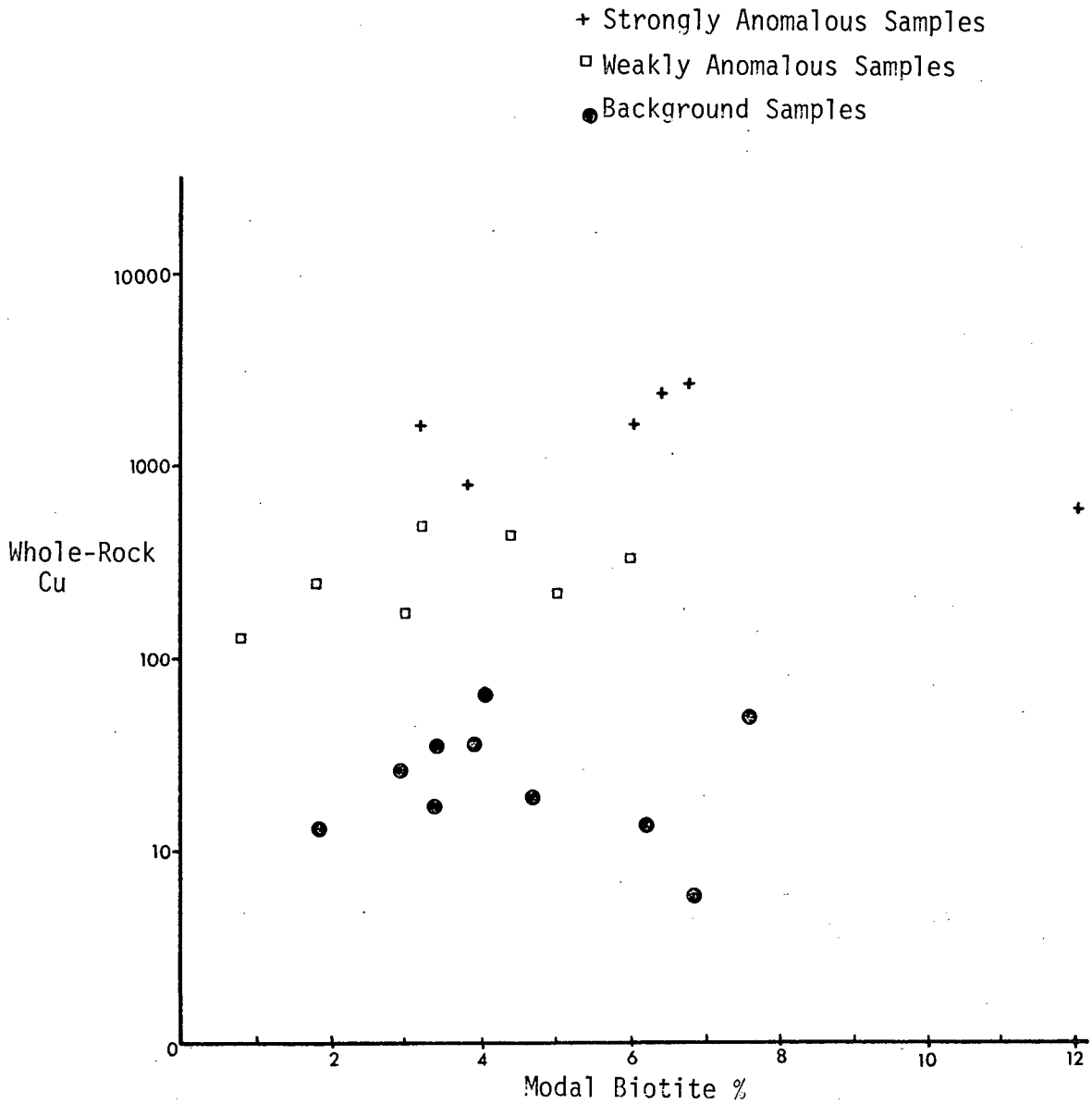


FIGURE 61: Relationship between whole-rock copper and modal proportions of biotite.

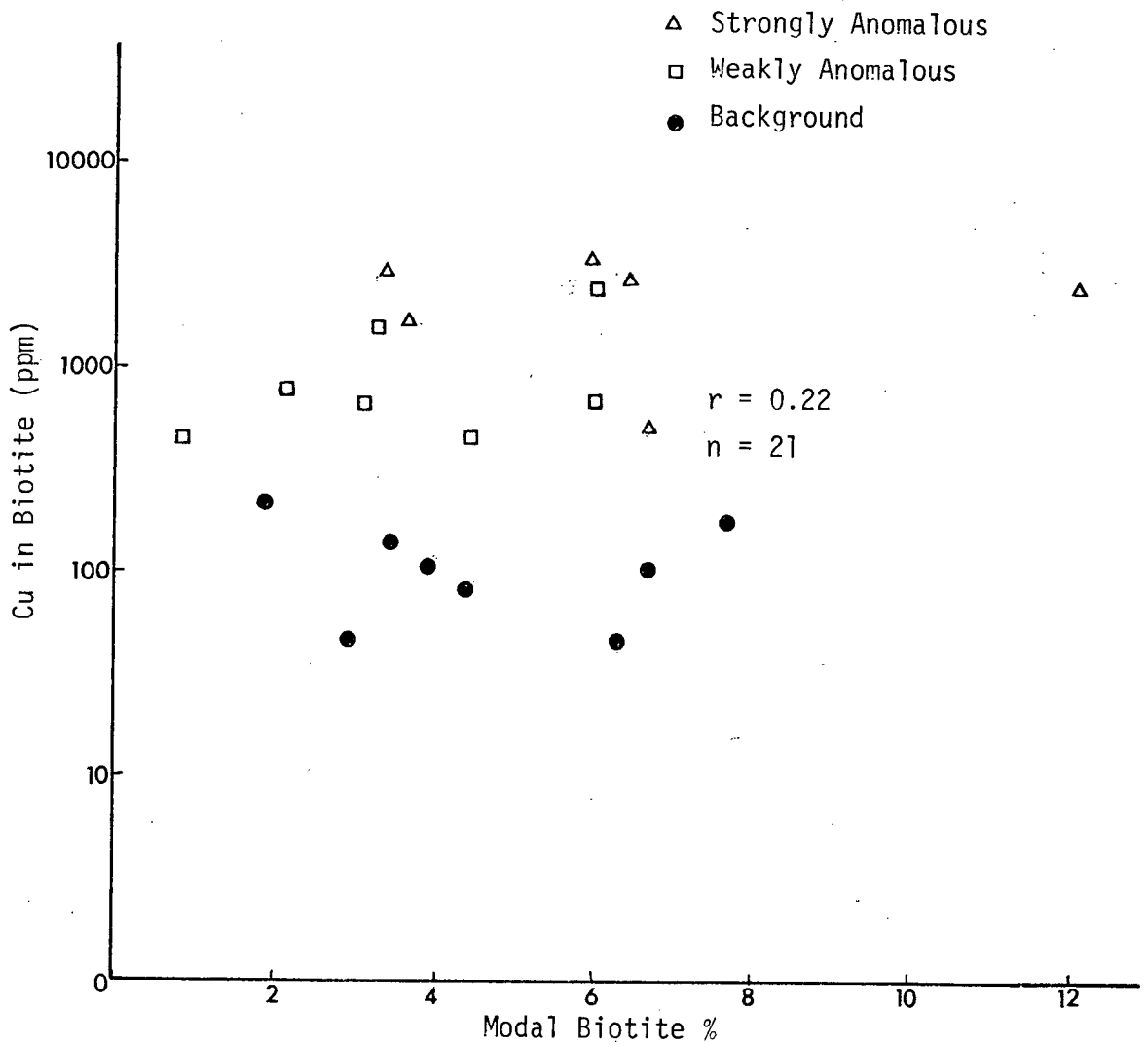


FIGURE 62: Relationship between modal and Copper contents of biotite.

All samples $r = 0.51$ $n = 21$
 Anomalous samples $r = 0.75$ $n = 13$
 Background samples $r = 0.60$ $n = 8$

△ Strongly anomalous
 □ Weakly anomalous
 ● Background

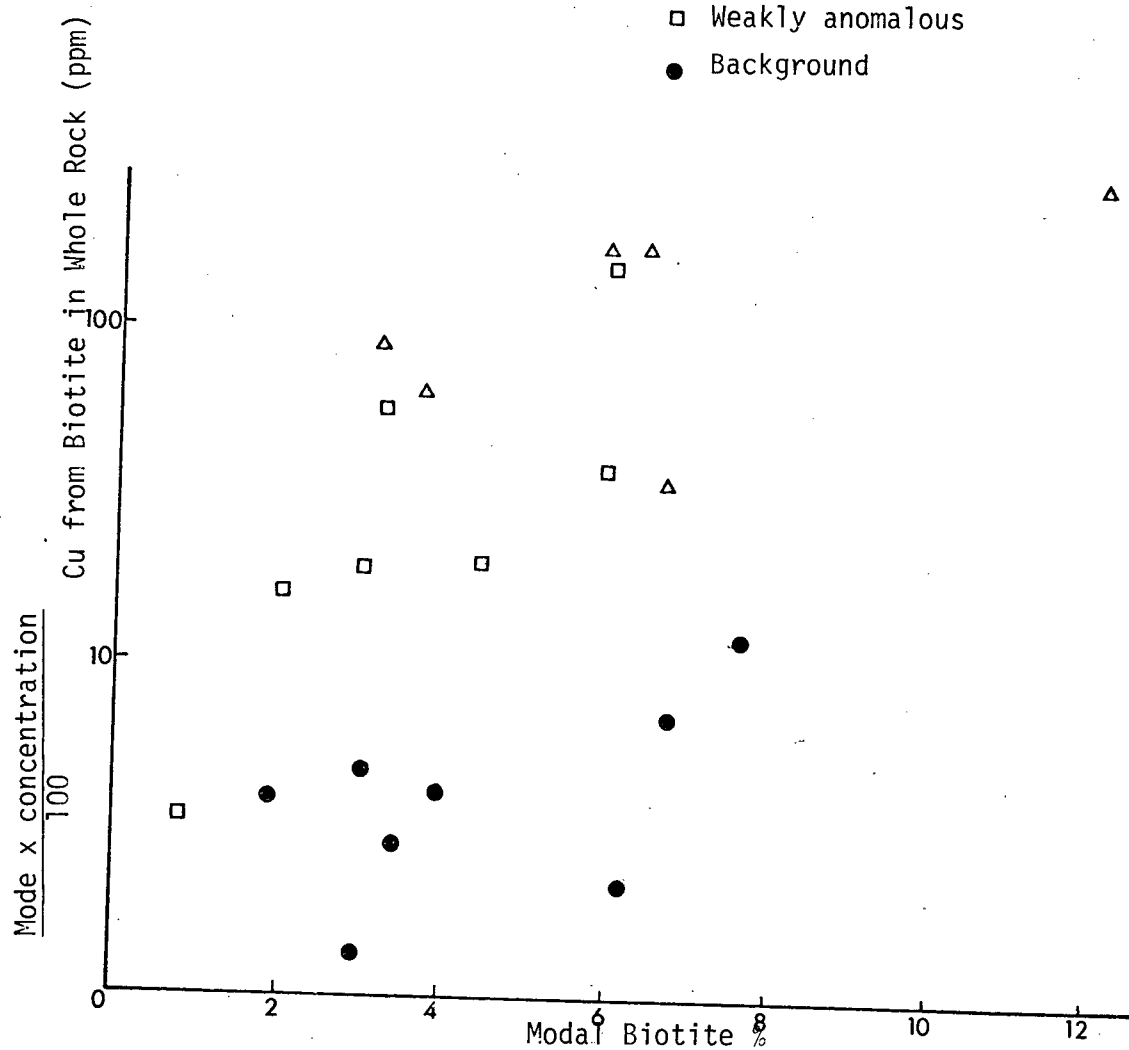


FIGURE 63: Plot of modal biotite versus Copper from biotite in whole rock

- + Strongly Anomalous
- Weakly Anomalous
- Background

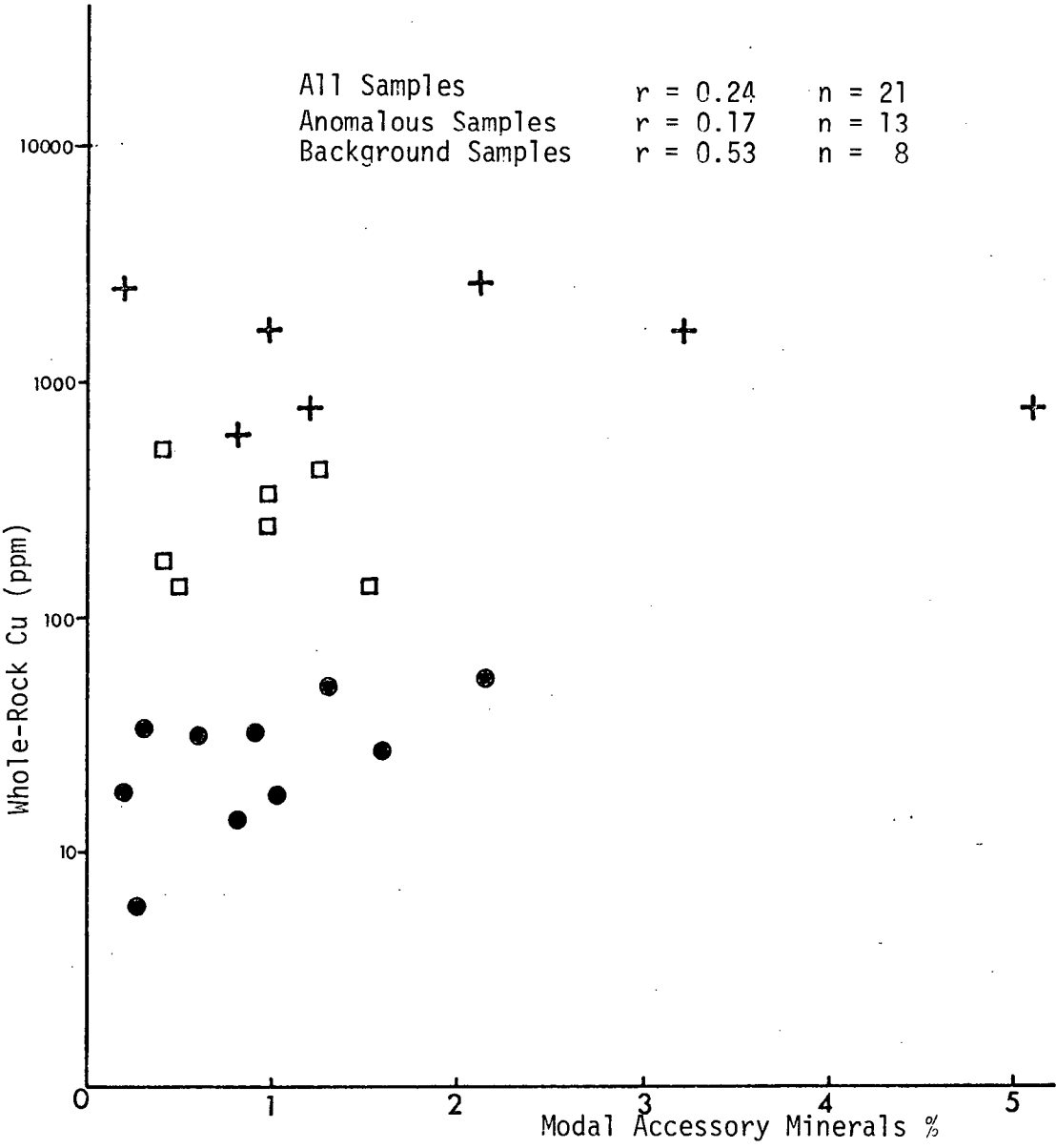


FIGURE 64: Relationship between whole-rock Copper and percent accessory minerals in rocks.

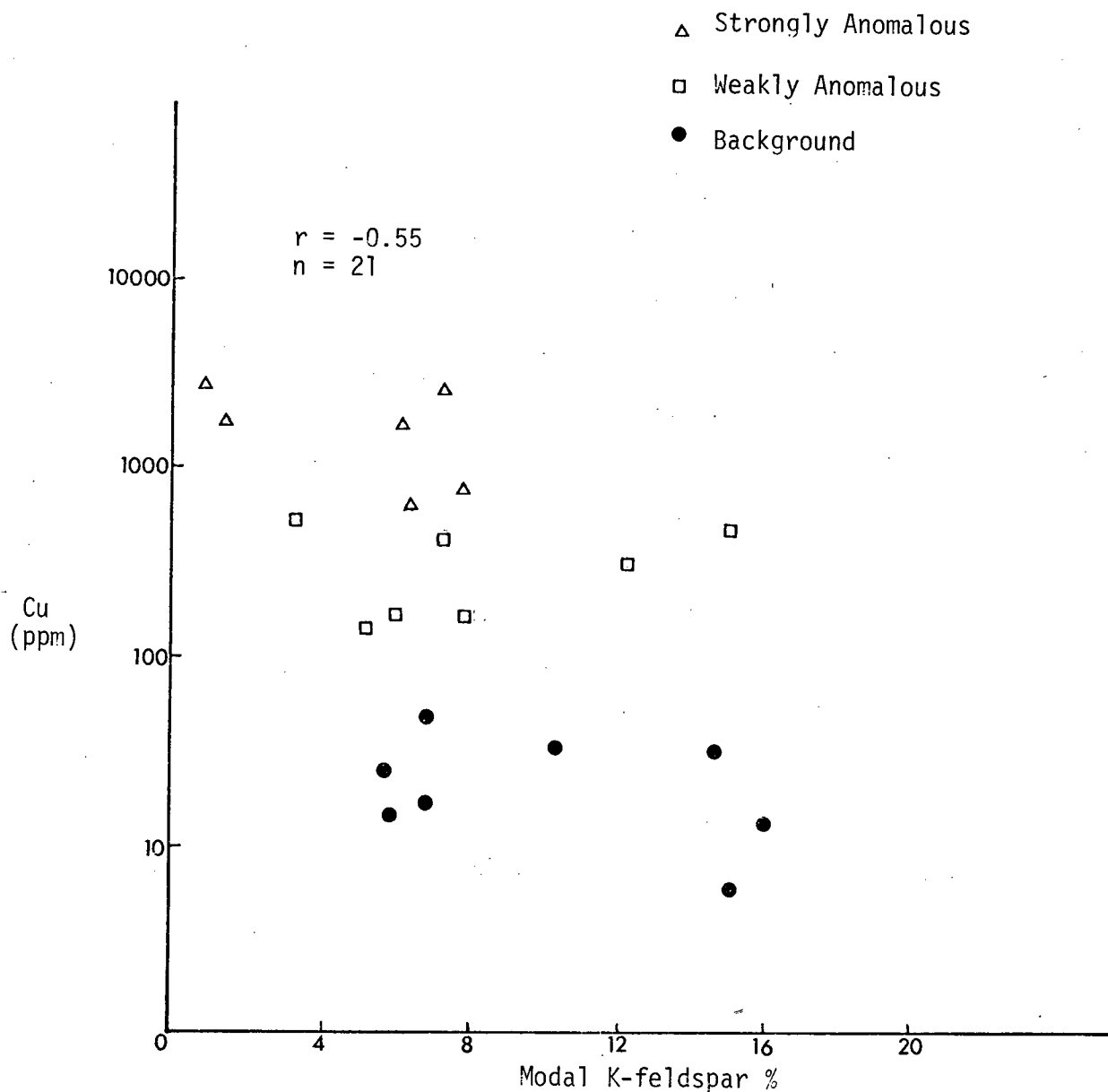


FIGURE 65: Covariance of Copper and modal K-feldspar in whole rocks.

in all samples (Table LXII), although a relatively weak positive correlation is apparent between whole-rock Zn and combined modal biotite and hornblende in anomalous samples. Nevertheless, the amount of Zn contributed to whole-rock samples by biotite increases with increasing modal biotite (Fig. 66).

(c) Variations Related to Chemical Composition of Mineral Phases

13 biotites were analyzed for Mg and Fe, and 26 quartz-feldspar fractions for Ca, Na and K (Table LIX). However, results for quartz-feldspar do not show any consistent relationships with trace elements, and consequently are not discussed further.

Biotites

Putman and Burnham (1963) have shown that major element composition of biotites can influence trace element content. Graybeal (1973) found no obvious correlation between Cu and major elements in biotite, although he obtained a weak positive correlation between Zn and Fe in biotite.

Biotites from mineralized samples are characterized by relatively high Fe and low Mg levels (Figs. 67 and 68). This reflects either the contribution of Fe from sulphide inclusions or suggest that hydrothermal processes during ore formation involved depletion of Mg and addition of Fe to biotites, probably derived from magnetite. Plots of Cu content against Fe and Mg show positive and weak negative relationships between Cu and Fe and Cu and Mg (Figs. 67 and 68) respectively. Zn and Co values generally increase with increasing Mg contents of biotites ($r = 0.50$ and 0.60 respectively).

TABLE LXII: Correlation Matrix for modal analysis and trace element
content of rocks and minerals - significant Correlations at
.05 confidence level.

Variable	WPCU	WPZN	BTCU	All samples		BT + HED	ACCESS	K-FSP
				BTZN	n=21 BT			
WRCU	1.0000							
WRZN	-0.1158	1.0000						
BTCU	0.8521	-0.2954	1.0000					
BTZN	-0.3948	<u>0.5217</u>	-0.3518	1.0000				
BT	0.2121	0.0780	0.2210	0.0520	1.0000			
BT + HED	0.1999	0.3248	0.1230	-0.0332	<u>0.7527</u>	1.0000		
ACCESS	0.2389	0.0127	0.1478	-0.1435	0.0019	0.3690	1.0000	
K-FSP	-0.5468	-0.1972	-0.3982	-0.0614	0.0829	-0.0006	-0.3048	1.0000

Anomalous Samples n = 13

Variable	WRCU	WRZN	BTCU	BTZN	BT	BT + HED	ACCESS	K-FSP
WRCU	1.0000							
WRZN	0.0814	1.0000						
BTCU	0.3808	-0.5584	1.0000					
BTZN	0.2189	0.4658	-0.2235	1.0000				
BT	0.3027	0.2218	0.3676	0.3766	1.0000			
BT + HED	0.1491	0.4671	0.1762	0.2549	<u>0.7566</u>	1.0000		
ACCESS	0.1748	-0.0253	0.0730	-0.2611	-0.0705	0.3453	1.0000	
K-FSP	-0.4214	-0.1895	0.1186	-0.2629	-0.0275	-0.0349	-0.1072	1.0000

Background Samples n = 8

Variable	WRCU	WRZN	BTCU	BTZN	BT	BT + HED	ACCESS	K-FSP
WRCU	1.0000							
WRZN	-0.1036	1.0000						
BTCU	0.1696	-0.0169	1.0000					
BTZN	-0.6992	0.5989	-0.0603	1.0000				
BT	-0.0724	-0.1325	-0.1462	-0.0697	1.0000			
BT + HED	0.1280	0.1723	-0.5550	-0.1387	<u>0.7280</u>	1.0000		
ACCESS	0.5273	0.2075	-0.1113	-0.0002	0.2123	0.4212	1.0000	
K-FSP	-0.3942	-0.3928	-0.2293	-0.2613	0.4392	0.2238	<u>-0.7186</u>	1.0000

All samples	$r = 0.73$	$n = 21$
Anomalous samples	$r = 0.88$	$n = 13$
Background samples	$r = 0.56$	$n = 8$

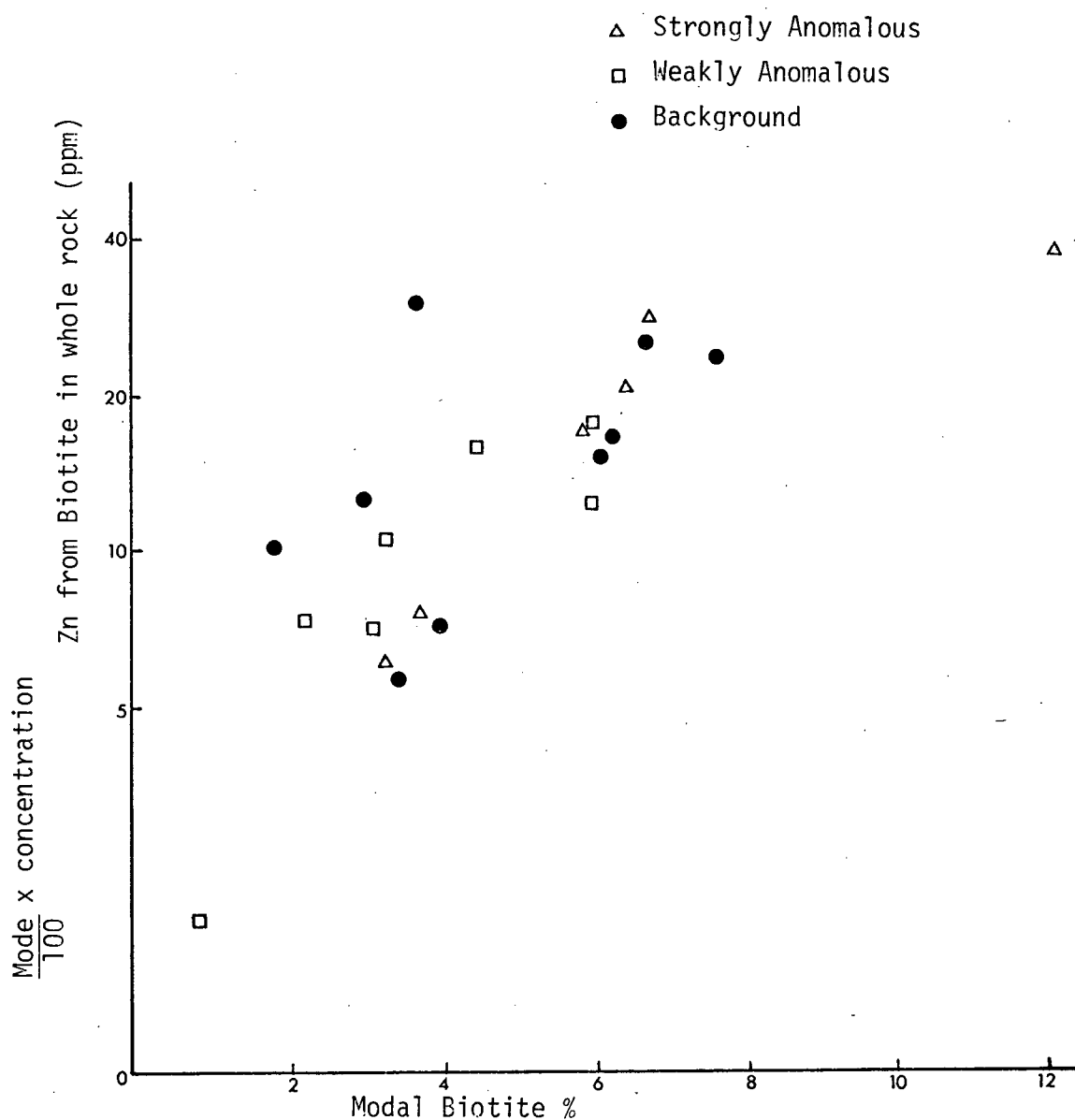


FIGURE 66: Plot of modal biotite versus Zinc from biotite in whole rocks.

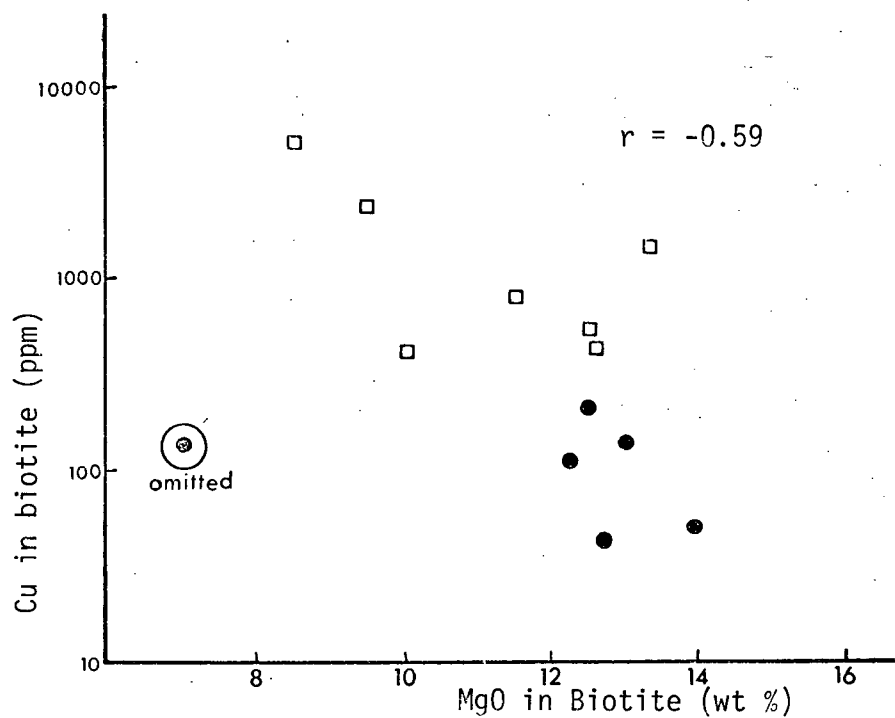


FIGURE 68: Copper versus Magnesium in biotites

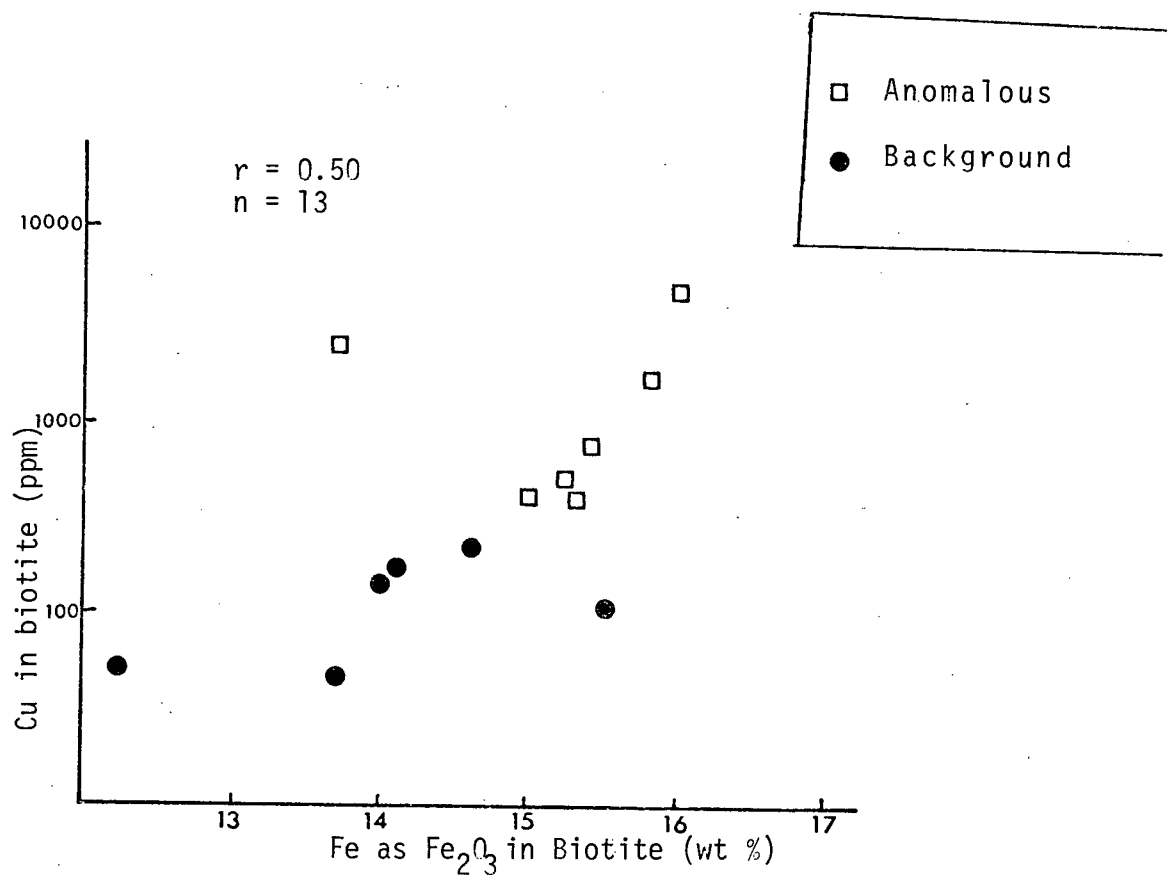


FIGURE 67: Copper versus Iron in biotites

This relationship is consistent with the ionic substitution of these elements for Mg in biotite lattices. Lack of correlation between Zn and Co, and Fe probably reflects the presence of epigenetic Fe as sulphide inclusions.

(d) Chemical Variations Related to Mineralization

Variations in trace element chemistry of minerals, if directly related to mineralization may be useful in geochemical exploration. In the anomalous samples examined in this study, all mineral phases are enriched in Cu which is principally present as sulphide inclusions (Figs. 69, 70 and 71; Table LIX). This is suggestive of an endogenous process producing a "blanket" enhancement effect on all rock constituents.

(i) Biotites

Biotites commonly are enriched in Cu which occurs dominantly as minute sulphide inclusions. Numerous workers (Lovering et al., 1970; Putman and Burnham, 1963; Al-Hashimi and Brownlow, 1970) have demonstrated that igneous biotites tend to have low Cu contents unless hydrothermal alteration and/or mineralization are associated with their host rock. This contention is supported by results of sulphide-selective leach (Fig. 58) and the strong positive correlation between whole-rock Cu and biotite Cu (Fig. 69). Petrographic evidence, which is consistent with chemical results, indicates that Cu occurs partly as small inclusions of bornite and chalcopyrite in biotite, and also along margins of ragged grains of femic minerals (Plates 14 and 15).

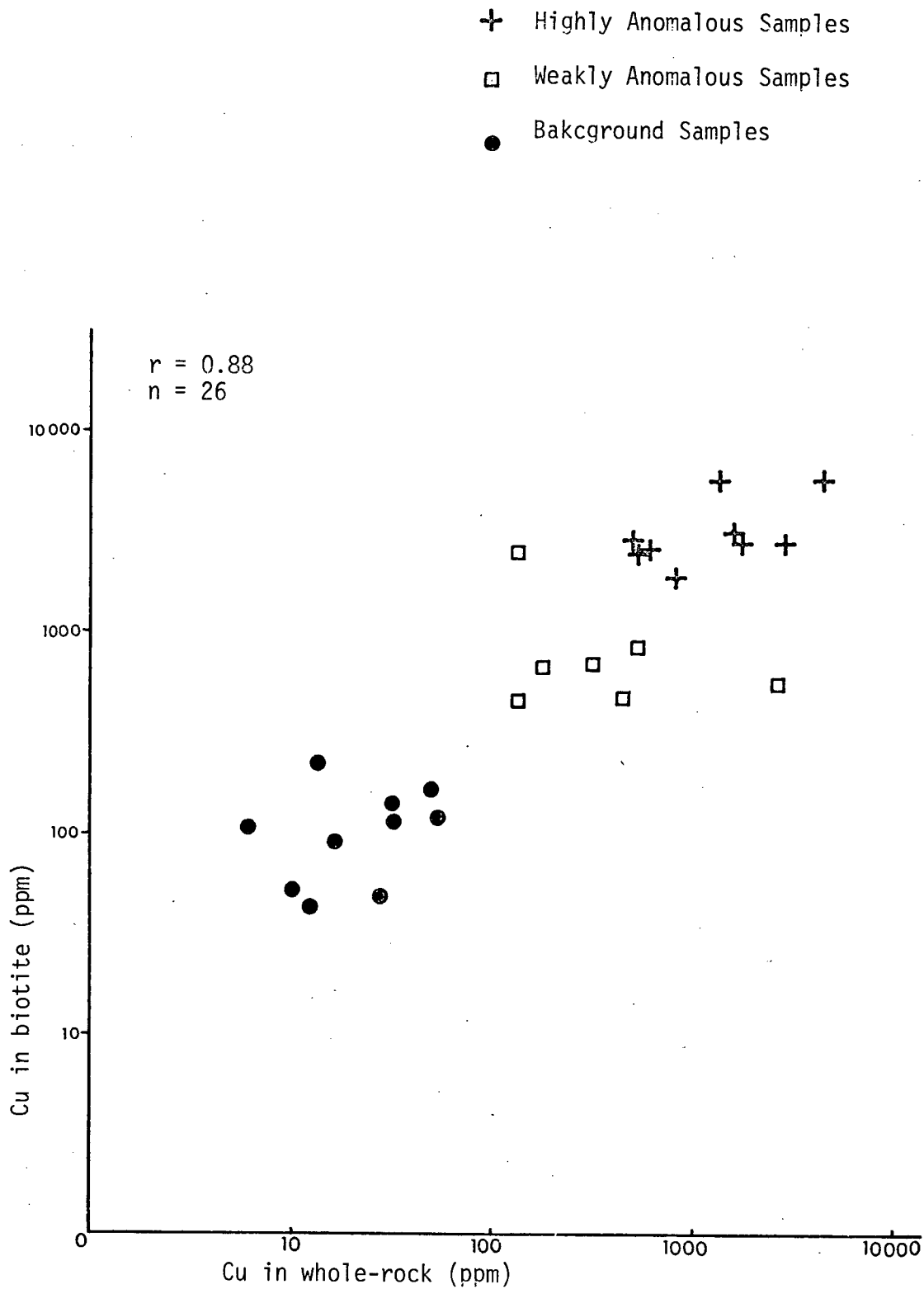


FIGURE 69: Relationship between total Copper in whole-rocks and biotites

The consistent tendency for lower Ni, Co, Zn, Mg and Mn levels in anomalous than background samples can be explained by leaching of these elements during hydrothermal and mineralization processes. This relationship corroborates field and bedrock geochemical evidence (Chapter 6) in which the aforementioned elements are leached from central zones of intense hydrothermal activity and concentrated at the outer margins of mineralized zones.

(ii) Magnetites

Magnetites from anomalous samples are characterized by enhanced Cu values relative to background samples (Fig. 70). Similar results have been reported by de Grys (1970) for magnetites associated with Cu-bearing intrusions in Ecuador. In mineralized environments, magnetite may occur in two forms: (1) as accessory primary magnetite; and (2) as epigenetic magnetite, intimately associated with sulphide phases.

Hewett (1972) undertook a mineralographic study of ore samples from Highland Valley porphyry Cu deposits. His results suggest that epigenetic magnetite is present in all the deposits, and that it is usually the first mineral in the paragenetic sequence of ore formation. Several of the photomicrographs presented by Hewett (1972) show inclusions of bornite in epigenetic magnetite. In this study no attempt was made to separate the two types of magnetite and the enhanced Cu content of magnetites from anomalous samples might simply reflect the epigenetic component as indicated by the results of sulphide-selective digestion (Fig. 59).

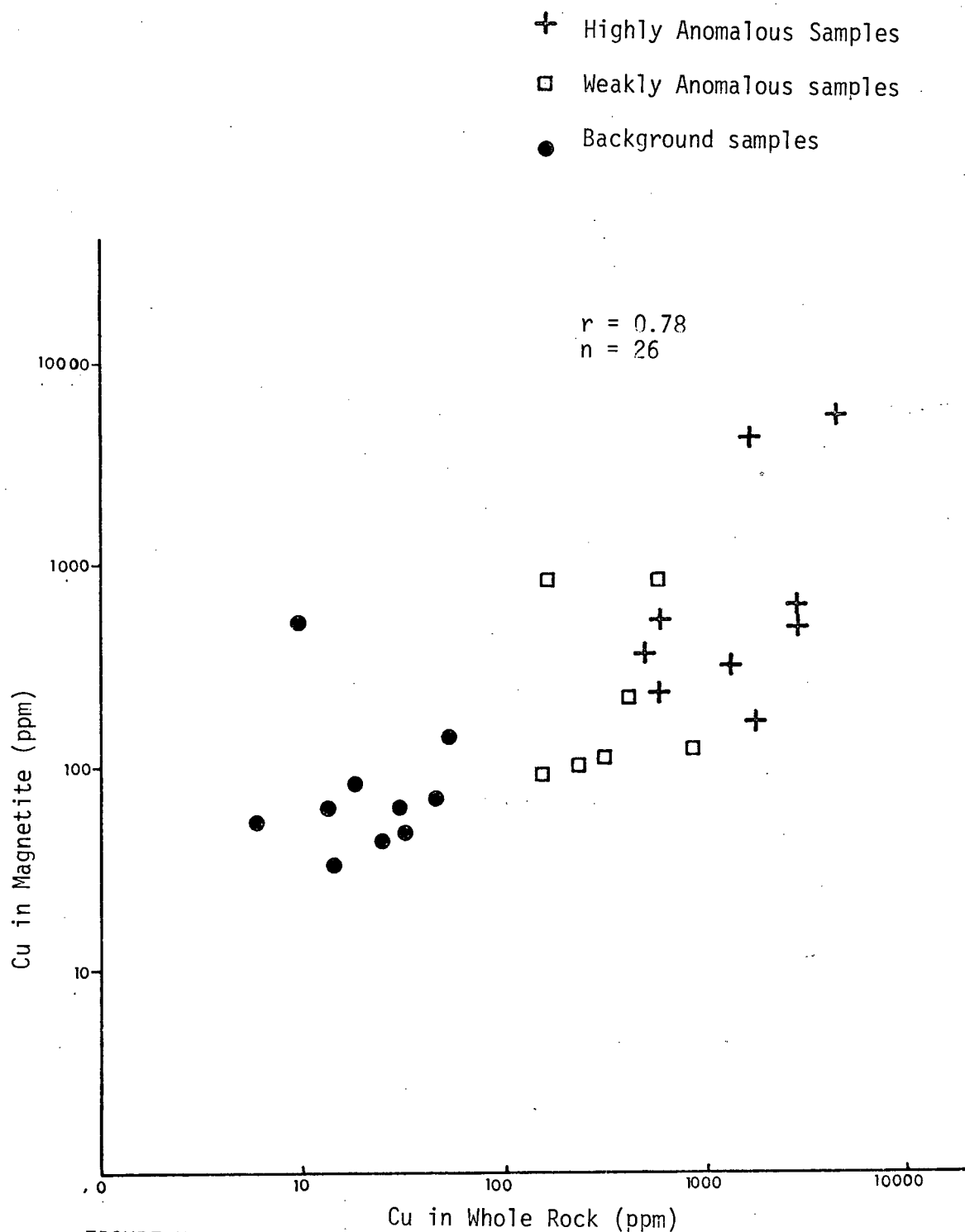


FIGURE 70: Relationship between Copper contents of whole rocks and magnetites.

Levels of Zn and Co are consistently lower in anomalous than background samples. This is suggestive of leaching of these elements from magnetite during hydrothermal alteration.

(iii) Quartz-Feldspar

Anomalous Cu and relatively low Zn values are characteristic of quartz-feldspar fractions from mineralized samples (Table LIX). As demonstrated earlier, enhanced Cu values are not due to contamination by biotite or magnetite. The strong positive correlation between Cu in whole rock and quartz-feldspar fractions reflects the high modal proportions (more than 80%) of these minerals in whole rocks (Fig. 71).

Several workers (Azzaria, 1963; Bradshaw, 1967; Bradshaw and Stoyel, 1968; Rabinovich and Badalov, 1968) have shown that quartz and feldspars in fresh granites contain appreciable Cu, although its mode of occurrence is not well understood. It may substitute for Fe and Mg, which commonly occur as impurities in feldspars of unmineralized igneous rocks (Wager and Mitchell, 1951), or occur directly as an impurity in quartz (Cutitta et al., 1960).

Results of sulphide selective leach suggest that Cu in anomalous samples principally occurs in sulphide form, mainly as inclusions in sericitized plagioclase and K-feldspar. Primary quartz probably contains little or no Cu, although hydrothermal quartz veinlets commonly carry opaque inclusions which may be sulphides.

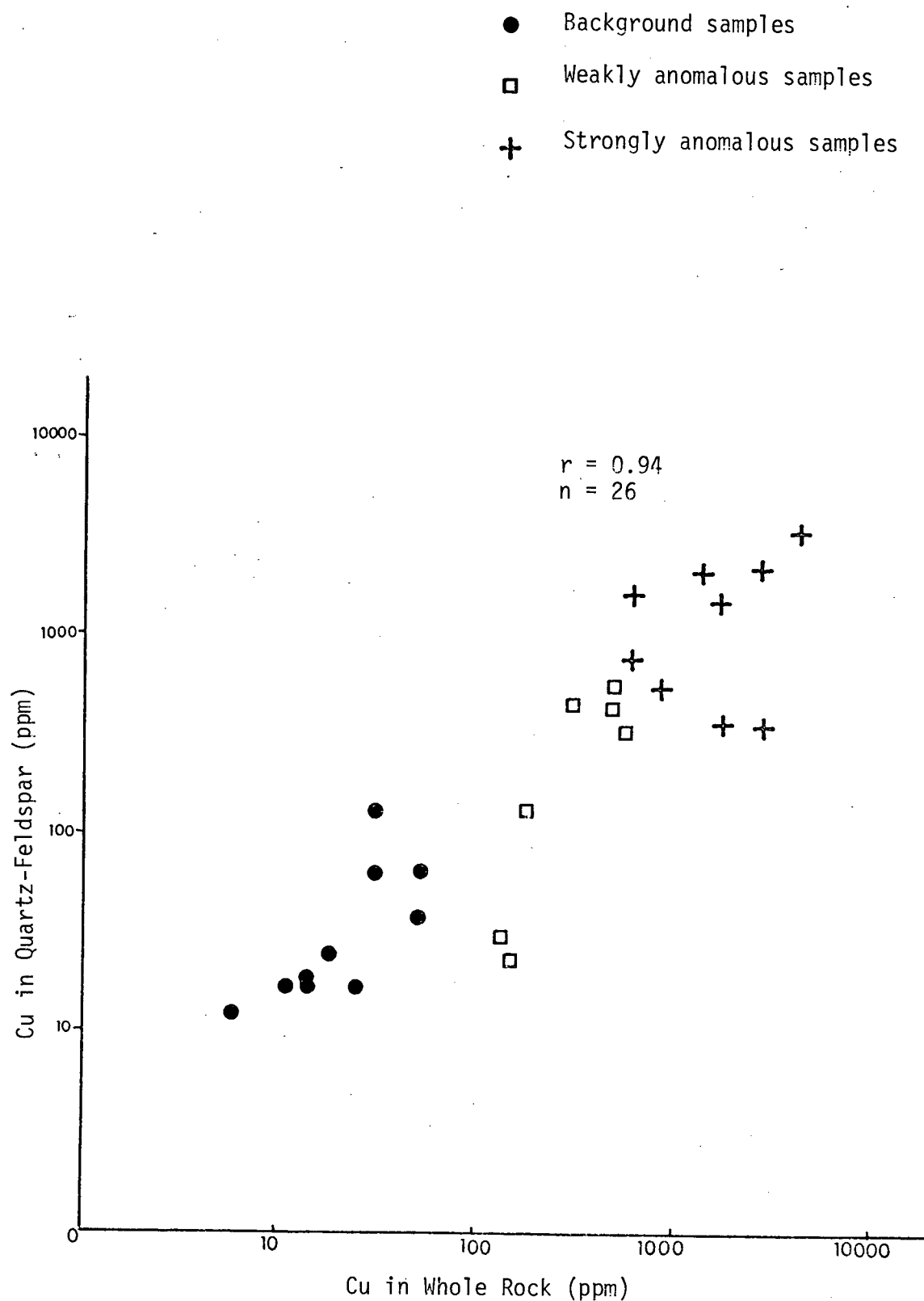


FIGURE 71: Relationship between Copper contents of whole rocks and quartz-feldspar fractions.

(iv) Nature of Mineralizing and Hydrothermal Processes

From the foregoing discussion, it is apparent that hydrothermal processes have produced pervasive enhancement in Cu content of most mineral constituents in mineralized rocks. This is in accordance with the model of mass flow of ore-forming solutions through grain boundaries, pores and other discontinuities in rocks (Korzhinskii, 1968). The overall effect of these processes is enrichment of Cu in most rock constituents. Results of mineral analysis further suggest that hydrothermal processes involve leaching of Ni, Zn, Mn, Co and Mg from femic minerals. This represents the incipient stage of large-scale metasomatic leaching documented in the analysis of whole rocks (Chapter 6), which culminates in the destruction of femic silicates and subsequent formation of hydrothermal alteration minerals. The leached metals are ultimately deposited at the periphery of mineralized zones by outward migrating solutions. These processes are further discussed in relation to genesis of mineralization in Chapter 8.

GEOCHEMICAL CONTRAST

Average geochemical contrast for Cu between background and anomalous samples in whole rock and mineral fractions is summarized in Table LXIII. KClO_3 -HCl digestion gives the best contrast in whole-rock analysis. Compared to whole-rock samples, all mineral phases give lower geochemical contrast for total and partial extractable Cu. Geochemical contrast in biotite is higher than that of quartz-feldspar, and contrast in both mineral phases considerably

TABLE LXIII: Comparison of geochemical contrast in whole rock and mineral separates (26 samples).

	HF-HClO ₄ -HNO ₃ Total Cu (p.p.m.)	KClO ₃ -HCl Ext. Cu (p.p.m.)	H ₂ O ₂ - Asc. Ext. Cu (p.p.m.)	Aqua Regia Ext. Cu (p.p.m.)	HNO ₃ -HClO ₄ Ext. Cu (p.p.m.)
(a) WHOLE ROCK					
R	6 - 4585	2 - 4281	3 - 1435	4 - 4963	4 - 4040
GM _B	21	11	14	19	16
Threshold	90	7	85	107	86
GM _A	745	697	568	721	618
Av. Contrast	8.3	9.8	6.7	6.7	7.2
(b) BIOTITE					
R	44 - 5617	26 - 5092	18-4253	34 - 4305	
GM _B	92	82	67	99	
Threshold	295	324	309	351	
GM	1624	1535	1483	1675	
Av. Contrast	5.5	4.8	4.8	4.8	
(c) QUARTZ- FELDSPAR					
R	12 - 3465	12 - 2605	7 - 1570	11 - 3292	
GM _B	29	21	18	24	
Threshold	146	103	101	127	
GM _A	619	434	419	527	
Av. Contrast	4.2	4.2	4.1	4.2	
(d) MAGNETITE					
R		14 - 1061		35 - 5451	
GM _B		35		67	
Threshold		101		198	
GM _A		176		401	
Av. Contrast		1.7		2.0	

R = Complete range

GM_B = Geometric mean; background, anomalous

Threshold = GM_B + 2 Standard Deviation

Av. Contrast = GM_A/threshold

exceed that of magnetite. In view of greater contrast obtained with whole-rock analysis, and difficulty of preparing mineral separates, their use appears to offer no advantages for mineral exploration in the Highland Valley.

SUMMARY AND CONCLUSIONS

(1) Cu contents of biotite, magnetite and quartz-feldspar fractions strongly correlate with whole-rock. This reflects the pervasive effect of epigenetic mineralization processes. Results of sulphide-selective leach suggest that significant amounts of Cu are present as sulphides in all mineral phases, from both anomalous and some background samples.

(2) With the exception of K-feldspar, modal proportions of minerals in whole rocks show no consistent relationship with trace-element contents. The inverse relationship between K-feldspar and whole-rock Cu reflects the increasing destruction of K-feldspar as intensity of mineralization increases.

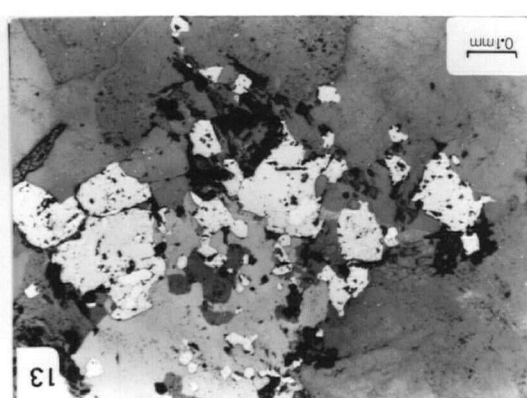
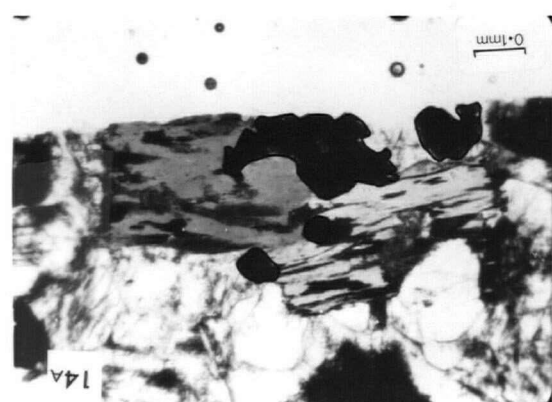
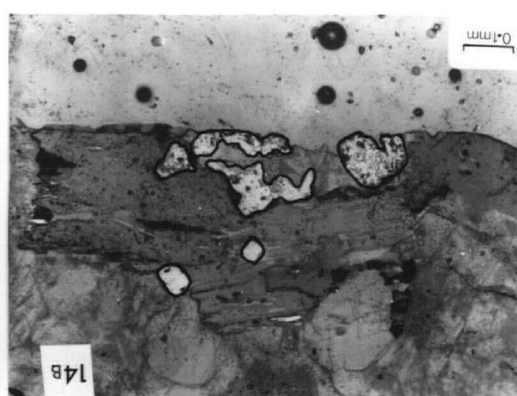
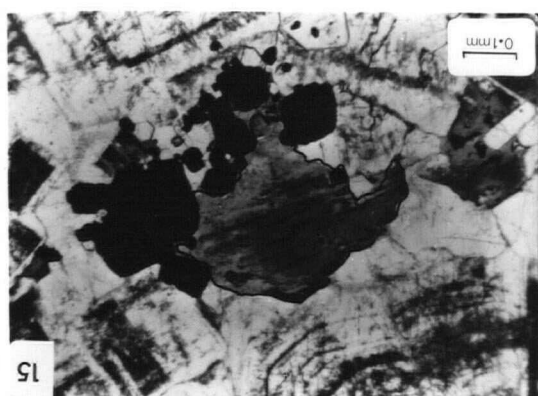
(3) Levels of Mg, Ni, Zn, Mn and Co in biotites and Zn and Co in magnetites are consistently lower in anomalous than background samples. This is consistent with incipient leaching of these elements during hydrothermal processes.

(4) Greater contrast was obtained with whole-rock than mineral analysis. Consequently, the use of mineral separates offers no advantages for mineral exploration in the Highland Valley.

PLATE 13: Disseminated sulphide grains (mainly bornite with minor chalcopyrite) in mineralized samples at Highmont (reflected light).

PLATE 14: Bornite inclusions in chloritized biotite (a) transmitted light (b) reflected light.

PLATE 15: Opaque grains (sulphide) occurring at the margins of a chloritized biotite (transmitted light).



CHAPTER EIGHT

ORE-FORMING PROCESSES AT HIGHLAND VALLEY

INTRODUCTION

(a) General Statement

In recent years numerous genetic models have been proposed for porphyry copper deposits (Burnham, 1967; Meyer and Hemley, 1967; Fournier, 1967, Nielsen, 1968; Lowell and Guilbert, 1970; White, 1968; Philips, 1973). Most of these models have not benefited from results of detailed bedrock geochemistry, which in conjunction with experimental studies are crucial to the understanding of chemical aspects of ore-forming processes in porphyry coppers.

The purpose of this portion of the study is to discuss ore-forming processes at Highland Valley in relation to lithochemical and isotopic data. Some suggestions on the physical aspects of ore genesis are speculative, and more definite conclusions must await results of extensive fluid inclusion studies underway at the University of Alberta (R.D. Morton, pers. comm.)

(b) Ore Genetic Models for Porphyry Copper Deposits

Various genetic models have been presented for porphyry copper deposits. All these models recognize the importance of magmatism in hydrothermal processes, and the main differences are in the depth of intrusion, the timing of hydrothermal processes and source of mineralizing fluids (Lowell and Guilbert, 1970).

In the orthomagmatic models (Burnham, 1967; Nielsen, 1968) an aqueous-rich volatile phase is released from the magma when internal

vapour pressure associated with saturation exceeds lithostatic pressure, or when the intrusive system is subjected to external stresses. Within this model, two different sources of ore metals have been advocated. Nielsen (1968) among others, suggests that metals were derived by differentiation of Cu-rich magma. In contrast, Noble (1970) and Sillitoe (1972) advocate a deep-seated source for ore metals, and consider the role of igneous intrusion in mineralization to be merely one of structural control rather than a source of ore metals. At the other end of the ore genetic 'spectrum' to the orthomagmatic models, White (1968) postulates an almost completely external source of mineralizing fluids - connate and/or meteoric hydrothermal solutions subject to convective processes by heat generated by subjacent intrusions. In this model, the pluton plays a passive role in mineralizing processes.

Various lines of evidence suggest that close relationships between mineralization at Highland Valley and evolution of the Guichon Creek batholith (Northcote, 1969; Brabec and White, 1971). Firstly, most of the major porphyry copper deposits are spatially associated with the younger and most differentiated rock units of the batholith - Bethsaida and Bethlehem Phases. Secondly, isotopic age determinations indicate temporal relationship between magmatism and hydrothermal processes. Results of K-Ar age determinations on hydrothermal sericites and biotites (Blanchflower, 1972; Jones et al., 1972; Dirom, 1965) indicate that, within limits of analytical error, mineralization and emplacement of the batholith are contemporaneous.

Despite the close spatial and temporal relationships between mineralization and evolution of Guichon Creek batholith, it is not clear whether the role of the pluton in mineralization is one of structural control or as a direct source of metals.

ORIGIN OF GUICHON CREEK BATHOLITH AND SOURCE OF METALS

One of the important tenets of the orthomagmatic model is that ore-forming fluids are by-products of magmas of the associated intrusion. If this supposition is correct, then the origin of Guichon Creek batholith is pertinent to ore genesis at Highland Valley. Relevant geochemical and isotopic data are reviewed in the following section.

(a) Provenance of Guichon Creek Magma and Associated Metals

Numerous workers have shown that K/Rb and Rb/Sr ratios set important constraints on the source materials of igneous masses (Hurley, 1968; Culbert, 1972). Results of regional geochemistry indicate that K/Rb ratios in rocks of the Guichon Creek batholith are relatively high (mean = 358) and largely outside the limit considered normal for continental plutonic rocks (Fig. 72). Furthermore, the Rb/Sr ratios are low and primitive, plotting in the region of basalts and andesites (Fig. 73). The mean Rb/Sr ratio of 0.05 is one-fifth the value cited for sialic crust (0.25; Faure and Hurley, 1963). Thus the copious Sr in the batholith is changing its $\text{Sr}^{87}/\text{Sr}^{86}$ ratio (by radioactive decay of Rb^{87}) by only .001 every 500 m.y. This reflects its primitive nature. Compared with other Mesozoic plutons in the Intermontane

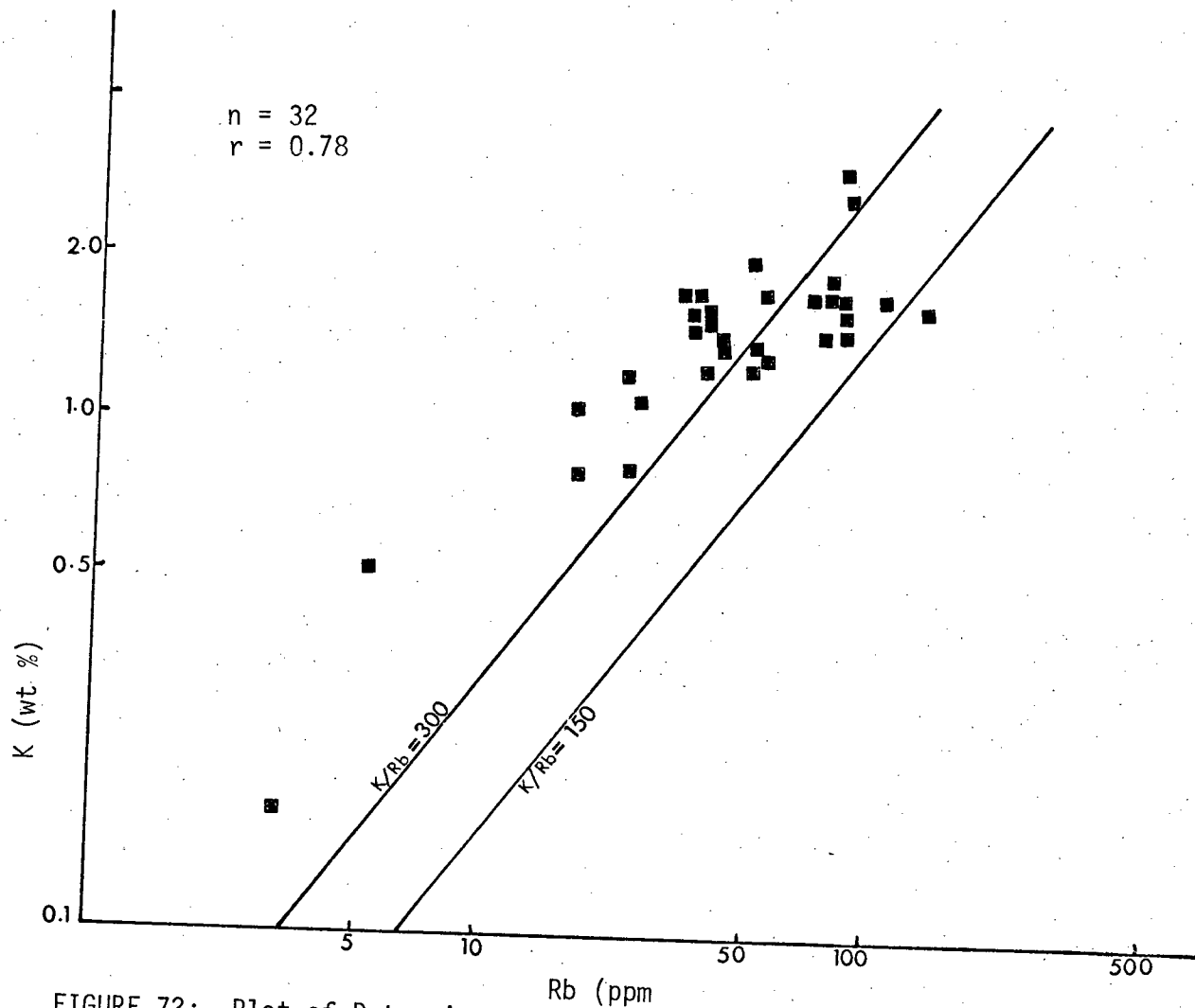


FIGURE 72: Plot of Potassium versus Rubidium and K/Rb ratios in rocks of Guichon Creek batholith. (Norman crustal K/Rb ratios = 150-300)

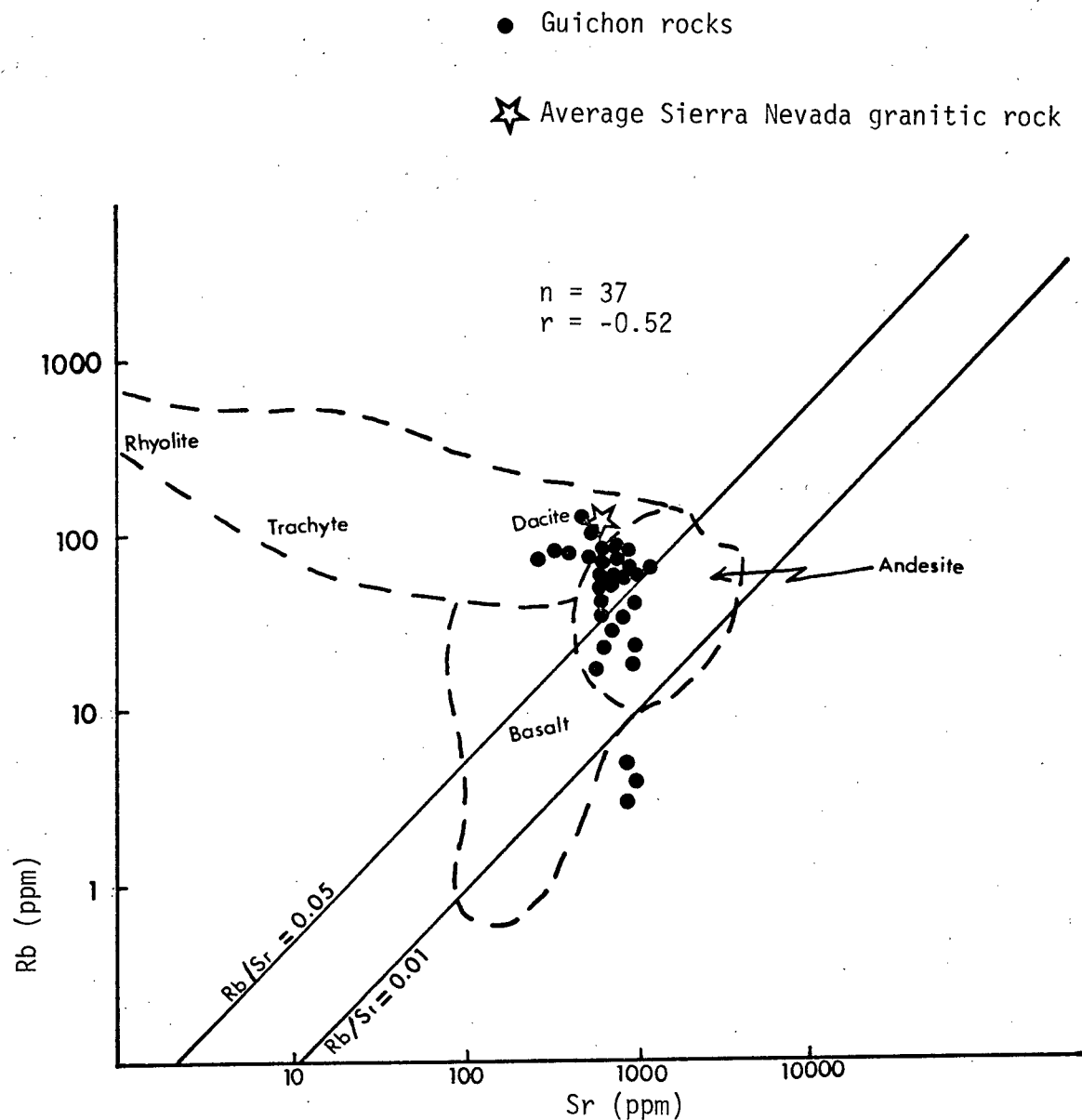


FIGURE 73: Plot of Rubidium versus Strontium in rocks of Guichon Creek batholith (Generalized geochemical relationships of Rb and Sr in certain types of rocks are shown for comparison; after Hedge, 1966)

Belt (Table LXIV), the Guichon Creek batholith is relatively impoverished in Rb and K, and characterized by higher K/Rb and lower Rb/Sr ratios. However, values obtained for the Guichon Creek batholith are similar to those reported by Culbert (1972) for the Coast Mountains batholith of the Coast Mountains Belt. The relatively high K/Rb and low Rb/Sr ratios in rocks of Guichon Creek batholith are not due to mineral fractionation, but reflect derivation from a subcrustal source region depleted in alkalis and enriched in Sr, most probably from subducted oceanic crust or upper mantle. This interpretation is consistent with the primitive initial Sr isotopic ratio ($\text{Sr}^{87}/\text{Sr}^{86} = 0.7037$) reported by Christmas et al., (1969)

Monger et al. (1972) and Dercourt (1972) have presented tectonic models for the evolution of the Canadian Cordillera which suggest that the Intermontane Belt, comprising extensive andesitic volcanic rocks and calc-alkaline plutons (including the Guichon Creek batholith), was the site of an ancient island arc generated by subduction of oceanic crust of the Pacific Plate beneath continental crust of the overriding North American Plate during the Mesozoic. In accordance with this model, the relatively early Mesozoic age of the Guichon Creek batholith - the oldest-dated Mesozoic pluton in the Canadian Cordillera - and its low K_2O content (mean = 1.85%) suggest derivation of the batholith from relatively shallow depths from the subduction zone (calculated as <130 km; Hatherton and Dickinson, 1969) close to the Triassic trench. In this context, the low alkalis in the batholith, high K/Rb and low Rb/Sr ratios are consistent with derivation from hydrated oceanic crust of probably

TABLE LXIV: *Means and ranges of Rb, Sr, Rb/Sr, K/Rb and $\text{Sr}^{87}/\text{Sr}^{86}$

ratios in some Mesozoic Cordilleran intrusions.

Intrusions	Rb (p.p.m.)	Sr (p.p.m.)	Rb/Sr	K/Rb	$\text{Sr}^{87}/\text{Sr}^{86}$	Age (m.y.)
Similkameen	95	390	0.151	250	0.7060	183
batholith	(52 - 152)	(147 - 639)	(0.081 - 1.01)	(172 - 309)	(0.7029-0.7091)	
Hogem	80	730	0.100	430		170
batholith	(55 - 118)	(468 - 1520)	(0.041-0.125)	(322 - 502)	-	
Nelson			0.175			171 - 49
batholith	-	-	(0.056 - 0.483)	-	0.7069	
White Creek	265	804	0.412	-	0.7250	126, 111
batholith	(196 - 357)	(435 - 1118)	(0.108-1.655)	-	(0.7076-0.7397)	
Bayonne						
batholith	-	-	0.246 (0.115 - 0.357)	-	0.7081 (0.7072-0.7090)	118, 110
Vernon	-	-	1.42	-	0.7064	
batholith			(0.108-2.84)			55
Coast Mountains	33	725	0.046	373	0.7038	
batholith	(4 - 150)	(25 - 795)	(0.11 - 0.60)	(225 - 628)	(0.7031-0.7050)	140, 84
Guichon Creek	35	686	0.05	358		
batholith	(3 - 132)	(249-1000)	(0.004 - 0.321)	(132 - 1030)	0.7037	200 \pm 5

*Modified after Peto (1974)

amphibolite composition (Jakes and White, 1970). Furthermore, results of sulphur isotopes in hydrothermal sulphides and sulphates, and deuterium and oxygen isotopes in hydrothermal sericites and kaolinites (Field et al., 1973; Jones et al., 1972; Sheppard et al., 1969) suggest a subcrustal source for mineralizing solutions and associated metals.

(b) Level of Emplacement and Volatile Pressures

Northcote (1969) has presented geologic evidence which suggests that the older intrusive units within the batholith were emplaced under mesozonal conditions, whereas the younger units, that are spatially associated with mineralization, were emplaced at relatively shallower levels in the crust (epizone). Westermann (1970), investigating the crystallization history of the batholith, found that in the older rock units, plagioclase crystallized earlier than quartz, whereas in the younger Bethlehem-Skeena and Bethsaida Phases, quartz was first to crystallize. Moreover, the quartz grains in the younger and more differentiated units are commonly fractured and occur dominantly as phenocrysts. According to Westermann (1970), these textural and mineralogical features are suggestive of increasing volatile pressures within the magma.

A rough estimate of volatile pressures during crystallization of the most differentiated and youngest unit (Bethsaida Phase) can be obtained by projecting normative compositions into the experimental system Ab-Or-Qz-H₂O (Fig. 74). All five samples of Bethsaida rocks plot in a restricted area close to the isobaric thermal trough for water vapour pressures around 6 to 7Kb. On the basis of

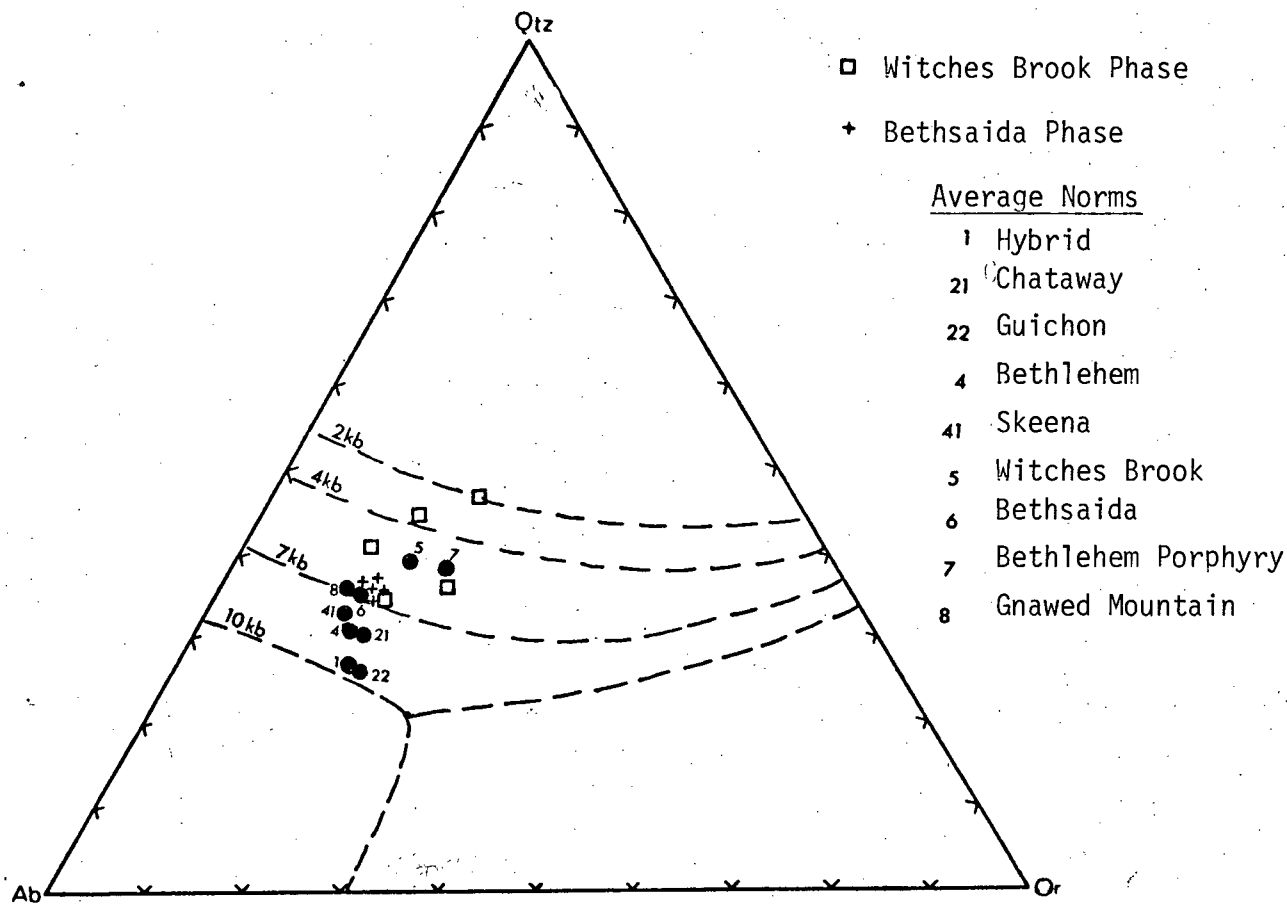


FIGURE 74: Plot of normative Ab-Or-Qz proportions for the Guichon Creek samples compared with boundary curves and minima at 2,4,7 and 10 Kb P_{H_2O} (von Platen and Holler, 1966) Ab/An ratio = 2.9

textural and field evidence Northcote (1969) has suggested that the Bethsaida Phase crystallized at relatively shallow depth (epizone), thus implying, at most 6 to 8km of cover which would produce a load pressure of about 2kb. If these estimates are correct, then the volatile pressures existing during emplacement of the Bethsaida Phase may be estimated as 4 to 5kb.

Burnham (1967) has suggested that the maximum content of H_2O in a granodiorite magma is about 6 wt. %, most of which is exsolved ('boiled off') between 10km and 3km depths. However at shallower depths, volatile pressures in excess of load pressure and tensile strength of the confining rocks may result in the development of shear fractures and micro-brecciation of cover rocks, permitting escape of 'fecund' aqueous solutions to form ore deposits. The porphyritic texture and fractured quartz phenocrysts in rocks of Bethsaida Phase (Westermann, 1970), and the presence of breccia pipes, are consistent with increasing volatile pressures during magmatic differentiation. However, no textures indicative of retrograde boiling have so far been documented, probably because of the difficulty of differentiating them from similar hydrothermal features (Philips, 1973).

From the foregoing discussion, it is evident that magmatic evolution of the batholith created the suitable structural and chemical environment for localization of mineralization within the batholith.

NATURE OF ALTERATION-MINERALIZATION PROCESSES

Extensive wall-rock alteration, that is so characteristic of porphyry copper deposits, constitutes the most visible evidence of interaction between host rocks and hydrothermal solutions. Meyer and Hemley (1967) among others, have demonstrated the close temporal and genetic relationships between sulphide deposition and wall-rock alteration at porphyry copper deposits.

(a) Mineral Stability Fields

Mineralogy of alteration assemblages at Highland Valley deposits provides evidence of the composition of mineralizing fluids. All the deposits of the Highland Valley contain sericite alteration either in association with kaolinite, quartz or K-feldspar. Argillization and sericitization of wall rocks require slight to moderate acidity ($\text{pH} < 6$) whereas abundant K-feldspar suggests pH exceeding 7 (Barnes and Czamanske, 1967). Cross-cutting vein relationships suggest that K-feldspar with or without quartz is generally early in the paragenetic sequence, and followed by sericite and argillic veins or selvages. This sequence suggests increasing acidity of hydrothermal fluids with increasing evolution. However, at Valley Copper, K-feldspar envelopes occur around sericite veins and in equilibrium with kaolinite. This relationship, which is contrary to the stability-field relationships established for these minerals by Hemley and Jones (1964), is attributed to a resurgence of abnormally high silica activities in ore-forming fluids shifting the mineral stability field to higher pH levels.

(b) Bedrock Geochemical Evidence

Results of bedrock and mineral geochemistry (Chapters 6 and 7) suggest that widespread chemical changes in wall rock are intimately associated with mineralization and hydrothermal alteration. Each deposit is characterized by central mineralized zones in which metasomatic activity is most intense.

In zones of intense argillic and phyllic alteration at Valley Copper, Lornex and Highmont, the base elements Ca, Na, Sr, Ba, Zn, Mn, Mg and Fe are depleted, whereas in potassic zones at the JA, Lornex and Valley Copper deposits K, Rb and Ba are relatively enriched. Calculations of chemical gain and loss of principal rock constituents through alteration and mineralization at Valley Copper (Fi . 75), suggest that in quartz-sericite and potassic zones, Ca, Mg, Fe, Na and Al are removed and K, Si and S added (for method of calculation, see Gresens, 1967). The obvious depletion of base cations in mineralized and altered zones is attributed to the break down of ferromagnesian minerals and plagioclase to sericite and kaolinite. Incipient stages of the above process are demonstrated by results of mineral analysis. Zn, Mn, Mg and Co levels in biotites and magnetites are consistently lower in mineralized and altered than in fresh samples. Cu and S concentrations, though erratic, are highest in zones of intense alteration and metallization, decreasing outwards to back round levels in fresh unmineralized host rocks.

DISCUSSION

The following modes of origin have been proposed for porphyry copper deposits, hence are relevant to the genesis of the

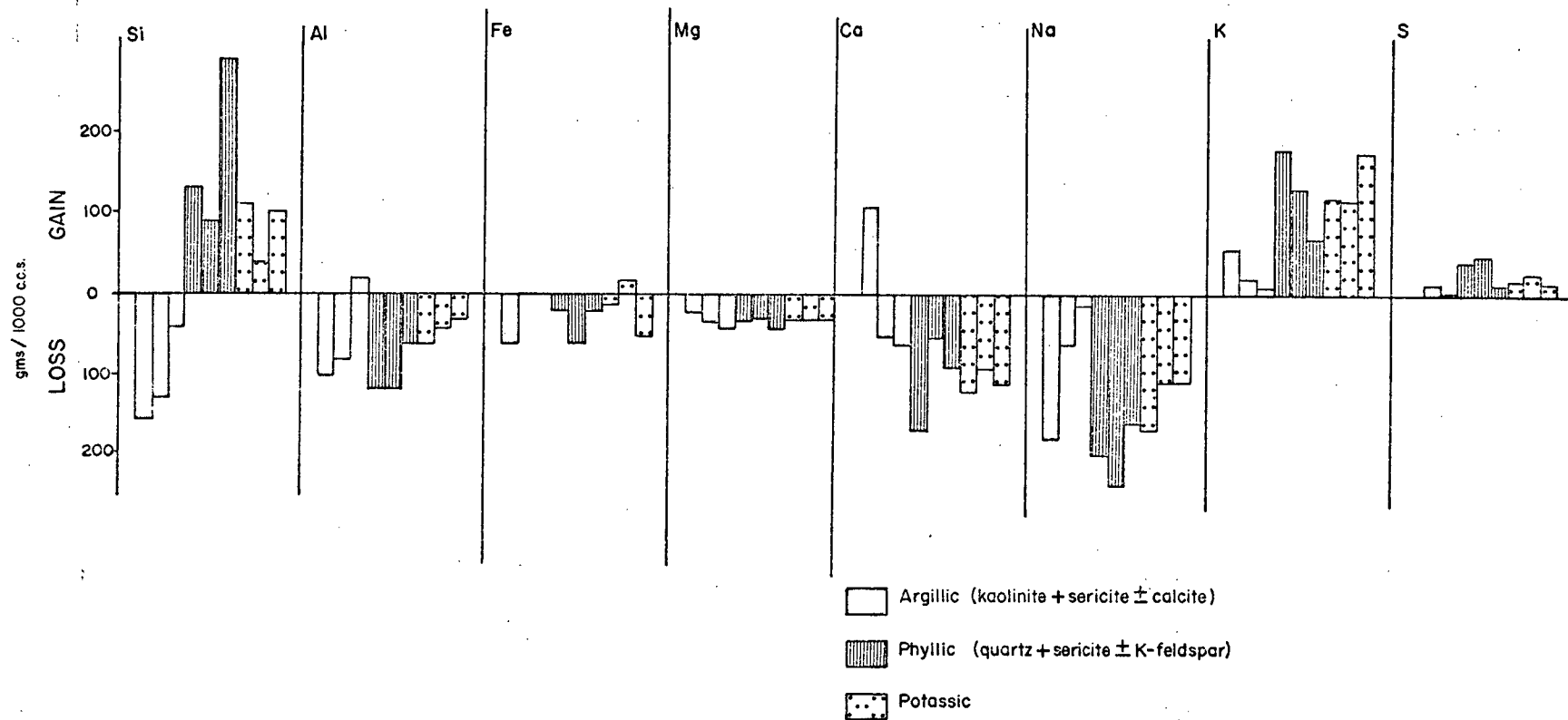


FIGURE 75: Gain and loss of principal rock constituents through alteration and mineralization, Valley Copper 3600 level.

Highland Valley deposits.

(i) Extraction of ore metals either by leaching of wall rocks by convecting meteoric waters as proposed by White (1968), or by deuteric alteration as proposed by Putman (1972).

(ii) Derivation of ore metals by assimilation of country rocks (Schau, 1970).

(iii) Concentration of ore metals by differentiation of a Cu-rich magma (Brabec and White, 1971; Nielsen, 1968; Burnham, 1967; Graybeal, 1973).

(iv) Derivation of ore metals by partial melting of subducted oceanic crust, and subsequent transportation to crustal levels, as an independent phase within calc-alkaline magmas (Sillitoe, 1972; Mitchell and Garson, 1972; Wright and McCurry, 1973; Noble, 1970).

On the basis of variations of Cu contents in the Guichon Creek batholith, Brabec and White (1971) postulated that the Highland Valley deposits were derived by differentiation of a Cu-rich magma. In contrast, Schau (1970) has suggested that Cu in the batholith was derived by assimilation of Nicola volcanic rocks. All the alternatives are now considered in light of regional, detailed bedrock and mineral geochemistry, and isotopic data.

The first hypothesis is least likely because results of detailed bedrock geochemistry around mineralized zones indicate that no zone of Cu and/or S depletion surrounds the orebodies at the level

of sampling, although the remote possibility that these elements could be extracted from channelways at greater depths is not ruled out. Moreover, results of mineral geochemistry suggest no obvious leaching of Cu from biotites, although such leaching of Zn, Mn, Ni, Co and other 'femic' elements is apparent in bedrock and minerals.

The second hypothesis has been proposed by Schau (1970) who postulated that ore metals were derived by assimilation of Nicola volcanic rocks. Brabec and White (1971) have criticized this hypothesis by demonstrating that the Hybrid Phase, the most contaminated unit within the batholith, is not significantly higher in Cu than uncontaminated rocks of the Guichon and Chataway Phases. Brabec (1970) further suggests that the relatively high Cu levels in the batholith would require selective assimilation of this metal from a large volume of country rocks. Field evidence do not support a large-scale contamination of the batholith beyond the outer margins (Northcote, 1969).

Available geochemical data are not consistent with the third hypothesis proposed by Brabec and White (1971), since (1) Cu in association with Zn, Mn, Ti, V, Ni, Co, Fe and Mg generally decrease with increasing fractionation or felsic composition of intrusive units. This geochemical pattern simply reflects normal differentiation trends observed in unmineralized intrusions. Sheraton and Black (1973), investigating trace element geochemistry of granitic intrusions unmineralized with respect to Cu, found that Cu concentrations decreased from more than 40 p.p.m. in granodiorite to less than 5 p.p.m. in more differentiated granites. In contrast,

studies on intrusions that are known to have generated immiscible sulphide phases such as the Skaergaard (Wager and Brown, 1967), and mineralized Laramide intrusions in Arizona (Graybeal, 1973), Cu contents of bedrock and mineral constituents generally increase with differentiation until Cu separates from the melt as an immiscible sulphide phase. Graybeal (1973), investigating the partitioning of Cu between co-existing biotite and hornblende found that, under equilibrium conditions, higher concentration of Cu within the magma was reflected by higher concentrations in the mineral phases. In the Guichon Creek batholith, results of Cu determinations in biotites and hornblendes (Brabec, 1970) suggest no appreciable variations throughout the batholith. From the foregoing discussions it is apparent that geochemical data do not support the hypothesis that ore metals at Highland Valley were derived by differentiation of a Cu-rich Guichon Creek magma. On the contrary, it is argued that the Guichon Creek magma became increasingly impoverished in Cu as a result of differentiation.

The fourth hypothesis, which regards mineralization as an independent by-product of magma generation rather than a direct result of differentiation processes, is consistent with geochemical data and in line with contemporary ideas of plate tectonics and ore genesis. Nevertheless, it must be emphasized that differentiation processes within a magma, provide the right chemical and physical environment for localization of ore metals.

High K/Rb and Sr values and low Rb, K, Rb/Sr and Sr isotopic ratios are consistent with derivation of Guichon Creek magma

from a deep-seated source, most probably subducted oceanic crust or upper mantle. Results of sulphur, oxygen and deuterium isotopes suggest a similar deep-seated source for mineralizing solutions and ore metals. Because of the temporal and spatial relationships between mineralization and magmatism, it is logical to presume that ore metals at the Highland Valley deposits were derived from a metal-rich portion of the subducted oceanic crust from which the Guichon Creek magma was generated. Sillitoe (1972) has demonstrated that there is enough Cu in oceanic basalts to generate metals in ore deposits. The ore metals derived from partial melting of subducted oceanic crust probably occur in a sulphide phase independent of the magma. Thus the role of the magma is believed to be one of structural control in channeling ore metals to crustal levels (Noble, 1970). Nevertheless, differentiation of the magma provided volatiles and structural openings, such as fractures, breccia zones, dyke swarms that facilitated the extraction of metals from the system and concentration as ore deposits.

Fig. 76 shows a comprehensive model that explains the evolution of the ore-forming fluids at the hydrothermal stage. The close spatial relationship between porphyry dykes or dyke swarms and ore deposits at Highland Valley, suggests that porphyries served as high-level structural 'outlets' for mineralizing solutions. The presence of saline fluid inclusions in quartz veins at Valley Copper Lornex and Highmont (R.D. Morton, pers. comm.) and enhanced values of B, F, Cl and S in ore zones suggest that the mineralizing fluids contained HCl, H_3BO_3 , HF, H_2S , H_2SO_4 and other volatile elements.

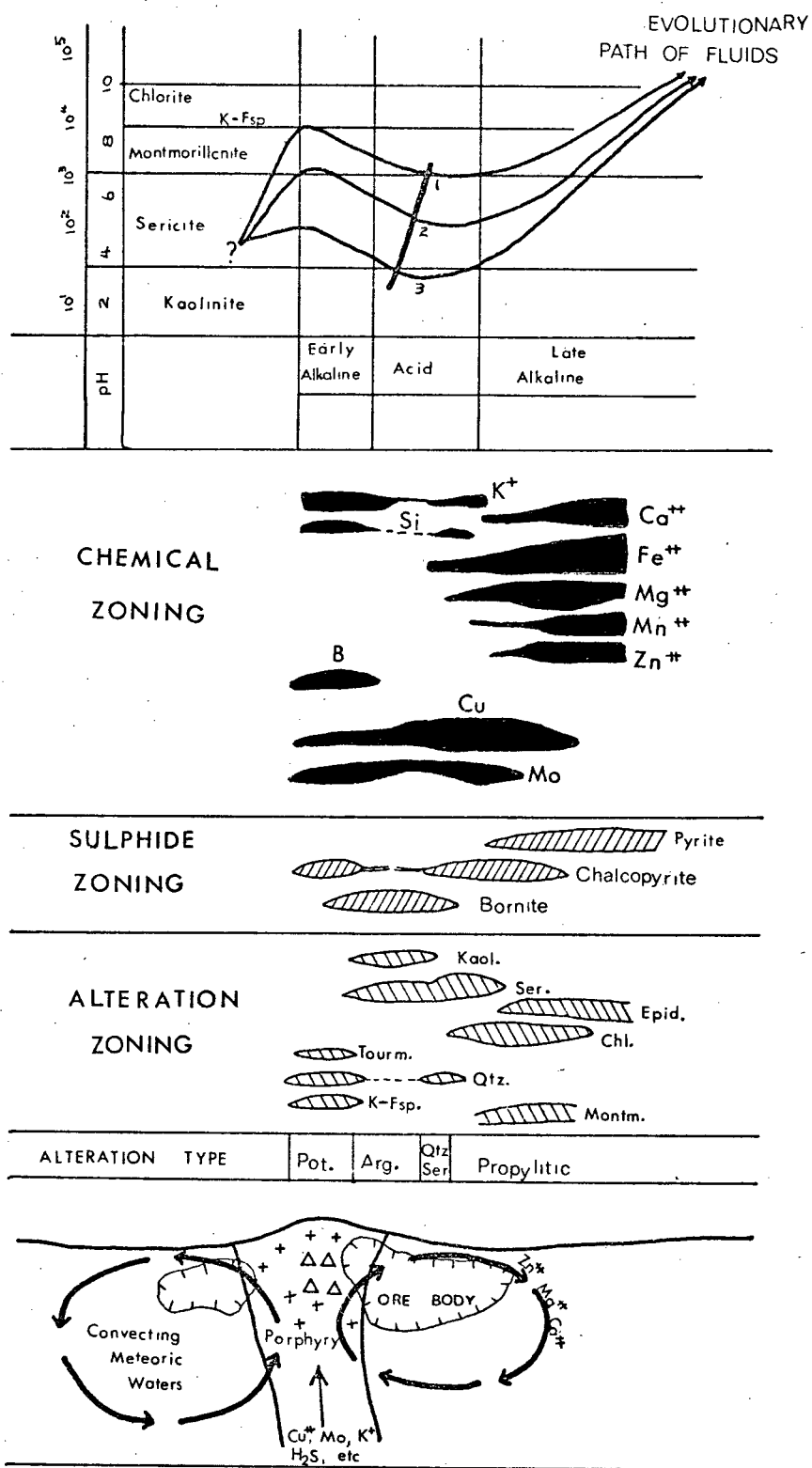


FIGURE 76: Model for chemical and mineral zoning and evolution of ore forming fluids.

Late stage differentiation products, such as K^+ , SiO_2 , Rb^+ and Na^+ were probably present. Extensive argillic and sericite alteration found around the deposits require that ore solutions be slightly to moderately acidic, and contain abundant H^+ , probably derived from dissociated H_2O and H_2S present in the juvenile fluids, or by admixture with convecting meteoric waters generated by heat from the porphyry dykes or stocks.

Helgeson (1970) has presented thermodynamic data which demonstrate that all equilibria in hydrothermal systems can be represented in terms of the ratio of activities of cations in the aqueous phase to that of the hydrogen ion. Changes in base cation/ H^+ activities as ore-forming fluids transgress the alteration zones are portrayed in Fig. 76. The evolutionary paths, designated 1, 2 and 3 in the diagram, represent different degrees of equilibration between ore fluids and wall rock. Formation of an early potassic zone (K -feldspar \pm quartz \pm sericite), that is commonly centred on porphyry dykes, requires a high base cation (K^+ , Na^+)/ H^+ activity ratio which could result from initial composition of mineralizing fluids (inherited from the magma) or less probably be derived at depths by H^+ consuming and base cation-releasing equilibrium reactions.

As the ore fluids rise and spread outwards they undergo adiabatic expansion, and in conjunction with reaction with wall rocks and/or mixing with meteoric waters, cool, causing dissociation of the most acidic components. This dissociation provides most of the abundant H^+ required for hydrolytic base leaching within the quartz-sericite and argillic zones, under acidic conditions. The

base cations (Mg^{++} , Ca^{++} , Fe^{++} , Na^{+} , Sr^{++} , Ba^{+} , Zn^{++} , Mn^{++}), released by leaching, are taken into the fluid and transferred to the outlying metasomatic front (Korzhinskii, 1968), as the solutions are cooled and neutralized.

Changes in base cation/ H^{+} activity ratios are generally accompanied by changes in pH and sulphur fugacity (Meyer and Hemley, 1967) which ultimately control sulphide deposition and zoning patterns. This accounts for the close association between sericite and argillic alteration, which require H^{+} consumption in their formation and sulphide mineralization, as amply demonstrated at Valley Copper, Lornex, Highmont and in parts of Bethlehem-JA.

From the foregoing discussion, it is apparent that regional, detailed bedrock and mineral geochemistry, and isotopic and tectonic evidence are consistent with the mode of origin proposed for the Guichon Creek batholith. Assuming the genetic model correct, it has far reaching implications in reconnaissance exploration for Cu deposits in calc-alkaline intrusions of the Intermontane Belt. Firstly, the apparent negative correlation between Cu contents and ore potential of the Guichon Creek batholith suggests that ore-bearing intrusions will probably not be enriched in Cu. Thus the suggestion by Warren and Delavault, (1960) that high Cu contents of intrusions reflect ore potential might not be generally applicable. Secondly, if ore metals in the Guichon Creek batholith were derived from subducted oceanic crust as an independent by-product of magma generation, it is most plausible that other calc-alkaline plutonic and volcanic rocks of similar age as the Guichon Creek batholith might originate

from the same metal-rich portion of subducted oceanic crust.

Such calc-alkaline intrusive and extrusive rocks within the Intermontane Belt can be identified by; (1) Their ages (Late Triassic - Early Jurassic); (2) their low Rb, Rb/Sr and high K/Rb ratios; and (3) their K_2O content which should reflect the relatively shallow depth of magma generation. Using the Guichon Creek batholith as a 'reference index', calc-alkaline intrusive and extrusive rocks which meet the above criteria might have considerable potential for porphyry Cu and/or massive sulphide deposits.

CONCLUSIONS

Regional, detailed bedrock and mineral geochemistry of the Guichon Creek batholith and associated mineralization is consistent with the hypothesis that ore metals did not arise as a direct result of differentiation processes within a Cu-rich magma, but rather as an independent by-product of magma generation from subducted oceanic crust of probably amphibolite composition. Nevertheless, chemical and mineral fractionation within the Guichon Creek magma led to the development of increased volatile contents and pressures that provided suitable chemical and structural environments for localization of ore deposits. Consequently not all ore-bearing plutons need be enriched in Cu.

CHAPTER NINE

SUMMARY AND CONCLUSIONS

SUMMARY AND CONCLUSIONS

More than 1500 bedrock and mineral samples collected from the vicinity of four major porphyry copper deposits in the Highland Valley together with 60 fresh regional samples (Northcote, 1968) were analyzed for more than 20 major, trace and potential pathfinder elements by total and partial extraction techniques.

Results and conclusions are summarized as follows:

(a) Regional Geochemistry

(1) Major element variations in rocks of the batholith suggest fractional crystallization of a calc-alkaline dioritic magma by progressive fractionation of plagioclase, biotite and hornblende. By this process, derivative fluids were enriched in Si and Na, and depleted in Ca, Fe, Mg and Ti. Ca-Na-K variation diagram indicates two trends of differentiation; normal calc-alkaline trend associated with K enrichment in dyke rocks of the Witches Brook Phase, and a trondhemitic trend associated with Na enrichment in the remainder of the batholith.

(2) In general, the batholith is relatively impoverished in K_2O and Rb (mean values 1.85% K_2O ; 35 p.p.m. Rb), and characterized by high K/Rb and low Rb/Sr ratios. These results are consistent with primitive initial Sr^{87}/Sr^{86} ratio (0.7037; Christmas et al., 1969) suggesting derivation of the magma from the upper mantle or subducted oceanic crust, in accordance with plate tectonic models.

(3) Variations in Mn, Zn, Ni, Co and V are intimately associated with degree of fractionation. These elements were progressively depleted in the Guichon Creek magma with increasing magmatic differentiation. Strong positive correlations with Fe and Mg suggest partitioning of these femic trace elements into silicate fractions during magmatic evolution.

(4) In accordance with results obtained by Brabec (1970), Cu concentrations decrease progressively from the relatively older and more mafic, to relatively younger and more felsic units. Minimum concentrations are encountered in the Bethsaida and Gnawed Mountain Phases that are spatially associated with Cu mineralization. The apparent tendency for Cu to decrease with increasing differentiation is commonly characteristic of unmineralized intrusions, and suggests that the Guichon Creek magma was probably not the direct source of metals concentrated by differentiation. This is in disagreement with the model proposed by Brabec (1970) and Brabec and White (1971), rather, it seems differentiation depleted the magma of metals.

(b) Detailed Bedrock Geochemistry

(5) Variations in concentrations of the 'femic group' of metals (Zn, Mn, Ti, V, Fe and M) around mineralization are controlled principally by primary lithologies. This is consistent with the geochemical affinity between these trace elements and Fe and Mg. However, it is apparent that in deposits where there is only one major host rock, such as at Valley Copper and Lornex,

Zn, Mn, Fe and Mg are leached in zones of intense argillic and phyllic alteration. This is attributed to the complete breakdown of ferromagnesian minerals to sericite and kaolinite. In contrast, propylitic zones with abundant chlorite, epidote, pyrite and carbonate are generally associated with enhanced values of femic metals.

(6) The lithophile elements Sr, Ba, Ca and Na are consistently depleted in zones of intense hydrothermal activity, especially where its character is phyllic or argillic. In contrast, Rb, K and less commonly Ba are enriched in zones of K-feldspar and sericite alteration. Rb/Sr and Ba/Sr ratios show consistent patterns related to alteration and mineralization.

(7) Cu and S, though erratic, show the highest contrast, and halos extending at least 0.5km from the core zones, and beyond visible alteration envelopes. Of these two elements, S seems to be less erratic than Cu as demonstrated by relatively lower coefficients of variation. Furthermore, dispersion trends for S are more consistent and smoother, partly because S occurs not only as Cu sulphides but also in pyrite which is most commonly disseminated at the periphery of porphyry-type deposits.

(8) Hg dispersion is not consistent at Highland Valley; a broad and pronounced halo is associated with Bethlehem-JA but is absent at Valley Copper. This behaviour is attributed to either higher temperature of ore formation or the clay and sericite

composition of alteration minerals at Valley Copper, which resulted in the loss or escape of volatile Hg.

(9) B anomalies are well developed at Lornex and Highmont, partly as a result of the spatial association of mineralization with tourmaline-bearing breccia pipes and porphyry dykes. Nevertheless, it is apparent that ore-forming solutions at Highmont and Lornex contained relatively abundant B. At Valley Copper and JA, B anomalies are less prominent.

(10) The halogens (Cl, F), either as total or water-extractable, are low in concentrations and do not show consistent relationship with hydrothermal alteration and/or mineralization. The absence of relationship between halogens and mineralization is most obvious at Valley Copper, and might suggest loss of halogens by volatilization. This is consistent with results reported by Kesler et al. (1972) suggesting no relationship between halogen content of intrusions and their Cu bearing potential.

(c) Mineral Geochemistry

(11) Cu contents of biotite, magnetite and quartz-feldspar fractions strongly correlate with whole-rock Cu in background and anomalous samples. Results of sulphide-selective leach are consistent with the principal mode of occurrence of Cu as sulphide inclusions in all mineral phases of both anomalous and some background samples.

(12) Levels of Mg, Ni, Zn, Mn and Co in biotites, and Zn

and Co in magnetites are generally lower in mineralized than background samples. This is consistent with incipient leaching of these elements during hydrothermal alteration.

(d) Sulphide Selective Digestion

(13) An efficacious sulphide-selective leach ($\text{KClO}_3\text{-HCl}$), not used previously in bedrock geochemistry, was developed during this study.

(14) Experimental results demonstrate that $\text{KClO}_3\text{-HCl}$ leach appears to be more sulphide selective for Cu than procedures such as $\text{H}_2\text{O}_2\text{-Ascorbic acid}$ and aqua regia digestion. Furthermore, hot concentrated acids are not involved, and the procedure is extremely rapid and simple and hence suited to routine application both in the field and laboratory.

(15) $\text{KClO}_3\text{-HCl}$ digestion gives a better geochemical contrast for Cu in bedrock, than either aqua regia, $\text{H}_2\text{O}_2\text{-Asc.}$, or total digestion.

(16) As expected, distribution of sulphide-held Cu using $\text{KClO}_3\text{-HCl}$ digestion at Valley Copper and JA is similar to that of total Cu because of the dominant occurrence of Cu as sulphide veins and disseminations. However, sulphide-held Fe delineates pyrite halos surrounding these deposits.

(e) Ore-forming Processes at Highland Valley.

(17) In view of established spatial and temporal relation-

ships between mineralization at Highland Valley and the evolution of the Guichon Creek magma, a modified orthomagmatic model is proposed for ore genesis at Highland Valley.

(18) Results of K, Rb and Sr determinations indicate relatively low abundances of these elements in fresh rocks of Guichon Creek batholith compared with other Mesozoic granitic rocks in the Canadian Cordillera. K/Rb ratios are relatively high, and largely outside the limits considered normal for crustal plutonic masses of granitic composition. Rb/Sr ratios are low, and similar to values reported for tholeiitic and 'primitive' calc-alkaline rocks of ancient island arcs. These results are consistent with low Sr isotopic ratios reported by Christmas et al. (1969), and suggest derivation of the batholith from a subcrustal source, most probably from subducted oceanic crust or upper mantle.

(19) A deep-seated source of the Guichon Creek magma has far-reaching implications for ore genesis. Various lines of isotopic evidence suggest derivation of sulphur and associated ore metals from a subcrustal source similar to that of the batholith, which is considered as a metal-rich portion of the subducted oceanic crust. Distribution of Cu in the batholith is similar to that of other femic elements, in that it differs from trends observed in intrusions that are reported to have produced immiscible sulphide phases, such as Skaergaard (Wager and Brown, 1967), and Laramide porphyritic intrusions of Arizona (Graybeal, 1973). Consequently, it is suggested that the role of Guichon Creek magma

in mineralization is merely one of structural control rather than a direct source of metals. However, differentiation of Guichon Creek magma provided adequate volatiles and structural 'traps' that led to the extraction of metals from the 'system'.

(20) Close spatial relationships between mineralization and porphyry dykes or stocks suggest that porphyries provided 'high-level' structural outlets for mineralizing solutions which subsequently reacted with wall rocks to produce the alteration and chemical patterns characteristic of porphyry-type deposits in the Highland Valley.

(21) The extensive leaching of 'base elements' (Ca, Na, Sr Ba) in zones of phyllic and argillic alteration is consistent with decreasing base cation/ H^+ ratios during the intense 'wave' of acidic processes associated with formation of H^+ consuming minerals such as sericite and kaolinite. The leached elements are concentrated at the outer margins of the metasomatic front (Korzhinskii, 1968) as solutions migrate outwards and are neutralized by reaction with wall rocks.

(f) Applications of Bedrock Geochemistry in Exploration

Results of this study suggest that bedrock geochemistry can be very useful for reconnaissance and detailed mineral exploration in the Guichon Creek batholith and similar calc-alkaline intrusions in the Canadian Cordillera.

(22) Assuming that the Guichon Creek magma and associated ore metals were derived from a metal-rich portion of subducted oceanic crust, the following criteria can be useful in reconnaissance exploration for Cordilleran intrusive and extrusive rocks generated from the same source region as the Guichon Creek batholith and with potential for porphyry coppers and/or massive sulphides.

(i) Late Triassic to Early Jurassic age; (ii) low K, Rb and Rb/Sr values, and high K/Rb ratios; and (iii) location in the Intermontane Belt of southern Canadian Cordillera.

(23) In view of the supposed role of magmatic differentiation in providing suitable chemical and structural environments for ore localization, petrochemical variation diagrams can be useful in identifying intrusive units that are most fractionated and capable of being spatially associated with mineralization.

(24) The close relationships between metal values and degree of fractionation in the Guichon Creek batholith suggest the need for assigning different background values to each intrusive phase and soils derived from them, during geochemical exploration programmes.

(25) For detailed exploration around porphyry copper prospects or deposits, Cu and S, because they show high contrast and extensive halos, constitute tools for delineating mineralized zones. S, however shows the more consistent or less erratic dispersion patterns. Pronounced S anomalies in bedrock suggest that SO_2 in soil gas or air can be useful in outlining mineralized zones at

Highland Valley. The intensity of such halos might be affected by bornite: chalcopyrite ratio; where this ratio is high (reflecting higher ore grade), intensity of gas anomalies will be diminished.

(26) Sulphide-held Cu shows a greater contrast than total Cu where a large number of fresh background samples are included in sampling programmes. Sulphide-held Fe as determined by $\text{KClO}_3\text{-HCl}$ will be useful in outlining pyrite halos that most commonly envelope porphyry coppers.

(27) In view of the close association between alteration and mineralization at porphyry coppers, the distribution of lithophile elements Rb, Sr and Ba, and/or K, Ca and Na, constitutes a reliable tool in delineating zones of intense alteration and mineralization. They are easily determined by routine analysis and their distribution more readily quantified than fine grained mineralogy characteristic of alteration zones. Furthermore, the use of ratios (e.g. Ba/Sr Rb/Sr) offer added advantages, in that it eliminates the influence of erratic data or local mineralogical control on metal distribution. At Highland Valley, Rb/Sr and Ba/Sr ratios exceeding 0.1 and 1 respectively delineate mineralized zones.

(28) Volatile elements have a limited application to exploration in the Highland Valley. Hg in bedrock, soil gas or air can be useful in detecting orebodies. similar to the Bethlehem-JA deposit. B is most useful in exploring for deposits associated with

breccia pipes and quartz porphyries. Because of the absence of pronounced Cl and F anomalies at the Highland Valley deposits, halogens in bedrock or as gaseous indicators have no exploration potential in the Highland Valley.

(29) Factor analysis constitutes a potent tool in deciphering the inter-relationships of metal distributions in multi-element geochemical studies. Metal associations obtained by factor analysis are consistent with subjective interpretations of geologic, hydrothermal and metallization processes.

(30) Greater contrast was achieved with whole-rock than mineral analysis, consequently the use of mineral separates offers no advantages for exploration in the Highland Valley.

REFERENCES

- Ager, C.A., Ulrych, J.J., and McMillan, W.J. 1973. A gravity model for the Guichon Creek batholith, south-central, British Columbia. *Can. J. Earth Sci.*, v. 10, pp. 920-935.
- Al-Hashimi, A.R.K. 1969. A study of copper dispersion in the Boulder batholith, Montana. Unpublished Ph.D. thesis, Boston University, 144 p.
- Al-Hashimi, A.R.K., and Brownlow, A.H. 1970. Copper content of biotites from the Boulder batholith, Montana. *Econ. Geol.*, v. 65, pp. 985-992.
- Allmann, R. and Korting, S. 1972. Fluorine in Handbook of Geochemistry, ed. K.H. Wedepohl, v. 3, pp. 9E-9F, Springer Verlag Publishers, New York.
- Armbrust, G.A., Munoz, J.O., and Farias, J.A. 1971. Rubidium as a guide to ore at El Teniente (Braden), Chile. (Abst), *Econ. Geol.*, v. 66, pp. 977.
- Azzaria, L.M. 1963. A study of the distribution of traces of copper, lead and zinc in the minerals of a Precambrian granite. *Can. Mineralogist*, v. 8, pp. 617-630.
- Baadsgaard, H., Folinsbee, R.E., and Lipson, J. 1961. Potassium-argon dates of biotites from Cordilleran granites. *Bull. Geol. Soc. Amer.*, v. 72, pp. 689-702.
- Bailey, G.B. and McCormick, G.R. 1974. Chemical halos as guides to lode deposits ore in the Park City district, Utah. *Econ. Geol.*, v. 69, pp. 377-382.
- Barnes, H.L., and Czamanske, G.K. 1967. Solubilities and transport of ore minerals. In *Geochemistry of Hydrothermal Ore Deposits*, ed. H.L. Barnes, pp. 334-381. Holt, Rinehart and Winston, New York.
- Bergey, W.R., Carr, J.M., and Reed, A.J. 1971. The Highmont copper-molybdenum deposits, Highland Valley, British Columbia. *Can. Inst. Min. Metall. Bull.*, v. 64, pp. 68-76.
- Blanchflower, J.D. 1972. Isotopic dating of copper mineralization at Alwin and Valley Properties, Highland Valley, B.C. Unpublished B. Sc. Thesis, 83 p.
- Blaxland, A.B. 1971. Occurrence of Zn in granitic biotites. *Mineralium Deposita*, v. 6, pp. 313-320.

- Bolter, E., and Al-Shaieb, Z. 1971. Trace-element anomalies in igneous wall rocks of hydrothermal veins. *Geochemical Exploration, CIM Spec. Vol. 11*, pp. 289-290.
- Boyle, R.W. 1961. The geology, geochemistry and origin of the gold deposits of the Yellowknife district. *Geol. Surv. Can. Mem. 310*.
- Boyle, R.W. 1965. Geology, geochemistry and origin of the lead-zinc-silver deposits of the Keno Hill-Galena Hill area, Yukon Territory, *Geol. Surv. Can. Bull. 111*.
- Boyle, R.W. 1967. Geochemical prospecting-retrospect and prospect. *Geol. Surv. Can. Paper 66-54*, pp. 30-43.
- Boyle, R.W., 1968. A source of metals and gangue elements in epigenetic deposits. *Mineralium Deposita*, v. 3, pp. 174-177.
- Boyle, R.W. 1971. Boron and boron minerals as indicators of mineral deposits. (Abst.), *Geochemical Exploration, CIM Spec. Vol. 11*, pp. 12.
- Boyle, R.W., and Garrett, R.G. 1970. Geochemical prospecting - A review of its status and future. *Earth Sci. Rev.*, v. 6, pp. 51-75.
- Brabec, D. 1970. A geochemical study of the Guichon Creek batholith, British Columbia. Unpublished Ph.D thesis, Univ. British Columbia, 146 p.
- Brabec, D. 1971. Aqua regia extractable vs. total copper and zinc content of granitic rocks. *Soc. Min. Eng. Trans.*, v. 250, pp. 94-97.
- Brabec, D., and White, W.H. 1971. Distribution of copper and zinc in rocks of the Guichon Creek batholith. *Geochemical Exploration, CIM Spec. Vol. 11*, pp. 291-297.
- Bradshaw, P.M.D. 1967. Distribution of selected elements in feldspar, biotite and muscovite from British granites in relation to mineralization. *Inst. Min. Metall. Trans.*, v. 76, pp. B137-148.
- Bradshaw, P.M.D., and Stoyel, A.J. 1968. Exploration for blind orebodies in southwest England by the use of geochemistry and fluid inclusions. *Inst. Min. Metall. Trans.*, v. 77, pp. B144-152.
- Bradshaw, P.M.D., Clews, D.R., and Walker, J.L. 1970. *Exploration Geochemistry, Part 4: Primary dispersion. Mining in Canada*, June, pp. 24-31.

- Bristol, C.C. 1968. The quantitative determination of minerals in some metamorphosed volcanic rocks by x-ray powder diffraction. *Can. J. Earth Sci.*, v. 5, pp. 235-242.
- Bristol, C.C. 1972. Quantitative determination of some carbonate minerals in greenschist facies meta-volcanic rocks. *Can. J. Earth Sci.*, v. 9, pp. 36-42.
- Brown, A.S. 1967. Investigation of mercury dispersion halos around mineral deposits in central British Columbia. *Geol. Surv. Can. Paper 66-54*, pp. 73-83.
- Burnham, C.W. 1967. Hydrothermal fluids at the magmatic stage. In *Geochemistry of Hydrothermal Deposits*, ed. L.H. Barnes, pp. 34-76.
- Burns, R.G., and Fyfe, W.S. 1967. Crystal field theory and the geochemistry of transition elements. In *Researches in Geochemistry*, ed. A.H. Abelson, v. 2, pp. 259-285. Wiley and Sons, New York.
- Cameron, E.M. 1972. Three geochemical standards of sulphide-bearing ultramafic rocks: UM.1, UM.2, UM.4. *Geol. Surv. Can. Paper 71-35*, 10 p.
- Carr, J.M. 1962. The geology of part of Thompson River Valley between Ashcroft and Spences Bridge. *Brit. Columbia Dept. Mines Pet. Res. Annual Rept.*, pp. 28-45.
- Carr, J.M. 1966. Geology of the Bethlehem and Craigmont copper deposits. In *Tectonic History and Mineral Deposits of the Western Cordillera*, CIM, Spec. Vol. 8, pp. 321-328.
- Carr, J.M. 1967. Lornex. *Brit. Columbia Dept. Mines Pet. Res. Annual Rept.*, pp. 157-158.
- Carson, D.J.T., and Jambor, J.L. 1974. Mineralogy, zonal relationships and economic significance of hydrothermal alteration at porphyry copper deposits, Babine Lake area, British Columbia. *Can. Inst. Min. Metall. Bull.*, v. 67, pp. 110-133.
- Christmas, L., Baadsgaard, H., Folinsbee, R.E., Fritz, P., Krouse, H.R., and Sasaki, A. 1969. Rb/Sr, S, and O isotopic analyses indicating source and date of contact metasomatic copper deposits, Craigmont, British Columbia, Canada. *Econ. Geol.*, v. 64, pp. 479-488.
- Coope, J.A. 1973. Geochemical prospecting for porphyry copper-type mineralization - a review. *J. Geochem. Explor.*, v. 2, pp. 81-102.

- Cornwall, H.R., and Rose, H.J. 1957. Minor elements in Keeweenawan lavas, Michigan. *Geochem. et Cosmochim. Acta*, v. 12, pp. 209-224.
- Culbert, R.R. 1972. Abnormalities in the distribution of K, Rb and Sr in the Coast Mountains batholith, British Columbia. *Geochim. et Cosmochim. Acta*, V. 36, pp. 1081-1100.
- Curtis, C.D. 1964. Applications of the crystal-field theory to the inclusion of trace transition elements in minerals during magmatic differentiation. *Geochim. et Cosmochim. Acta*, v. 28, pp. 389-403.
- Cuttita, F., Senftle, F.F., and Walker, E.C. 1960. Preliminary tests on isotopic fractionation of copper absorbed on quartz and sphalerite. U.S. Geol. Surv. Prof. Paper 400B, pp. 44-53.
- Danner, W.R., and Nestell, M.K. 1971. Permian-Triassic of the Western Cordilleran eugeosyncline. (Abst), *Bull. Can. Pet. Geol.*, v. 19, pp. 324-325.
- Darling, R. 1971. Preliminary study of the distribution of minor and trace elements in biotite from quartz monzonite associated with contact-metasomatic tungsten-molybdenum-copper ore, California, U.S.A. *Geochemical Exploration, CIM Spec. Vol. 11*, pp. 315-322.
- Dass, A.S., Boyle, R.W., and Tupper, W.M. 1973. Endogenic halos of the native silver deposits, Cobalt, Ontario Canada. *Geochemical Exploration 1972*, pp. 25-35. Inst. Min. Metall. London.
- Davis, J.D., and Guilbert, J.M. 1973. Distribution of the radioelements potassium, uranium and thorium in selected porphyry copper deposits. *Econ. Geol.*, v. 68, pp. 145-160.
- De Grys, A. 1970. Copper and zinc in alluvial magnetites from central Ecuador. *Econ. Geol.*, v. 65, pp. 714-717.
- Dercourt, J. 1972. The Canadian Cordillera, the Hellenides, and the sea-floor spreading theory. *Can. J. Earth Sci.*, v. 9, pp. 709-743.
- Dirom, G.E. 1965. K-Ar age determination in biotites and amphiboles, Bethlehem Copper property, B.C. Unpublished M.A.Sc. thesis, Univ. British Columbia.
- Dolezal, J., Povondra, P., and Sulcek, Z. 1966. Decomposition techniques in inorganic analysis, Iliffe Books Ltd. London, 224 p.

- Doyle, P.J. 1972. Regional stream sediment reconnaissance and trace element content of rock, soil and plant material in eastern Yukon Territory. Unpublished M.Sc. thesis, Univ. British Columbia, 132 p.
- Faure, G., and Hurley, P.M. 1963. The isotopic compositions of strontium in oceanic and continental basalts; Application to the origin of igneous rocks. *J. Petrol.*, v. 4, pp. 31-50.
- Field, C.W., Jones, M.B., and Bruce, W.R. 1973. Porphyry copper-molybdenum deposits in the Pacific Northwest. A.I.M.E. Preprint 73-S-69.
- Fipkie, C.E. 1972. Some aspects of the hydrothermal mineralogy of the Lornex porphyry copper deposit, Highland Valley, B.C. Unpublished B.Sc. thesis, Univ. British Columbia, 99 p.
- Flanagan, F.J. 1973. 1972 values for international geochemical reference samples. *Geochim. Cosmochim. Acta.*, v. 37, pp. 1189-1200.
- Folinsbee, R.E., Baadsgaard, H., and Lipson, J. 1960. Potassium-argon time scale, Rept. XXI, Int. Geol. Cong., Norden, Pt. III, pp. 7-17.
- Foster, J.R. 1973. The efficiency of various digestion procedures in the extraction of metals from rocks and rock-forming minerals. *Can. Inst. Min. Metall. Bull.*, v. 66, pp. 85-92.
- Fountain, R.J. 1972. Geological relationships in the Panguna porphyry copper deposit, Bougainville Island, New Guinea. *Econ. Geol.*, v. 67, pp. 1049-1064.
- Fournier, R.O. 1967. The porphyry copper deposit exposed in the Liberty open-pit mine near Ely, Nevada. *Econ. Geol.*, v. 62, pp. 57-81.
- Friedrich, G.H. 1971. Use of mercury in geochemical exploration. *Geol. Mijnbouw*, v. 50, pp. 768-770.
- Garrett, R.G. 1969. The determination of sampling and analytical errors in exploration geochemistry. *Econ. Geol.*, v. 64, pp. 568-569; discussion, v. 68, pp. 281-283 (1973).
- Garrett, R.G. 1971. Molybdenum, tungsten and uranium in acid plutonic rocks as a guide to regional exploration, S.E. Yukon, *Can. Min. Journ.*, April, pp. 37-40.
- Goldschmidt, V.M. 1954. *Geochemistry*. Oxford University Press.

- Goodfellow, W.D. 1974. Major and minor element halos in volcanic rocks at Brunswick No. 12 sulphide deposit, N.B. Canada. (Abst.) Proc. 5th Intern. Geochem. Explor. Symp., April 1974, Vancouver, pp. 34-35.
- Gott, G.B., and McCarthy, Jr., A.H. 1966. Distribution of gold, silver, tellurium and mercury in the Ely mining district, White Pine County, Nevada. U.S. Geol. Surv. Circ. 535, 5 p.
- Graybeal, F.T. 1973. Copper, manganese, and zinc in coexisting mafic minerals from Laramide intrusive rocks in Arizona. Econ. Geol., v. 68, pp. 785-798.
- Gresens, R.L. 1967. Composition-volume relationships of metasomatism. Chem. Geol., v.2, pp. 47-65.
- Guilbert, J.M., and Lowell, J.D. 1973. Potassic alteration in porphyry copper deposits. (Abst.), Econ. Geol., v. 68, pp. 703.
- Gunton, J.E., and Nichol, I. 1974. Chemical zoning associated with the Ingerbelle-Copper Mountain mineralization, Princeton, British Columbia. (Abst.), Proc. 5th Intern. Geochem. Explor. Symp., April, Vancouver, pp. 38-39.
- Haack, U. 1969. Spurenelemente in biotiten aus graniten and gneisen. Contrib. Min. Pet., v. 22, pp. 83-126.
- Hamil, B.M., and Nackowski, M.P. 1971. Trace-element distribution in accessory magnetite from quartz monzonite intrusives and in relation to sulfide mineralization in the Basin and Range Province of Utah and Nevada - a preliminary report. Geochemical Exploration. CIM Spec. Vol. 11, pp. 331-333.
- Hatherton, T., and Dickinson, W.R. 1969. The relationship between andesitic volcanism and seismicity in Indonesia, the Lesser Antilles and other island arcs. J. Geophys. Res., v. 74, pp. 5301-5310.
- Hausen, D.M. and Kerr, P.F. 1971. X-ray diffraction methods in evaluating potassium silicate alteration in porphyry mineralization. Geochemical Exploration. CIM Spec. Vol. 11, pp. 334-340.
- Hawkes, H.E., and Webb, J.S. 1962. Geochemistry in Mineral Exploration. Harper and Row, 415 p.
- Haynes, S.J., and Clark, A.H. 1972. A rapid method for the determination of chlorine in silicate rocks using ion-selective electrodes. Econ. Geol., v. 67, pp. 378-382.

- Hedge, C.E. 1966. Variations in radiogenic strontium found in volcanic rocks. *J. Geophys. Res.*, v. 71, pp. 6119-6126.
- Heier, K.S., and Adams, J.A.S. 1964. The geochemistry of the alkali metals. *Phys. Chem. Earth*, v. 5, pp. 253-381.
- Helgeson, H.C. 1970. A chemical and thermodynamic model of ore deposition in hydrothermal systems. *Mineral. Soc. Amer. Spec. Paper 3*, pp. 155-186.
- Hemley, J.J., and Jones, W.R. 1964. Chemical aspects of hydrothermal alteration with emphasis on hydrogen metasomatism. *Econ. Geol.*, v. 59, pp. 538-569.
- Hewett, F.G. 1972. Mineral deposits of the Highland Valley. Unpublished report, Geol. 409 course, Univ. British Columbia, 45 p.
- Hoffman, S.J. 1972. Geochemical dispersion in bedrock and glacial overburden around a copper property in south-central B.C. Unpublished M.Sc. thesis, Univ. British Columbia, 209 p.
- Holland, H.D. 1972. Granites, solutions and base metal deposits. *Econ. Geol.* v. 67, pp. 281-301.
- Huff, L.C. 1971. A comparison of alluvial exploration techniques for porphyry copper deposits. *Geochemical Exploration. CIM Spec. Vol. 11*, pp. 190-194.
- Hurley, P.M. 1968. Absolute abundances and distribution of Rb, K and Sr in the earth. *Geochim. Cosmochim. Acta*, v. 32, pp. 273-283.
- Ineson, P.A. 1969. Trace-element aureoles in limestone wall rocks adjacent to lead-zinc-barite-fluorite mineralization in the northern Pennine and Derbyshire ore-fields. *Inst. Min. Metall. Trans.*, v. 78, pp. B29-B40.
- Ineson, P.A. 1970. Trace-element aureoles in limestone wall rocks adjacent to fissure veins in the Eyam area of the Derbyshire ore-field. *Inst. Min. Metall. Trans.*, v. 79, pp. B238-B245.
- Jakes, P., and White, A.J.R. 1970. K/Rb ratios of rocks from island arcs. *Geochim. Cosmochim. Acta*, v. 34, pp. 849-856.
- Jonasson, I.R., Lynch, J.J. and Trip, L.J. 1973. Field and laboratory methods used by the Geological Survey of Canada in geochemical surveys, 12. Mercury in ores, rocks, soils, sediments and water. *Geol. Surv. Can. Paper 73-21*, 22 p.

- Jones, M.B., Allen, J.M., and Field, C.W. 1972. Hydrothermal alteration and mineralization, Valley Copper deposit, British Columbia. (Abst.), Econ. Geol., v. 67, pp. 1006.
- Kesler, S.E., Van Loon, J.C., and Moore, C.M. 1973. Evaluation of ore potential of granodioritic rocks using water extractable chloride and fluoride. Can. Inst. Min. Metall. Bull., v. 66, pp. 56-60.
- Kesler, S.E., Van Loon, J.C. and Bateson, J.H. 1973. Analysis of fluoride in rocks and an application to exploration. J. Geochem. Explor., v. 2, pp. 11-17.
- Kistler, R.W., Evernden, J.F., and Shaw, H.R. 1971. Sierra Nevada plutonic cycle: Part 1, Origin of composite granitic batholiths. Geol. Soc. Amer. Bull., v. 82, pp. 853-868.
- Korzhinskii, D.S. 1968. The theory of metasomatic zoning. Mineralium Deposita, v. 3, pp. 222-231.
- Krauskopf, K.B. 1967. Source rock for metal-bearing fluids. In Geochemistry of Hydrothermal Ore Deposits, ed. H.L. Barnes, pp. 1-33, Holt, Rinehart and Winston, New York.
- Kuroda, P.K., and Sandell, E.B. 1953. Chlorine in igneous rocks, Geol. Soc. Amer. Bull., v. 64, pp. 879-896.
- Larsen, E.S.J., and Poldervaart, A. 1961. Petrologic study of Bald Rock batholith, near Badwell Bar, California. Geol. Soc. Amer. Bull., v. 72, pp. 69-92.
- Leech, G.B., Lowdon, J.A., Stockwell, C.H., and Wanless, R.K. 1963. Age determinations and geological studies. Geol. Surv. Can. Paper 63-17.
- Levinson, A.A. 1974. Introduction to Exploration Geochemistry. Applied Publishing Ltd., Calgary.
- Lovering, T.G., Cooper, J.R., Drewes, H., and Cone, G.C. 1970. Copper in biotite from igneous rocks in southern Arizona as an ore indicator. U.S. Geol. Surv. Prof. Paper 700-B, pp. B1-8.
- Lowell, J.D., and Guilbert, J.M. 1970. Lateral and vertical alteration-mineralization zoning in porphyry ore deposits. Econ. Geol., v. 64, pp. 373-408.
- Luth, W.C., Jahns, R.H., and Tuttle, D.F. 1964. The granitic system at pressures of 4 - 10kb. J. Geophys. Res., v. 69, pp. 759-773.

- Lyakhovich, V.V. 1959. Some data on composition of accessory magnetites: I.G.E.M. Academy of Science U.S.S.R., v. 3, pp. 89-103 (in Russian).
- Lynch, J.J. 1971. The determination of copper, nickel and cobalt in rocks by atomic absorption spectrometry using a cold leach. *Geochemical Exploration. CIM Spec. Vol. 11*, pp. 313-314.
- McCarthy, J.H. 1972. Mercury vapor and other volatile components in the air as guides to ore deposits. *J. Geochem. Explor.*, v. 1, pp. 143-162.
- McDougall, I., and Lovering, J.F., 1963. Fractionation of Cr, Ni, Co and Cu in differentiated dolerite-lamprophyre sequence at Red Hill, Tasmania. *Geol. Soc. Aust. Jour.*, v. 10, pp. 325-338.
- McMillan, W.J. 1971. Valley Copper. *In* *Geology, Exploration and Mining in British Columbia, 1970*, BCDM Rpt., pp. 354-369.
- McMillan, W.J. 1972. The Highland Valley porphyry copper district. *Guidebook, No. 9, Intern. Geol. Cong.*, pp. 53-69.
- McMillan, W.J. 1973. Geological Map of the Highland Valley. BCDM Rept., (in press).
- McNerney, J.J., and Buseck, P.R. 1973. Geochemical exploration using mercury vapor. *Econ. Geol.*, v. 68, pp. 1313-1320.
- Meyer, C., and Hemley, J.J. 1967. Wall-rock alteration. *In* *Geochemistry of Hydrothermal Ore Deposits*, ed. H.L. Barnes, pp. 166-236. Holt, Rinehart and Winston, New York.
- Mitchell, A.H.G., and Carson, M.S. 1972. Relationship of porphyry copper and circum-Pacific tin deposits to palaeo-Benioff zones. *Inst. Min. Metall. Trans.*, v. 81, pp. B10-B25.
- Monger, J.W., Souther, J.G., and Gabrielse, H. 1972. Evolution of the Canadian Cordillera: A plate tectonic model. *Am. Jour. Sci.* v. 272, pp. 577-602.
- Nairis, B. 1971. Endogene dispersion aureoles around the Rudtjebacken sulphide ore in the Adak area, northern Sweden. *Geochemical Exploration. CIM Spec. Vol. 11*, pp. 357-374.
- Nielsen, R.L. 1968. Hypogene texture and mineral zoning in a copper-bearing granodiorite porphyry stock, Santa Rita, New Mexico. *Econ. Geol.*, v. 63, pp. 37-50.
- Noble, J.A. 1970. Metal provinces of the western United States. *Geol. Soc. Amer. Bull.*, v. 81, pp. 1607-1624.

- Nockolds, S.R., and Allen, R. 1953. The geochemistry of some igneous rock series. *Geochim. Cosmochim. Acta*, v. 4, pp. 105-142.
- Norrish, K., and Hutton, J. 1969. An accurate X-ray spectrographic method for the analysis of a wide range of geological samples. *Geochim. Cosmochim. Acta*, v. 33, pp. 431-453.
- Northcote, K.E. 1968. Geology and geochemistry of the Guichon Creek batholith. Unpublished Ph.D thesis, Univ. British Columbia, 186 p.
- Northcote, K.E. 1969. Geology and geochronology of the Guichon Creek batholith. *British Columbia Dept. Mines Pet. Res., Rept.*, 56, 73p.
- Olade, M., and Fletcher, K. 1974. Potassium chlorate-hydrochloric acid; A sulphide-selective leach for bedrock geochemistry. *J. Geochem. Expl.*, v. 3, (in press).
- Olade, M.A. and Fletcher, W.K. 1974. Primary dispersion of rubidium and strontium around porphyry copper deposits, Highland Valley, B.C. *Econ. Geol.*, (in press).
- Olade, M., Fletcher, K., and H.V. Warren. 1974. Barium-strontium relationships at Highland Valley porphyry copper deposits, B.C. *Western Miner* (in press).
- Orion Research 1970. Manual on specific ion meters. Orion Research, 26 p.
- Oyarzun, J.M. 1974. Rubidium and strontium as a guide to copper mineralization emplaced in some Chilean andesitic rocks. (Abst.), *Proc. 5th Intern. Geochem. Explor. Symp.*, April, Vancouver, pp. 48.
- Pantazis, Th.M., and Govett, G.J.S. 1973. Interpretation of a detailed rock geochemical survey around Mathiati mine, Cyprus. *Jour. Geochem. Explor.*, v. 2, pp. 25-36.
- Parry, W.T. 1972. Chlorine in biotite from Basin and Range plutons. *Econ. Geol.*, v. 67, pp. 972-975.
- Parry, W.T., and Nackowski, M.P. 1963. Copper, lead and zinc in biotites from Basin and Range quartz monzonites. *Econ. Geol.*, v. 58, pp. 1126-1144.
- Peto, P. 1973. Petrochemical study of the Similkameen batholith, British Columbia. *Geol. Soc. Amer. Bull.*, v. 84, pp. 3977-3984.
- Peto, P. 1974. Plutonic evolution of the Canadian Cordillera. *Geol. Soc. Amer. Bull.*, v. 85, pp. 1269-1276.

- Philips, W.J. 1973. Mechanical effects of retrograde boiling and its probable importance in the formation of some porphyry copper deposits. *Inst. Min. Metall. Trans.*, v. 82, pp. B90-B98.
- Putman, G.W. 1972. Base metal distribution in granitic rocks: Data from the Rocky Hill and Lights Creek stocks, California. *Econ. Geol.*, v. 67, pp. 511-527.
- Putman, G.W. 1973. Biotite-sulfide equilibrium in granitic rocks: a revision. *Econ. Geol.*, v. 68, pp. 884-891.
- Putman, G.W., and Burnham, C.W. 1963. Trace elements in igneous rocks, northwestern and central Arizona. *Geochim. Cosmochim. Acta*, v. 27, pp. 53-106.
- Rabinovich, A.V., and Badalov, S.I. 1968. Geochemistry of copper in some intrusives of Karamazar and West Uzbekistan. *Geochem. Intern.* v. 8, pp. 146-150.
- Rabinovich, A.V., Muravera, A.N., and Zhdanova, M.V. 1958. Molybdenum content of certain rocks and minerals in the intrusives of Eastern Transbaikalia. *Geochem. Intern.*, v. 2, pp. 155-162.
- Ringwood, A.E. 1955. The principles governing trace element distribution during magmatic crystallization. *Geochim. Cosmochim. Acta*, v. 17, pp. 189-202; 242-254.
- Rose, A.W. 1970. Zonal relations of wall rock alteration and sulfide distribution at porphyry copper deposits. *Econ. Geol.*, v. 63, pp. 920-936.
- Rouse, G.E., and Stevens, D.M. 1971. The use of sulfur dioxide gas geochemistry in the detection of sulfide deposits. Paper presented at AIME Ann. Gen. Meeting, March 1971.
- Sakrison, H.C. 1971. Rock geochemistry - its current usefulness on the Canadian Shield. *Can. Inst. Min. Metall. Bull.*, v. 64, pp. 28-31.
- Schau, M. 1970. Discussion of paper by Christmas *et al.*, 1969. *Econ. Geol.*, v. 65, pp. 62-63; reply to discussion, pp. 63-64.
- Sheppard, S.M.F., Nielsen, R.L., and Taylor, Jr., H.P. 1969. Oxygen and hydrogen isotope ratios of clay minerals from porphyry copper deposits. *Econ. Geol.*, v. 64, pp. 755-777.
- Sheraton, J.W., and Black, L.P. 1973. Geochemistry of mineralized granitic rocks of northeast Queensland. *Jour. Geochem. Explor.*, v. 2, pp. 331-348.

- Shikawa, H., Kuroda, R., and Sudo, T. 1962. Minor elements in some altered zones of Kuroko (black ore) deposits in Japan. *Econ. Geol.*, v. 57, pp. 785-789.
- Shikawa, H., Tono, N., and Wakasa, K. 1974. Geochemical exploration for the Kuroko deposits in the northeast Honshu, Japan. (Abst.), *Proc. 5th Int. Geochem. Explor. Symp.*, April, Vancouver, pp. 55-56.
- Sillitoe, R.H. 1972. A plate tectonic model for the origin of porphyry copper deposits. *Econ. Geol.*, v. 67, pp. 184-197.
- Sinclair, A.J. 1974. Selection of threshold values in geochemical data using probability plots. *Jour. Geochem. Explor.*, v. 3, pp. 129-149.
- Smith, T.E. 1974. The geochemistry of the granitic rocks of Halifax County, Nova Scotia. *Can. J. Earth Sci.*, v. 11, pp. 650-656.
- Stanley, A. 1964. Relation of copper to rock types in an area of known economic mineralization. *Econ. Geol.*, v. 59, pp. 1492-1496.
- Stanton, R.E. 1966. *Rapid Methods of Trace Analysis for Geochemical Application*. E. Arnold, London, 96 p.
- Taubeneck, W.H. 1965. An appraisal of some potassium-rubidium ratios in igneous rocks. *Jour. Geophys. Res.*, v. 70, pp. 475-478.
- Taubeneck, W.H. 1967. Petrology of Cornucopia Tonalite Unit, Cornucopia stock, Wallowa Mountains, northeastern Oregon. *Geol. Soc. Amer. Spec. Paper* 91, 56 p.
- Tauson, L.V., Sheremet, Y.M., and Antipin, V.S. 1970. Trends in the distribution of molybdenum in Mesozoic granitoids of northeastern Transbakykalia. *Geochem. Intern.*, v. 8, pp. 637-642.
- Theobald, Jr., P.K., Overstreet, W.C., and Thompson, C.E. 1962. Minor elements in alluvial magnetite from the Inner Piedmont Belt, North and South Carolina. *U.S. Geol. Surv. Prof. Paper* 554-A, 34p.
- Theodore, T.G., and Nash, J.T. 1973. Geochemical and fluid zonation at Copper Canyon, Lander County, Nevada. *Econ. Geol.*, v. 68, pp. 565-570.
- Thurlow, J.G. 1974. Lithogeochemistry of the Buchans massive sulphide deposits. (Abst.), Paper presented at CIM Ann. Gen. Mtg, April 1974, Montreal.

- Tooker, E.W. 1963. Altered wall rocks in the central part of the fault Range Mineral Belt, Gulpin and Clear Creek counties, Colorado. U.S. Geol. Surv. Prof. Paper 439, 102p.
- Turekian, K.L. and Kulp, J.L. 1956. The geochemistry of strontium. *Geochim. Cosmochim. Acta*, v. 10, pp. 245-296.
- Turekian, K.L., and Wedepohl, K.H. 1961. Distribution of the elements in some major units of the Earth's crust. *Geol. Soc. Amer. Bull.*, v. 72, pp. 641-664.
- Tuttle, O.F., and Bowen, N.L. 1958. Origin of granite in the light of experimental studies in the system $\text{NaAlSi}_3\text{O}_8$ - KAlSi_3O_8 - SiO_2 - H_2O . *Geol. Soc. Amer. Mem.* 74.
- Van Loon, J.C., Kesler, S.E., and Moore, C.M. 1973. Analysis of water-extractable chloride in rocks by use of a selective ion electrode. *Geochemical Exploration 1972*, pp. 429-434. IMM, London.
- Wager, L.R., and Mitchell, R.L. 1951. The distribution of trace elements during strong fractionation of basic magma - a further study of the Skaergaard intrusion, East Greenland. *Geochim. Cosmochim. Acta*, v. 1, pp. 129-208.
- Wager, L.R., and Brown, G.M. 1967. *Layered Igneous Rocks*. Oliver and Boyd, Edinburgh and London, 588 p.
- Warren, H.V., and Delavault, R.E. 1960. Readily extractable copper in eruptive rocks as a guide for prospecting. *Econ. Geol.*, v. 54, pp. 1291-1297.
- Warren, H.V., Church, B.N., and Northcote, K.G. 1974. Barium-strontium relationships; possible geochemical tool in search for orebodies, *Western Miner*, April, pp. 107-111.
- Westermann, C.J. 1970. A petrogenetic study of the Guichon Creek batholith, B.C. Unpublished M.Sc. thesis, Univ. British Columbia, 116 p.
- White, W.H., Thompson, R.M., and McTaggart, K.C. 1957. The geology and mineral deposits of Highland Valley, B.C. *Can. Inst. Min. Metall. Trans.*, v. 60, pp. 273-289.
- White, D.E. 1968. Environment of generation of some base metal deposits. *Econ. Geol.* v. 63, p. 301-335.
- Wright, J.B., and McCurry, P. 1973. Magmas, mineralization and sea-floor spreading. *Geol. Rundsch.*, v. 62, pp. 116-125.

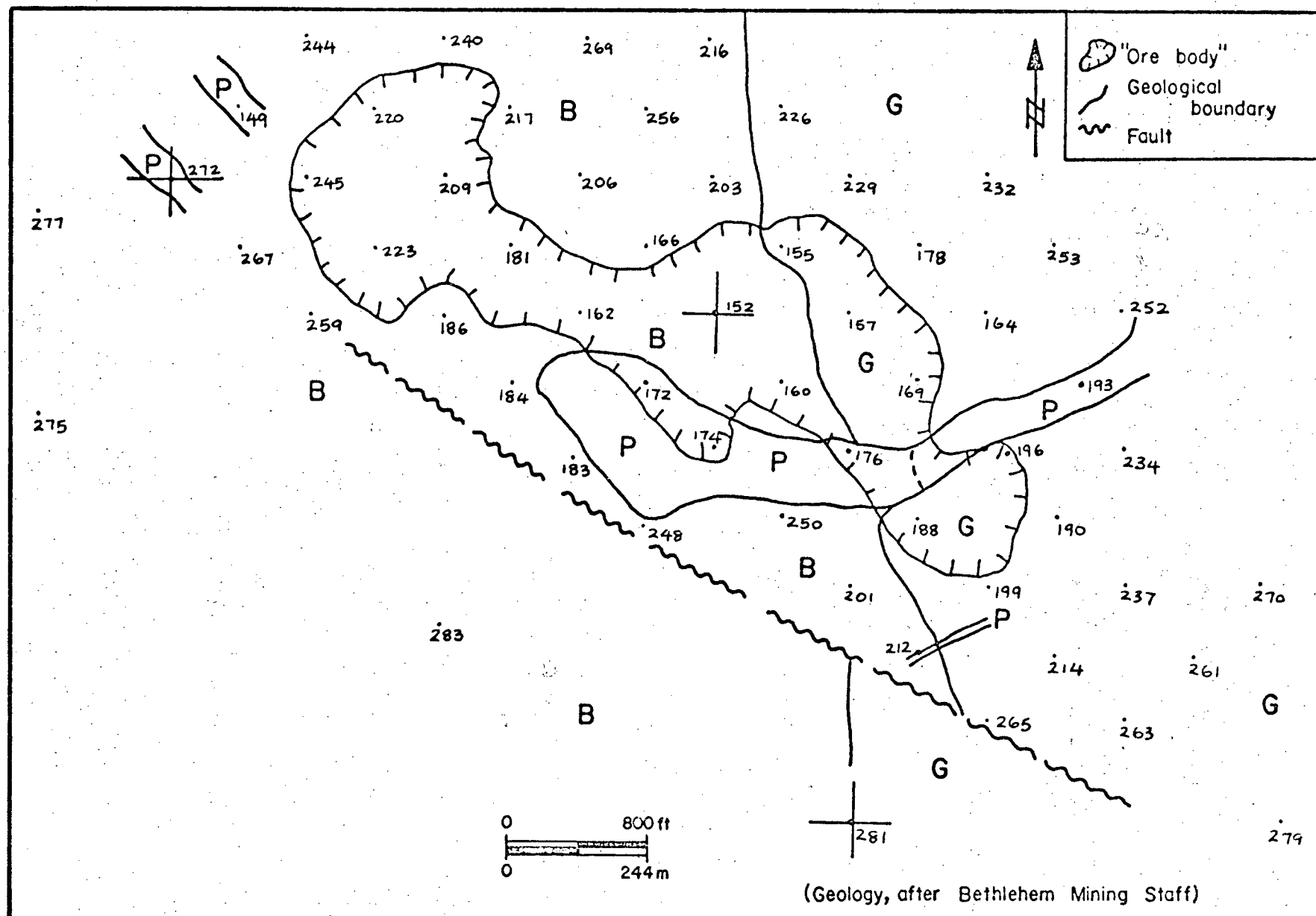
Zlobin, B.I., et al. 1967. Copper in intrusions of the central part of northern Tian-Shan as related to the problems of metallogeny. *Geologiya Rudnyh Mestorozhdenii*, No. 1, pp. 45-56 (in Russian).

APPENDICES

APPENDIX A

Bethlehem-JA

(Sample locations and Analytical Results)



BETHLEHEM-JA SUBOUTCROP LEVEL

ATOMIC ABSORPTION ANALYSIS (HNO₃-HClO₄ DIGESTION)
(VALUES IN PPM)

SAMP.	#	LOC.COORD	CU	ZN	MN	AG	NI	PB
149	200	600	1692.837	15.914	131.765	0.0	0.0	0.0
152	550	450	1775.473	14.713	101.506	0.0	0.0	0.0
155	600	500	6535.980	22.217	196.577	1.092	4.295	0.0
157	650	450	6220.469	61.356	254.251	0.0	19.172	0.0
160	600	400	19547.449	19.620	357.867	5.567	0.0	0.0
162	450	450	5117.715	11.450	99.178	0.0	0.0	0.0
164	750	450	1166.666	56.146	476.038	0.0	12.911	0.0
166	500	500	328.860	12.060	114.882	0.0	3.215	0.0
169	700	400	6725.117	28.951	205.626	0.0	11.643	0.0
172	500	400	3973.669	6.517	54.929	0.0	0.0	0.0
174	550	350	5311.582	4.557	200.474	4.606	0.0	0.0
176	650	350	103.444	11.883	130.648	0.0	0.0	0.0
178	700	500	118.827	19.086	140.775	0.0	4.236	0.0
181	400	500	2754.736	13.202	123.633	0.0	0.0	0.0
183	450	350	3510.393	23.316	126.070	0.0	2.926	0.0
184	400	400	700.666	5.103	39.525	0.0	0.0	0.0
186	350	450	361.314	12.586	101.003	0.0	0.0	0.0
188	700	300	4953.898	23.316	189.032	0.0	5.221	0.0
190	800	300	605.170	23.117	169.087	0.0	3.777	0.0
193	800	400	1077.945	12.301	85.228	0.0	0.0	0.0
196	750	350	5036.199	14.596	136.469	0.0	6.045	0.0
199	750	250	1419.913	33.305	213.640	0.0	8.262	0.0
201	650	250	2403.555	25.278	224.554	0.0	5.781	0.0
203	550	550	1128.453	11.216	129.731	0.0	0.0	0.0
206	450	550	3210.041	9.996	68.462	0.0	3.253	0.0
209	350	550	2762.178	10.977	77.261	0.0	0.0	0.0
212	700	200	664.644	36.836	347.589	0.0	12.878	0.0
214	800	200	1280.636	31.923	249.638	0.0	7.698	0.0
216	550	650	1527.321	16.479	94.433	0.0	0.0	0.0
217	400	600	8908.797	16.508	105.800	0.0	0.0	0.0
220	300	600	326.573	16.143	103.098	0.0	0.0	0.0
223	300	500	1947.921	12.017	103.098	0.0	0.0	0.0
226	600	600	135.017	18.414	120.747	0.0	0.0	0.0
229	650	550	4013.349	15.285	134.628	0.0	4.893	0.0
232	750	550	877.136	18.377	111.820	0.0	9.693	0.0
234	850	350	732.641	48.547	338.685	0.0	7.698	0.0
237	850	250	191.453	49.668	283.006	0.0	5.485	0.0
240	350	650	723.205	21.971	147.257	0.0	9.860	0.0
243	250	650	1795.757	17.557	129.120	0.0	0.0	0.0
245	250	550	2988.712	14.370	124.546	0.0	0.0	0.0
248	500	300	223.611	17.931	153.149	0.0	0.0	0.0
250	600	300	3851.349	15.644	122.417	0.0	0.0	0.0
252	850	450	213.480	19.680	185.846	0.0	6.045	0.0
253	800	500	205.794	19.286	190.626	0.0	5.221	0.0
256	500	600	4657.453	22.459	224.882	0.0	0.0	0.0
259	250	450	237.677	28.608	236.709	0.0	0.0	0.0
261	900	200	1580.017	19.313	173.265	0.0	0.0	0.0
263	850	150	493.235	46.022	252.838	0.0	0.0	0.0
265	750	150	2444.422	35.302	269.409	0.0	0.0	0.0
267	200	500	2733.765	21.815	201.566	0.0	0.0	0.0
269	450	650	613.838	15.757	56.919	0.0	0.0	0.0
270	950	250	359.223	28.406	232.058	0.0	0.0	0.0
272	150	550	175.158	15.688	143.645	0.0	0.0	0.0
275	50	375	1125.930	16.056	124.503	0.0	0.0	0.0
277	050	525	1059.831	16.787	98.787	0.0	0.0	0.0
279	965	75	69.011	22.381	172.363	0.0	0.0	0.0
281	650	75	224.076	26.152	171.160	0.0	0.0	0.0
283	350	225	2086.849	33.876	212.065	0.0	0.0	0.0

BETHLEHEM-JA SUBOUTCROP LEVEL

SPECTROGRAPHIC ANALYSIS

(VALUES IN PPM)

SAMP. #	B	SR	TI	IN	V	MO	BA	BIGA	SN
149	0	700	600	50	30	0	600	020	0
152	20	500	1500	50	40	4	500	020	0
155	15	700	1000	50	50	0	400	020	0
157	15	500	2001	50	80	30	300	020	0
160	30	100	500	50	30		1500	020	0
162	60	400	2000	50	50	150	500	020	0
164	20	500	2001	50	80	100	200	020	0
166	0	700	700	50	30	0	500	020	0
169	10	800	2001	50	100	10	600	020	0
172	0	300	700	50	30	0	500	020	0
174	60	100	1000	50	20	400	400	020	0
176	20	400	500	50	15	10	500	020	0
178	15	800	1000	50	50	0	500	020	0
181	10	800	800	50	30	10	400	020	0
183	0	500	1000	50	30	0	600	020	0
184	0	200	500	50	10	40	300	020	0
186	0	700	500	50	20	0	500	020	0
188	0	600	700	50	40	5	500	020	0
190	0	600	1000	50	40	0	500	020	0
193	10	500	1000	50	30	0	500	020	0
196	0	1000	2000	50	50	20	500	020	0
199	10	800	1000	50	50	20	500	020	0
201	20	800	800	50	40	50	500	020	0
203	10	1000	2000	50	30	10	300	020	0
206	10	600	1000	50	20	0	500	020	0
209	0	1000	1000	50	30	15	600	020	0
212	20	1000	2001	50	70	15	500	020	0
214	10	1000	1500	50	60	0	1000	020	0
216	0	1000	700	50	30	0	600	020	0
217	0	700	1000	50	30	0	600	020	0
220	0	1000	1000	50	40	0	700	020	0
223	10	800	800	50	38	5	600	020	0
226	30	800	1000	50	50	0	500	020	0
229	30	600	2000	50	50	15	400	020	0
232	10	1000	1500	50	50	0	600	020	0
234	20	700	1500	50	50	0	500	020	0
237	10	700	1000	50	50	0	600	020	0
240	10	800	2001	50	40	8	400	020	0
243	0	700	1000	50	40	0	500	020	0
245	0	700	1000	50	50	15	400	020	0
248	10	700	600	50	30	0	300	020	0
250	10	400	2001	50	40	15	500	020	0
252	10	900	2000	50	60	0	500	020	0
253	15	700	1000	50	30	0	500	020	0
256	15	600	2000	50	60	10	1500	020	0
259	0	600	1000	50	30	10	400	020	0
261	15	800	1500	50	70	0	500	020	0
263	0	1000	2001	50	80	0	500	020	0
265	0	800	2000	50	50	0	400	020	0
267	20	400	1000	50	40	0	400	020	0
269	10	800	2001	50	60	0	400	020	0
270	10	800	2001	50	60	0	400	020	0
272	20	600	1000	50	40	0	500	020	0
275	0	600	1500	50	50	15	500	020	0
277	0	600	700	50	30	0	600	020	0
279	10	1000	2000	50	60	0	500	020	0
281	0	500	2000	50	50	0	400	020	0
283	0	800	900	50	30	0	400	020	10

BETHLEHEM-JA 2800 LEVEL

ATOMIC ABSORPTION ANALYSIS (HNO3-HClO4 DIGESTION)
(VALUES IN PPM)

SAMP.	#	LOC.	COORD	CU	ZN	MN	AG	NI	PB
150	200	600		985.699	13.329	94.863	0.0	0.0	0.0
153	550	450		3339.367	14.642	108.180	0.0	0.0	0.0
156	600	500		3313.963	13.023	65.304	0.0	0.0	0.0
158	650	450		4460.469	19.526	129.051	0.0	6.154	0.0
160	600	400		19547.449	19.620	357.867	5.567	0.0	0.0
162	450	450		5117.715	11.450	99.178	0.0	0.0	0.0
165	750	450		890.089	27.557	188.107	0.0	6.776	0.0
167	500	500		899.189	8.601	77.717	0.0	2.600	0.0
170	700	400		2056.387	36.377	275.696	0.0	0.0	0.0
172	500	400		3973.669	6.517	54.929	0.0	0.0	0.
174	550	350		5311.582	4.557	200.474	4.606	0.0	0.0
176	650	350		103.444	11.883	130.648	0.0	0.0	0.0
179	700	500		566.357	18.218	92.498	0.0	6.870	0.0
181	400	500		2754.736	13.202	123.633	0.0	0.0	0.0
184	400	400		700.666	5.103	39.525	0.0	0.0	0.0
186	350	450		361.314	12.586	101.003	0.0	0.0	0.0
188	700	300		4953.898	23.316	189.032	0.0	5.221	0.0
191	800	300		936.281	22.508	220.309	0.0	0.0	0.0
194	800	400		231.847	20.156	161.565	0.0	13.114	0.0
197	750	350		9212.871	14.104	107.302	0.0	8.861	0.0
199	750	250		1419.913	33.305	213.640	0.0	8.262	0.0
201	650	250		2403.555	25.278	224.554	0.0	5.781	0.0
204	550	550		129.453	14.497	139.235	0.0	0.0	0.0
207	450	550		674.802	9.840	134.475	0.0	0.0	0.0
210	350	550		2038.765	12.058	187.438	0.0	0.0	0.0
212	700	200		664.644	36.836	347.589	0.0	12.878	0.0
214	800	200		1280.636	31.923	249.638	0.0	7.698	0.0
218	400	600		3144.409	19.812	130.648	0.0	0.0	0.0
221	300	600		2096.329	15.378	102.200	0.0	0.0	0.0
224	300	500		6248.395	13.312	131.260	0.0	3.417	0.0
227	600	600		252.816	22.280	222.593	0.0	10.528	0.0
230	650	550		356.683	20.580	185.846	0.0	4.893	0.0
233	750	550		23.622	18.490	179.815	0.0	6.705	0.0
235	850	350		1583.558	28.416	196.064	0.0	5.551	0.0
238	850	250		2670.732	31.670	264.706	0.0	5.057	0.0
241	350	650		1914.531	16.699	102.499	0.0	0.0	0.0
244	250	650		563.530	17.766	347.232	0.0	0.0	0.0
246	250	550		2096.329	16.890	180.132	0.0	0.0	0.0
248	500	300		223.611	17.931	153.149	0.0	0.0	0.0
250	600	300		3851.349	15.644	122.417	0.0	0.0	0.0
254	800	500		397.143	33.225	401.691	0.0	4.728	0.0
257	500	600		1738.952	19.703	224.882	0.0	0.0	0.0
259	250	450		237.677	28.608	236.709	0.0	0.0	0.0
261	900	200		1580.017	19.313	173.265	0.0	0.0	0.0
263	850	150		493.235	46.022	252.838	0.0	0.0	0.0
266	750	150		573.549	27.937	176.883	0.0	0.0	0.0
267	200	500		2733.765	21.815	201.566	0.0	0.0	0.0
271	950	250		645.205	25.695	159.787	0.0	0.0	0.0
273	150	550		309.216	18.107	124.503	0.0	0.0	0.0
275	50	375		1125.930	16.056	124.503	0.0	0.0	0.0
277	050	525		1059.831	16.787	98.787	0.0	0.0	0.0
279	965	75		69.011	22.381	172.363	0.0	0.0	0.0
281	650	75		224.076	26.152	171.160	0.0	0.0	0.0
283	350	225		2086.849	33.876	212.065	0.0	0.0	0.0

BETHLEHEM-JA 2800 LEVEL

ATOMIC ABSORPTION ANALYSIS (TOTAL DIGESTION)
(VALUES IN WEIGHT %)

SAMP. #			CAO	MGO	FE2O3	NA2O	K2O
150	0	0	3.055	1.126	3.310	3.733	1.441
153	0	0	3.012	0.968	2.207	3.968	1.525
156	0	0	2.444	0.991	6.517	1.178	2.655
158	0	0	3.155	1.655	3.441	3.776	1.205
160	0	0	1.535	0.822	3.931	2.030	6.121
162	0	0	1.748	0.923	2.276	2.602	2.966
165	0	0	2.742	1.880	4.497	3.824	2.147
167	0	0	5.471	0.855	2.276	2.165	0.631
170	0	0	3.126	2.544	4.966	3.896	1.365
172	0	0	1.037	0.349	1.828	3.054	4.002
174	0	0	1.208	0.191	0.897	1.130	4.275
176	0	0	1.208	0.383	1.517	4.089	3.154
179	0	0	1.833	1.362	4.000	2.718	2.495
181	0	0	2.288	0.889	1.979	6.494	1.271
184	0	0	0.782	0.146	0.862	3.276	4.096
186	0	0	2.458	0.720	2.186	6.975	1.761
188	0	0	2.984	1.745	3.524	4.040	1.836
191	0	0	2.842	1.688	3.448	4.089	1.177
194	0	0	2.586	2.645	2.621	6.494	1.789
197	0	0	2.032	1.576	2.600	3.757	3.390
199	0	0	3.652	2.004	4.345	4.040	2.043
201	0	0	2.842	1.418	3.662	3.343	1.620
204	0	0	2.814	1.114	2.931	6.013	1.318
207	0	0	2.814	0.889	2.600	4.618	0.772
210	0	0	2.600	0.923	2.400	3.535	1.789
212	0	0	3.197	2.285	4.214	5.532	1.365
214	0	0	3.481	2.420	4.524	6.013	1.761
218	0	0	2.387	0.687	1.862	3.535	1.742
221	0	0	2.373	1.013	2.586	3.992	1.554
224	0	0	2.174	1.002	1.862	3.896	1.836
227	0	0	4.206	2.330	3.766	7.456	1.365
230	0	0	2.998	1.610	3.579	5.772	1.337
233	0	0	2.941	1.745	3.138	6.494	1.196
235	0	0	2.302	1.936	5.724	3.088	2.618
238	0	0	3.226	2.026	4.317	4.089	1.601
241	0	0	2.799	1.283	3.076	4.570	1.337
244	0	0	3.737	1.216	3.345	3.992	1.620
246	0	0	2.757	1.385	3.193	5.772	1.460
248	0	0	3.169	1.204	2.972	3.968	0.989
250	0	0	2.231	0.923	1.517	3.824	1.930
254	0	0	3.183	2.082	3.586	6.253	1.196
257	0	0	3.012	1.227	2.979	5.051	1.384
259	0	0	3.425	1.193	3.097	3.559	1.224
261	0	0	4.718	1.947	5.586	3.992	1.761
263	0	0	4.050	2.701	5.317	3.848	1.987
266	0	0	2.927	1.891	3.503	4.064	1.365
267	0	0	3.140	1.249	3.386	3.463	2.213
271	0	0	3.069	1.981	4.469	3.848	1.930
273	0	0	2.160	1.249	3.000	6.253	1.940
275	0	0	3.297	0.878	3.379	3.944	1.507
277	0	0	2.757	1.272	3.276	5.291	1.742
279	0	0	3.766	1.936	4.676	6.494	1.290
281	0	0	3.694	2.184	4.828	3.752	1.516
283	0	0	2.757	1.092	3.241	4.089	1.723

BETHLEHEM-JA 2800 LEVEL

SPECTROGRAPHIC ANALYSIS
(VALUES IN PPM)

SAMP. #	B SR	TI	IN	V	MO	BA	BICA	SN
150	0 700	1500	50	50	0 500	020	0	
153	0 700	1000	50	50	15 500	020	0	
156	10 500	2001	50	60	50 500	020	0	
158	10 700	1000	50	50	6 400	020	0	
160	30 100	500	50	30	1500	020	0	
162	60 400	2000	50	50	150 500	020	0	
165	0 600	1000	50	40	0 600	020	0	
167	0 600	1000	50	50	20 700	020	0	
170	101200	2000	50	100	0 700	020	0	
172	0 300	700	50	30	0 500	020	0	
174	60 100	1000	50	20	400 400	020	0	
176	20 400	500	50	15	10 500	020	0	
179	20 500	1000	50	40	7 500	020	0	
181	10 800	800	50	30	10 400	020	0	
184	0 200	500	50	10	40 300	020	0	
186	0 700	500	50	20	0 500	020	0	
188	0 600	700	50	40	5 500	020	0	
191	10 600	1500	50	40	0 400	020	0	
194	0 500	1000	50	50	0 500	020	0	
197	0 400	1500	50	50	30 500	020	0	
199	10 800	1000	50	50	20 500	020	0	
201	20 800	800	50	40	50 500	020	0	
204	0 600	1000	50	30	0 600	020	0	
207	0 800	1000	50	30	0 500	020	0	
210	40 800	1500	50	40	20 500	020	0	
212	201000	2001	50	70	15 500	020	0	
214	101000	1500	50	60	01000	020	0	
218	40 600	1000	50	40	80 500	020	0	
221	0 800	1000	50	30	0 500	020	0	
224	0 700	1000	50	50	20 400	020	0	
227	0 500	1000	50	50	50 400	020	0	
230	101000	2000	50	50	0 400	020	0	
233	20 500	1500	50	50	20 300	020	0	
235	15 700	1500	50	60	0 800	020	0	
238	151000	1500	50	50	0 500	020	0	
241	0 800	2000	50	40	10 400	020	0	
244	15 700	1000	50	50	10 500	020	0	
246	15 500	1000	50	40	20 300	020	0	
248	10 700	600	50	30	0 300	020	0	
250	10 400	2001	50	40	15 500	020	0	
254	10 600	1500	50	40	0 400	020	0	
257	0 800	1500	50	40	0 600	020	0	
259	0 600	1000	50	30	10 400	020	0	
261	15 800	1500	50	70	0 500	020	0	
263	01000	2001	50	80	0 500	020	0	
266	0 800	2000	50	50	8 600	020	0	
267	20 400	1000	50	40	0 400	020	0	
271	0 600	1500	50	50	0 400	020	0	
273	20 600	500	50	30	0 600	020	15	
275	0 600	1500	50	50	15 500	020	0	
277	0 600	700	50	30	0 600	020	0	
279	101000	2000	50	60	0 500	020	0	
281	0 500	2000	50	50	0 400	020	0	
283	0 800	900	50	30	0 400	020	10	

BETHLEHEM-JA 2800 LEVEL

(VALUES IN PPM EXCEPT FOR HG (PPB) AND SIO2 & S (WT.%))

SAMP. #	RB	SR	RB/SR	SIO2	S	HG	CL	F	HEXCL	HEX-P
150	40	639	10863.44	.21	15	384	148	6.3	10.	
153	47	688	6862.38	.76	13	496	280	4.0	8.	
156	70	339	20658.77	6.6	100	352	240	22.	4.7	
158	38	658	5862.47	2.22	98	608	336	20.	3.2	
160	141	100	141052.89	2.74	128	368	412	3.	5.6	
162	90	392	23062.33	1.0	38	640	296	16.	10.1	
165	58	620	9460.64	.23	60	480	396	19.	6.2	
167	28	653	4361.04	.25	35	432	156	5.6	7.	
170	40	762	5260.97	.82	27	384	328	19.	6.3	
172	84	242	34768.34	.56	84	168	128	3.	30.	
174	85	115	73973.88	.60	53	32	64	2.7	10.	
176	76	372	20469.76	.02	2					
179	70	476	14763.42	1.77	1	200	116	5.1	9.	
181	37	751	4964.82	.42	1	240	140	2.8	6.	
184	91	216	42164.62	.17	176	384	72	4.0	10.	
186	58	829	7067.04	.05	190	320	128	20.	7.4	
188	53	755	7063.13	.50	1	352	280	34.3	5.	
191	39	860	4563.25	.09	1	480	284	14.0	6.	
194	55	536	10357.60	.12	6	512	296	4.2	7.1	
197	86	662	13061.68	1.17	7	368	256	3.8	5.	
199	45	803	5660.21	.27	9	256	240	5.7	5.8	
201	74	576	12860.99	.24	12	352	288	4.6	6.5	
204	34	735	4664.05	.21	6	280	260	12.	3.	
207	27	932	2963.65	.11	5	340	256	4.4	12.	
210	61	586	10460.42	.50	5	416	180	16.2	10.	
212	42	756	5657.86	.1	7	160	360	3.6	12.0	
214	55	892	6258.41	.21	5	368	256	3.6	6.0	
218	57	520	11060.95	1.57	17	172	472	16.0	3.5	
221	43	805	5362.94	.82	1	180	388	3.8	5.	
224	56	627	8962.87	.56	1	168	372	4.1	7.2	
227	56	511	11056.62	1.34	12	196	192	6.	8.5	
230	37	730	4963.14	.22	1	188	452	7.	11.	
233	45	546	8261.07	.01	1	196	460	3.8	11.1	
235	66	488	13563.82	.91	8	220	204	8.	8.5	
238	43	639	6761.4	.24	7	196	360	5.	8.4	
241	37	746	5064.17	.56	7	200	92	7.6	9.	
244	32	600	5358.15	.1	8	180	260	2.8	7.0	
246	43	559	7762.94	.33	10	196	252	11.0	12.	
24"	33	691	4861.53	.66	15	156	336	3.	6.6	
250	48	553	8764.63	.22	1	168	360	11.0	9.	
254	39	677	5863.81	.01	4	212	76	4.7	11.0	
257	36	780	4662.86	.51	1	216	44	3.6	4.4	
259	32	654	5062.84	.19	22	224	172	14.0	6.2	
261	51	663	7755.94	.37	1	260	208	6.8	8.6	
263	45	725	6259.06	.07	7	182	344	3.3	9.2	
271	56	643	8764.54	.12	2	216	120	5.6	8.5	
273	56	717	7864.36	.04	5	176	272	3.8	9.0	
275	37	739	5062.82	.14	8	180	324	1.7	6.2	
277	48	769	6264.79	.03	1	228	40	4.3	7.4	
279	37	883	4260.18	.01	1	224	68	1.6	5.6	
281	47	562	8461.54	.02	1	240	384	15.0	4.9	
283	44	768	8766.05	.19	1	184	256	4.6	6.2	

BETHLEHEM-JA 2400 LEVEL

ATOMIC ABSORPTION ANALYSIS (HNO₃-HClO₄ DIGESTION)

(VALUES IN PPM)

SAMP.	#	LOC.COORD	CU	ZN	MN	AG	NI	PB
151	200	600	727.165	24.427	173.045	0.0	0.0	0.0
154	550	450	5400.781	15.506	113.540	0.0	0.0	0.0
159	650	450	5057.133	24.744	204.737	0.0	7.088	0.0
163	450	450	4675.551	16.710	15.362	0.0	0.0	0.0
168	500	500	2976.465	14.756	101.506	0.0	1.374	0.0
171	700	400	2307.012	15.914	127.696	0.0	0.0	0.0
173	500	400	6850.141	6.002	182.486	1.162	0.0	0.0
175	550	350	6172.984	7.253	92.945	0.0	0.0	0.0
177	650	350	212.518	9.595	83.159	0.0	0.0	0.0
180	700	500	169.646	15.565	117.562	0.0	18.862	0.0
182	400	500	3372.431	18.263	90.269	0.0	3.253	0.0
185	400	400	1133.037	8.626	143.241	0.0	0.0	0.0
187	350	450	148.990	10.583	114.537	0.0	0.0	0.0
189	700	300	4923.797	20.313	183.304	0.0	0.0	0.0
192	800	300	4282.523	24.389	199.272	0.0	6.870	0.0
195	800	400	845.344	19.117	164.380	0.0	8.728	0.0
198	750	350	1928.842	26.797	190.946	0.0	6.210	0.0
200	750	250	3546.295	24.644	196.705	0.0	8.628	0.0
202	650	250	1663.475	19.147	115.141	0.0	0.0	0.0
205	550	550	826.200	11.163	86.117	0.0	0.0	0.0
208	450	550	1302.155	8.651	72.561	0.0	0.0	0.0
211	350	550	1165.238	12.627	94.135	0.0	0.0	0.0
213	700	200	963.617	7.253	135.702	0.0	0.0	0.0
215	800	200	2236.109	32.649	258.323	0.0	9.027	0.0
219	400	600	3742.283	14.146	82.272	0.0	0.0	0.0
222	300	600	1850.313	13.133	116.957	0.0	0.0	0.0
225	300	500	4144.883	9.428	139.543	0.0	0.0	0.0
228	600	600	191.930	24.440	218.679	0.0	9.310	0.0
231	650	550	930.627	21.008	160.783	0.0	6.210	0.0
236	850	350	894.822	36.687	400.762	0.0	8.861	0.0
239	850	250	2357.317	30.938	213.153	0.0	5.057	0.0
242	350	650	1243.653	17.483	123.026	0.0	0.0	0.0
247	250	550	3505.272	12.804	131.872	0.0	0.0	0.0
249	500	300	194.792	23.616	248.972	0.0	0.0	0.0
251	600	300	3726.749	18.597	182.668	0.0	0.0	0.0
255	800	500	70.516	23.816	197.186	0.0	4.728	0.
258	500	600	2091.526	17.393	135.855	0.0	0.0	0.0
260	250	450	398.575	19.147	135.855	0.0	0.0	0.0
262	900	200	902.378	22.889	158.595	0.0	0.0	0.0
264	850	150	2352.045	9.822	90.278	0.0	0.0	0.0
268	200	500	1300.885	10.550	86.749	0.0	0.0	0.0
274	150	550	3162.533	27.866	221.243	0.0	0.0	0.0
276	50	375	961.462	23.257	212.995	0.0	0.0	0.0
278	50	525	193.880	13.298	92.967	0.0	0.0	0.0
280	965	75	345.656	27.480	195.428	0.0	0.0	0.0
282	650	75	584.937	8.301	84.496	0.0	0.0	0.0
284	350	225	142.139	7.634	90.419	0.0	0.0	0.0

BETHLEHEM-JA 2400 LEVEL
SPECTROGRAPHIC ANALYSIS
(VALUES IN PPM)

SAMP. #	B SR	TI	IN	V	MO	BA	BIGA	SN
151	0 700	700	50	30	0 700	020	0	
154	0 800	800	50	30	8 600	020	0	
159	0 600	1000	50	60	10 500	020	0	
163	10 600	700	50	30	1001000	020	0	
168	0 800	1000	50	40	0 600	020	0	
171	101000	2000	50	40	300 400	020	0	
173	50 400	1000	50	50	200 400	020	0	
175	30 200	800	50	20	200 500	020	0	
177	10 400	600	50	20	0 500	020	0	
180	201500	1500	50	500	0 100	020	0	
182	0 800	700	50	30	10 600	020	0	
185	10 200	600	50	30	0 400	020	0	
187	10 700	600	50	30	0 400	020	0	
189	10 500	1000	50	40	50 200	020	0	
192	01000	1000	50	50	7 600	020	0	
195	0 700	2000	50	60	0 500	020	0	
198	01000	2000	50	50	10 500	020	0	
200	15 700	2000	50	40	0 200	020	0	
202	0 700	1000	50	30	0 600	020	0	
205	10 800	1000	50	30	15 500	020	0	
208	101500	1000	50	40	01000	020	0	
211	01500	2000	50	50	0 500	020	0	
213	50 200	1000	50	20	50 400	020	0	
215	151000	800	50	40	0 500	020	0	
219	20 400	1500	50	50	40 500	020	0	
222	50 500	1500	50	40	800 500	020	0	
225	20 500	200	50	30	20 500	020	0	
228	15 800	2000	50	50	0 400	020	0	
231	101000	1500	50	50	0 500	020	0	
236	20 800	2001	50	70	30 100	020	0	
239	01000	2001	50	70	30 400	020	0	
242	0 700	500	50	30	10 400	020	0	
247	20 900	2001	50	50	20 400	020	0	
249	10 400	1000	50	30	8 400	020	0	
251	10 400	600	50	20	0 500	020	0	
255	0 700	800	50	30	4 400	020	0	
258	0 800	1000	50	30	0 500	020	0	
260	01000	1500	50	40	8 500	020	0	
262	01000	2001	50	50	0 500	020	0	
264	151000	2000	50	60	8 500	020	0	
268	0 800	1500	50	40	8 600	020	0	
274	15 600	1500	50	50	10 400	020	0	
276	0 700	1000	50	30	15 500	020	0	
278	0 600	1000	50	30	5 500	020	0	
280	101200	2000	50	50	0 500	020	0	
282	10 150	700	50	10	0 300	020	0	
284	15 200	600	50	10	5 300	020	5	

APPENDIX B

Valley Copper

(Sample locations and analytical results)

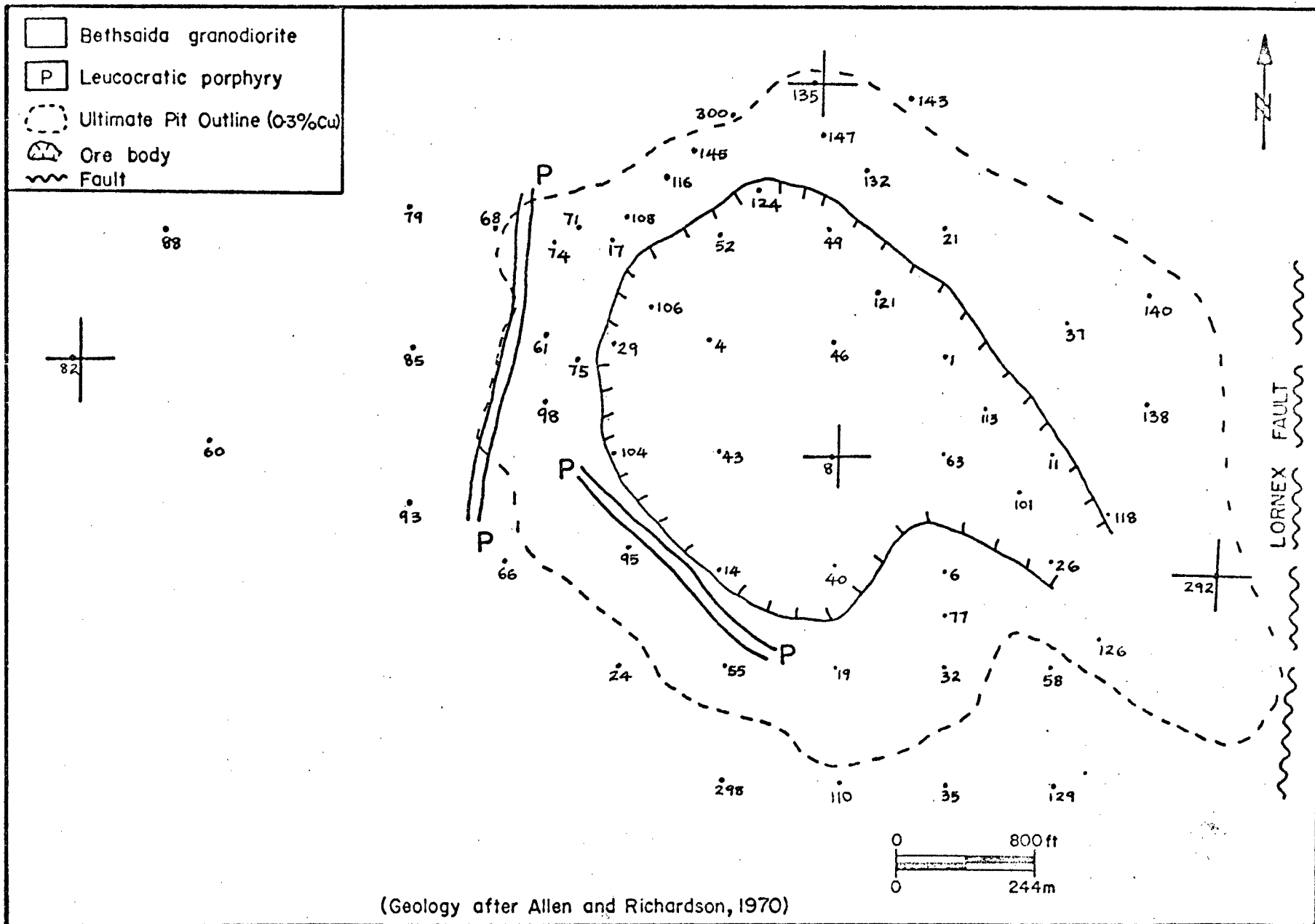


FIGURE 80: Location of samples, Valley Copper Suboutcrop Level

VALLEY COPPER SUBOUTCROP LEVEL

ATOMIC ABSORPTION ANALYSIS (HNO3-HClO4 DIGESTION)
(VALUES IN PPM)

SAMP.	#	LOC.COORD	CU	ZN	MN	AG	NI	PB
1	375	212	5404.191	41.337	493.321	1.308	1.003	0.0
4	285	218	3568.929	12.443	202.550	0.844	0.617	0.0
6	375	131	3424.768	11.441	278.611	0.0	0.0	0.0
8	333	175	829.821	17.405	161.065	0.0	0.0	0.0
11	415	175	1529.498	26.601	203.739	0.452	0.0	0.0
14	290	131	2122.148	16.004	201.362	1.060	0.0	0.0
17	250	257	3117.681	20.009	213.672	0.0	0.0	0.0
19	333	95	1389.874	17.981	74.271	0.0	0.0	0.0
21	375	260	5564.070	10.356	53.770	1.329	0.0	0.0
24	251	95	2214.659	14.606	964.061	0.0	0.0	0.0
26	415	135	2022.325	27.067	235.323	0.0	0.0	0.0
29	250	217	7350.621	26.359	288.146	2.699	0.0	0.0
32	375	95	1765.783	18.693	166.877	0.0	0.0	0.0
35	375	50	699.095	24.536	158.746	0.0	0.0	0.0
37	420	225	6522.184	19.101	268.717	0.0	0.0	0.0
40	333	134	4804.105	37.709	120.346	0.0	0.0	0.0
43	290	175	5099.324	15.416	154.502	1.208	0.0	0.0
46	333	217	4478.520	14.227	81.282	0.080	0.0	0.0
49	330	260	4792.617	14.575	73.167	0.0	0.0	0.0
52	290	257	2447.569	11.570	300.241	0.0	0.0	0.0
55	292	95	2004.448	21.236	311.999	0.0	0.0	0.0
58	415	95	1347.661	16.976	147.196	0.0	0.0	0.0
60	100	180	54.337	26.230	286.069	0.0	0.0	0.0
61	225	220	2724.894	9.919	151.037	0.603	0.0	0.0
63	375	175	6646.320	12.663	161.453	1.270	0.0	0.0
66	210	135	1542.012	11.153	138.009	0.0	0.0	0.0
68	207	260	2147.808	17.437	370.903	0.0	0.0	0.0
71	237	260	2261.061	17.756	282.751	1.518	0.0	0.0
74	228	255	3862.698	5.785	132.292	0.0	0.0	0.0
75	236	211	2767.040	20.729	200.571	0.0	0.0	0.0
77	375	115	2158.081	35.899	238.150	0.0	0.0	0.0
79	174	268	359.896	34.630	348.179	0.0	0.0	0.0
82	50	212	11.278	24.788	264.405	0.0	0.0	0.0
85	175	215	45.865	28.012	356.369	0.0	0.0	0.0
88	84	260	151.450	24.860	197.015	0.0	0.0	0.0
93	174	156	1247.331	18.812	183.187	0.0	0.0	0.0
95	255	140	3631.027	10.780	292.916	1.179	0.0	0.0
98	225	195	2154.846	16.724	207.586	0.0	0.0	0.0
101	402	160	7406.465	24.393	233.459	0.658	0.0	0.0
104	250	175	1019.937	14.428	235.272	0.0	0.0	0.0
106	265	230	4173.414	14.971	242.545	0.0	0.0	0.0
108	255	265	4311.160	21.889	249.119	0.0	0.0	0.0
110	334	51	3036.520	14.642	237.086	0.0	0.0	0.0
113	390	193	2370.130	25.393	223.706	0.0	0.0	0.0
116	270	280	1714.048	24.393	337.980	0.0	0.0	0.0
118	435	152	7005.930	14.300	279.424	0.0	0.0	0.0
121	350	237	5195.066	18.781	138.911	0.0	0.0	0.0
124	305	275	1898.817	24.444	213.656	0.0	0.0	0.0
126	432	105	2986.460	3.732	391.586	0.536	0.0	0.0
129	427	55	538.624	11.248	306.907	0.0	0.0	0.0
132	345	282	2219.927	14.957	137.547	0.0	0.0	0.0
135	327	315	3415.737	22.861	285.031	0.0	0.0	0.0
138	450	194	3723.940	23.799	272.721	0.0	0.0	0.0
140	450	235	6903.949	33.801	357.867	0.901	0.0	0.0
143	362	310	6627.395	15.101	291.788	4.944	0.0	0.0
145	280	290	2336.121	23.900	266.047	0.0	0.0	0.0
147	327	296	3124.426	23.395	308.047	0.0	0.0	0.0
292	475	130	6159.180	16.632	323.104	0.0	0.0	
295	415	50	10941.070	21.301	192.675	0.0	0.0	
298	290	52	1537.919	25.041	359.518	0.0	0.0	
300	292	310	2062.914	27.928	385.779	0.0	0.0	

VALLEY COPPER SUBOUTCROP LEVEL

SPECTROGRAPHIC ANALYSIS

(VALUES IN PPM)

SAMP. #	B	SR	TI	IN	V	MO	BA	BIGA	SN
1	15	150	1000	50	50	10	500	020	0
4	10	200	1500	50	30	10	400	020	0
6	10	1500	2000	50	30	10	500	020	0
8	0	500	600	50	20	0	500	020	0
11	0	500	500	50	20	0	700	020	0
14	10	400	1000	50	30	0	800	020	0
17	10	400	1000	50	40	5	700	020	0
19	0	600	700	50	20	0	1000	020	0
21	0	300	1000	50	30	5	600	020	0
24	15	300	1500	50	40	10	500	020	0
26	0	500	2000	50	30	0	700	020	0
29	15	200	2000	50	40	15	500	020	0
32	10	500	1000	50	20	0	500	020	0
35	0	800	700	50	20	0	500	020	0
37	0	300	800	50	40	4	600	020	0
40	0	300	1000	50	30	0	700	020	0
43	0	300	500	50	20	0	500	020	0
46	0	300	500	50	20	10	500	020	0
49	10	400	1000	50	30	20	500	020	0
52	20	400	1000	50	50	0	500	020	0
55	10	200	1000	50	30	0	400	020	0
58	0	700	1500	50	20	0	1000	020	0
60	0	700	800	50	20	0	600	020	0
61	20	400	800	50	30	5	600	020	0
63	15	300	1000	50	40	60	500	020	0
66	0	300	800	50	15	100	500	020	0
68	20	300	2001	50	30	80	600	020	0
71	10	400	800	50	20	400	500	020	0
74	20	300	1500	50	30	20	800	020	0
75	10	500	800	50	30	0	800	020	0
77	0	500	1500	50	30	0	1000	020	0
79	0	700	500	50	20	4	700	020	0
82	0	800	500	50	20	0	700	020	0
85	0	500	1000	50	20	0	800	020	0
88	0	500	700	50	20	0	500	020	0
93	10	500	700	50	20	30	500	020	0
95	10	400	800	50	30	4	500	020	0
98	0	500	700	50	20	0	800	020	0
101	0	400	2001	50	50	40	600	020	0
104	0	400	500	50	20	0	500	020	0
106	0	400	1000	50	40	0	500	020	0
108	0	500	1000	50	30	0	700	020	0
110	20	300	1500	50	30	0	600	020	0
113	0	500	1000	50	40	0	600	020	0
116	15	400	500	50	20	5	500	020	0
118	10	300	2000	50	40	0	500	020	0
121	10	200	500	50	30	5	500	020	0
124	10	500	500	50	20	0	500	020	0
126	20	200	2001	50	30	40	200	020	0
129	20	300	1000	50	30	0	400	020	0
132	0	400	700	50	30	10	500	020	0
135	0	400	2000	50	40	8	600	020	0
138	0	1500	1000	50	40	8	500	020	0
140	0	400	800	50	30	150	500	020	0
143	15	1000	600	50	30	100	400	020	0
145	0	500	700	50	30	6	700	020	0
147	0	400	700	50	30	0	600	020	0
292	10	500	1000	50	30	15	400	020	0
295	10	400	1000	50	40	30	600	020	0
298	20	400	1000	50	30	20	1000	020	0
300	0	500	2000	50	30	10	500	020	0

VALLEY COPPER 3600 LEVEL

ATOMIC ABSORPTION ANALYSIS (HNO₃-HClO₄ DIGESTION)
(VALUES IN PPM)

SAMP.	#	LOC.COORD	CU	ZN	MN	AG	NI	PB
2	375	212	4795.492	16.392	340.455	1.194	0.0	0.0
5	285	218	4168.574	5.393	217.663	0.852	0.0	0.0
7	375	131	2442.377	15.632	147.196	0.0	0.0	0.0
9	333	175	3934.639	4.336	32.784	0.592	0.0	0.0
12	415	175	4179.773	14.303	231.696	0.428	0.0	0.0
15	290	131	8915.070	17.008	141.065	1.654	0.0	0.0
18	250	257	8672.949	15.232	201.757	0.847	0.0	0.0
20	333	95	4879.008	5.995	145.086	0.656	0.0	0.0
22	375	260	3160.536	22.837	201.757	0.509	0.0	0.0
25	251	95	1454.594	16.379	131.531	0.0	0.0	0.0
27	415	135	3016.187	23.451	162.807	0.080	0.0	0.0
30	250	217	2250.734	19.959	203.739	0.0	0.0	0.0
33	375	95	3533.487	8.477	193.859	0.0	0.0	0.0
36	375	50	1780.947	20.209	226.069	0.0	0.0	0.0
38	420	225	6159.813	13.403	120.912	0.375	0.0	0.0
41	333	134	1574.561	15.833	108.478	0.0	0.0	0.0
44	290	175	4672.180	16.473	156.816	0.0	0.0	0.0
47	333	217	3176.616	10.639	99.117	0.0	0.0	0.0
50	330	260	3533.487	17.532	128.111	0.107	0.0	0.0
53	290	257	3929.087	17.804	167.266	0.0	0.0	0.0
56	292	95	6374.113	13.313	144.511	0.0	0.0	0.0
59	415	95	454.177	20.864	171.151	0.0	0.0	0.0
62	225	220	2952.335	10.427	153.346	0.0	0.0	0.0
64	375	175	4095.922	25.981	88.692	2.291	0.0	0.0
67	210	135	435.083	19.545	335.325	0.0	0.0	0.0
69	207	260	2656.572	17.724	471.050	0.0	0.0	0.0
72	237	260	4297.684	18.693	248.686	0.0	0.0	0.0
76	236	211	956.369	10.639	212.876	0.0	0.0	0.0
78	375	115	2489.233	13.671	112.991	0.0	0.0	0.0
80	174	268	112.783	24.232	282.336	0.0	0.0	0.0
83	50	212	81.165	17.024	609.589	0.0	0.0	0.0
86	175	215	67.711	28.875	298.569	0.0	0.0	0.0
89	84	260	10.955	31.594	430.566	0.450	0.0	0.0
91	100	180	926.470	3.886	527.682	0.0	0.0	0.0
94	174	156	1145.979	30.955	246.925	0.0	0.0	0.0
96	255	140	449.402	24.138	244.004	1.057	0.0	0.0
99	225	195	2856.825	19.840	262.720	0.637	0.0	0.0
102	402	160	3900.533	126.356	156.575	1.528	0.0	0.0
105	250	175	4551.625	11.221	124.652	0.0	0.0	0.0
107	265	230	4783.902	16.016	202.960	0.0	0.0	0.0
109	255	265	1582.364	10.581	423.182	0.0	0.0	0.0
111	334	51	6951.875	1031.626	322.942	0.0	0.0	5.730
114	390	193	5727.238	11.369	155.022	3.034	0.0	0.0
117	270	280	409.435	35.459	452.094	0.0	0.0	0.0
119	435	152	4157.574	22.595	273.836	0.502	0.0	0.0
122	350	237	3061.598	148.565	263.459	0.0	0.0	0.0
125	305	275	4183.988	15.826	238.540	0.0	0.0	0.0
127	432	105	3879.675	9.530	282.412	1.318	0.0	0.0
130	427	55	396.049	9.987	246.925	0.936	0.0	0.0
133	345	282	3682.602	17.849	352.383	0.0	0.0	0.0
136	327	315	2774.952	16.680	206.161	0.849	0.0	0.0
138	450	194	3723.940	23.799	272.721	0.0	0.0	0.0
141	450	235	958.333	93.349	609.424	0.0	0.0	0.0
143	362	310	6627.395	15.101	291.788	4.944	0.0	0.0
146	280	290	2394.440	22.299	611.269	0.0	0.0	0.0
293	475	130	3801.205	34.554	499.842	0.0	0.0	0.0
296	415	50	306.953	19.425	296.892	0.0	0.0	0.0
299	290	52	1702.081	19.254	174.170	0.0	0.0	0.0
301	292	310	897.856	27.341	420.536	0.0	0.0	0.0

VALLEY COPPER 3600 LEVEL

ATOMIC ABSORPTION ANALYSIS (TOTAL DIGESTION)
(VALUES IN WEIGHT %)

SAMP. #			CAO	MGO	FE2O3	NA2O	K2O
2	0	0	1.066	0.383	1.655	1.914	3.955
5	0	0	2.202	0.428	1.655	1.352	3.343
7	0	0	1.336	0.371	1.241	3.175	2.401
9	0	0	0.469	0.248	1.103	2.237	3.719
12	0	0	1.634	0.428	2.207	2.165	3.249
15	0	0	1.307	0.371	1.793	1.539	3.013
18	0	0	1.591	0.462	2.207	2.357	2.872
20	0	0	1.563	0.304	1.310	2.405	2.354
22	0	0	1.805	0.675	2.407	3.415	2.646
25	0	0	1.052	0.428	1.517	4.906	2.024
27	0	0	1.734	0.473	1.724	3.535	2.363
30	0	0	1.890	0.405	1.586	3.127	2.345
33	0	0	1.620	0.270	1.241	2.492	2.599
36	0	0	1.876	0.315	1.028	3.583	2.213
38	0	0	1.151	0.304	1.862	2.453	2.024
41	0	0	0.767	0.332	0.897	3.583	1.648
44	0	0	1.023	0.371	1.724	2.386	3.183
47	0	0	1.037	0.281	1.379	2.116	3.861
50	0	0	0.668	0.562	1.931	2.646	3.531
53	0	0	1.606	0.416	2.207	2.049	2.693
56	0	0	1.350	0.439	1.793	1.861	3.154
59	0	0	1.947	0.371	1.103	3.175	1.460
62	0	0	2.032	0.315	1.517	2.958	2.401
64	0	0	0.554	0.295	1.483	0.322	2.806
67	0	0	2.202	0.360	1.793	3.896	2.213
69	0	0	3.638	0.409	1.862	2.973	1.911
72	0	0	1.847	0.439	2.414	2.391	3.305
76	0	0	1.876	0.464	2.345	3.511	2.175
78	0	0	1.321	0.405	1.172	2.694	2.589
80	0	0	2.629	0.360	1.586	4.906	1.761
83	0	0	4.419	0.585	1.103	0.202	2.335
86	0	0	2.188	0.270	1.862	4.570	2.147
89	0	0	2.657	0.518	1.862	4.570	1.864
91	0	0	2.316	0.392	1.931	3.896	2.024
94	0	0	2.103	0.462	1.207	0.890	3.908
96	0	0	1.847	0.422	1.931	4.666	1.742
99	0	0	1.918	0.411	2.207	3.131	3.154
102	0	0	1.137	0.360	1.517	2.621	3.644
105	0	0	1.137	0.360	1.517	2.621	3.644
107	0	0	2.245	0.377	1.828	1.756	3.089
109	0	0	2.771	0.428	2.138	1.914	3.390
111	0	0	2.018	0.563	2.483	1.318	4.218
114	0	0	0.952	0.326	1.793	1.669	3.004
117	0	0	2.629	0.822	3.310	3.824	2.260
119	0	0	2.018	0.529	2.276	2.742	3.296
122	0	0	2.501	0.490	2.483	2.405	3.625
125	0	0	1.705	0.540	2.345	1.785	3.719
127	0	0	2.984	0.433	1.897	1.299	3.089
130	0	0	2.359	0.280	1.103	2.573	1.902
133	0	0	2.018	0.360	1.793	4.089	1.911
136	0	0	3.169	0.473	2.345	3.040	3.041
138	0	0	2.700	0.546	2.669	2.650	4.218
141	0	0	2.771	0.552	2.834	2.453	2.806
143	0	0	3.979	0.231	1.483	1.231	2.448
146	0	0	2.487	0.523	2.359	3.415	3.220
293	0	0	2.998	0.439	2.586	2.650	3.315
296	0	0	2.416	0.371	1.207	3.088	2.637
299	0	0	1.805	0.473	1.724	6.975	1.648
301	0	0	1.762	0.585	2.690	3.656	3.060

VALLEY COPPER 3600 LEVEL

SPECTROGRAPHIC ANALYSIS

(VALUES IN PPM)

SAMP. #	B SR	TI	IN	V	MO	BA	BIGA	SN
2	0 300	1000	50	20	0 400	020	0	
5	102001	1000	50	50	0 400	020	0	
7	0 400	2000	50	20	20 500	020	0	
9	0 300	1000	50	20	40 400	020	0	
12	15 300	1000	50	30	0 600	020	0	
15	10 600	1000	50	40	0 800	020	0	
18	101000	1000	50	40	0 500	020	0	
20	0 200	800	50	30	0 400	020	0	
22	0 500	700	50	20	5 500	020	0	
25	0 600	800	50	15	20 500	020	0	
27	0 500	1500	50	30	15 500	020	0	
30	10 500	2000	50	30	0 500	020	0	
33	10 500	1000	50	40	0 400	020	0	
36	0 500	700	50	20	0 700	020	0	
38	0 300	500	50	20	50 500	020	0	
41	0 400	1000	50	15	4 500	020	0	
44	0 500	1000	50	40	10 500	020	0	
47	0 300	600	50	20	0 400	020	0	
50	0 400	1000	50	40	0 500	020	0	
53	10 500	2000	50	50	0 500	020	0	
56	10 400	1000	50	40	0 500	020	0	
59	0 800	1500	50	20	5 600	020	0	
62	20 400	800	50	20	15 600	020	0	
64	20 150	2000	50	50	100 500	020	0	
67	10 400	900	50	20	5 600	020	0	
69	0 400	1500	50	30	40 600	020	0	
72	01500	1000	50	30	200 500	020	0	
76	15 400	800	50	30	5 800	020	0	
78	0 500	700	50	20	0 800	020	0	
80	0 600	800	50	20	0 500	020	0	
83	60 500	1000	50	30	0 500	020	0	
86	0 700	1000	50	20	0 700	020	0	
89	01500	700	50	20	0 600	020	0	
91	10 700	800	50	20	0 500	020	0	
94	0 600	1000	50	20	30 600	020	0	
96	0 800	1000	50	30	0 500	020	0	
99	102001	1000	50	30	5 600	020	0	
102	10 300	600	50	20	0 500	020	0	
105	0 800	800	50	30	0 500	020	0	
107	0 900	1000	50	30	0 600	020	0	
109	15 400	1000	50	30	20 700	020	0	
111	15 300	1000	50	50	0 700	020	0	
114	10 400	800	50	30	20 500	020	0	
117	01000	1000	50	30	10 600	020	0	
119	01500	500	50	30	40 600	020	0	
122	10 200	1000	50	30	20 400	020	0	
125	0 300	2000	50	40	30 500	020	0	
127	20 800	1000	50	30	151000	020	0	
130	20 400	1000	50	30	0 600	020	0	
133	10 300	700	50	40	4 500	020	0	
136	01000	1000	50	50	15 600	020	0	
138	01500	1000	50	40	8 500	020	0	
141	10 400	2001	50	30	40 500	020	0	
143	151000	600	50	30	100 400	020	0	
146	0 500	800	50	40	0 700	020	0	
293	0 600	700	50	30	5 400	020	0	
296	10 500	1000	50	30	0 400	020	0	
299	01000	700	50	20	101000	020	0	
301	20 500	2001	50	50	20 800	020	0	

VALLEY COPPER 3600 LEVEL

(VALUES IN PPM EXCEPT FOR HG (PPE) AND SIO2 & S (WT.%))

SAMP. #	RB	SR	RB/SR	SIO2	S	HG	CL	F	HEXCL	HEX-F
2	73	328	22267.37	.27	1	490	409	10.7	11.0	
5	69	2223	3166.8	.31	1	256	440	2.3	10.0	
7	47	501	9372.8	.21	1	220	616	2.2	9.0	
9	67	369	18173.94	.46	2	312	460	4.2	5.2	
12	65	269	24164.23	.47	5	228	406	4.7	10.5	
15	62	72	86166.17	.39	1	344	412	2.2	10.3	
18	69	883	7865.69	.84	1	220	288	1.5	7.3	
20	61	483	12666.71	.23	1	232	694	7.2	8.1	
22	59	625	9466.96	.17	6	240	304	3.1	9.8	
25	50	729	6968.93	.12	7	260	348	7.0	6.2	
27	45	581	7771.39	.13	1	196	240	3.0	6.0	
30	59	496	11967.44	.12	2	190	540	2.6	7.0	
33	50	443	11370.80	.21	1	220	436	2.2	5.1	
36	53	580	9167.93	.17	10	224	212	2.0	6.2	
38	62	334	18668.33	.27	10	364	480	1.4	2.5	
41	44	496	8975.44	.10	1	320	324	2.3	4.6	
44	70	681	10371.47	.26	1	296	408	2.6	5.6	
47	72	342	2175.06	.32	1	480	436	2.5	6.3	
50	82	440	18669.69	.12	1	276	328	1.6	2.8	
53	71	627	11365.92	.30	1	224	312	1.9	5.8	
56	61	346	17668.28	.28	7	172	236	3.5	4.5	
59	34	800	4271.41	.05	3	460	292	1.7	3.7	
62	63	495	12765.96	.38	5	280	306	3.2	5.4	
64	76	161	47270.43	.40	22	396	360	2.7	2.7	
67	52	549	9565.44	.06	6	316	236	6.3	6.0	
69	64	432	14862.26	.36	5	220	348	5.6	6.8	
72	72	1680	4364.89	1.17	46	222	318	7.1	8.2	
75	52	585	8965.55	.47	1	320	272	5.4	7.8	
78	41	542	7674.61	.33	2	225	528	5.6	5.3	
80	43	839	5165.00	.02	1	220	152	1.8	4.3	
83	87	464	18663.17	.03	7	280	376	1.2	4.1	
86	62	715	8765.46	.04	1	296	312	5.3	5.0	
89	45	1460	3166.68	.09	1	270	264	2.3	6.5	
91	52	675	7763.57	.16	11	320	336	7.2	6.4	
94	49	741	6668.15	.17	7	376	220	1.4	7.4	
96	39	1031	3865.95	.04	4	340	328	1.8	5.2	
99	55	2402	2364.23	.28	12	141	600	1.9	4.8	
105	58	883	6671.47	.23	4	68	408	1.8	4.3	
107	65	871	7566.72	.20	1	232	600	1.4	4.1	
109	82	462	17761.76	.20	1	208	285	3.2	4.1	
111	77	278	27763.72	.28	1	264	408	1.2	3.9	
114	55	272	20274.62	.57	1	216	404	1.2	4.8	
117	48	908	5368.51	.04	2	204	700	1.2	6.2	
119	59	1471	4062.77	.20	7	196	448	1.2	3.5	
122	78	199	39269.75	.36	26	220	660	1.6	3.6	
125	76	279	27267.25	.36	7	192	564	1.0	6.	
127	60	900	6761.18	.10	1	175	452	2.0	5.	
130	48	393	12271.09	.11	1	168	472	1.4	5.8	
133	75	276	27163.15	.44	1	212	252	3.6	5.2	
136	61	893	6860.88	2.63	1	200	700	1.0	1.5	
138	70	1386	5159.07	1.89	1	210	653	1.1	1.8	
141	70	377	18660.12	.33	5	212	624	2.4	4.0	
143	59	759	7871.74	1.07	1	152	460	1.0	3.5	
146	71	624	11362.01	.99	1	181	725	1.3	3.7	
293	61	681	9057.98	.24	1	176	604	1.0	4.2	
296	58	681	8566.36	.18	6	326	270	2.5	4.5	
299	36	765	4769.89	.16	1	200	265	1.8	4.6	
301	70	423	16562.48	.18	5	176	700	1.3	6.0	

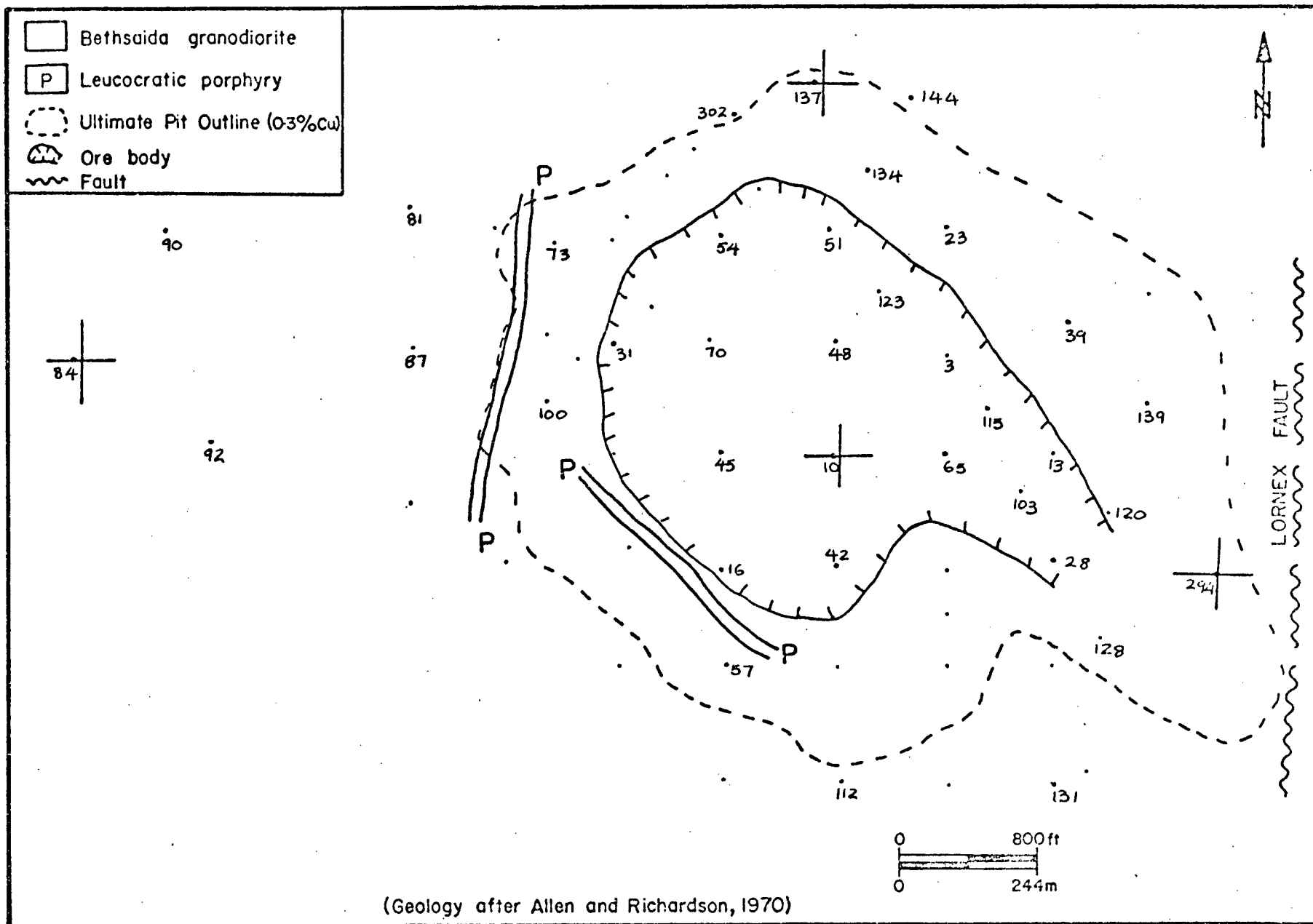


FIGURE 82: Location of samples, Valley Copper 3300 Level.

VALLEY COPPER 3300 LEVEL

ATOMIC ABSORPTION ANALYSIS (HNO₃-HClO₄ DIGESTION)

(VALUES IN PPM)

SAMP.	#	LOC.COORD	CU	ZN	MN	AG	NI	PB
3	375	212	5257.129	14.454	185.996	0.901	1.505	0.0
10	333	275	2819.834	11.874	172.318	0.294	0.0	0.0
13	415	175	3940.172	20.948	205.323	0.683	0.0	0.0
16	290	131	3807.497	16.191	132.673	0.0	0.0	0.0
23	375	260	1046.838	17.580	180.903	0.844	0.0	0.0
28	415	135	5842.004	5.315	192.677	0.616	0.0	0.0
31	250	217	4154.602	24.143	190.316	0.0	0.0	0.0
34	375	95	225.977	11.039	232.502	0.0	0.0	0.0
39	420	225	3101.618	18.255	207.705	0.0	0.0	0.0
42	333	134	665.327	8.641	227.675	0.0	0.0	0.0
45	290	175	4646.469	25.678	231.696	0.267	0.0	0.0
48	333	217	7605.289	14.682	109.230	0.987	0.0	0.0
51	330	260	3489.944	4.953	311.578	1.208	0.0	0.0
54	290	257	4068.029	17.756	182.274	0.0	0.0	0.0
57	292	95	3354.378	20.009	163.389	0.281	0.0	0.0
65	375	175	1029.696	19.512	151.037	0.214	0.0	0.0
70	285	218	6708.621	12.958	115.626	0.0	0.0	0.0
73	237	210	102.970	25.132	268.305	0.0	0.0	0.0
81	174	268	150.950	30.639	289.601	0.0	0.0	0.0
84	50	212	16.046	24.411	238.150	0.0	0.0	0.0
87	175	215	1138.918	67.218	325.108	0.0	0.0	0.0
90	84	260	27.477	25.620	323.710	0.0	0.0	0.0
92	100	180	52.227	25.620	293.294	1.277	0.0	0.0
97	255	140	406.281	3.080	256.823	0.0	0.0	0.0
100	225	195	3564.146	18.797	292.916	0.0	0.0	0.0
103	402	160	2653.940	10.621	200.119	0.0	0.0	0.0
112	334	51	1568.299	13.078	445.023	0.0	0.0	0.0
115	390	143	3538.494	15.260	191.277	0.797	0.0	0.0
120	435	152	2111.572	13.078	151.237	0.0	0.0	0.0
123	350	237	8984.219	12.815	166.782	1.562	0.0	0.0
128	432	105	1335.231	17.127	262.535	5.943	0.0	0.0
131	427	55	3172.285	8.755	375.628	0.0	0.0	0.0
134	345	282	2321.562	13.162	170.258	0.0	0.0	0.0
137	327	315	5557.781	9.147	242.545	1.092	0.0	0.0
139	450	194	9635.844	8.767	261.982	4.588	0.0	0.0
142	450	235	2589.996	22.620	265.677	0.0	0.0	0.0
144	362	310	953.776	6.308	311.090	0.0	0.0	0.0
148	327	296	382.764	24.189	248.387	0.0	0.0	0.0
294	475	130	2704.168	37.064	233.475	0.0	0.0	
297	415	50	1584.689	4.759	322.936	0.0	0.0	
302	292	310	949.996	27.271	349.847	0.0	0.0	

VALLEY COPPER 3300 LEVEL

SPECTROGRAPHIC ANALYSIS

(VALUES IN PPM)

SAMP. #	B SR	TI	IN	V	MO	BA	BIGA	SN
3	0 500	1000	50	30	0 500	020	0	
10	0 600	1000	50	30	4 500	020	0	
13	10 400	2000	50	30	10 600	020	0	
16	0 400	1000	50	30	30 700	020	0	
23	10 700	500	50	30	01000	020	0	
28	10 300	800	50	40	0 500	020	0	
31	02001	500	50	20	0 500	020	0	
34	0 500	1000	50	20	0 400	020	0	
39	0 400	1000	50	40	30 400	020	0	
42	0 300	700	50	20	0 600	020	0	
45	0 500	1000	50	40	10 500	020	0	
48	0 400	800	50	40	0 500	020	0	
51	10 500	500	50	30	0 500	020	0	
54	0 500	1000	50	30	0 500	020	0	
57	0 700	1000	50	40	5 800	020	0	
65	0 400	1000	50	20	0 600	020	0	
70	0 400	1500	50	40	15 600	020	0	
73	01000	1500	50	30	0 900	020	0	
81	10 700	1500	50	30	3 600	020	0	
84	10 800	500	50	15	0 700	020	0	
87	10 400	700	50	10	5 300	015	0	
90	10 700	800	50	20	0 500	020	0	
92	0 600	1000	50	30	0 500	020	0	
97	10 700	1000	50	20	3 400	020	0	
100	0 400	800	50	30	0 500	020	0	
103	0 400	1000	50	30	0 600	020	0	
112	15 400	700	50	30	0 500	020	0	
115	102001	1000	50	40	300 700	020	0	
120	01000	500	50	30	20 500	020	7	
123	10 400	500	50	40	0 500	020	0	
128	0 500	500	50	30	20 800	020	0	
131	20 400	1000	50	40	0 600	020	0	
134	0 500	1500	50	30	20 600	020	0	
137	0 700	1000	50	50	5 500	020	0	
139	10 100	1500	50	50	8 500	020	0	
142	0 500	1500	50	30	15 500	020	0	
144	20 400	1000	50	40	6 500	020	0	
148	0 600	600	50	20	15 800	020	0	
294	0 400	700	50	20	01000	020	0	
297	20 400	1000	50	30	02000	020	0	
302	0 800	2000	50	40	30 700	020	0	

APPENDIX C

Lornex

(Sample locations and analytical results)

FIGURE 83

Location of samples. Lornex Surface (in pocket)

LORNEX SURFACE SAMPLES

ATOMIC ABSORPTION (TOTAL DIGESTION -RAPID TEFLON TUBE PROCEDURE)

(VALUES IN PPM FOR TRACE ELEMENTS AND WT. % FOR MAJOR ELEMENTS)

SAMP. #	LOC.COORD	CU	ZN	FE2O3	CAO	NA2O	K2O
72LS	72705540393	16	28	1.9	3.3	3.9	1.4
72LS	72805440393	13	35	2.1	3.3	4.0	1.3
72LS	72905550370	26	25	3.4	3.6	4.0	1.3
72LS	73005360414	11	24	2.0	3.4	3.5	1.6
72LS	73105310424	414	41	2.1	3.0	3.7	1.4
72LS	73203100465	31	27	1.6	2.4	4.1	1.5
72LS	73302970468	6	19	1.3	2.5	4.3	.5
72LS	73403010456	30	25	1.4	2.4	4.3	1.4
72LS	73502940450	7	28	1.2	2.4	3.8	1.5
72LS	73602830461	4	17	1.3	3.0	4.3	.1
72LS	73702750459	7	28	1.5	2.5	3.9	1.6
72LS	73802730452	8	30	1.8	2.7	4.2	2.2
72LS	73902670442	18	25	1.4	2.4	4.2	1.8
72LS	74002620435	2	35	1.4	2.5	4.1	1.3
72LS	74102770425	5	39	1.3	2.7	4.5	1.5
72LS	74203100455	3	17	2.0	4.1	4.8	.3
72LS	74303110426	189	29	1.7	2.8	4.4	1.2
72LS	74403100435	48	36	1.4	2.4	3.7	1.7
72LS	74502570423	4	34	1.3	2.4	4.0	1.4
72LS	74602550407	4	33	1.5	2.5	3.7	1.4
72LS	74702170464	27	32	1.6	2.6	4.0	1.5
72LS	74803050 44	15	34	1.5	2.4	3.8	1.6
72LS	74903130478	32	26	1.5	2.4	4.0	1.5
72LS	75002920481	120	27	1.4	2.4	3.9	1.5
72LS	75102800495	15	30	1.4	2.8	4.1	1.5
72LS	75202600 95	6	28	1.4	2.6	4.2	1.6
72LS	75302900600	3	15	1.3	3.0	4.2	.2
72LS	75403020580	4	19	1.6	4.0	4.7	.7
72LS	75502330606	8	24	1.7	4.0	4.1	1.5
72LS	75602210612	76	22	1.3	2.5	3.8	1.4
72LS	75701920630	120	22	1.5	2.2	3.8	1.5
72LS	75801870614	69	26	1.4	2.4	3.8	1.7
72LS	75901920582	14	26	1.4	2.8	4.2	.3
72LS	76001900560	423	28	1.5	2.4	4.1	1.6
72LS	76101820521	68	24	1.5	2.5	3.8	1.6
72LS	76202220545	80	27	1.5	2.4	3.7	1.6
72LS	76302520 56	2	26	1.5	2.6	3.7	1.4
72LS	76402610 40	6	23	1.5	2.6	3.5	1.5
72LS	76506270618	5	38	1.8	3.3	3.6	1.3
72LS	76606170575	9	40	1.9	3.1	3.3	1.5
72LS	76706160567	29	35	1.8	3.0	3.3	1.5
72LS	76806120 56	10	36	2.0	3.2	3.9	1.6
72LS	76906280584	15	27	1.9	2.5	4.1	1.7
72LS	77006660572	11	26	2.7	4.2	3.9	2.2
72LS	77106460577	12	27	2.1	3.9	4.0	1.5
72LS	77207030486	135	50	4.0	4.8	2.8	1.7
72LS	77306830 92	6	34	1.2	4.2	4.1	.4
72LS	77406960527	4	18	2.1	3.7	3.8	1.0
72LS	77506790544	8	33	1.3	3.2	3.5	.5
72LS	77606620552	538	24	1.8	3.7	3.2	1.6

SAMP. # LOC.COORD	CU	ZN	FE203	CAO	NA2O	K2O
72LS 77706250595	14	42	2.3	3.6	3.8	1.3
72LS 77805170567	7	31	1.8	3.4	3.8	1.0
72LS 77905020 47	66	31	1.3	3.5	4.4	.5
72LS 78005000365	372	57	1.4	3.2	4.3	.8
72LS 78104310507	265	45	2.3	2.9	3.5	1.6
72LS 78204960322	1520	37	1.0	2.8	3.9	.5
72LS 78304680295	1290	22	.8	2.5	2.7	1.0
72LS 78404570215	546	20	1.2	3.0	1.4	2.4
72LS 78504660219	2100	31	1.3	4.3	.5	3.7
72LS 78604800305	2900	19	.6	2.5	3.0	.8
72LS 78704520209	1400	17	1.6	2.1	2.2	1.8
72LS 78804990300	3260	46	.8	2.6	3.3	.8
72LS 78905120365	510	47	2.6	3.6	4.0	1.9
72LS 79004150385	228	22	0.9	2.4	2.1	1.9
72LS 79104720428	67	43	2.5	3.3	4.1	2.1
72LS 79204580487	128	210	3.3	5.4	3.8	1.6
72LS 79305110330	760	85	3.0	2.5	4.0	1.3
72LS 79404400486	1530	55	2.5	2.9	4.2	1.6
72LS 79503940463	5000	55	2.1	2.2	2.8	1.9
72LS 79604850385	1130	41	2.4	2.7	3.7	2.0
72LS 79704830447	136	52	2.9	3.2	3.8	1.7
72LS 79804460245	580	18	.6	2.5	4.0	1.9
72LS 79905150348	18	41	1.1	4.7	4.9	.5
72LS 80004170364	1470	28	1.9	1.6	3.5	2.3
72LS 80103530483	11	16	2.2	3.5	4.3	1.5
72LS 80205020385	254	39	2.8	3.3	3.7	2.2
72LS 80304210 48	3500	14	1.2	2.3	1.8	2.1
72LS 80503990212	45	33	1.5	2.2	4.3	1.7
72LS 80604540 45	5500	33	1.7	2.4	1.1	2.7
72LS 80704010528	6000	82	2.7	2.6	1.5	1.8
72LS 80804150214	330	15	1.0	1.9	3.7	1.2
72LS 80904200527	105	53	2.8	3.0	3.9	1.5
72LS 81004980272	2020	20	0.6	2.4	2.8	.8
72LS 81103970549	166	43	2.3	2.4	3.7	2.0
72LS 81204910298	4360	28	0.8	2.1	3.7	1.0
72LS 81306450519	35	24	2.6	3.8	4.1	.4
72LS 81506060525	33	50	2.8	3.4	4.0	1.9
72LS 81606200493	18	25	2.5	3.4	4.3	1.3
72LS 81706540490	13	27	2.7	3.6	4.3	1.8
72LS 81804600464	1220	99	2.4	2.5	3.7	1.8
72LS 81904920423	1060	60	2.8	2.8	3.7	1.6
72LS 82004750465	93	99	3.1	3.7	4.0	1.8
72LS 82106530560	97	38	3.6	3.9	3.8	1.6
72LS 82206000560	13	31	2.5	3.2	3.9	1.5
72LS 82306010550	7	28	2.1	2.7	3.8	1.6
72LS 82405730550	18	27	2.6	3.7	3.8	1.5
72LS 82505520535	11	37	2.5	3.5	4.1	1.6
72LS 82605400499	178	24	2.4	3.0	2.9	1.9
72LS 82705400468	7	33	2.4	3.0	4.0	1.4
72LS 82804330348	600	23	1.0	2.2	3.2	1.7
72LS 82906300590	20	22	2.6	5.0	3.7	2.2
72HS 88402950316	10	27	2.2	3.0	4.4	1.5
72HS 88902860362	20	24	1.6	2.4	3.8	1.3

LORNEX SURFACE SAMPLES

ATOMIC ABSORPTION ANALYSIS (HNO₃-HClO₄ DIGESTION)
(VALUES IN PPM)

SAMP. #	LOC.COORD	AG	NI	ZN	PB	CO	CD	MN	CU
727	0 0	0.0	0.0	15.926	0.0	1.000	0.0	182.753	5.976
728	0 0	0.0	2.474	22.222	0.0	0.0	0.0	238.004	6.375
729	0 0	0.0	2.474	20.741	0.0	0.0	0.0	216.754	15.538
730	0 0	0.0	1.237	11.852	0.0	0.0	0.0	110.502	5.578
731	0 0	0.0	1.237	29.259	6.667	2.000	0.264	276.255	501.992
732	0 0	0.0	0.0	20.741	0.0	0.0	0.0	318.755	8.765
733	0 0	0.0	0.0	14.074	0.0	0.0	0.0	216.754	3.984
734	0 0	0.0	0.0	20.370	0.0	0.0	0.0	340.006	29.482
735	0 0	0.0	0.0	22.963	0.0	0.0	0.264	327.255	7.171
736	0 0	0.0	1.237	12.222	0.0	1.000	0.0	212.504	3.984
737	0 0	0.0	0.0	20.741	0.0	0.0	0.0	293.255	7.570
738	0 0	2.500	0.0	21.481	6.667	0.0	0.0	284.755	3.187
739	0 0	0.0	0.0	18.148	0.0	0.0	0.0	263.504	20.319
740	0 0	0.0	0.0	24.444	0.0	0.0	1.055	331.505	3.586
741	0 0	0.0	0.0	25.926	0.0	0.0	0.0	344.256	3.187
742	0 0	0.0	0.0	12.963	0.0	0.0	0.0	238.004	3.586
743	0 0	0.0	0.0	16.667	0.0	0.0	0.0	242.254	167.331
744	0 0	0.0	0.0	24.444	0.0	0.0	0.0	318.755	40.637
745	0 0	0.0	0.0	26.296	0.0	0.0	0.264	344.256	3.984
746	0 0	0.0	0.0	26.667	0.0	0.0	0.0	340.006	3.984
747	0 0	0.0	2.474	22.963	0.0	1.000	0.0	310.255	28.685
748	0 0	0.0	0.0	29.630	0.0	0.0	0.264	382.506	15.139
749	0 0	0.0	0.0	20.741	0.0	0.0	0.0	340.006	33.068
750	0 0	0.0	0.0	24.074	0.0	0.0	0.0	340.006	117.530
751	0 0	0.0	0.0	20.000	0.0	0.0	0.396	284.755	11.952
752	0 0	0.0	0.0	22.593	0.0	0.0	0.0	297.505	5.179
753	0 0	0.0	2.000	13.333	0.0	2.000	0.0	164.849	1.724
754	0 0	0.0	0.0	15.190	0.0	2.000	0.0	187.475	3.103
755	0 0	0.0	1.000	19.409	0.0	3.000	0.0	226.263	6.207
756	0 0	0.0	2.000	17.215	0.0	1.000	0.0	223.030	70.690
757	0 0	0.0	4.000	16.878	0.0	1.000	0.0	203.636	117.241
758	0 0	0.0	2.000	19.916	0.0	1.000	0.0	216.566	65.517
759	0 0	0.0	1.000	21.097	0.0	2.000	0.0	210.101	10.345
760	0 0	0.0	2.000	21.941	0.0	1.000	0.0	239.192	379.310
761	0 0	0.0	2.000	18.565	0.0	0.0	0.0	219.798	71.724
762	0 0	0.0	1.000	19.409	0.0	0.0	0.0	223.030	74.138
763	0 0	0.0	1.000	21.941	0.0	1.000	0.0	261.818	2.414
764	0 0	0.0	2.000	19.409	0.0	0.0	0.0	223.030	3.793
765	0 0	0.0	2.000	24.473	0.0	3.000	0.0	168.081	3.793
766	0 0	0.0	3.000	24.135	0.0	2.000	0.0	187.475	6.207
767	0 0	0.0	3.000	23.629	0.0	2.000	0.0	197.172	24.138
768	0 0	0.0	4.000	23.797	0.0	2.000	0.0	197.172	6.897
769	0 0	0.0	3.000	19.072	0.0	1.000	0.0	138.990	15.517
770	0 0	0.0	3.000	14.852	0.0	2.000	0.0	164.849	11.034
771	0 0	0.0	3.000	17.722	0.0	2.000	0.0	155.152	12.069
772	0 0	0.0	12.000	25.148	0.0	9.000	0.0	171.313	110.345
773	0 0	0.500	2.000	26.667	12.500	2.000	0.472	219.798	4.483
774	0 0	0.0	3.000	10.127	0.0	1.000	0.0	90.505	3.103
775	0 0	0.0	2.000	25.316	0.0	0.0	0.0	190.707	3.448
776	0 0	0.0	3.000	16.878	0.0	2.000	0.0	126.061	475.862
777	0 0	0.0	4.000	25.316	0.0	3.000	0.0	155.152	8.966

778	0	0	0.0	2.000	20.253	0.0	2.000	0.0	203.636	8.276
779	0	0	0.0	1.000	23.629	0.0	0.0	0.0	242.424	72.414
780	0	0	0.0	2.000	42.194	5.000	0.0	0.094	239.192	344.828
781	0	0	0.0	3.000	30.380	0.0	3.000	0.0	232.727	251.724
782	0	0	0.0	1.000	30.717	2.500	0.0	0.0	245.657	1344.828
783	0	0	0.0	0.0	20.422	0.0	0.0	0.0	248.889	1137.932
784	0	0	0.0	2.000	14.346	0.0	2.000	0.0	969.697	500.000
785	0	0	0.250	2.000	17.722	0.0	1.000	0.0	1131.313	2000.000
786	0	0	0.0	1.000	24.473	0.0	0.0	0.0	193.940	2586.208
787	0	0	0.0	0.0	13.502	0.0	0.0	0.0	184.243	1275.863
788	0	0	0.0	3.000	40.506	5.000	1.000	0.0	226.263	3103.449
789	0	0	0.0	4.000	38.819	2.500	3.000	0.0	397.576	465.517
790	0	0	0.0	2.000	11.814	0.0	0.0	0.0	581.818	241.379
791	0	0	0.0	4.000	29.536	0.0	2.000	0.0	239.192	63.793
792	0	0	0.0	3.000	160.338	5.000	2.000	0.189	387.879	125.862
793	0	0	0.0	3.000	60.760	2.500	2.000	0.0	268.282	603.448
794	0	0	0.0	2.000	37.131	0.0	3.000	0.0	142.222	1258.621
795	0	0	1.000	2.000	40.506	0.0	2.000	0.0	213.333	4137.930
796	0	0	0.0	2.000	32.068	0.0	1.000	0.0	265.050	982.759
797	0	0	0.0	3.000	38.819	0.0	2.000	0.0	297.374	120.690
798	0	0	0.0	0.0	8.439	0.0	0.0	0.0	229.495	458.621
799	0	0	0.0	0.0	35.177	0.0	0.0	0.0	337.349	7.921
800	0	0	0.0	3.333	28.936	0.0	0.0	0.0	245.783	1309.978
801	0	0	0.0	3.333	13.050	0.0	0.0	0.0	134.940	2.437
802	0	0	0.0	0.0	32.340	0.0	1.250	0.0	236.145	213.252
803	0	0	0.667	3.333	7.943	0.0	0.0	0.0	337.349	2924.601
805	0	0	0.0	0.0	22.695	0.0	2.500	0.0	255.422	15.842
806	0	0	1.000	0.0	23.262	0.0	0.0	0.0	269.879	4874.332
807	0	0	0.667	0.0	56.738	0.0	2.500	0.0	771.084	5178.977
808	0	0	0.0	5.000	8.624	6.667	0.0	0.0	130.121	280.274
809	0	0	0.0	0.0	39.716	0.0	3.750	0.0	212.048	97.487
810	0	0	0.0	5.000	16.454	3.333	0.0	0.0	269.879	1645.088
811	0	0	0.0	0.0	36.312	0.0	0.0	0.0	265.060	152.323
812	0	0	0.667	3.333	22.695	0.0	0.0	0.0	149.398	3716.680
813	0	0	0.0	0.0	17.021	0.0	0.0	0.0	154.217	12.186
815	0	0	0.0	0.0	34.610	0.0	2.500	0.0	216.867	12.186
816	0	0	0.0	3.333	17.021	0.0	3.750	0.0	163.855	7.312
817	0	0	0.0	1.667	15.319	0.0	2.500	0.0	134.940	3.046
818	0	0	0.667	3.333	81.702	0.0	2.500	0.0	361.446	974.867
819	0	0	0.667	5.000	51.064	6.667	1.250	0.0	380.723	883.473
820	0	0	0.0	0.0	96.454	0.0	2.500	0.469	506.024	79.208
821	0	0	0.0	3.333	30.638	6.667	0.0	0.0	375.903	79.208
822	0	0	0.0	0.0	20.426	0.0	1.250	0.0	192.771	3.656
823	0	0	0.0	3.333	18.156	0.0	1.250	0.0	168.675	3.656
824	0	0	0.0	3.333	17.021	0.0	1.250	0.0	183.133	3.046
825	0	0	0.0	5.000	20.426	0.0	0.0	0.0	178.313	5.484
826	0	0	0.0	1.667	15.319	0.0	1.250	0.0	163.855	170.602
827	0	0	0.0	3.333	20.993	0.0	2.500	0.0	149.398	1.828
828	0	0	0.0	1.667	9.645	0.0	0.0	0.0	255.422	456.969
829	0	0	0.0	1.667	18.156	0.0	1.250	0.0	168.675	21.935
884	0	0	0.0	0.0	18.462	0.0	0.0	0.0	216.446	3.279
889	0	0	0.0	3.333	23.496	0.0	1.250	0.0	263.130	8.743

LORNEX SURFACE SAMPLES

SPECTROGRAPHIC ANALYSIS

(VALUES IN PPM)

SAMP. #	B	SR	TI	IN	V	MO	BA	BIGA	SN
727		500	500	50	30		500	20	
728	20	500	1000	50	40		400	20	
729		600	1000	50	40		500	20	
730		500	500	50	30		500	20	
731		500	500	50	20		500	20	
732		500	800	50	20		500	20	
733		600	200	50	15		200	20	
734		500	400	50	15		500	20	
735		700	800	50	20		800	20	
736		1000	1000	50	20		400	20	
737		600	900	50	20		600	20	
738		700	1000	50	20		500	20	
739		700	800	50	30		1000	20	
740		800	800	50	30		600	20	
741		800	500	50	20		1000	20200	
742		1000	800	50	20		500	20	
743		800	500	50	20		500	20	
744		500	1000	50	30		600	20	
745		500	200	50	15		600	20	
746		600	700	50	20		600	20	
747		600	300	50	15		500	20	
748		600	500	50	15		400	15	
749		600	900	50	20		500	20	
750-2		600	600	50	20		500	20	
751		600	400	50	20		500	20	
752		500	500	50	20		400	20	
753		1000	500	50	15		200	20	
754		800	600	50	20		500	20	
755		500	150	50	10		800	20	
756		400	200	50	10		500	20	
757		400	300	50	15		500	20	
758		400	1000	50	20		600	20	
759		900	600	50	15		400	20	
760		500	500	50	10		500	20	
761		500	600	50	10		500	20	
762		500	600	50	15		600	20	
763		500	500	50	15		400	20	
764		500	500	50	15		500	20	
765		500	700	50	40		500	20	
766		500	700	50	30		500	20	
767		500	500	50	30		500	20	
768		700	600	50	30		500	20	
769		500	700	50	30		500	20	
770		500	800	50	40		600	20	
771		600	500	50	30		600	20	
772		500	800	50	50		400	20	
773		1000	2000	50	40		150	20	
774		800	1000	50	40		400	20	
775		700	1000	50	30		150	20	
776		500	700	50	20		500	20	

SAMP. #	B	SR	TI	IN	V	MO	BA	BICA	SN
777		1000	600	50	40		500	20	
778		800	700	50	40		400	20	
779		10 800	800	50	40		200	20	
780		15 700	700	50	40		300	20	
781		500	1000	50	40		600	20	
782		15 800	1000	50	40	20 200	20		
783		15 500	1500	50	30	5 200	20		
784		30 200	2000	50	40	5 500	20		
785		50 100	1000	50	50	20 400	20		
786		15 300	800	50	40	15 300	20		
787		50 300	800	50	20	10 500	20		
788		15 700	1000	50	40	20 200	20		
789		10 600	1000	50	50	500	20		
790		50 200	800	50	30	500	20		
791		600	800	50	30	500	20		
792		10 600	800	50	40	500	20		
793		10 600	700	60	30	500	20		
794		600	900	50	40	500	20		
795		400	1500	50	50	30 500	20		
796		700	1000	50	50	20 600	20		
797		1000	2000	50	40	800	20		
798		400 300	2000	50	20	200 200	20		
799		151000	1000	50	30	200	20		
800-1		700	700	50	30	1000	20		
801		700	1000	50	40	600	20		
802		10 600	2000	50	30	800	20		
803		50 300	700	50	40	20 500	20		
805		15 500	500	50	20	500	20		
806		40 200	2000	50	50	40 600	20		
807		20 500	2000	50	50	500 500	20		
808		50 400	900	50	20	4 500	20		
809		700	1000	50	50	700	20		
810		20 400	700	50	30	10 200	20		
811		700	800	50	30	600	20		
812		10 700	1000	50	40	150 200	20		
813		800	1500	50	50	600	20		
815		10 800	1000	50	40	200	20		
816		500	1500	50	50	600	20		
817		900	1000	50	30	200	10		
818		700	2000	50	40	600	20		
819		20 700	1000	50	40	5 700	20		
820		15 600	1000	50	50	600	20		
821		10 700	1000	50	30	500	20		
822		15 700	1000	50	40	500	20		
823		600	1000	50	30	500	20		
824		800	900	50	30	400	20		
825		800	800	50	40	400	20		
826		10 500	1000	50	30	600	20		
827		900	1500	50	40	600	20		
828		20 400	800	50	20	500	20		
829		600	700	50	40	500	20		
884B		600	1000	50	30	600	20		
889		800		50	30	800	20		

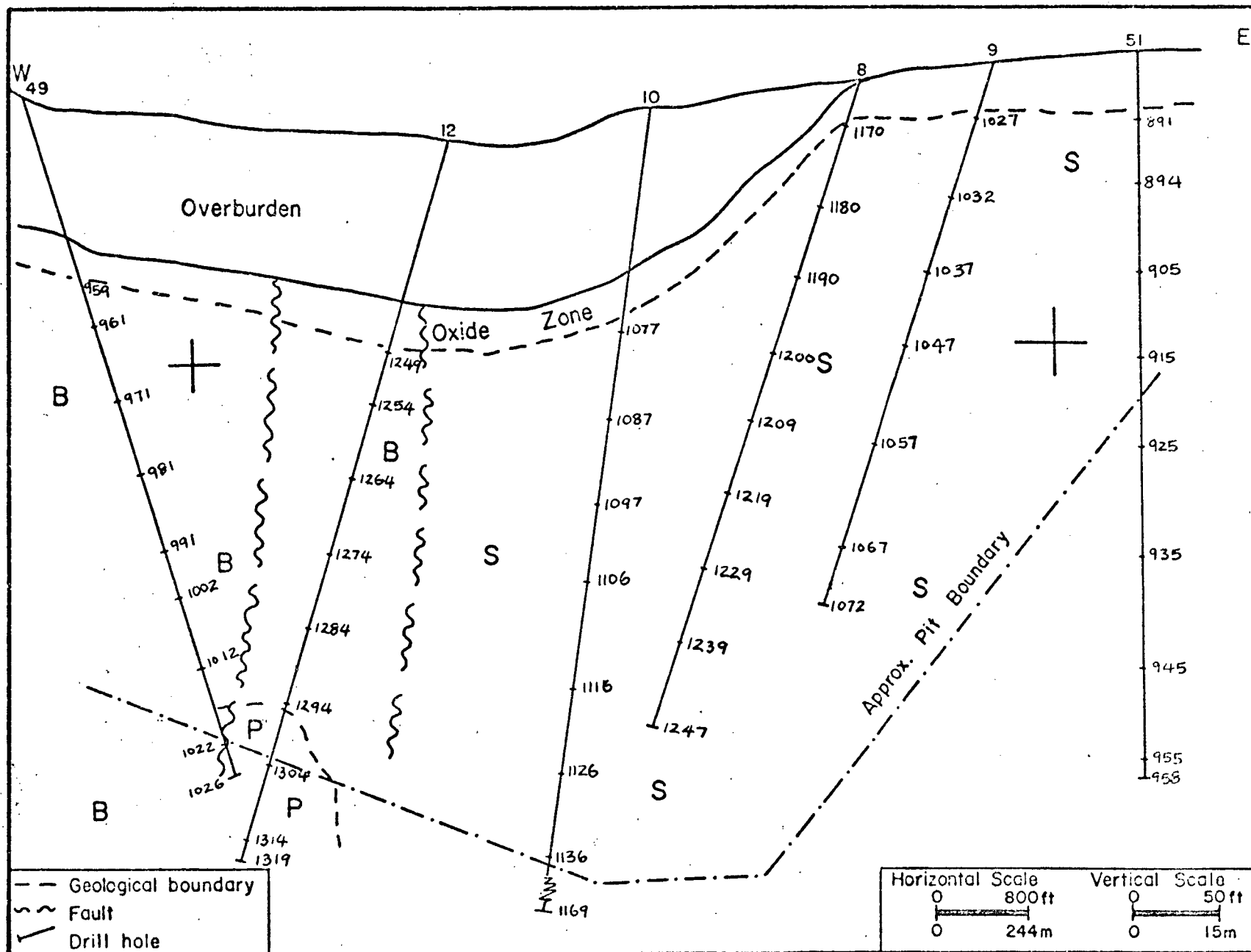


FIGURE 84: Location of drill core samples, Lornex mine (every 10th sample)

ATOMIC ABSORPTION (TOTAL DIGESTION -RAPID TEFLON TUBE PROCEDURE)

(VALUES IN PPM FOR TRACE ELEMENTS AND WT. % FOR MAJOR ELEMENTS)

DRILL-HOLE 51

SAMP. #	LOC.COORD	CU	ZN	FE2O3	CAO	NA2O	K2O
72LZ	89114200660	51	29	1.7	3.6	3.9	1.5
72LZ	89214200655	268	40	2.1	2.8	3.7	1.2
72LZ	89314200650	200	58	2.2	3.7	3.6	2.1
72LZ	89414200645	106	49	2.1	2.8	3.5	1.3
72LZ	89514200640	308	35	2.2	3.3	3.5	1.6
72LZ	89614200635	131	35	2.2	3.0	3.5	1.4
72LZ	89714200630	1080	35	1.8	4.9	3.4	.9
72LZ	89814200625	561	52	1.9	3.5	3.5	1.3
72LZ	89914200620	4310	33	1.7	1.9	2.0	2.4
72LZ	90014200615	2690	46	1.7	3.1	2.7	1.6
72LZ	90114200610	621	42	1.3	3.2	3.2	.9
72LZ	90214200605	487	46	1.8	3.0	3.3	.8
72LZ	90314200600	560	34	1.2	5.1	.3	3.3
72LZ	90414200595	1510	31	1.2	4.9	.3	3.2
72LZ	90514200590	4030	10	1.2	1.3	.1	.8
72LZ	90614200585	751	34	1.1	2.7	3.4	1.0
72LZ	90714200580	431	44	2.8	3.6	3.5	1.9
72LZ	90814200575	880	57	2.3	2.5	3.4	1.5
72LZ	90914200570	67	35	1.9	2.9	3.7	1.7
72LZ	91014200565	201	38	2.3	3.0	3.6	1.7
72LZ	91114200560	125	41	3.2	4.0	3.6	1.6
72LZ	91214200555	237	52	2.0	2.2	1.6	1.2
72LZ	91314200550	1400	79	2.4	2.4	3.0	.3
72LZ	91414200545	312	37	2.2	3.3	2.4	2.1
72LZ	91514200540	1870	41	2.3	2.0	3.2	1.8
72LZ	91614200535	507	34	1.2	1.3	3.0	2.3
72LZ	91714200530	1450	34	1.1	1.1	2.8	2.7
72LZ	91814200525	940	37	1.2	1.5	3.2	2.4
72LZ	91914200520	557	26	1.3	1.9	3.3	2.0
72LZ	92014200515	48	33	1.4	2.9	3.8	2.0
72LZ	92114200510	2400	51	1.7	2.2	3.3	1.2
72LZ	92214200505	194	42	2.0	3.2	3.6	1.0
72LZ	92314200500	232	36	2.5	3.3	3.5	1.6
72LZ	92414200495	230	43	2.1	3.1	3.4	1.8
72LZ	92514200490	930	47	2.5	2.9	3.3	2.3
72LZ	92614200485	158	51	2.2	3.0	3.3	1.6
72LZ	92714200480	212	33	2.3	2.7	3.4	1.7
72LZ	92814200475	179	38	2.1	2.9	3.2	1.6
72LZ	92914200470	261	40	2.8	2.2	3.4	1.7
72LZ	93014200465	1620	49	2.2	2.1	3.0	1.7
72LZ	93114200460	1880	51	2.4	2.2	3.2	1.8
72LZ	93214200455	521	45	2.2	2.5	3.2	1.5
72LZ	93314200440	423	67	2.0	2.2	3.2	1.7
72LZ	93414200435	1540	46	2.1	2.5	3.1	1.8
72LZ	93514200430	2640	58	2.7	2.6	2.5	2.0
72LZ	93614200425	1250	48	2.4	2.7	3.0	1.8
72LZ	93714200420	759	56	2.5	2.3	3.2	1.9
72LZ	93814200415	744	41	2.6	2.8	3.3	1.9
72LZ	93914200410	1400	80	2.3	2.7	2.9	1.8
72LZ	94014200405	3250	89	2.7	2.5	2.9	1.9
72LZ	94114200400	2670	69	3.0	2.7	2.6	2.3
72LZ	94214200395	820.	40	2.2	2.6	3.3	1.2
72LZ	94314200390	578	52	2.4	2.5	3.0	1.6
72LZ	94414200385	281	68	2.3	3.0	3.2	1.6
72LZ	94514200380	2130	64	1.5	2.1	2.6	2.0
72LZ	94614200375	42	81	2.1	3.0	3.6	1.5
72LZ	94714200355	93	32	2.0	3.1	3.4	1.6
72LZ	94814200350	21	40	2.0	3.3	3.6	1.5
72LZ	94914200345	860	43	1.8	2.4	3.8	1.2
72LZ	95014200340	570	44	2.1	2.9	3.7	1.6
72LZ	95114200335	2550	39	2.0	2.5	2.5	1.9
72LZ	95314200325	2700	54	2.4	2.4	3.5	1.6
72LZ	95414200320	820	44	2.0	2.7	3.7	1.3
72LZ	95514200315	880	49	2.2	3.2	3.5	1.2
72LZ	95614200310	850	36	3.0	2.6	2.6	1.9
72LZ	95714200305	254	32	2.1	3.2	2.7	1.7
72LZ	95814200300	7000	29	2.8	1.2	.3	2.9

SAMP. #	LOC.COORD	CU	ZN	FE203	CAO	NA2O	K2O
72LZ	95902050573	22	27	1.4	2.7	4.4	1.6
72LZ	96002080569	9	23	1.1	2.2	3.9	1.8
72LZ	96102100565	8	25	1.3	2.1	3.9	1.6
72LZ	96202130560	11	29	1.4	2.1	4.0	1.5
72LZ	96302150556	7	24	1.2	2.2	3.9	1.6
72LZ	96402180552	8	19	1.0	1.6	4.0	1.3
72LZ	96502200547	7	16	.9	2.3	4.1	.9
72LZ	96602230543	5	28	1.6	1.8	4.0	1.3
72LZ	96702250539	9	19	1.3	1.8	3.6	1.5
72LZ	96802280535	1	24	1.2	2.8	3.5	1.9
72LZ	96902300530	2	36	1.5	1.5	3.1	1.2
72LZ	97002330526	2	19	1.2	2.2	3.9	1.4
72LZ	97102360522	4	23	1.4	1.3	2.0	1.6
72LZ	97202390517	3	25	1.2	2.1	3.3	1.5
72LZ	97302410513	2	27	1.2	2.5	3.2	1.5
72LZ	97402440509	4	22	1.3	1.8	2.6	1.8
72LZ	97502470504	2	74	3.2	2.0	3.3	2.2
72LZ	95214200330	305	36	2.2	3.1	3.7	1.4
72LZ	97602490500	5	30	1.4	1.8	1.0	1.5
72LZ	97702520496	1	19	1.3	1.7	.4	.5
72LZ	97802540492	2	12	.5	1.1	.3	.4
72LZ	97902570488	1	29	1.6	3.0	1.8	1.3
72LZ	98002600483	4	29	1.3	2.4	3.6	1.6
72LZ	98102620479	1	19	1.2	2.1	3.8	1.3
72LZ	98202640475	2	23	1.3	2.3	3.8	1.5
72LZ	98302670470	3	28	1.4	2.6	4.0	1.6
72LZ	98402700466	3	22	1.2	2.3	3.9	1.5
72LZ	98502720462	2	25	1.2	2.5	3.8	1.6
72LZ	98602750459	3	29	1.2	2.0	3.6	1.9
72LZ	98702780455	6	27	1.3	2.3	4.1	1.4
72LZ	98802800449	3	24	1.3	2.6	3.8	1.4
72LZ	98902820445	6	22	1.5	2.5	4.1	1.6
72LZ	99002850440	8	21	1.4	2.9	4.2	1.6
72LZ	99102880436	6	25	1.5	2.7	4.1	1.6
72LZ	99202900432	7	50	1.5	2.2	3.3	1.6
72LZ	99302930428	9	57	1.3	2.5	3.9	1.2
72LZ	99402950424	6	23	1.8	3.1	4.4	1.5
72LZ	99502980419	20	54	1.7	3.3	3.7	1.6
72LZ	99603000415	13	26	1.6	2.9	3.7	1.5
72LZ	99703030411	6	36	1.6	2.2	3.9	1.2
72LZ	99803050407	6	26	1.3	2.4	4.1	1.3
72LZ	99903080403	5	79	1.5	2.5	3.8	1.3
72LZ	100003110398	13	62	2.3	2.3	2.9	1.4
72LZ	100103140394	16	83	1.5	2.4	2.4	1.8
72LZ	100203160389	3	22	1.3	2.3	4.3	1.1
72LZ	100303190385	5	53	1.5	2.2	3.9	1.3
72LZ	100403210381	16	63	1.6	2.5	3.3	1.6
72LZ	100503240376	13	19	1.4	2.2	3.8	1.3
72LZ	100603260372	7	20	1.5	2.6	3.0	2.1
72LZ	100703280368	28	420	1.1	2.1	.2	2.9
72LZ	100803310363	65	930	1.0	2.3	.3	3.0
72LZ	100903340359	89	1230	1.4	.7	.2	2.7
72LZ	101003370355	56	1230	1.2	.9	.2	2.8
72LZ	101103390351	64	990	1.0	.9	.1	3.0
72LZ	101203420347	54	890	1.1	1.1	.2	2.7
72LZ	101303440342	33	820	1.0	1.2	.3	2.8
72LZ	101403470338	47	820	1.1	1.6	.2	2.5
72LZ	101503500333	29	450	.9	1.5	.1	2.8
72LZ	101603520329	57	1090	1.1	1.2	.2	2.9
72LZ	101703550325	34	900	1.1	.9	.1	2.7
72LZ	101803580320	72	1210	1.1	.7	.1	2.8
72LZ	101903600316	47	1220	1.3	1.1	.2	2.8
72LZ	102003630312	21	370	.9	1.4	.1	3.0
72LZ	102103650308	19	360	.9	1.2	.1	2.8
72LZ	102203670304	15	1070	1.2	1.8	.2	2.7
72LZ	102303700300	58	1230	1.1	1.4	.2	2.9
72LZ	102403730295	73	1070	1.6	1.3	.2	2.7
72LZ	102503750291	6440	35	1.3	1.2	1.1	2.3
72LZ	102603780287	1260	20	1.2	1.4	3.5	2.0

DRILL-HOLE 9

SAMP. # LOC.COORD	CU	ZN	FE2O3	CAO	NA2O	K2O
72LZ102712330650	3250	52	1.2	2.0	2.1	2.1
72LZ102812300645	1900	44	2.1	2.7	3.4	2.3
72LZ102912270641	5370	67	2.5	3.6	1.6	1.9
72LZ103012240637	6490	60	2.8	2.4	2.2	2.5
72LZ103112210633	3250	45	2.4	2.4	2.9	2.1
72LZ103212180629	1770	44	2.1	2.1	3.4	1.9
72LZ103312150625	3800	46	2.2	2.3	2.6	2.0
72LZ103412130620	6550	13	2.3	.3	.3	3.3
72LZ103512100616	3940	28	2.0	.6	1.4	2.5
72LZ103612070612	1390	43	2.0	1.6	2.5	1.6
72LZ103712040608	710	26	1.4	1.0	3.5	1.2
72LZ103812010604	2400	33	2.3	1.3	1.8	1.7
72LZ103911980600	1200	40	2.4	2.0	3.2	1.7
72LZ104011950595	1520	34	2.1	2.6	2.7	2.1
72LZ104111920591	644	48	2.3	2.7	3.2	1.6
72LZ104211900587	4490	50	2.0	1.2	1.2	2.2
72LZ104311870583	3140	36	2.3	1.6	3.2	1.8
72LZ104411840579	7510	46	2.4	1.0	2.2	1.8
72LZ104511810575	1900	52	2.2	1.7	2.9	1.6
72LZ104611790571	1900	58	2.1	1.7	3.2	1.8
72LZ104711760567	6570	38	2.3	1.0	.5	2.6
72LZ104811740563	3660	36	1.8	.6	1.3	3.4
72LZ104911710559	4220	40	2.1	2.3	2.7	1.9
72LZ105011680554	6470	50	1.9	1.4	1.3	2.7
72LZ105111650550	3420	34	1.3	.4	.9	4.2
72LZ105211620546	3550	56	1.3	.9	2.2	2.6
72LZ105311600542	5270	26	1.3	1.0	2.6	3.1
72LZ105411570538	6020	29	1.7	1.5	2.7	3.6
72LZ105511540534	2540	30	1.3	1.1	3.0	3.9
72LZ105611510530	4110	29	1.4	1.2	3.1	2.5
72LZ105711490526	2500	40	1.7	1.2	3.2	3.1
72LZ105811460522	3170	45	2.1	1.7	3.0	2.5
72LZ105911430518	3810	53	2.5	1.4	3.3	2.3
72LZ106011400514	2340	27	1.7	0.8	3.1	3.2
72LZ106111370510	6570	43	2.9	0.8	1.3	5.4
72LZ106211340505	2670	61	2.4	1.2	2.9	2.7
72LZ106311310500	6530	69	2.4	1.9	1.8	2.8
72LZ106411280496	6560	92	2.6	0.8	1.5	2.9
72LZ106510780422	6570	82	2.3	0.9	2.9	1.5
72LZ106610750417	3960	46	1.5	1.2	3.3	1.5
72LZ106710730413	3520	55	2.7	1.2	2.1	1.9
72LZ106810700409	6560	86	5.3	1.0	.9	5.9
72LZ106910670405	1810	36	2.2	0.8	3.1	2.3
72LZ107010640400	1070	44	1.2	1.4	3.7	1.4
72LZ107110610396	383	43	2.2	1.9	3.4	1.5
72LZ107210590392	720	49	1.9	1.1	3.5	2.5
72LZ107310560388	850	58	2.2	1.1	3.4	2.2
72LZ107410530383	2000	56	1.7	1.4	2.8	1.9
72LZ107510500379	1280	40	2.0	1.4	3.5	2.1

SAMP. #	LOC.COORD	CU	ZN	FE203	CAO	NA2O	K2O
72LZ107608220539		3340	39	1.2	1.0	3.1	3.6
72LZ107708210534		4980	66	3.0	1.0	1.9	2.3
72LZ107808200529		1510	45	1.1	1.4	3.4	1.5
72LZ107908180524		1630	49	2.0	1.5	3.3	1.3
72LZ108008160519		2060	69	2.0	1.3	3.0	1.8
72LZ108108150515		3460	48	1.7	1.3	2.5	1.5
72LZ108208140510		3480	42	1.1	1.0	2.9	2.0
72LZ108308130505		3000	47	1.5	1.1	3.2	1.5
72LZ108408110501		3540	64	2.1	1.4	2.9	2.5
72LZ108508100496		2390	45	1.3	.9	3.1	1.7
72LZ108608080491		1900	28	1.1	1.3	4.2	1.9
72LZ108708070487		4190	41	1.6	1.0	3.0	1.9
72LZ108808050482		2040	53	1.6	.9	3.7	2.0
72LZ108908040477		6450	39	1.8	.9	2.4	2.8
72LZ109008030472		2430	46	1.3	1.2	3.5	3.5
72LZ109108010467		4520	36	1.3	.8	2.3	3.0
72LZ109208000463		3180	46	1.2	1.8	1.9	2.0
72LZ109307980458		3450	21	.7	1.2	1.1	1.2
72LZ109407970453		3870	30	1.5	1.9	2.4	2.0
72LZ109507950448		3700	32	1.5	.5	1.0	3.3
72LZ109607940444		1840	30	1.3	3.7	4.1	1.3
72LZ109707930439		3020	33	1.0	2.0	3.4	1.5
72LZ109807910434		2940	39	1.1	1.9	4.0	1.1
72LZ109907900429		3660	46	1.2	2.4	3.6	.9
72LZ110007880424		1270	32	.8	3.3	4.0	.8
72LZ110107860419		9600	32	2.1	1.5	.9	2.2
72LZ110207850415		2890	35	1.1	2.0	3.0	1.7
72LZ110307840410		4000	62	1.4	2.6	3.4	1.2
72LZ110407830405		2250	40	1.5	2.2	3.9	.9
72LZ110507810400		3500	60	1.8	2.9	2.9	1.9
72LZ110607800395		2690	49	1.4	2.4	3.3	1.2
72LZ110707780390		4040	50	1.5	1.9	3.6	1.3
72LZ110807760385		4600	42	1.5	1.8	3.4	1.4
72LZ110907750381		3050	29	1.1	2.5	3.0	1.4
72LZ111007740377		3550	39	1.5	2.8	3.6	1.5
72LZ111107730372		3200	45	1.6	1.5	3.6	1.4
72LZ111207710367		4120	53	1.5	1.9	3.0	1.2
72LZ111307690362		2260	44	1.3	3.2	4.1	1.1
72LZ111407650347		3800	32	1.4	1.7	2.8	2.5
72LZ111507630343		4700	180	2.0	3.0	2.5	1.7
72LZ111607600334		3400	48	1.8	3.8	3.1	1.6
72LZ111707590329		4180	49	1.3	3.1	1.9	2.2
72LZ111807570324		4000	32	1.3	1.6	3.5	1.3
72LZ111907560320		4360	27	1.8	3.0	3.3	1.8
72LZ112007550315		2990	44	1.0	1.7	3.2	1.4
72LZ112107540310		2930	50	1.0	2.6	3.3	1.2
72LZ112207520305		3800	44	1.5	2.4	3.4	1.1
72LZ112307500300		8600	41	2.2	2.9	.9	2.8
72LZ112407490295		2970	38	1.1	2.5	3.5	1.0
72LZ112507470291		3080	44	1.6	5.1	4.0	.8
72LZ112607460286		3690	45	2.2	4.2	3.4	1.2
72LZ112707450281		2990	44	1.4	3.1	3.3	1.0
72LZ112807440277		4900	25	1.7	5.9	.8	3.0
72LZ112907420272		3300	39	2.2	4.1	3.5	.8
72LZ113007400267		5000	43	2.1	4.5	2.9	1.8
72LZ113107390262		2320	35	1.3	9.0	3.9	1.7
72LZ113207380257		4400	41	1.6	6.3	3.0	2.1
72LZ113307360252		3690	39	1.8	3.4	2.3	2.0
72LZ113407350248		4160	57	2.0	3.9	2.5	1.9
72LZ113507330244		4000	33	1.5	5.0	1.1	2.7
72LZ113607310239		4000	35	1.5	8.1	1.6	2.6
72LZ113707300234		3590	51	1.3	8.8	3.3	1.7
72LZ113807290229		5500	170	1.6	5.4	.8	2.5
72LZ113907280224		10200	160	2.8	6.4	1.8	2.4
72LZ114007260220		4000	49	2.1	3.7	2.5	1.8
72LZ114107250215		13200	21	2.7	2.7	1.0	2.4
72LZ114207230210		4000	42	2.8	4.4	3.2	1.5
72LZ114307220205		2860	25	1.3	4.3	3.6	1.3
72LZ114407200200		3600	29	1.7	4.3	2.4	1.8
72LZ114507190195		15800	34	3.3	3.7	2.0	1.3
72LZ114607170190		2840	45	1.3	3.5	3.1	1.5
72LZ114707160186		2950	48	1.5	4.0	3.2	1.5
72LZ114807150181		3120	28	1.7	5.1	1.7	1.8
72LZ114907130176		3600	41	2.1	3.6	1.9	2.1
72LZ115007120171		5600	19	1.7	4.2	.4	2.9
72LZ115107100167		5300	32	1.3	6.0	3.7	1.4
72LZ115207090162		3330	37	1.1	3.5	3.6	.9
72LZ115307070157		5000	60	1.8	3.3	2.5	1.3
72LZ115407050153		3120	38	1.6	4.9	3.5	1.2
72LZ115507040147		3800	31	1.3	4.4	2.4	1.2
72LZ115607030143		4300	38	1.7	3.8	3.3	1.3
72LZ115707020138		3650	34	1.4	3.3	3.7	.9
72LZ115807000134		3680	31	1.4	3.6	2.5	1.8
72LZ115906980129		5700	27	1.7	3.2	1.1	2.4
72LZ116006970124		3800	33	1.4	3.9	1.6	1.6
72LZ116106960119		3830	36	1.2	6.0	2.0	1.3
72LZ116206950115		3900	26	1.3	4.9	2.8	1.6
72LZ116306930110		2920	27	1.2	2.6	2.5	1.5
72LZ116406910105		3230	41	1.7	4.0	1.3	2.1
72LZ116506900100		4120	4200	10.6	.3	.4	2.1
72LZ116606890095		2790	23	1.4	3.7	2.3	1.5
72LZ116706870090		1660	38	1.0	3.2	1.8	2.0
72LZ116806850085		2980	27	1.1	1.2	2.8	1.9
72LZ116906830080		3620	64	2.2	4.0	1.9	1.4

DRILL-HOLE 8

SAMP. #	LOC.COORD	CU	ZN	FE2O3	CAO	NA2O	K2O
72LZ117010790646		2380	36	1.3	1.3	3.4	1.7
72LZ117110770642		8400	27	1.9	.8	1.5	2.3
72LZ117210740638		2130	24	1.6	.5	1.9	2.4
72LZ117310710634	13000	26	1.6	.5	2.0	2.5	
72LZ117410680630	3500	22	1.8	.6	2.9	2.5	
72LZ117510650625	6300	49	2.3	2.5	2.6	1.9	
72LZ117610630621	5700	59	3.0	1.3	3.0	2.0	
72LZ117710600617	2670	57	2.4	1.7	3.7	1.6	
72LZ117810570612	3600	49	2.6	2.2	3.1	1.8	
72LZ117910550608	3870	39	1.3	1.8	3.2	1.2	
72LZ118010520604	4070	55	1.7	1.4	3.0	1.8	
72LZ118110490600	5900	75	2.7	2.0	3.2	1.8	
72LZ118210470596	4150	57	2.3	2.0	4.2	2.1	
72LZ118310440592	2080	57	2.1	3.2	3.3	1.9	
72LZ118410410588	2240	49	1.7	3.0	3.8	1.3	
72LZ118510380584	2920	48	2.8	1.6	1.9	2.5	
72LZ118610350580	4130	28	1.3	1.5	3.1	1.6	
72LZ118710330576	3250	51	2.8	2.6	3.2	1.9	
72LZ118810300572	2500	44	2.6	2.3	3.1	2.0	
72LZ118910280568	3260	39	2.4	2.6	3.1	1.7	
72LZ119010250564	1880	46	2.8	3.1	3.3	1.7	
72LZ119110200559	4020	52	2.0	1.6	3.4	1.9	
72LZ119210190555	550	51	1.9	3.5	3.6	1.2	
72LZ119310160550	3260	52	2.0	1.5	3.4	1.4	
72LZ119410130546	2610	35	1.8	1.5	2.5	2.1	
72LZ119510100542	1320	42	2.3	.8	3.8	1.6	
72LZ119610080538	2830	24	2.5	2.1	2.9	1.8	
72LZ119710050534	18000	24	2.6	.1	.3	3.0	
72LZ119810020530	4100	19	1.3	.2	1.3	2.4	
72LZ119909990526	4440	18	1.5	.4	2.0	1.9	
72LZ120009970522	3860	21	1.0	.4	2.2	1.6	
72LZ120109940518	4400	22	1.0	.1	0.3	2.9	
72LZ120209910514	5700	30	1.4	2.2	.3	5.0	
72LZ120309880510	4600	33	1.2	0.3	.2	3.0	
72LZ120409850505	10500	21	2.7	.4	.3	3.8	
72LZ120509830500	5600	24	1.4	.2	.7	3.6	
72LZ120609800496	13700	28	2.0	1.2	.9	1.9	
72LZ120709780492	2340	72	1.8	2.4	3.5	1.1	
72LZ120809750488	7000	55	2.0	1.0	2.1	3.5	
72LZ120909720484	2380	53	2.1	1.5	2.9	2.0	
72LZ121009690480	3500	45	2.0	1.1	2.5	1.9	
72LZ121109660476	2070	45	2.1	2.1	2.7	2.0	
72LZ121209630472	6500	92	2.2	1.7	2.6	1.5	
72LZ121309600468	1670	61	1.8	2.3	3.4	1.2	
72LZ121409580464	2570	40	2.1	1.6	3.2	1.6	
72LZ121509550460	1940	58	1.9	1.5	3.5	1.4	
72LZ121609520455	4340	62	1.5	2.5	3.1	1.1	
72LZ121709500451	3350	62	2.1	2.7	2.8	1.7	
72LZ121809470447	2100	46	1.8	2.1	3.0	1.7	
72LZ121909440443	10100	97	2.2	.8	1.3	3.0	
72LZ122009410438	2170	56	1.7	1.3	3.3	1.7	
72LZ122109390434	3350	38	1.8	1.6	1.8	1.7	
72LZ122209360430	3980	62	1.5	4.9	3.0	1.4	
72LZ122309330426	4600	76	1.5	3.5	3.1	1.6	
72LZ122409300422	2760	32	.8	3.4	3.2	1.1	
72LZ122509270418	5400	42	1.4	3.8	3.0	1.2	
72LZ122609250414	4600	22	1.0	4.4	2.7	1.2	
72LZ122709220410	2770	42	.8	3.6	3.5	.7	
72LZ122809190405	2600	35	1.3	2.9	2.7	1.3	
72LZ122909160401	3580	36	1.1	3.5	2.3	1.4	
72LZ123009130397	4900	65	1.7	2.6	3.1	1.3	
72LZ123109100393	3070	44	1.9	3.3	2.3	1.9	
72LZ123209080389	4500	49	1.4	3.1	2.1	1.3	
72LZ123309050385	3250	54	2.1	3.3	3.1	.9	
72LZ123409020380	3850	73	2.3	3.3	2.9	1.9	
72LZ123508990376	1630	46	1.3	3.3	3.3	1.1	
72LZ123608960372	4300	53	1.6	2.5	3.0	1.3	
72LZ123708940368	3640	50	1.9	3.3	2.8	1.2	
72LZ123808910364	3030	53	1.4	2.9	3.2	1.1	
72LZ123908890360	3890	48	1.1	2.5	3.0	.9	
72LZ124008860356	4060	46	1.2	3.9	2.8	1.2	
72LZ124108830352	3220	62	1.6	3.7	2.8	1.1	
72LZ124208800348	2030	56	1.2	4.3	3.0	.9	
72LZ124308780343	2400	53	1.4	4.1	2.9	1.1	
72LZ124408750339	2470	47	1.4	3.8	2.9	1.2	
72LZ124508720335	2450	47	1.1	3.1	3.2	.7	
72LZ124608690331	4800	64	1.4	2.8	3.0	.7	
72LZ124708670327	2570	43	1.3	2.9	3.0	.9	

DRILL-HOLE 12

SAMP. #	LOC.COORD	CU	ZN	FE2O3	CAO	NA2O	K2O
72LZ124805530523		1180	36	1.8	3.4	1.2	2.2
72LZ124905500518		1900	42	1.8	2.4	2.5	1.8
72LZ125005480514	10100	46	2.9	5.4	.7	2.6	
72LZ125105450510	2390	32	1.6	2.5	2.7	1.8	
72LZ125205430505	810	36	2.0	4.6	3.7	1.3	
72LZ125305400501	1590	32	1.7	2.8	2.1	1.3	
72LZ125405380497	9000	32	2.7	1.4	.2	3.0	
72LZ125505350493	4500	28	1.9	4.5	2.5	1.7	
72LZ125605330488	2870	30	2.8	4.1	2.8	1.4	
72LZ125705300484	1920	28	1.2	2.2	2.9	1.1	
72LZ125805270480	3760	25	2.0	4.5	2.9	1.0	
72LZ125905250476	3070	36	1.9	2.7	1.9	2.3	
72LZ126005220472	4600	31	2.8	2.5	2.3	3.2	
72LZ126105200468	5200	33	2.0	1.4	1.8	2.4	
72LZ126205180463	1930	31	1.6	1.0	1.8	1.9	
72LZ126305150459	1820	32	1.5	1.6	2.8	1.4	
72LZ126405120455	2340	28	1.2	1.7	2.6	1.2	
72LZ126505100450	3500	36	1.9	2.2	2.6	1.5	
72LZ126605070446	3690	34	2.1	2.6	2.5	2.4	
72LZ126705050442	4460	36	2.0	3.7	2.4	1.3	
72LZ126805020438	6100	30	1.9	2.6	1.9	2.2	
72LZ126904990434	5800	43	1.4	1.2	2.3	1.7	
72LZ127004960430	1540	18	1.1	2.9	3.1	1.6	
72LZ127104940425	2480	21	1.1	1.6	2.1	2.1	
72LZ127204910420	1000	32	1.2	1.3	2.4	1.4	
72LZ127304890416	6000	35	1.8	.9	1.1	4.9	
72LZ127404860412	5100	32	1.6	1.9	1.8	2.8	
72LZ127504840408	3480	32	1.5	2.2	1.6	3.4	
72LZ127604810404	2470	32	1.5	2.6	2.6	1.9	
72LZ127704790400	1330	33	1.4	3.6	2.8	3.4	
72LZ127804760396	1550	27	1.2	2.4	2.9	1.4	
72LZ127904740391	3890	32	1.8	2.4	2.4	2.3	
72LZ128004710386	6700	30	1.7	2.4	2.4	2.3	
72LZ128104680382	2140	29	1.4	1.8	2.6	1.5	
72LZ128204650378	3410	36	1.6	2.6	1.8	2.5	
72LZ128304630373	4700	29	1.5	2.8	.4	3.4	
72LZ128404610369	2670	25	1.2	3.8	.3	3.3	
72LZ128504580365	2960	28	1.3	4.2	.6	4.1	
72LZ128604550361	2470	41	1.7	4.3	1.6	2.5	
72LZ128704530357	2500	29	1.7	4.9	.6	3.7	
72LZ128804500353	3810	25	1.7	4.3	.5	3.1	
72LZ128904470348	1100	27	1.8	3.4	2.3	2.3	
72LZ129004450344	1500	29	1.7	2.4	2.9	1.4	
72LZ129104430340	5200	27	1.3	2.2	.3	2.5	
72LZ129204400335	5400	43	1.6	2.4	.8	2.2	
72LZ129304370331	2440	30	1.5	1.9	2.6	2.0	
72LZ129404340327	2560	27	1.3	2.0	2.6	2.0	
72LZ129504320323	6000	30	1.6	2.2	2.5	2.3	
72LZ129604300319	6600	33	1.7	1.1	1.5	2.8	
72LZ129704270315	4260	22	1.5	2.5	2.3	2.2	
72LZ129804250310	8300	42	2.1	1.8	2.2	3.4	
72LZ129904220306	6200	28	1.4	2.1	2.3	2.7	
72LZ130004200302	3410	34	2.0	2.3	2.8	2.1	
72LZ130104170297	9800	58	2.3	2.1	1.7	2.4	
72LZ130204140293	13300	52	1.6	1.7	1.0	2.0	
72LZ130304110289	10100	41	1.2	.8	.6	2.1	
72LZ130404090285	3550	31	2.0	3.0	2.4	2.0	
72LZ130504060280	2310	23	1.4	2.5	2.3	1.7	
72LZ130604040276	350	26	2.1	3.3	3.6	1.5	
72LZ130704010272	351	31	1.9	4.3	3.2	1.9	
72LZ130803990268	4180	31	2.5	3.5	2.7	2.2	
72LZ130903960264	1750	28	1.4	2.3	3.4	2.1	
72LZ131003940259	2230	25	2.1	4.8	3.1	2.0	
72LZ131103910255	1700	22	1.4	3.2	3.3	2.5	
72LZ131203890250	6050	30	3.7	3.9	2.2	3.2	
72LZ131303860246	2080	18	.8	.8	2.5	1.8	
72LZ131403840242	1150	42	1.8	3.5	1.9	2.3	
72LZ131503810238	1370	41	2.4	3.6	2.6	2.1	
72LZ131603780234	3250	17	1.3	2.5	1.6	2.8	
72LZ131703750230	2730	38	2.9	4.6	3.5	2.5	
72LZ131803730225	4370	28	2.5	3.9	1.6	2.0	
72LZ131903700220	8200	25	4.0	3.9	2.3	1.9	

ATOMIC ABSORPTION ANALYSIS (HN03-HCLO4 DIGESTION)
(EVERY FIFTH SAMPLE - ALL DRILL HOLES)

(VALUES IN PPM)

SAMP.	#	LOC.COORD	AG	NI	ZN	PB	CO	CD	MN	CU
894	0	0	0.0	3.333	36.364	0.0	1.250	0.0	271.618	95.628
899	0	0	0.0	3.333	22.378	0.0	2.500	0.0	190.982	3770.490
900	0	0	0.0	1.667	41.399	0.0	1.250	0.0	280.106	2404.371
905	0	0	0.0	1.667	6.378	6.845	3.750	0.0	72.149	4808.742
910	0	0	0.0	1.667	33.566	0.0	1.250	0.0	216.446	218.579
915	0	0	0.0	0.0	34.685	0.0	0.0	0.0	331.034	1803.280
920	0	0	0.0	0.0	20.699	0.0	3.750	0.0	169.761	38.798
925	0	0	0.0	3.333	363.636	0.0	0.0	0.0	241.910	792.350
930	0	0	0.0	3.333	45.874	0.0	1.250	0.0	292.838	1420.766
935	0	0	0.0	0.0	53.706	0.0	3.750	0.0	466.844	2459.017
940	0	0	0.0	3.333	76.084	0.0	2.500	0.0	254.642	2841.530
945	0	0	0.0	3.333	60.420	0.0	1.250	0.0	415.915	2021.858
950	0	0	0.0	1.667	48.112	0.0	2.500	0.0	594.165	508.197
951	0	0	0.0	5.000	31.329	0.0	3.750	0.0	348.010	2404.371
956	0	0	0.0	3.333	30.769	0.0	1.250	0.0	420.159	792.350
961	0	0	0.0	0.0	19.580	0.0	1.250	0.0	233.422	2.732
966	0	0	0.0	0.0	18.462	0.0	0.0	0.0	339.522	2.186
971	0	0	0.0	3.333	19.580	0.0	0.0	0.0	288.594	1.639
976	0	0	0.0	0.0	27.413	0.0	0.0	0.0	386.207	2.186
981	0	0	0.0	0.0	16.224	0.0	0.0	0.0	246.154	2.186
986	0	0	0.0	0.0	17.902	0.0	0.0	0.0	271.618	1.639
991	0	0	0.0	0.0	21.259	0.0	0.0	0.0	530.504	1.639
996	0	0	0.0	3.333	20.140	0.0	0.0	0.0	891.247	8.743
1000	0	0	0.133	0.0	49.231	82.139	0.0	0.0	1188.329	13.115
1002	0	0	0.0	0.0	18.462	0.0	3.750	0.0	331.034	1.093
1007	0	0	0.199	0.0	369.231	92.406	0.0	8.197	2716.179	22.951
1012	0	0	0.332	0.0	928.671	71.872	0.0	19.126	12307.695	65.574
1017	0	0	0.332	0.0	951.049	273.797	0.0	20.219	9973.477	40.984
1022	0	0	0.266	0.0	1118.881	889.840	0.0	25.137	8063.664	16.940
1027	0	0	0.0	3.333	44.755	0.0	0.0	0.0	305.570	3114.756
1032	0	0	0.0	0.0	42.517	0.0	1.250	0.0	212.202	1803.280
1037	0	0	0.0	0.0	19.021	0.0	1.250	0.0	118.833	683.060
1043	0	0	0.0	1.667	31.888	0.0	0.0	0.0	280.106	3005.464
1048	0	0	0.0	0.0	23.496	0.0	2.500	0.0	237.666	3825.138
1052	0	0	0.0	0.0	55.944	0.0	0.0	0.0	114.589	3551.914
1057	0	0	0.0	0.0	35.804	0.0	0.0	0.0	174.005	2513.662
1062	0	0	0.0	3.333	59.301	0.0	2.500	0.0	386.207	2622.951
1067	0	0	0.0	3.333	39.161	0.0	2.500	0.0	157.029	3278.690
1072	0	0	0.0	3.333	40.280	0.0	1.250	0.0	199.470	737.705
1077	0	0	0.199	3.333	54.825	0.0	0.0	0.0	93.369	4808.742
1082	0	0	0.0	0.0	36.923	0.0	0.0	0.0	169.761	2622.951
1087	0	0	0.0	1.667	32.448	0.0	0.0	0.0	157.029	4316.938
1092	0	0	0.133	0.0	36.923	0.0	0.0	0.0	97.613	3387.979
1097	0	0	0.0	0.0	21.818	0.0	0.0	0.0	161.273	2896.175
1101	0	0	0.199	0.0	16.783	0.0	0.0	0.0	135.809	10109.289
1106	0	0	0.0	0.0	42.517	0.0	0.0	0.0	233.422	2841.530
1111	0	0	0.0	0.0	34.685	0.0	0.0	0.0	169.761	4098.359
1116	0	0	0.133	0.0	4.364	0.0	0.0	0.0	174.005	3770.490
1121	0	0	0.0	0.0	34.126	0.0	0.0	0.0	250.398	3005.464
1126	0	0	0.066	0.0	37.483	0.0	0.0	0.0	224.934	3825.138
1131	0	0	0.066	0.0	30.210	6.845	2.500	0.0	195.226	2185.793
1136	0	0	0.266	3.333	29.650	10.267	1.250	0.0	318.302	4808.742
1141	0	0	0.465	3.333	13.427	3.422	0.0	0.0	216.446	15847.000
1146	0	0	0.0	1.667	38.601	0.0	2.500	0.0	241.910	2732.240
1150	0	0	0.266	3.333	7.385	3.422	0.0	0.0	289.594	6994.535
1155	0	0	0.066	0.0	25.734	6.845	0.0	0.0	161.273	4316.938
1160	0	0	0.133	0.0	27.972	6.845	0.0	0.0	199.470	4371.582
1165	0	0	2.855	6.667	4475.523	13.690	0.0	92.896	42.440	40983.617
1170	0	0	0.0	0.0	34.126	3.422	6.250	0.0	157.029	2732.240
1175	0	0	0.332	0.0	31.329	0.0	0.0	0.0	106.101	7377.051
1180	0	0	0.0	1.667	49.231	0.0	0.0	0.0	207.958	4535.516
1185	0	0	0.0	3.333	31.888	0.0	2.500	0.0	488.063	2896.175
1190	0	0	0.0	3.333	38.042	0.0	1.250	0.0	212.202	1857.924
1195	0	0	0.0	0.0	29.091	0.0	2.500	0.0	250.398	1256.831
1200	0	0	0.133	0.0	7.832	0.0	0.0	0.0	12.308	4098.359
1204	0	0	0.598	3.333	11.189	0.0	0.0	0.0	16.127	10655.742
1209	0	0	0.0	0.0	43.636	0.0	0.0	0.0	288.594	2021.858
1214	0	0	0.0	0.0	22.378	0.0	0.0	0.0	80.637	2459.017
1219	0	0	0.531	0.0	89.510	3.422	0.0	5.464	55.172	10382.516
1224	0	0	0.0	0.0	20.699	3.422	2.500	3.279	229.178	2622.951
1229	0	0	0.0	1.667	22.378	6.845	0.0	2.732	267.374	3661.201
1234	0	0	0.332	0.0	82.797	3.422	0.0	2.732	318.302	3825.138
1239	0	0	0.133	1.667	46.993	0.0	0.0	0.0	301.326	3879.781
1244	0	0	0.0	0.0	48.112	0.0	0.0	0.0	275.862	2568.306
1249	0	0	0.0	0.0	27.413	3.422	0.0	0.0	174.005	1912.569
1254	0	0	0.266	3.333	22.378	6.845	0.0	0.0	233.422	9289.617
1259	0	0	0.0	0.0	21.818	0.0	1.250	0.0	263.130	2950.821
1264	0	0	0.0	0.0	19.021	0.0	0.0	0.0	46.684	2568.306
1269	0	0	0.0	1.667	27.413	10.267	0.0	0.0	216.446	5737.703
1274	0	0	0.066	0.0	18.462	0.0	0.0	0.0	445.623	5519.121
1279	0	0	0.0	0.0	19.580	0.0	0.0	0.0	280.106	3879.781
1284	0	0	0.133	3.333	5.035	6.845	0.0	3.825	976.128	3005.464
1289	0	0	0.0	0.0	16.783	3.422	1.250	2.732	785.146	1256.831
1294	0	0	0.199	0.0	22.378	0.0	0.0	0.0	420.159	2732.240
1299	0	0	0.531	0.0	21.259	0.0	0.0	0.0	339.522	6448.086

LORNEX DRILL-CORE SAMPLES

SPECTROGRAPHIC ANALYSIS

377

(EVERY FIFTH SAMPLE - ALL DRILL HOLES)

(VALUES IN PPM)

SAMP. #	B	SR	TI	IN	V	MO	BA	BIGA	SN
894		700	1500	50	40	600	20		
899	15	400	1000	50	30	600	20		
900	20	500	1000	50	40	30 200	20		
905	15	100	700	40	20	200		5	
910		800	700	50	30	600	20		
915	20	400	2000	50	40	5 500	20		
920		600	1000	50	30	800	20		
925		700	1000	50	30	700	20		
930		600	1000	50	30	600	20		
935		600	1000	50	30	5 600	20		
940		700	1000	50	40	5 600	20		
945	20	500	700	50	30	500	20		
950	20	600	700	50	30	500	20		
951	20	400	1000	50	30	50 500	20		
956	20	400	1000	50	30	400	20		
961		600	600	50	20	800	20		
966	20	500	500	50	20	300	20		
971	20	600	800	50	20	500	20		
976	20	1200	1000	50	20	600	20		
981		600	1000	50	30	700	20		
986		600	1500	50	40	2000	20		
991	10	700	800	50	30	900	20		
996		400	800	60	30	600	20		
1000	15	400	1500	60	30	40 500	20		
1002		500	800	50	20	600	20		
1007	50	400	1000	80	15	15 400	20	4	
1012	50	150	700	300		5 300	20	10	
1017	40	200	600	100		5 300	10	4	
1022	50	300	500	200	1	5 200	20	4	
1027	20	300	1000	50	50	700	20	2	
1032	10	500	1000	50	50	10 800	20	1	
1037	20	300	1500	50	20	500	20	1	
1043	15	400	1500	50	30	50 600	20		
1048	50	200	1000	50	30	5 400	20		
1052	40	300	1000	50	20	500	20		
1057	10	500	1500	50	40	5 600	20		
1062	20	400	1000	50	50	500	20		
1067	20	500	2000	50	50	30 300	20		
1072	10	500	1000	50	20	10 500	20		
1077	50	400	1000	50	40	15 600	20		
1082	20	400	2000	50	40	5 500	20		
1087	30	400	2000	50	40	5 300	20		
1092	60	300	2000	50	40	400 150	20		
1097	15	500	1000	50	40	200 200	20		
1101	20	200	1000	50	50	20 200	20		
1106	10	600	1000	50	50	20 150	20		
1121	20	2001	2001	50	50	40 150	20		
1126	20	700	1000	50	40	10 300	20		
1131	15	1500	1000	50	100	2001 150	20		
1136	30	600	800	50	60	500 150	20		
1141	20	300	1000	50	50	200 500	20		
1146	20	600	1000	50	50	30 300	20		
1150	50	400	1500	50	50	10 500	20		
1155	15	500	800	50	50	700 200	20		
1160	10	500	1000	50	50	500 200	20		
1165	20	300	800	50	20	50 150	15		
1170		400	900	50	30	10 600	20		
1175	20	300	1500	50	40	20 500	20		
1180		500	2000	50	40	10 500	20		
1185	30	200	1500	50	30	3 500	20		
1190		600	1000	50	40	5 500	20		
1195	20	400	1000	50	30	4 500	20		
1200	30	300	1000	50	30	40 400	20		
1204	40		2000	50	50	30 500	20		
1209	20	400	1000	50	30	500	20		
1214	20	300	1500	50	40	10 400	20		
1219	15	200	1000	50	50	40 500	20		
1224	20	800	800	50	40	200	20		
1229	20	500	2000	50	50	500	20		
1234	10	800	700	50	50	8 800	20		
1239	10	800	1500	50	50	20 150	20		
1244	10	1000	1500	50	50	10 150	20		
1249	20	600	2000	50	30	5 500	20		
1254	40	200	2000	50	40	200 700	20		
1259	20	400	2000	50	40	4 400	20		
1264	15	600	2000	50	30	400	20		
1269	15	500	1500	50	40	600	20		
1274	15	500	1500	50	40	600	20		
1279	15	800	2001	50	50	10 800	20		
1284	50	200	1000	50	40	15 300	20		
1289	20	400	2000	50	50	20 500	20		
1294	10	600	1000	50	40	800	20		
1299		500	1000	50	50	700	20		

APPENDIX D

Highmont

(Sample locations and analytical results)

FIGURE 85

Location of samples, Highmont Surface (in pocket)

HIGHMONT SURFACE SAMPLES

ATOMIC ABSORPTION (TOTAL DIGESTION -RAPID TEFLON TUBE PROCEDURE)

(VALUES IN PPM FOR TRACE ELEMENTS AND WT. % FOR MAJOR ELEMENTS)

SAMP. #	LOC.COORD	CU	ZN	FE2O3	CAO	NA2O	K2O
72HS	114290488	1190	75	1.2	2.0	4.1	1.9
72HS	221430474	23	35	1.0	1.5	3.9	1.7
72HS	310370745	397	48	2.2	1.9	2.9	2.0
72HS	505471127	340	36	4.2	3.1	2.7	1.7
72HS	610790467	1050	40	1.6	2.4	3.9	.6
72HS	710750508	2660	34	2.1	2.4	3.3	1.4
72HS	810840548	383	35	1.5	2.0	3.6	1.9
72HS	911150513	8	29	1.0	1.6	3.9	1.4
72HS	1011610490	4	29	1.6	1.8	5.0	.5
72HS	1111680515	47	43	3.2	2.5	4.0	.2
72HS	1212110484	2	26	1.1	1.8	5.0	.5
72HS	1312040368	85	48	3.2	3.5	3.2	1.7
72HS	1412170411	17	37	2.1	2.5	3.2	1.3
72HS	1512200422	407	26	.9	1.8	3.8	1.7
72HS	1612690443	8	21	.9	1.9	4.2	.5
72HS	1712840425	8	27	1.0	1.7	4.0	2.0
72HS	1812750402	9	29	1.5	2.2	4.3	1.2
72HS	1913800477	499	38	1.9	2.3	3.0	1.5
72HS	2013400482	120	36	2.9	2.0	4.3	1.0
72HS	2113410434	48	33	1.8	2.6	4.3	.9
72HS	2213800590	427	35	2.4	2.7	2.9	2.0
72HS	2313800633	97	48	3.9	3.2	3.1	1.9
72HS	2413150507	13	34	2.2	2.1	3.8	1.2
72HS	2513200505	350	37	2.2	2.7	3.3	1.3
72HS	2614110447	27	28	1.3	1.3	4.6	0.8
72HS	2710400530	9	20	2.3	2.4	2.9	1.6
72HS	2810490588	520	22	0.8	1.8	4.0	1.6
72HS	2910270587	2700	24	.8	1.9	3.9	1.9
72HS	3010230555	3820	19	2.0	2.8	3.5	1.5
72HS	3110500484	4260	31	1.8	2.0	3.2	1.4
72HS	3209750385	2410	28	2.1	2.2	3.2	2.4
72HS	3310490452	0007	20	2.6	2.5	3.6	1.2
72HS	3410150468	18	37	1.5	3.0	3.3	1.4
72HS	3510300543	1250	34	2.8	2.6	3.4	2.1
72HS	3608550455	28	30	2.6	3.2	3.6	1.6
72HS	3709360430	100	34	2.5	2.7	3.6	1.9
72HS	3808800487	70	28	2.6	2.6	3.4	2.0
72HS	3909340515	250	30	2.2	2.8	3.8	1.4
72HS	4008960467	107	28	2.2	2.3	3.3	1.7
72HS	4106001124	72	30	2.4	2.9	3.9	1.4
72HS	4202250467	4	15	1.4	3.2	4.0	.1
72HS	4310940844	426	26	2.2	3.2	3.5	1.3
72HS	4406751108	166	26	2.3	3.3	3.5	1.3
72HS	4507000982	141	24	2.5	2.6	3.2	1.5
72HS	4610950807	213	25	2.3	3.3	3.8	1.6
72HS	4704660370	98	30	2.5	3.9	3.9	1.4
72HS	4808700796	40100	61	2.9	4.3	1.4	.6
72HS	4905531101	310	14	1.7	3.1	3.4	1.2
72HS	5005281008	1820	24	2.7	3.8	3.3	1.3
72HS	5107051130	255	21	2.5	3.4	3.5	1.4

SAMP. #	LOC.COORD	CU	ZN	FE2O3	CAO	NA2O	K2O
72HS	5207530959	36	33	2.6	3.7	3.5	1.6
72HS	5311480876	1930	20	1.4	2.4	3.7	1.2
72HS	5406200999	49	20	2.5	3.1	3.4	1.5
72HS	5506751157	111	26	2.4	3.2	3.8	1.4
72HS	5605720999	114	21	2.1	3.1	4.1	1.2
72HS	5704050537	225	24	1.8	2.8	3.8	0.9
72HS	5809320923	134	32	2.5	2.9	3.5	1.5
72HS	5909240958	39	25	2.2	3.4	3.5	1.1
72HS	6008000977	80	23	2.3	2.8	3.4	1.5
72HS	6103700545	830	27	2.5	3.5	3.3	1.3
72HS	6205490549	165	35	2.0	3.4	3.5	2.0
72HS	6305500260	14	23	2.3	2.9	4.1	1.2
72HS	6406100550	44	20	2.1	2.9	3.4	1.6
72HS	6506210770	510	30	2.6	3.8	3.7	1.9
72HS	6606321040	141	25	2.3	3.3	3.7	1.5
72HS	6704121103	196	32	2.5	2.8	3.9	1.9
72HS	6802660696	750	28	2.0	3.3	3.7	1.6
72HS	6902300832	1760	26	1.8	2.4	3.6	2.2
72HS	7004360684	464	46	2.1	2.5	3.2	1.7
72HS	7104100685	168	26	2.6	3.2	3.9	1.7
72HS	7205390683	110	30	2.6	3.4	3.9	2.0
72HS	7301500744	64	19	1.5	2.9	3.7	1.1
72HS	7406360684	1330	29	2.2	2.5	3.3	1.5
72HS	7508380555	164	33	2.0	2.6	3.2	1.6
72HS	7608520560	205	40	2.6	3.3	4.2	1.9
72HS	7707050499	22	28	2.2	3.1	3.9	1.7
72HS	7808230525	93	40	2.2	3.4	3.8	1.3
72HS	7908420648	80	29	2.1	3.1	4.0	1.2
72HS	8008650642	273	22	.7	2.4	4.2	.6
72HS	8108570660	190	21	.6	1.8	4.5	.4
72HS	8208660617	275	41	2.1	2.8	3.6	1.3
72HS	8307900573	670	27	1.9	2.8	3.3	1.7
72HS	8407680578	37	42	2.5	3.8	3.7	1.5
72HS	8508050645	277	29	2.0	3.2	3.5	1.3
72HS	8608290664	32	23	2.3	3.3	3.6	1.5
72HS	8707570666	15	29	2.1	3.3	3.6	1.4
72HS	8807250645	571	25	2.4	2.7	3.8	1.4
72HS	8906900635	137	32	2.7	3.1	3.8	1.5
72HS	9007660612	12	30	2.4	3.0	3.8	1.8
72HS	9108040694	9	20	2.3	3.8	4.4	1.5
72HS	9207950710	110	32	1.9	2.8	3.8	1.5
72HS	9308660683	16	36	2.1	3.3	3.8	1.1
72HS	9408410682	24	35	1.8	2.7	4.0	1.4
72HS	9508320699	150	22	1.9	2.4	4.3	.4
72HS	9608340710	71	34	1.4	2.8	3.8	1.4
72HS	9708420734	99	29	1.4	2.1	4.3	.6
72HS	9808430721	115	21	.7	2.4	4.5	.2
72HS	9908550745	212	21	1.1	2.3	4.5	.3
72HS	10008630770	101	20	1.0	2.1	4.5	.8
72HS	10108720737	205	21	0.6	1.3	4.4	1.2
72HS	10209130732	280	19	0.5	1.6	4.3	.5
72HS	10307680744	16	16	1.0	1.7	4.3	1.2
72HS	10407830740	71	21	1.1	2.0	4.3	1.6
72HS	10507880754	17	32	1.8	3.2	3.9	1.4
72HS	10607950764	8	13	.4	2.8	4.9	.2
72HS	10707990781	8	15	.4	1.8	5.0	.4
72HS	10809250690	2100	13	3.2	.4	2.0	.2

SAMP. #	LOC.COORD	CU	ZN	FE203	CAO	NA2O	K2O
72HS	10909630717	274	18	.5	2.3	3.9	.4
72HS	11010000684	1000	21	.7	1.9	3.9	1.0
72HS	11110640612	707	24	1.0	1.9	3.8	1.6
72HS	11210650629	1307	30	.8	1.8	3.8	1.7
72HS	11310930649	524	32	.9	1.9	4.1	1.3
72HS	11410270648	152	31	.6	1.6	3.8	2.1
72HS	11511440615	473	32	.9	1.5	3.8	1.2
72HS	11611560588	292	32	.8	2.0	4.0	1.6
72HS	11712100598	2690	28	1.3	2.6	3.5	1.4
72HS	11812990669	249	28	1.8	1.9	4.0	1.2
72HS	11911870617	1510	26	.6	1.7	4.1	1.4
72HS	12012130643	556	27	1.5	1.8	3.3	1.5
72HS	12112470724	43	32	1.7	2.2	3.4	1.5
72HS	12213190791	447	47	3.4	5.3	5.9	1.1
72HS	12307960755	244	22	1.7	3.1	3.9	.5
72HS	12411650671	47	29	1.5	2.3	3.5	.9
72HS	12508700796	3370	26	1.9	2.5	3.6	1.6
72HS	12607710663	125	33	2.1	2.9	3.7	1.2
72HS	12707220715	590	27	2.2	3.1	3.7	1.1
72HS	12810910875	158	34	2.3	2.9	3.4	1.2
72HS	12904820734	3520	16	1.0	1.4	.9	2.5
72HS	13004400735	1240	34	1.1	3.1	3.1	2.0
72HS	13107750694	801	37	2.5	3.0	3.5	1.9
72HS	13407480771	481	28	1.3	2.7	3.4	1.3
72HS	13505630835	51	20	1.4	3.0	4.0	.5
72HS	13707400573	267	24	2.0	3.1	3.7	1.7
72HS	13804780635	37	26	2.1	3.0	3.4	1.5
72HS	13908881087	6	23	2.2	3.2	3.8	1.0
72HS	14009560919	672	26	2.2	2.4	3.7	1.4
72HS	14108001012	290	24	1.9	3.0	3.9	1.3
72HS	14206490917	344	27	1.9	2.2	3.5	1.2
72HS	14305760679	221	21	2.1	3.3	3.6	1.3
72HS	14406770737	21	21	1.9	2.9	3.7	1.4
72HS	14507350530	21	24	2.0	3.1	2.6	1.3
72HS	14605070709	121	21	1.7	3.0	4.0	.6
72HS	14704801038	167	26	1.8	3.3	3.6	.8
72HS	14804621100	347	25	2.0	2.8	3.4	1.7
72HS	14908450795	191	26	1.7	3.0	4.2	.5
72HS	15004620761	294	22	1.5	3.4	3.8	.9
72HS	15109341024	4	28	2.2	3.7	3.7	1.3
72HS	15206990950	233	27	2.1	3.0	3.8	1.1
72HS	15304901150	272	25	1.6	3.1	3.9	1.8
72HS	15410370915	314	29	2.6	3.8	3.6	1.1
72HS	15502050527	2920	68	1.3	2.3	1.7	2.7
72HS	15601480552	14	22	1.3	3.2	4.0	.5
72HS	15701630550	51	24	1.4	3.2	4.6	.3
72HS	15802130500	7	15	.9	3.3	4.0	.1
72HS	15901850575	3	18	1.3	3.9	3.7	.2
72HS	16001750600	41	37	1.1	2.3	4.7	.2
72HS	16105271082	146	37	2.1	3.2	3.6	.6
72HS	16204931075	32	26	2.0	2.7	3.7	1.1
72HS	16306960874	153	29	2.1	3.5	3.8	1.1
72HS	16501980575	89	18	1.2	2.3	4.5	.5
72HS	16605761030	320	31	2.3	3.1	3.4	1.0
72HS	16702120780	217	24	2.5	2.8	3.5	1.3
72HS	16801600813	121	19	1.2	1.7	3.3	2.0
72HS	16902130814	210	22	2.2	2.6	3.6	1.7

SAMP. # LOC.COORD	CU	ZN	FE203	CAO	NA2O	K2O
72HS 17002330733	68	21	1.6	2.4	3.6	1.6
72HS 17101350740	23	18	1.3	2.4	4.2	.3
72HS 17201390670	12	24	1.4	1.9	4.2	.4
72HS 17301140664	24	20	1.5	2.3	3.6	.4
72HS 17401551002	22	17	.7	2.1	4.2	.4
72HS 17510250305	37	27	2.2	2.4	3.5	1.5
72HS 17611500290	40	29	2.1	2.5	3.3	1.5
72HS 17712360252	231	28	2.1	2.5	3.5	1.3
72HS 17810250381	108	34	2.2	2.2	3.4	1.5
72HS 17909620608	304	14	1.2	.8	4.1	2.1
72HS 18009500578	338	33	2.0	2.0	3.1	1.6
72HS 18109251250	4	27	2.2	2.6	3.8	1.2
72HS 18209001212	9	30	2.2	2.7	3.7	1.4
72HS 18309441208	4	37	2.0	2.8	3.6	1.3
72HS 18409511220	5	19	2.1	2.9	3.7	1.4
72HS 18509921162	7	25	2.1	3.0	3.6	1.3
72HS 18608351275	5	24	2.2	2.8	3.4	1.5
72HS 18708001230	4	25	1.8	2.6	3.9	.9
72HS 38608100690	132	22	2.5	3.1	3.7	1.2
72HS 33012450925	18	27	2.3	2.9	3.8	1.7
72HS 33113250924	64	21	2.7	3.2	3.6	1.6
72HS 33213420898	14	27	2.5	2.9	3.9	1.7
72HS 33313880925	17	21	2.6	3.2	3.7	2.1
72HS 44508680830	950	26	2.4	3.7	3.5	1.3
72HS 47308950934	179	31	3.2	3.8	4.2	1.2
72HS 61208940874	2160	26	1.8	2.0	4.3	1.2
72HS 66704901101	169	22	1.6	1.6	3.7	2.0
72HS 66810410832	980	29	2.1	2.5	3.6	1.6
72HS 66910400780	364	32	2.4	3.1	3.9	1.8
72HS 67007450690	860	31	1.2	4.2	2.2	1.5
72HS 67108600945	205	27	1.9	2.7	4.2	1.6
72HS 67308950934	629	27	1.5	3.6	3.4	1.5
72HS 67509430785	438	29	2.0	2.7	4.0	1.0
72HS 68909900934	870	29	1.9	2.9	3.9	1.4
72HS 88001160844	374	16	1.9	2.7	3.9	2.6
73HS 51216500505			3.2	3.0	3.1	1.9
73HS 51316200590			3.0	2.8	3.4	2.0
73HS 51416400650			2.9	2.8	3.6	1.9
73HS 51715500800			2.3	3.0	3.6	1.9
73HS 51816500820			2.4	2.9	3.7	2.0
73HS 51915800700			2.6	2.9	3.7	1.8
73HS 52015500940			2.5	3.0	3.8	1.7
73HS 52112501050			2.3	2.9	3.6	1.9

HIGHMONT SURFACE SAMPLES

ATOMIC ABSORPTION ANALYSIS (HNO₃-HClO₄ DIGESTION)

(VALUES IN PPM)

SAMP.	#	LOC.COORD	AG	NI	ZN	PB	CO	CD	MN	CU
1	0	0	0.0	2.000	87.500	110.000	0.0	0.179	251.867	1279.462
2	0	0	0.0	6.000	18.750	5.000	0.0	0.0	200.202	13.468
3	0	0	0.0	8.000	53.125	0.0	0.0	0.0	413.320	336.700
5	0	0	0.0	6.000	40.625	0.0	0.0	0.0	691.020	303.030
6	0	0	0.0	10.000	40.625	0.0	0.0	0.0	381.029	848.485
7	0	0	0.0	4.000	31.250	0.0	0.0	0.357	251.867	2289.562
8	0	0	0.0	6.000	25.000	0.0	0.0	0.0	284.157	336.700
9	0	0	0.0	2.000	25.000	0.0	6.667	0.0	219.576	8.081
10	0	0	0.0	10.000	31.250	0.0	0.0	0.0	290.615	5.387
11	0	0	0.0	6.000	53.125	0.0	10.000	0.179	374.571	64.646
12	0	0	0.0	4.000	25.000	0.0	0.0	0.0	238.951	4.714
13	0	0	0.0	8.000	21.875	0.0	0.0	0.357	232.492	96.296
14	0	0	0.0	4.000	31.250	0.0	0.0	0.357	355.197	841.751
15	0	0	0.0	0.0	12.500	0.0	0.0	0.0	187.286	7.407
16	0	0	0.0	4.000	18.750	0.0	6.667	0.0	180.828	7.407
17	0	0	0.0	0.0	18.750	0.0	0.0	0.0	213.118	4.040
18	0	0	0.0	4.000	21.875	15.000	0.0	0.0	290.615	5.387
19	0	0	0.0	8.000	40.625	0.0	0.0	0.0	257.008	471.381
20	0	0	0.0	10.000	40.625	0.0	0.0	0.0	302.362	63.973
21	0	0	0.0	2.000	46.875	0.0	0.0	0.0	347.716	35.017
22	0	0	0.0	2.000	28.125	0.0	0.0	0.357	226.772	390.573
23	0	0	0.0	18.000	37.500	0.0	0.0	0.179	257.008	84.175
24	0	0	0.0	6.000	31.250	0.0	3.333	0.0	257.008	12.121
25	0	0	0.0	8.000	37.500	0.0	6.667	0.0	287.244	350.168
26	0	0	0.0	6.000	31.250	0.0	0.0	0.0	216.693	22.896
27	0	0	0.0	2.000	18.750	0.0	0.0	0.0	131.024	8.081
28	0	0	0.0	0.0	15.625	0.0	0.0	0.0	156.221	572.391
29	0	0	0.0	0.0	12.500	0.0	6.667	0.179	136.063	2356.903
30	0	0	0.0	0.0	15.625	0.0	0.0	0.0	85.669	10.774
31	0	0	1.500	6.000	31.250	0.0	0.0	0.0	236.850	4040.405
32	0	0	0.0	2.000	21.875	0.0	0.0	0.0	206.614	1481.482
33	0	0	0.0	4.000	18.750	0.0	0.0	0.357	191.496	8.754
34	0	0	0.0	2.000	28.125	0.0	3.333	0.0	181.417	18.855
35	0	0	0.0	2.000	28.125	0.0	0.0	0.0	241.890	1245.792
36	0	0	0.0	0.0	25.000	0.0	0.0	0.0	160.000	26.936
37	0	0	0.0	0.0	28.125	0.0	0.0	0.0	185.000	117.845
38	0	0	0.0	0.0	21.875	0.0	0.0	0.0	180.000	77.441
39	0	0	0.0	6.000	25.000	0.0	0.0	0.0	175.000	228.956
40	0	0	0.0	0.0	25.000	0.0	0.0	0.0	205.000	103.704
41	0	0	0.0	8.000	65.625	0.0	6.667	6.071	230.000	42.424
42	0	0	0.0	6.000	6.250	0.0	0.0	0.0	110.000	5.387
43	0	0	0.0	10.000	25.000	10.000	0.0	0.0	175.000	370.370
44	0	0	0.0	6.000	21.875	0.0	0.0	0.0	180.000	161.616
45	0	0	0.0	4.000	9.375	0.0	0.0	0.0	120.000	134.680
46	0	0	0.0	8.000	18.750	0.0	0.0	0.0	170.000	188.552
47	0	0	0.0	6.000	28.125	10.000	6.667	0.0	210.000	28.283
48	0	0	10.500	10.000	68.750	70.000	0.0	0.0	235.000	37037.047
49	0	0	0.0	4.000	150.000	0.0	0.0	0.0	210.000	309.764
50	0	0	0.0	8.000	18.750	0.0	0.0	0.0	205.000	1481.482
51	0	0	0.0	2.000	6.250	0.0	0.0	0.0	155.000	235.690

SAMP.	#	LOC.	COORD	AG	NI	ZN	PB	CO	CD	MN	CU
52	0	0		0.0	6.000	15.625	0.0	0.0	0.0	190.000	27.609
53	0	0		0.0	2.000	15.625	0.0	0.0	0.0	140.000	1414.142
54	0	0		0.0	4.000	12.500	0.0	6.667	0.0	135.000	29.630
55	0	0		0.0	6.000	25.000	10.000	0.0	0.0	235.000	101.010
56	0	0		0.0	8.000	12.500	0.0	0.0	0.0	170.000	108.271
57	0	0		0.0	6.000	25.000	0.0	6.667	0.0	235.000	227.235
58	0	0		0.0	6.000	31.250	0.0	0.0	0.0	235.000	127.652
59	0	0		0.0	0.0	9.375	0.0	0.0	0.0	105.000	30.075
60	0	0		0.0	6.000	12.500	0.0	0.0	0.0	165.000	62.824
61	0	0		0.0	6.000	34.375	0.0	0.0	0.0	180.000	735.171
62	0	0		0.0	2.000	21.875	0.0	0.0	0.0	210.000	140.351
63	0	0		0.0	2.000	12.500	0.0	0.0	0.0	185.000	10.693
64	0	0		0.0	10.000	12.500	0.0	6.667	0.0	140.000	44.110
65	0	0		0.0	8.000	18.750	0.0	0.0	0.0	155.000	467.836
66	0	0		0.0	2.000	15.625	0.0	0.0	0.0	145.000	83.542
67	0	0		0.0	6.000	25.000	0.0	0.0	0.0	175.000	160.401
68	0	0		0.0	8.000	21.875	0.0	6.667	0.0	195.000	802.005
69	0	0		0.0	16.000	25.000	0.0	6.667	0.0	155.000	1604.010
70	0	0		0.0	6.000	50.000	0.0	0.0	0.0	320.000	421.052
71	0	0		0.0	6.000	18.750	0.0	0.0	0.0	160.000	137.009
72	0	0		0.0	6.000	21.875	0.0	0.0	0.0	150.000	110.276
73	0	0		0.0	4.000	25.000	0.0	0.0	0.0	210.000	70.175
74	0	0		0.0	2.000	25.000	0.0	0.0	0.0	140.000	1403.509
75	0	0		0.0	6.780	16.068	5.714	2.520	0.0	145.535	124.808
76	0	0		0.0	6.780	19.450	0.0	2.520	0.0	212.978	130.946
77	0	0		0.0	2.712	11.416	0.0	0.0	0.0	110.039	7.775
78	0	0		0.0	4.068	17.590	0.0	0.0	0.0	177.482	85.115
79	0	0		0.0	1.356	13.784	0.0	2.520	0.0	113.589	64.655
80	0	0		0.0	1.356	10.825	0.0	0.0	0.0	78.092	245.524
81	0	0		0.0	1.356	10.148	0.0	0.0	0.0	70.993	146.496
82	0	0		0.0	5.424	22.410	5.714	3.780	0.331	145.535	159.591
83	0	0	0.571	0.0	5.424	14.799	0.0	0.0	0.0	152.635	699.744
84	0	0		0.0	1.356	19.873	0.0	0.0	0.0	166.833	31.509
85	0	0		0.0	1.356	15.645	0.0	0.0	0.0	124.237	204.604
86	0	0		0.0	4.068	8.118	0.0	0.0	0.0	85.191	5.729
87	0	0		0.0	4.068	9.556	0.0	2.520	0.0	85.191	13.913
88	0	0		0.0	5.424	13.446	2.857	0.0	0.0	127.787	396.931
89	0	0		0.0	6.780	14.545	0.0	0.0	0.0	159.734	112.532
90	0	0		0.0	2.712	11.586	0.0	0.0	0.0	106.489	380.563
91	0	0		0.0	1.356	6.004	2.857	2.520	0.0	49.695	3.683
92	0	0		0.0	4.068	12.883	0.0	0.0	0.0	124.237	51.969
93	0	0		0.0	2.712	8.986	0.0	2.520	0.0	117.138	13.095
94	0	0		0.0	1.356	15.905	0.0	1.260	0.031	152.635	12.276
95	0	0		0.0	1.356	8.748	0.0	0.0	0.0	88.741	130.128
96	0	0		0.0	5.424	15.507	0.0	0.0	0.0	156.184	56.061
97	0	0		0.0	4.068	12.724	0.0	0.0	0.0	141.986	103.120
98	0	0		0.0	2.712	10.099	0.0	0.0	0.0	85.191	114.578
99	0	0		0.0	5.424	11.133	0.0	2.520	0.0	102.940	204.604
100	0	0		0.0	1.356	9.145	0.0	0.0	0.016	92.291	53.197
101	0	0		0.0	0.0	9.940	0.0	0.0	0.0	92.291	163.683
102	0	0		0.0	1.356	8.986	0.0	0.0	0.0	81.642	265.985
103	0	0		0.0	2.712	7.952	0.0	0.0	0.0	102.940	6.138
104	0	0		0.0	1.356	8.907	0.0	0.0	0.0	106.489	54.425
105	0	0		0.0	2.712	13.917	0.0	0.0	0.031	156.184	9.821
106	0	0		0.0	1.356	5.567	0.0	0.0	0.0	63.894	5.320
107	0	0		0.0	2.712	5.567	0.0	0.0	0.0	60.344	5.729
108	0	0		0.0	1.356	3.579	0.0	0.0	0.0	56.794	2250.639

SAMP.	#	LOC.	COORD	AG	NI	ZN	PB	CO	CD	MN	CU
109	0	0		0.0	1.356	10.179	5.714	0.0	0.0	92.291	270.077
110	0	0		0.0	4.068	12.406	0.0	2.520	0.0	110.039	879.795
111	0	0		0.571	4.068	12.962	5.714	2.520	0.0	145.535	748.849
112	0	0		0.571	0.0	15.189	0.0	0.0	0.031	120.688	1207.161
113	0	0		0.0	0.486	14.630	0.0	0.0	0.0	134.886	511.509
114	0	0		0.0	0.0	9.979	0.0	0.0	0.0	78.092	130.946
115	0	0		0.286	0.243	19.619	0.0	0.0	0.047	152.635	511.509
116	0	0		0.0	0.0	16.068	5.714	0.0	0.0	149.085	278.261
117	0	0		0.0	0.729	17.252	14.286	0.0	0.0	170.383	2127.878
118	0	0		0.0	0.729	16.913	0.0	0.0	0.0	184.581	225.064
119	0	0		0.0	0.0	14.799	0.0	0.0	0.0	124.237	1350.384
120	0	0		0.571	0.973	20.127	0.0	2.520	0.031	181.032	634.271
121	0	0		0.571	1.216	22.495	0.0	2.520	0.047	198.780	46.240
122	0	0		0.0	0.729	19.027	0.0	2.520	0.0	184.581	184.143
123	0	0		0.0	0.973	16.913	5.714	0.0	0.0	170.383	278.261
124	0	0		0.571	0.486	23.848	0.0	0.0	0.062	216.528	48.696
125	0	0		0.0	0.973	19.873	0.0	0.0	0.031	202.329	3069.053
126	0	0		0.571	0.243	21.987	0.0	2.520	0.031	234.276	115.806
127	0	0		0.0	0.486	19.535	0.0	2.520	0.016	234.276	654.731
128	0	0		0.857	0.243	24.947	5.714	1.260	0.047	262.673	163.683
129	0	0		0.0	0.0	3.383	0.0	0.0	0.0	134.886	3069.053
130	0	0		0.0	0.0	22.833	0.0	0.0	0.031	255.574	1084.399
131	0	0		0.571	5.424	24.693	0.0	2.520	0.221	372.712	789.874
134	0	0		0.0	2.712	18.605	0.0	0.0	0.0	404.659	567.089
135	0	0		0.0	1.356	12.770	0.0	0.0	0.0	207.654	57.114
137	0	0		0.0	5.424	13.192	0.0	2.520	0.0	228.952	214.684
138	0	0		0.0	4.068	14.884	0.0	2.520	0.0	218.303	44.962
139	0	0		0.0	2.712	11.924	0.0	0.0	0.0	250.250	4.051
140	0	0		0.0	2.712	16.237	0.0	1.260	0.0	282.196	757.469
141	0	0		0.0	1.356	14.630	0.0	2.520	0.0	266.223	186.329
142	0	0		0.0	2.712	10.233	0.0	0.0	0.0	186.356	206.582
143	0	0		0.0	2.712	18.605	5.714	1.260	0.0	314.143	405.063
144	0	0		0.0	0.0	12.600	0.0	0.0	0.0	244.925	27.949
145	0	0		0.0	4.068	13.108	0.0	0.0	0.0	287.521	18.633
146	0	0		0.0	2.712	14.884	0.0	0.0	0.0	298.170	137.722
147	0	0		0.0	0.0	18.858	0.0	0.0	0.221	335.440	186.329
148	0	0		0.0	1.356	15.222	0.0	0.0	0.0	260.898	388.861
149	0	0		0.0	2.712	21.226	0.0	0.0	0.221	356.739	222.785
150	0	0		0.0	3.711	20.686	5.424	2.000	0.0	247.589	396.694
151	0	0		0.0	4.948	15.394	0.0	0.0	0.0	186.540	7.052
152	0	0		0.0	3.711	22.129	0.0	1.000	0.0	257.764	282.094
153	0	0		0.0	2.474	16.356	0.0	2.000	0.0	193.323	308.540
154	0	0		0.0	3.711	18.761	0.0	1.000	0.0	230.630	401.102
155	0	0		2.712	1.237	62.538	16.271	0.0	0.263	830.949	3129.476
156	0	0		0.0	1.237	15.586	0.0	2.000	0.0	193.323	11.901
157	0	0		0.0	2.474	20.204	0.0	0.0	0.0	206.889	60.826
158	0	0		0.0	1.237	9.621	0.0	0.0	0.0	128.882	14.545
159	0	0		0.0	3.711	12.989	0.0	2.000	0.0	166.190	5.289
160	0	0		0.0	1.237	30.788	0.0	1.000	0.263	169.581	47.603
161	0	0		0.0	4.948	29.826	0.0	3.000	0.0	440.912	167.493
162	0	0		0.0	2.474	18.280	0.0	2.000	0.0	220.456	39.669
163	0	0		0.0	8.660	17.318	0.0	3.000	0.0	193.323	198.347
165	0	0		0.0	2.474	13.470	0.0	1.000	0.0	189.931	112.397
166	0	0		0.0	4.948	24.053	0.0	1.000	0.263	210.281	370.248
167	0	0		0.0	6.186	20.686	0.0	2.000	0.0	244.197	255.647
168	0	0		0.0	2.474	13.470	0.0	0.0	0.0	149.232	141.047
169	0	0		0.0	4.948	17.799	0.0	2.000	0.0	213.672	215.978

SAMP.	#	LOC.COORD	AG	NI	ZN	PB	CU	CD	MN	CU
170	0	0	0.0	3.711	12.989	0.0	1.000	0.0	172.973	77.135
171	0	0	0.0	2.474	14.913	0.0	0.0	0.0	169.581	30.854
172	0	0	0.0	2.474	18.761	0.0	1.000	0.0	176.365	11.019
173	0	0	0.0	2.474	10.968	0.0	2.000	0.0	139.057	26.006
174	0	0	0.0	3.711	11.930	0.0	0.0	0.0	149.232	29.972
175	0	0	0.0	4.948	17.318	0.0	2.000	0.0	200.106	52.011
176	0	0	0.0	3.711	16.356	0.0	0.0	0.0	220.456	39.669
177	0	0	0.0	2.474	17.318	5.424	0.0	0.0	217.064	220.386
178	0	0	0.0	1.237	20.686	0.0	1.000	0.263	220.456	127.824
179	0	0	0.0	0.0	7.505	0.0	2.000	0.0	91.574	352.617
180	0	0	0.542	4.948	23.572	5.424	2.000	0.263	291.680	453.995
181	0	0	0.0	2.474	14.817	0.0	0.0	0.0	200.106	8.815
182	0	0	0.0	2.474	18.569	0.0	0.0	0.0	237.414	11.901
183	0	0	0.0	2.474	23.860	0.0	0.0	0.132	234.022	7.493
184	0	0	0.0	1.237	9.140	0.0	0.0	0.0	115.315	7.052
185	0	0	0.0	3.711	12.989	0.0	0.0	0.0	159.407	12.342
186	0	0	0.0	2.474	12.989	0.0	0.0	0.0	186.540	10.138
187	0	0	0.0	3.711	17.607	0.0	0.0	0.0	234.022	8.815
386	0	0	0.0	3.711	16.837	0.0	1.000	0.0	169.581	136.639
330	0	0	0.0	2.474	15.875	0.0	2.000	0.0	142.448	15.868
331	0	0	0.0	1.237	12.123	0.0	0.0	0.0	122.099	62.149
332	0	0	0.0	3.711	15.201	0.0	0.0	0.0	145.840	14.545
333	0	0	0.0	4.948	11.064	0.0	0.0	0.0	108.532	14.545
345	0	0	0.542	2.474	17.318	5.424	2.000	0.0	122.099	850.689
473	0	0	0.0	3.711	19.242	2.712	1.000	0.0	210.281	143.251
612	0	0	0.542	2.474	21.648	5.424	2.000	0.0	176.365	2203.857
667	0	0	0.0	1.237	12.508	0.0	0.0	0.0	108.532	189.532
668	0	0	0.0	3.711	20.686	0.0	2.000	0.526	206.889	903.582
669	0	0	0.0	4.948	19.050	0.0	2.000	0.0	149.232	387.879
670	0	0	0.0	1.237	21.648	0.0	1.000	0.395	240.805	907.990
671	0	0	0.0	1.237	12.508	0.0	0.0	0.0	125.490	176.309
673	0	0	0.0	1.237	19.242	5.424	0.0	0.0	261.155	683.196
675	0	0	0.0	1.237	19.435	0.0	0.0	0.0	189.931	409.917
689	0	0	0.0	3.711	19.242	0.0	2.000	0.0	172.973	771.350
880	0	0	0.0	0.0	10.629	0.0	0.0	0.0	106.101	382.514
512			0.	1.123	21.270	0.0	0.0	0.0	186.275	349.232
513			0.0	0.545	16.491	0.0	0.0	0.0	146.740	308.214
514			0.0	0.954	39.486	2.114	0.0	0.0	233.948	74.936
517			0.0	.	16.378	1.0	0.0	0.0	156.810	55.945
518			0.	0.	20.786	.0	0.0	0.	200.335	34.974
519			0.0	.0	20.283	0.0	0.0	0.0	177.941	38.791
520			0.0	0.0	17.572	1.114	0.0	0.0	145.856	17.021
521			0.0	0.0	17.243	0.842	0.0	0.0	149.546	15.426

HIGHMONT SURFACE SAMPLES
SPECTROGRAPHIC ANALYSIS
(VALUES IN PPM)

1	10 700	1000	40	20	700	20
2A	101000	2001	60	50	1000	15
3	50 500	2001	60	60	15 400	30
5	50 40	2000	50	50	300	20 10
6	20 500	2001	60	50	400	20
7	20 800	2000	60	40	800	20
8	30 800	2001	50	40	81000	20
9	20 700	2000	60	30	1000	20
10	2001 400	2001	60	60	100	20
11	2001 400	2001	60	70		30
12	401000	2000	70	40	150	20
13	101000	2000	70	60	800	20
14	201000	2001	60	60	1500	20
15	501000	1000	60	40	1500	20
16	201000	1000	60	20	500	20
17	15 500	700	60	10	700	20
18	10 800	1000	50	20	1000	20
19	1500	2000	60	50	800	20
20	151200	2000	50	20	1000	20
21	20011000	2000	60	20	300	20
22	1500	2000	50	50	800	20
23	151200	2000	50	50	1000	20
24	201200	2000	50	50	5 800	20
25	101200	2000	50	50	1000	20
26	151000	2000	50	50	101000	20
27	1000	2000	50	50	500	20
28	50 150	2000	40	50	15 400	20
29	400 800	2000	50	50	200	20
30	1000	2000	50	50	700	20
31	101000	2000	50	60	1000	20
32	10 800	2000	40	50	1000	20
33	1000	1000	50	30	500	15
34	800	1500	50	40	500	15
35	20 800	2001	60	50	1000	20
36	800	2001	40	40	800	20
37	700	2001	50	40	1000	15
38	1000	2001	40	40	1000	15
39	800	2001	40	40	5 800	20
40	700	2001	40	40	20 700	20
41	10 800	2001	50	40	500	20
42	101000	1501	50	30	300	20
43	20 400	2001	50	40	15 400	20
44	600	2000	60	40	800	15
45	20 700	2000	60	40	600	20
46	700	2000	60	40	5 600	20
47	800	2000	60	40	500	20
48	600	1500	50	402001	500	10
49	15 600	2000	50	30	4 400	20
50	1000	2000	50	40	20 400	20
51	1000	2001	50	50	3 800	20

SAMP. #	B	SR	TI	IN	V	MO	BA	BIG	SN
52		800	1000	50	30		1000	20	
53	20	500	1000	50	30		400	15	
54		800	2000	50	50		700	20	
55		700	2001	50	50		400	20	
56		900	2000	50	50	15	800	20	
57		700	2001	50	60	5	400	20	
58		700	1500	50	50		800	20	
59		700	2000	50	50		900	20	
60		600	2000	50	50		700	20	
61		800	2000	50	50		1000	20	
62		700	800	50	30		800	15	
63		600	2001	50	50		500	15	
64		800	2000	50	50		700	20	
65		700	2001	50	50	7	700	20	
66		700	2000	50	50		600	20	
67		800	2001	50	50	7	700	20	
68		800	2001	50	50		1000	20	
69		700	2001	50	50	10	800	20	
70	15	300	2000	60	50	30	300	20	
71		500	2000	50	40		600	15	
72		700	2000	50	60	10	800	15	
73	10	700	2000	50	50	15	1000	20	
74		800	2001	50	60	40	700	20	
75		1000	2000	60	50		800	20	
76		101000	2001	50	60	30	800	20	
77		10 800	2000	50	50		700	20	
0-		077	5777	17	27		277	57	
79		151000	2001	50	50		700	20	
80		101500	2000	50	30		400	20	
81		751000	2000	50	30		300	20	
82		151000	2001	50	60		1000	20	
83		700	2000	50	50	10	800	20	
84		600	1500	50	40		700	20	
85		800	2000	50	50		800	20	
86		600	2000	50	40		700	15	
87		600	2001	50	40		700	15	
88		201000	1500	50	30		500	20	
89		201500	600	60	20		400	20	
90		151000	1000	50	20		400	20	
91		201000	1500	50	30		800	20	
92		20 500	800	50	20		700	20	
93		10 800	1000	50	20		300	20	
94		10 700	800	50	20		700	20	
95		10 800	600	50	20		800	20	
96		1000	2000	50	50		700	20	
97		601000	1000	50	30		200	20	
98		101000	2000	60	50		1000	20	
99		101000	2001	60	50		1000	20	
100		201000	2000	50	40		500	20	
101		101000	2000	60	50		700	20	
102		1000	2000	60	60		1000	20	
103		1000	2000	60	40		700	20	
104		201000	800	60	20		400	20	
105		101000	1500	50	40		800	20	
106		101000	800	50	30		700	20	
107		1000	1000	50	40		600	20	
108		2001 150	1000	50	10	15	300	30	

SAMP. #	B SR	TI	IN	V	MO	BA	BIGA	SN
109	301500	800	60	30		500	20	
110	30 800	1000	50	30		1000	20	
111	15 700	2000	50	40		101500	20	
112	20 700	1000	50	30		1000	20	
113	15 900	1000	50	20		800	20	
114	15 500	700	50	15		800	20	
115	15 800	2000	50	40		1000	20	
116	30 700	1500	50	30		1000	20	
117	20 800	1500	50	40		81000	20	
118	201500	1500	50	40		1500	20	
119	201000	800	50	20		800	20	
120	201000	700	50	30		800	20	
121	201000	2000	50	40		700	20	
122	101500	1000	50	40		1000	20	
123	201500	1000	50	40		400	20	
124	20 800	2000	50	50		300	20	
125	15 800	800	50	50		15 500	20	
126	15 800	2000	50	50		10 600	20	
127	151500	1000	60	40		1500	20	
128	30 600	2001	50	50		600	20	
129	60 150	2000	50	30		2001 500	20	
130	50 400	2001	50	50		300 500	20	
131	1000	2000	50	50		101000	20	
134	15 400	800	50	30		300	20	
135	101000	800	50	40		400	20	
137	800	1500	60	40		15 700	20	
138	700	1500	50	50		800	20	
139	700	2000	50	40		1000	20	
140	10 800	1000	50	40		1500	20	
141	800	1500	50	40		800	20	
142	800	1500	50	50		800	20	
143	700	1500	50	50		400	15	
144	201000	2001	60	60		5 800	20	
145	201000	2001	60	60		800	20	
146	501000	2000	60	50		150 300	20	
147	151000	2000	60	50		5 400	20	
148	15 800	2000	60	50		5 800	20	
149	15 800	2001	60	50		200	20	
150	201000	2001	60	50		40 700	20	
151	101000	2000	60	50		1000	20	
152	151000	1500	50	40		400	20	
153	10 500	800	50	40		700	20	
154	101000	2000	50	50		20 700	20	
155	50 400	2000	60	40		50 500	20	
156	201000	2001	60	40		200	20	
157	101000	1000	50	30		300	20	
158	1500	1000	50	30		200	20	
159	1000	800	50	30		400	20	
160	151000	1000	50	20		4 400	20	
161	101000	1000	50	40		400	20	
162	201000	1500	50	50		41500	20	
163	201500	2001	50	60		15 700	20	
165	101000	800	60	20		300	20	
166	1000	2000	50	50		4 600	20	
167	101000	2001	50	80		700	20	
168	600	1000	50	30		700	20	
169	20 800	700	50	30		600	20	

SAMP. #	B	SR	TI	IN	V	MC	BA	BIGA	SN
170		700	800	50	30		600	20	
171		151000	1500	50	20		150	15	
172		101000	800	50	20		1000	20	
173		600	800	50	20		800	20	
174		800	700	50	20	20	500	20	
175		700	2000	50	40		41000	20	
176		800	1000	50	30		700	20	
177		700	1000	50	30		700	20	
178		700	2000	50	40		800	20	
179	500	300	1000	50	15	51	1000	20	
180	15	500	1000	50	40		800	20	
181	10	600	700	50	30		800	20	
182		600	1000	50	50		800	20	
183		500	1500	50	40		500	20	
184		600	1000	50	30		500	20	
185	10	600	700	50	40		800	20	
186		600	1000	50	50		800	20	
187	40	600	1000	50	30		600	20	
386		151000	1000	50	40	600	800	20	
330		500	1500	50	50		500	20	
331		1000	1000	50	40		1000	20	
332		800	1000	50	40		800	20	
333		800	1000	50	40		1000	20	
345	20	150	2000	50	40		500	20	
473		601200	1000	50	50	51	500	20	
612	40	800	2000	50	50		300	20	
667	10	400	1000	50	20		600	20	
668	10	800	2001	50	40	10	400	20	
669	50	1000	2000	50	50		500	20	
670	40	400	2000	50	50	4	500	20	
671	40	800	1500	50	40		600	20	
673	20	700	2000	50	50	10	500	20	
675		1000	1500	50	40		300	20	
689		800	700	50	40		500	20	
880		600	600	50	20		700	20	
512	0	600	1500	50	40	50	700	020	0
513	0	600	1000	50	30	0	700	020	0
514	0	500	1500	50	30	20	800	020	0
517	0	600	1500	50	40	0	700	020	0
518	0	700	1000	50	30	0	800	020	0
519	0	600	1500	50	30	0	800	020	0
520	0	600	1000	50	30	0	800	020	0
521	0	500	800	50	30	0	700	020	0

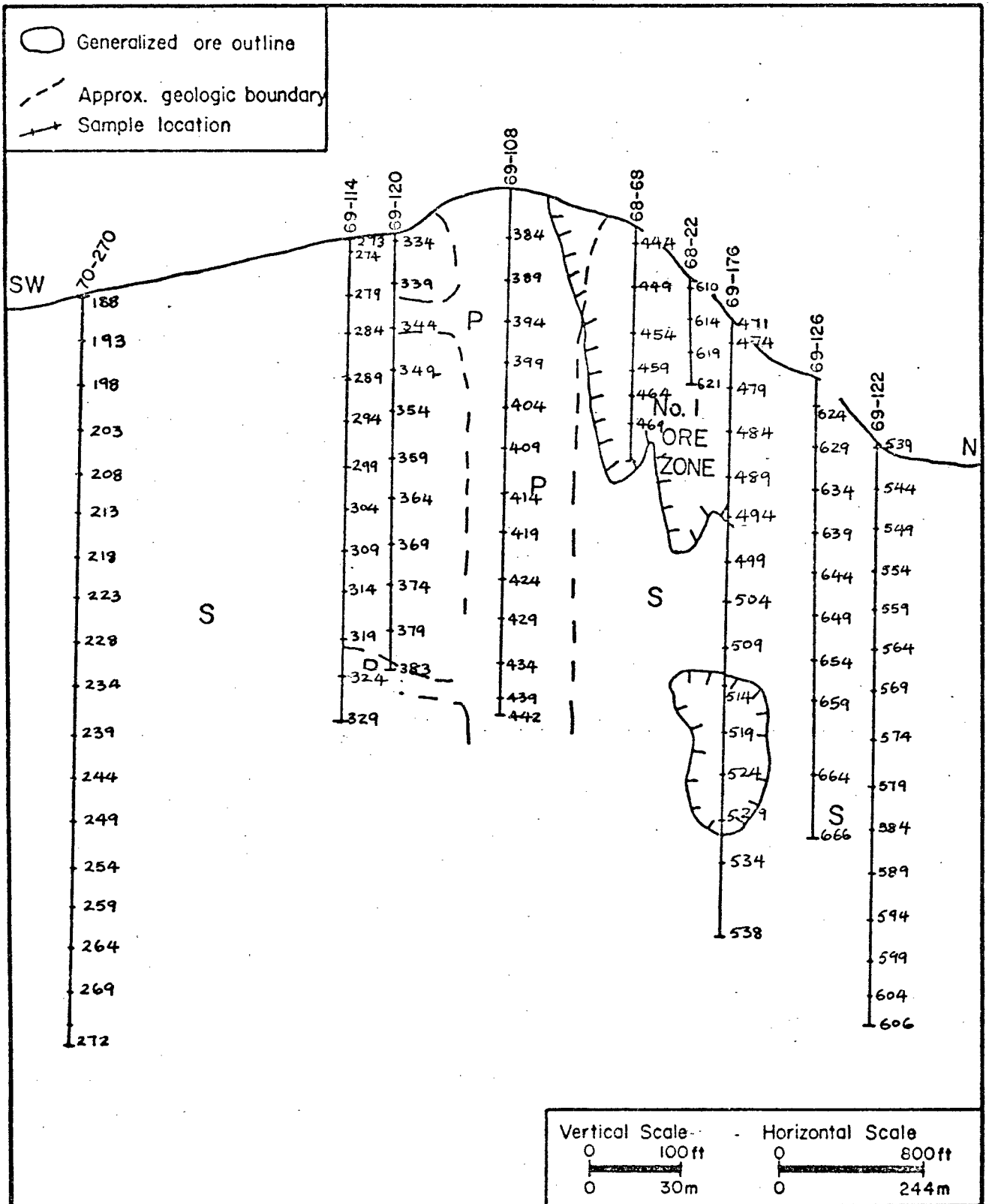


FIGURE 86: Location of drill-core samples, Highmont property (every 5th sample)

(VALUES IN PPM FOR TRACE ELEMENTS
AND WT. % FOR MAJOR ELEMENTS)

DRILL-HOLE 70-270

SAMP. #	LOC.COORD	CU	ZN	FE2O3	CAO	NA2O	K2O
72HZ	18800500505	4	27	2.6	4.0	3.1	1.3
72HZ	18900500500	7	21	2.0	3.1	3.5	1.4
72HZ	19000500495	8	22	2.1	2.8	3.6	1.3
72HZ	19100500490	9	24	2.1	3.0	3.5	1.2
72HZ	19200500485	13	22	2.3	2.8	3.7	.6
72HZ	19300500480	8	22	1.8	2.7	3.4	2.2
72HZ	19400500475	7	22	1.9	3.0	3.8	1.3
72HZ	19500500470	6	25	1.9	2.8	3.6	1.3
72HZ	19600500465	7	28	2.0	2.7	3.8	1.6
72HZ	19700500460	1	24	1.9	2.8	3.7	1.5
72HZ	19800500455	1	26	1.9	2.7	3.7	1.6
72HZ	19900500450	4	26	2.0	2.9	3.8	1.4
72HZ	20000500445	8	24	2.1	2.7	3.9	1.0
72HZ	20100500440	152	24	2.0	2.7	3.7	1.3
72HZ	20200500435	140	37	1.9	1.6	4.5	.5
72HZ	20300500430	3	25	2.0	3.0	3.7	1.0
72HZ	20400500425	11	26	2.0	2.7	3.5	1.1
72HZ	20500500420	234	30	1.6	3.3	3.9	0.6
72HZ	20600500415	41	27	2.0	3.5	3.6	0.7
72HZ	20700500410	13	20	2.1	2.9	3.7	1.0
72HZ	20800500405	14	25	2.3	2.8	3.4	1.2
72HZ	20900500400	10	24	2.1	2.8	3.9	1.2
72HZ	21000500395	599	26	2.1	3.2	3.2	1.2
72HZ	21100500390	45	36	2.1	2.6	3.8	0.9
72HZ	21200500385	8	22	1.9	2.8	3.3	1.2
72HZ	21300500380	1140	23	2.1	2.3	3.2	1.3
72HZ	21400500375	14	20	2.4	2.4	2.6	1.1
72HZ	21500500370	6	26	1.8	2.7	3.3	1.3
72HZ	21600500365	6	20	2.0	2.5	3.5	1.2
72HZ	21700500360	6	15	1.9	2.6	3.5	1.2
72HZ	21800500355	3	17	1.5	2.3	3.2	1.7
72HZ	21900500350	13	20	1.6	2.2	3.0	1.8
72HZ	22000500345	7	28	1.9	2.9	3.3	1.1
72HZ	22100500340	12	25	1.4	2.1	3.2	1.5
72HZ	22200500335	138	21	1.5	2.1	3.2	1.6
72HZ	22300500330	5	21	1.7	2.3	2.9	1.4
72HZ	22400500325	990	31	1.7	2.7	3.7	1.0
72HZ	22500500320	30	32	1.5	2.0	3.5	0.7
72HZ	22600500315	4	22	1.8	2.7	3.7	1.7
72HZ	22700500310	8	18	1.8	2.5	3.8	1.6
72HZ	22800500305	22	23	1.7	3.4	4.0	.9
72HZ	22900500300	6	25	2.0	2.6	3.9	1.1
72HZ	23000500295	7	22	1.9	3.0	3.5	1.4
72HZ	23100500290	10	23	1.9	3.0	4.0	1.7
72HZ	23200500285	9	24	2.1	2.8	3.9	1.6
72HZ	23300500280	4	20	1.9	3.2	4.1	1.5
72HZ	23400500275	6	18	1.6	3.1	3.8	1.5
72HZ	23500500270	5	13	1.3	1.9	3.9	3.4
72HZ	23600500265	4	12	1.3	2.3	4.4	1.0
72HZ	23700500260	26	17	1.9	3.1	4.0	1.7
72HZ	23800500255	16	22	1.5	2.3	4.1	1.0
72HZ	23900500250	10	20	2.1	2.5	4.1	1.9
72HZ	24000500245	1100	18	1.7	3.0	3.5	1.2
72HZ	24100500240	24	20	1.9	2.1	4.2	1.5
72HZ	24200500235	32	22	1.6	2.4	4.2	0.8
72HZ	24300500230	14	16	1.0	3.6	1.2	0.9
72HZ	24400500225	18	30	1.9	6.1	3.1	1.0
72HZ	24500500220	5	23	1.6	2.9	4.6	1.4
72HZ	24600500215	2	18	1.8	3.0	3.9	1.3
72HZ	24700500210	7	27	1.9	2.9	3.9	1.2
72HZ	24800500205	8	25	2.0	2.4	3.8	1.6
72HZ	24900500200	3	18	1.8	2.7	3.8	1.5
72HZ	25000500195	154	34	2.1	3.4	2.4	1.0
72HZ	25100500190	12	26	2.1	2.8	3.9	1.5
72HZ	25200500185	9	27	2.0	2.7	4.5	1.0
72HZ	25300500180	34	28	1.7	3.2	4.8	0.8
72HZ	25400500175	36	18	1.6	4.5	3.5	1.2
72HZ	25500500170	2	18	2.1	2.9	4.0	1.4
72HZ	25600500165	4	25	2.4	3.1	4.1	1.7
72HZ	25700500160	2	21	2.2	3.2	3.9	1.5
72HZ	25800500155	6	24	2.2	3.0	4.3	1.6
72HZ	25900500150	183	18	2.1	2.6	3.7	1.7
72HZ	26000500145	13	20	2.5	3.3	4.0	1.6
72HZ	26100500140	10	25	2.1	3.7	4.9	.4
72HZ	26200500135	13	18	2.0	3.1	4.0	1.4
72HZ	26300500130	11	27	2.3	3.0	4.2	1.2
72HZ	26400500125	64	28	1.9	3.1	4.8	.8
72HZ	26500500120	8	29	2.3	3.4	3.6	1.0
72HZ	26600500115	5	25	2.2	3.6	4.4	.7
72HZ	26700500110	7	29	2.3	3.9	3.9	1.4
72HZ	26800500105	8	31	2.2	3.2	4.0	1.5
72HZ	26900500100	8	25	2.0	5.2	3.8	1.2
72HZ	27000500095	5	25	2.1	2.9	4.2	0.7
72HZ	27100500090	6	31	2.3	1.8	5.7	0.7
72HZ	27200500085	8	26	2.7	2.9	4.7	0.6

DRILL-HOLE 69-114

SAMP. # LOC.COORD	CU	ZN	FE2O3	CAO	NA2O	K2O
72HZ 27303650540	35	21	2.2	3.4	4.4	1.5
72HZ 27403650535	56	24	2.5	3.4	4.4	1.4
72HZ 27503650530	19	29	2.3	3.4	4.3	1.6
72HZ 27603650525	242	33	2.7	5.2	4.0	1.1
72HZ 27703650520	94	35	1.7	3.6	4.7	1.2
72HZ 27803650515	124	16	1.1	1.2	5.4	1.5
72HZ 27903650510	134	32	1.8	2.9	5.2	0.7
72HZ 28003650505	168	30	2.1	2.8	4.9	0.8
72HZ 28103650500	345	27	1.8	2.0	5.5	0.7
72HZ 28203650495	83	28	2.3	2.3	4.8	1.0
72HZ 28303650490	147	29	2.2	1.3	4.6	1.2
72HZ 28403650485	138	28	2.2	2.7	4.8	1.1
72HZ 28503650480	43	21	2.1	2.4	2.9	1.7
72HZ 28603650475	99	30	2.4	2.7	4.3	1.5
72HZ 28703650470	18	24	2.4	2.9	4.0	1.6
72HZ 28803650465	17	22	1.2	5.0	5.4	1.3
72HZ 28903650460	4140	17	2.4	15.6	2.5	0.8
72HZ 29003650455	49	20	1.9	2.6	3.9	1.8
72HZ 29103650450	216	33	1.6	3.1	4.3	1.6
72HZ 29203650445	203	30	1.7	2.7	3.7	1.7
72HZ 29303650440	67	20	1.7	2.9	3.6	1.6
72HZ 29403650435	217	28	2.1	2.9	4.5	1.1
72HZ 29503650430	92	38	2.4	2.9	5.0	.9
72HZ 29603650425	187	31	1.3	3.2	3.4	.8
72HZ 29703650420	58	29	1.7	3.2	4.5	.9
72HZ 29803650415	135	27	2.0	4.1	4.6	.8
72HZ 29903650410	452	42	2.1	2.2	4.3	.8
72HZ 30003650405	12300	40	2.0	4.4	2.5	1.5
72HZ 30103650400	118	22	1.9	2.7	3.9	1.8
72HZ 30203650395	97	32	2.0	2.7	3.7	1.8
72HZ 30303650390	34	23	2.2	3.0	4.4	1.7
72HZ 30403650385	40	30	2.5	2.9	3.7	1.8
72HZ 30503650380	26	34	2.3	3.0	3.7	1.7
72HZ 30603650375	118	23	2.2	2.8	4.3	1.8
72HZ 30703650370	241	29	1.7	1.9	3.7	1.4
72HZ 30803650365	29	32	2.1	3.2	3.9	1.3
72HZ 30903650360	50	31	2.1	2.0	4.7	1.4
72HZ 31003650355	21	26	2.3	3.1	3.8	1.7
72HZ 31103650350	182	31	2.2	2.9	3.8	1.7
72HZ 31203650345	56	26	2.1	3.5	4.0	1.5
72HZ 31303650340	13	18	2.2	3.0	3.4	1.6
72HZ 31403650335	291	26	2.0	3.7	3.6	1.0
72HZ 31503650330	82	26	1.9	2.7	4.1	1.4
72HZ 31603650325	35	42	2.2	3.3	3.8	2.2
72HZ 31703650320	33	39	2.1	3.6	4.0	1.2
72HZ 31803650315	113	39	2.0	2.3	3.9	1.5
72HZ 31903650310	4610	34	2.2	3.5	2.0	3.4
72HZ 32003650305	176	42	2.1	2.3	3.8	2.0
72HZ 32103650300	372	35	2.2	2.3	4.4	1.0
72HZ 32203650295	126	24	1.9	2.4	3.6	1.8
72HZ 32303650290	540	31	2.5	6.7	3.0	1.4
72HZ 32403650285	1940	23	2.1	3.0	3.7	2.2
72HZ 32503650280	780	27	2.1	3.3	3.8	2.3
72HZ 32603650275	212	29	2.3	4.2	3.6	1.8
72HZ 32703650270	13	29	2.4	3.3	3.5	2.1
72HZ 32803650265	80	18	2.1	2.6	3.1	1.8
72HZ 32903650260	980	33	2.1	2.9	2.9	1.8

DRILL-HOLE 69-120

SAMP. #	LOC.COORD	CU	ZN	FE2O3	CAO	NA2O	K2O
72HZ	33404150540	193	29	2.7	2.2	3.6	1.8
72HZ	33504150535	177	22	1.7	2.0	3.9	1.4
72HZ	33604150530	570	23	2.7	3.4	3.7	1.5
72HZ	33704150525	353	25	2.7	3.4	3.9	1.4
72HZ	33804150520	219	26	2.6	3.3	4.0	1.6
72HZ	33904150515	417	27	2.8	2.3	4.0	1.8
72HZ	34004150510	670	26	2.8	2.9	3.7	1.3
72HZ	34104150505	277	21	2.7	2.9	3.8	1.6
72HZ	34204150500	318	25	2.3	3.0	3.6	1.6
72HZ	34304150495	333	21	2.0	1.4	3.2	1.6
72HZ	34404150490	381	24	2.4	2.7	3.7	1.7
72HZ	34504150485	2070	22	1.3	2.5	.7	2.5
72HZ	34604150480	4450	27	2.3	2.5	3.8	1.2
72HZ	34704150475	550	27	1.6	2.6	4.2	1.1
72HZ	34804150470	470	26	2.4	2.8	3.9	1.3
72HZ	34904150465	210	22	2.0	2.3	4.2	1.3
72HZ	35004150460	2560	25	2.6	2.7	3.9	1.6
72HZ	35104150455	160	20	1.5	2.0	3.7	2.4
72HZ	35204150450	710	23	2.0	1.9	3.8	1.7
72HZ	35304150445	530	21	2.2	2.8	4.0	1.6
72HZ	35404150440	910	27	2.1	3.3	3.6	1.1
72HZ	35504150434	660	24	1.8	2.2	3.8	2.2
72HZ	35604150430	540	26	2.2	2.5	4.1	1.8
72HZ	35704150425	850	29	2.0	2.1	4.2	1.0
72HZ	35804150420	730	30	2.1	2.1	4.3	1.4
72HZ	35904150415	276	20	1.8	2.3	3.5	2.3
72HZ	36004150410	1070	27	2.2	3.4	3.4	1.9
72HZ	36104150405	1010	21	1.9	2.6	3.8	1.8
72HZ	36204150400	890	29	2.1	2.7	3.9	1.0
72HZ	36304150395	1010	35	2.1	2.6	3.4	1.6
72HZ	36404150390	1020	29	2.0	2.0	3.9	1.3
72HZ	36504150385	376	38	2.4	3.4	3.0	1.8
72HZ	36604150380	398	23	1.7	2.7	3.7	1.9
72HZ	36704150375	630	26	1.9	2.6	3.5	1.6
72HZ	36804150370	270	27	1.5	1.9	4.0	1.0
72HZ	36904150365	750	29	2.2	2.6	4.1	1.6
72HZ	37004150360	830	27	1.8	2.4	4.1	1.4
72HZ	37104150355	408	28	1.9	2.4	4.3	1.0
72HZ	37204150350	352	34	2.0	2.2	4.3	0.7
72HZ	37304150345	286	31	2.4	3.4	3.5	1.0
72HZ	37404150340	307	32	2.0	2.1	4.4	.8
72HZ	37504150335	700	26	2.4	2.8	3.9	1.3
72HZ	37604150330	349	31	2.2	2.5	4.3	.8
72HZ	37704150325	760	38	2.2	2.2	4.8	.8
72HZ	37804150320	980	26	2.2	3.2	3.1	1.6
72HZ	37904150315	156	18	1.1	2.0	2.5	1.5
72HZ	38004150310	630	30	1.8	2.7	3.7	2.3
72HZ	38104150305	1040	24	1.8	1.8	2.9	1.7
72HZ	38204150300	810	22	1.6	2.1	3.5	1.2
72HZ	38304150295	960	16	1.8	2.1	3.4	2.9

DRILL-HOLE 69-108

SAMP. #	LOC. COORD	CU	ZN	FE2O3	CAO	NA2O	K2O
72HZ	38405500570	236	25	2.4	2.9	3.8	1.5
72HZ	38505500565	890	24	2.3	2.8	4.0	1.2
72HZ	38605500560	132	22	2.5	3.1	3.7	1.2
72HZ	38705500555	29	26	2.8	3.5	3.9	1.2
72HZ	38805500550	36	27	2.3	2.7	4.0	.8
72HZ	38905500545	1460	23	1.4	2.2	4.1	1.4
72HZ	39005500540	2440	23	2.0	2.4	3.1	1.6
72HZ	39105500535	491	19	1.5	2.0	4.1	1.8
72HZ	39205500530	2040	23	2.0	1.8	4.3	1.5
72HZ	39305500525	469	21	1.5	2.3	4.3	1.8
72HZ	39405500520	189	40	3.3	2.7	3.5	1.2
72HZ	39505500515	510	35	1.9	2.5	4.4	.9
72HZ	39605500510	1340	27	1.2	1.4	3.9	1.4
72HZ	39705500505	66	29	1.3	2.3	4.3	1.0
72HZ	39805500500	94	32	1.4	2.2	4.8	2.0
72HZ	39905500495	620	26	1.6	1.4	3.1	1.4
72HZ	40005500490	1820	30	1.9	2.3	2.5	.8
72HZ	40105500485	670	31	2.1	2.4	3.7	1.8
72HZ	40205500480	314	37	3.2	2.8	2.9	1.5
72HZ	40305500475	27	35	3.0	3.0	3.5	1.4
72HZ	40405500470	72	37	1.8	3.9	3.4	0.9
72HZ	40505500465	99	43	2.1	2.9	3.8	1.6
72HZ	40605500460	188	45	3.2	2.8	4.0	1.5
72HZ	40705500455	466	22	2.0	2.9	3.7	1.9
72HZ	40805500450	73	28	2.1	3.4	3.9	1.0
72HZ	40905500445	57	27	2.4	3.3	4.0	1.4
72HZ	41005500440	190	36	2.5	3.5	2.4	.8
72HZ	41105500435	39	35	3.0	2.4	4.2	1.5
72HZ	41205500430	1450	32	1.8	2.7	3.7	1.5
72HZ	41305500425	527	27	1.9	2.5	4.0	1.2
72HZ	41405500420	15	34	1.8	4.2	3.1	.9
72HZ	41505500415	1780	24	1.4	2.4	4.1	1.3
72HZ	41605500410	860	31	1.8	2.7	4.4	1.3
72HZ	41705500405	135	26	1.5	2.7	4.5	1.6
72HZ	41805500400	14	22	1.1	2.6	3.6	1.5
72HZ	41905500395	24	25	1.3	2.4	4.0	1.7
72HZ	42005500390	271	24	1.3	3.1	3.9	1.4
72HZ	42105500385	77	26	1.3	2.1	3.8	1.6
72HZ	42205500380	89	97	.9	1.1	.8	1.3
72HZ	42305500375	85	22	1.3	2.2	4.2	1.2
72HZ	42405500370	89	16	1.0	2.6	3.9	1.5
72HZ	42505500365	574	16	1.0	2.5	2.8	.9
72HZ	42605500360	236	19	1.1	2.9	4.4	.6
72HZ	42705500355	93	21	1.5	2.4	4.3	.9
72HZ	42805500350	89	19	1.3	2.7	4.2	1.5
72HZ	42905500345	9	20	1.4	2.5	4.6	.7
72HZ	43005500340	222	30	1.7	3.6	3.8	.7
72HZ	43105500335	138	30	2.2	2.9	3.8	.7
72HZ	43205500330	870	22	1.4	2.6	4.2	.6
72HZ	43305500325	387	13	2.1	4.6	2.2	1.0
72HZ	43405500320	489	21	1.3	2.4	4.1	.5
72HZ	43505500315	154	21	1.0	3.1	3.9	1.0
72HZ	43605500310	306	23	1.6	2.7	4.1	1.2
72HZ	43705500305	35	10	.6	1.0	3.2	2.9
72HZ	43805500300	44	29	1.7	2.5	4.4	1.3
72HZ	43905500295	32	26	1.5	2.2	4.5	1.6
72HZ	44005500290	71	24	1.5	2.3	4.1	1.6
72HZ	44105500285	34	33	1.9	2.6	4.5	1.5
72HZ	44205500280	205	26	1.5	3.3	3.7	1.2

DRILL-HOLE 68-68

SAMP. #	LOC.COORD	CU	ZN	FE2O3	CAO	NA2O	K2O
72HZ	44307000545	396	38	2.9	3.4	3.9	1.4
72HZ	44407000540	6680	20	1.2	4.5	0.8	1.4
72HZ	44507000535	950	26	2.4	3.7	3.5	1.3
72HZ	44607000530	2100	29	2.4	3.1	3.7	1.4
72HZ	44707000525	1180	32	2.7	3.4	3.8	1.3
72HZ	44807000520	6150	29	2.8	3.2	3.7	1.8
72HZ	44907000515	6350	32	2.0	2.0	4.6	2.5
72HZ	45007000510	249	33	1.5	2.7	4.6	1.3
72HZ	45107000505	1670	26	2.2	3.3	4.2	1.0
72HZ	45207000500	1800	23	2.6	3.2	4.1	1.0
72HZ	45307000495	1030	26	2.5	3.1	4.0	1.0
72HZ	45407000490	2120	32	3.8	3.8	3.2	.9
72HZ	45507000485	1950	19	2.0	2.9	3.9	.6
72HZ	45607000480	3550	27	2.1	2.3	3.8	1.1
72HZ	45707000475	444	23	2.1	3.7	3.8	1.1
72HZ	45807000470	2550	28	3.0	2.4	3.8	1.2
72HZ	45907000465	66	23	2.6	3.5	4.2	.9
72HZ	46007000460	368	29	2.6	2.7	4.2	1.2
72HZ	46107000455	199	36	2.8	3.3	4.1	1.4
72HZ	46207000450	214	29	2.5	3.4	3.8	1.1
72HZ	46307000445	2448	30	2.4	3.1	4.0	1.4
72HZ	46407000440	116	28	2.5	3.2	4.0	1.5
72HZ	46507000435	4300	22	2.2	3.0	3.7	1.6
72HZ	46607000430	1610	24	2.3	3.3	4.0	1.7
72HZ	46707000425	3050	28	1.9	3.4	3.4	1.6
72HZ	46807000420	3550	26	2.8	3.7	4.0	1.8

DRILL-HOLE 69-176

SAMP. #	LOC.COORD	CU	ZN	FE2O3	CAO	NA2O	K2O
72HZ	47108100495	1400	27	3.8	1.8	6.1	.8
72HZ	47208100490	2880	35	3.1	2.4	5.1	.8
72HZ	47308100485	179	31	3.2	3.8	4.2	1.2
72HZ	47408100480	83	32	3.1	3.3	3.8	1.5
72HZ	47508100475	62	33	2.6	3.3	4.0	1.5
72HZ	47608100470	17	37	2.5	3.3	4.3	1.5
72HZ	47708100465	233	29	2.4	2.8	4.0	1.4
72HZ	47808100460	1910	38	2.3	3.5	4.3	1.3
72HZ	47908100455	33	33	2.5	3.4	4.1	1.5
72HZ	48008100450	9	32	2.4	3.7	4.4	1.5
72HZ	48108100445	28	39	2.8	3.5	4.2	1.4
72HZ	48208100440	164	31	2.4	2.8	4.0	1.4
72HZ	48308100435	61	33	2.4	3.0	4.0	1.4
72HZ	48408100430	107	40	2.6	3.1	4.2	1.6
72HZ	48508100425	268	31	2.4	2.8	3.8	1.5
72HZ	48608100420	1400	45	2.3	3.4	1.6	2.4
72HZ	48708100415	114	28	2.6	2.8	4.0	1.1
72HZ	48808100410	6260	22	2.0	2.6	4.2	.7
72HZ	48908100405	548	32	2.8	3.0	3.9	1.4

72HZ	49008100400	489	30	2.7	2.9	3.9	1.5
72HZ	49108100395	468	31	2.7	3.1	3.8	1.4
72HZ	49208100390	425	33	2.8	2.8	3.9	1.5
72HZ	49308100385	1530	34	2.7	2.9	3.9	1.5
72HZ	49408100380	1160	30	2.1	2.8	4.3	1.3
72HZ	49508100375	382	29	2.5	3.0	3.8	1.6
72HZ	49608100370	580	31	2.5	2.9	3.9	1.7
72HZ	49708100365	88	31	2.5	2.6	3.8	1.5
72HZ	49808100360	216	30	2.5	3.1	3.8	1.6
72HZ	49908100355	330	32	2.5	3.2	4.1	1.2
72HZ	50008100350	6850	24	2.3	2.0	0.7	4.5
72HZ	50108100345	67	28	2.2	3.3	4.5	1.6
72HZ	50208100340	42	28	2.3	3.3	4.5	1.5
72HZ	50308100335	2440	35	2.2	2.7	4.4	1.6
72HZ	50408100330	290	32	2.3	3.0	4.2	1.3
72HZ	50508100325	76	29	2.3	3.1	4.1	1.5
72HZ	50608100320	323	33	2.1	2.6	4.5	1.3
72HZ	50708100315	6850	35	2.4	2.3	2.4	2.1
72HZ	50808100310	435	27	2.2	3.1	3.9	1.0
72HZ	50908100305	154	28	2.3	3.3	3.6	1.4
72HZ	51008100300	25	27	2.3	3.4	4.0	1.3
72HZ	51108100295	1380	38	2.3	2.8	4.0	1.4
72HZ	51208100290	229	30	2.3	3.2	3.7	1.3
72HZ	51308100285	256	33	2.0	2.4	4.0	1.3
72HZ	51408100280	3260	25	2.2	2.7	3.9	1.5
72HZ	51508100275	2030	33	2.1	2.7	4.0	1.5
72HZ	51608100270	630	36	2.0	2.4	4.7	1.3
72HZ	51708100265	467	31	1.8	2.6	4.0	1.8
72HZ	51808100260	1890	35	1.9	2.5	4.2	1.2
72HZ	51908100255	630	36	2.1	2.8	4.0	1.5
72HZ	52008100250	133	27	2.0	2.5	4.1	1.5
72HZ	52108100245	890	25	1.6	2.7	4.1	1.7
72HZ	52208100240	301	27	1.9	2.9	3.9	1.7
72HZ	52308100235	1340	39	1.6	2.2	3.2	3.8
72HZ	52408100230	720	25	1.6	2.1	3.9	1.9
72HZ	52508100225	2110	32	1.8	2.5	3.9	1.4
72HZ	52608100220	376	30	1.8	3.0	3.9	1.4
72HZ	52708100215	286	26	1.4	2.4	4.0	1.8
72HZ	52808100210	12	28	2.1	2.9	4.0	1.3
72HZ	52908100205	438	23	2.6	5.1	4.7	1.8
72HZ	53008100200	148	15	3.1	8.1	5.6	1.3
72HZ	53108100195	399	25	2.0	3.2	4.1	1.3
72HZ	53208100190	112	22	1.9	3.0	3.1	.9
72HZ	53308100185	640	29	2.0	2.2	4.0	1.6
72HZ	53408100180	410	23	1.5	2.7	3.4	1.0
72HZ	53508100175	525	22	2.0	2.6	3.3	1.5
72HZ	53608100170	840	25	2.1	2.5	3.5	1.5
72HZ	53708100165	1550	23	1.8	2.6	4.0	1.1
72HZ	53808100160	1160	24	1.6	2.7	3.5	1.5

DRILL-HOLE 69-122

SAMP. #	LOC.COORD	CU	ZN	FE2O3	CAO	NA2O	K2O
72HZ	53909850425	15	23	2.3	2.8	4.4	1.1

72HZ	54009850420	5	25	2.2	3.0	4.0	1.0
72HZ	54109850415	25	20	1.1	2.1	3.8	1.0
72HZ	54209850410	142	20	1.7	2.7	4.0	1.5
72HZ	54309850405	442	19	1.7	2.7	4.0	1.5
72HZ	54409850400	1500	18	1.7	2.2	4.0	1.6
72HZ	54509850395	35	17	1.6	2.4	4.1	1.7
72HZ	54609850390	2100	17	2.5	1.3	3.8	2.1
72HZ	54709850385	430	20	2.9	2.2	3.5	2.0
72HZ	54809850380	90	25	1.9	2.8	4.1	1.4
72HZ	54909850375	930	21	1.7	2.9	4.1	1.1
72HZ	55009850370	474	22	1.6	2.7	4.0	1.1
72HZ	55109850365	650	20	1.3	2.5	4.3	1.2
72HZ	55209850360	29	27	2.4	3.0	4.1	1.3
72HZ	55309850355	9	21	2.1	4.0	3.7	1.3
72HZ	55409850350	21	20	1.9	3.3	3.7	1.3
72HZ	55509850345	31	24	2.6	3.1	3.8	1.3
72HZ	55609850340	17	18	2.6	3.0	3.7	1.6
72HZ	55709850335	55	23	3.0	3.4	4.1	1.3
72HZ	55809850330	960	63	3.3	5.5	4.1	1.4
72HZ	55909850325	36	22	2.5	2.8	4.0	1.0
72HZ	56009850320	208	24	2.4	3.2	4.0	1.2
72HZ	56109850315	165	27	2.6	2.9	3.7	1.2
72HZ	56209850310	12	27	2.3	3.0	3.9	1.1
72HZ	56309850305	9	27	2.3	3.4	3.8	1.4
72HZ	56409850300	33	18	1.7	1.7	3.5	2.4
72HZ	56509850295	49	24	2.8	3.6	3.8	1.4
72HZ	56609850290	8	24	1.8	3.3	3.9	1.3
72HZ	56709850285	143	23	2.1	3.6	4.0	1.2
72HZ	56809850280	10	27	2.2	3.3	4.0	1.3
72HZ	56909850275	11	23	1.8	3.6	4.1	1.4
72HZ	57009850270	17	25	2.6	3.1	3.7	1.0
72HZ	57109850265	9	20	2.0	2.4	4.0	1.2
72HZ	57209850260	10	23	2.0	3.9	3.6	1.2
72HZ	57309850255	11	28	2.0	7.7	.9	0.9
72HZ	57409850250	102	23	2.2	3.5	3.8	1.1
72HZ	57509850245	8	19	1.4	1.6	3.6	2.0
72HZ	57609850235	5	23	2.3	3.2	3.8	1.2
72HZ	57709850230	399	23	2.8	2.7	1.3	1.8
72HZ	57809850225	77	20	2.7	2.6	3.9	1.5
72HZ	57909850220	25	22	2.2	2.9	4.0	1.6
72HZ	58009850215	8	22	1.9	2.8	4.0	1.3
72HZ	58109850210	146	18	2.1	2.9	4.0	1.4
72HZ	58209850205	10	119	1.9	2.9	4.0	1.6
72HZ	58309850200	8	27	2.0	3.0	4.0	1.4
72HZ	58409850195	146	24	1.8	3.1	4.1	1.5
72HZ	58509850190	10	24	2.3	3.2	3.8	1.2
72HZ	58609850185	8	24	2.3	2.7	3.8	1.3
72HZ	58709850180	17	21	1.7	3.0	3.8	1.5
72HZ	58809850175	8	25	2.3	3.1	3.9	1.3
72HZ	58909850170	11	28	2.5	2.9	3.9	1.4
72HZ	59009850165	11	31	2.3	3.5	3.8	1.2
72HZ	59109850160	14	30	2.3	3.2	3.9	1.3
72HZ	59209850155	83	31	2.1	3.1	4.0	1.4
72HZ	59309850150	37	33	1.7	2.9	4.0	1.3
72HZ	59409850145	9	41	2.4	3.0	4.1	1.3
72HZ	59509850140	7	42	2.3	3.2	4.0	1.4
72HZ	59609850135	6	44	2.0	2.7	4.0	1.3
72HZ	59709850130	135	48	1.7	2.6	3.9	1.5
72HZ	59809850125	780	110	2.3	2.8	3.8	1.4
72HZ	59909850120	590	31	3.5	2.2	2.7	1.8
72HZ	60009850115	503	97	2.6	2.7	3.5	1.6
72HZ	60109850110	213	41	1.8	3.3	4.0	1.3
72HZ	60209850105	154	38	2.4	2.8	3.6	1.6
72HZ	60309850100	91	27	1.4	2.7	3.9	2.1
72HZ	60409850095	268	30	1.8	2.7	3.8	1.8
72HZ	60509850090	150	34	1.8	3.1	3.6	1.6
72HZ	60609850085	64	37	2.0	3.2	4.2	1.6

DRILL-HOLE 68-22

SAMP. #	LOC.COORD	CU	ZN	FE2O3	CAO	NA2O	K2O
72HZ	61007650520	1010	18	1.1	2.1	4.7	1.2
72HZ	61107650515	373	22	2.0	2.6	4.4	1.1
72HZ	61207650510	2160	26	1.8	2.0	4.3	1.2
72HZ	61307650505	295	24	2.3	3.1	3.9	1.2
72HZ	61407650500	521	23	2.3	3.0	4.1	1.4
72HZ	61507650495	169	25	2.3	3.1	4.0	1.9
72HZ	61607650490	254	30	2.2	2.8	3.9	1.3
72HZ	61707650485	383	31	2.5	2.1	4.0	1.4
72HZ	61807650480	540	31	2.4	3.0	3.9	1.6
72HZ	61907650475	700	32	2.4	2.8	3.4	1.5
72HZ	62007650470	528	32	2.5	2.6	3.7	1.5
72HZ	62107650465	548	27	1.9	2.8	3.9	1.2

DRILL-HOLE 69-126

SAMP. #	LOC.COORD	CU	ZN	FE2O3	CAO	NA2O	K2O
72HZ	62209150460	21	25	1.9	3.1	3.9	1.4
72HZ	62309150455	9	25	1.7	3.2	3.8	1.1
72HZ	62409150450	8	23	2.1	3.4	3.9	1.3
72HZ	62509150445	14	15	1.3	2.5	3.6	.7
72HZ	62609150440	10	20	1.7	4.0	4.1	.4
72HZ	62709150435	39	12	.9	2.8	3.8	.4
72HZ	62809150430	6	18	.9	3.4	3.8	.3
72HZ	62909150425	542	23	1.3	4.0	4.1	.3
72HZ	63009150420	51	22	1.5	4.0	3.8	.6
72HZ	63109150415	318	25	2.0	3.2	4.3	1.3
72HZ	63209150410	256	20	1.8	4.8	4.0	.4
72HZ	63309150405	14	20	1.6	4.8	4.4	.3
72HZ	63409150400	61	17	1.5	4.5	3.9	.3
72HZ	63509150395	10	15	1.8	5.6	3.3	.6
72HZ	63609150390	21	15	1.4	3.9	4.6	.2
72HZ	63709150385	6	19	1.4	4.2	3.7	.4
72HZ	63809150380	53	19	1.9	3.8	4.2	.6
72HZ	63909150375	790	19	1.8	3.5	4.3	.6
72HZ	64009150370	13	18	1.6	4.3	4.0	.7
72HZ	64109250365	18	19	1.7	3.8	4.2	.6
72HZ	64209150360	59	18	1.4	2.6	3.7	1.4
72HZ	64309150355	682	13	.9	2.4	4.1	1.0
72HZ	64409150350	234	19	1.2	3.5	4.1	1.0
72HZ	64509150345	165	11	.8	5.0	1.9	.5
72HZ	64609150340	1030	16	1.1	3.5	4.3	.5
72HZ	64709150335	41	17	1.2	3.4	4.1	.7
72HZ	64809150330	291	18	1.5	3.2	3.8	.7
72HZ	64909150325	120	17	1.3	4.0	4.0	.5
72HZ	65009150320	700	21	1.5	2.6	4.4	.7
72HZ	65109150315	354	22	2.1	3.3	4.2	.9
72HZ	65209150310	35	20	1.4	3.6	3.9	.5
72HZ	65309150305	8	17	1.2	4.0	7.1	.7
72HZ	65409150300	17	21	1.7	3.1	4.0	1.3
72HZ	65509150295	23	14	1.4	3.9	3.8	.7
72HZ	65609150290	71	13	1.6	3.5	4.1	.6
72HZ	65709150285	89	20	1.6	2.9	3.8	1.8
72HZ	65809150280	599	21	1.9	2.7	3.8	1.6
72HZ	65909150275	384	26	1.7	2.5	4.4	1.3
72HZ	66009150270	7960	24	2.3	3.0	4.0	1.5
72HZ	66109150265	463	21	1.7	2.5	4.0	1.5
72HZ	66209150260	431	22	1.7	2.9	4.0	1.6
72HZ	66309150255	247	24	2.2	2.5	3.9	1.2
72HZ	66409150250	5	20	2.2	3.8	4.1	1.9
72HZ	66509150245	346	23	1.4	3.8	4.6	1.2
72HZ	66609150240	12	20	2.1	3.3	3.9	1.6

HIGHMONT DRILL-CORE SAMPLES

ATOMIC ABSORPTION ANALYSIS (HNO3-HClO4 DIGESTION)

(VALUES IN PPM)

(EVERY FIFTH SAMPLE - ALL DRILL HOLES)

SAMP. #	LOC.COORD	AG	NI	ZN	PB	CO	CD	MN	CU
188	0 0	0.0	2.474	18.280	0.0	2.000	0.0	308.638	7.934
193	0 0	0.0	1.237	12.026	0.0	0.0	0.0	118.707	4.408
198	0 0	0.0	1.237	15.394	0.0	0.0	0.0	189.931	3.967
203	0 0	0.0	1.237	19.242	0.0	0.0	0.263	193.323	6.171
208	0 0	0.0	0.0	18.761	0.0	2.000	0.0	203.498	7.934
213	0 0	0.0	3.711	20.974	5.424	2.000	0.0	206.889	1410.469
218	0 0	0.0	1.237	18.280	0.0	2.000	0.0	206.889	4.408
223	0 0	0.0	0.0	11.545	0.0	0.0	0.0	145.840	3.526
228	0 0	0.0	2.474	20.204	0.0	0.0	0.395	203.498	24.242
234	0 0	0.0	1.237	14.432	0.0	0.0	0.0	169.581	7.493
239	0 0	0.0	4.948	16.296	0.0	1.000	0.0	212.504	8.367
244	0 0	1.250	3.711	25.556	10.000	1.000	0.0	531.259	13.147
249	0 0	0.0	2.474	17.037	0.0	1.000	0.0	212.504	3.187
254	0 0	0.0	3.711	15.185	6.667	0.0	0.264	403.757	32.669
259	0 0	0.0	2.474	14.815	0.0	0.0	0.0	233.754	159.363
264	0 0	0.0	3.711	24.444	0.0	2.000	0.0	340.006	75.697
269	0 0	0.0	3.711	21.111	6.667	1.000	0.0	467.508	13.546
274	0 0	0.0	2.474	12.593	0.0	0.0	0.0	148.753	59.761
279	0 0	0.0	4.948	25.556	0.0	2.000	0.0	382.506	130.677
284	0 0	0.0	2.474	22.222	0.0	1.000	0.0	318.755	139.442
289	0 0	0.0	1.237	15.556	0.0	0.0	0.0	255.004	68.526
294	0 0	0.0	2.474	21.111	0.0	2.000	0.0	276.255	203.187
299	0 0	0.0	2.474	43.704	0.0	2.000	0.0	391.006	529.880
304	0 0	0.0	1.237	20.741	0.0	2.000	0.0	284.755	44.622
309	0 0	0.0	3.711	24.074	0.0	1.000	0.0	340.006	52.191
314	0 0	0.0	0.0	22.222	0.0	0.0	0.0	446.257	278.884
319	0 0	1.250	2.474	18.148	10.000	0.0	0.0	450.507	3864.540
324	0 0	0.0	1.237	19.630	3.333	0.0	0.0	310.255	1792.830
329	0 0	0.0	1.237	27.778	0.0	0.0	0.0	382.506	1095.618
334	0 0	0.0	0.0	22.593	0.0	1.000	0.0	318.755	199.203
339	0 0	0.0	3.711	21.481	0.0	0.0	0.0	327.255	398.406
344	0 0	0.0	2.474	18.889	0.0	2.000	0.0	306.005	410.358
349	0 0	1.250	1.237	20.000	6.667	3.000	0.0	297.505	235.060
354	0 0	0.0	2.474	27.407	0.0	3.000	0.0	318.755	908.367
359	0 0	0.0	3.711	15.926	0.0	2.000	0.0	250.754	294.821
364	0 0	0.0	4.948	22.593	0.0	2.000	0.0	340.006	1047.809
369	0 0	0.0	1.237	23.333	0.0	0.0	0.0	318.755	637.450
374	0 0	0.0	2.474	29.630	0.0	2.000	0.264	323.005	354.582
379	0 0	0.0	0.0	14.074	0.0	0.0	0.0	204.003	159.363
384	0 0	0.0	3.711	21.481	0.0	2.000	0.0	318.755	270.916
389	0 0	0.0	1.237	19.630	0.0	0.0	0.0	276.255	1414.343
394	0 0	0.0	2.474	31.111	0.0	0.0	0.264	374.006	219.123
399	0 0	0.0	1.237	16.296	0.0	0.0	0.0	216.754	569.721
404	0 0	0.0	2.474	27.407	0.0	0.0	0.0	510.008	72.908
409	0 0	0.0	1.237	21.481	0.0	0.0	0.0	369.756	76.494
414	0 0	0.0	2.474	24.074	0.0	0.0	0.0	437.757	12.749
419	0 0	0.0	3.711	10.741	0.0	1.000	0.0	182.753	25.498
424	0 0	0.0	0.0	8.889	0.0	0.0	0.0	170.003	83.665

SAMP.	#	LOC.COORD	AG	NI	ZN	PB	CO	CD	MN	CU
429	0	0	0.0	1.237	13.704	0.0	0.0	0.0	174.253	11.155
434	0	0	0.0	2.474	33.333	3.333	0.0	0.132	263.504	470.120
439	0	0	0.0	3.711	16.296	0.0	1.000	0.0	225.254	36.255
444	0	0	0.0	1.237	11.111	0.0	0.0	0.0	276.255	5976.094
449	0	0	0.0	2.474	14.074	0.0	1.000	0.0	195.503	5418.324
454	0	0	0.0	3.711	24.815	0.0	3.000	0.0	361.256	1952.192
459	0	0	0.0	2.474	18.148	0.0	2.000	0.0	280.504	59.761
464	0	0	0.0	3.711	19.259	0.0	1.000	0.0	255.004	113.546
474	0	0	1.250	3.711	21.111	6.667	2.000	0.0	310.255	93.626
479	0	0	0.0	2.474	18.889	0.0	1.000	0.0	233.754	24.701
484	0	0	0.0	2.474	24.074	0.0	2.000	0.0	297.505	103.586
489	0	0	0.0	3.711	22.963	0.0	3.000	0.0	284.755	498.008
494	0	0	0.0	1.237	23.704	0.0	2.000	0.0	335.756	1095.618
499	0	0	0.0	4.948	28.518	0.0	2.000	0.264	433.507	290.836
504	0	0	0.0	3.000	28.692	0.0	4.000	0.0	258.586	268.965
509	0	0	0.0	2.000	21.941	0.0	3.000	0.0	181.010	137.931
514	0	0	0.500	3.000	25.316	0.0	3.000	0.0	226.263	3275.862
519	0	0	0.0	4.000	28.692	5.000	3.000	0.0	255.354	586.207
524	0	0	0.0	3.000	22.278	0.0	2.000	0.0	223.030	706.897
529	0	0	0.0	3.000	27.848	5.000	2.000	0.0	226.263	1068.966
534	0	0	0.0	4.000	21.603	0.0	3.000	0.0	210.101	396.552
539	0	0	0.0	5.000	16.203	0.0	6.000	0.0	145.455	8.621
544	0	0	0.500	3.000	16.878	0.0	3.000	0.0	142.222	1344.828
549	0	0	0.0	4.000	19.409	0.0	4.000	0.0	164.849	844.828
554	0	0	0.0	2.000	17.722	0.0	2.000	0.0	200.404	13.793
559	0	0	0.0	3.000	23.629	0.0	3.000	0.0	213.333	39.655
564	0	0	0.0	3.000	13.840	0.0	4.000	0.0	106.667	37.931
569	0	0	0.0	5.000	15.696	0.0	4.000	0.0	126.061	6.897
574	0	0	0.0	3.000	20.253	0.0	4.000	0.0	164.849	106.897
579	0	0	0.0	3.000	16.878	0.0	3.000	0.0	148.687	24.138
584	0	0	0.0	4.000	18.228	0.0	5.000	0.0	155.152	4.828
589	0	0	0.0	3.000	22.785	0.0	2.000	0.0	200.404	11.724
594	0	0	0.0	3.000	25.485	0.0	3.000	0.0	193.940	6.207
599	0	0	0.0	4.000	24.641	0.0	8.000	0.0	210.101	706.897
604	0	0	0.0	4.000	25.654	0.0	5.000	0.0	177.778	279.310
610	0	0	0.0	0.0	20.253	0.0	2.000	0.0	177.778	1000.000
614	0	0	0.0	3.000	21.941	0.0	4.000	0.0	174.546	551.724
619	0	0	0.0	5.000	27.004	5.000	4.000	0.283	213.333	672.414
624	0	0	0.0	4.000	12.152	0.0	3.000	0.0	100.202	4.483
629	0	0	0.0	2.000	17.215	0.0	2.000	0.0	126.061	534.483
634	0	0	0.0	3.000	8.439	0.0	3.000	0.0	67.879	32.759
639	0	0	0.0	2.000	12.827	0.0	4.000	0.0	109.899	793.104
644	0	0	0.0	2.000	11.477	0.0	3.000	0.0	77.576	237.931
649	0	0	0.0	3.000	15.190	0.0	2.000	0.0	113.131	94.828
654	0	0	0.0	2.000	18.903	0.0	3.000	0.0	187.475	12.069
659	0	0	0.0	3.000	21.097	0.0	4.000	0.0	158.384	362.069
664	0	0	0.0	4.000	16.034	0.0	3.000	0.0	187.475	4.828

HIGHMONT DRILL-CORE SAMPLES
SPECTROGRAPHIC ANALYSIS

(VALUES IN PPM)

(EVERY FIFTH SAMPLE - ALL DRILL HOLES)

SAMP. #	B	SR	TI	IN	V	MO	BA	BIG	SN
188		1000	2000	50	60		700		20
193		700	1000	60	30		1000		20
198		700	1000	50	40		600		20
203	15	800	1000	50	40		500		20
208		800	2000	50	50		700		20
213	15	1000	1000	50	40		1000	1520	
218		500	1500	50	30		800		20
223	10	800	1000	50	30		700		20
228	10	800	1500	50	40		150		20
234		1000	700	50	30		500		20
239	10	600	500	50	30		500		15
244	15	500	700	50	40		800		15
249		800	1000	50	40		600		15
254	10	400	1000	50	40		400		15
259		500	1000	50	30		700		15
264		400	1000	50	30	5	400		15
269		500	1000	50	30		300		15
274		500	700	50	30	5	400		15
279	20	200	900	50	30	8	500		15
284	50	400	900	50	40	15	400		15
289	20	500	2000	50	30		300		20
294	40	700	2000	50	30	4	400		20
299	30	700	1000	50	30		100		20
304	15	700	1000	50	40		700		20
309	15	600	700	50	30		500		20
314	20	500	1000	50	40		300		20
319	30	300	2001	50	50	2001	1000		20
324	15	1000	2000	50	40	50	800		20
329	40	600	1000	50	40	5	200		20
334	40	600	1000	50	40	5	200		20
339	10	700	2000	50	40	5	500		20
344		1000	1000	50	30	15	500		20
349	10	900	1500	50	30	4	500		20
354		1000	1500	50	40	10	200		20
359		500	2000	50	40	10	1000		20
364	15	800	2001	50	40	15	2000		20
369	15	800	2001	50	40	15	2000		20
374		1000	1000	50	30	4	100		20
379	15	500	1000	50	20	20	500		20
384	20	500	1500	50	30		500		20
389	20	400	1500	50	20	10	800		20
394	20	700	1000	50	50		900		20
399	80	400	800	50	20	4	500		20
404	15	300	400	20	10		100		10
409	20	700	2000	50	50		500		20
414	10	800	2000	50	50		1000		20
419	15	400	500	50	20		500		20
424		600	1000	50	30		600		20

SAMP. #	B	SR	TI	IN	V	MO	BA	BIG	SN
429	15	500	500	50	20	5	200	20	
434		500	1000	50	30	20	200	20	
439		500	500	50	20		500	20	
444	40	400	2000	50	50	50	200	20	
449	20	300	700	50	30	8	400	20	
454	500	1000	1000	50	50	40	1000	20	
459	15	500	1500	50	30		300	20	
464		700	1000	50	30		600	20	
474	80	600	900	50	30		800	20	
479		600	1000	50	30		700	20	
484		600	1000	50	30		500	20	
489		500	800	50	30		500	20	
494	10	600	1000	50	40	60	500	20	
499	15	500	1000	50	30		700	20	
504	10	700	500	50	40		400	20	
509		700	700	50	30		500	20	
514	15	800	1000	50	40	5	300	20	
519		600	1000	50	40		800	20	
524	20	500	2000	50	50	5	900	20	
529	10	600	1000	50	40	10	1000	20	
534	15	800	1000	50	40	50	1000	20	
539		700	1500	50	50		1000	20	
544		700	500	50	30	4	1000	20	
549		700	1000	50	40		800	20	
554		600	500	50	30		500	20	
559		600	700	50	30		300	20	
564	10	400	1000	50	30		300	20	
569		800	900	50	40		700	20	
574	10	1000	2000	50	50	5	700	20	
579		800	900	50	30		600	20	
584		800	900	50	30		700	20	
589		800	1000	50	40		600	20	
594		800	1000	50	40		700	20	
599	10	500	1000	50	30	50	600	20	
604		700	700	50	30		700	20	
610	50	500	700	50	40	10	300	20	
614	10	600	500	50	30		500	20	
619		500	1000	50	40		500	20	
624		700	800	50	30		500	20	
629	10	800	1000	50	40		300	20	
634		900	500	50	20		200	20	
639	10	1000	500	50	20		500	20	
644		800	500	50	30		500	20	
649	10	1000	800	50	30		300	20	
654	15	500	1000	50	30		400	20	
659		400	800	50	30		300	20	
664		600	800	50	40	5	700	20	

VOLUME II

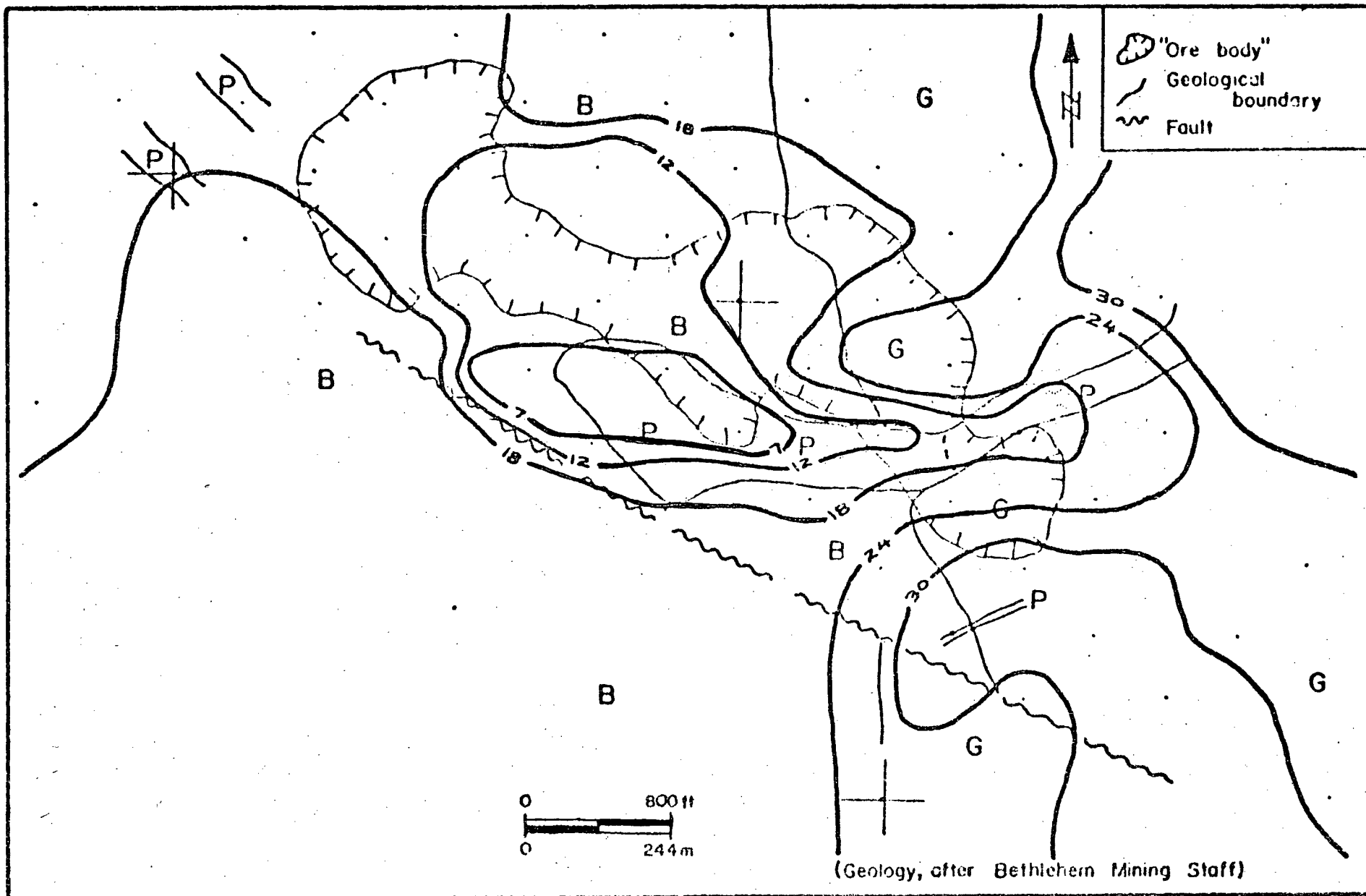


FIGURE A1: Distribution of Zn (ppm), Bethlehem-JA 2800 Level

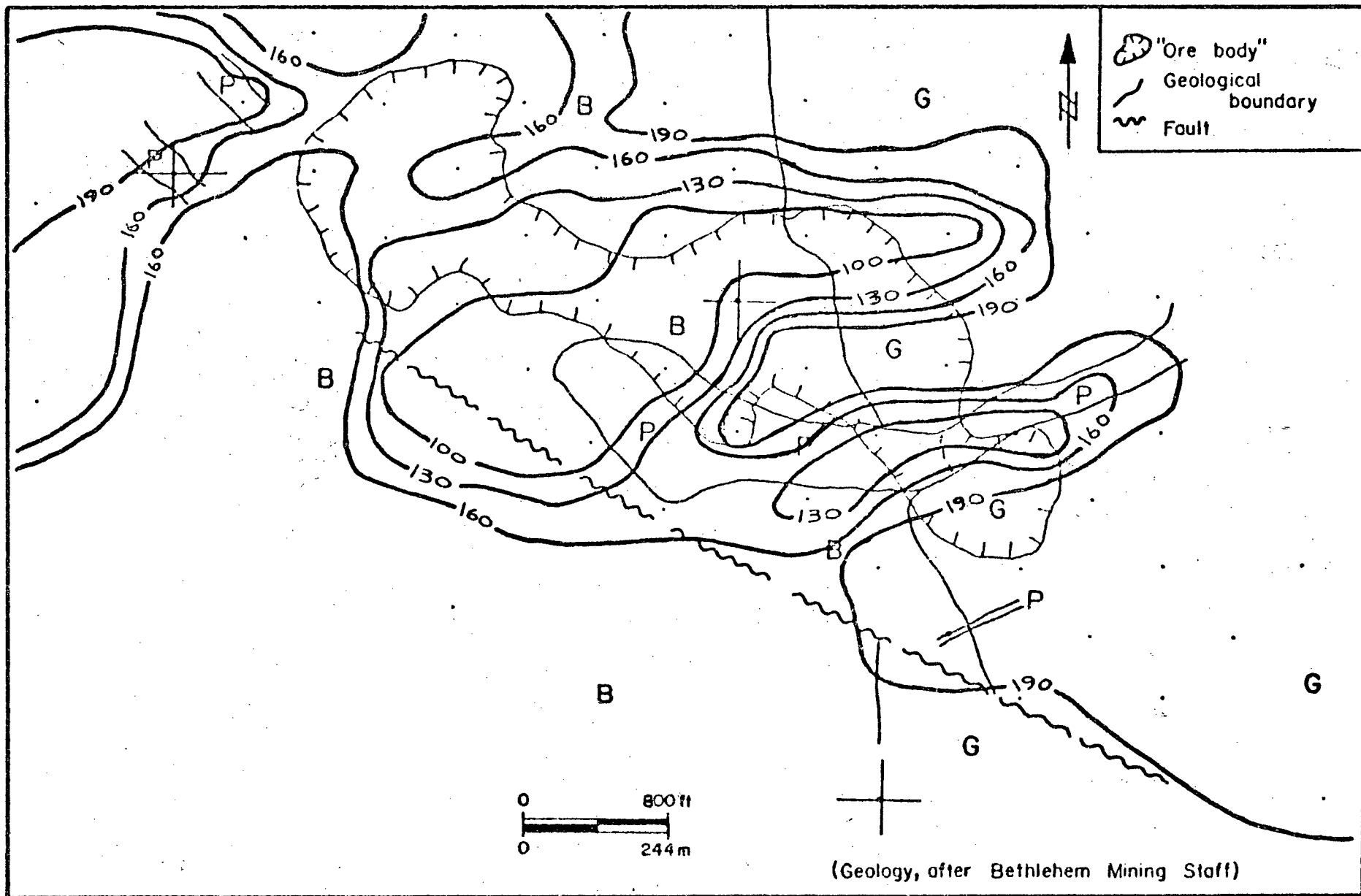


FIGURE A2: Distribution of Mn (ppm), Bethlehem-JA 2800 Level

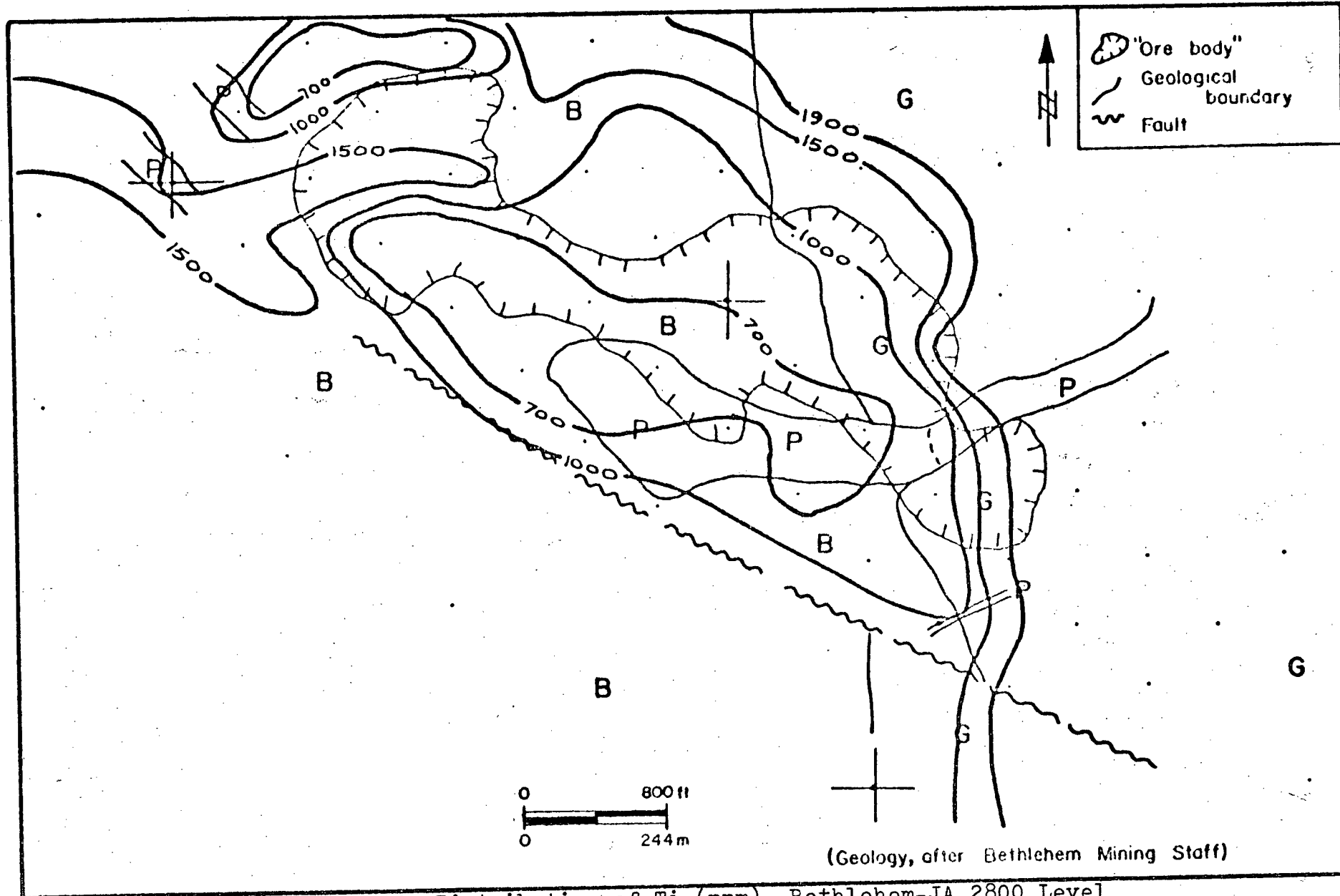


FIGURE A3: Distribution of Ti (ppm), Bethlehem-JA 2800 Level

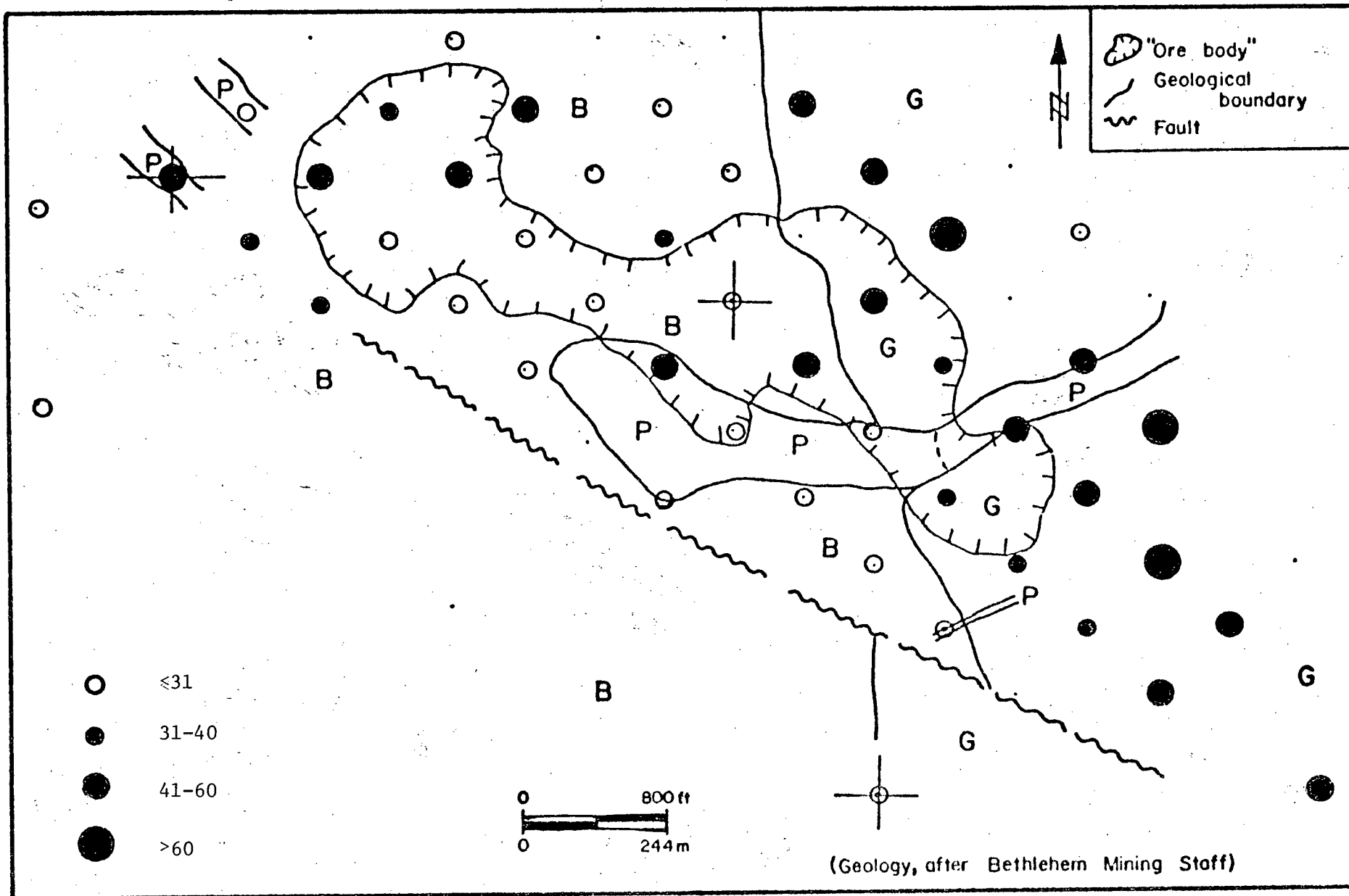


FIGURE A4: Distribution of V (ppm), Bethlehem-JA 2800 Level

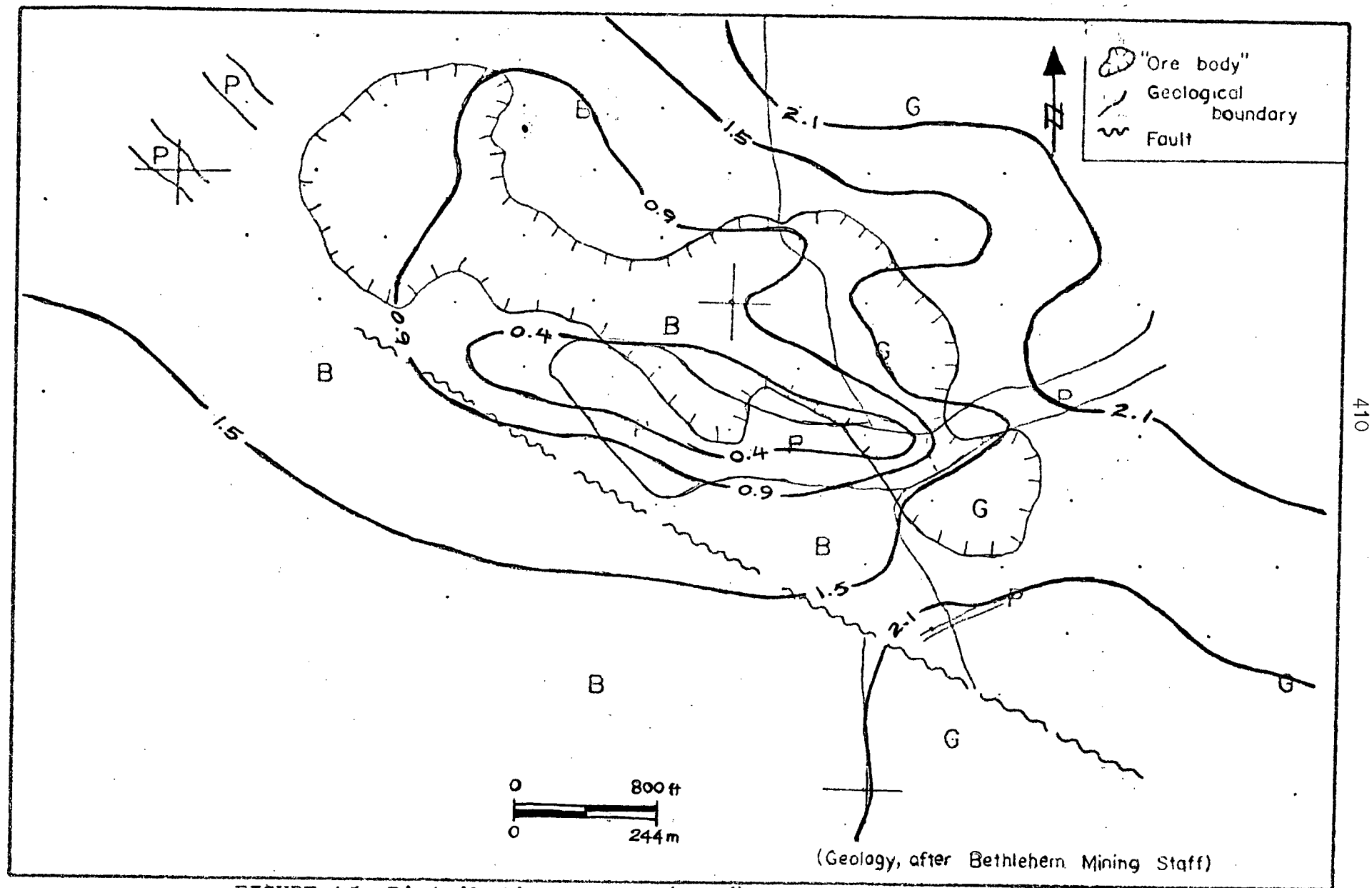


FIGURE A5: Distribution of MgO (Wt.%), Bethlehem-JA 2800 Level

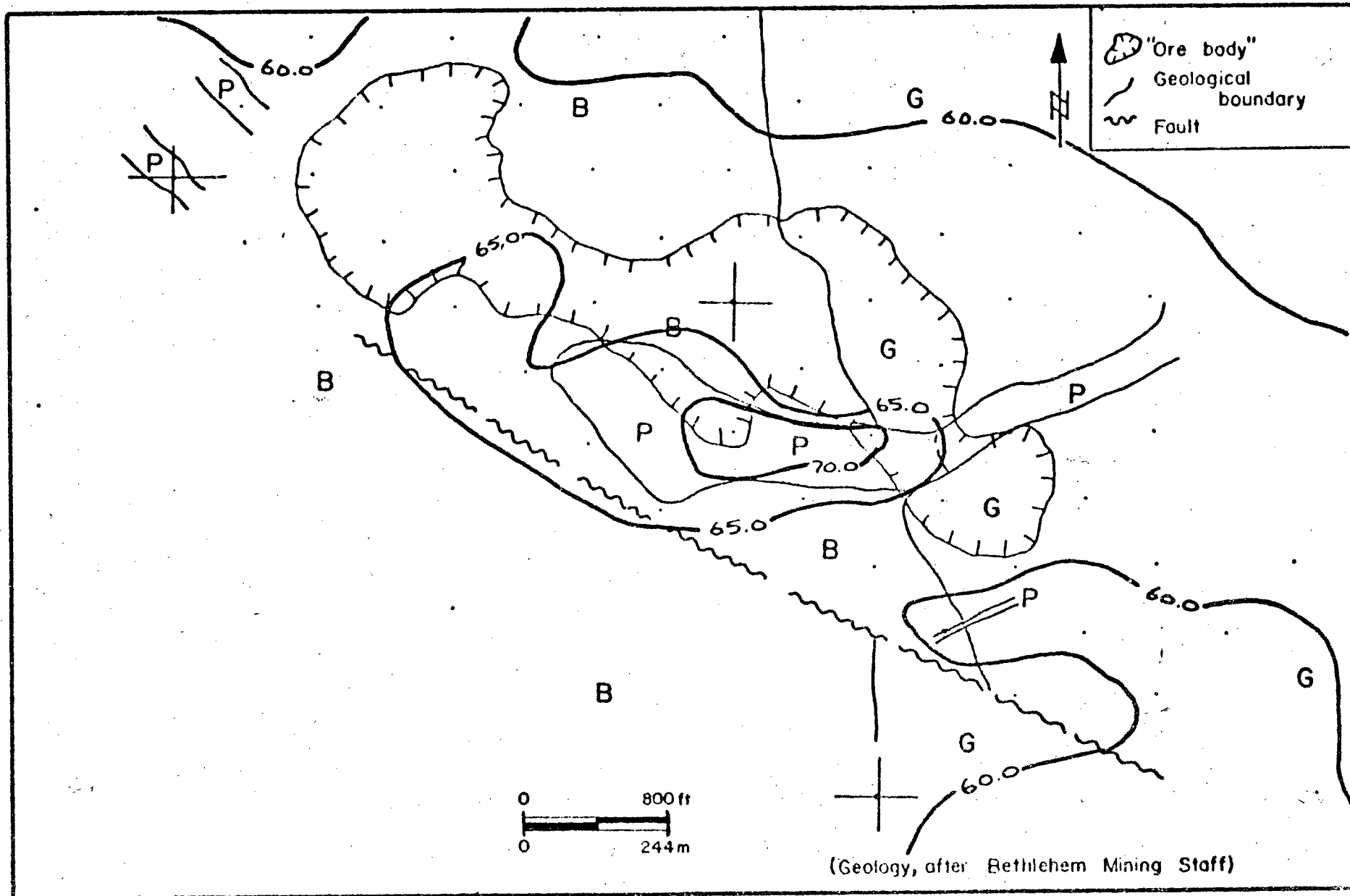


FIGURE A6: Distribution of SiO_2 (wt.%), Bethlehem-JA 2800 Level

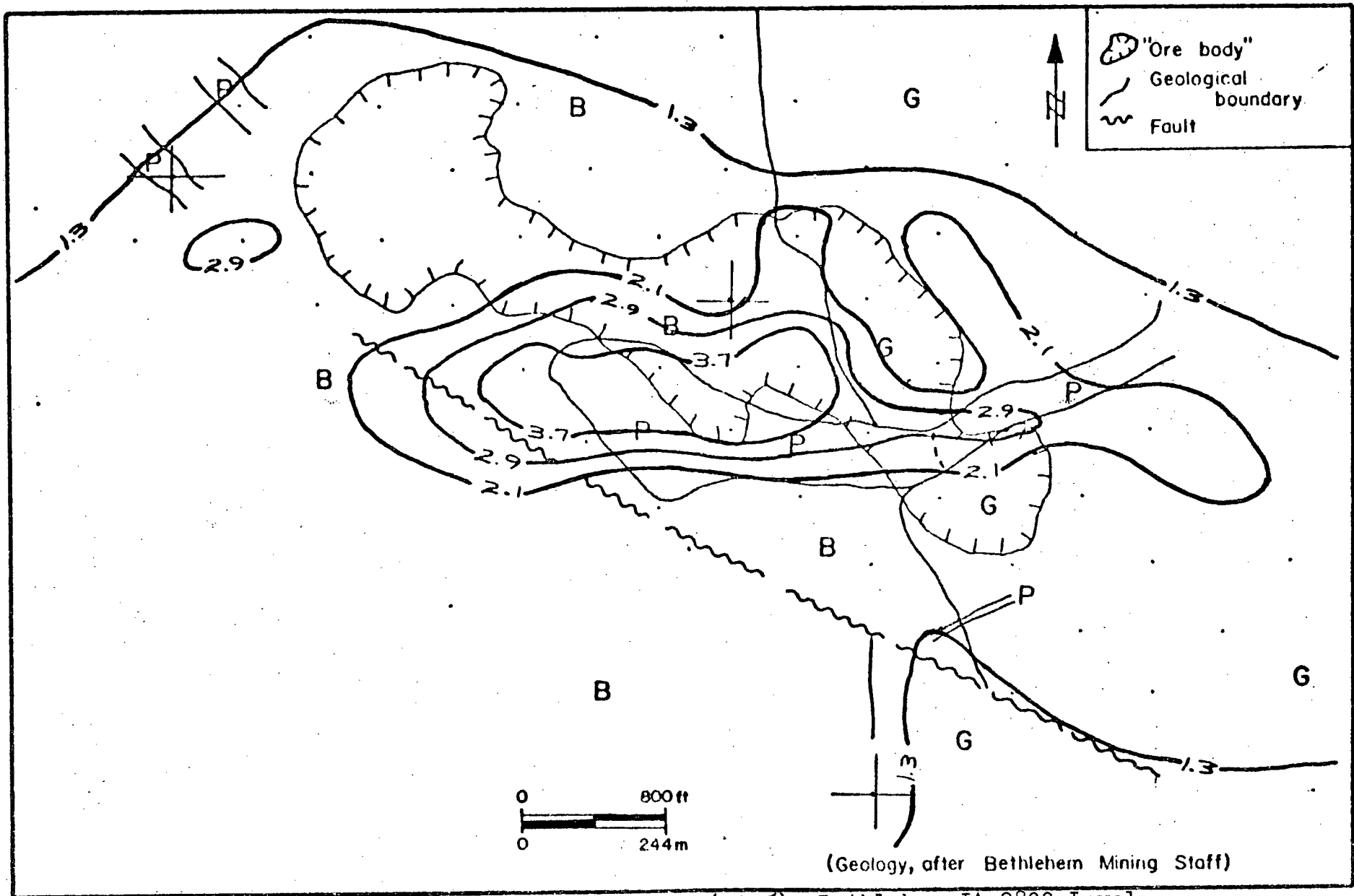


FIGURE A7: Distribution of K_2O (wt.%), Bethlehem-JA 2800 Level

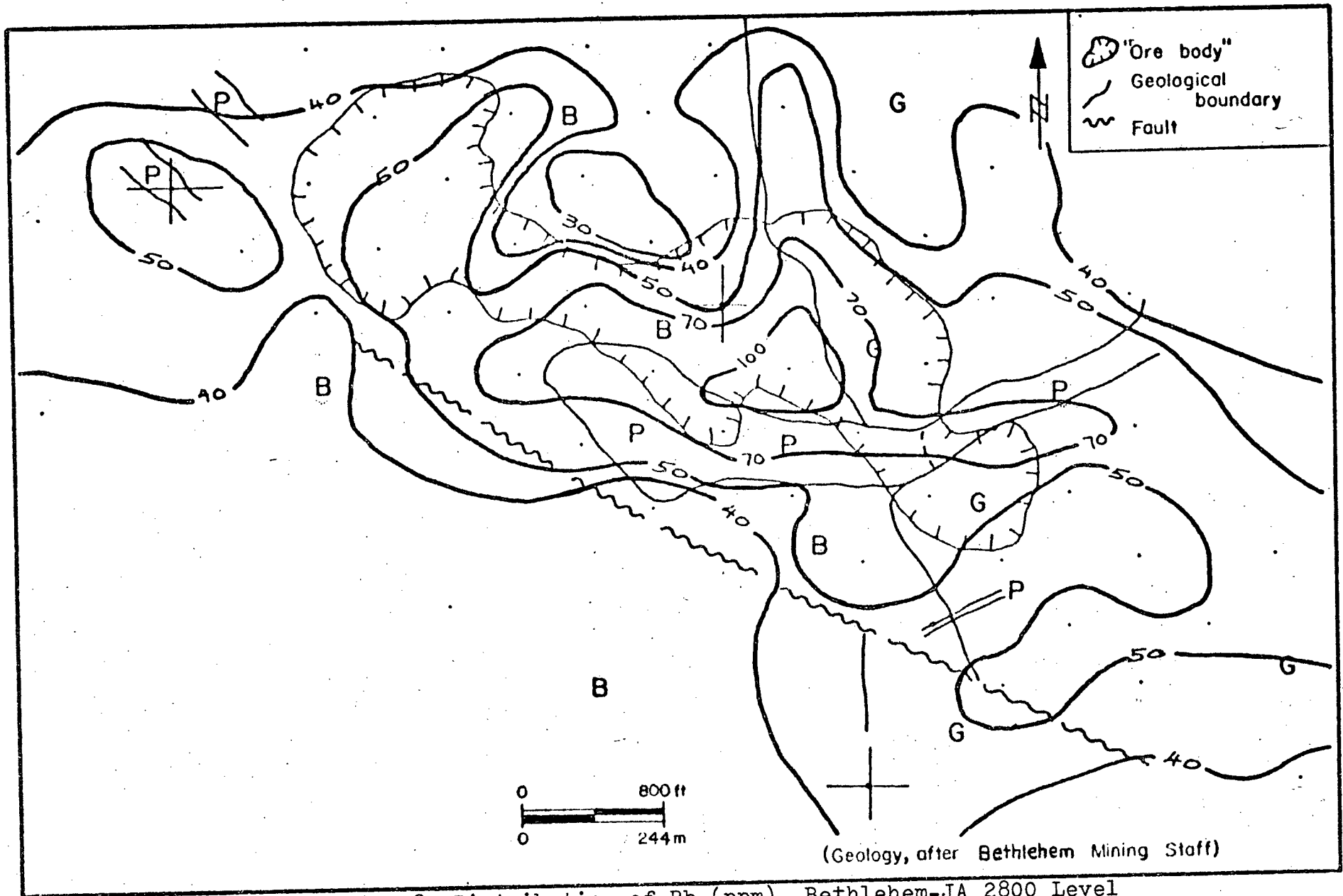


FIGURE A8: Distribution of Rb (ppm), Bethlehem-JA 2800 Level

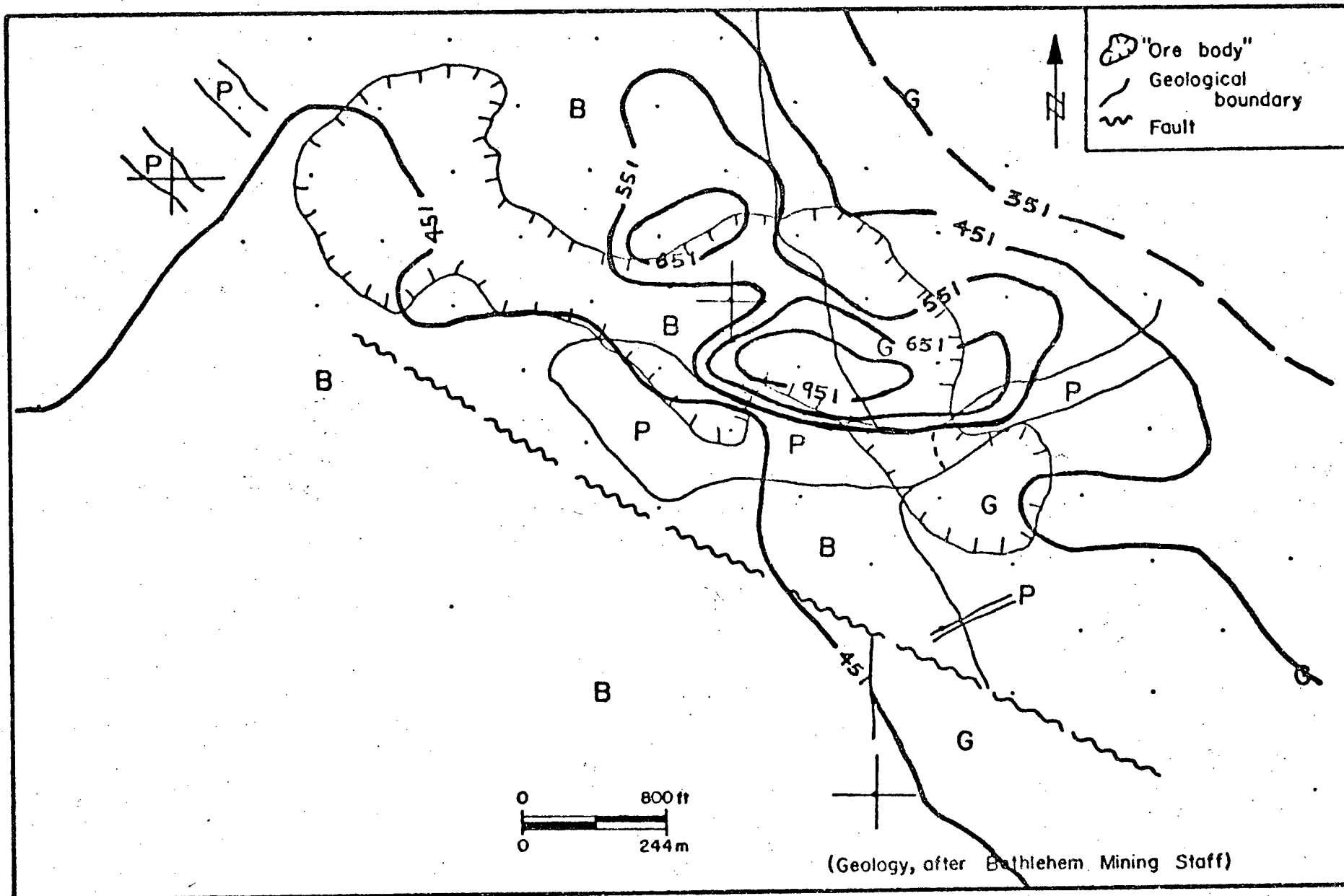


FIGURE A9: Distribution of Ba (ppm), Bethlehem-JA 2800 Level

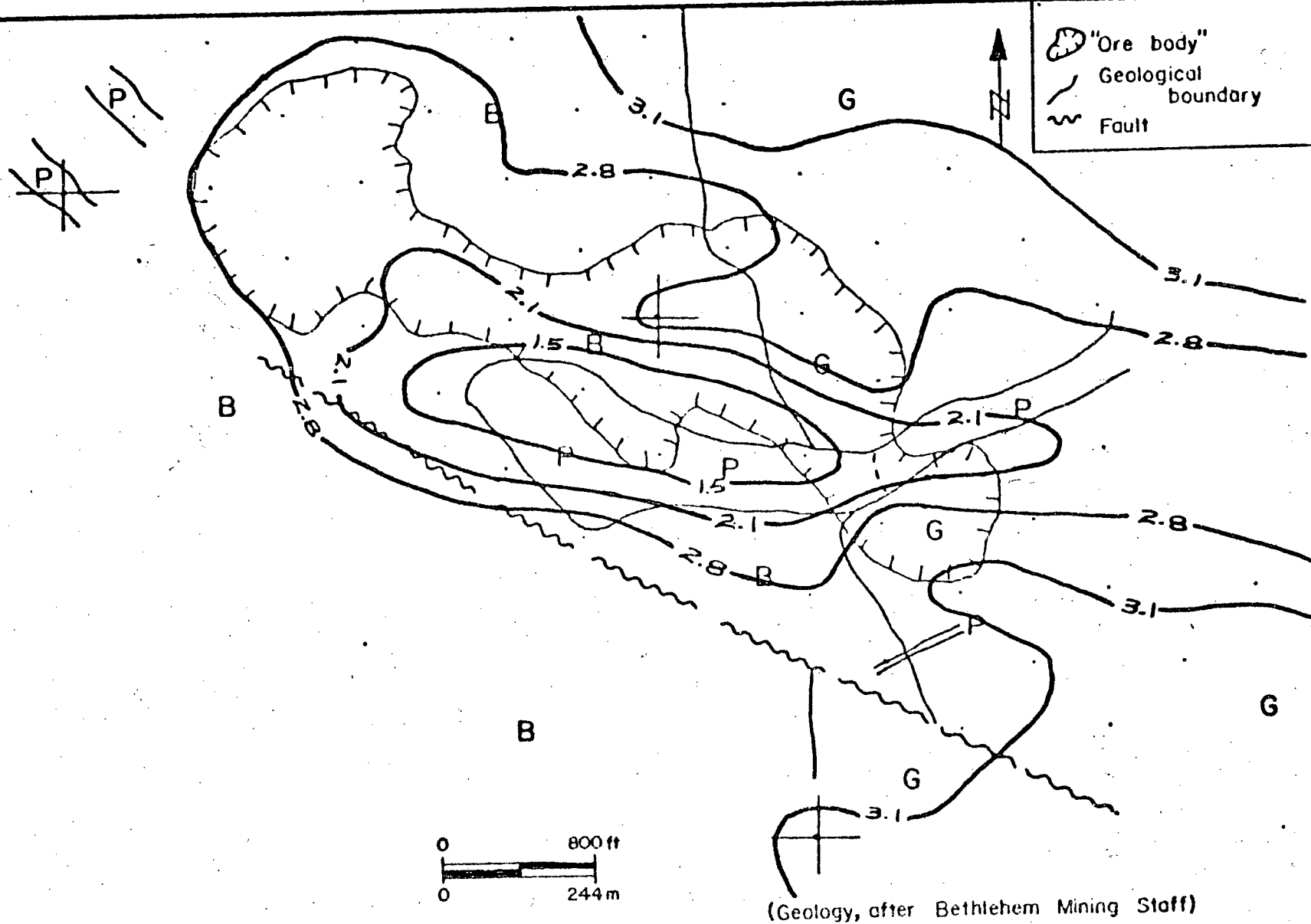


FIGURE A10: Distribution of CaO (wt.%), Bethlehem-JA 2800 Level

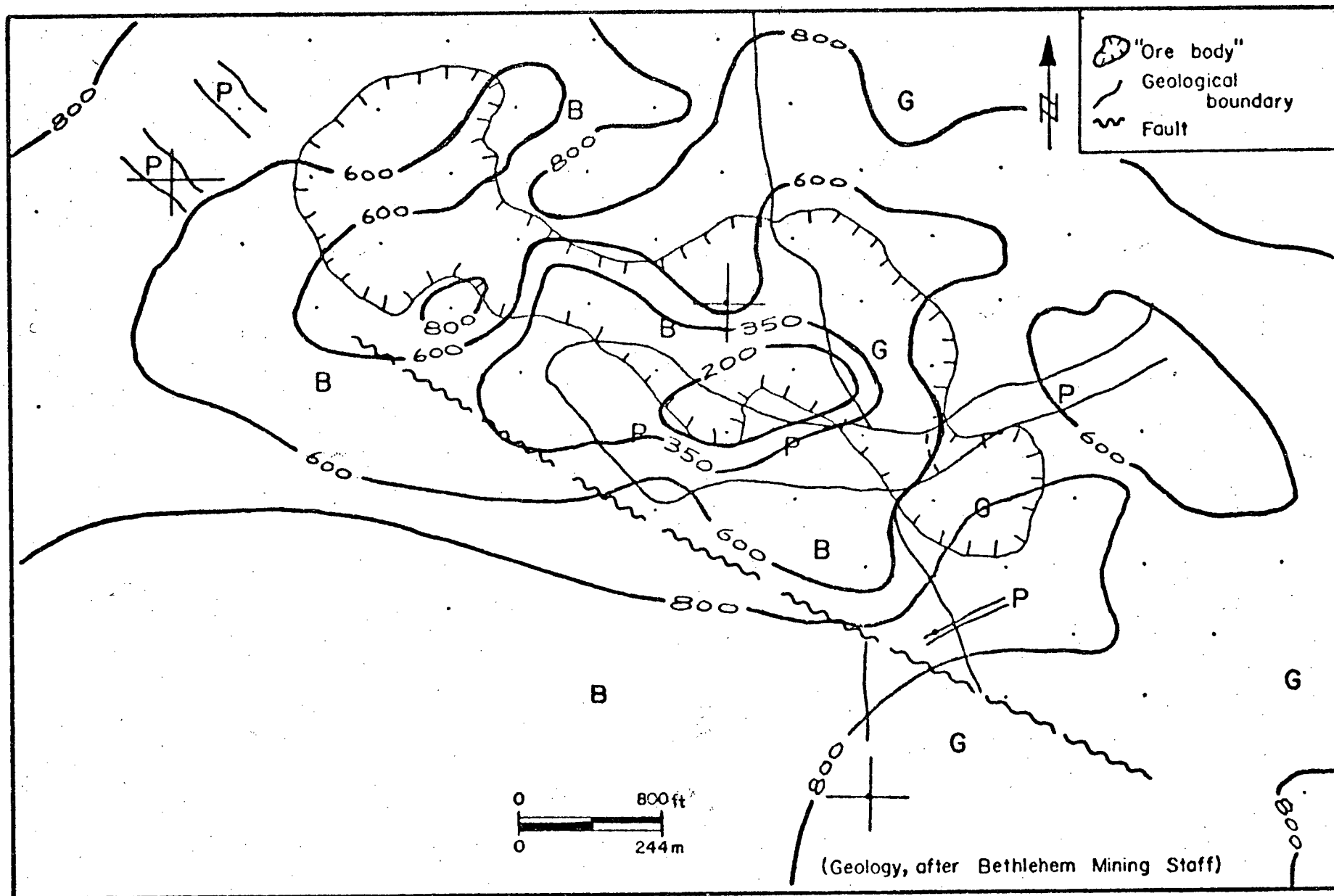


FIGURE All: Distribution of Sr (ppm), Bethlehem-JA 2800 Level

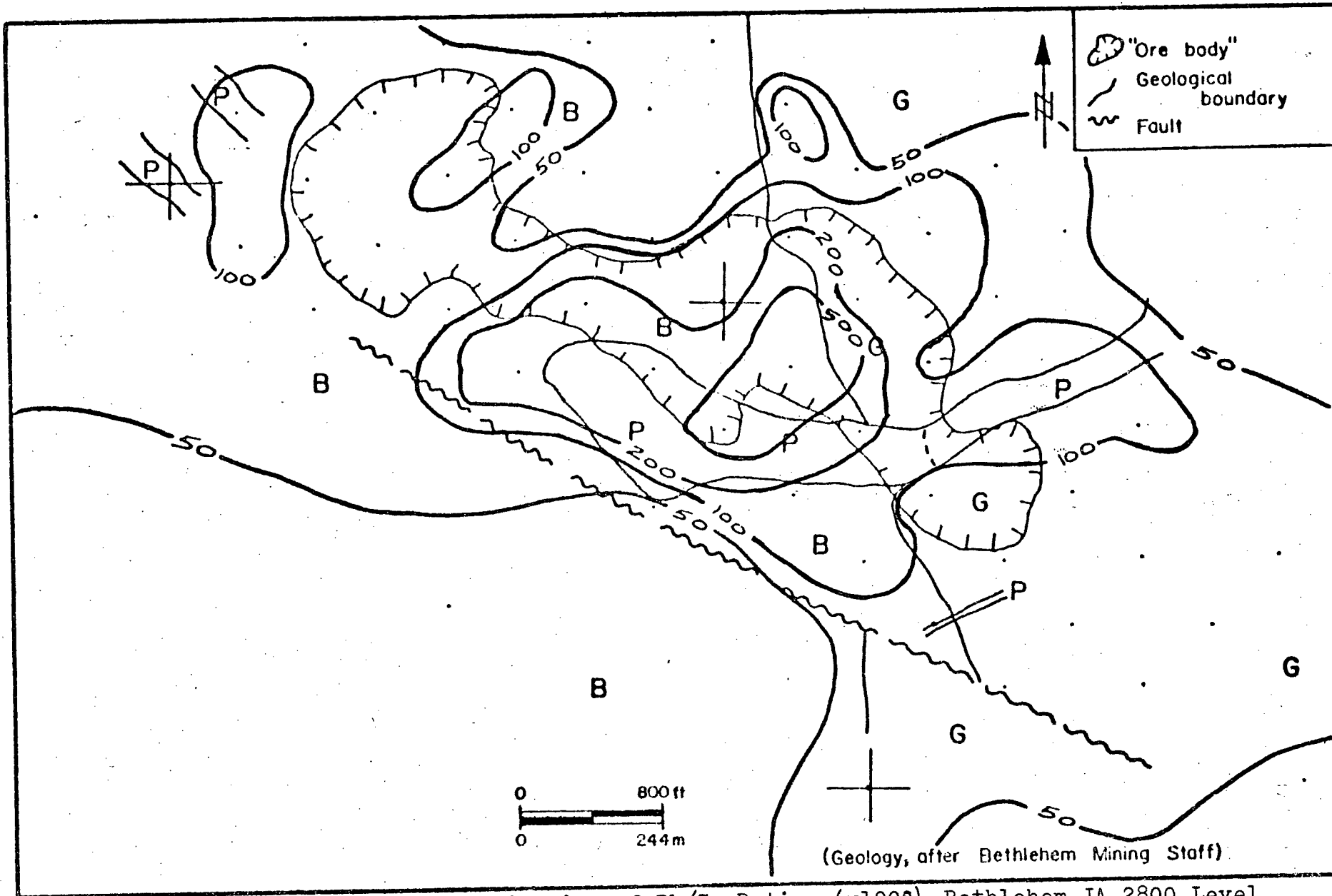


FIGURE A12a: Distribution of Rb/Sr Ratios (x1000), Bethlehem-JA 2800 Level

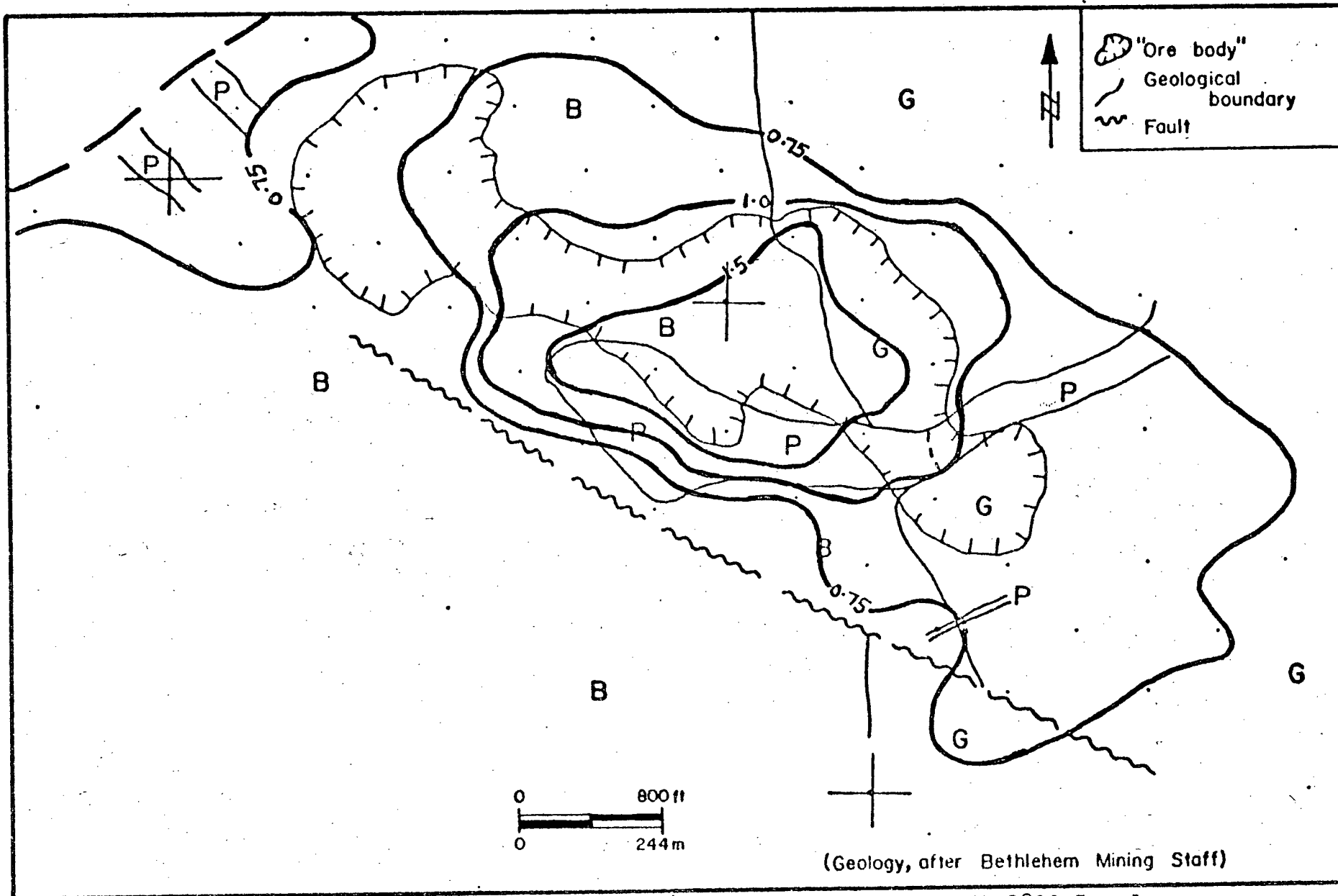


FIGURE A12b: Distribution of Ba/Sr Ratios, Bethlehem-JA 2800 Level

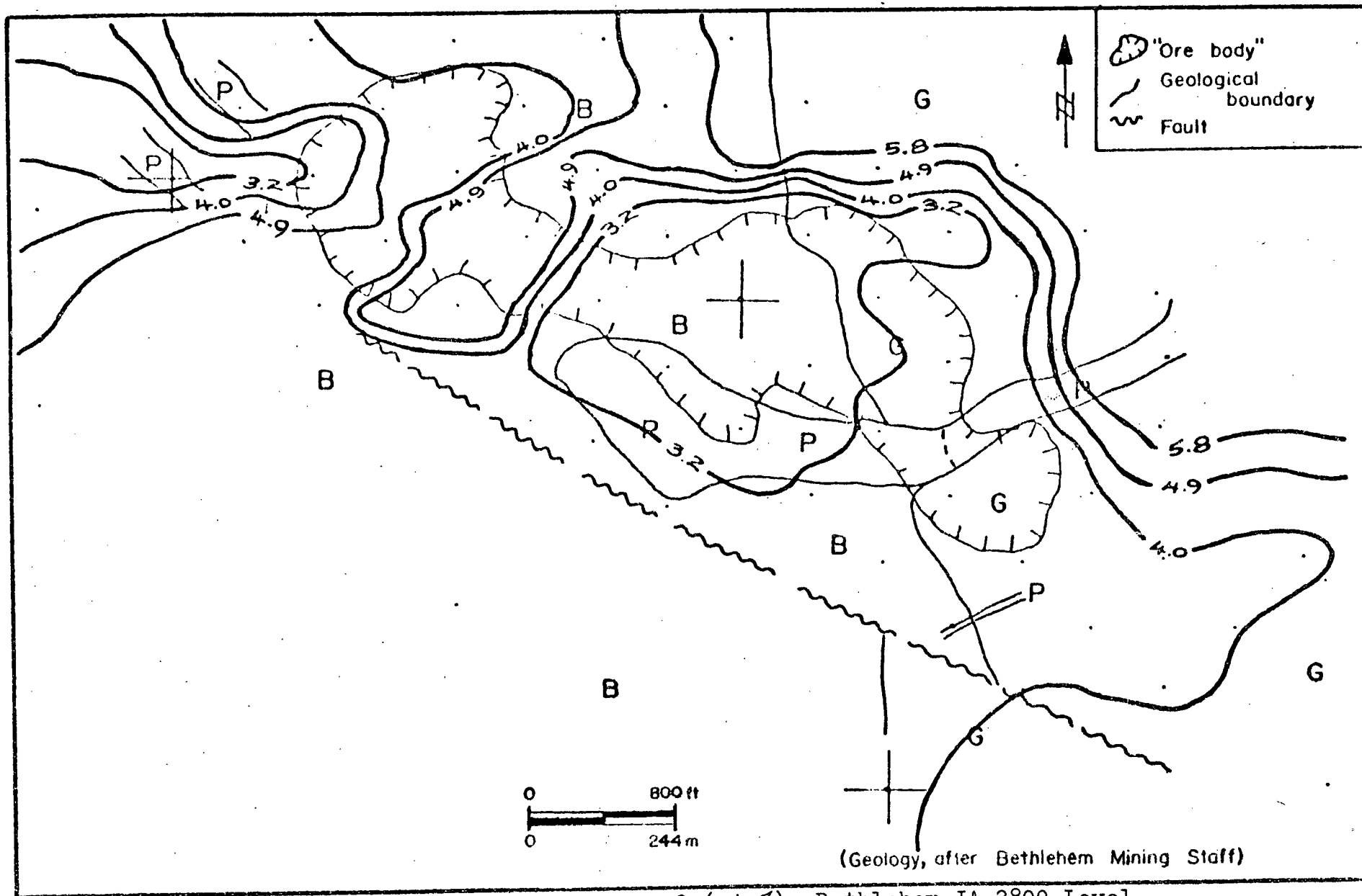


FIGURE A13, Distribution of Na_2O (wt.%), Bethlehem-JA 2800 Level

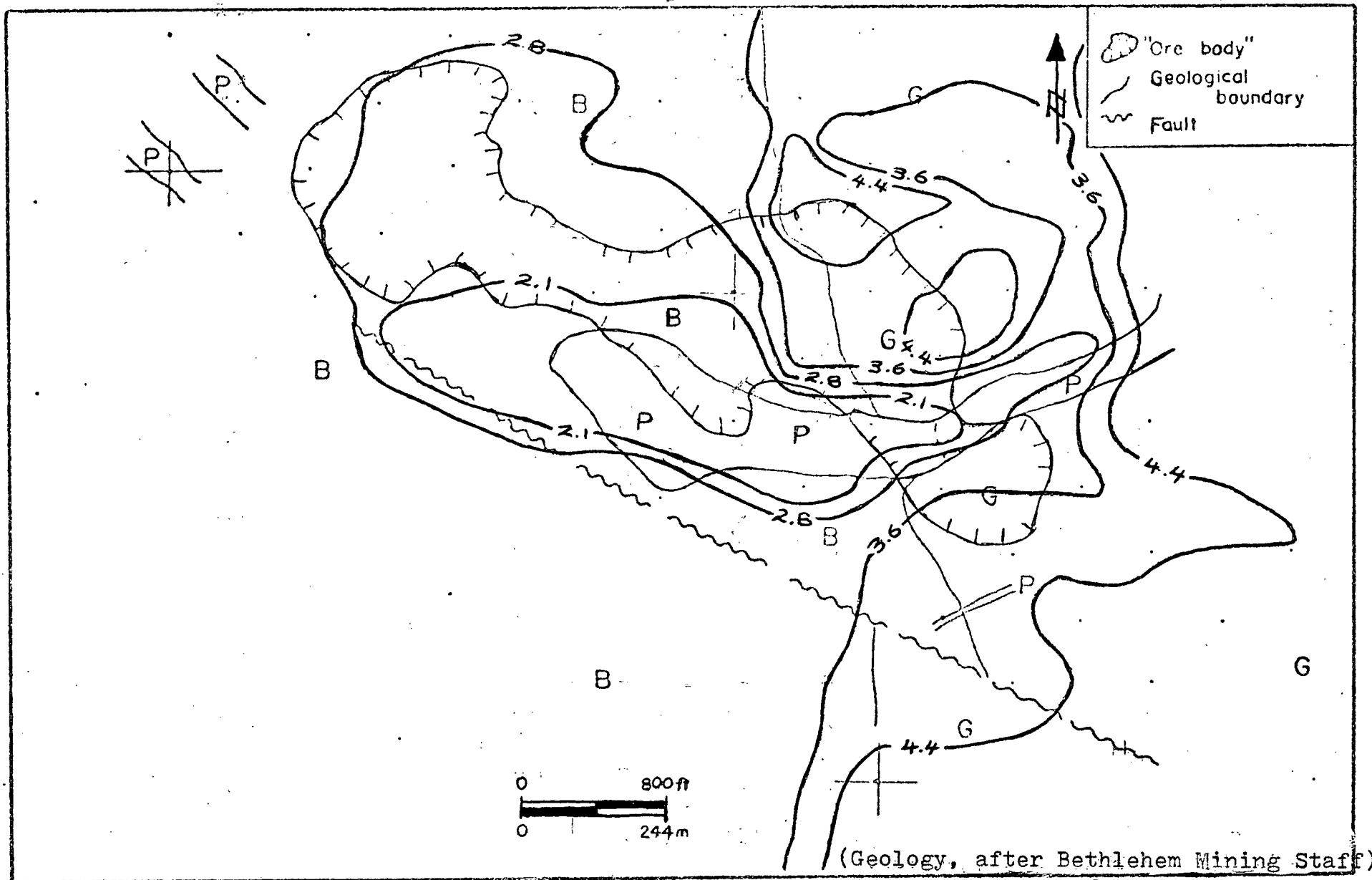


FIGURE A14: Distribution of Total Fe as Fe_2O_3 (wt.%), Bethlehem-JA 2800 Level

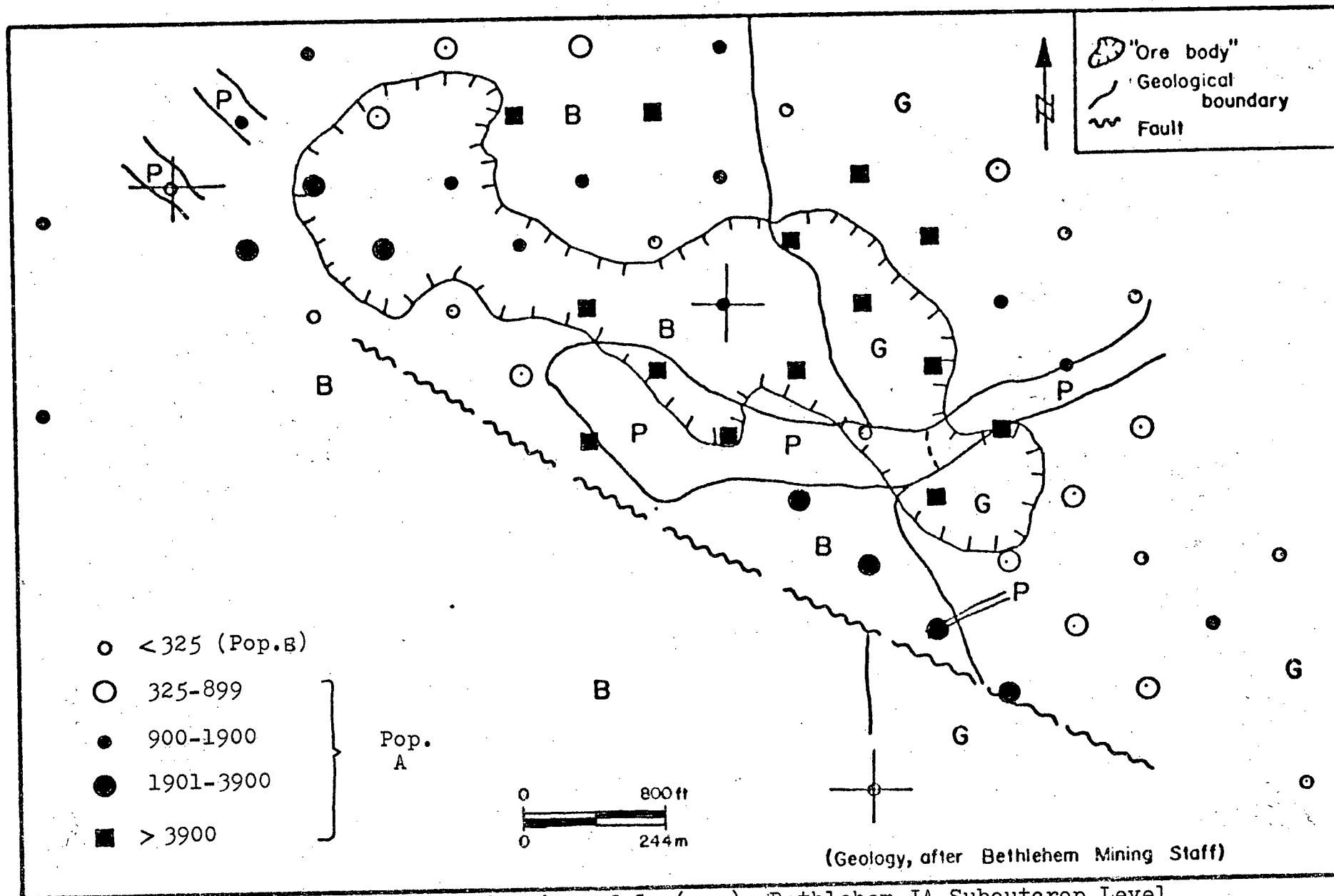


FIGURE A15: Distribution of Cu (ppm), Bethlehem-JA Suboutcrop Level

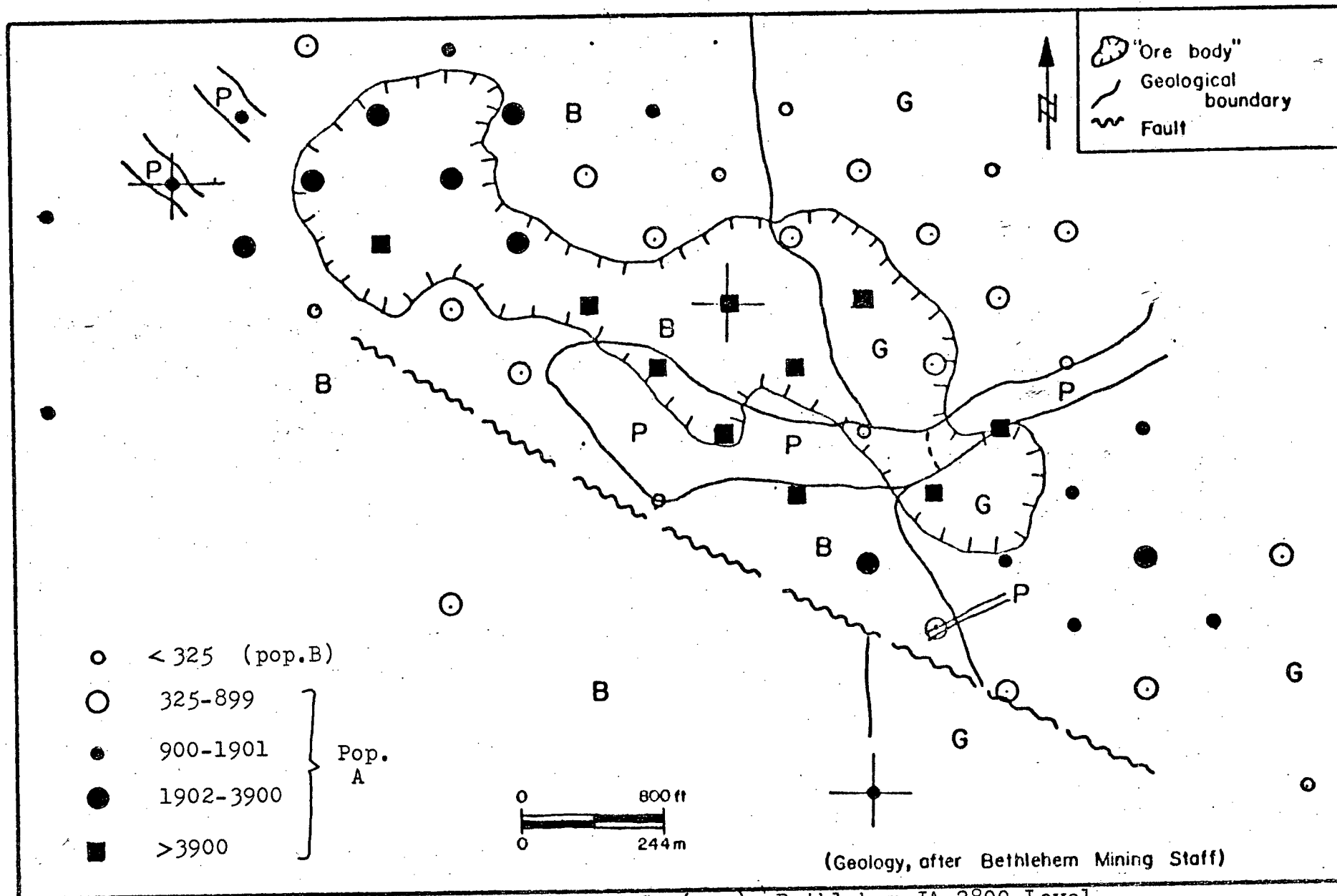


FIGURE A16: Distribution of Cu (ppm), Bethlehem-JA 2800 Level

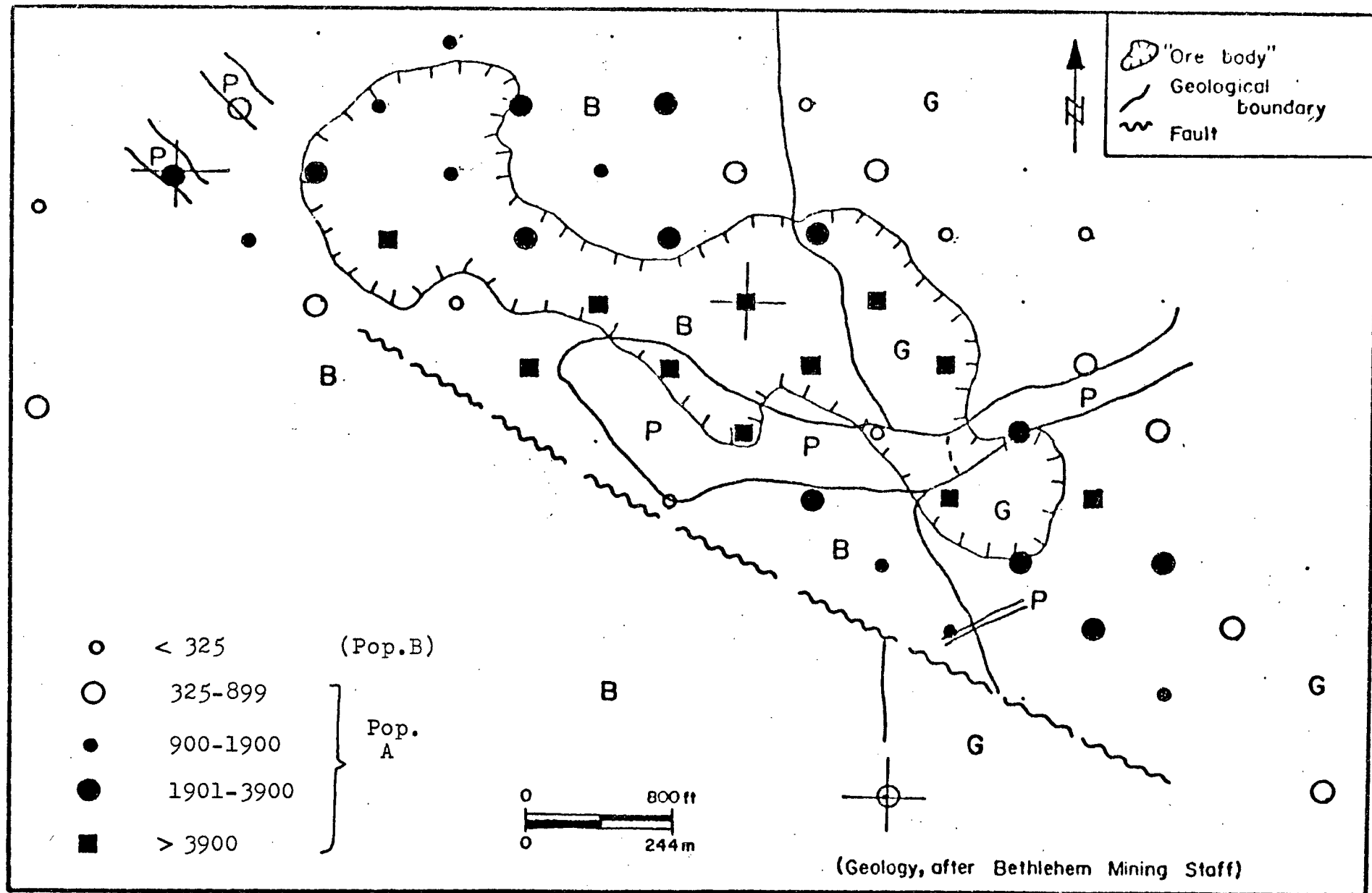


FIGURE A17: Distribution of Cu (ppm), Bethlehem-JA 2400 Level

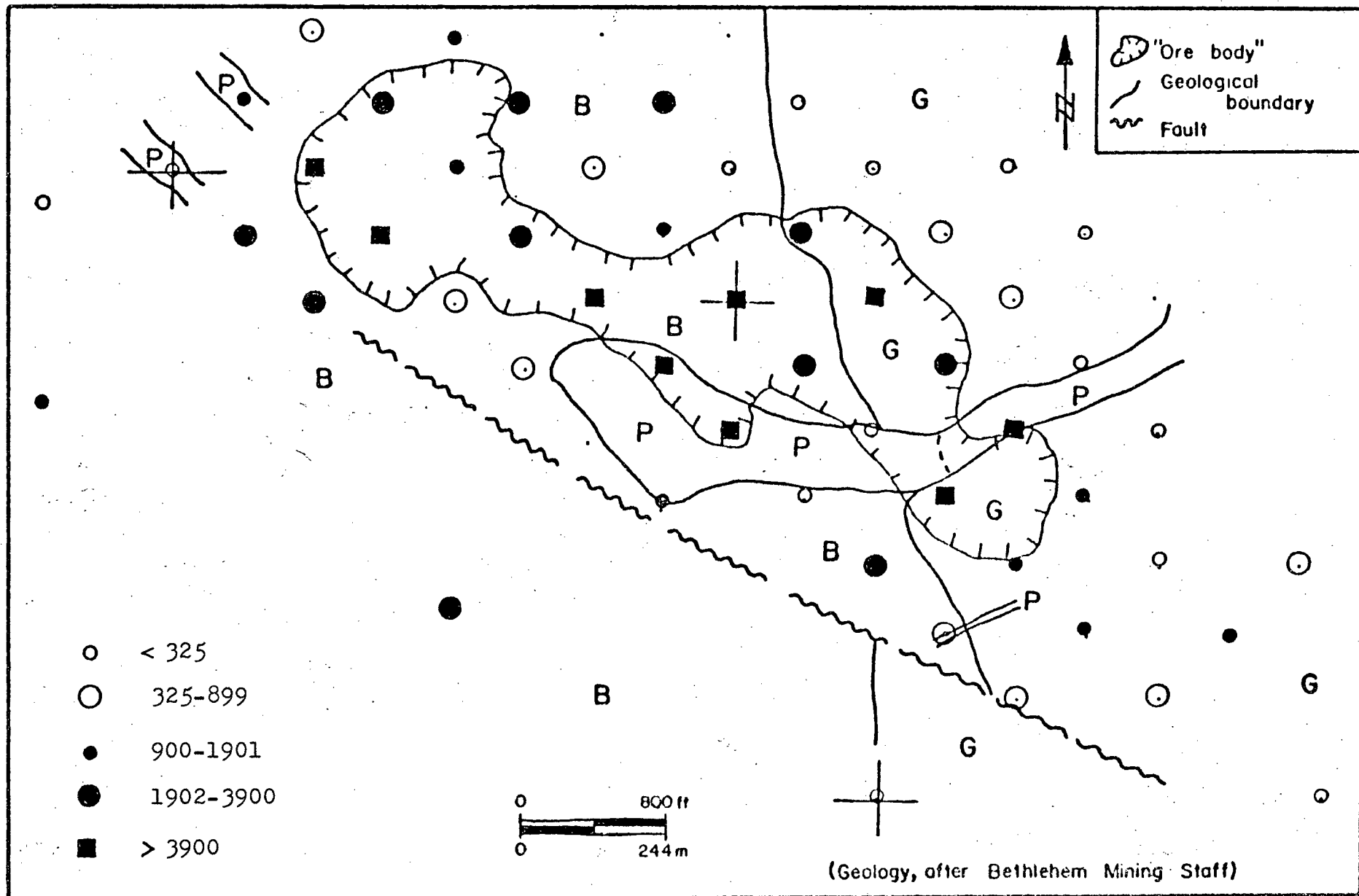


FIGURE A18: Distribution of Sulphide-held Cu (ppm), Bethlehem-JA 2800 Level

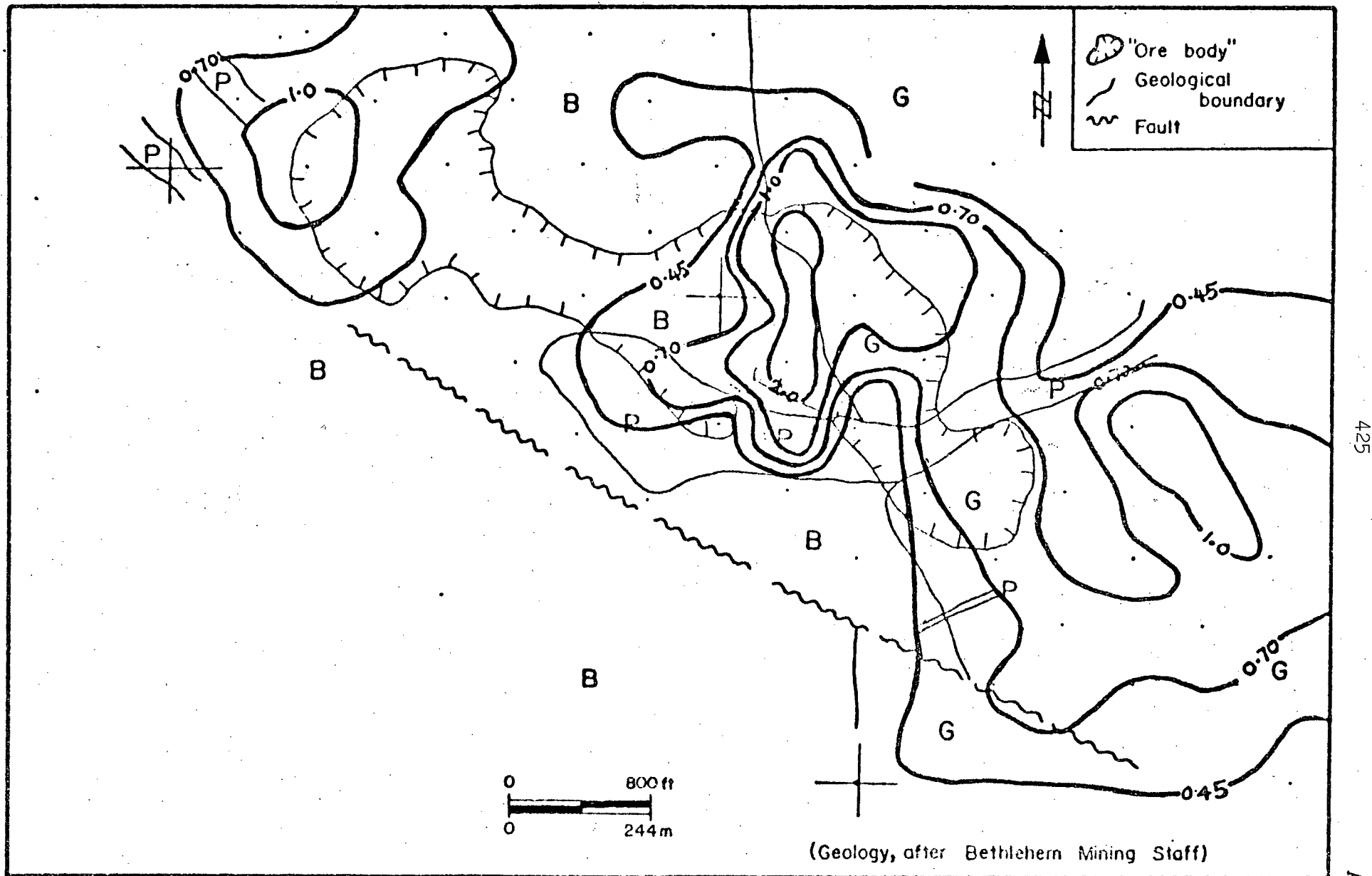


FIGURE A19: Distribution of Sulphide-held Fe (wt.%), Bethlehem-JA 2800 Level

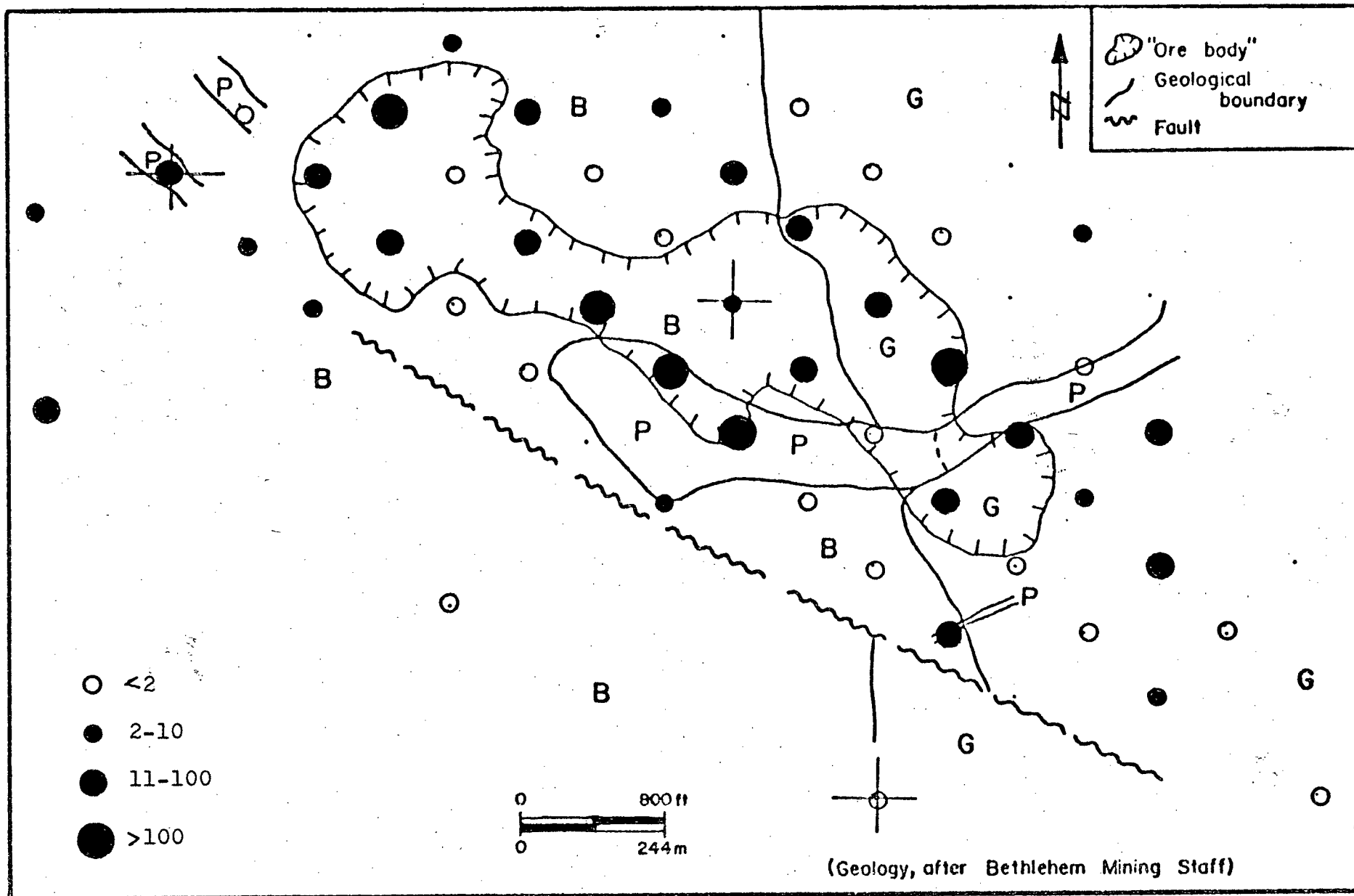


FIGURE A20: Distribution of Mo (ppm), Bethlehem-JA 2800 Level

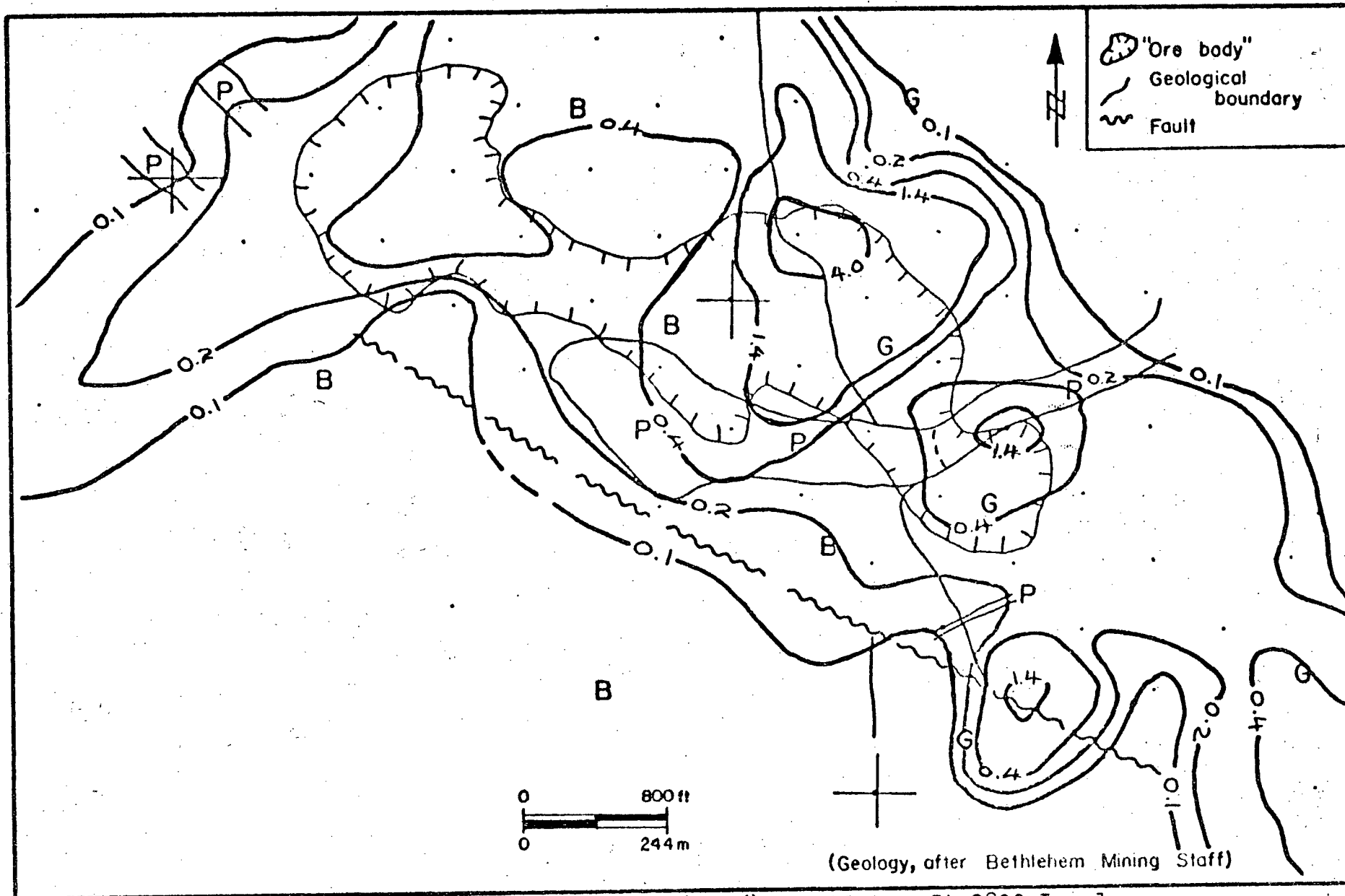


FIGURE A21: Distribution of S (wt.%), Bethlehem-JA 2800 Level

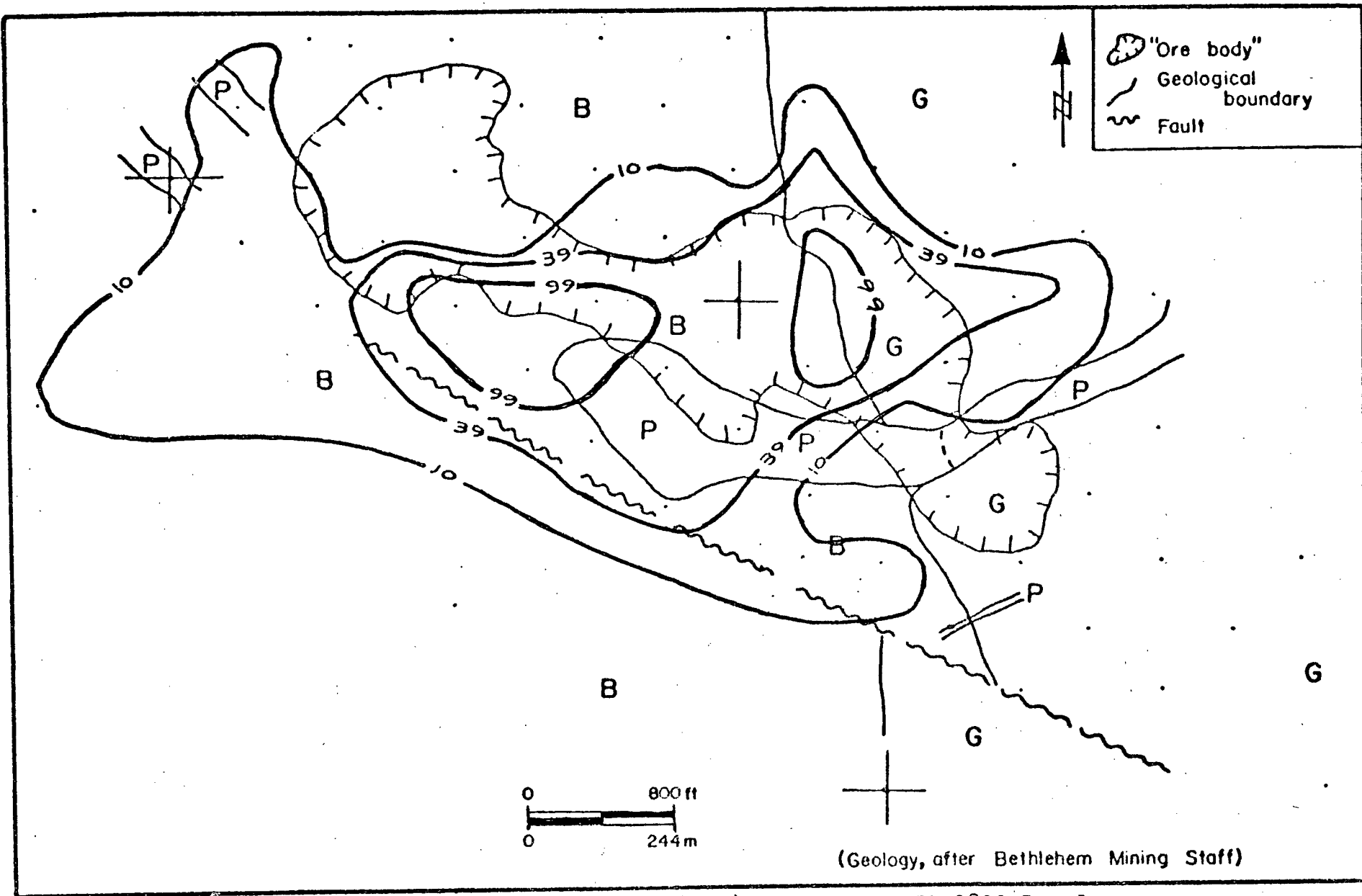


FIGURE A22: Distribution of Hg (ppb), Bethlehem-JA 2800 Level

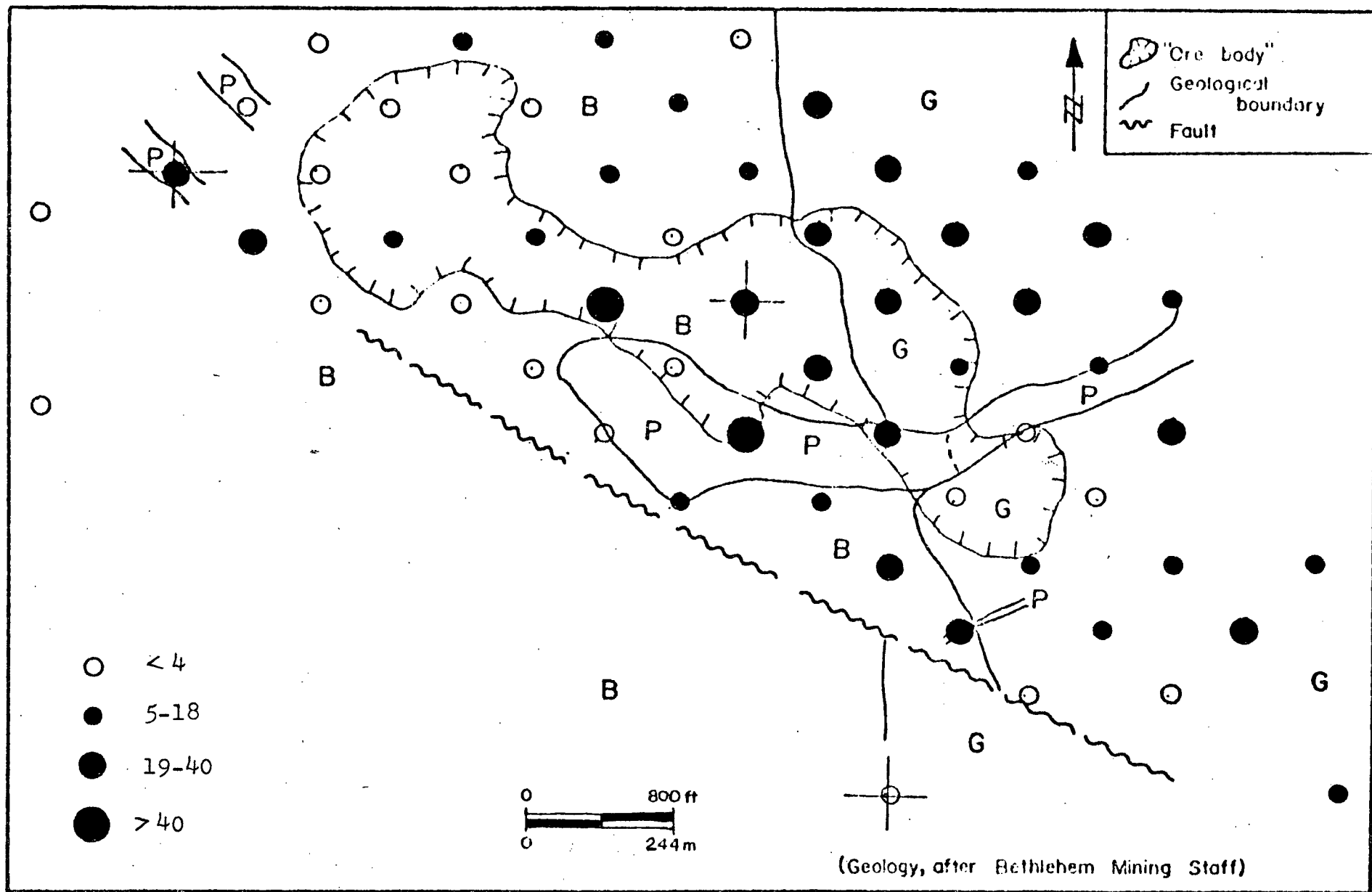


FIGURE A23: Distribution of B (ppm), Bethlehem-JA 2800 Level

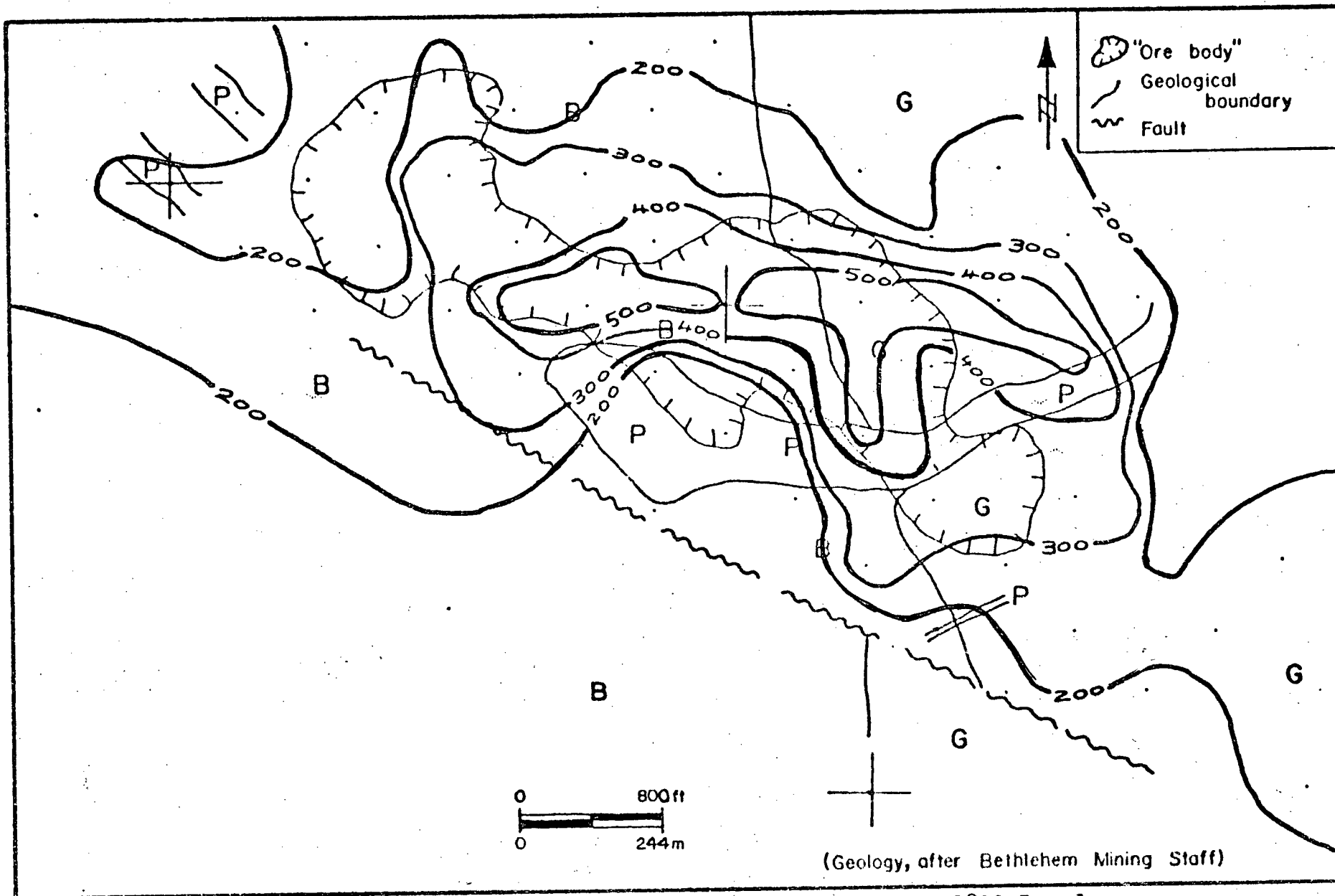


FIGURE A24: Distribution of Cl (ppm), Bethlehem-JA 2800 Level

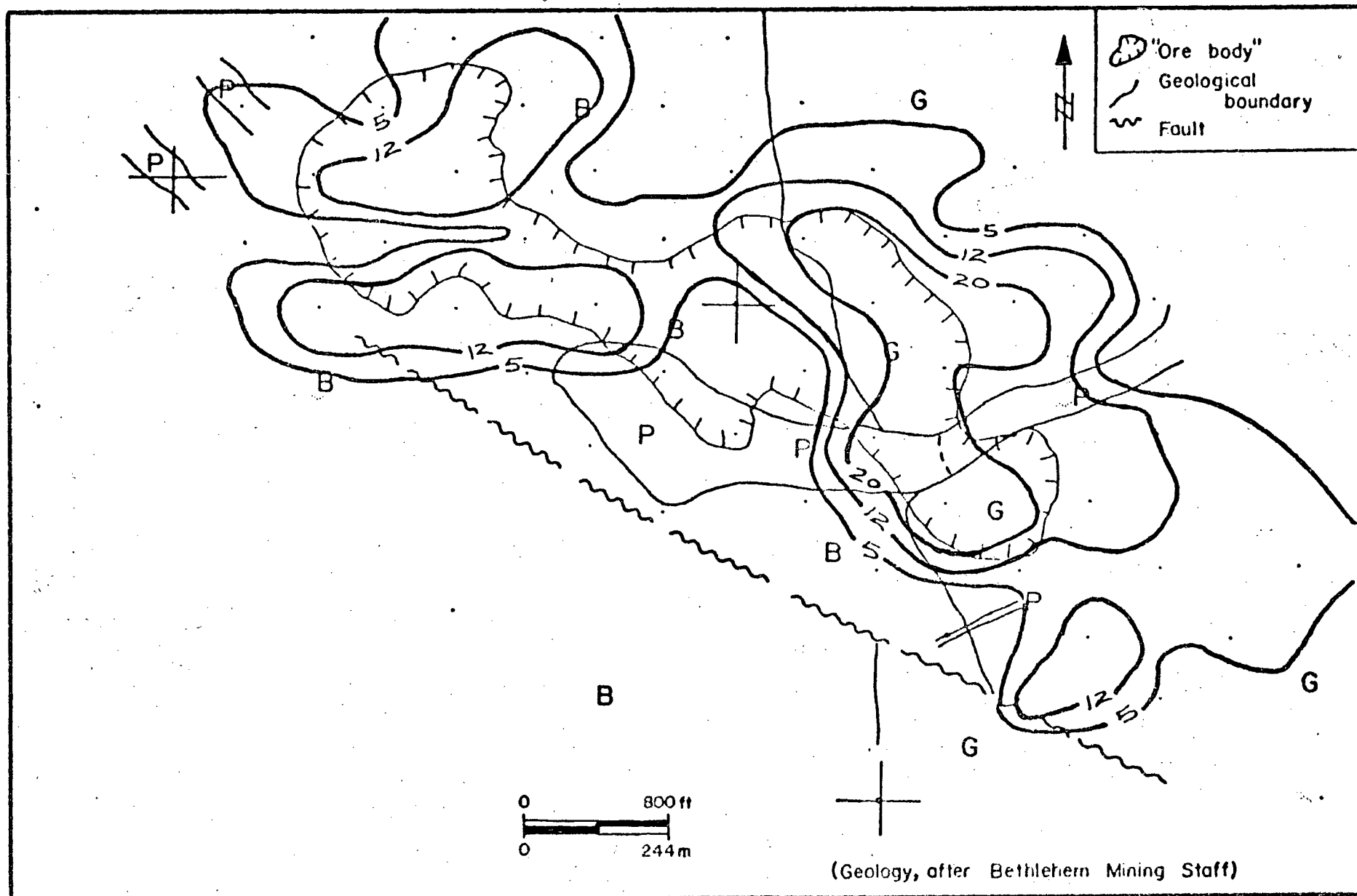


FIGURE A25: Distribution of Water-extractable Cl (ppm), Bethlehem-JA 2800 Level

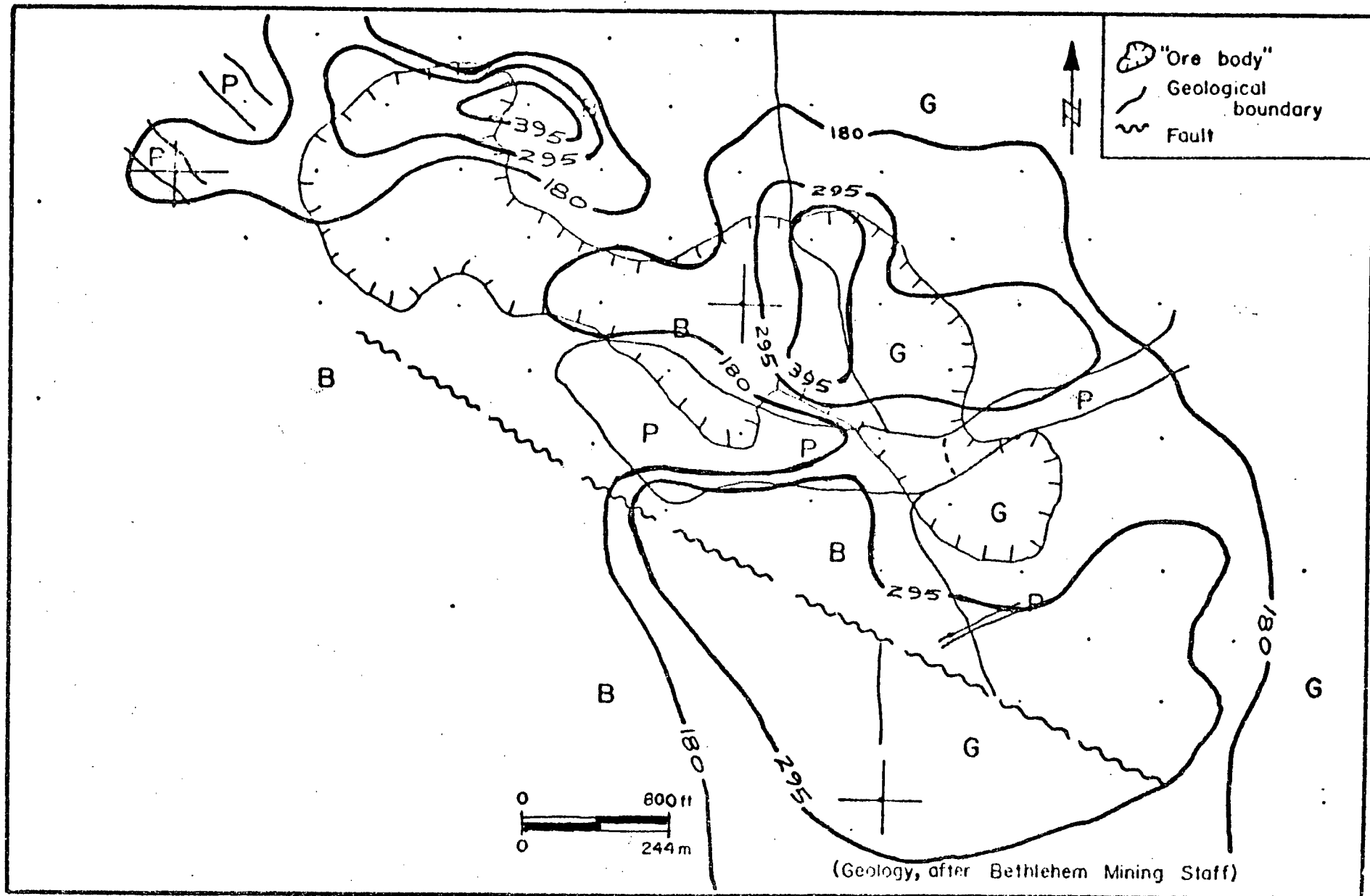


FIGURE A26: Distribution of F (ppm), Bethlehem-JA 2800 Level

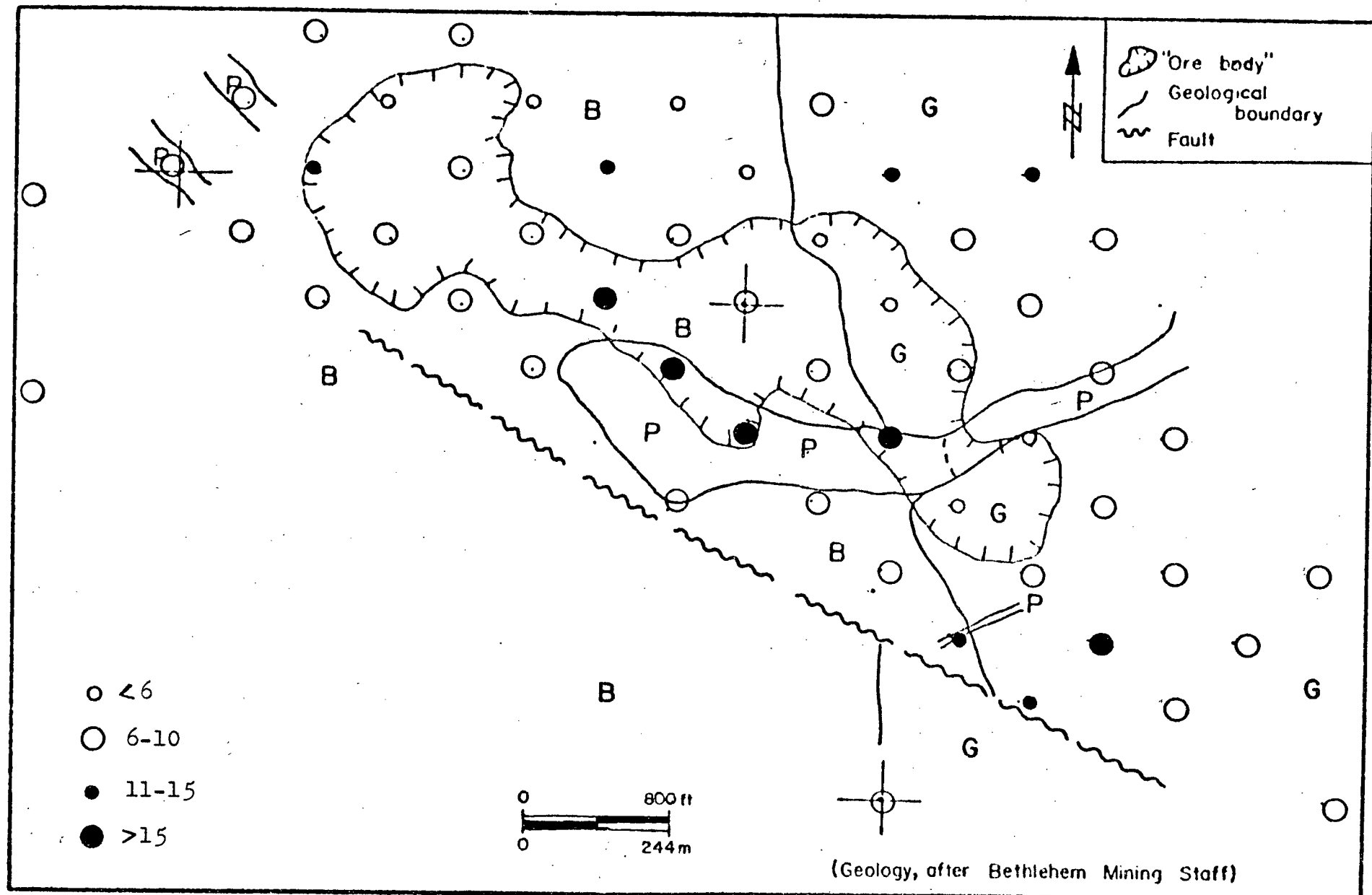


FIGURE A27: Distribution of water-extractable F (ppm), Bethlehem-JA 2800 Level

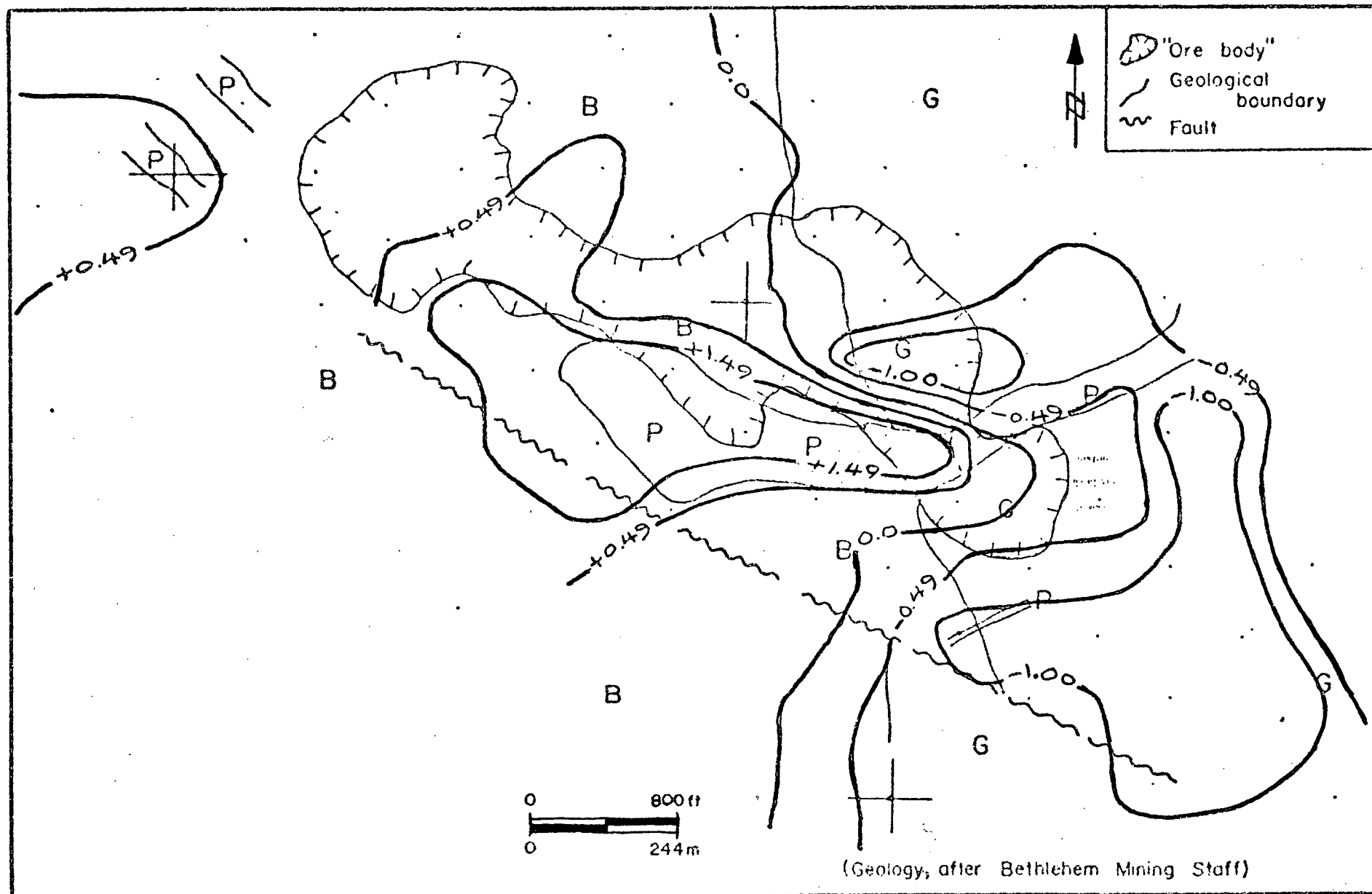


FIGURE A28: Scores of Factor R-1 (V,Fe,Mg,Zn,Mn,Ca,Ti vs Si), Bethlehem-JA 2800 Level

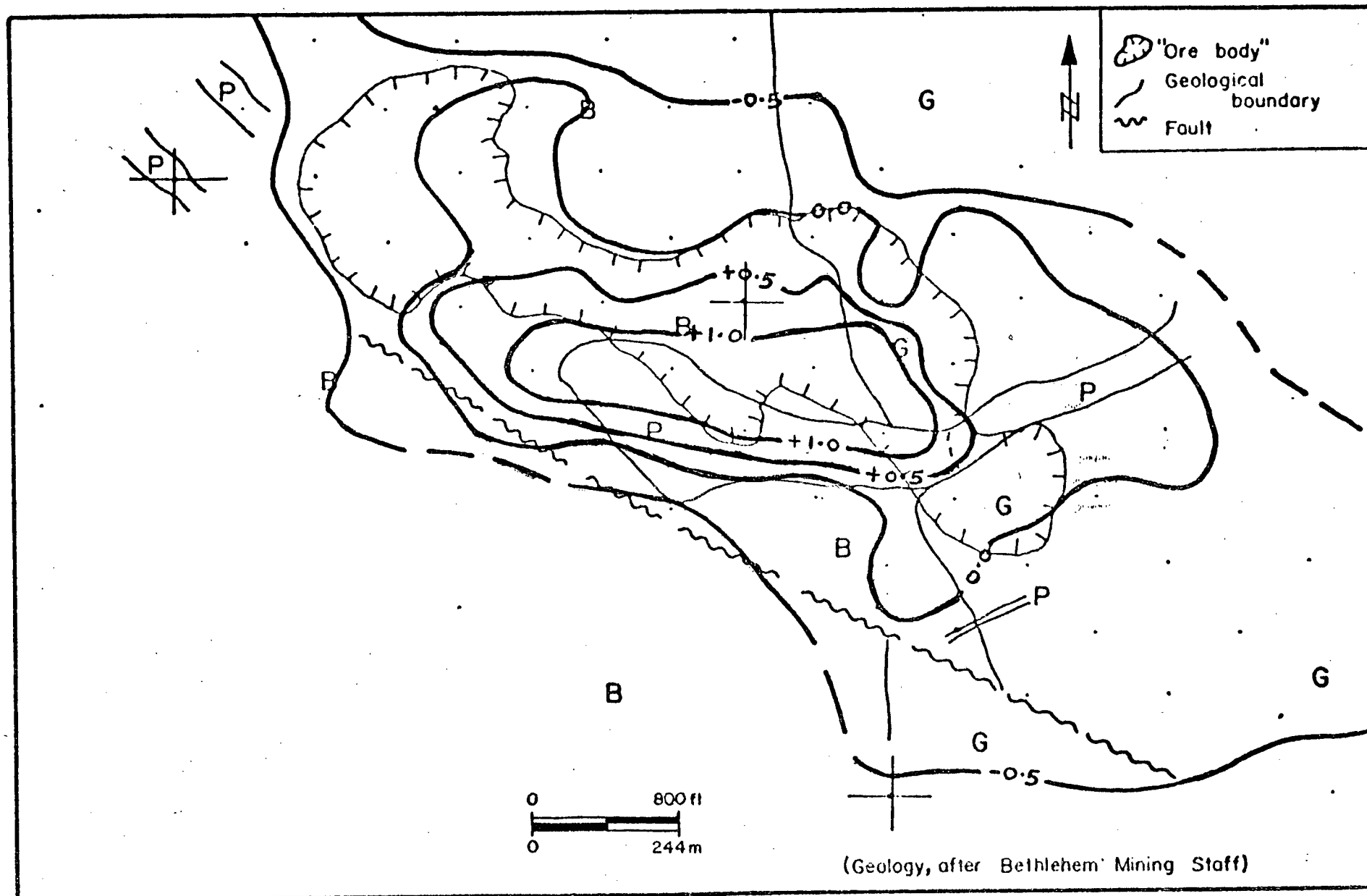


FIGURE A29: Scores of Factor R-2 (K,Rb vs Ti,Ca,Sr), Bethlehem-JA 2800 Level

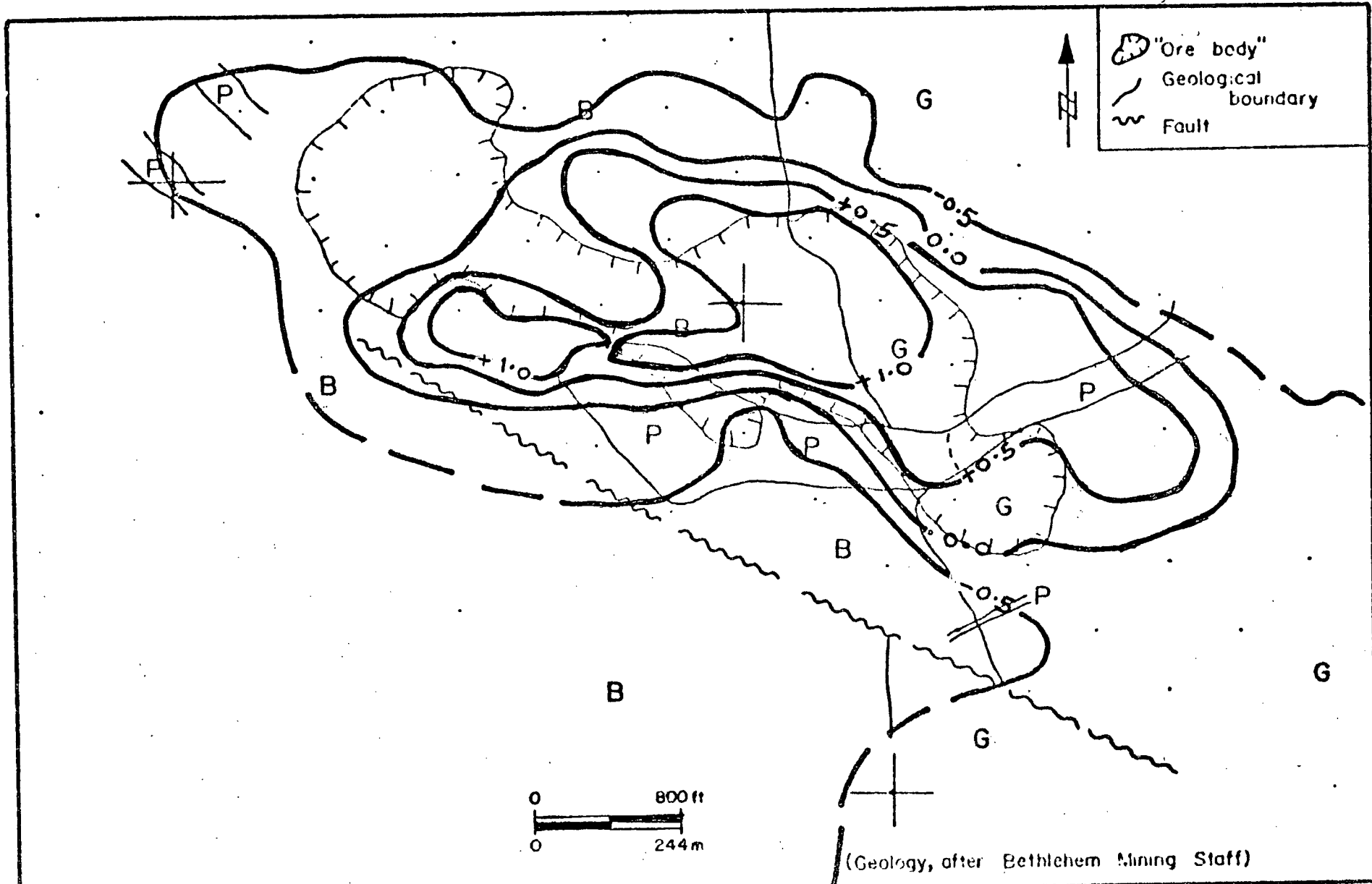


FIGURE A30: Scores of Factor R-3 (Hg,Cl vs B), Bethlehem-JA 2800 Level

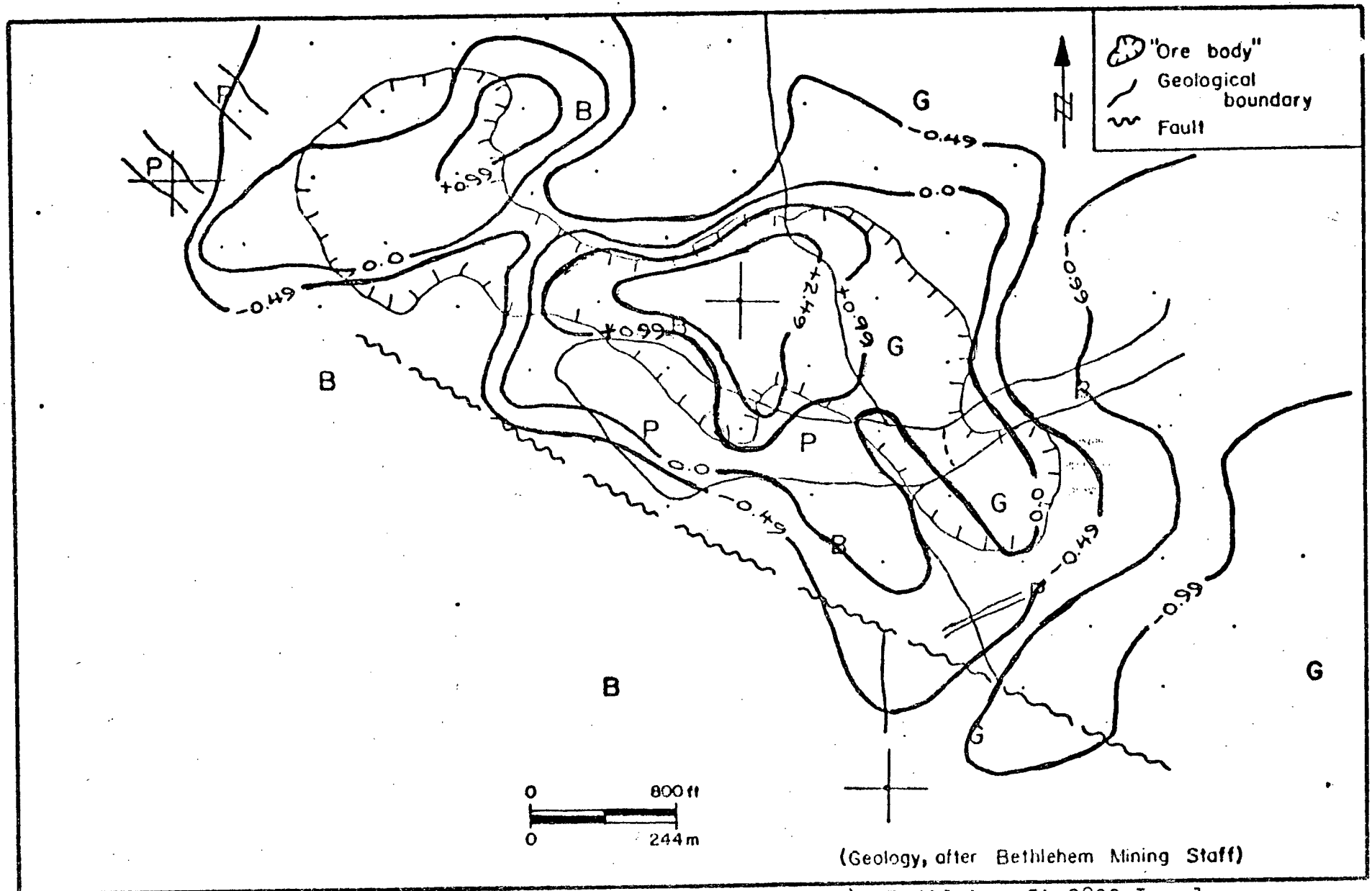


FIGURE A31: Scores of Factor R-4 (Mo,S,Cu vs Na), Bethlehem-JA 2800 Level

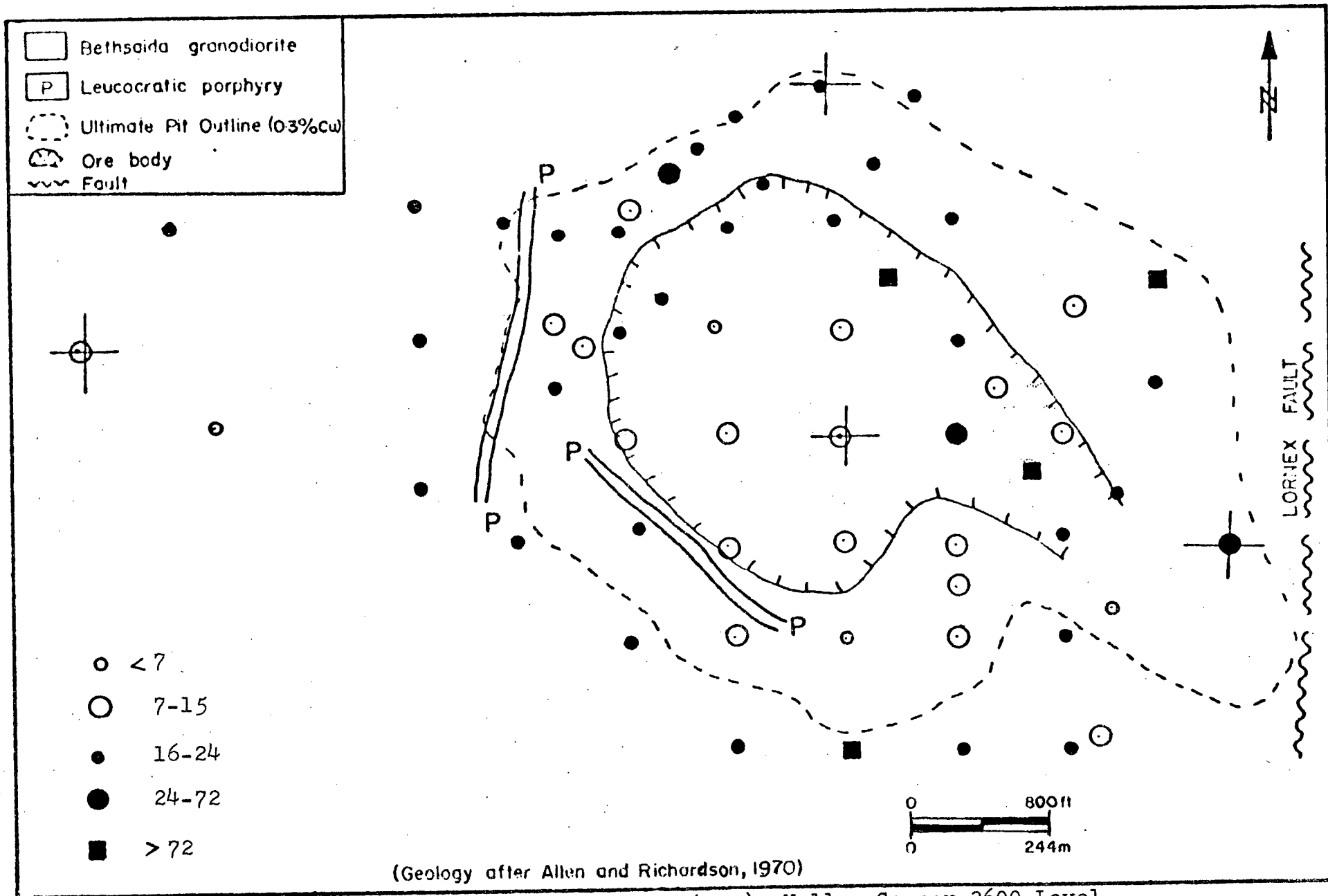


FIGURE A32: Distribution of Zn (ppm), Valley Copper 3600 Level

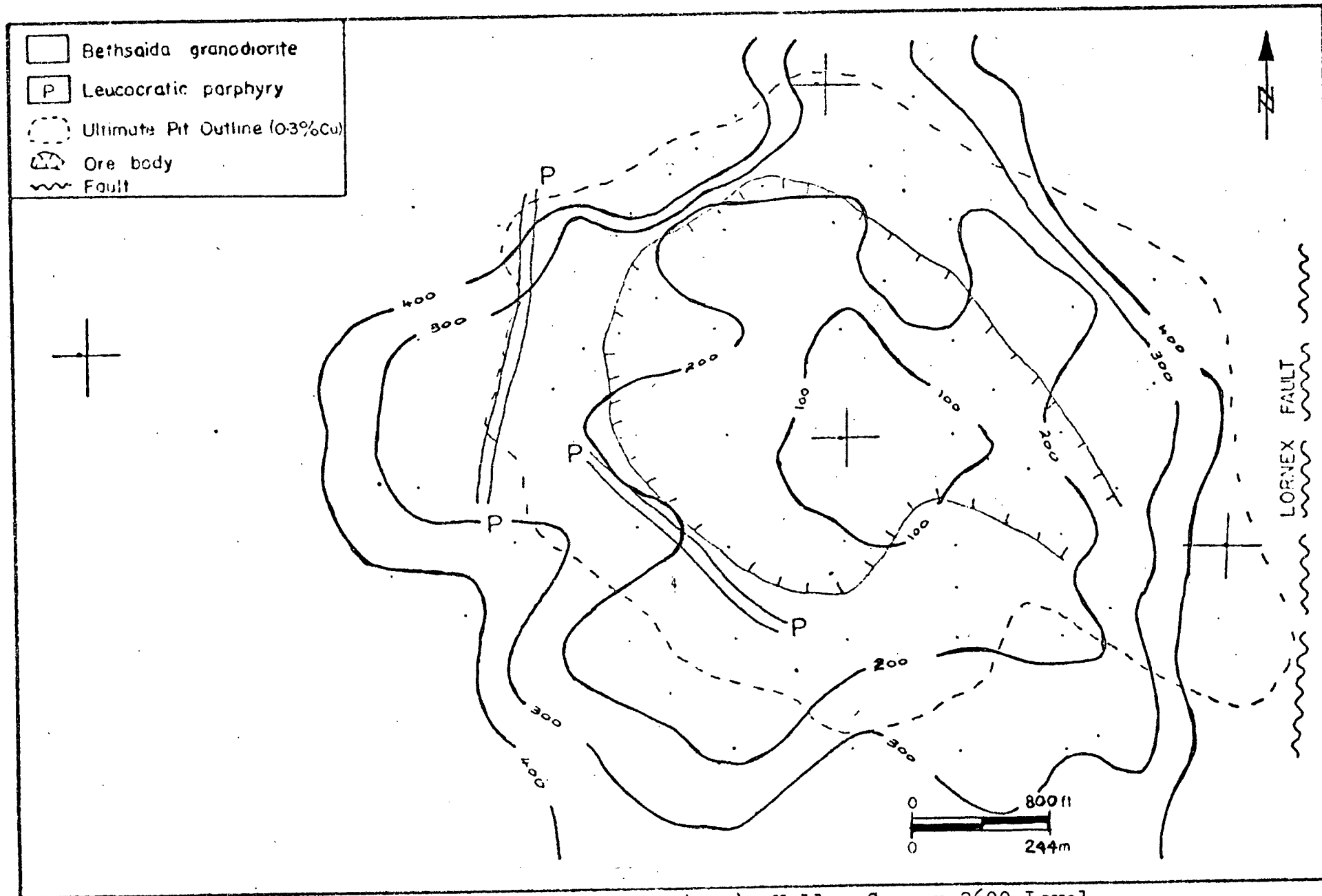


FIGURE A33: Distribution of Mn (ppm), Valley Copper 3600 Level

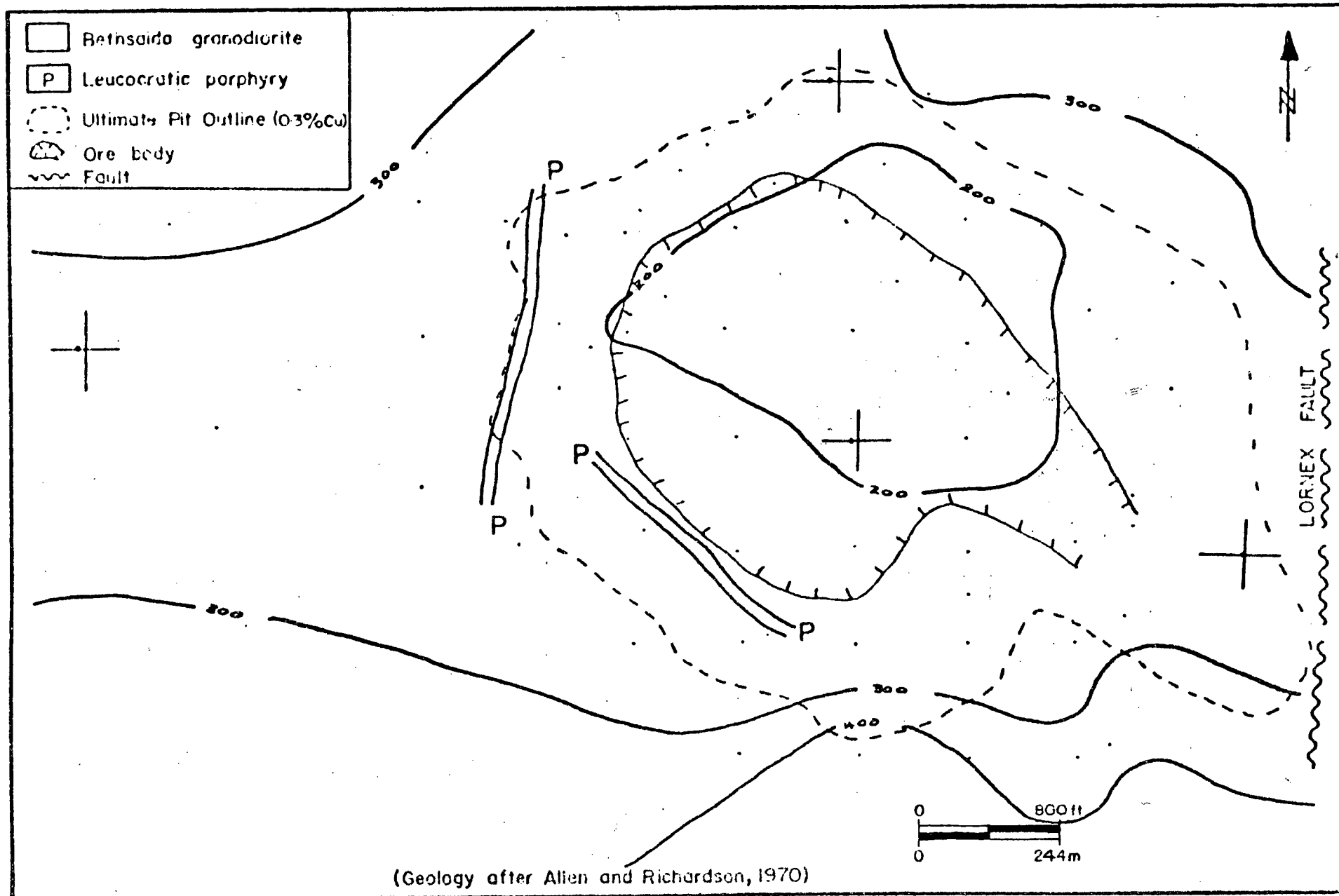


FIGURE A34: Distribution of Mn (ppm), Valley Copper 3300 Level

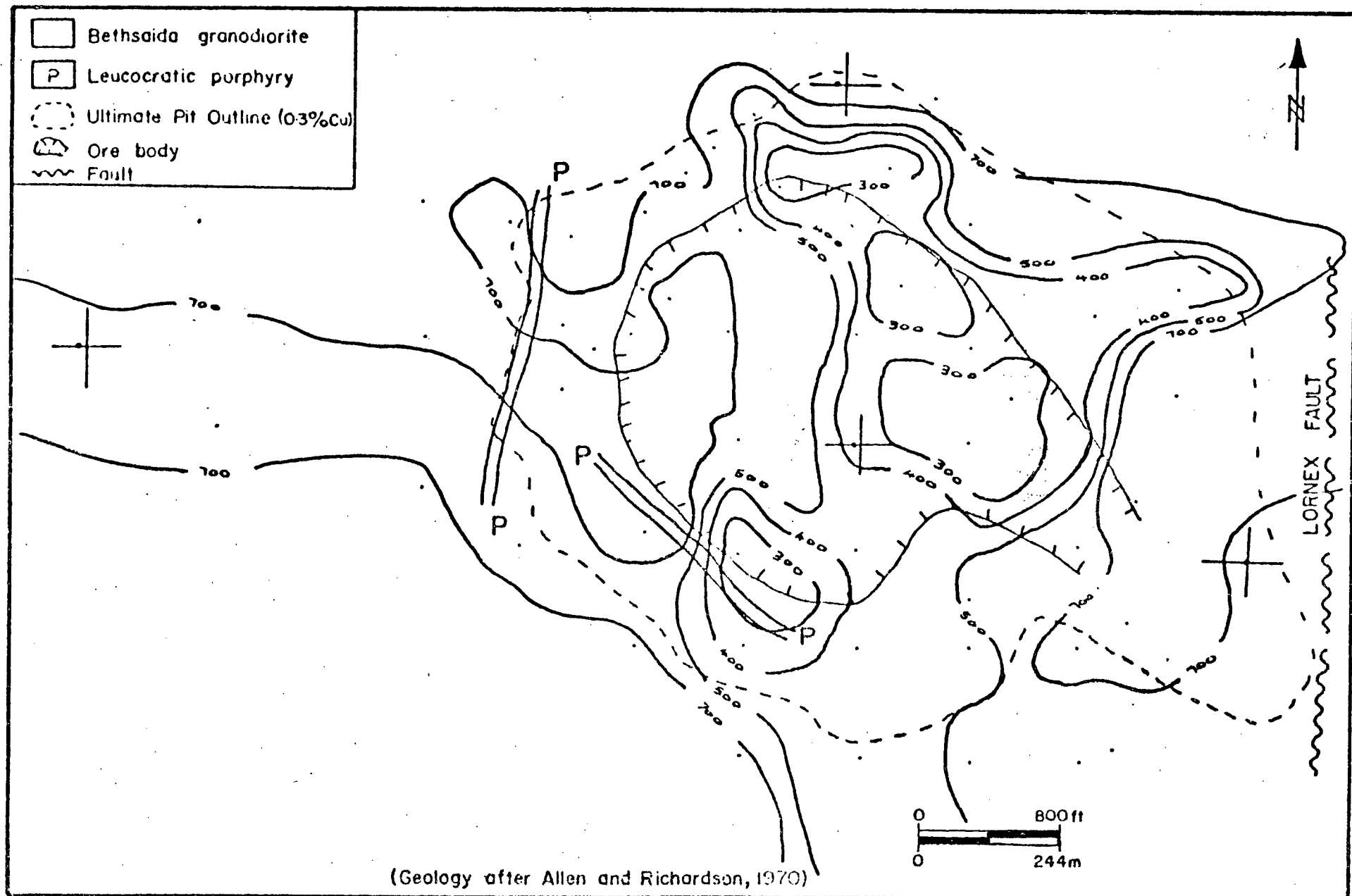


FIGURE A35: Distribution of Sr (ppm), Valley Copper 3600 Level

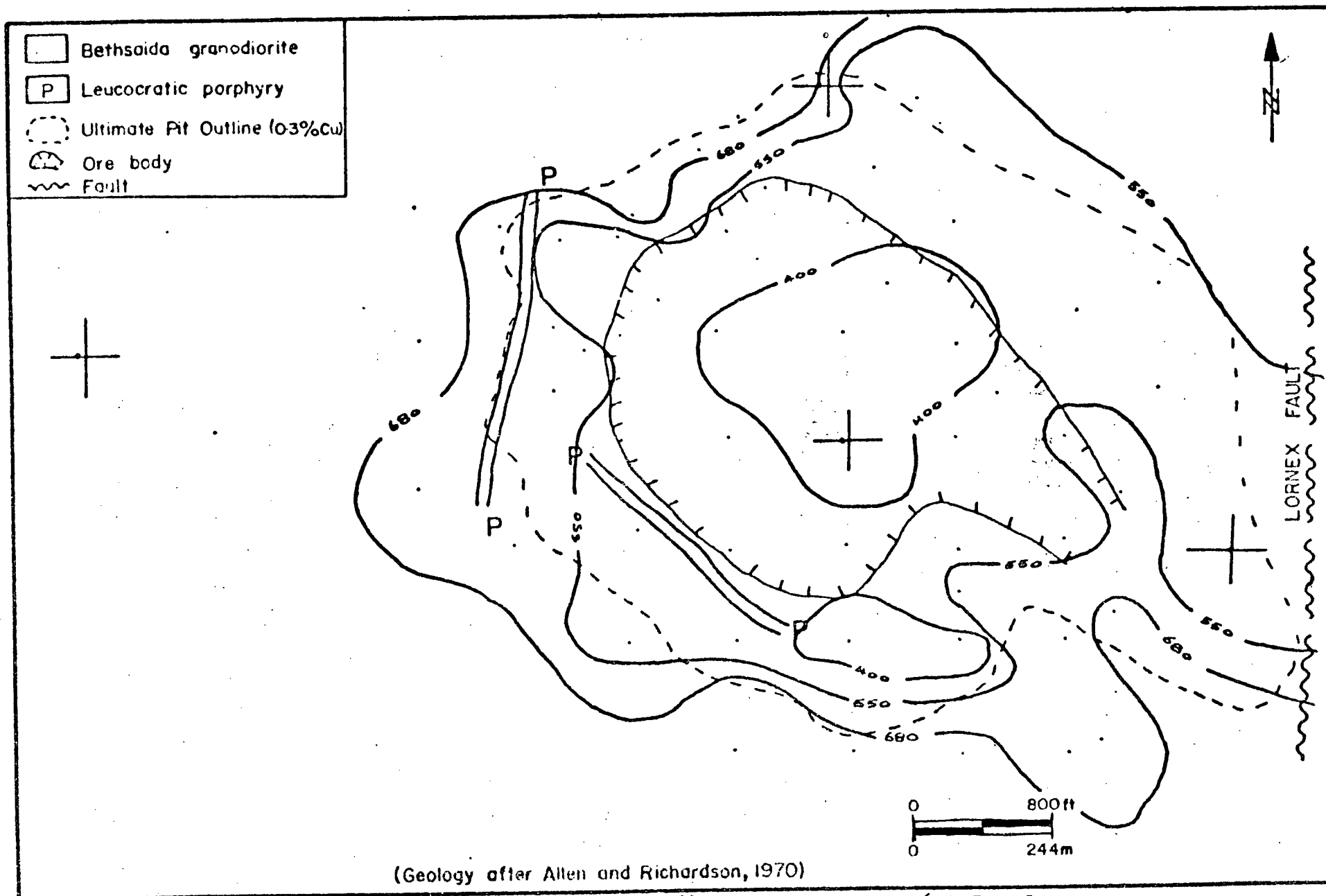


FIGURE A36a: Distribution of Ba (ppm), Valley Copper 3600 Level

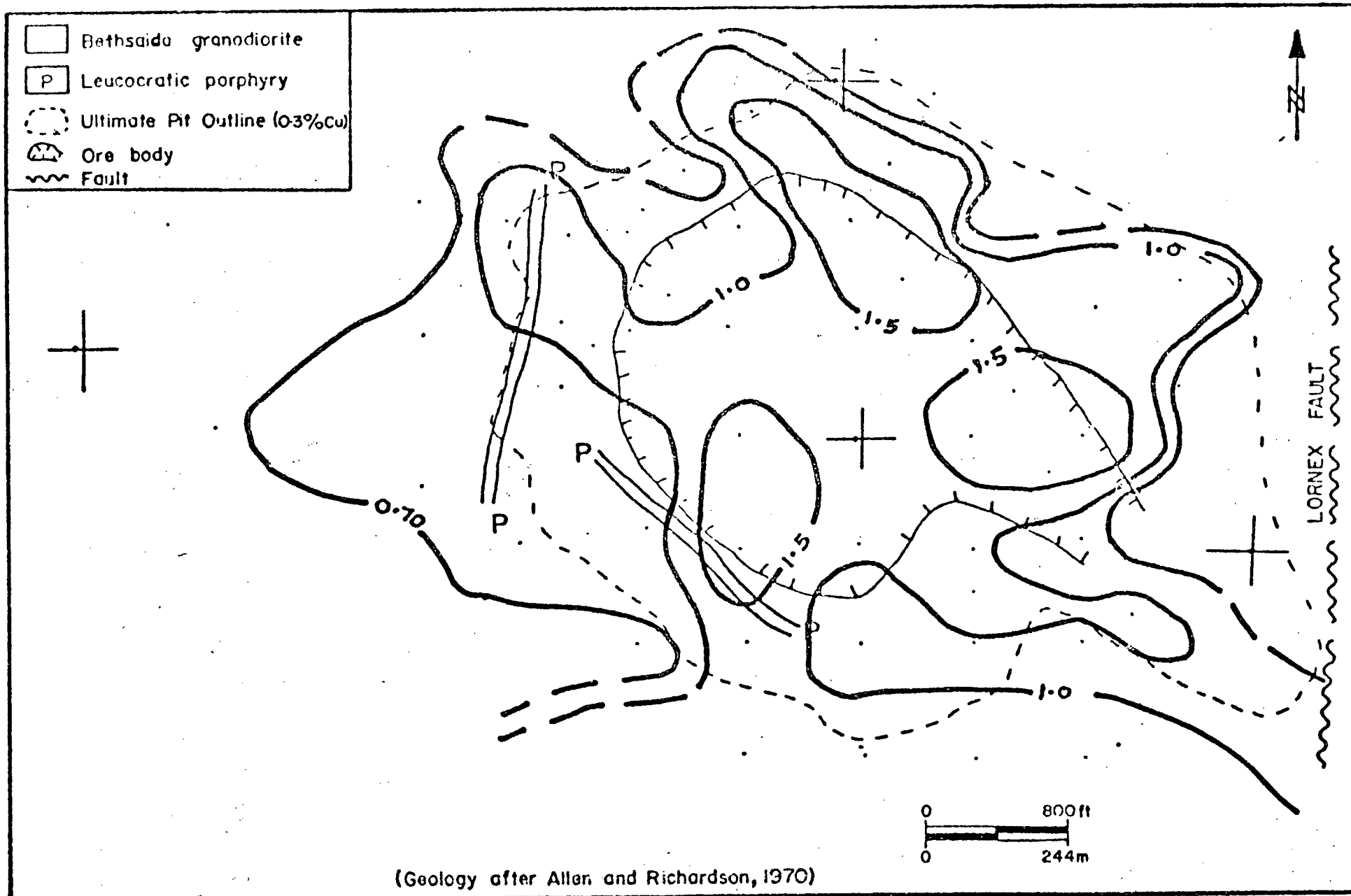


FIGURE A36b: Distribution of Ba/Sr Ratios, Valley Copper 3600 Level

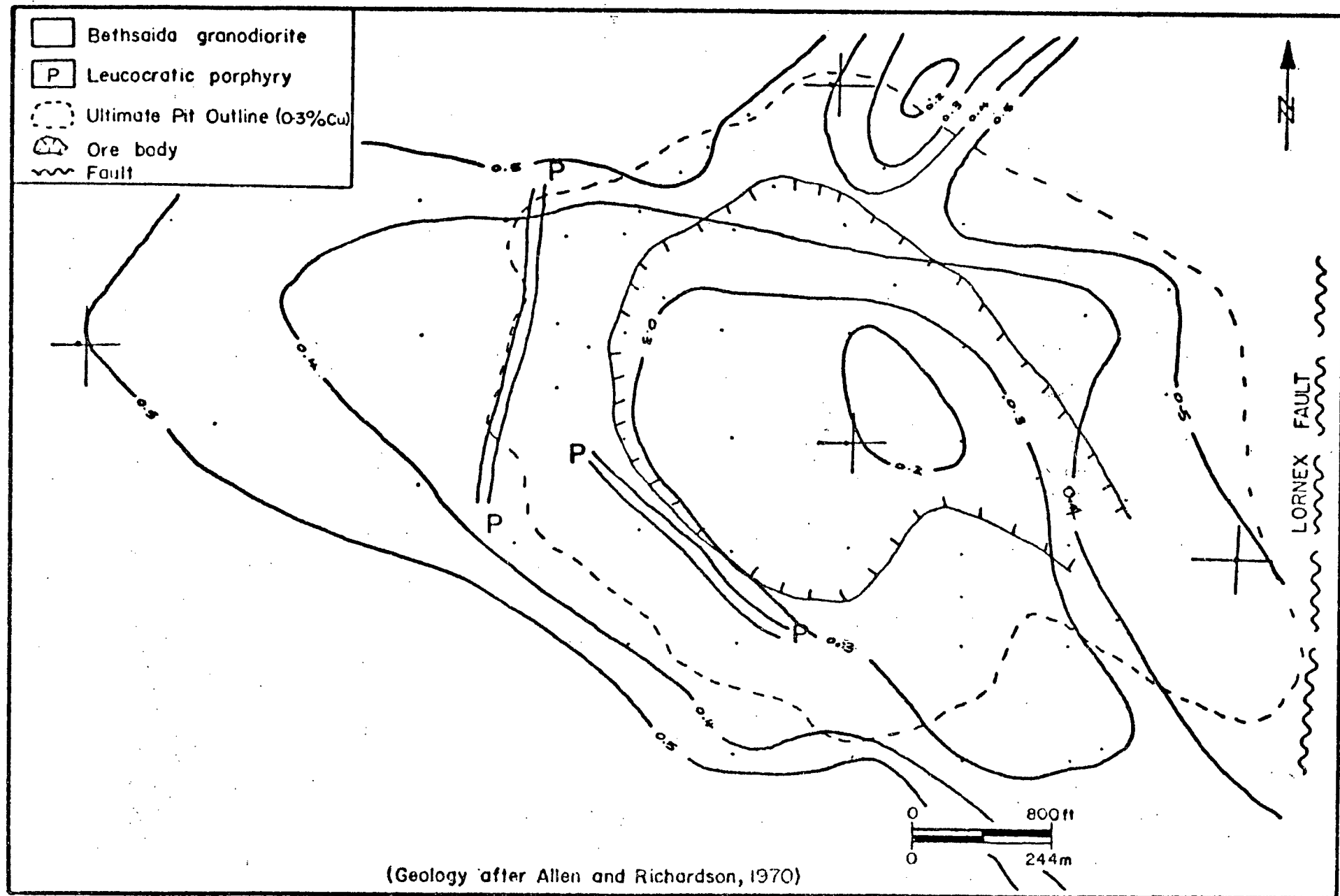


FIGURE A37: Distribution of MgO (wt.%), Valley Copper 3600 Level

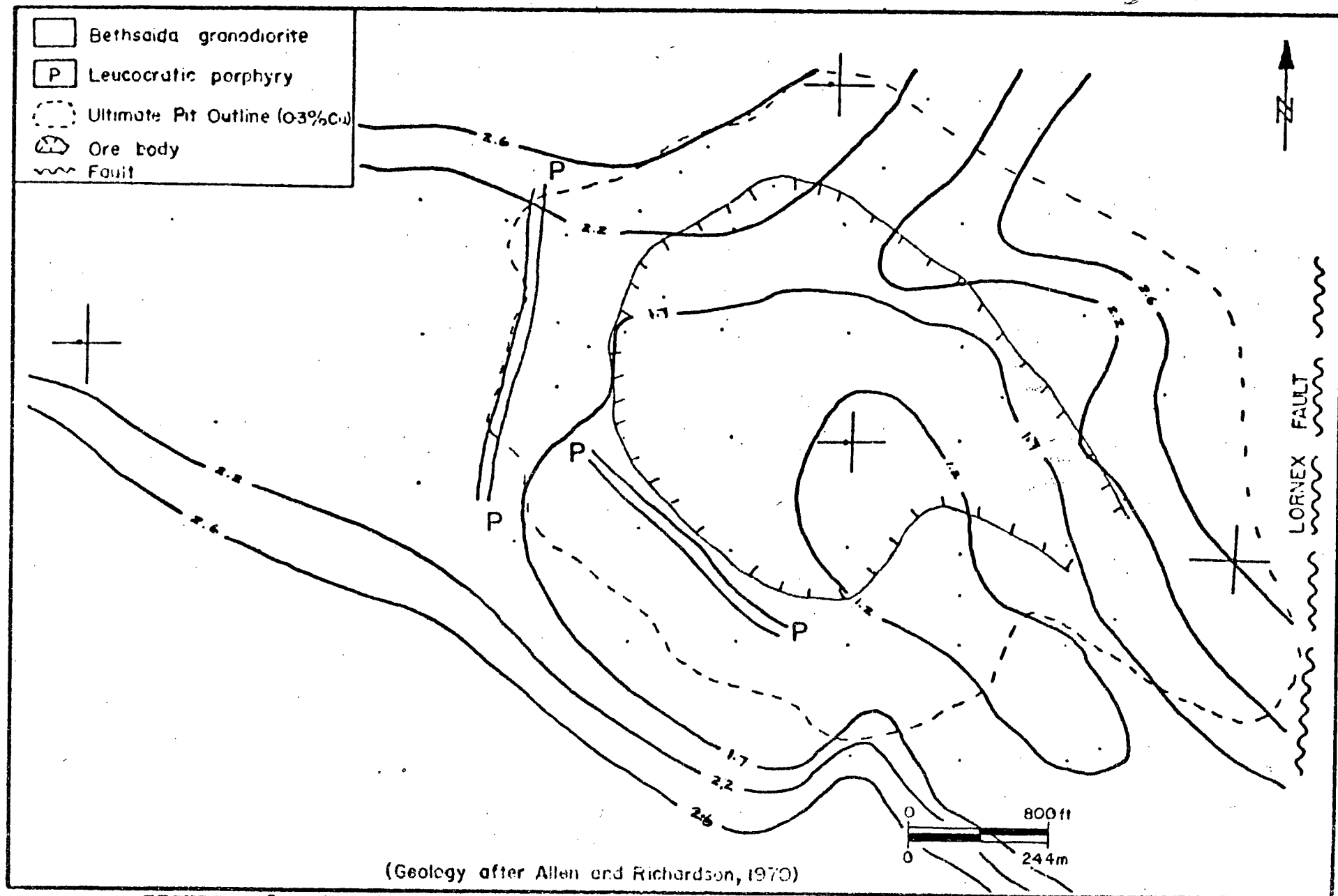


FIGURE A38: Distribution of Total Fe as Fe_2O_3 (wt.%), Valley Copper 3600 Level

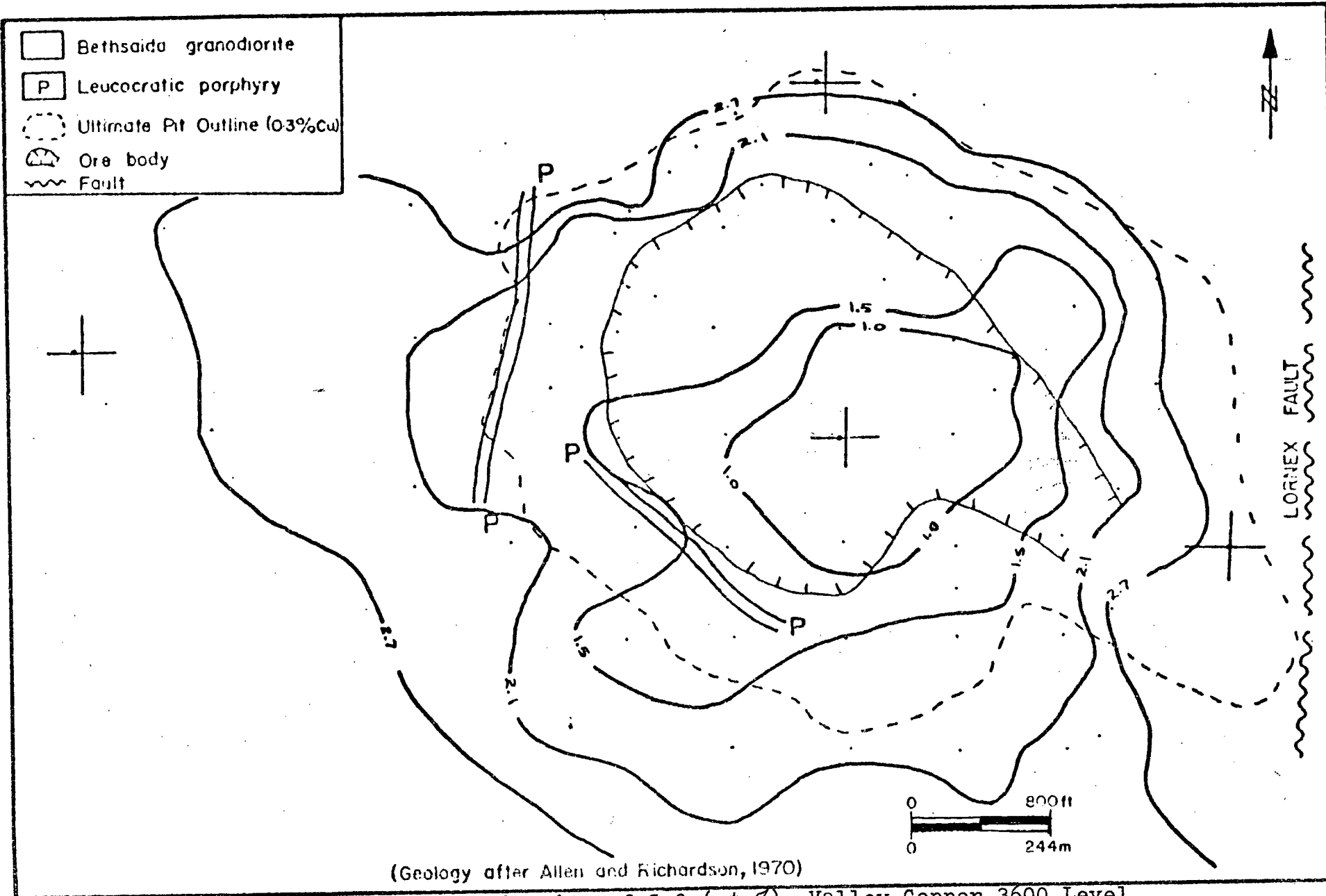


FIGURE A40: Distribution of CaO (wt.%), Valley Copper 3600 Level

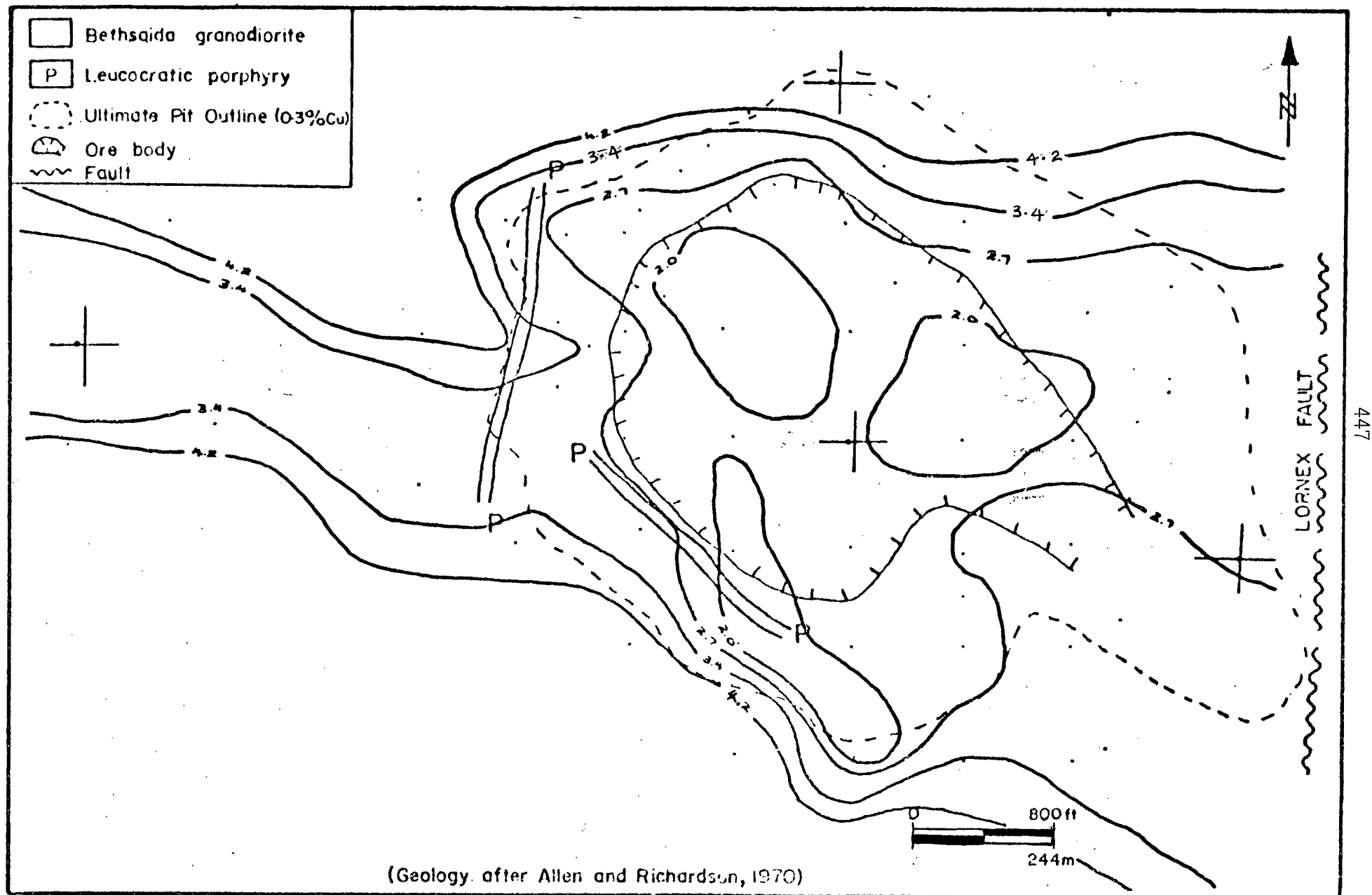


FIGURE A41: Distribution of Na_2O (wt.%), Valley Copper 3600 Level

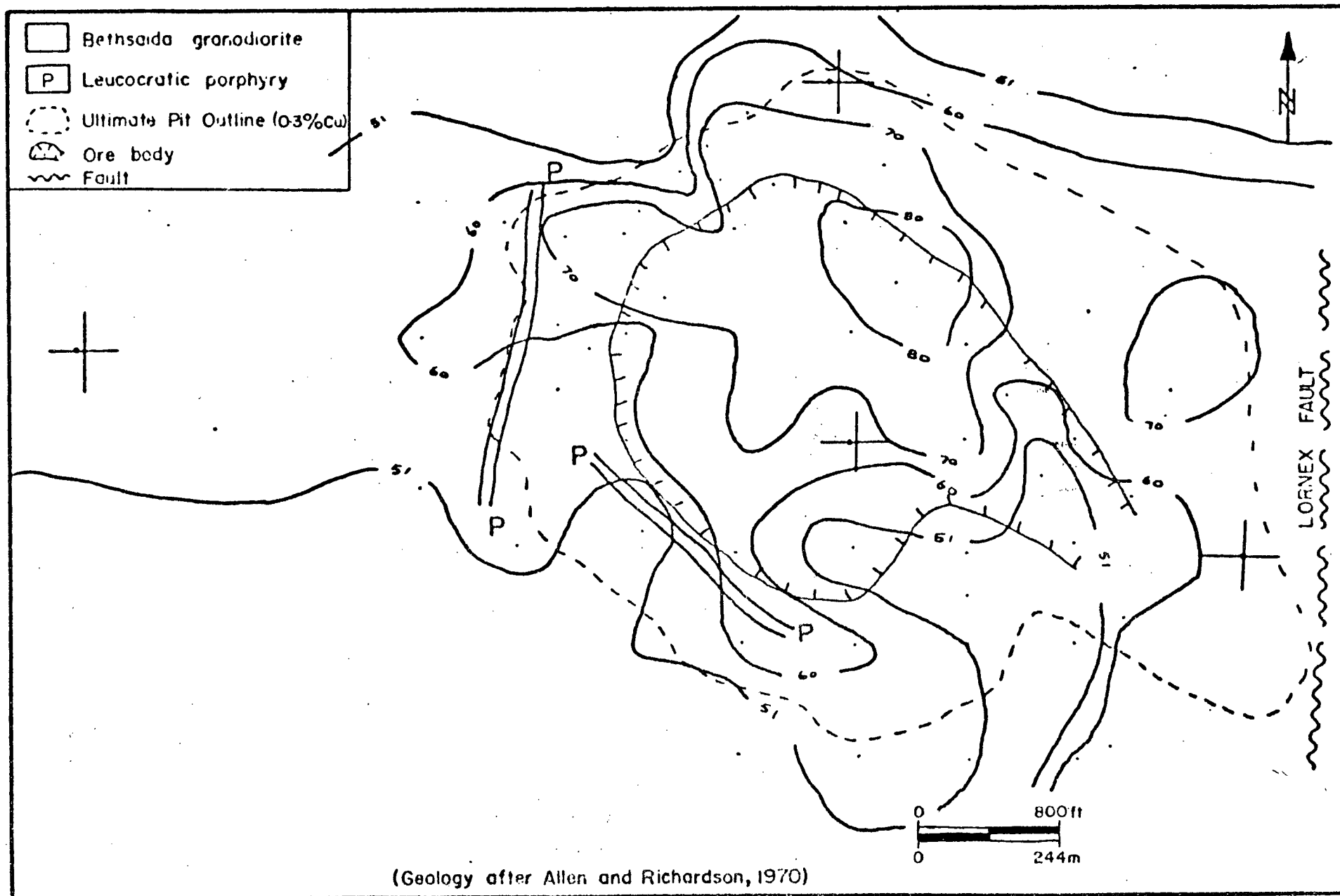


FIGURE A42: Distribution of Rb (ppm), Valley Copper 3600 Level

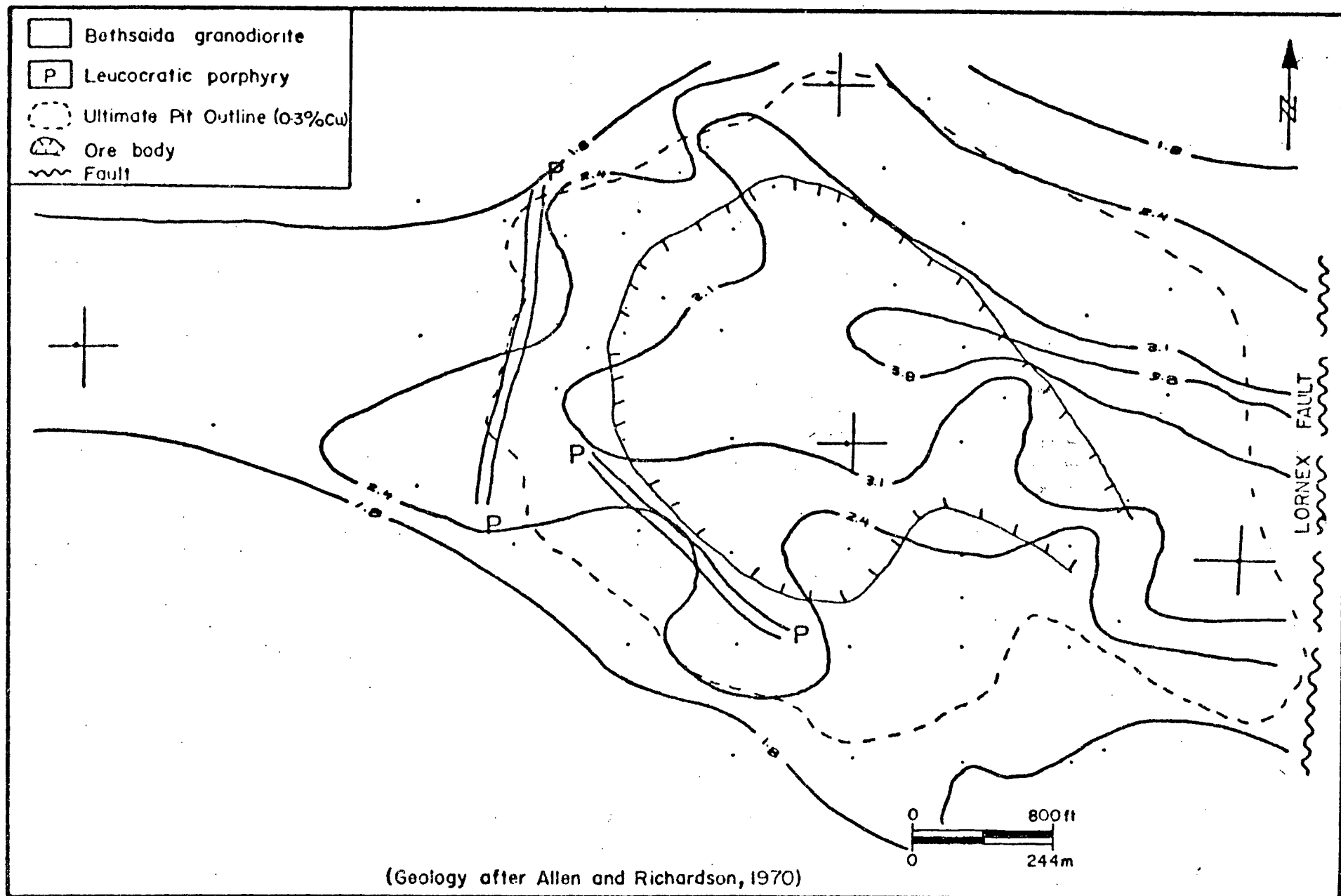


FIGURE A43: Distribution of K_2O (wt.%), Valley Copper 3600 Level

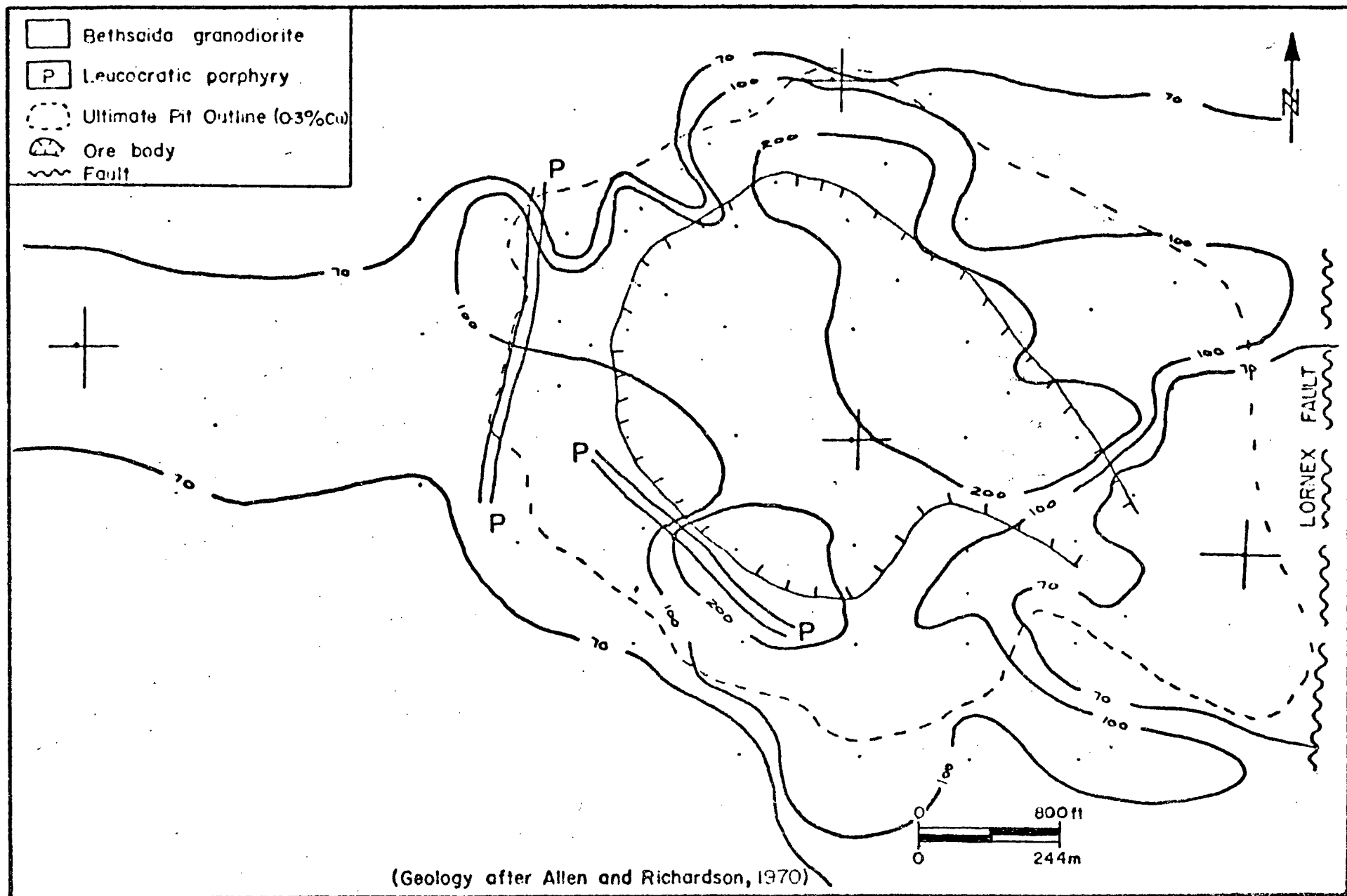


FIGURE A44: Distribution of Rb/Sr Ratios (x1000), Valley Copper 3600 Level

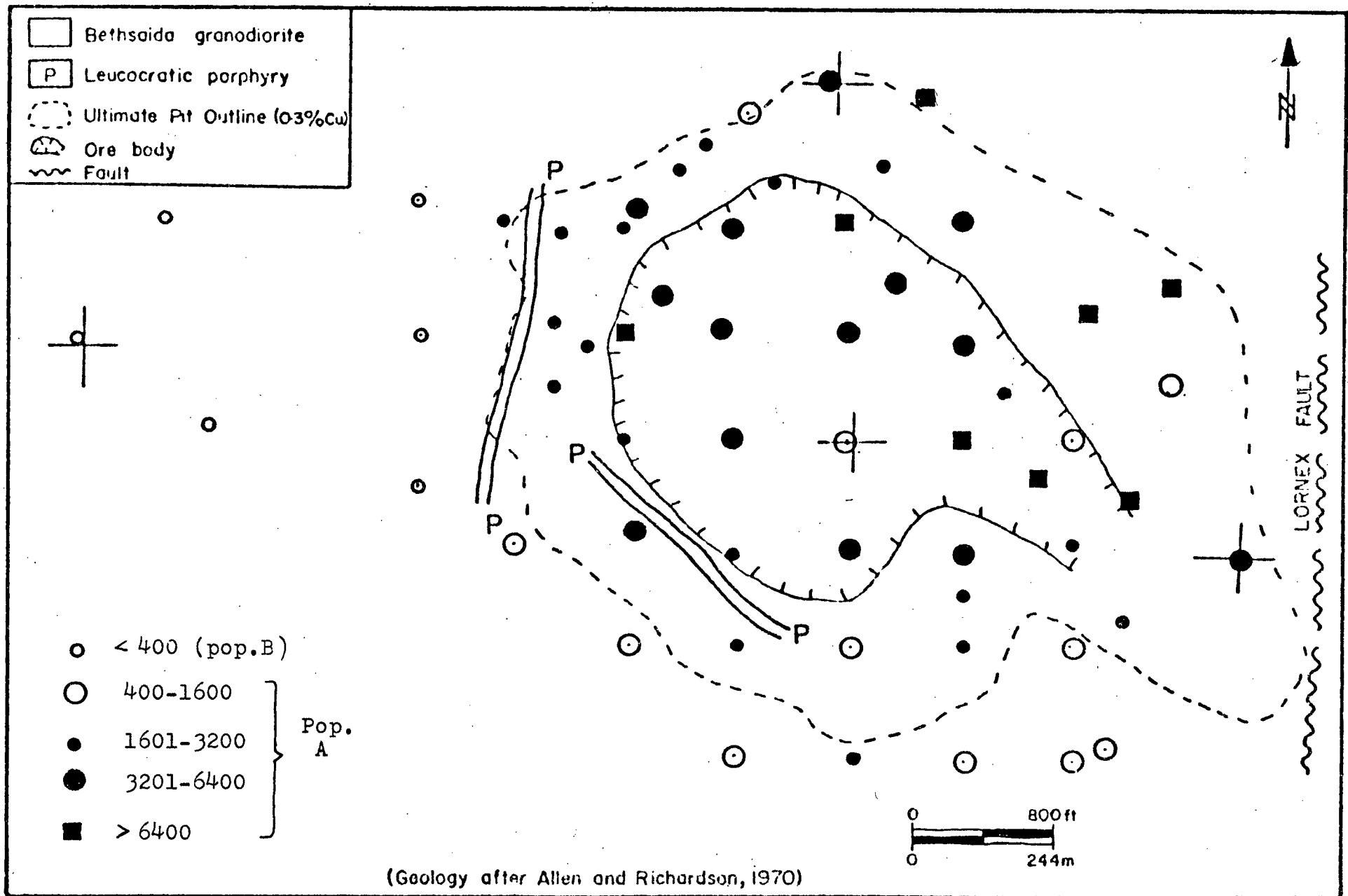


FIGURE A46: Distribution of Cu (ppm), Valley Copper Suboutcrop Level

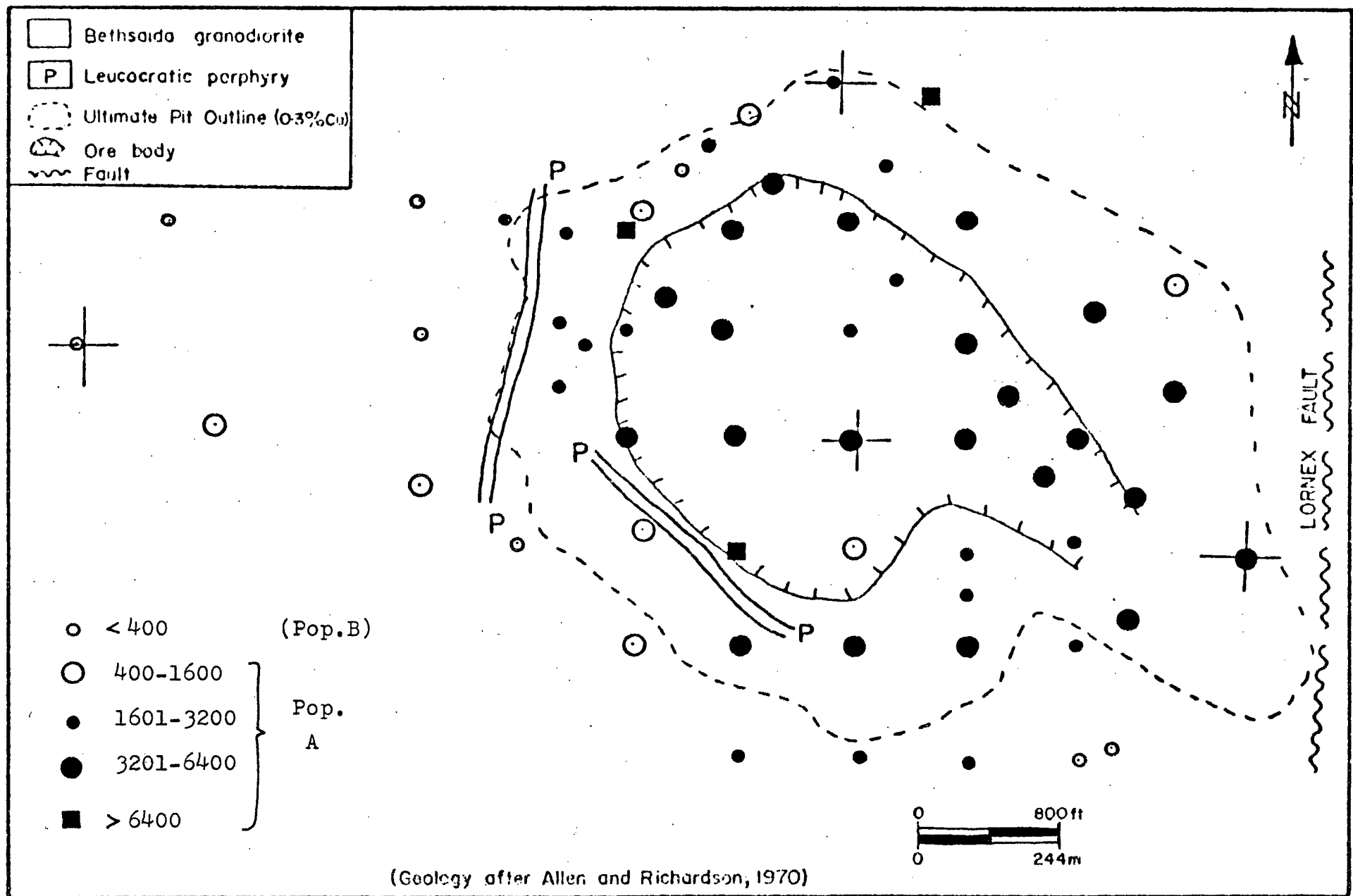


FIGURE A47: Distribution of Cu (ppm), Valley Copper 3600 Level

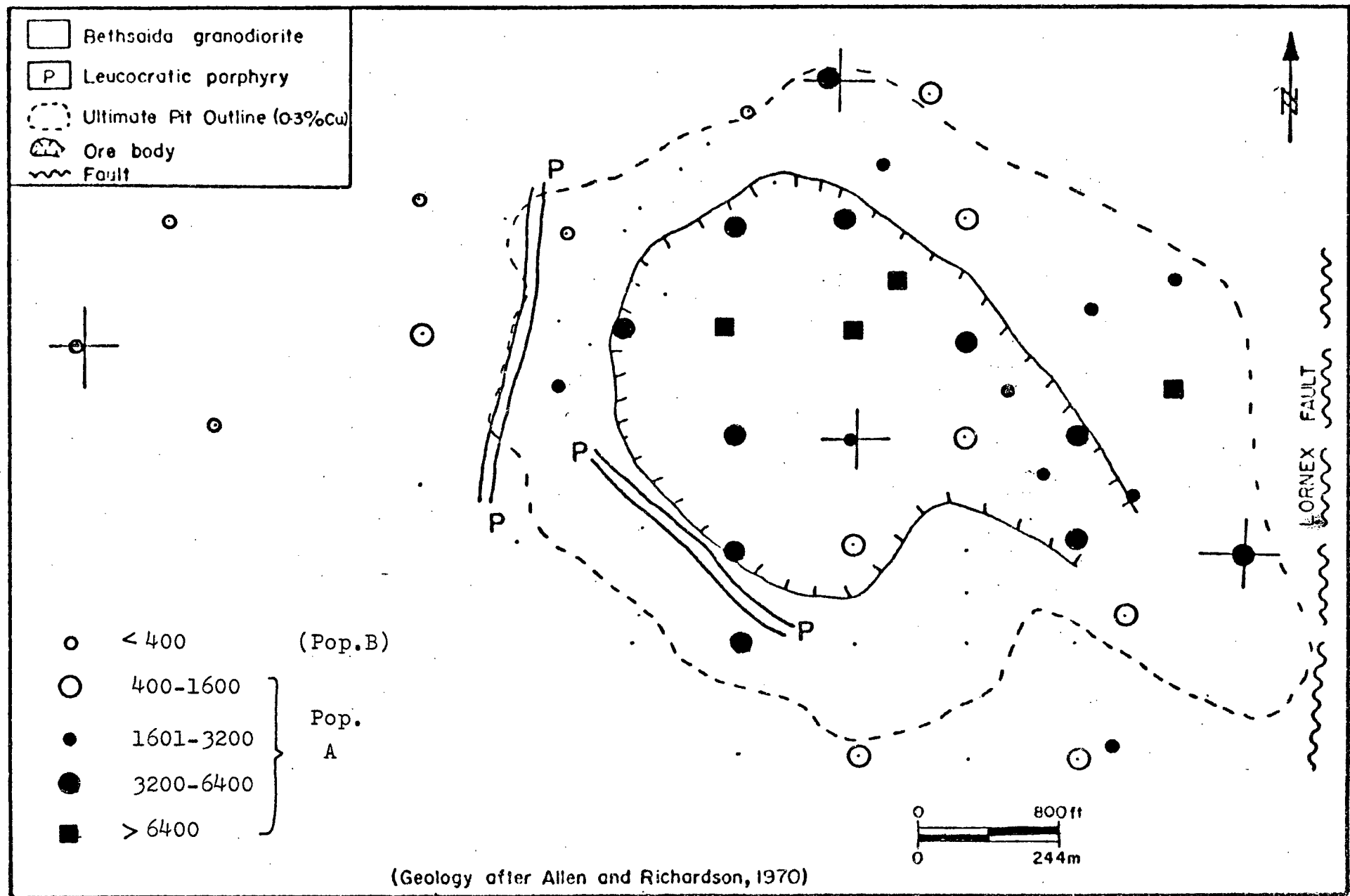


FIGURE A48: Distribution of Cu(ppm), Valley Copper 3300 Level

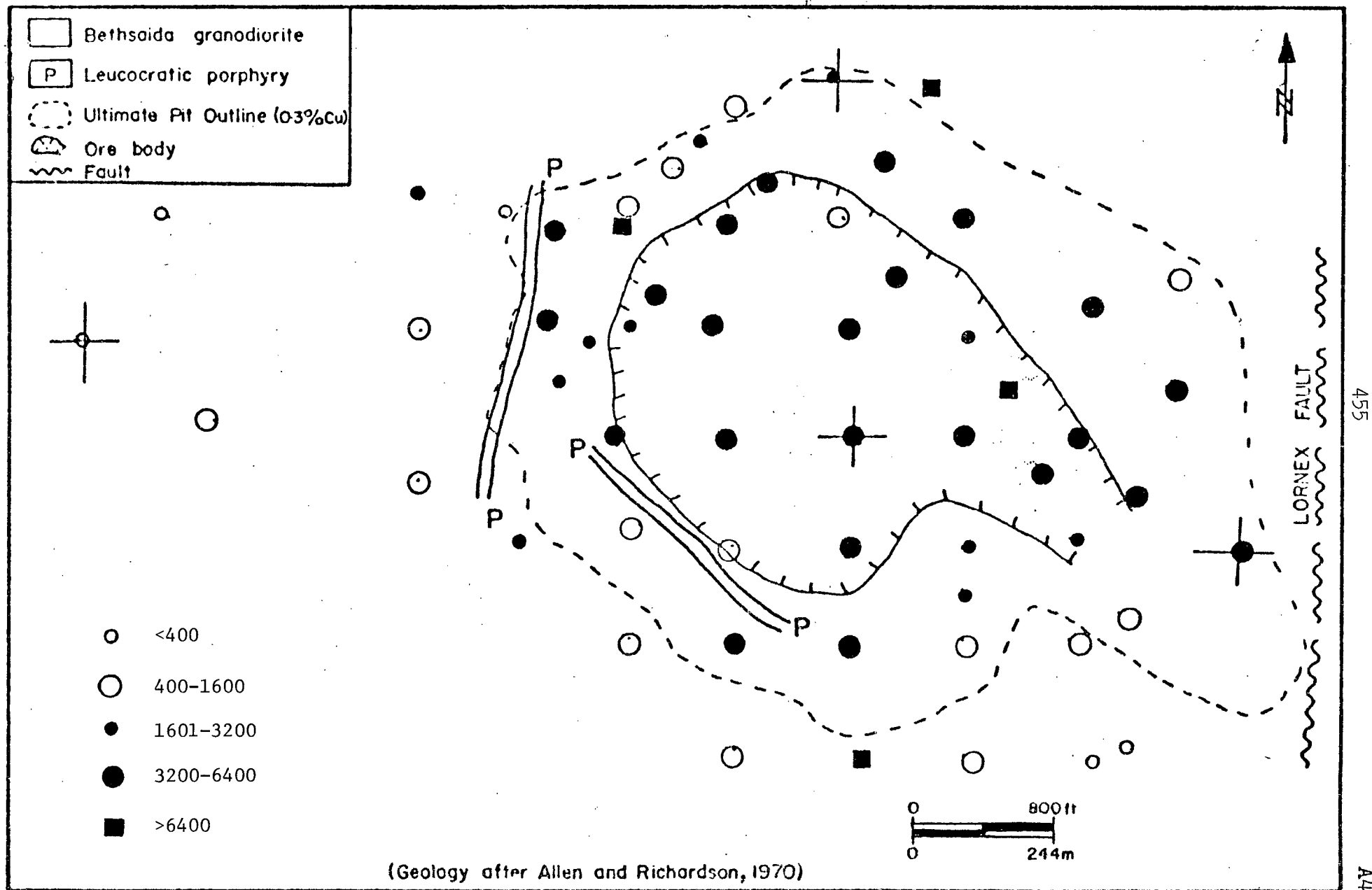


FIGURE A49: Distribution of Sulphide-held Cu (ppm), Valley Copper 3600 Level

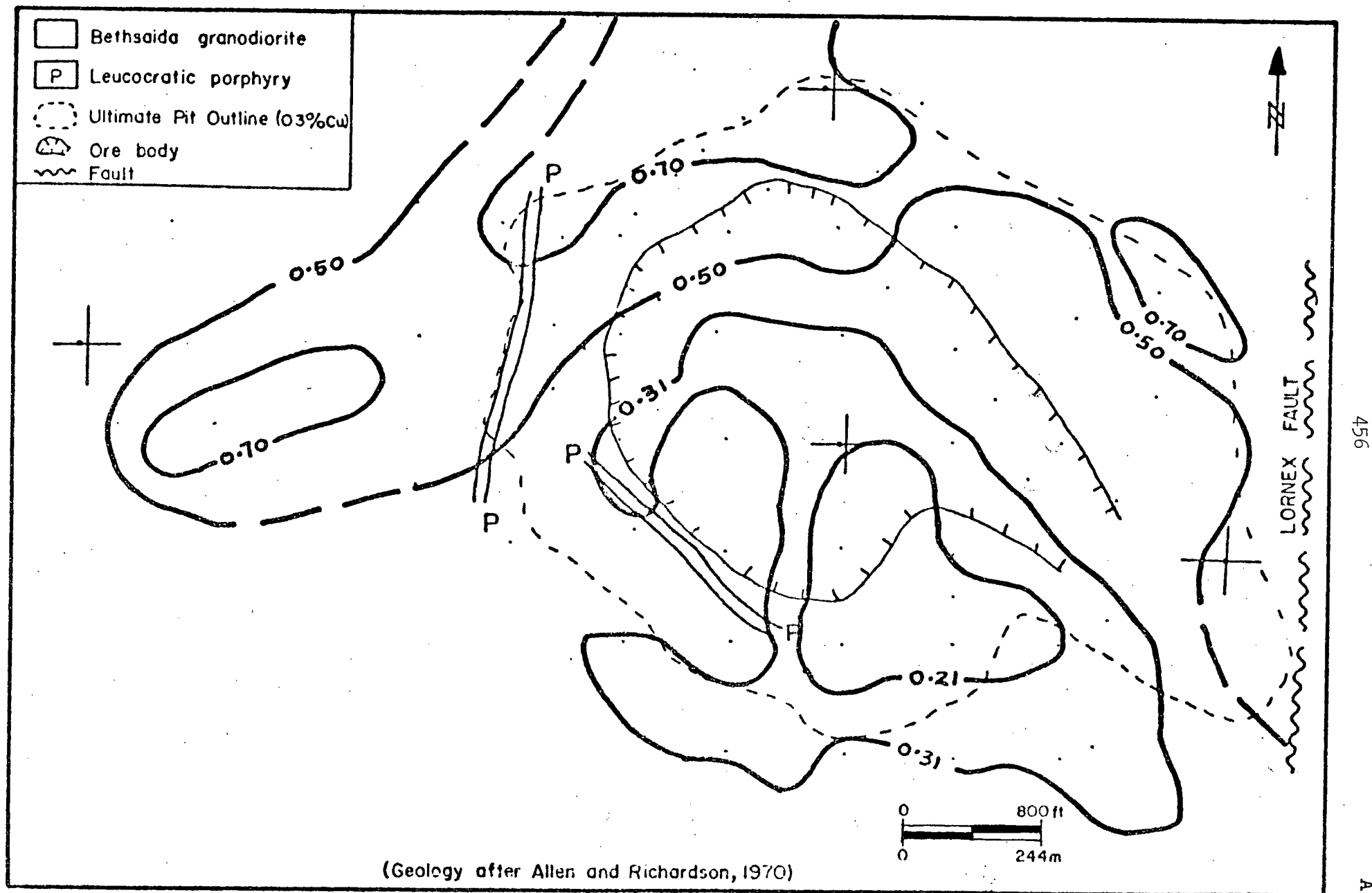
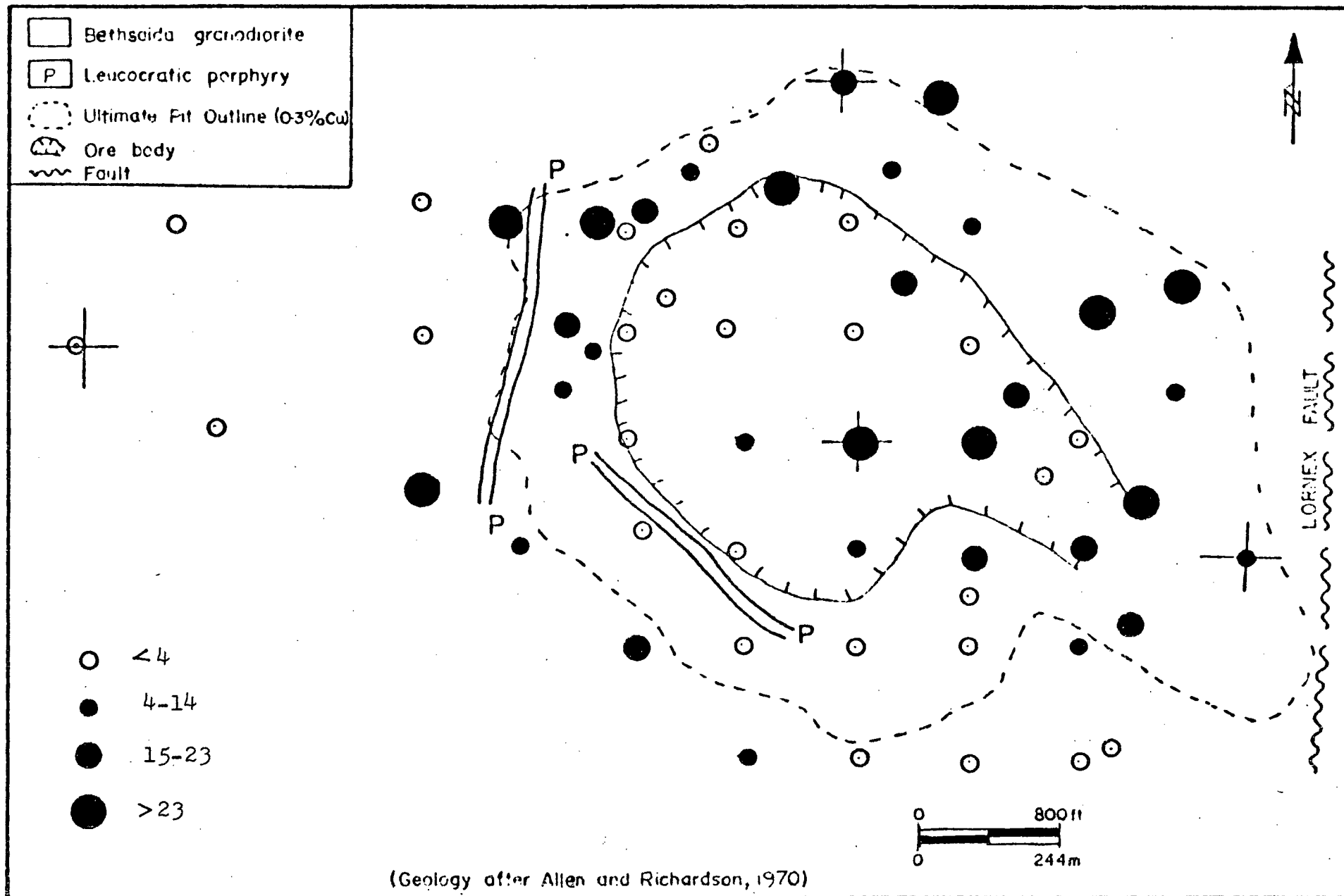


FIGURE A50: Distribution of Sulphide-held Fe (wt.%), Valley Copper 3600 Level



(Geology after Allen and Richardson, 1970)

FIGURE A51: Distribution of Mo (ppm), Valley Copper 3600 Level

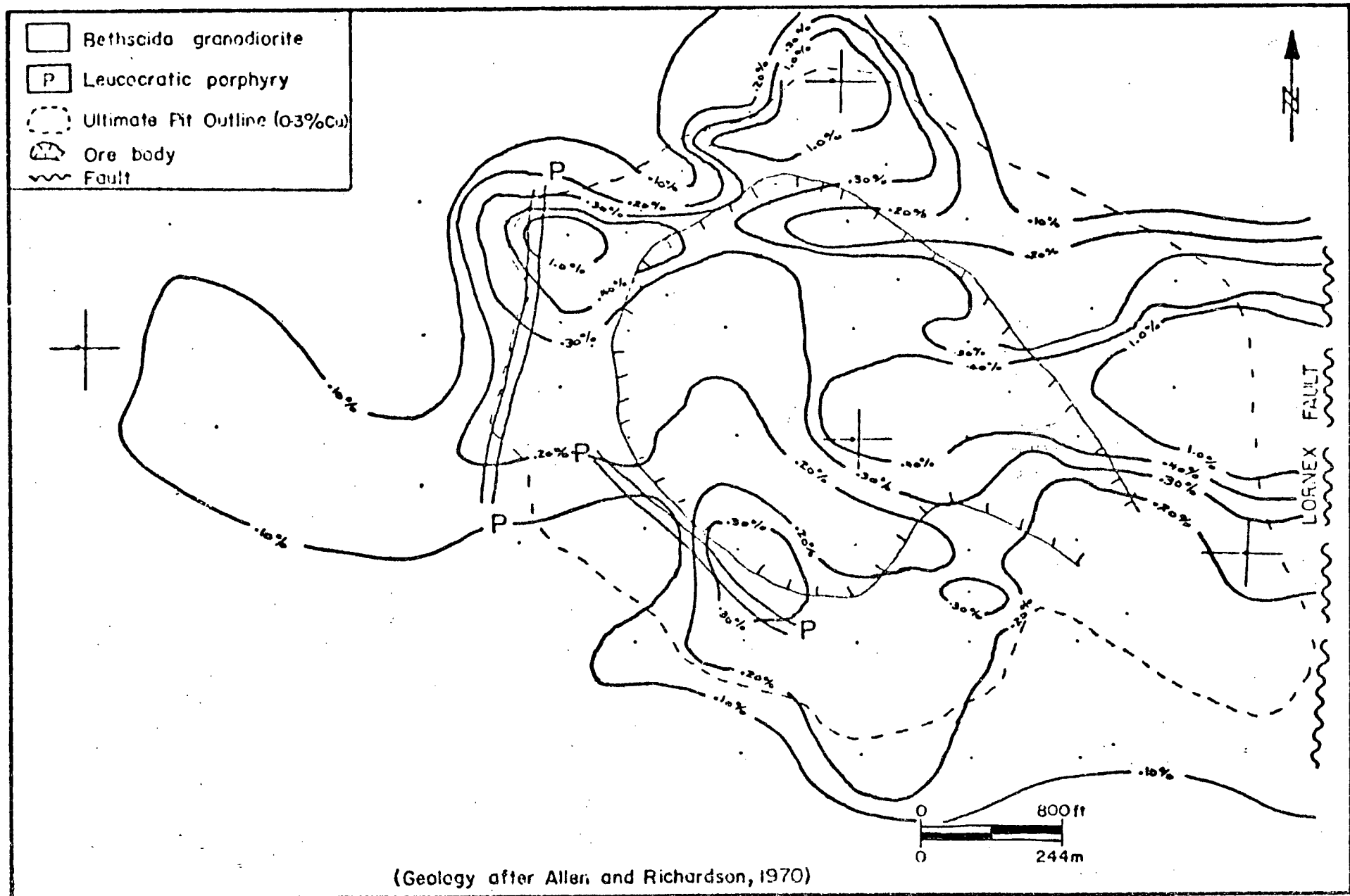
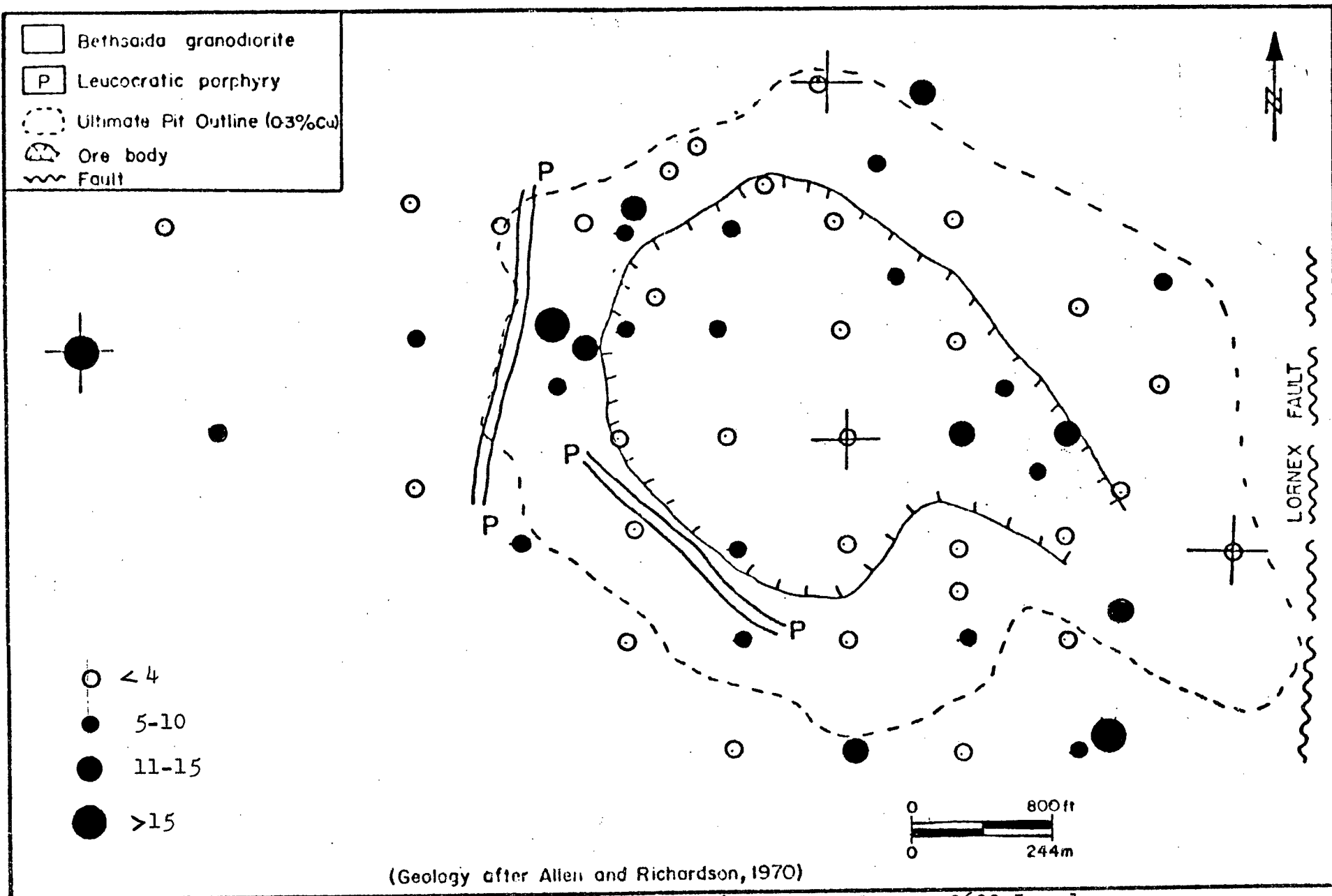


FIGURE A52: Distribution of S (wt.%), Valley Copper 3600 Level



(Geology after Allen and Richardson, 1970)

FIGURE A53: Distribution of B (ppm), Valley Copper 3600 Level

459

A53

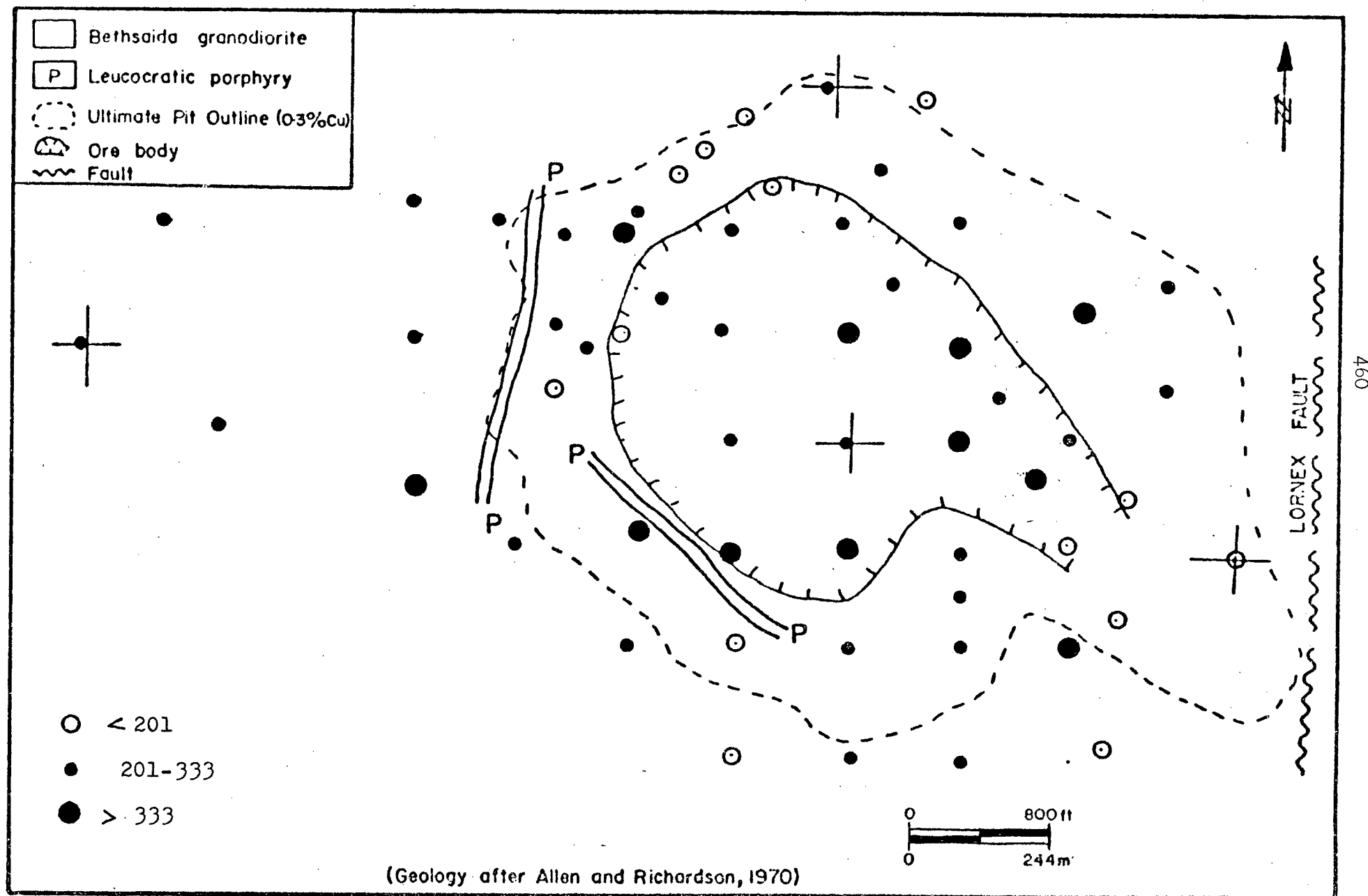


FIGURE A54: Distribution of Cl (ppm), Valley Copper 3600 Level

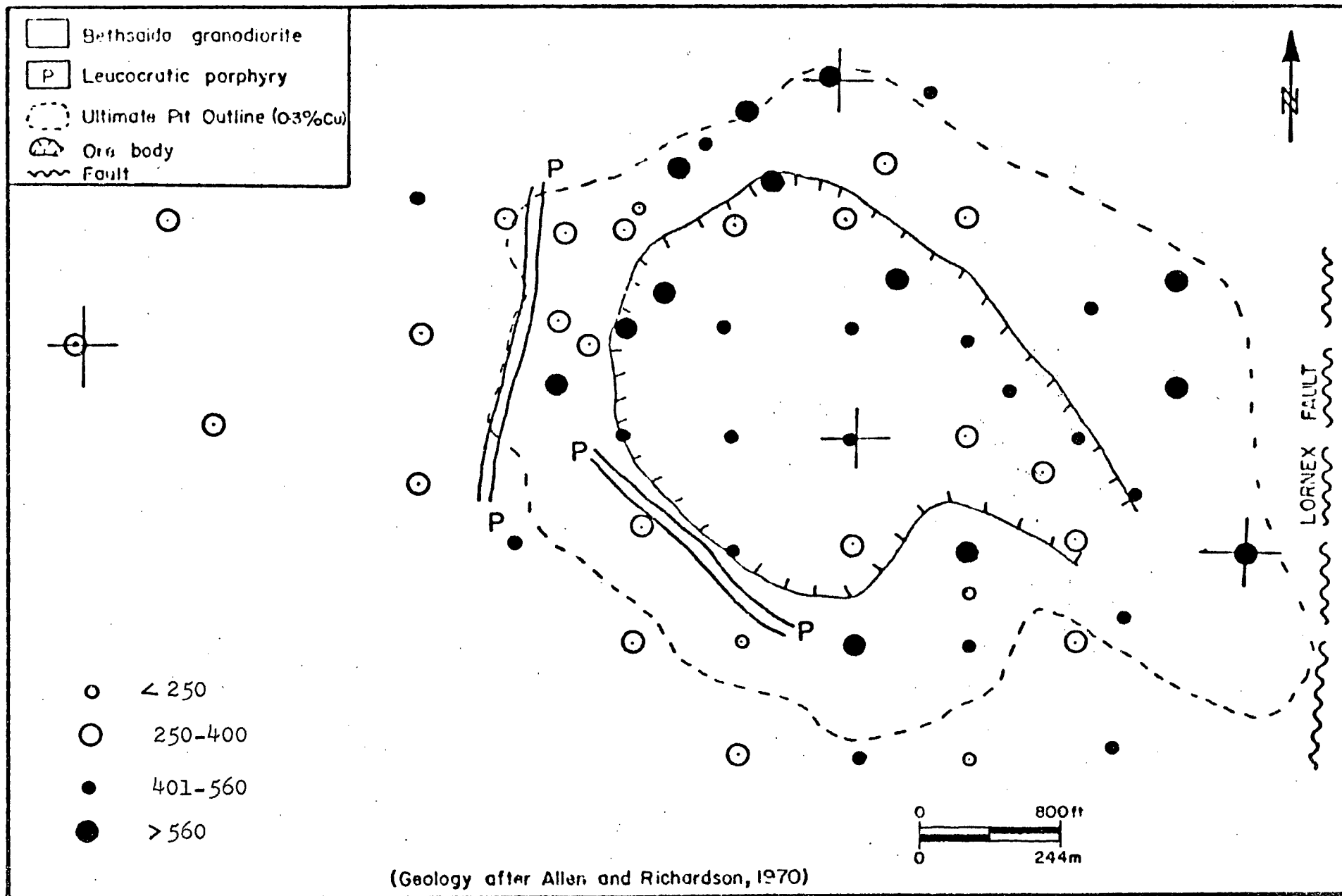


FIGURE A55: Distribution of F (ppm), Valley Copper 3600 Level

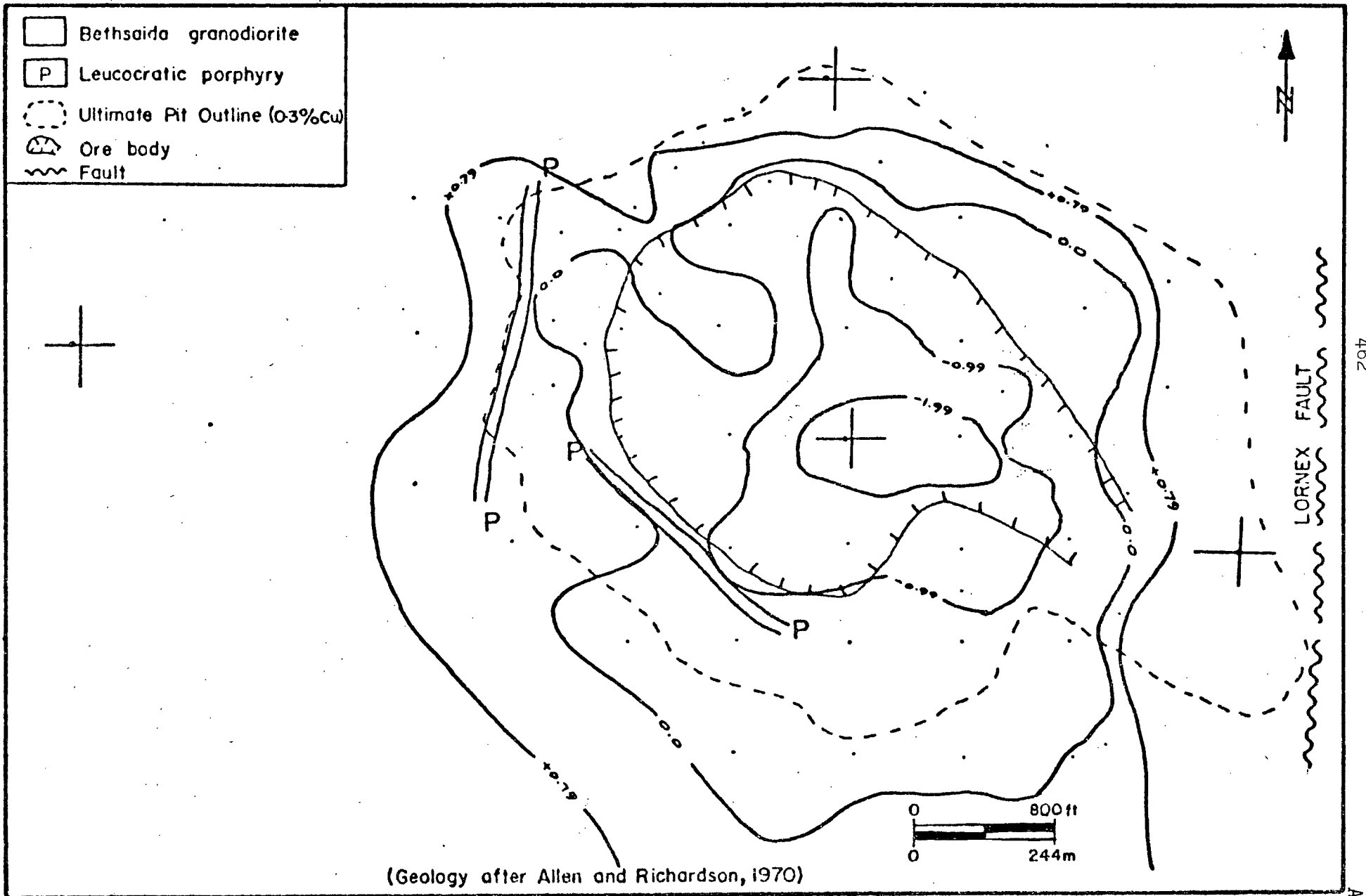


FIGURE A56: Scores for Factor R-1 (Ca, Mn, Sr), Valley Copper 3600 Level

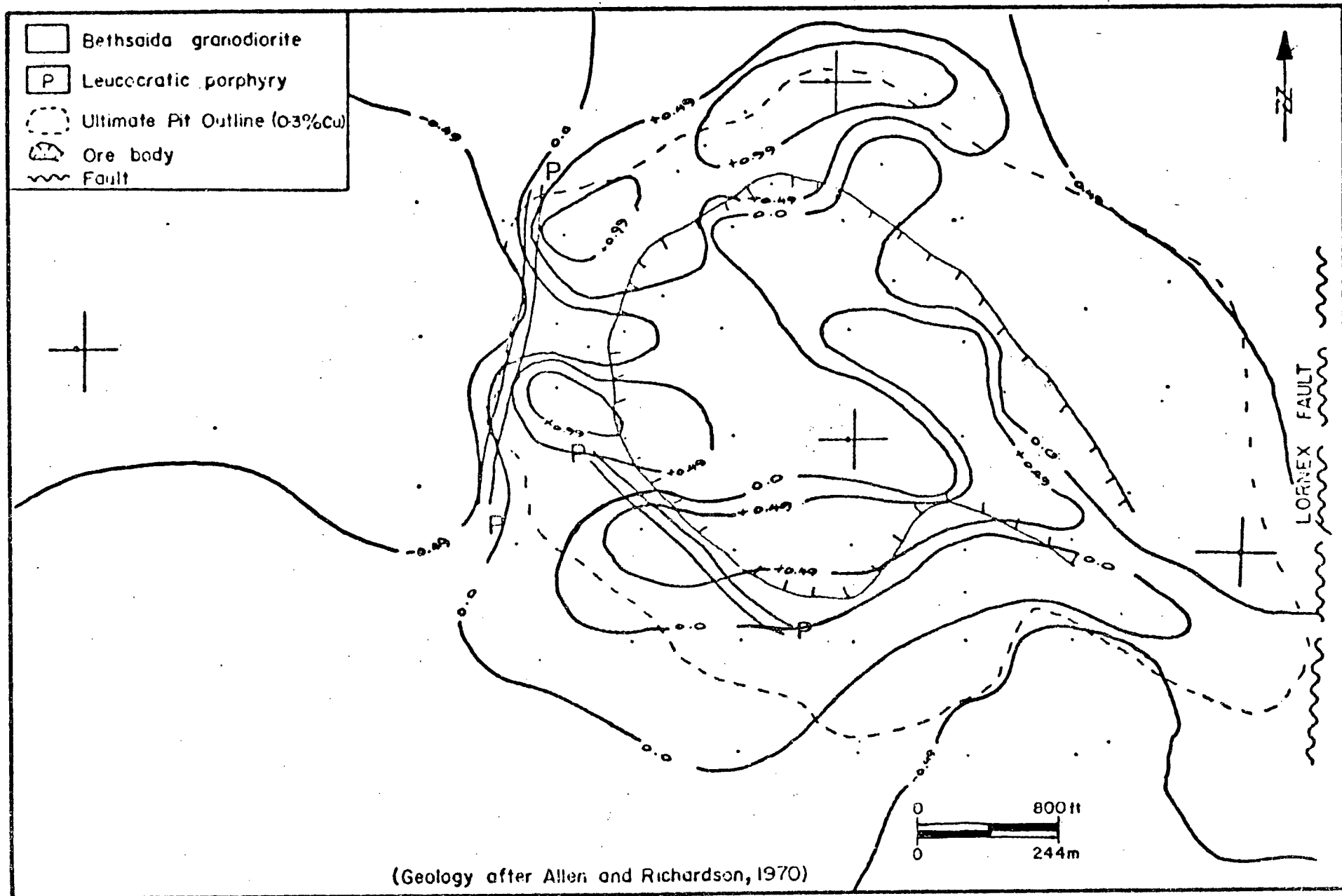


FIGURE A57: Scores for Factor R-2 (S,Cu,F,Fe,K vs Cl), Valley Copper 3600 Level

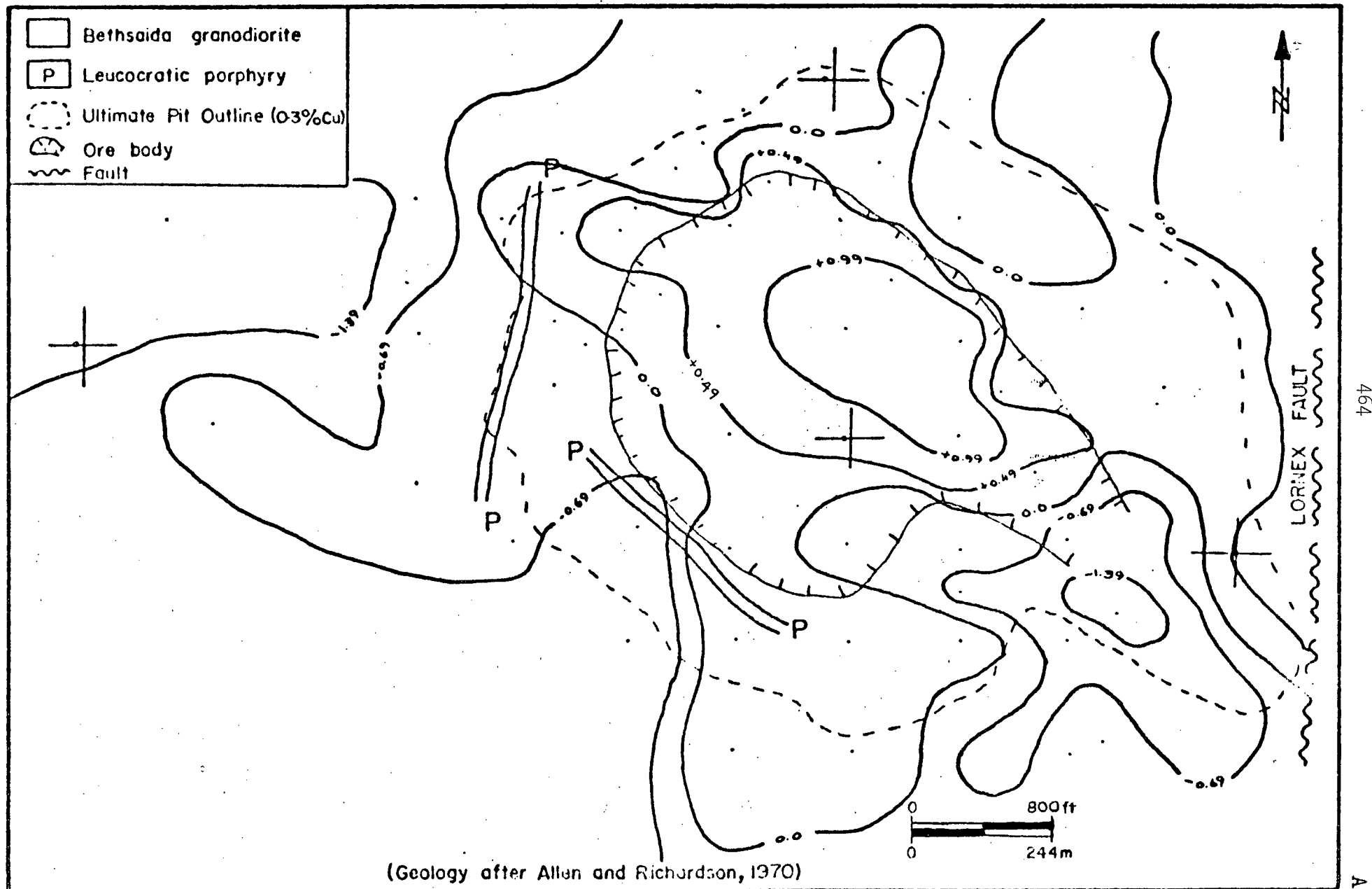


FIGURE A58: Scores for Factor R-3 (Rb,K), Valley Copper 3600 Level

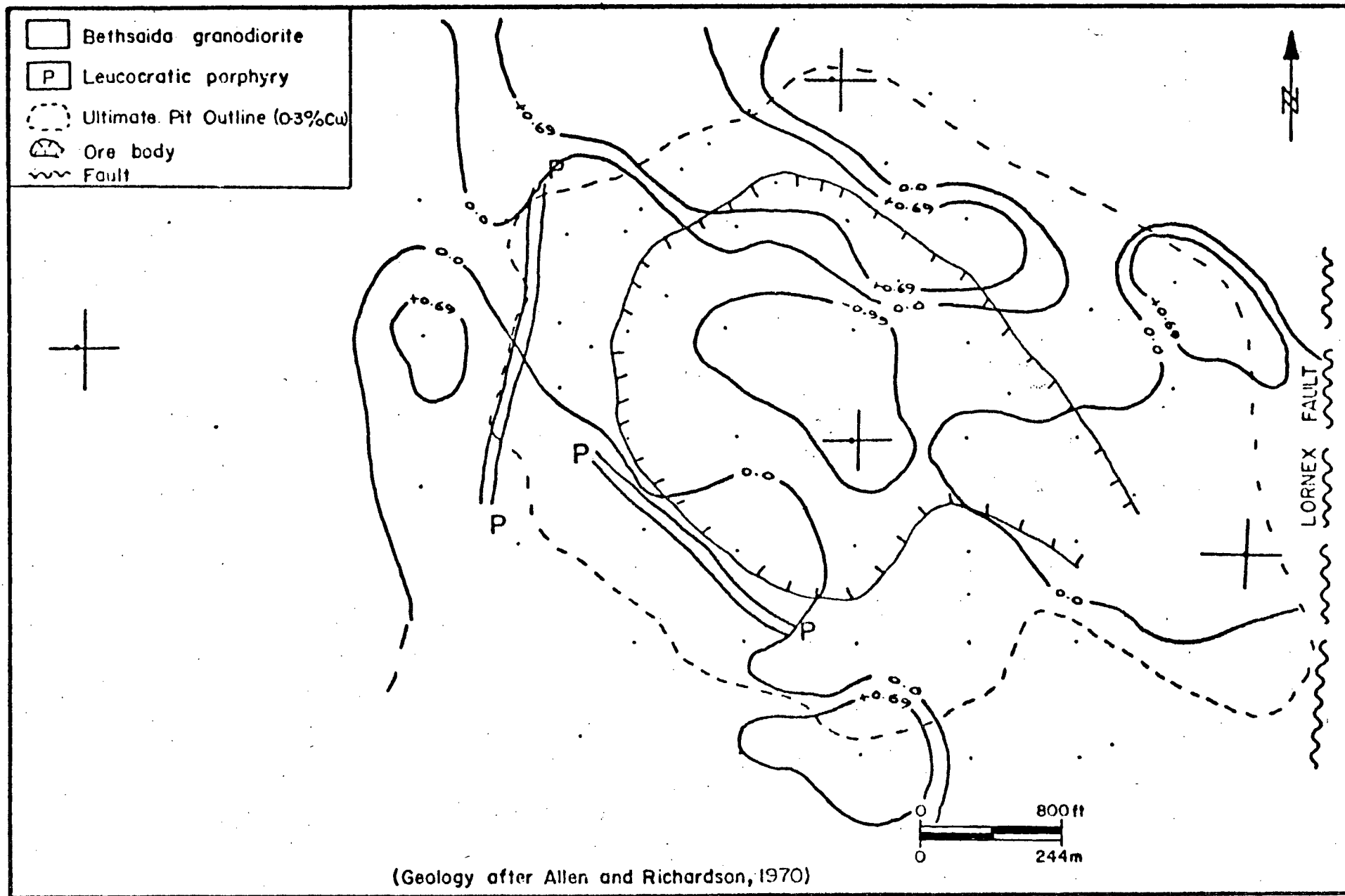


FIGURE A59: Scores for Factor R-4 (Zn,Mg,Fe), Valley Copper 3600 Level

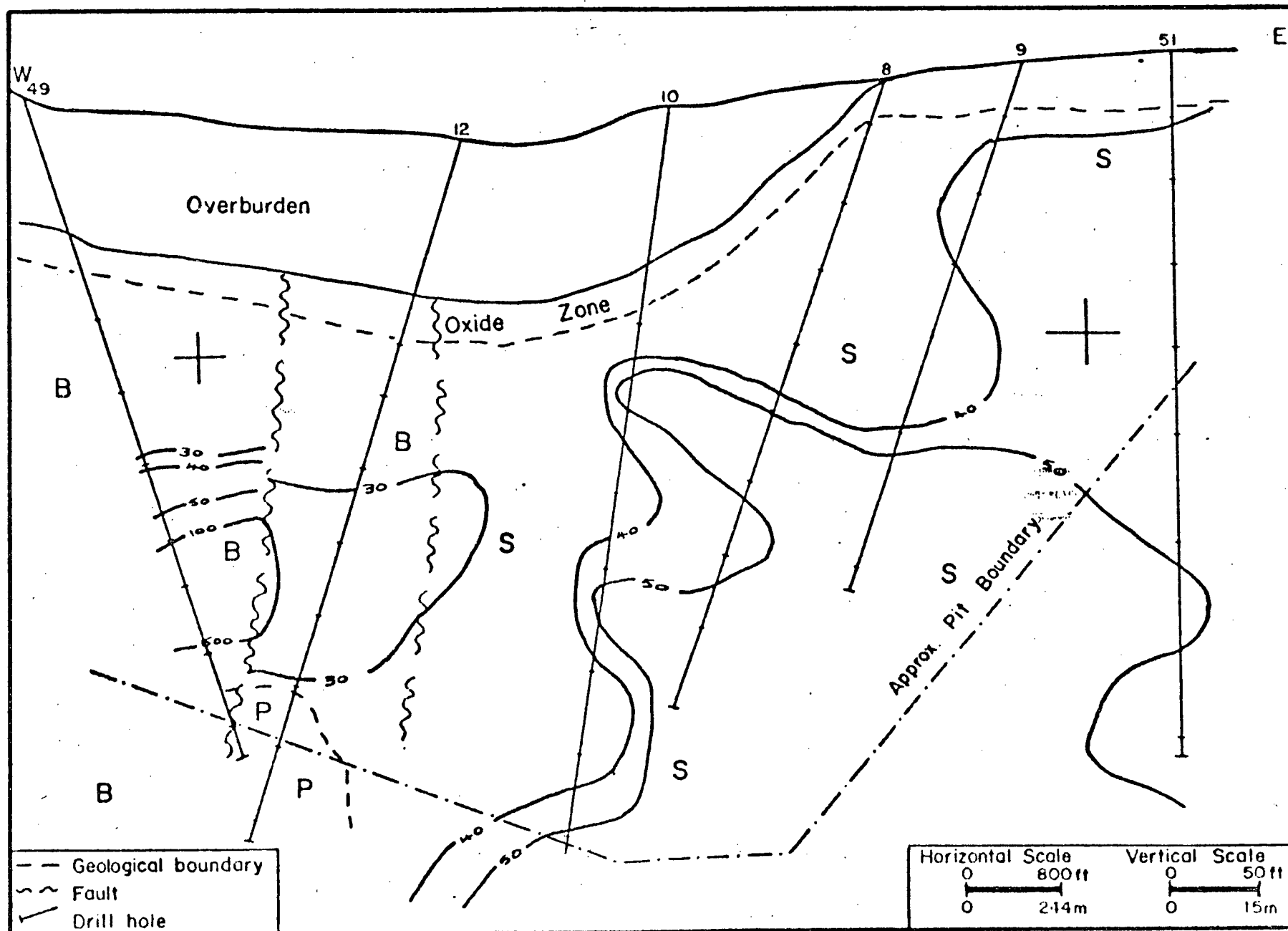


FIGURE A60: Distribution of Zn (ppm), Lornex Subsurface

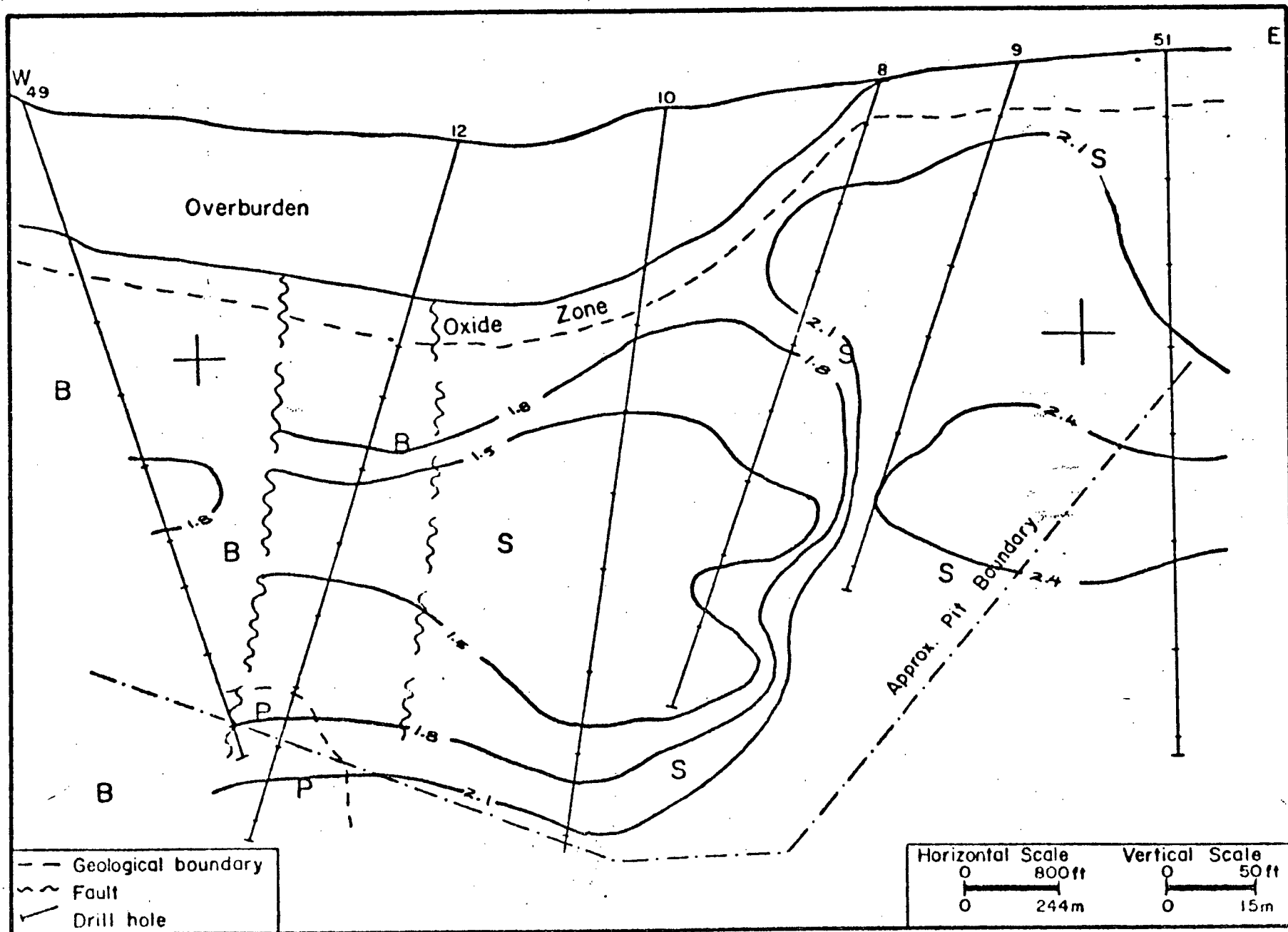


FIGURE A61: Distribution of Total Fe as Fe_2O_3 (wt.%), Lornex Subsurface

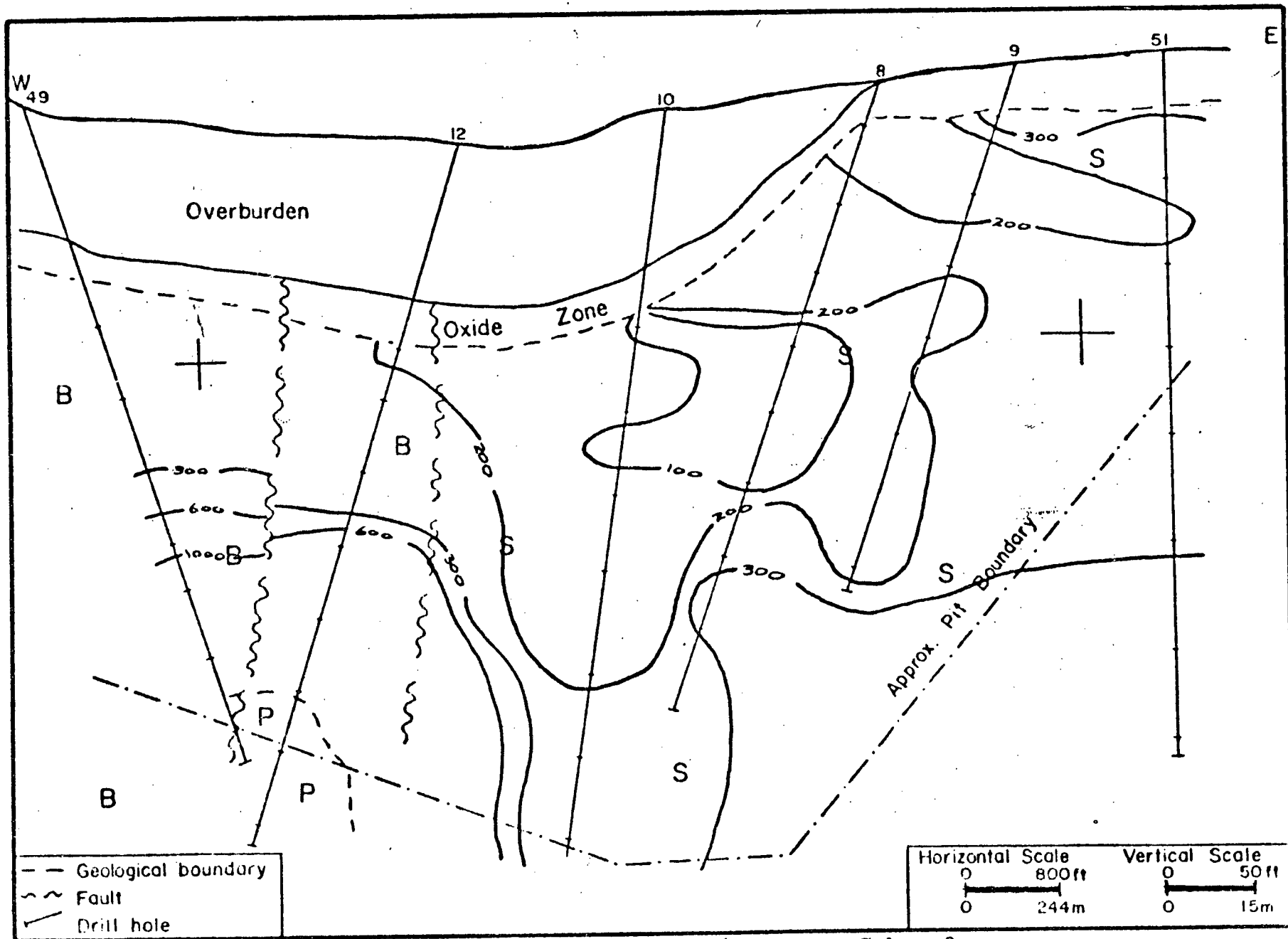


FIGURE A62: Distribution of Mn (ppm), Lornex Subsurface

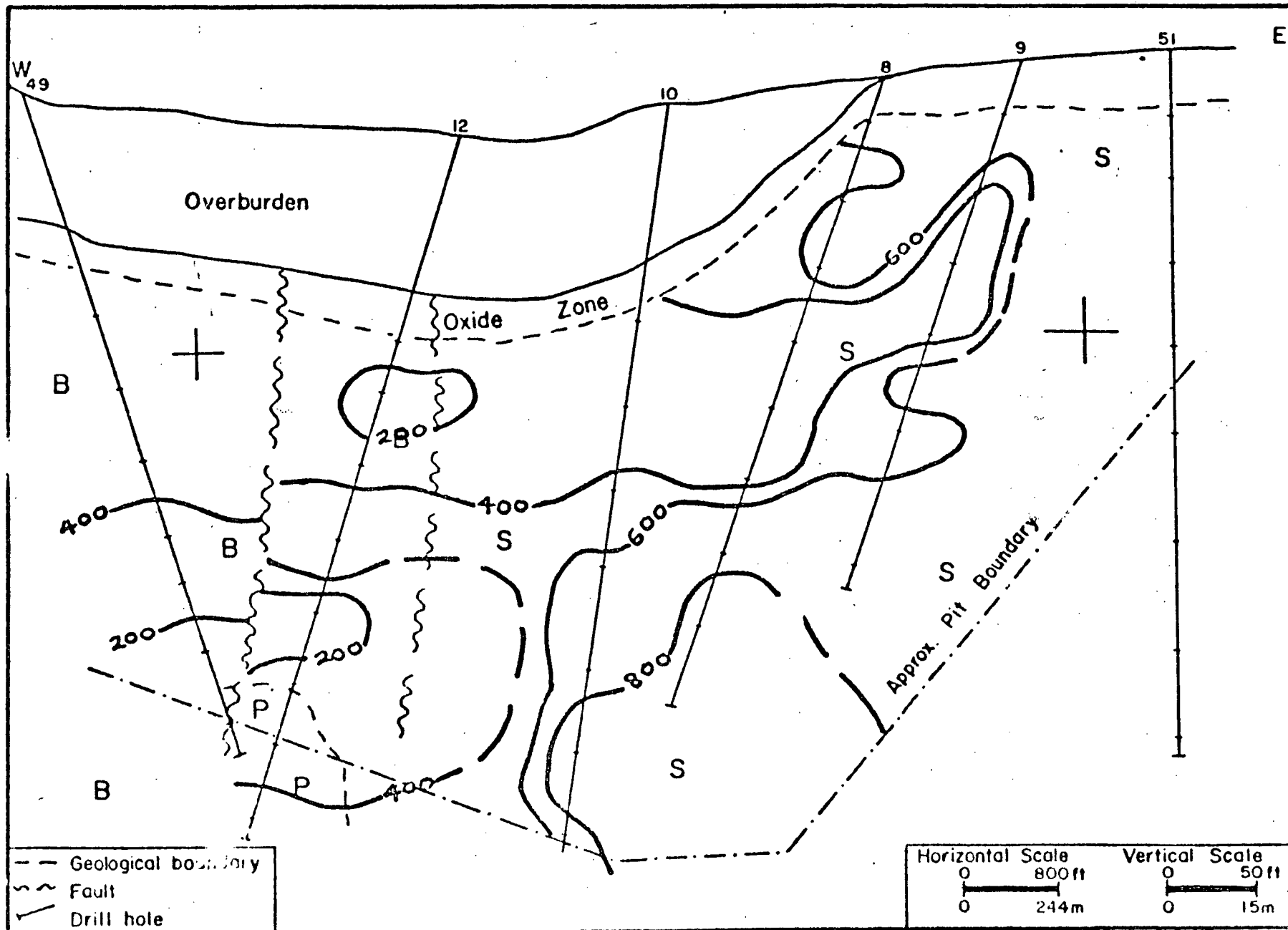


FIGURE A63a: Distribution of Sr (ppm), Lornex Subsurface

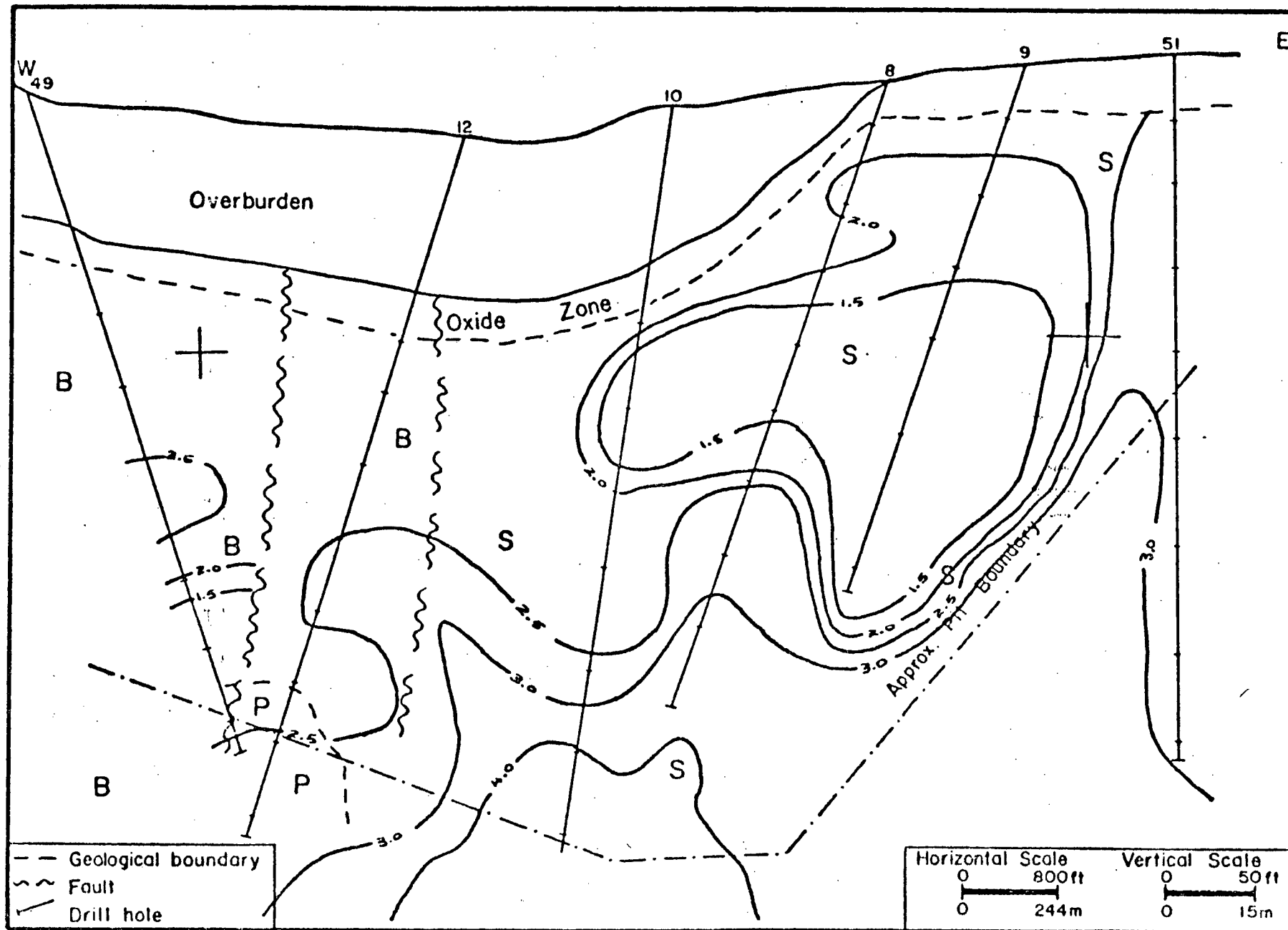


FIGURE A63: Distribution of CaO (wt.%), Lornex Subsurface

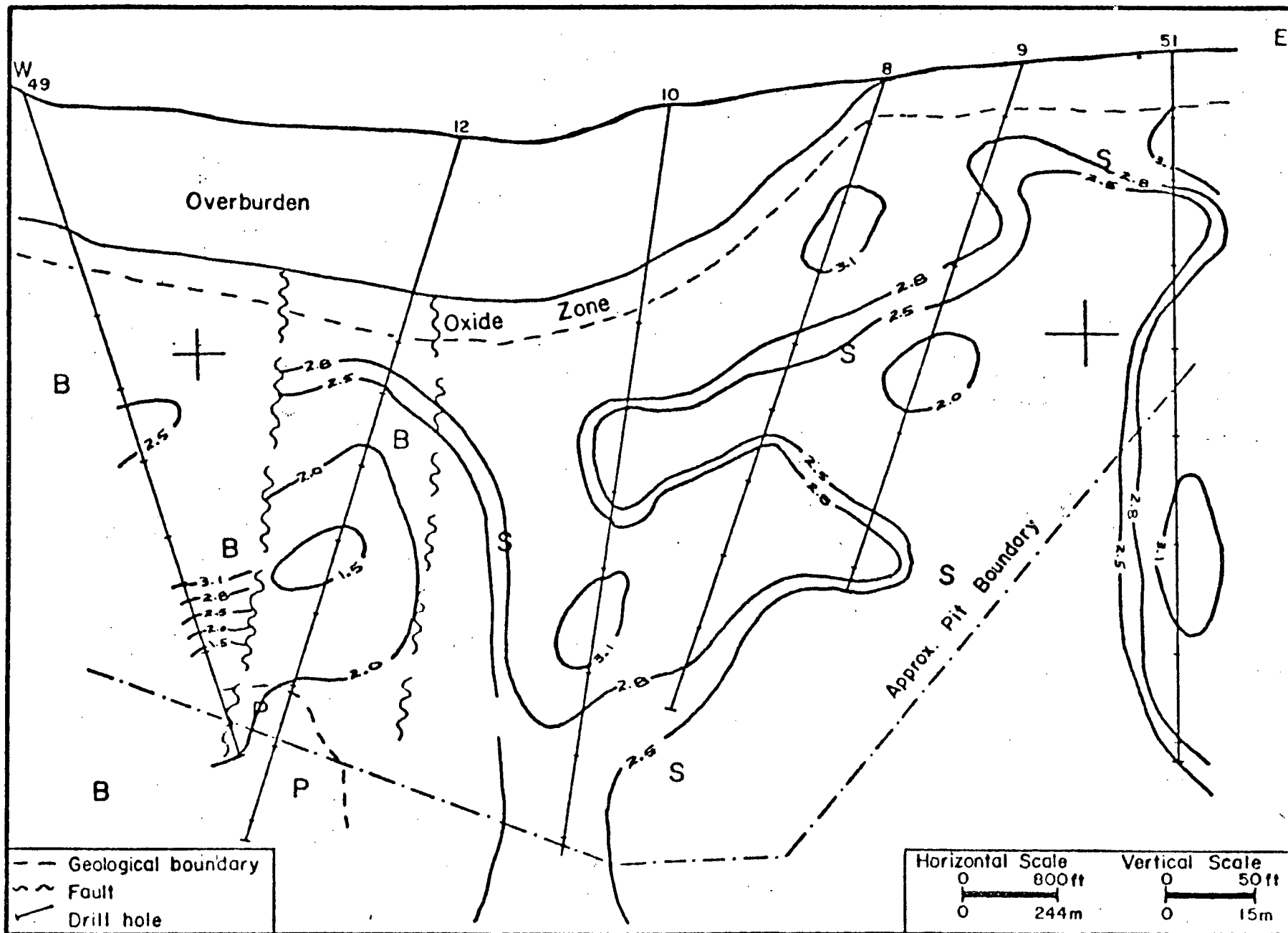


FIGURE A64: Distribution of Na_2O (wt.%,) Lornex Subsurface

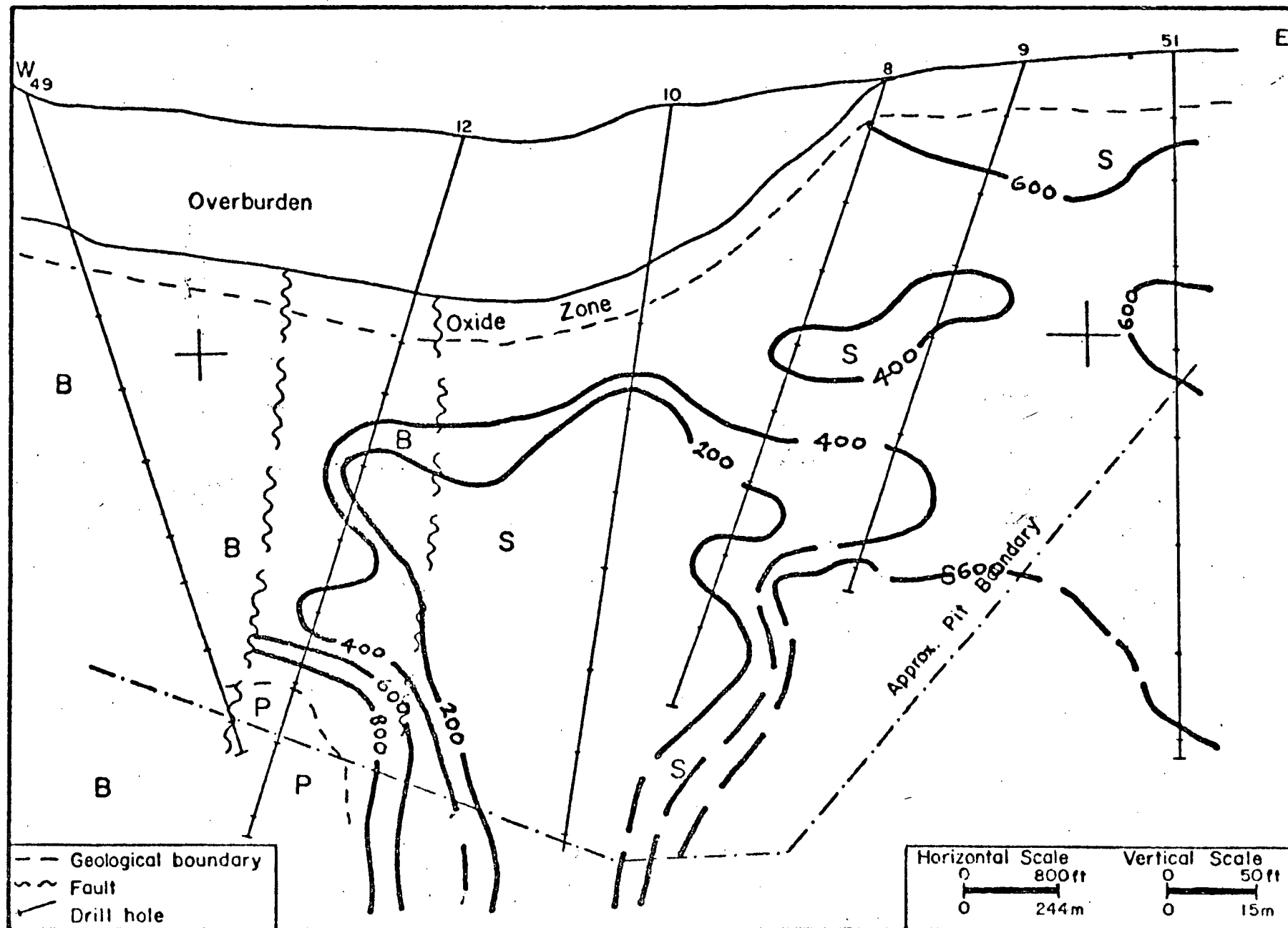


FIGURE A65a: Distribution of Ba (ppm), Lornex Subsurface

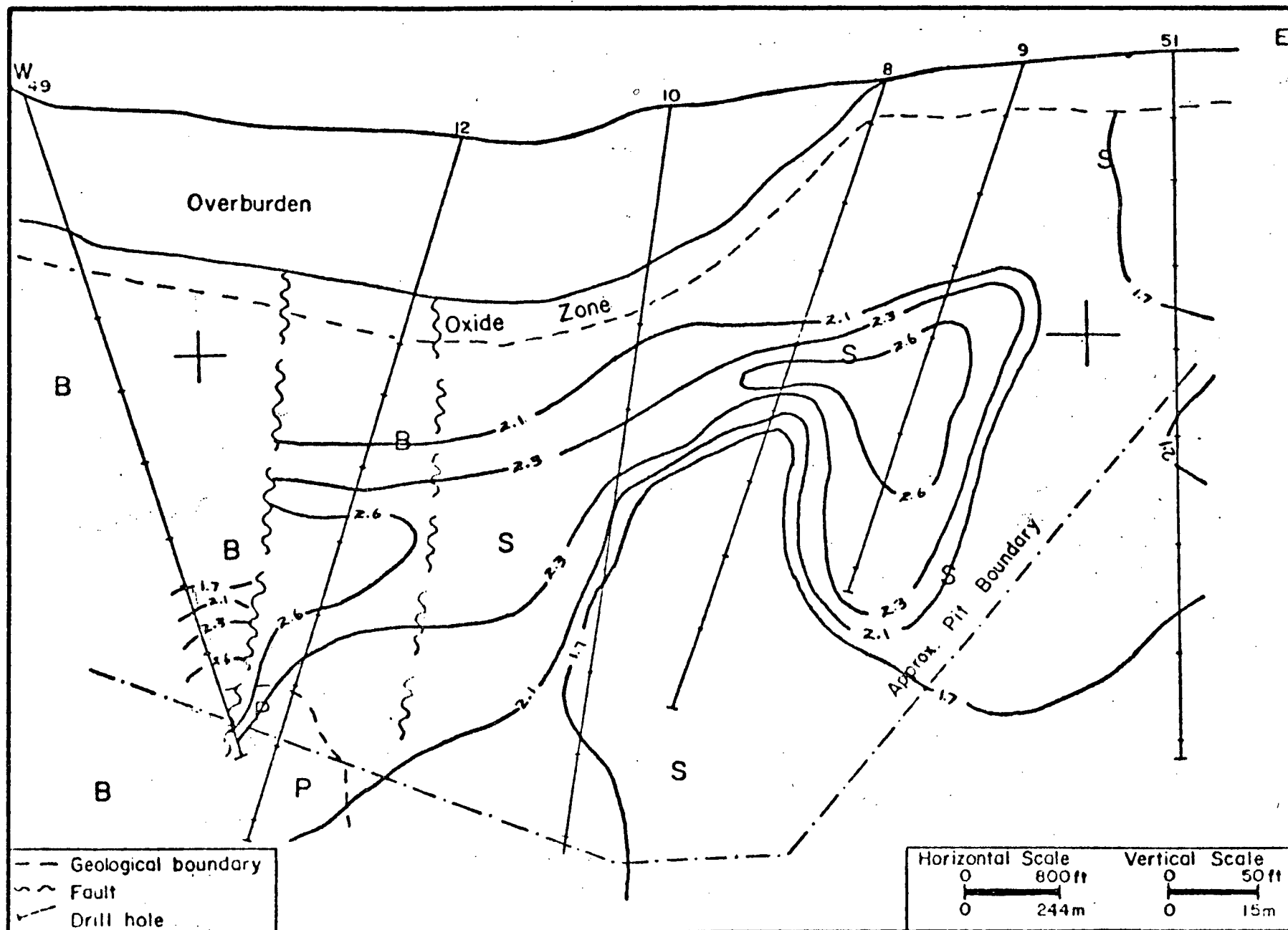


FIGURE A65b: Distribution of K_2O (wt.%), Lornex Subsurface

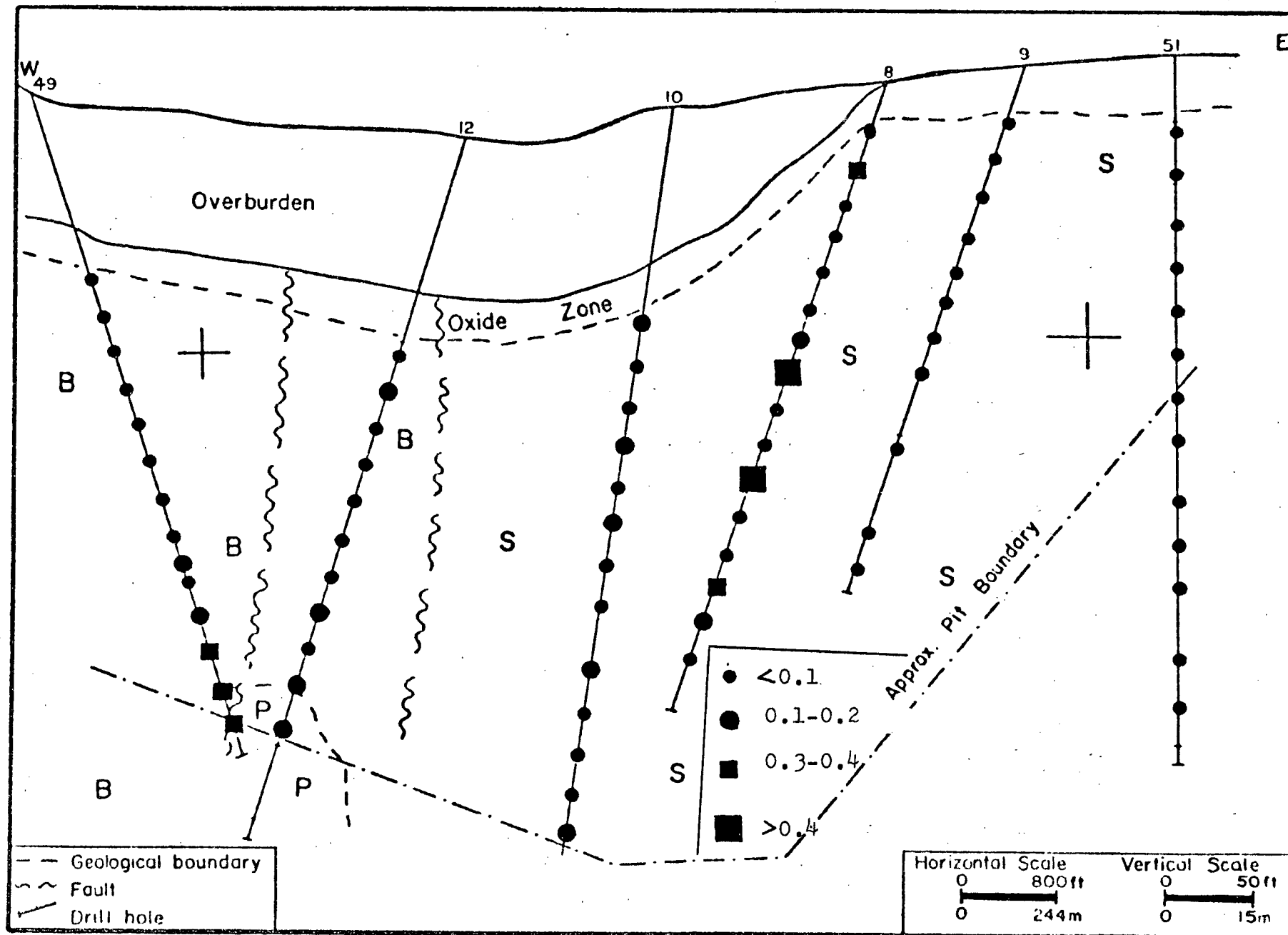


FIGURE A66: Distribution of Ag (ppm), Lornex Subsurface

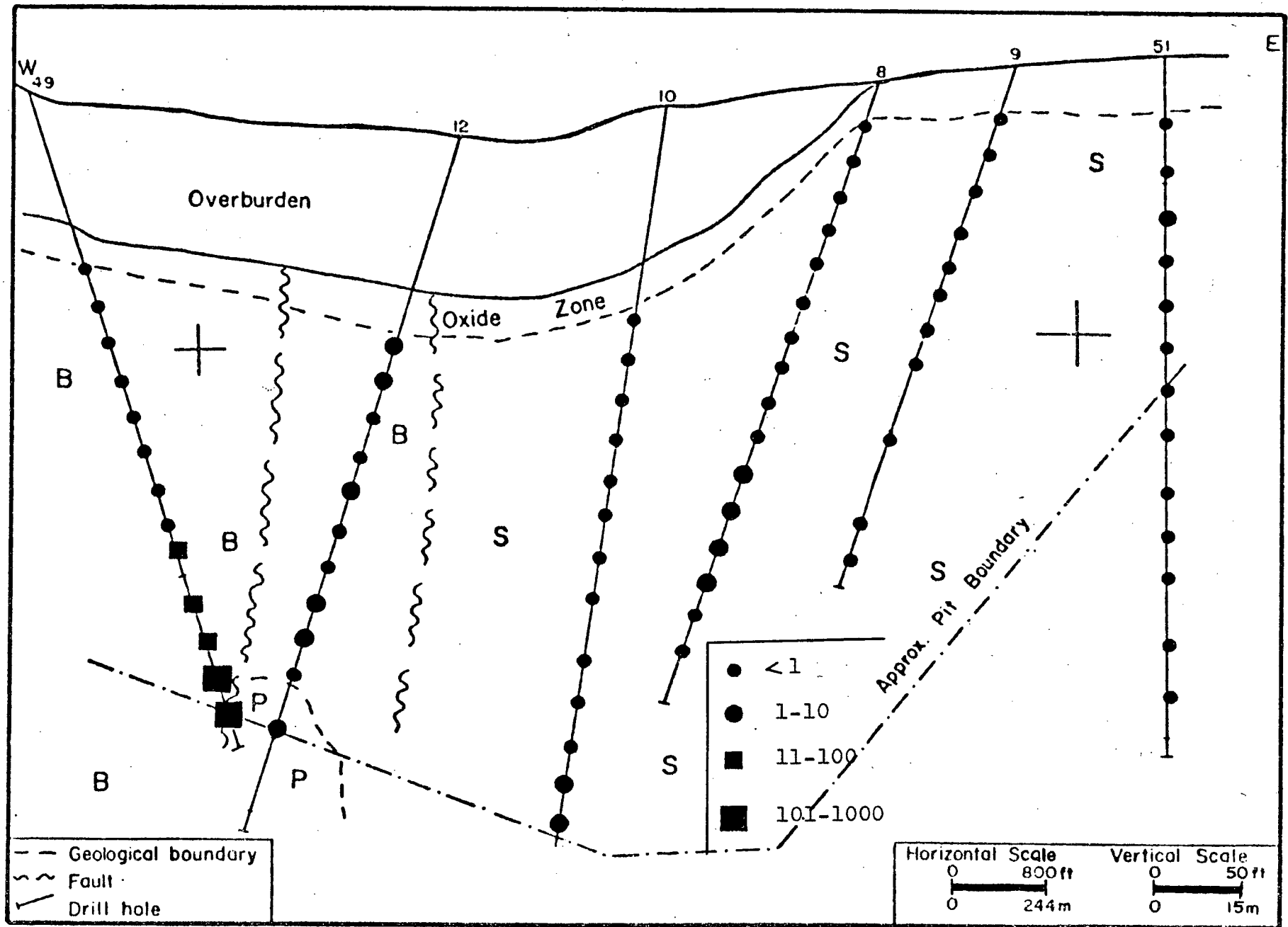


FIGURE A67: Distribution of Pb (ppm), Lornex Subsurface

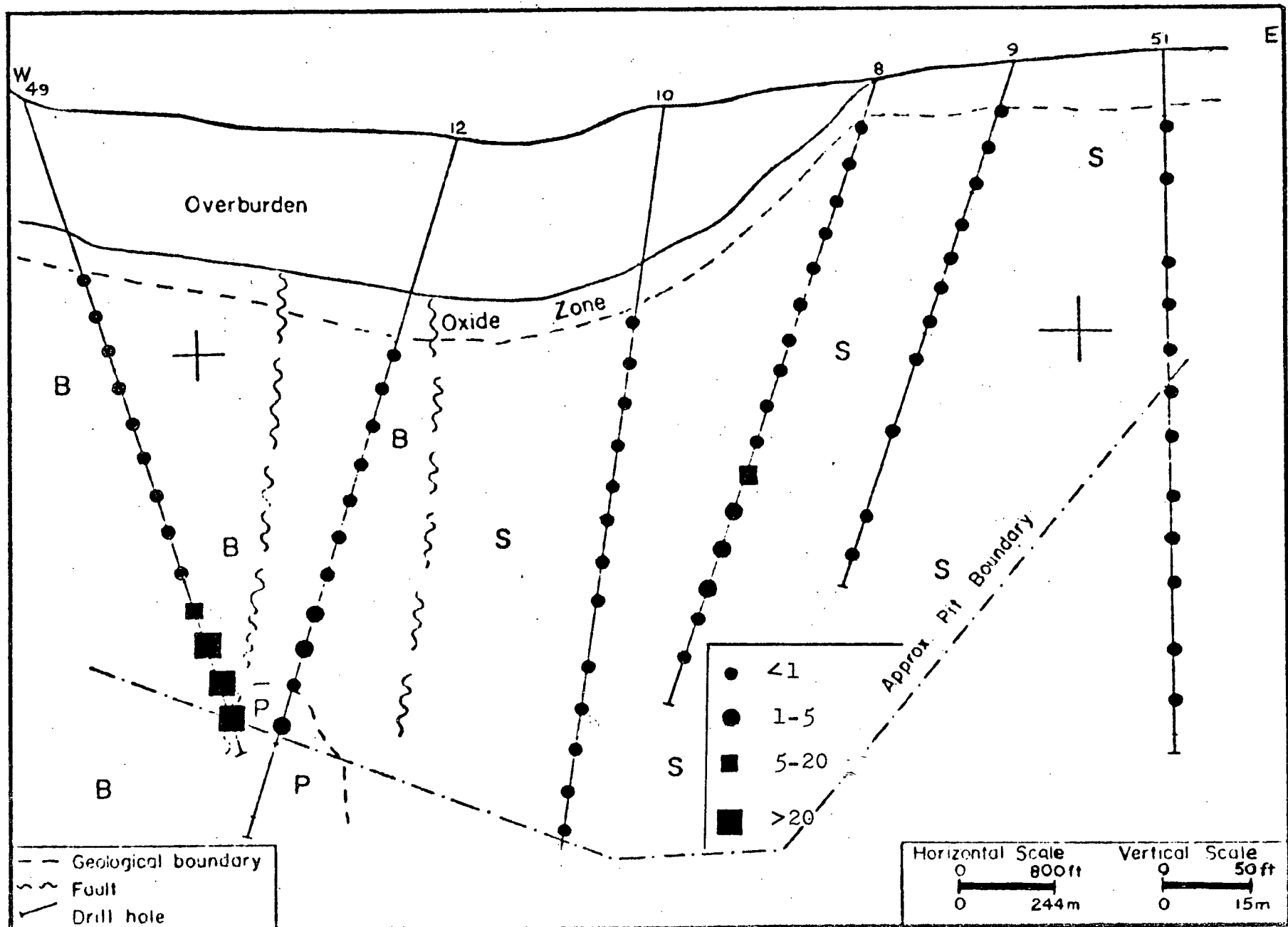


FIGURE A68: Distribution of Cd (ppm), Lornex Subsurface

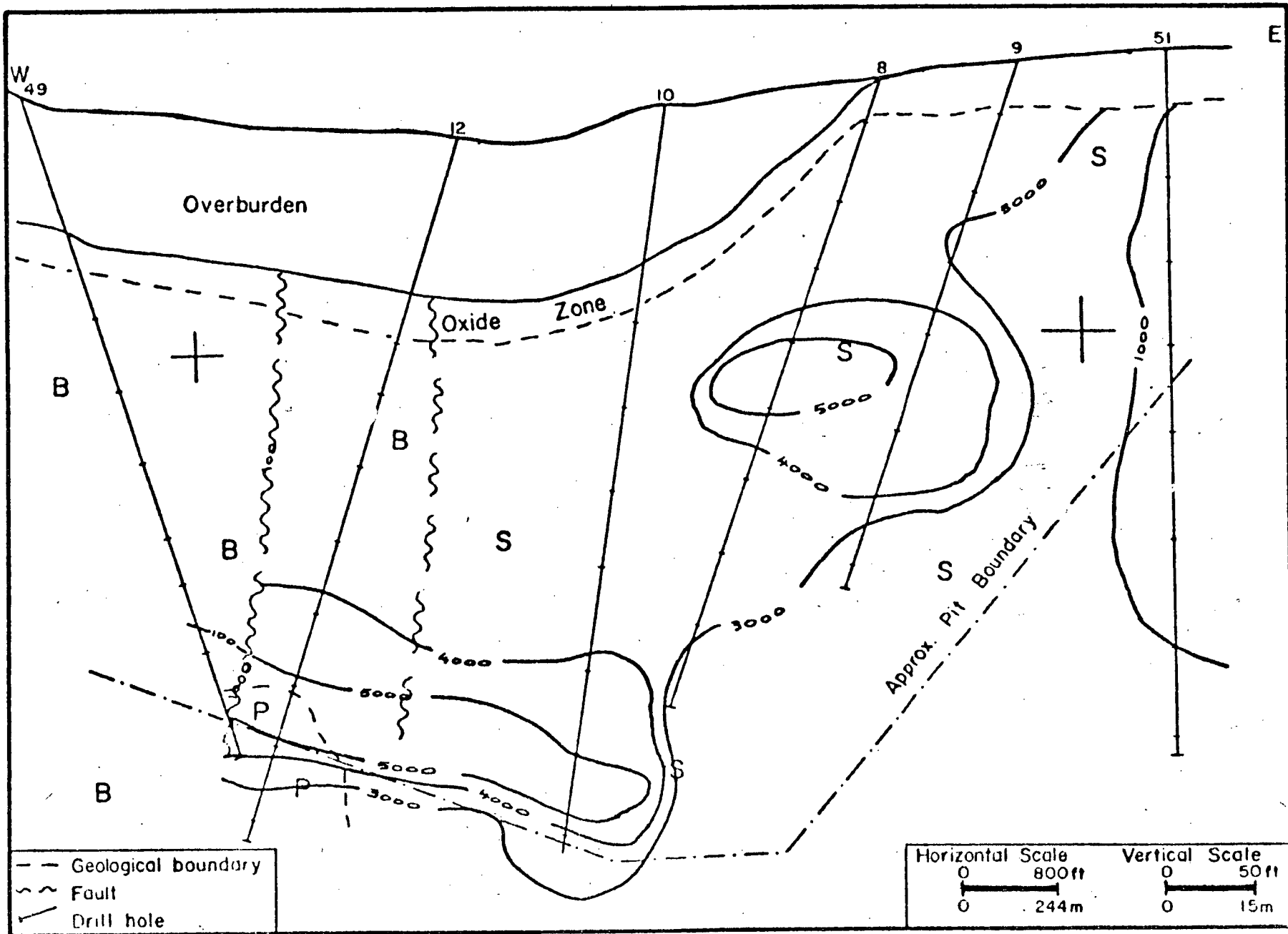


FIGURE A70: Distribution of Cu (ppm), Lornex Subsurface

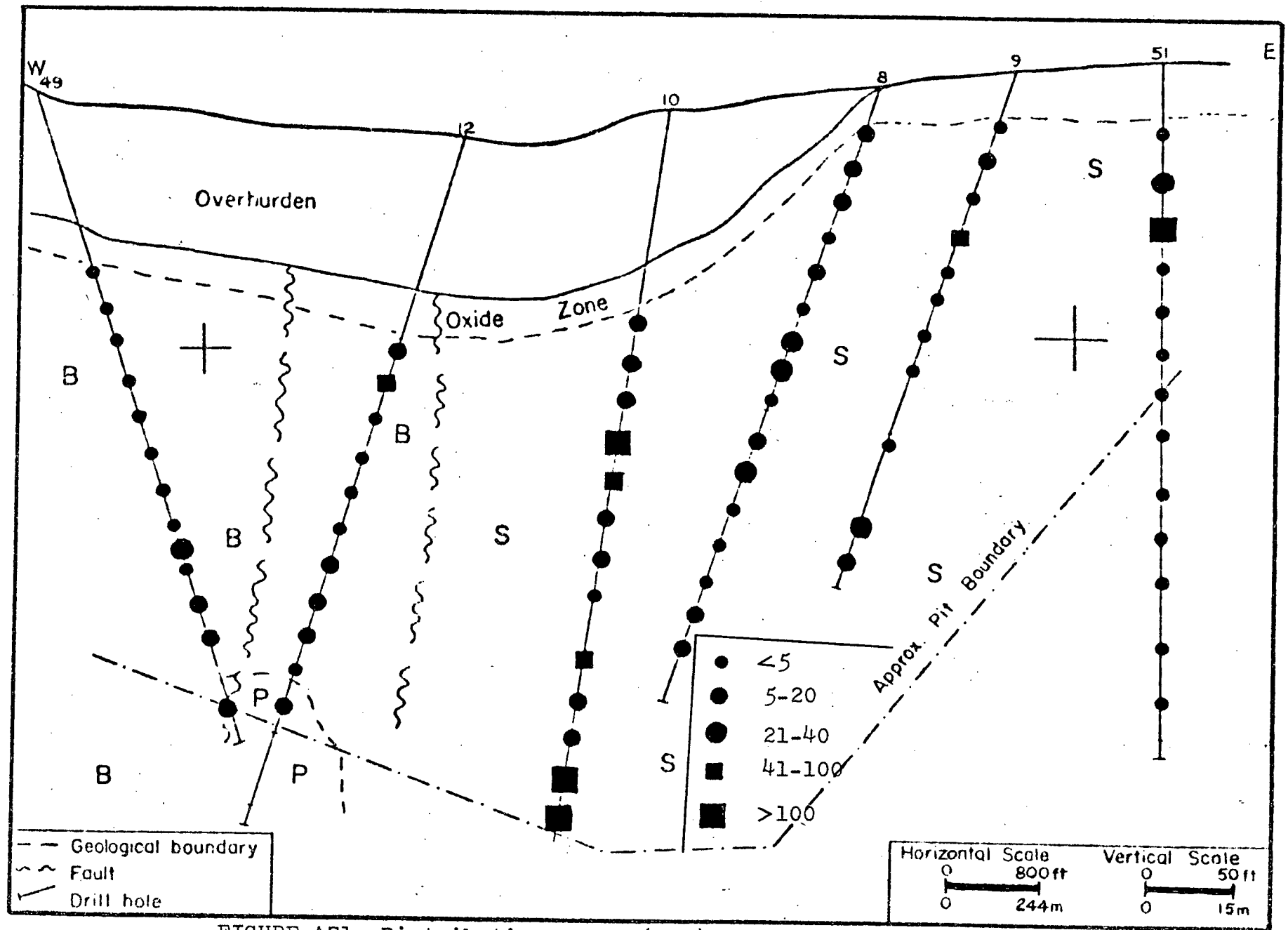


FIGURE A71: Distribution of Mo (ppm), Lornex Subsurface

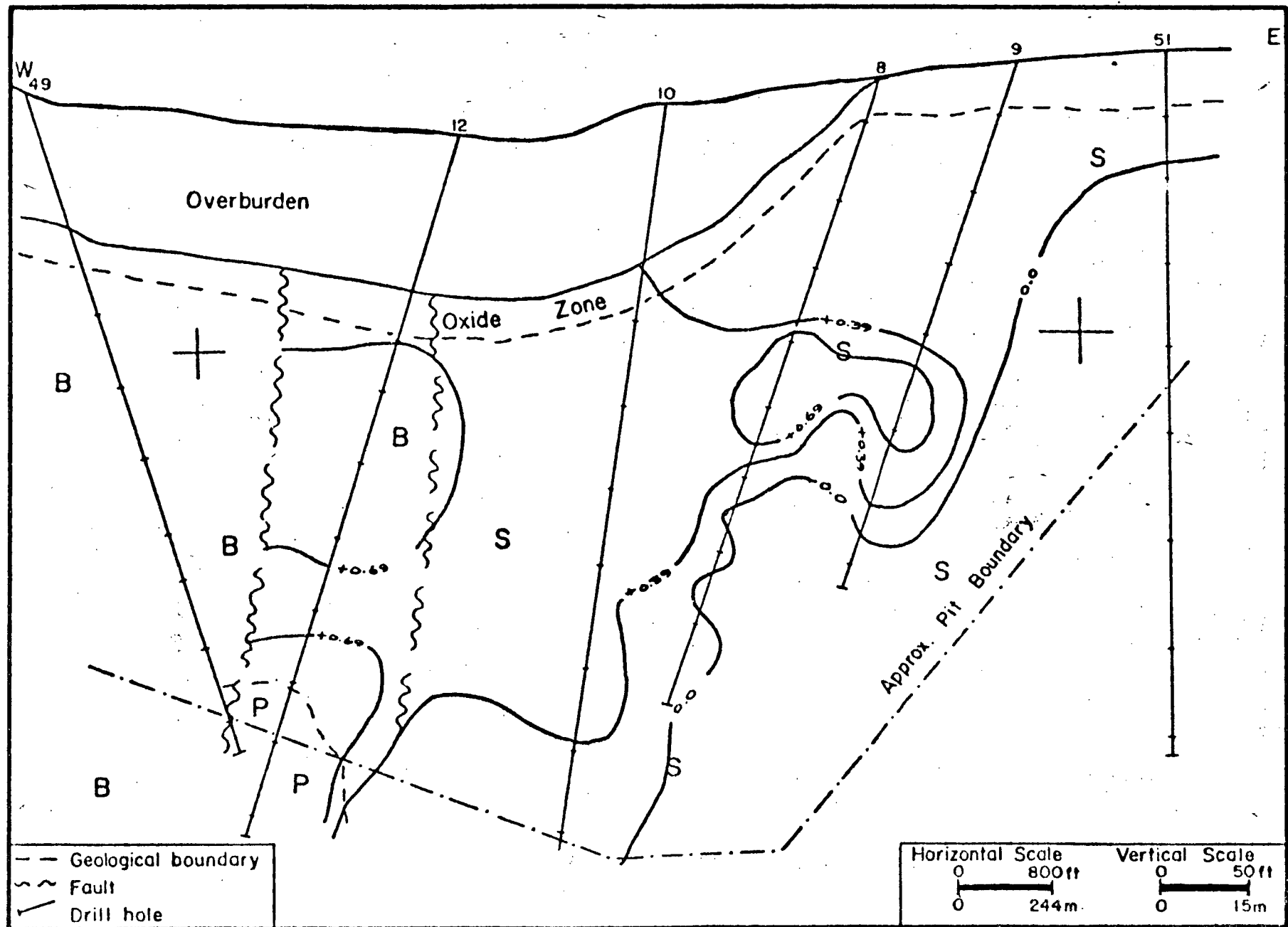


FIGURE A73: Scores for Factor R-2 (V,Ti,Ca vs Mn,Zn), Lornex Subsurface

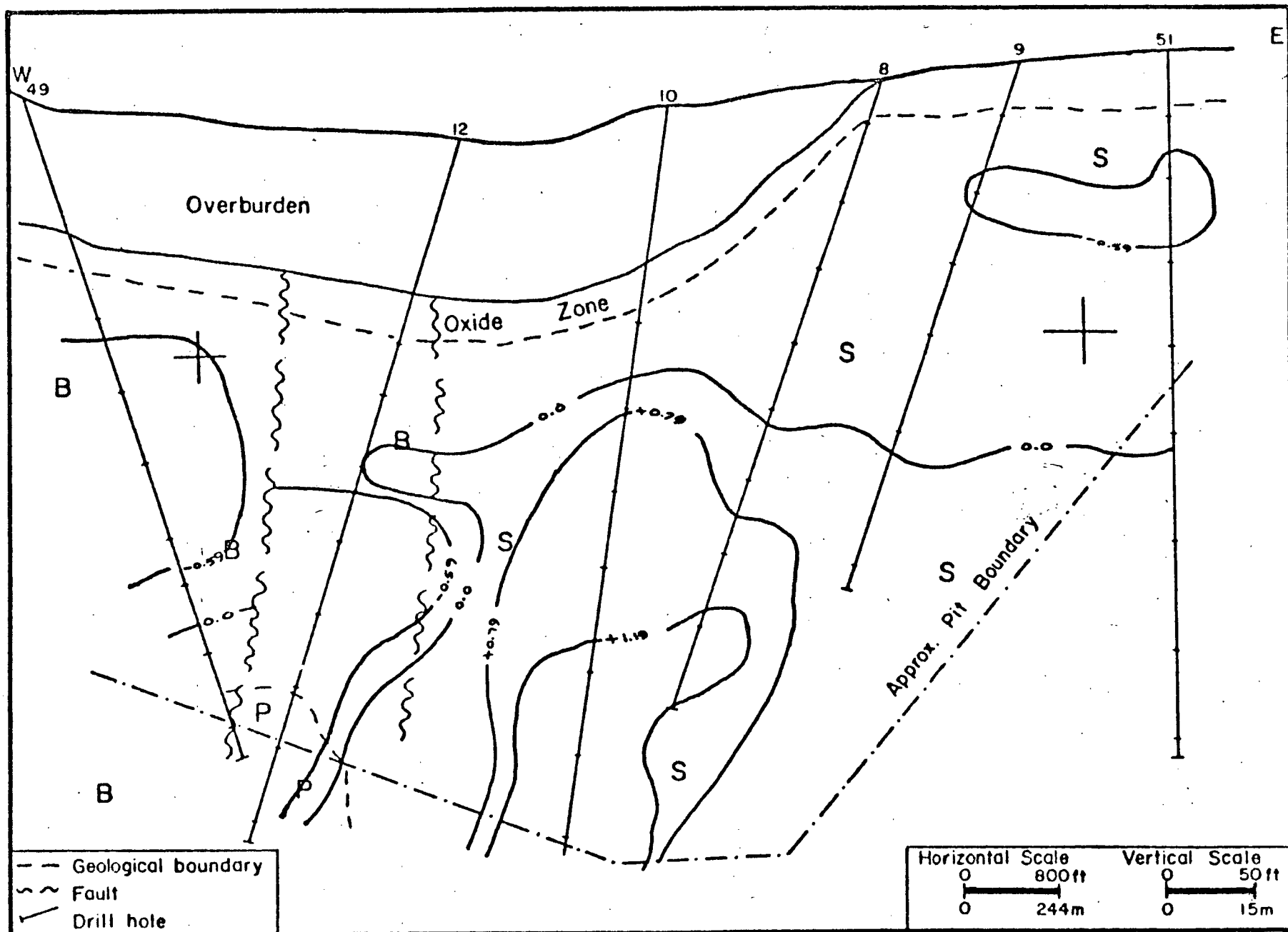


FIGURE A74; Scores for Factor R-3 (Mo, Fe vs Bu), Lornex Subsurface

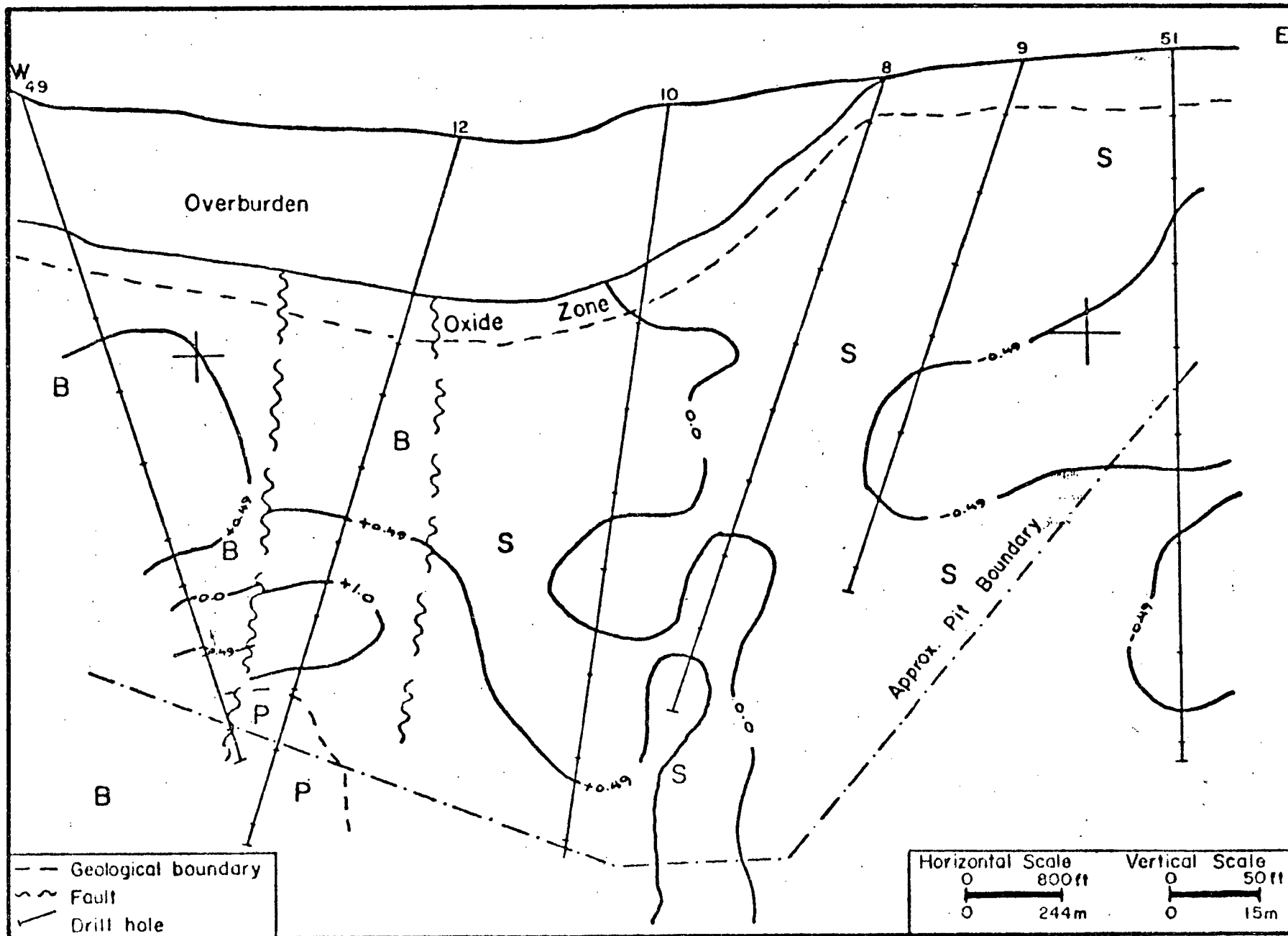


FIGURE A75: Scores for Factor R-4 (Ca,Zn), Lornex Subsurface

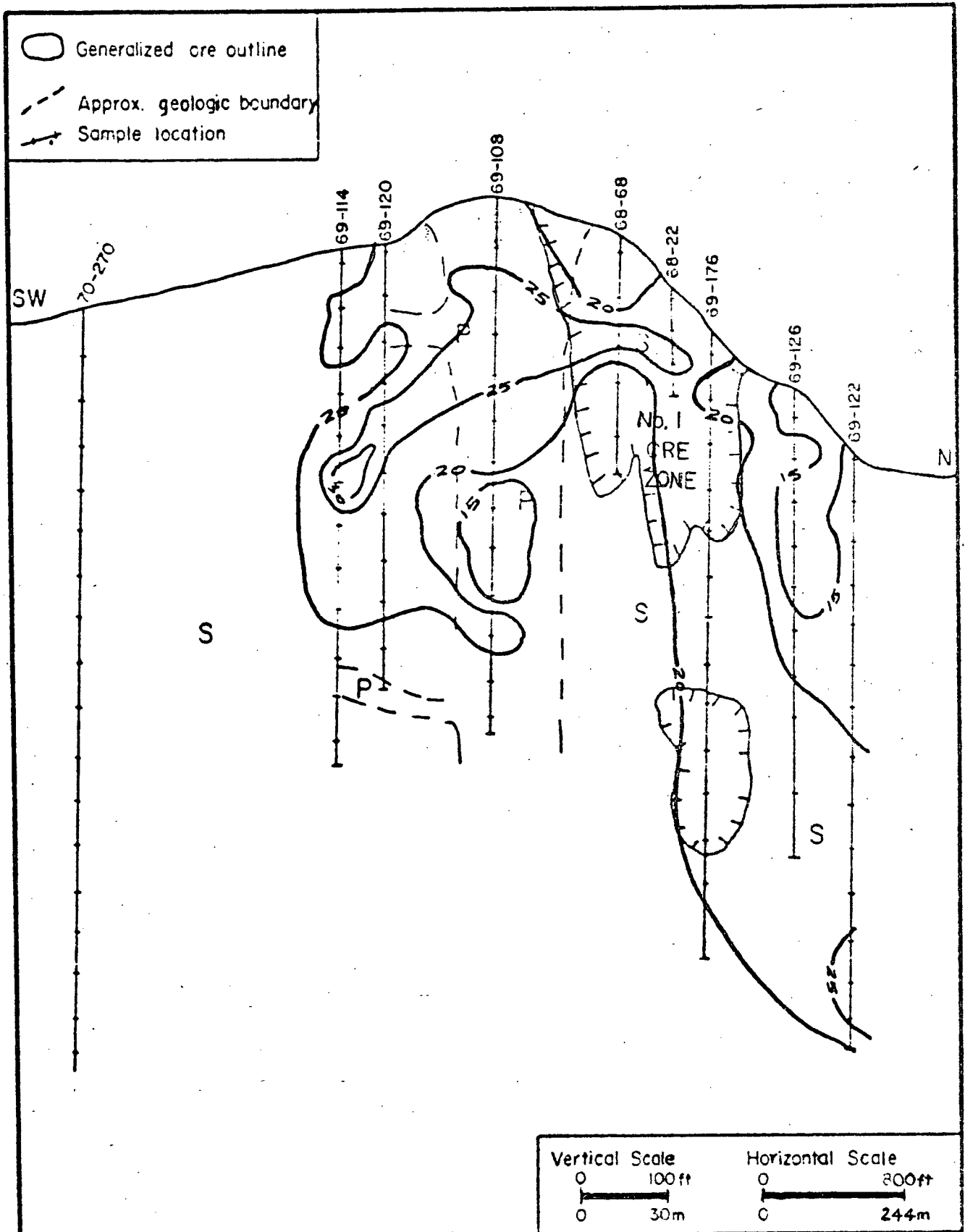


FIGURE A76: Distribution of Zn (ppm), Highmont Subsurface

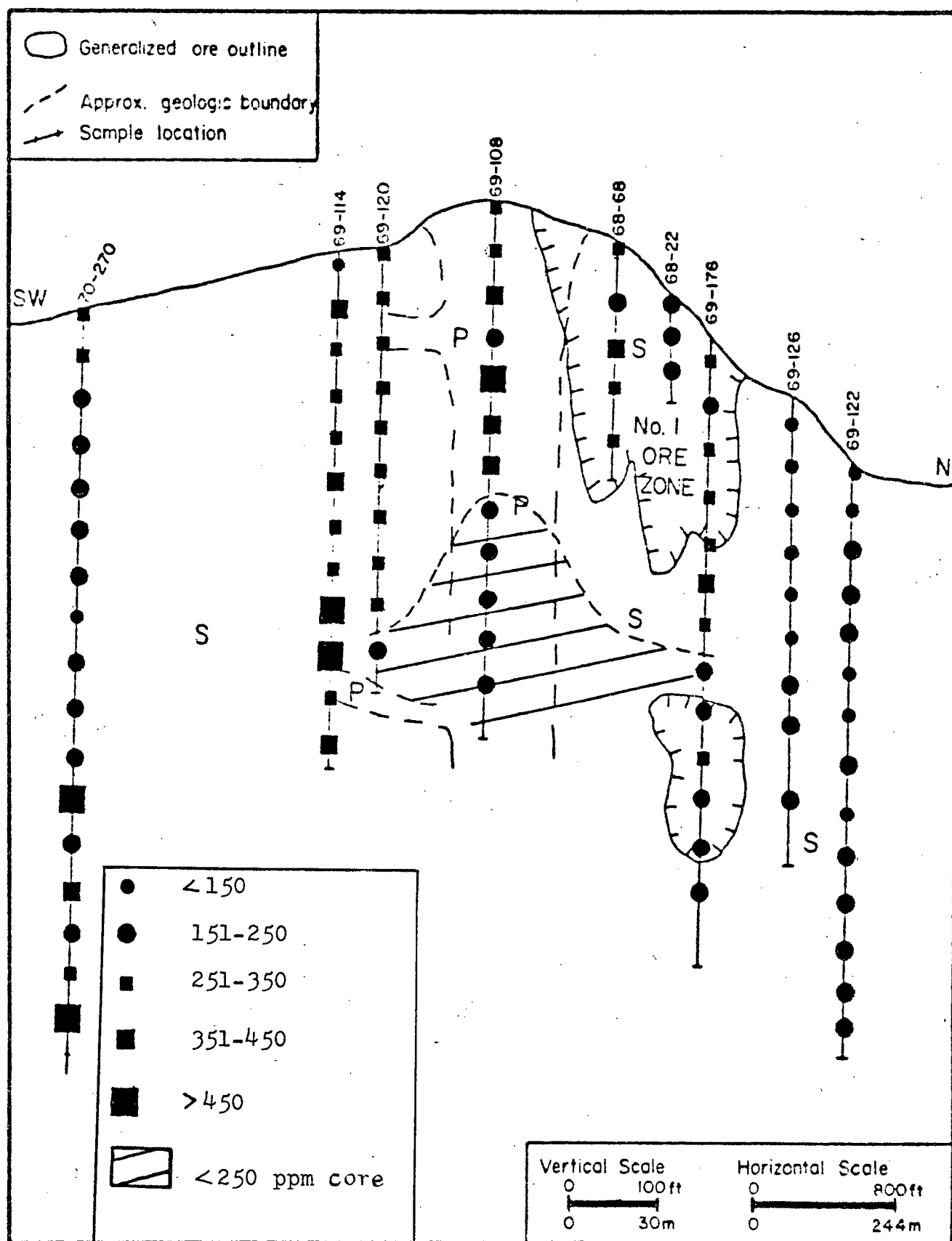


FIGURE A77: Distribution of Mn (ppm), Highmont Subsurface

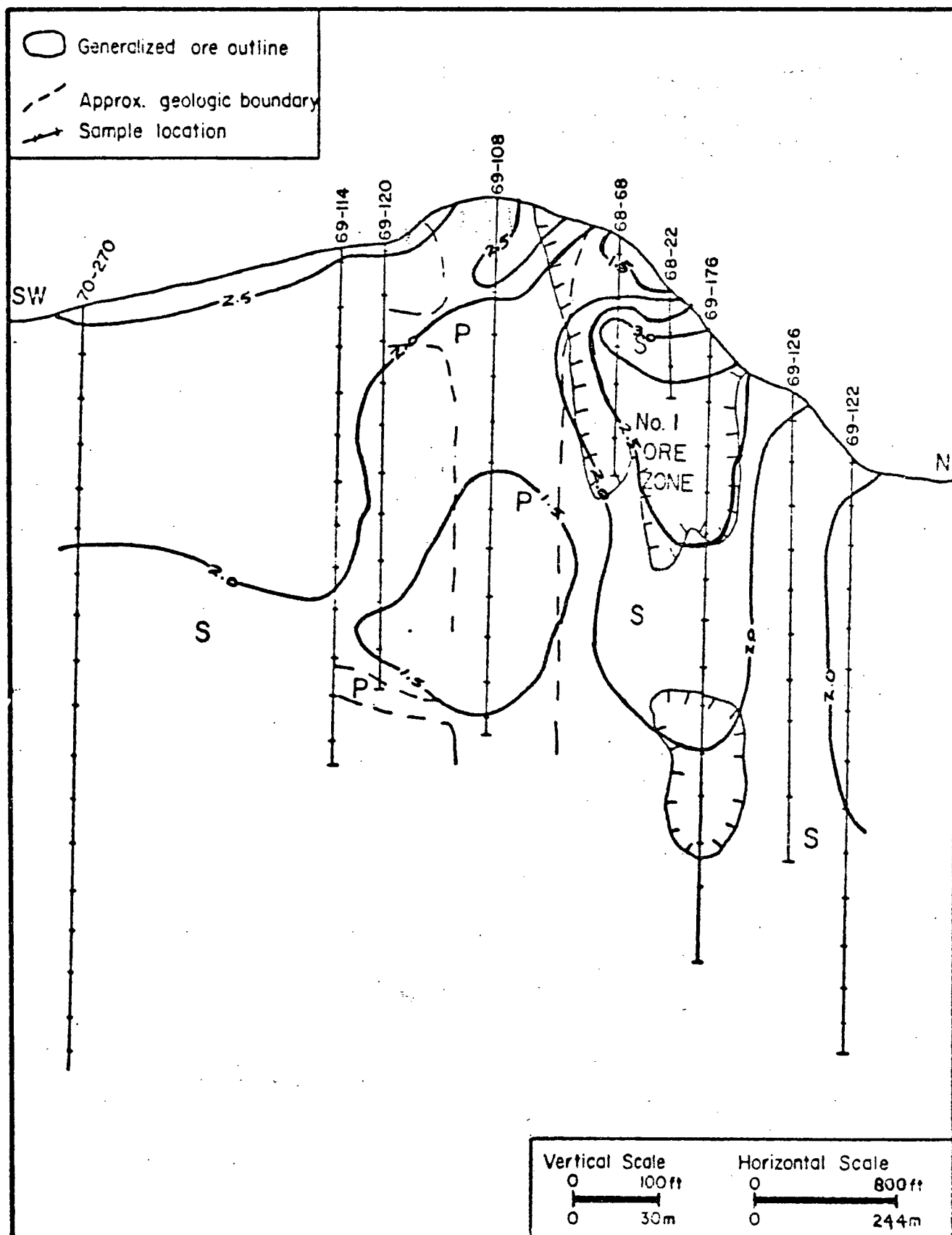


FIGURE A78: Distribution of Total Fe as Fe_2O_3 (wt.%) Highmont Subsurface

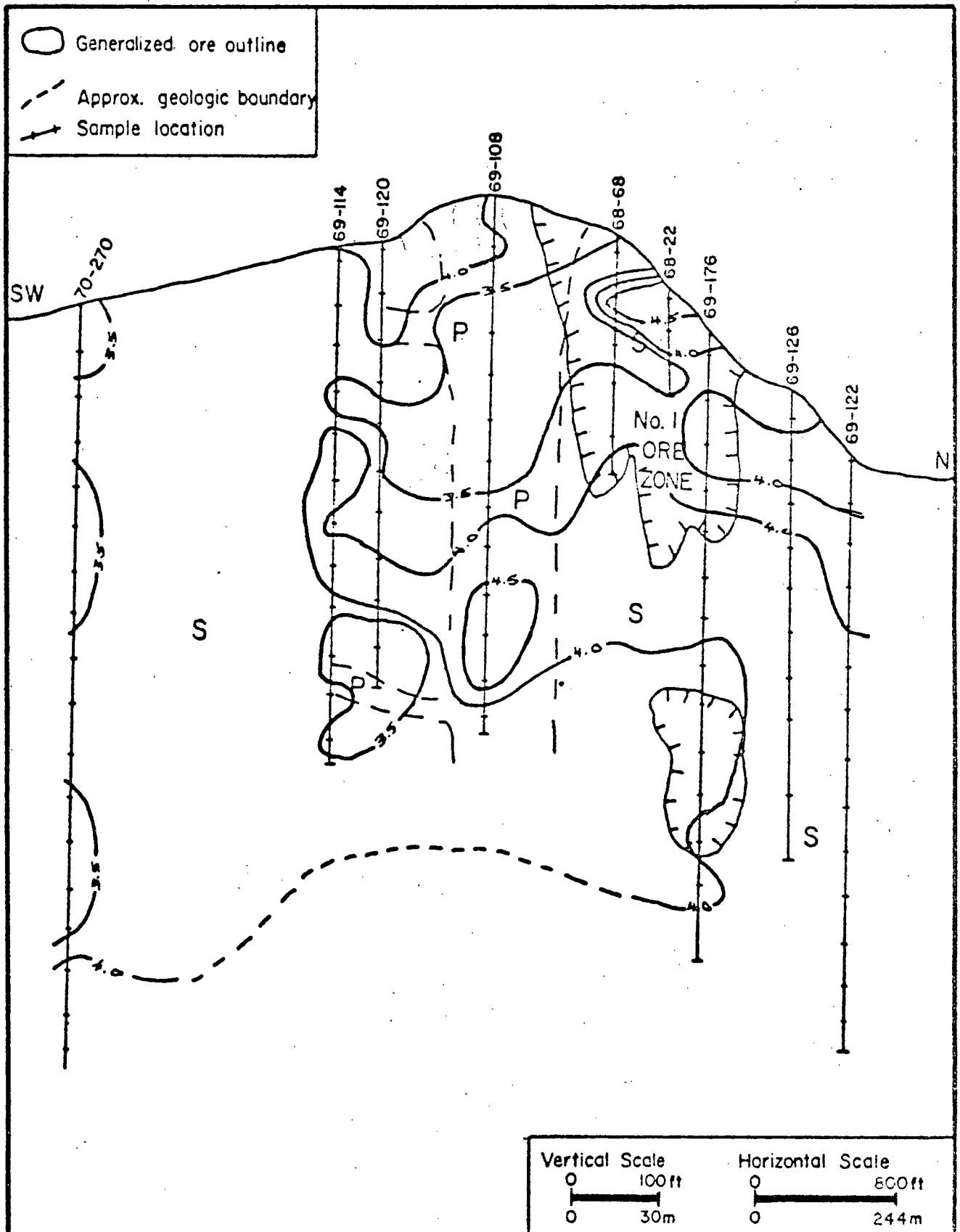


FIGURE A79: Distribution of Na_2O (wt.%), Highmont Subsurface

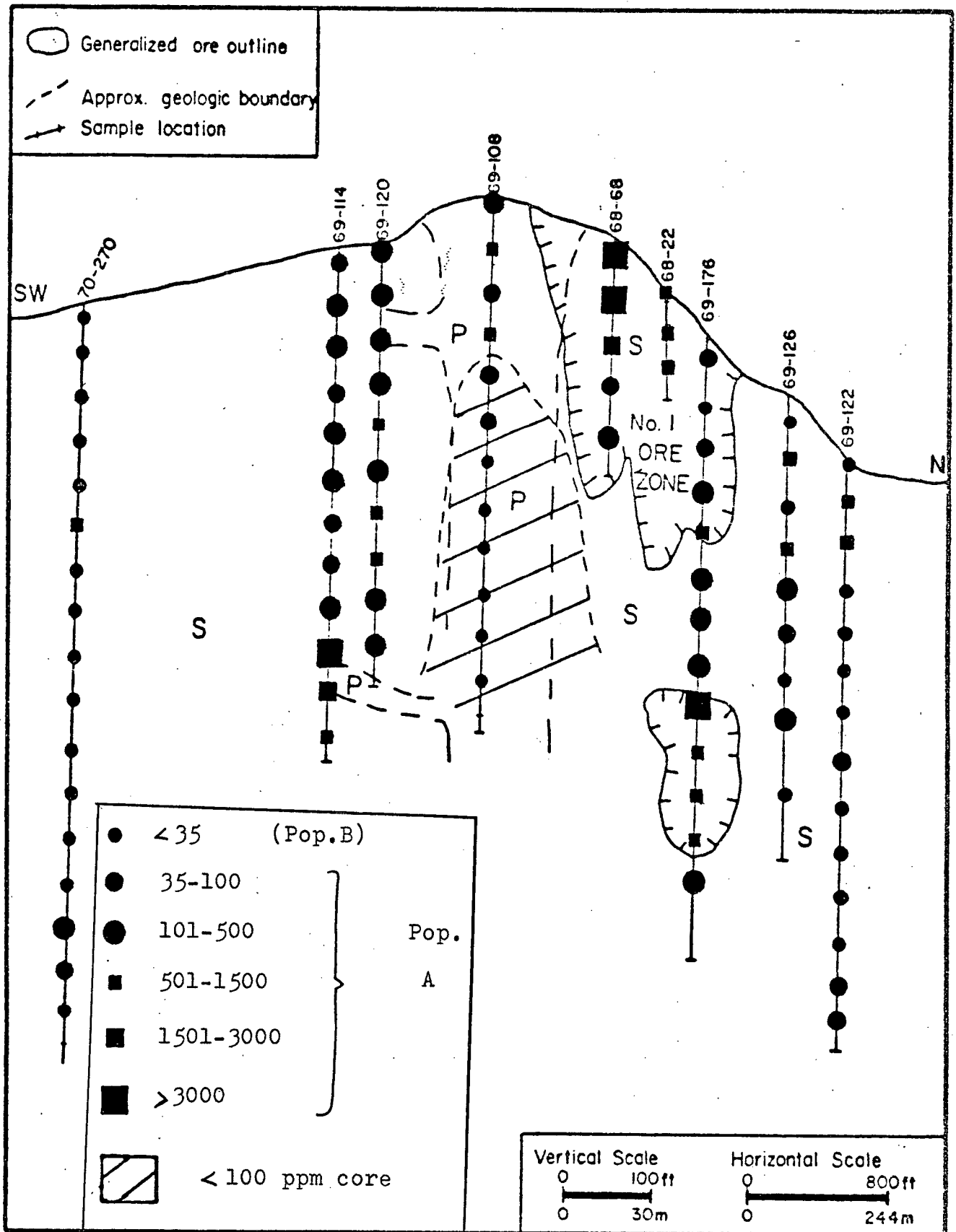


FIGURE A81: Distribution of Cu (ppm), Highmont Subsurface

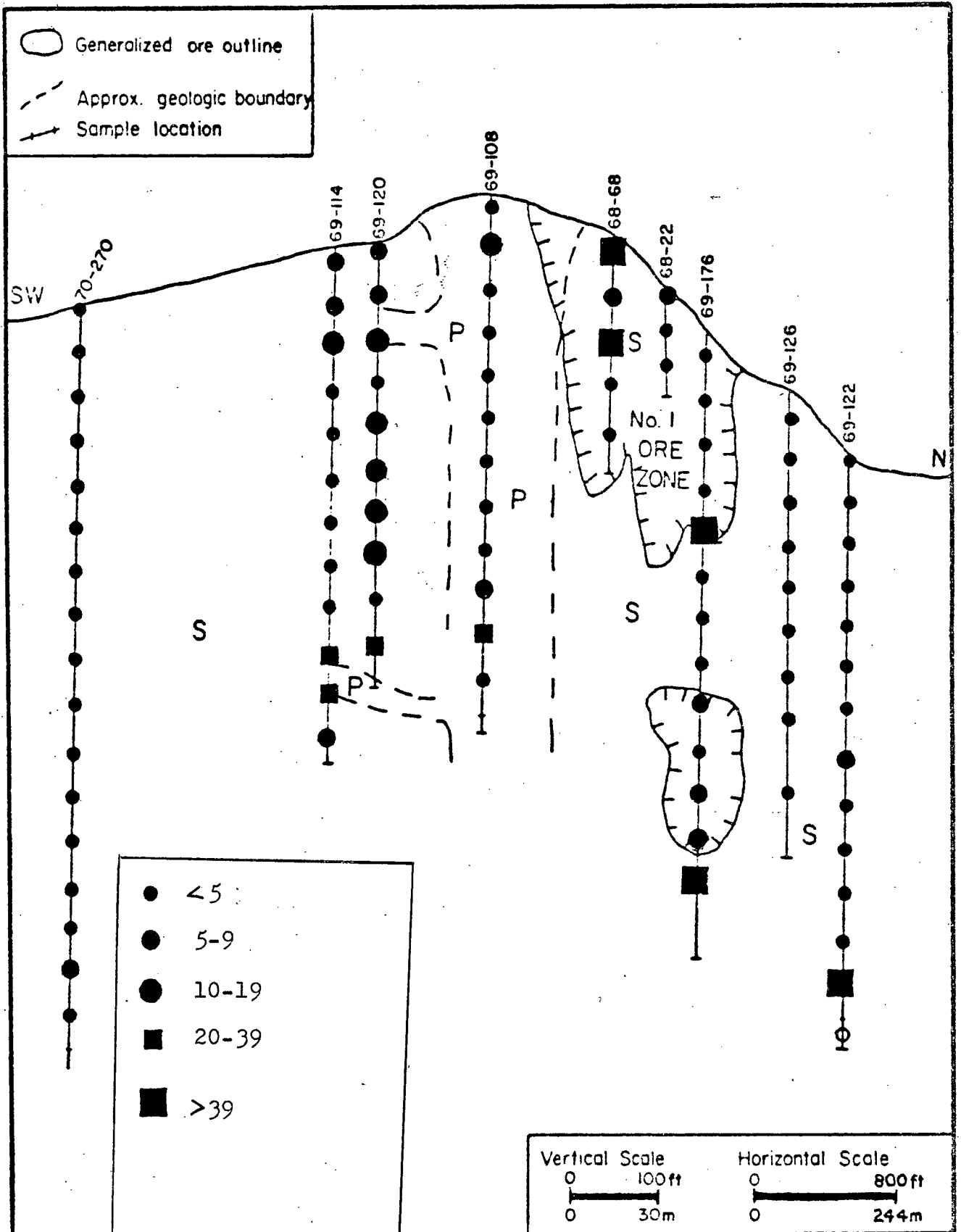


FIGURE A82: Distribution of Mo (ppm), Highmont Subsurface

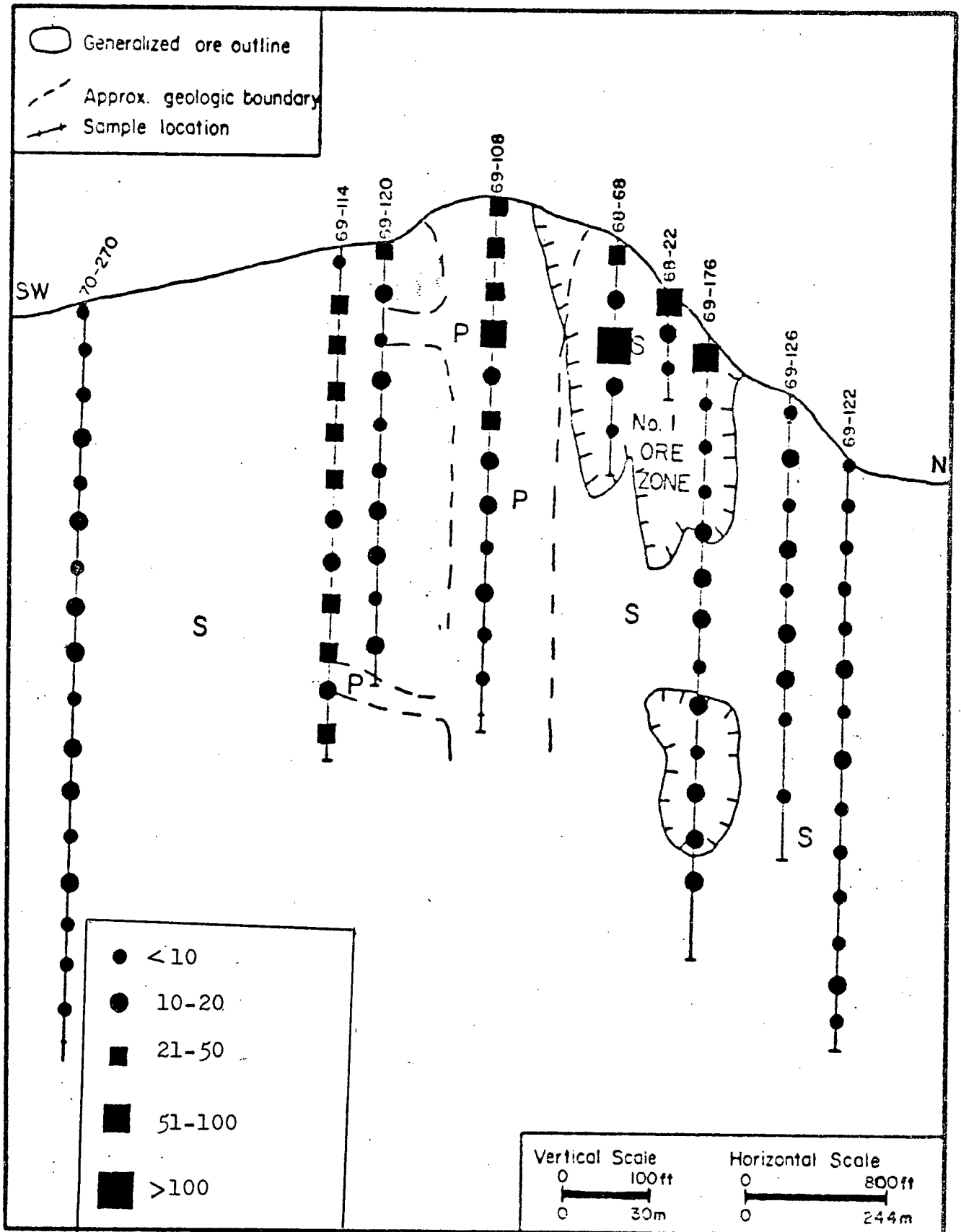


FIGURE A84: Distribution of B (ppm), Highmont Subsurface

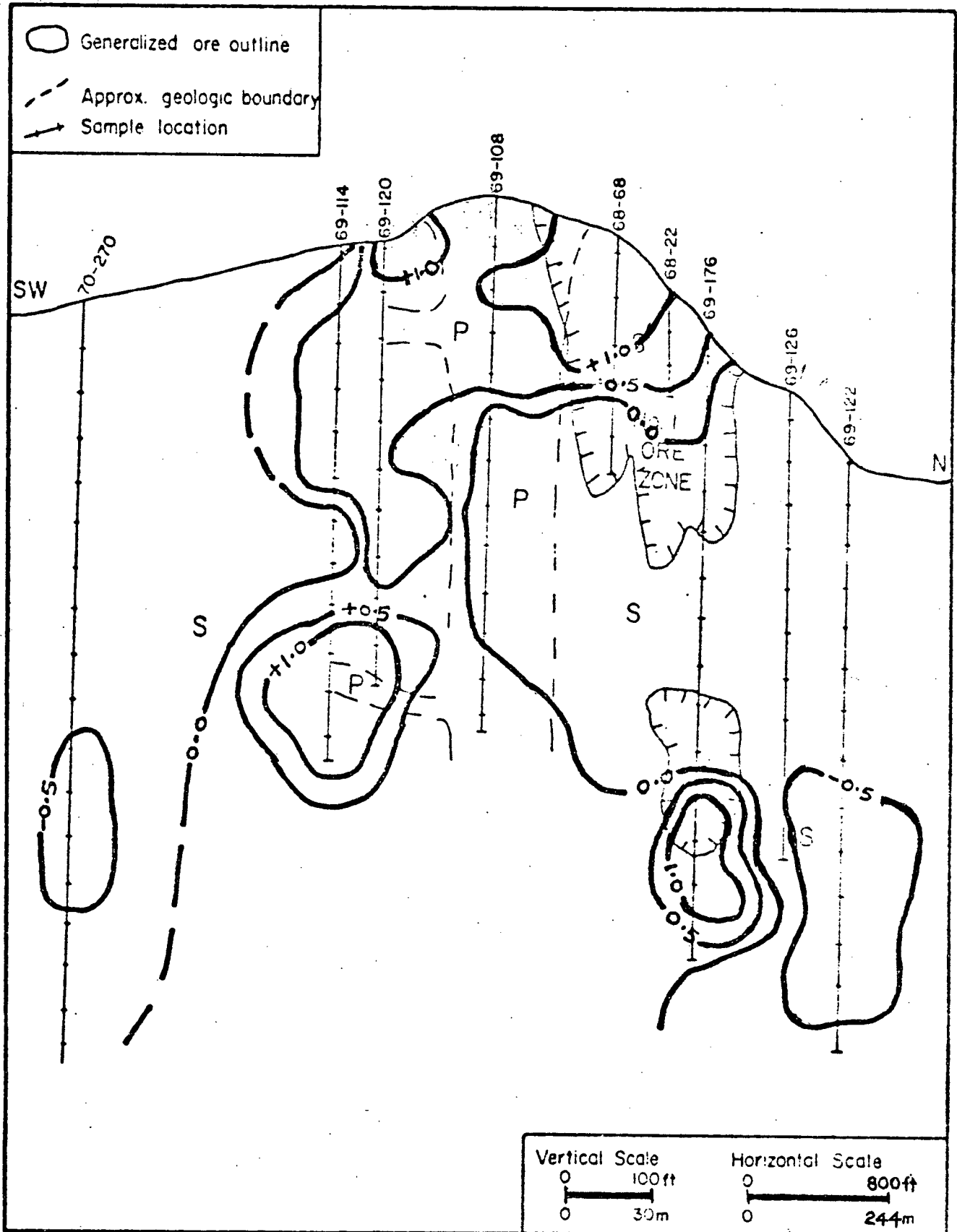


FIGURE A85: Scores of Factor R-1 (Cu,Mo,B), Highmont Subsurface

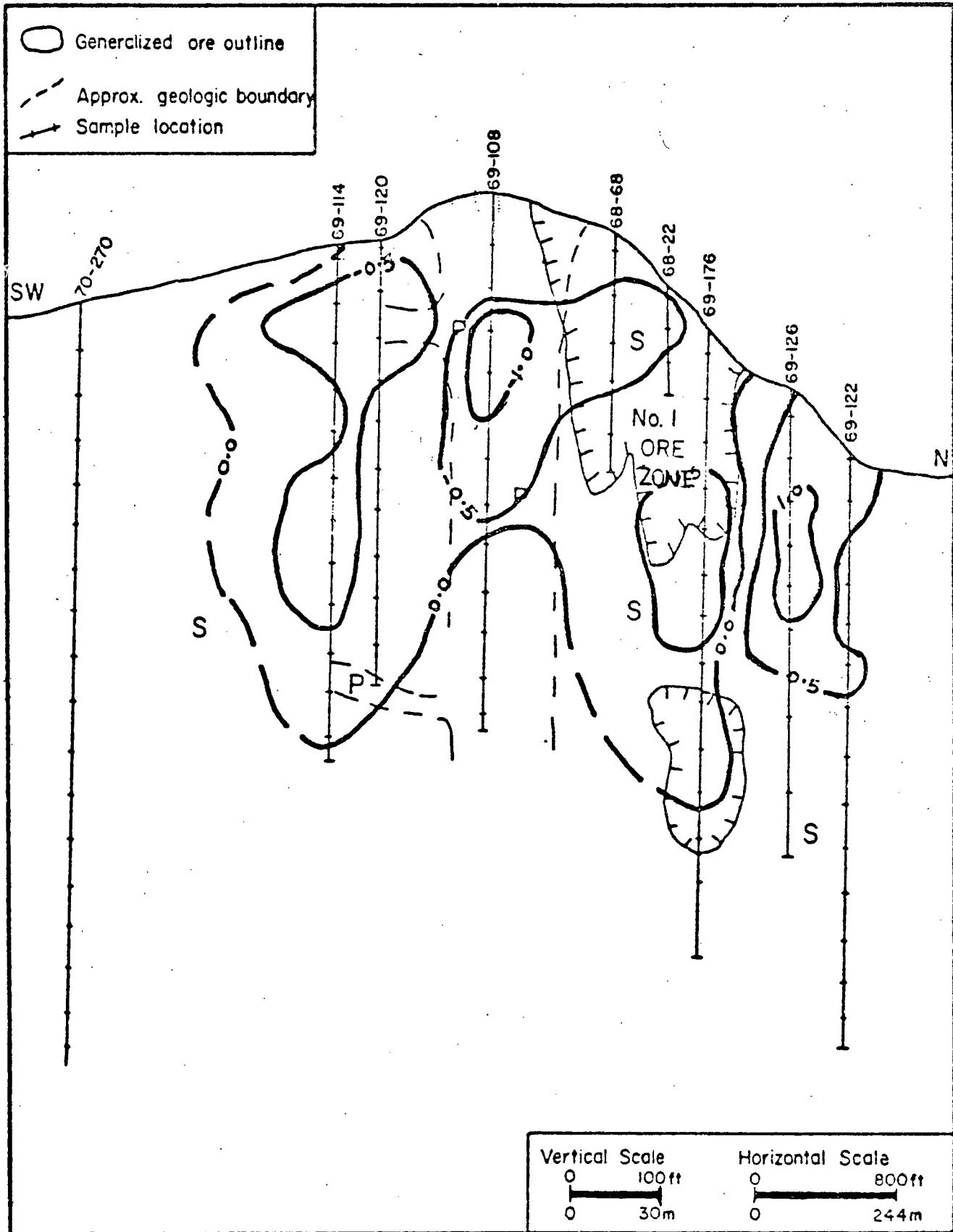


FIGURE A86: Scores of Factor R-2 (Zn, Mn, Ca), Highmont Subsurface

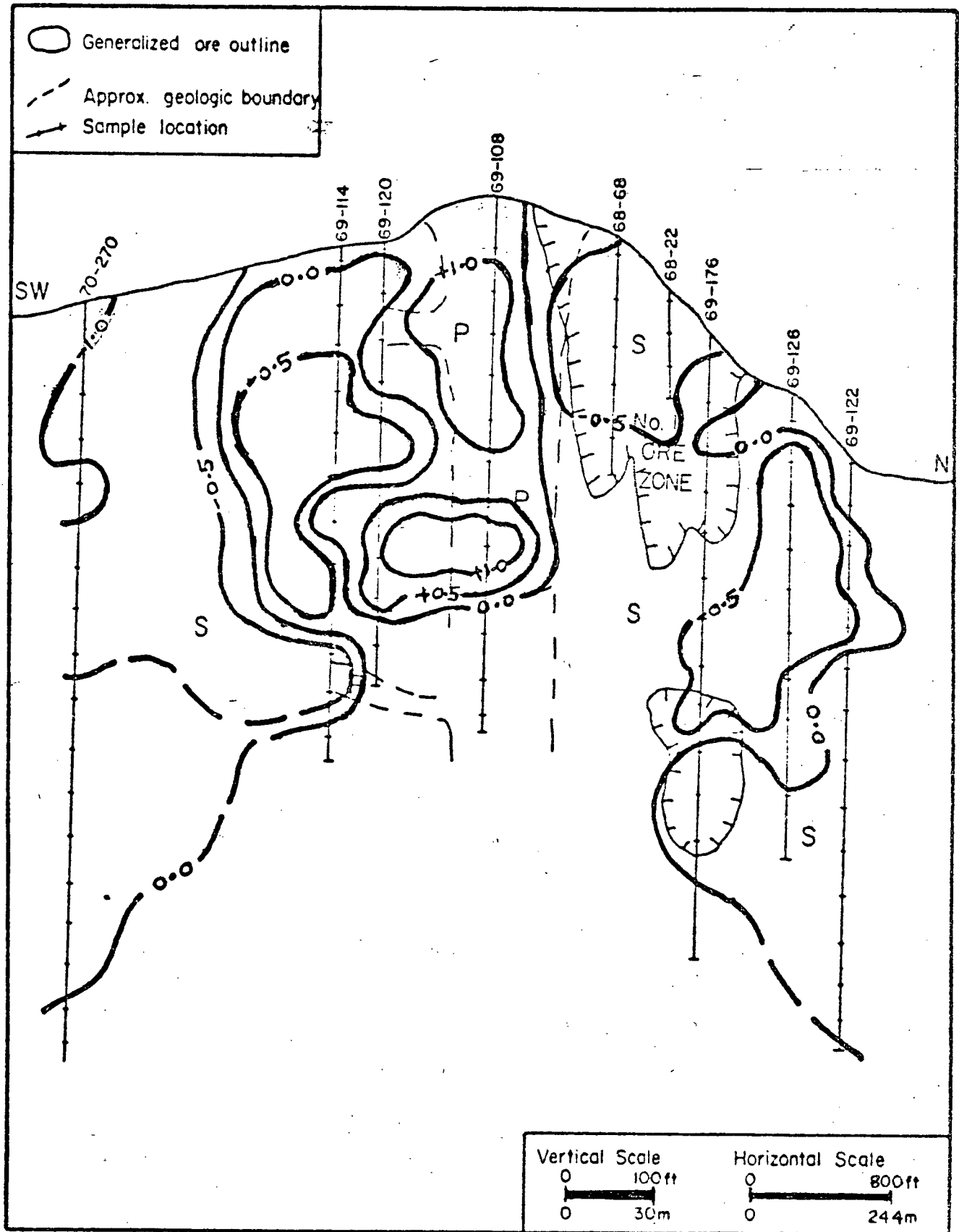


FIGURE A87: Scores of Factor R-3 (K,Ba), Highmont Subsurface

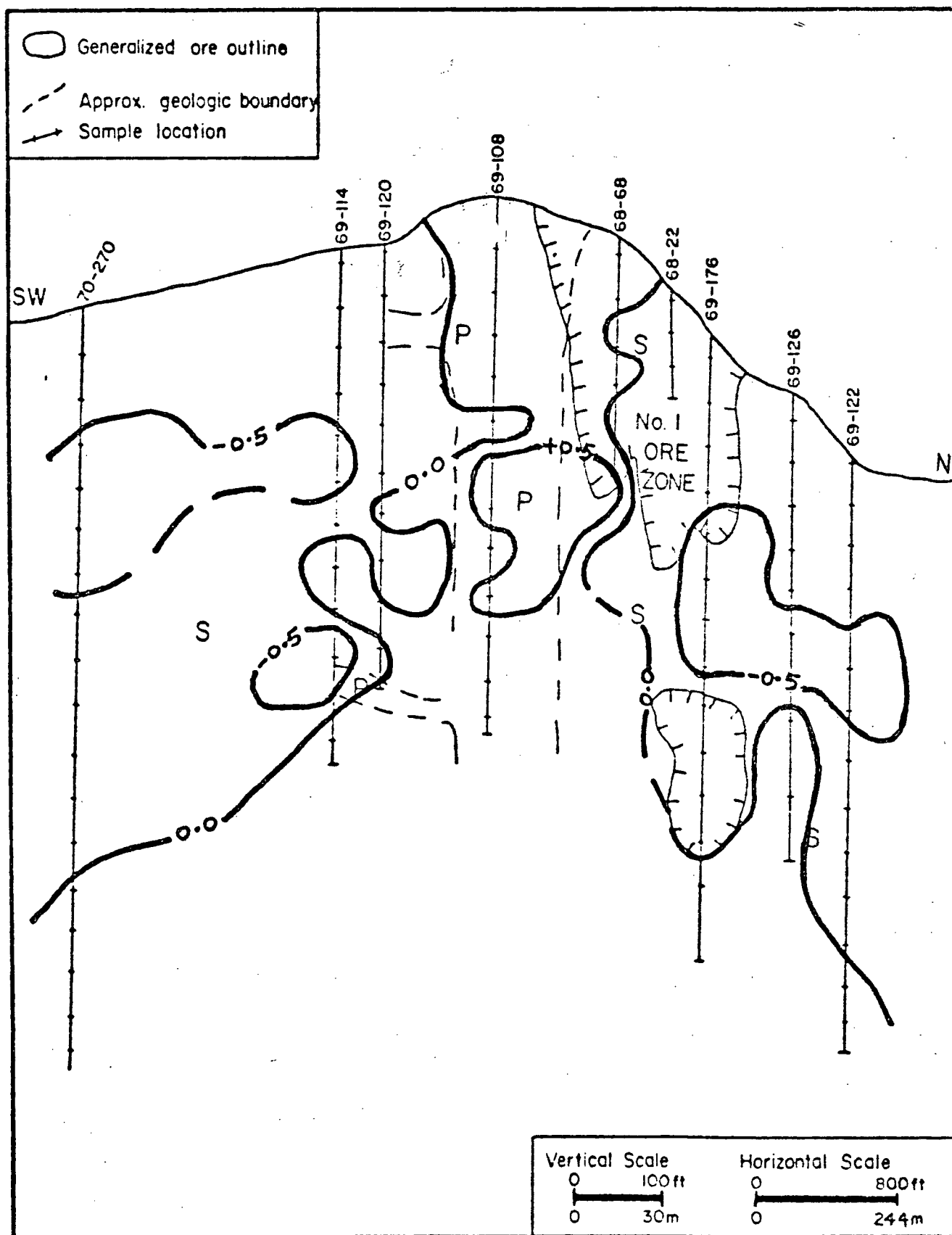


FIGURE A88: Scores of Factor R-4 (Sr,Ti,V), Highmont Subsurface

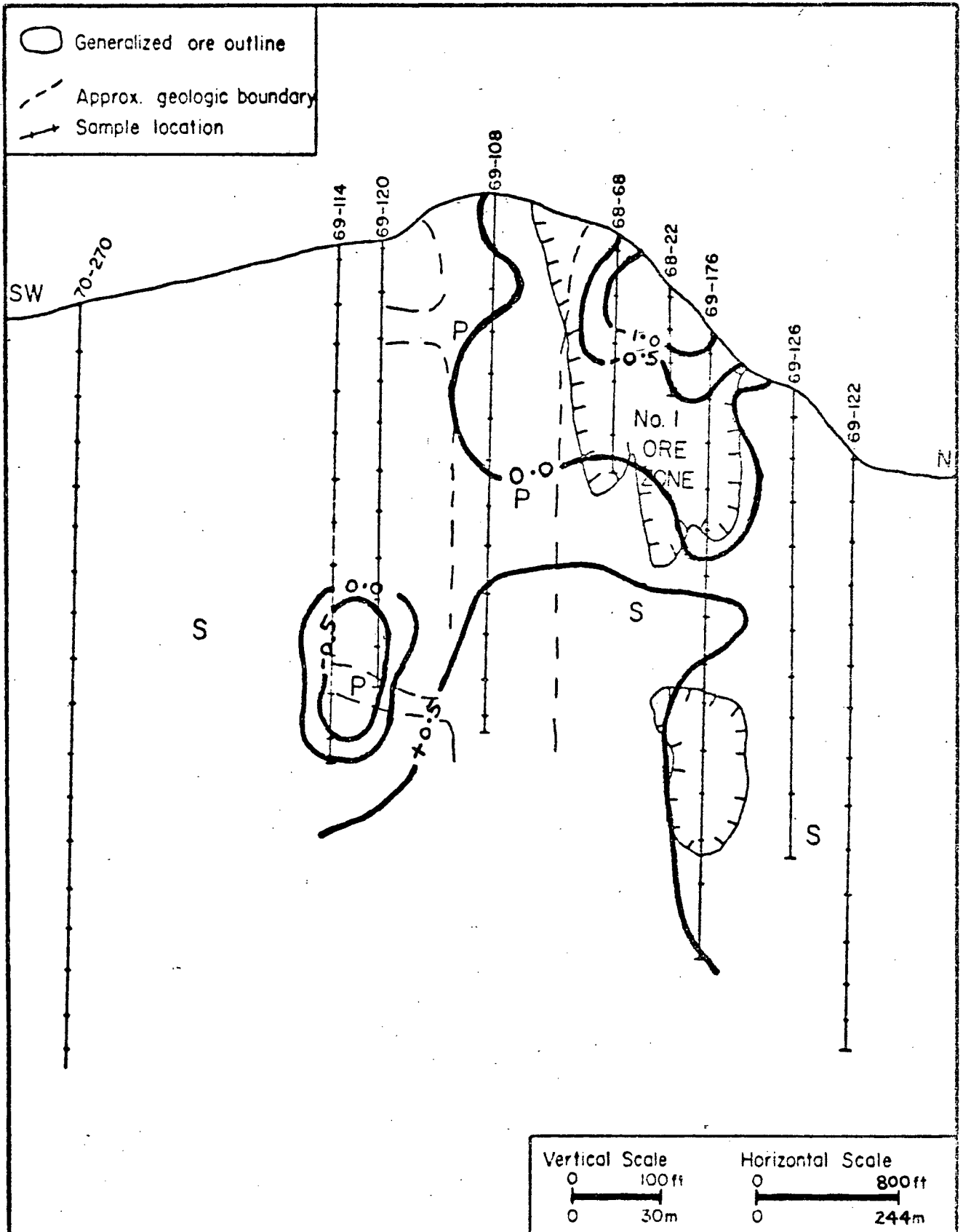


FIGURE A89: Scores of Factor R-5 (Fe,Na), Highmont Subsurface

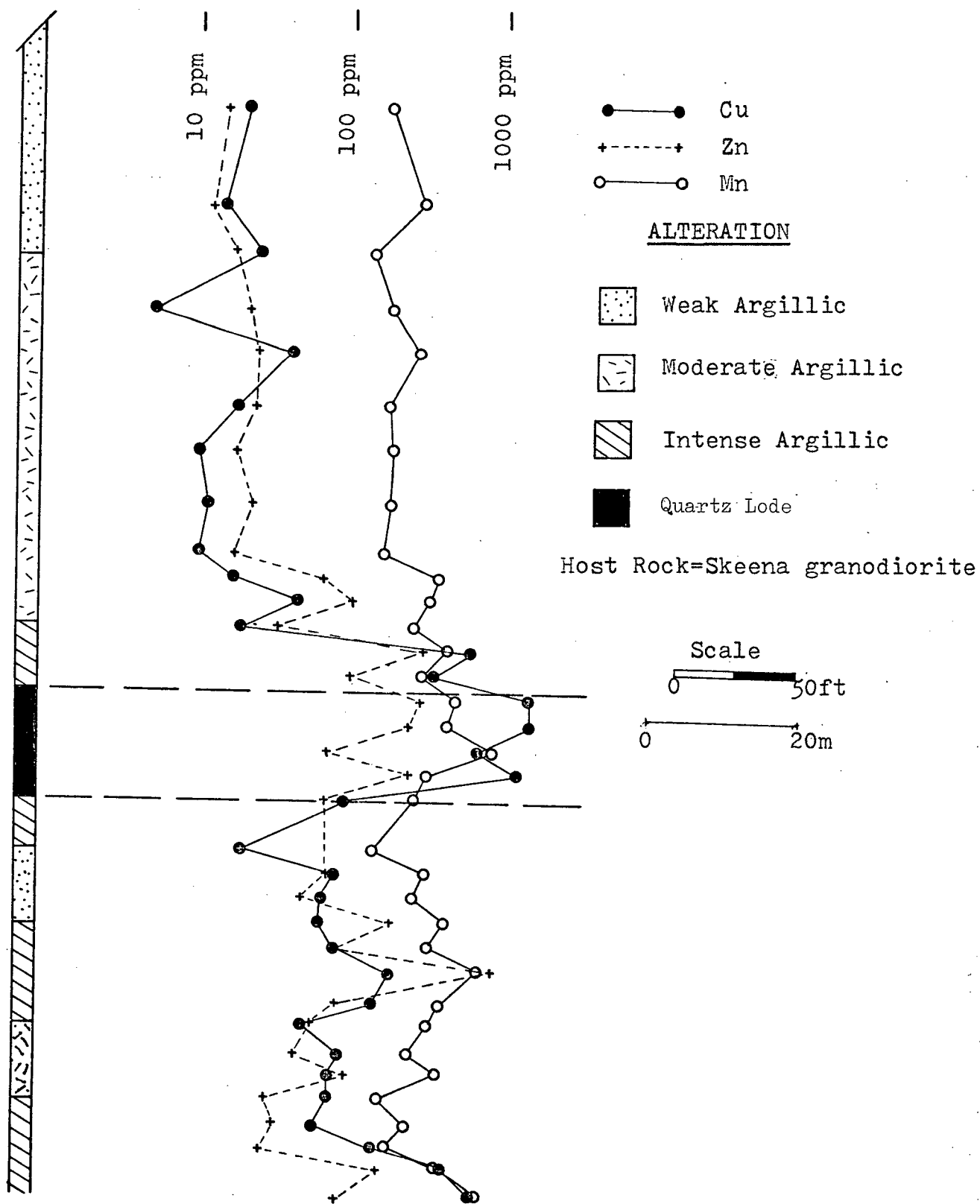


FIGURE A90: Distribution of Cu,Zn,Mn (ppm) along
Drill-Hole 69-2, Skeena Vein

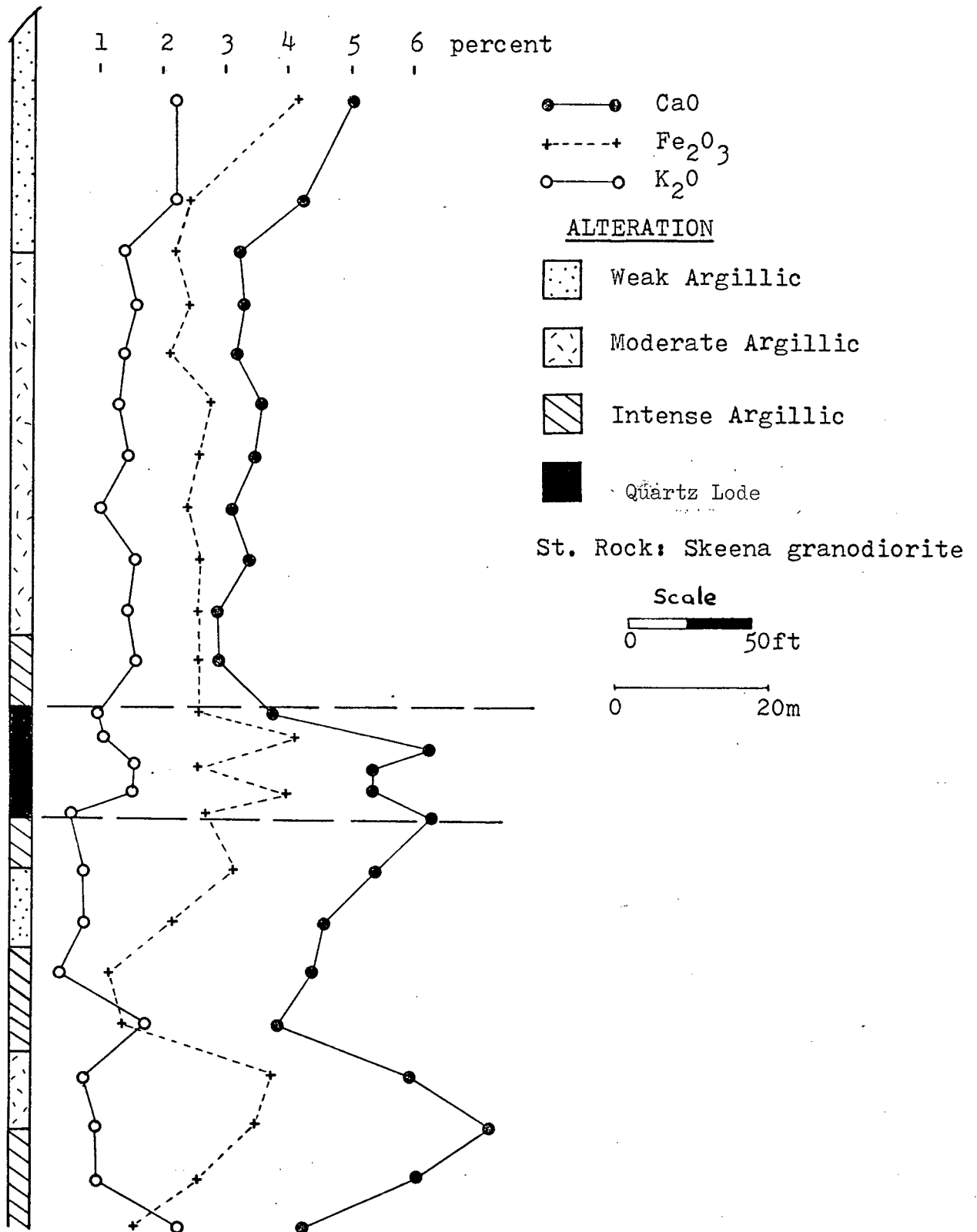


FIGURE A91: Distribution of CaO, Fe as Fe₂O₃ and K₂O (wt.%) along Drill-Hole 69-2, Skeena Vein

PUBLICATIONS

- Olade, M.A.D. (1969). Phases of hypogene tin mineralization in Nigeria. Ibad. Geol., v. 1, pp. 30-36.
- Olade, M.A.D., and Morton, R.D. (1972) Observations on the Proterozoic Seton Formation, East Arm of Great Slave Lake, Northwest Territories. Can. J. Earth Sci., v. 9, pp. 1110-1123.
- Baadsgaard, H., Morton, R.D., and Olade, M.A.D. (1973) Rb/Sr isotopic age for the Precambrian lavas of the Seton Formation, East Arm of Great Slave Lake, Northwest Territories. Can. J. Earth Sci., v. 10, pp. 1579-1582.
- Olade, M., and Fletcher, K. (1974) Potassium chlorate-hydrochloric acid: A sulphide-selective leach for bedrock geochemistry Journ. Geochem. Explor. v. 2, no. 3 (in press)
- Olade, M.A.D. (1974) Trace-element and isotopic data and their bearing on the genesis of Precambrian spilites, Athapuscow aulacogen. Great Slave Lake, Canada. Geol. Mag. (in press)
- Olade, M.A., and Fletcher, W.K. (1974) Primary dispersion of rubidium and strontium around porphyry copper deposits, Highland Valley, B.C. Econ. Geol. (in press)
- Olade, M., Fletcher, K., and Warren, H.V. (1974) Barium-strontium relationships at porphyry copper deposits, Highland Valley, B.C. Western Miner (in press)
- Olade, M., and Fletcher, K. Distribution of ore elements - sulphur, sulphide-held copper and iron at porphyry copper deposits, Highland Valley, B.C. (in preparation)
- Olade, M., and Fletcher, K. Regional and detailed bedrock geochemistry of porphyry copper deposits, Highland Valley, B.C. (in preparation)
- Olade, M., and Fletcher, K. Micro-dispersion of trace elements in minerals from porphyry copper deposits, Highland Valley. B.C. (in preparation)
- Olade, M., and Fletcher, K. Factor analysis of bedrock geochemical data from porphyry copper deposits, Highland Valley, B.C. (in preparation)
- Olade, M.A. Ore-forming processes at porphyry copper deposits in light of geochemical and isotopic data, Highland Valley, B.C. (in preparation).